0 0 0 0 4 9 0 1 9 8 1

uc-38

LBL-6890

c.1

RECEIVED
LAWRENCE
BERKELEY LABORATORY

APR 20 1978

LIBRARY AND
DOCUMENTS SECTION

For Reference

Not to be taken from this room

Energy and Environment Division

Turbulent Heat Transport In Two- And Three-Dimensional Temperature Fields

Don Sarath Abesiri Samaraweera

Ph.D. thesis

March 1978

Lawrence Berkeley Laboratory University of California/Berkeley

Prepared for the U.S. Department of Energy under Contract No. W-7405-ENG-48

LBL-6890

c.1

38

LEGAL NOTICE

This report was prepared as an account of work sponsored by the United States Government. Neither the United States nor the Department of Energy, nor any of their employees, nor any of their contractors, subcontractors, or their employees, makes any warranty, express or implied, or assumes any legal liability or responsibility for the accuracy, completeness or usefulness of any information, apparatus, product or process disclosed, or represents that its use would not infringe privately owned rights.

0 0 0 0 4 9 0 1 9 8 2

TURBULENT HEAT TRANSPORT IN TWO-AND THREE-DIMENSIONAL TEMPERATURE FIELDS

by

Don Sarath Abesiri Samaraweera

B.Sc.(Eng.), M.Sc.(Eng.), D.I.C.

Thesis submitted for the degree of

Doctor of Philosophy

in the Faculty of Engineering of the

University of London

March 1978

Department of Mechanical Engineering,
Imperial College of Science and Technology,
London SW7 2BX.

ABSTRACT

This Thesis presents a fundamental numerical study of turbulent heat and mass transport processes in two-and three-dimensional convective flows. The model of turbulence employed is of the type referred to as a second-order closure. In this scheme transport equations for all non-zero components of the Reynolds stress tensor, for the isotropic dissipation rate of turbulent kinetic energy, for all non-zero scalar flux tensor components and for the mean square scalar fluctuations are solved by a finite difference method along with the mean momentum and mean enthalpy (or concentration) equations. The model used for the stresses has been developed in an earlier work. In the present study parallel ideas were utilised in obtaining a model for turbulent heat and mass transfer processes.

The study has focused especially on the problem of non axi-symmetric convective heat and mass transport in pipes, which arises when the boundary conditions are not axi-symmetric. The few available experimental data on such situations have indicated anisotropy in effective diffusivities. To expand the available data base an experiment was conducted to obtain heat transfer measurements in strong three-dimensional heating conditions.

Numerical procedures, especially suitable for incorporation of second-order turbulent closure models have been developed. The effect of circumferential conduction in the tube material, (which is influential in the asymmetric heating data currently available) was accounted for directly by extending the finite difference calculations into the pipe wall.

The principal goal of predicting three-dimensional scalar transfer has been achieved. The predictions of the mean temperature field are in much closer agreement with experiment than an earlier study using

isotropic diffusion coefficients. The prediction of free shear flows have been only partially successful. The present model does not fully account for the variation in effective Prandtl number, among free shear flows observed in experiments. The prediction of wall flows indicate that the turbulent time scales of velocity and scalar fields are not proportional in the vicinity of adiabatic (or impermeable) surfaces. The implications of this result for the further refinement of the model is discussed.

ACKNOWLEDGEMENTS

It is with pleasure and sincere thanks that I acknowledge the sound guidance provided by Professor B.E. Launder during the course of my research work. His active interest and amazing appetite for progress had a considerable influence on the completion of this work. His constructive criticism and understanding during the write-up period, and also the kind hospitality shown by his family, especially during our early days in Davis, California, are much appreciated.

Dr. M.M. Gibson is thanked for the guidance provided by him during Professor Launder's absence from Imperial College. Later in University of California at Davis, during the summer of '77, Professors J.W. Baughn and M.A. Hoffman supervised my experimental investigation. They are thanked for providing their expertise on those lines.

I also thank my colleagues: Dr. G.J. Reece and Mr. D. Bryant, for providing their computer codes for my use which helped me a great deal in developing the present versions; Mr. S. El-Tahry, Drs. R. Schiestel, B.I. Sharma and S.A. Syed, for the pleasant and useful discussions we had; Mr. A. Giesbrecht and A. Mokhtarani, for their contributions towards the completion of my experimental work within a short time.

The computations reported here were performed at the University of London computer centre, Imperial College computer centre, University of California at Davis computer centre and at Lawrence Berkeley Laboratory computer centre. The help given by their consulting staff is much appreciated.

The Tea Research Institute of Sri Lanka is gratefully acknowledged for granting post graduate study leave which enabled me to carry out the work described in this Thesis.

Support for the research has been provided by the United Kingdom Science Research Council through grant No. B/RG/78011 and by Division of Basic Energy Sciences of the U.S. Department of Energy. This support is gratefully acknowledged.

My wife, Damayanthi, for whom I am especially thankful provided constant encouragement throughout the course of the work and finally took over the challenging task of typing my scribbles.

CONTENTS

		Page
Abstract		2
Acknowledgements		4
Contents		6
List of Tables		12
List of Figures		13
Nomenclature		19
CHAPTER 1:	INTRODUCTION	27
1.1	Introduction	27
1.2	Equations of Fluid Motion and Scalar Transport	29
1.3	Closure Levels	32
1.3.1	Mean-Field Closure Models	34
1.3.2	Turbulent Transport Models	35
1.3.3	Higher Order Closures	37
1.3.4	Other Closures	37
1.4	Evaluation of Available Models	38
1.4.1	Eddy Viscosity Models	38
1.4.2	Eddy Diffusivity Models and Turbulent Prandtl (or Schmidt) Number	40
1.4.3	Reynolds Stress Models	43
1.4.4	Scalar Flux Models	44
1.5	Present Contribution	45
1.5.1	Theoretical Contribution	45
1.5.2	Choice of Turbulence Model	45
1.5.3	Path for Verification of the Turbulence Model	46
1.5.4	Numerical Contribution	48
1.5.5	Experimental Contribution	50

		Page
CHAPTER 2:	TURBULENCE MODEL	51
2.1	Introduction	51
2.2	Reynolds Stress Equation and its Trace	52
	2.2.1 The Viscous Destruction Term	54
	2.2.2 The Diffusion Term	55
	2.2.3 The Pressure-Strain Term	58
	2.2.4 Wall Effects on the Pressure-Strain Term	62
2.3	Transport Equation for Isotropic Dissipation Rate	67
2.4	The Scalar Flux Equation	71
	2.4.1 The Diffusion Term	73
	2.4.2 The Pressure-Scalar Gradient Correlation	74
	2.4.3 Wall Effects on the Pressure-Scalar Gradient Term	79
2.5	The Transport Equation for Scalar Fluctuations	83
2.6	A Summary of the Models to be Investigated	85
2.7	Modelled Equations in Cartesian Tensor Form	90
	2.7.1 Reynolds Stress Equations	90
	2.7.2 Isotropic Dissipation Rate Equation	91
	2.7.3 Scalar Flux Equations	92
	2.7.4 Scalar Fluctuation Equation	93
CHAPTER 3:	NUMERICAL PROCEDURES	94
3.1	Introduction	94
3.2	The Patankar-Spalding Procedure for Two-Dimensional Boundary Layers	96
	3.2.1 Main Features	96
	3.2.2 Treatment of Turbulent Shear Stress and Scalar Flux	98
	3.2.3 Instability in Solution and a Possible Remedy	99

Page

3.3 Description and Application of the Three-Dimensional (θ, r, z) Boundary Layer Procedure 101

3.3.1 Finite Difference Grid 102

3.3.2 Derivation of Finite Difference Equations 103

3.3.3 Assembly of Finite Difference Terms 105

3.3.4 Finite Difference Equation for Velocity Components and SIMPLE Algorithm 106

3.3.5 The Case of Axi-Symmetric (or Plane-Symmetric) Confined Flow 110

3.4 An Ideal Grid 111

3.5 Staggered Grid Arrangement for $(\theta\text{-}r\text{-}z)$ Procedure: for Three-and Two-Dimensional Scalar Transport in a Two-Dimensional Hydrodynamic Field 113

3.5.1 Staggered Grid Arrangement for $(x\text{-}\Psi)$ Procedure 114

3.6 Cell Layout and Boundary Conditions 115

3.6.1 Wall Boundary Condition 116

3.6.2 Symmetric Axis (or Plane) Boundary Condition 119

3.6.3 Free-Stream Boundary Condition 119

3.7 Treatment of Conducting Wall in the Numerical Procedure 121

CHAPTER 4: REVIEW OF EXPERIMENTAL DATA 124

4.1 Introduction 124

4.2 Data Required and Criteria for Assessment 126

4.2.1 Criteria for Assessment of Data 128

4.3 Characteristics of Free Shear Flows 129

4.3.1 Integral Forms of Mean Equations 129

4.3.2 Definition of Self Similarity and Decay Laws 130

4.3.3 Expressions for Shear Stress and Scalar Flux for Self Similar Flows 134

		Page
4.4	Review of Data for Free Shear Flows	136
	4.4.1 Plane Jet	136
	4.4.2 Plane Mixing Layer	138
	4.4.3 Plane Wake	141
4.5	Characteristics of Flows Affected by Walls	144
	4.5.1 Turbulent Prandtl Number in the Near-Wall Logarithmic Region	145
4.6	Review of Data for Wall Flows	147
	4.6.1 Flat Plate Boundary Layer	147
	4.6.2 Pipe Flow	150
4.7	Review of Data on Three-Dimensional Scalar Transport	152
CHAPTER 5:	EXPERIMENTAL INVESTIGATION	157
5.1	Preliminary Considerations	157
	5.1.1 Aim of the Experimental Investigation	157
	5.1.2 Facilities Available and Level of Measurements	158
	5.1.3 Method of Obtaining Circumferentially Non-Uniform Heating Rates	158
	5.1.4 Choice of Tube Material	160
	5.1.5 Choice of Fluid	161
5.2	Experimental Equipment	162
	5.2.1 Design of the Tube	162
	5.2.2 Thermocouple Installation	164
	5.2.3 Power Measurement	165
	5.2.4 Flow Measurement	165
5.3	Preliminary Measurements	167
	5.3.1 Verification of Uniformity of the Silver Coating	167

Page

5.3.2 Uncertainties in Measurements 168

5.4 Experimental Results 170

CHAPTER 6: PREDICTION OF TWO-DIMENSIONAL SCALAR TRANSPORT 171

6.1 Introduction 171

6.2 Prediction of Free Shear Flows 172

6.2.1 The Plane Jet 172

6.2.2 The Plane Wake 175

6.2.3 The Plane Mixing Layer 176

6.2.4 Conclusions 179

6.3 Flat Plate Boundary Layer 181

6.3.1 Hydrodynamic Predictions 182

6.3.2 Scalar Transport Predictions 184

6.4 Pipe Flow 188

6.4.1 Hydrodynamic Predictions 188

6.4.2 Scalar Transport Predictions 189

6.4.3 Conclusions 191

CHAPTER 7: PREDICTION OF THREE-DIMENSIONAL SCALAR TRANSPORT 193

7.1 Introduction 193

7.2 Verification of the Three-Dimensional Solution Procedure 195

7.2.1 Check for Numerically Induced Asymmetry in Scalar Field 195

7.2.2 Check for the Conservation of Mean Scalar 196

7.2.3 Check for Grid Independence of the Solution 197

7.3 Comparison of Predicted Results with Experimental Data 198

7.4 Conclusions 206

		Page
CHAPTER 8:	CONCLUDING REMARKS	207
8.1	Achievements and Limitations of Present Work	207
8.2	Suggestions for Future Work	210
References		212
Figures for Chapters (1) - (8)		220
APPENDIX A:	A Form for the Near-Wall Effect Function in Cylindrical Geometry	294
APPENDIX B:	Simulation of the Diffusive Transport of $\overline{u_i c}$ and $\overline{c^2}$	296
APPENDIX C:	Derivation of the Exact Equation for Pressure-Scalar Gradient Correlation	299
APPENDIX D:	Modelled Reynolds Stress and Scalar Flux Equations in Cylindrical Polar Coordinates	302
APPENDIX E:	Derivation of Finite Difference Equation for Variables Stored in Staggered $(x\text{-}\Psi)$ Grid	309
APPENDIX F:	Computer Program for the Solution of Two-and Three-Dimensional Scalar Transport Problem	316
F.1	Introduction	316
	F.1.1 Base Case	317
	F.1.2 The Grid System	317
F.2	Listing of FORTRAN Symbols	319
F.3	Description of Subroutines and Common Block	328
F.4	Listing of the Computer Program	338
Figures for Appendices (A) - (F)		386

LIST OF TABLES

			Page
Table 2.1	:	Hydrodynamic models used in the present study	86
Table 2.2	:	Scalar transport models investigated in the present study	88
Table 3.1	:	Variable locations in an ideal grid	112
Table 4.1	:	Data reviewed and their relative importance	127
Table 4.2	:	Decay Laws	133
Table 4.3	:	Self similar shear stress and scalar flux relations	135
Table 4.4	:	Scalar measurements in plane jets	137
Table 4.5	:	Scalar measurements in plane mixing layers	139
Table 4.6	:	Scalar measurements in plane wake	142
Table 4.7	:	Scalar measurements in smooth flat plate boundary layers	148
Table 4.8	:	Three-dimensional scalar experiments in fully developed pipe flows	153
Table 7.1	:	Measuring stations for Quarmby and Anand's experiments	198
Table D.1	:	Modelled Reynolds stress equations in cylindrical polar coordinates	303
Table D.2	:	Modelled scalar flux equations in cylindrical polar coordinates	306
Table F.1	:	Listing of FORTRAN symbols	319
Table F.2	:	Contents of comdeck COMALL	329

LIST OF FIGURES

			Page
Figure 3.1	:	Control volumes in Patankar-Spalding method	220
Figure 3.2	:	Conventional grid arrangement	220
Figure 3.3	:	Grid layout in the cross stream	221
Figure 3.4	:	Cell mass balance	221
Figure 3.5	:	Three orthogonal views of control volumes with ideal orientation of stress and fluxes (A Cartesian non expanding grid is shown here for clarity)	222
Figure 3.6	:	Idealised grid system for three-dimensional boundary layer flows	223
Figure 3.7	:	Modified grid system for the present problem	224
Figure 3.8	:	Typical grid pattern in the near-wall region	225
Figure 3.9	:	False-source term technique	225
Figure 3.10	:	Treatment of a conducting thick wall	226
Figure 4.1	:	Notation for velocity and scalar field configurations	227
Figure 5.1	:	Adhesive tape strips	229
Figure 5.2	:	Silver coating on the tube	229
Figure 5.3	:	Electrical connections to the silver coating	229
Figure 5.4	:	Thermocouple arrangement around the tube	230
Figure 5.5	:	Thermocouple circuit	230
Figure 5.6	:	Electrical power circuit	231
Figure 5.7	:	Heat flux variation (ideal)	232
Figure 5.8	:	A more plausible heat flux variation	232
Figure 6.1	:	The plane jet in stagnant surroundings: Mean velocity profiles	233
Figure 6.2	:	The plane jet in stagnant surroundings: Shear stress profiles	233
Figure 6.3	:	The palne jet in stagnant surroundings: Turbulence intensity profiles	234

		Page
Figure 6.4 :	The plane jet in stagnant surroundings; Mean temperature profiles	235
Figure 6.5 :	The plane jet in stagnant surroundings; Cross-stream heat flux profiles	235
Figure 6.6 :	The plane jet in stagnant surroundings: The ratio of streamwise to cross-stream scalar fluxes	236
Figure 6.7 :	The plane jet in stagnant surroundings: Turbulent Prandtl number profiles	236
Figure 6.8 :	The plane wake: Mean velocity profiles	237
Figure 6.9 :	The plane wake: Shear stress profiles	237
Figure 6.10 :	The plane wake: Turbulence intensity profiles	238
Figure 6.11 :	The plane wake: Mean temperature profiles	239
Figure 6.12 :	The plane wake: Cross-stream heat flux profiles	239
Figure 6.13 :	The plane wake: The ratio of streamwise to cross-stream scalar fluxes	240
Figure 6.14 :	The plane wake: Turbulent Prandtl number profiles	240
Figure 6.15 :	The plane wake: Streamwise heat flux profiles	241
Figure 6.16 :	The plane wake: Temperature fluctuations	241
Figure 6.17 :	The plane mixing layer with $\frac{U_1}{U_2} = 0.5$: Mean velocity profiles	242
Figure 6.18 :	The plane mixing layer with $\frac{U_1}{U_2} = 0.5$: Shear stress profiles	243
Figure 6.19 :	The plane mixing layer with $\frac{U_1}{U_2} = 0.5$: Turbulence intensity profiles	244
Figure 6.20 :	The plane mixing layer with $\frac{U_1}{U_2} = 0.5$: Mean temperature profiles	245
Figure 6.21 :	The plane mixing layer with $\frac{U_1}{U_2} = 0.5$: Cross-stream scalar flux profiles	245
Figure 6.22 :	The plane mixing layer with $\frac{U_1}{U_2} = 0.5$: The ratio of streamwise to cross-stream scalar fluxes	246
Figure 6.23 :	The plane mixing layer with $\frac{U_1}{U_2} = 0.5$: Turbulent Prandtl number profiles	246

			Page
Figure 6.24	:	The plane mixing layer with $\frac{U_1}{U_2} \approx 0$: Mean velocity profiles	247
Figure 6.25	:	The plane mixing layer with $\frac{U_1}{U_2} \approx 0$: Shear stress profiles	247
Figure 6.26	:	The plane mixing layer with $\frac{U_1}{U_2} \approx 0$: Mean temperature profiles	248
Figure 6.27	:	The plane mixing layer with $\frac{U_1}{U_2} \approx 0$: Cross-stream scalar flux profiles	248
Figure 6.28	:	The plane mixing layer with $\frac{U_1}{U_2} \approx 0$: The ratio of streamwise to cross-stream scalar fluxes	249
Figure 6.29	:	The plane mixing layer with $\frac{U_1}{U_2} \approx 0$: Turbulent Prandtl number profiles	249
Figure 6.30	:	Flat plate boundary layer: Mean velocity profiles	250
Figure 6.31	:	Flat plate boundary layer: Shear stress profiles	250
Figure 6.32	:	Flat plate boundary layer: Turbulence intensity profiles - comparison of two near-wall effect models	251
Figure 6.33	:	Flat plate boundary layer: Turbulence intensity profiles - comparison of two near-wall functions	252
Figure 6.34	:	Flat plate boundary layer: Turbulence intensity profiles - comparison of two diffusion modes	253
Figure 6.35	:	Flat plate boundary layer: Shear correlation coefficient - comparison of two diffusion models	254
Figure 6.36	:	Flat plate boundary layer - step in wall heat flux: Mean temperature profiles	255
Figure 6.37	:	Flat plate boundary layer - step in wall heat flux: Temperature defect profiles	256
Figure 6.38	:	Flat plate boundary layer - step in wall heat flux: Turbulent Prandtl number profiles	257
Figure 6.39	:	Flat plate boundary layer - step in wall heat flux: Cross-stream heat flux profiles	258
Figure 6.40	:	Flat plate boundary layer - step in wall heat Flux: Streamwise heat flux profiles	259

			Page
Figure 6.41	:	Flat plate boundary layer - step in wall heat flux: Temperature fluctuations profiles	260
Figure 6.42	:	Fully developed pipe flow: Mean velocity profiles	261
Figure 6.43	:	Fully developed pipe flow: Shear stress profiles	261
Figure 6.44	:	Fully developed pipe flow: Turbulence intensity profiles - comparison of two near-wall effect models	262
Figure 6.45	:	Fully developed pipe flow: Turbulence intensity profiles - comparison of two diffusion models	263
Figure 6.46	:	Fully developed pipe flow: Mean temperature profiles	264
Figure 6.47	:	Fully developed pipe flow: Cross-stream heat flux profiles	264
Figure 6.48	:	Fully developed pipe flow: Streamwise heat flux profiles	265
Figure 6.49	:	Fully developed pipe flow: Turbulent Prandtl number profiles	265
Figure 6.50	:	Fully developed pipe flow: Concentration profiles downstream of a short mass transfer region	266
Figure 6.51	:	Turbulent Schmidt number profiles downstream of a short mass transfer section in the wall - pipe flow	267
Figure 7.1	:	Comparison of streamwise development of near-wall concentration levels in QUARMBY and ANAND's [59] experiment	268
Figure 7.2	:	The angular variation of (a) wall heat fluxes, (b) wall temperature and (c) Nusselt number, $Nu(\omega, X/D)$, BLACK and SPARROW's [13] experiment, Re = 40500	269
Figure 7.3	:	The angular variation of (a) wall heat fluxes, (b) wall temperature and (c) Nusselt number, $Nu(\omega, X/D)$, BLACK and SPARROW's [13] experiment, Re = 16800	270
Figure 7.4	:	Non-dimensional temperature $\frac{C - C_{min}}{C_{max} - C_{min}}$ contours: Black and Sparrow's experiment, Re = 40500	271

			Page
Figure 7.5	:	Non-dimensional temperature $\frac{C - C_{min}}{C_{max} - C_{min}}$ contours: Black and Sparrow's experiment, Re = 16800	272
Figure 7.6	:	Non-dimensional temperature profiles in BLACK and SPARROW's [13] experiment, X/D = 52	273
Figure 7.7	:	Streamwise development of Nusselt numbers at several angular locations - BLACK and SPARROW's [13] experiment , Re = 40500	274
Figure 7.8	:	Streamwise development of Nusselt number at several angular locations - BLACK and SPARROW's [13] experiment, Re = 16800	275
Figure 7.9	:	Heat flux through the outer and inner surface of the tube, (a) $Re \simeq 20000$, (b) $Re \simeq 40000$, (c) $Re \simeq 90000$	276
Figure 7.10	:	Temperature profiles at the outer surface of the tube wall : Present experimental situation; Both halves heating, $Re \simeq 20000$	277
Figure 7.11	:	Temperature profiles at the outer surface of the tube wall: Present experimental situation; Both halves heating, $Re \simeq 40000$	278
Figure 7.12	:	Temperature profiles at the outer surface of the tube wall: Present experimental situation; Both halves heating, $Re \simeq 90000$	279
Figure 7.13	:	Streamwise variation of Nusselt number: Present experimental investigation, Both halves heating, $Re \simeq 20000$	280
Figure 7.14	:	Predicted non-dimensional temperature $\frac{C - C_{min}}{C_{max} - C_{min}}$ Contours: Present experimental situation; Both halves heating, $Re \simeq 40000$	281
Figure 7.15	:	Variation of (a) heat fluxes and (b) local Nusselt number, around the tube wall, $Re \simeq 20000$	284
Figure 7.16	:	Temperature profiles at the outer surface of the tube wall: Present experimental situation, $Re \simeq 20000$	285
Figure 7.17	:	Variation of (a) heat fluxes and (b) local Nusselt number, around the tube wall, $Re \simeq 40000$	286
Figure 7.18	:	Temperature profiles at the outer surface of the tube wall: Present experimental situation, $Re \simeq 40000$	287
Figure 7.19	:	Variation of (a) heat fluxes and (b) local Nusselt number, around the tube wall, $Re \simeq 90000$	288

			Page
Figure 7.20	:	Temperature profiles at the outer surface of the tube wall: Present experimental situation, $Re \simeq 90000$	289
Figure 7.21	:	Predicted non-dimensional temperature $\frac{C - C_{min}}{C_{max} - C_{min}}$ contours: Present experimental situation: Only right half heating, $Re \simeq 40000$	290
Figure 7.22	:	Ratio of diffusivity of heat in tangential to radial direction: Prediction of Black and Sparrow's flow, $Re = 40500$	293
Figure 7.23	:	Ratio of diffusivity of heat in tangential to radial direction: Prediction of present experiment, $Re \simeq 40000$	293
Figure A.1	:	Near-wall geometries	386
Figure E.1	:	Staggered grid in ω-space	387
Figure F.1	:	Calculation Domain	388
Figure F.2	:	Grid and related dimensions	389

NOMENCLATURE

A	:	Coefficient in equation (3.3)
A^{Φ}	:	Coefficient in the finite difference equation for Φ (equation (3.16))
a	:	Area of a control volume surface
a^{mi}_{lj}	:	Fourth-order tensor defined in equation (2.13)
B	:	Coefficient in equation (3.3)
B_c	:	Coefficient in logarithmic law for scalar (equation (4.15))
b	:	Non-dimensional radius, also as in equation (2.39)
b_{ij}	:	Anisotropy of the stress tensor (i and $j = x$, y , z or θ , r , z or 1 , 2 , 3)
b^{mi}_{ij}	:	Fourth-order tensor defined in equations (2.20) and (2.21)
b^{Φ}	:	Coefficient in linearised source term (equation (3.15))
C	:	Time averaged value of scalar property, also, coefficient in equation (3.3)
$\hat{C}$	:	Instantaneous value of scalar property
C_c	:	Coefficient in modelled velocity-velocity-scalar correlation (equation (2.45))
C_{c1}	:	Coefficient in modelled form of ϕ_{ic1} (equation (2.48))
C'_{c1}	:	Coefficient in modelled form of ϕ_{ic1} (equation (2.61))
C_{c1w}	:	Coefficient in modelled form of ϕ_{ic1w} (equation (2.67))
C_{c2}	:	Coefficient in modelled form of ϕ_{ic2} (equation (2.58))
C_g	:	Coefficient in modelled velocity-scalar-scalar correlation (equation (2.77))
C_{g2}	:	Coefficient in modelled form of ε_c (Table (2.2))
C_s	:	Coefficient in modelled triple velocity correlation (equation (2.6))
C'_s	:	Coefficient in modelled triple velocity correlation (equation (2.8))
C_{s1}	:	Coefficient in modelled form of ϕ_{ij1} (equation (2.11))
C_{s1w}	:	Coefficient in modelled form of ϕ_{ij1w} (equation (2.21))

C_{s2}	:	Coefficient in modelled form of ϕ_{ij2} (equation (2.17))
C_{s2w}	:	Coefficient in modelled form of ϕ_{ij2w} (equation (2.21))
C_{ε}	:	Coefficient in modelled form of $\overline{u_k \varepsilon'}$ (equation (2.34))
$C_{\varepsilon 1}$	:	Coefficient in modelled production of ε (equation (2.33))
$C_{\varepsilon 2}$	:	Coefficient in modelled destruction term of ε (equation (2.33))
C^{Φ}	:	Coefficient in linearised source term (equation (3.15))
C_{τ}	:	Friction temperature or friction concentration
$\overline{c^2}$	:	Time averaged value of scalar fluctuation squared
c^m_{ni}	:	Third-order tensor defined in equation (2.51)
c_p	:	Specific heat of fluid
D_{c1}	:	A gradient diffusion model for scalar flux (Table (2.2))
D_{c2}	:	A gradient diffusion model for scalar flux (Table (2.2))
D_{c3}	:	Tensor invariant model for scalar flux (Table (2.2))
D_{ij}	:	A production of Reynolds stress like term (equation (2.16))
D_{s1}	:	Tensor invariant diffusion model for stresses (Table (2.1))
D_{s2}	:	Gradient diffusion model for stresses (Table (2.1))
d	:	Suffix denoting the down-stream location
d^m_{li}	:	Third-order tensor defined by equations (2.66) and (2.67)
E	:	Coefficient in logarithmic law of the wall for velocity (equation (3.30))
E_c	:	Coefficient in logarithmic law of the wall for scalar (equation (3.31))
f	:	Near-wall effect function in modelling ϕ_{ij} and ϕ_{ic} terms, also, dimensionless velocity profile (Section (4.3.2))
g	:	Dimensionless cross-stream velocity (Section (4.3.2))
g_i	:	Gravitational vector ($i = x$, y , z or θ , r , z or 1 , 2 , 3)
h	:	Dimensionless shear stress (Section (4.3.2))
$\dot{J}''$	:	Flux through a boundary

K_f : Thermal conductivity of fluid

K_w : Thermal conductivity of tube wall

k : Turbulent kinetic energy

L : Convection through boundaries (Appendix (E))

l : Mixing length

l_ε : Dissipation length scale

m : Mass flow rate, also, dimensionless mean scalar (Section (Section (4.3.2))

Nu : Nusselt number

n : Exponent in decay of turbulence, also, dimensionless cross-stream scalar flux (Section (4.3.2))

n_a : Unit normal vector ($a = x$, y , z)

P : Time averaged value of pressure, also, production of turbulent kinetic energy

$\hat{P}$: Instantaneous value of pressure

P_c : Production of scalar fluctuations (Section (2.7.4))

Pe : Peclet number

P_{ic} : Production of scalar fluxes (Section (2.7.3))

P_{ij} : Production of Reynolds stress tensor (equation (2.15))

Pr : Molecular Prandtl number

Pr_t : Turbulent Prandtl number

p : Fluctuations in pressure, also, pressure and dimensionless streamwise scalar flux (Section (4.3.2))

p' : Pressure correction

q : Dimensionless difference between streamwise and cross-stream normal stress (Section (4.3.2))

$\dot{q}''$: Wall flux of C

R : Radius of pipe, also, ratio of time scales of turbulent scalar and velocity fields

R_{cw1} : A near-wall effect model for ϕ_{ic} (Table (2.2))

R_{cw2} : A near-wall effect model for ϕ_{ic} (Table (2.2))

R_{c1} : A model for pressure-scalar gradient correlation (Table (2.2))

R_{c2} : A model for pressure-scalar gradient correlation (Table (2.2))

Re : Reynolds number

R_i : Inner radius of tube

R_o : Outer radius of tube

R_{sw1} : Launder et al. near-wall model (Table (2.1))

R_{sw2} : Gibson-Launder near-wall model (Table (2.1))

R_{s1} : Launder et al. isotropic model (Table (2.1))

R_{s2} : Launder et al. Simple model (Table (2.1))

r : Radius

S : Time averaged generation of C per unit volume, also, spreading parameter in a wake (equation (4.12))

$\hat{S}$: Instantaneous generation of C per unit volume

S_{ci} : Surface integral term in equation (2.47)

S_i : Surface integral term in equation (C.9)

S_{ij} : Surface integral term in equation (2.9)

S_{ik} : Surface integral term in equation (C.10)

S^{Φ} : Source of Φ in equation (3.9)

Sc_t : Turbulent Schmidt number

St : Stanton number

T : A period of time (equation (1.5)), also Transport coefficient of Φ (Appendix(E))

T_i : Diffusion term in equation (2.41) (equation (2.44))

T_{ij} : Diffusion term in equation (2.2) (Section (2.2.2))

t : Time variable

U : Streamwise mean velocity

U_i : Time averaged velocity component ($i = x$, y , z or θ , r , z or 1 , 2 , 3)

$\hat{U}_i$: Instantaneous value of velocity component ($i = x$, y ; z or θ , r , z or 1 , 2 , 3)

U_τ : Friction velocity

u : Suffix denoting the upstream plane

$\overline{u^2}$: Streamwise conponent of Reynolds normal stress

u_i : Fluctuations in velocity ($i = x, y, z$ or θ, r, z or $1, 2, 3$)

$\overline{u_i c}$: Time averaged components of scalar flux ($i = x, y, z$ or θ, r, z or $1, 2, 3$)

$\overline{u_i c^2}$: Time averaged correlation of velocity-scalar-scalar ($i = x, y, z$ or θ, r, z or $1, 2, 3$)

$\overline{u_i u_j}$: Time averaged components of Reynolds stress (i and $j = x, y, z$ or θ, r, z or $1, 2, 3$)

$\overline{u_i u_j c}$: Time averaged correlation of velocity-velocity-scalar (i and $j = x, y, z$ or θ, r, z or $1, 2, 3$)

$\overline{u_i u_j u_k}$: Time averaged triple velocity correlation (i, j and $k = x, y, z$ or θ, r, z or $1, 2, 3$)

$\overline{u_i u_j u_k u_l}$: Quadruple velocity correlation

$\overline{u_k \varepsilon'}$: Time averaged correlation between velocity and dissipation fluctuations ($i = x, y, z$ or θ, r, z or $1, 2, 3$)

$\overline{uc}$: Streamwise scalar flux

$\overline{uv}$: Reynolds shear stress

V : Cross-stream velocity

$\overline{v^2}$: Cross-stream component of Reynolds normal stress

$\overline{vc}$: Cross-stream scalar flux

W : Streamwise mean velocity in θ, r, z coordinates

$\overline{w^2}$: Transverse component of Reynolds normal stress

X_i, x_i : Displacement vector ($= x, y, z$ or $i = \theta, r, z$ or $1, 2, 3$)

X_o : Distance to the virtual origin

x_2 : Cross stream direction

y : Distance in cross-stream direction

y^+ : Non dimensional distance away from a wall

y_o : Effective distance to the wall (equation (A.3))

z : Distance in z-direction

GREEK SYMBOLS

α	:	Coefficient in modelled form of ϕ_{ij2} (equation (2.14))
α_c	:	Coefficient in the linear form of c^m_{ni} (equation (2.55))
α'_c	:	Coefficient in the linear form of d^m_{li} (equation (2.68))
β	:	Coefficient in modelled form of ϕ_{ij2} (equation (2.14))
β_{ab}	:	Wall-effect tensor in Daly-Harlow model (a and $b = x$, y , z) (equation (2.23))
β_c	:	Coefficient in the linear form of c^m_{ni} (equation (2.55))
β'_c	:	Coefficient in the linear form of d^m_{li} (equation (2.68))
Γ	:	Diffusion coefficient
Γ_i	:	Diffusion coefficient of Φ in the direction-i
Γ_t	:	Turbulent diffusivity of scalar property
Γ^Φ	:	Kinematic diffusivity of scalar property
γ	:	Coefficient in modelled form of ϕ_{ij2} (equation (2.19))
δ	:	Characteristic length for the hydrodynamic field
δ_c	:	Characteristic length for the scalar field
δ_{ij}	:	Kronecker delta (= 1 for $i = j$, = 0 for $i \neq j$)
ε	:	Dissipation rate of turbulent kinetic energy
ε_c	:	Dissipation rate of scalar fluctuations
ε_{ij}	:	Dissipation tensor (i and $j = x$, y , z or θ , r , z or 1 , 2 , 3)
ζ	:	Weighting factor in hybrid difference formula (equation (3.13))
ζ_w	:	Coefficient in modelled form of ϕ_{ij2w} (equation (2.22))
η	:	Coefficient in modelled form of ϕ_{ij2} (equation (2.14)), also, dimensionless distance for hydrodynamic field
η_c	:	Dimensionless distance for scalar field
κ	:	The von Kármán constant
κ_c	:	Coefficient in the logarithmic law for C
λ	:	Ratio of free stream velocities in a mixing layer

μ : Dynamic viscosity of fluid

ν : Kinematic viscosity of fluid

ν_t : Turbulent viscosity

ν_c : Coefficient in the linear form of c^m_{ni} (equation (2.55))

ν'_c : Coefficient in the linear form of d^m_{ni} (equation (2.68))

ξ_i : Cartesian components of position vector ($i = x$, y , z), also, the weighting factor in equation (3.11)

Π : Net flux of Φ in equation (3.13)

π : Angle of 180° expressed in radians

ρ : Density of fluid

σ_t : Turbulent Prandtl number or Schmidt number

τ : Characteristic time scale of decay of turbulence

Φ : Any dependent variable

$\overline{\Phi}$: Interpolated value of variable Φ at regular grid node

ϕ_{ic} : Pressure-scalar gradient correlation

ϕ_{ic1} : Turbulent part of ϕ_{ic}

ϕ_{ic2} : Mean strain of ϕ_{ic}

ϕ_{ic1w} : Turbulent part of the near-wall effects of ϕ_{ic}

ϕ_{ic2w} : Mean strain part of the near-wall effects of ϕ_{ic}

ϕ_{ij} : Pressure-strain correlation

ϕ_{ij1} : Turbulent part of ϕ_{ij}

ϕ_{ij2} : Mean strain part of ϕ_{ij}

ϕ_{ij1w} : Turbulent part of the near-wall effects of ϕ_{ij}

ϕ_{ij2w} : Mean strain part of the near-wall effects of ϕ_{ij}

Ψ : Stream function

ψ : Near-wall effect function in equation (2.25)

Ω : Weighting factor (Appendix (E))

Ω_c : Equals $\frac{C_c k}{\varepsilon}$ (Appendix (D))

Ω_s	:	Equals $\frac{C_s k}{\varepsilon}$ (Appendex (D))
ω	:	Non dimensional stream function (equation (3.1))

OTHER SYMBOLS AND NOTATIONS

$D(\ )$	:	Diffusion of ( )
$\frac{D}{Dt}(\ )$	:	Substantial derivative equals $\frac{\partial}{\partial t}(\ ) + U_j \frac{\partial}{\partial x_j}(\ )$
E	:	'Exterior' boundary
eff	:	Effective
I	:	'Interior' boundary
(I)	:	Ith grid position in θ-direction or ω-direction
$(I+i)$	:	$(I+i)$ the grid position in θ-direction or ω-direction ($i = +1$, $+\frac{1}{2}$, -1 , $-\frac{1}{2}$ etc)
i	:	Inside surface of the tube
(J)	:	Jth grid position in r-direction
$(J+j)$	:	$(J+j)$th grid position in r-direction ($j = +1$, $+\frac{1}{2}$, -1 , $-\frac{1}{2}$ etc.)
(K)	:	Kth grid position in z-direction
$(K+k)$	:	$(K+k)$th grid position in z-direction ($k = +\frac{1}{2}$ and $-\frac{1}{2}$)
o	:	Outer surface of the tube, also, characteristic value
tot	:	Total
$turb$	:	Turbulent
$wall$	:	At the wall
$\Sigma(\ )$	:	Summation of ( )
$\Delta(\ )$	:	Increment in ( )
$+$	:	Position on the higher side of displacement component
$-$	:	Position on the lower side of displacement component
$,$	:	e.g. $f_{,i}$ means the covariant differential of f with respect to direction-x_i

CHAPTER 1

INTRODUCTION

1.1 Introduction

Most fluid flows and heat transfer processes of practical interest to engineers involve turbulence. Methods for quantitative evaluation of turbulent flows are thus needed for optimum designing of the equipment involved. Before the advent of large electronic computers, this need was meet by experimental investigations of the gross flow characteristics and empirical correlation of the same. The applicability of such information was limited and could at best provide broad guide-lines for the flow evaluation. Analytical and semi-empirical methods available to the designer were based mainly on intuitive ideas on turbulence phenomena. These again had limited applicability. No general analytical solution of the equations governing fluid and heat flow processes are available to date, but the numerical solution of these equations, facilitated by the advent of computers, has become a reality. During the last two decades a considerable proportion of fluid dynamic and heat transfer researchers have directed their efforts on numerical solution of the flow and heat-transfer equations; considerable success has been achieved. Now, with the ever increasing computational capability, it has become possible to embark into the investigation of increasingly complex flow situations, including three-dimensional flows.

It has long been assumed that the Navier-Stokes equations which comprise a closed set of equations for instantaneous velocity and pressure field govern the motion of both laminar and turbulent flows. For a laminar flow, with a set of well defined boundary conditions, these Navier-Stokes equations, at least in principle, can be numerically

solved to any required degree of accuracy. In the case of turbulent flows, meaningful results for the instantaneous velocity and pressure fields from a numerical precedure can be expected only if the numerical discretisation is finer than the smallest scales of turbulence. This would demand computer storage and time, several orders of magnitude larger than the capabilities of present day computers. An alternative approach based on an averaged form of the governing equations together with a model of the statistical parameters appearing in them is utilised in the numerical analysis of turbulent flows; this approach is well within the capabilities of modern computers.

1.2 Equations of Fluid Motion and Scalar Transport

Since the equations are needed in their general three-dimensional form, the Cartesian tensor notation is used for compactness, ignoring the distinction between covariant and contravariant tensors and using the repeated-suffix summation convention so that

$$a_i b_i \equiv a_1 b_1 + a_2 b_2 + a_3 b_3 .$$

Further, the compact comma suffix notation is used for differentiation, so that

$$f_{,i} \equiv \frac{\partial f}{\partial x_i} .$$

For a Newtonian fluid of uniform density ρ and kinematic viscosity ν, the Navier-Stokes equations derived from Newton's second law applied to a unit control volume, in the absence of body forces, take the form,

$$\hat{U}_{i,t} + (\hat{U}_i \hat{U}_j)_{,j} = - \frac{1}{\rho} \hat{P}_{,i} + \nu \hat{U}_{i,jj} \tag{1.1}$$

where $\hat{U}_i$ is the component of velocity in the direction x_i , $\hat{P}$ is the pressure and t is the time variable.

For an incompressible fluid, the continuity equation assumes the form,

$$\hat{U}_{i,i} = 0. \tag{1.2}$$

The instantaneous momentum equations obtained by applying (1.2) in (1.1) are,

$$\hat{U}_{i,t} + \hat{U}_j \hat{U}_{i,j} = - \frac{1}{\rho} \hat{P}_{,i} + \nu \hat{U}_{i,jj} . \tag{1.3}$$

Correspondingly, the low-speed transport of heat or passive matter

is describable by the following equation.

$$\hat{C}_{,t} + \hat{U}_j \hat{C}_{,j} = \hat{S} + \Gamma \hat{C}_{,jj} \tag{1.4}$$

where $\hat{C}$ is the passive scalar (e.g. enthalpy, concentration of a chemical species etc.), Γ is the kinematic diffusivity of the property and $\hat{S}$ is the generation of $\hat{C}$ per unit volume (for example, by chemical reaction) at the point considered.

Now taking the statistical average of variables $\hat{U}_i$, $\hat{C}$ and $\hat{P}$ with respect to time, obtain

$$U_i = Lt_{T\to\infty} \frac{1}{T} \int_{t_o}^{t_o+T} \hat{U}_i \, dt \qquad \text{etc..} \tag{1.5}$$

Here the equation (1.5) should be convergent and independent of t_o. Further, T denotes a period of time larger than the time scale of the slowest fluctuations and smaller than the time scale over which significant variations in the averaged quantities occur. Equation (1.5) implies that the fluctuations u_i etc. of the variables defined by,

$$u_i = \hat{U}_i - U_i \qquad \text{etc.} \tag{1.6}$$

should satisfy,

$$0 = Lt_{T\to\infty} \frac{1}{T} \int_{t_o}^{t_o+T} u_i \, dt \qquad \text{etc..} \tag{1.7}$$

Now substituting (1.6) in the instantaneous equations (1.3) and (1.4) with the above definitions yields,

$$U_{i,t} + U_j U_{i,j} = -\frac{1}{\rho} P_{,i} + \nu U_{i,jj} - (\overline{u_i u_j})_{,j} \tag{1.8}$$

and

$$C_{,t} + U_j C_{,j} = S + \Gamma C_{,jj} - (\overline{u_j c})_{,j} \tag{1.9}$$

The equations for mean momentum (1.8), differ from the equations for the instantaneous momentum due to the appearence of the fluctuating velocity correlation tensor, $\overline{u_i u_j}$, known as turbulent or Reynolds stress. Similarly (1.9) has additional dependent variable, $\overline{u_j c}$, representing the turbulent scalar flux in direction x_j. Thus differences between the laminar fluid flows and passive scalar transport to that of their turbulent counterparts should be solely attributed to the effects of the turbulent stresses and fluxes. In laminar flows equation (1.3) with the continuity relation (1.2) form a closed set which in principle may be solved; this in turn allows the solution of (1.4). To solve equations (1.8) and (1.9), however, additional equations or expressions are needed determining $\overline{u_i u_j}$ and $\overline{u_j c}$. The provision of a model for these correlations forms a significant fraction of this thesis.

1.3 Closure Levels

In order to solve the mean momentum and mean scalar equations in turbulent motion one needs to have some information regarding the correlations $\overline{u_i u_j}$ and $\overline{u_j c}$. It is this information that is supplied in a turbulent closure model. At the practical level most proposals for turbulence closures have been on Boussinesq's idea of a "turbulent viscosity". He suggested in 1877 that the local turbulent shear stress (i.e. the cross correlation of fluctuating velocities) could be expressed as the product of the turbulent (eddy) viscosity and the local mean velocity gradient, a clear analogy with laminar stresses. The turbulent viscosity was considered to be a function of the flow field rather than a property of the fluid. Thus, in a simple shear flow where $U_1 = U_1 \{ x_2 \}$,

$$- \overline{u_1 u_2} = \nu_t \, U_{1,2} \quad , \tag{1.10}$$

the minus sign ensuring that momentum is diffused down the velocity gradient as in laminar flow. The idea of a turbulent viscosity was conceived to deal with situations where only one shear stress component exists. In practice there are many relatively simple but important flows where such a situation prevails. Implied in (1.10) is the notion that the turbulent shear stress vanishes in the absence of a gradient in mean velocity.

As a tensorial extension of (1.10) one may write

$$\overline{u_i u_j} = - \nu_t \, (U_{i,j} + U_{j,i}) + \frac{1}{3} \delta_{ij} \, \overline{u_m u_m} \tag{1.11}$$

which relates all the components of the stress tensor to the mean strain field and the turbulent kinetic energy. In (1.11) the turbulent viscosity ν_t is a scalar quantity. The term $\frac{1}{3} \delta_{ij} \, \overline{u_m u_m}$ to the right hand side of (1.11) accounts for the fact that, in the absence of mean strain, the normal stresses do not vanish and that they are equal in magnitude.

Even for weak turbulent shear flows this is not exactly true.

Alternatively, considering the turbulent viscosity as a second-order tensor, one may write,

$$- \overline{u_i u_j} = (\nu_t)_{ik} (U_{j,k} + U_{k,j}) \tag{1.11a}$$

or even assuming a fourth-order tensor for the turbulent viscosity,

$$- \overline{u_i u_j} = (\nu_t)_{ijkl} (U_{k,l} + U_{l,k}) \tag{1.11b}$$

The components of the turbulent viscosities in (1.11a) and (1.11b), however, should satisfy the conditions imposed by the incompressibility of fluid and symmetry of $\overline{u_i u_j}$ tensor.

The scalar counterpart of equation (1.10) is the definition of eddy diffusivity of heat or matter given by,

$$- \overline{u_2 c} = \Gamma_t C_{,2} \quad . \tag{1.12}$$

The tensorial extensions of the equation (1.12) can be written in forms parallel to (1.11) and (1.11a).

In practice it is often the ratio of eddy viscosity and eddy diffusivity, denoted by turbulent Prandtl number, that is used in describing the scalar fluxes. This quantity

$$Pr_t = \frac{\nu_t}{\Gamma_t} \tag{1.13}$$

should merely be considered as the ratio of diffusivities in a direction where non-zero mean gradients are present, or else if Pr_t is considered as a tensor, then it's components should be permitted to take finite, infinite or indefinite magnitudes.

1.3.1 Mean-Field Closure Models

In mean-field closure models, the turbulent stresses and scalar fluxes are expressed by algebraic expressions containing mean quantities only. Most of these models are based on the eddy viscosity-eddy diffusivity concept described in the previous section. An example of an algebraic formula for the turbulent viscosity is provided by Prandtl's mixing length hypothesis,

$$\nu_t = l^2 U_{1,2} \quad . \tag{1.14}$$

Here again in order to find ν_t , the mixing length l , should be prescribed. For example in wall boundary layer flows, the mixing length l may be expressed by two separate expressions covering the "inner" and "outer" regions. These expressions have been extensively tested mainly for turbulent wall boundary layer flow calculations where it seem to perform very well. Numerous empirical and intuitive formulae are available which include various physical effects like that of low Reynolds number, the transition region, compressibility, mass transfer, pressure gradient, transverse curvature etc. on the behaviour of the wall boundary layer. A useful account of this is given by REYNOLDS and CEBECI [1].

The corresponding closure of the scalar equation is generally achieved by specification of Pr_t as a function of geometrical and flow parameters. Several formulations of eddy viscosity generalized to three-dimensional compressible and incompressible wall layers are also given in [1].

In the case of free shear layers it is the specification of ν_t (assumed constant at any section in the shear flow) rather than the mixing length l , that is common. Some empirical formula for ν_t , as functions of characteristic flow parameters, which will give best agreement with self preserved mean profiles in simple free shear flows can be found in [1].

1.3.2 Turbulent Transport Models

In turbulent transport models one or more additional partial differential equations will be supplied. These partial differential equations will implicitly or explicitly determine the shear stress $\overline{u_1 u_2}$ and scalar flux $\overline{u_2 c}$. These closure models can further be classified according to the number of additional partial differential equations considered for determining ν_t.

(a) One-Equation Models

Usually a transport equation for the turbulent kinetic energy forms the basis of one-equation models. Now, instead of ν_t being related to mean flow quantities, it is expressed in terms of turbulent velocity and length scales as

$$\nu_t \propto k^{\frac{1}{2}} l \quad . \tag{1.15}$$

Further, in order to solve the partial differential equation for turbulent kinetic energy a length scale has to be prescribed in approximating the dissipation term. As with zero-equation models the length scale is prescribed here with prior knowledge of behaviour of the flow.

(b) Two-Equation Viscosity Models

The use of an additional turbulence partial differential equation for the length scale l or a related variable eliminates the need for prescribing one to facilitate solution of turbulence kinetic energy equation. Transport equations for several length scale related quantities were studied by researchers, a summary of this is given in LAUNDER and SPALDING [2]. The most successful one which is now tested in a vast range of flow conditions is the transport equation for the isotropic dissipation rate ε. (The modelling of this equation supplementary to the Reynolds stress model is given in the next Chapter).

Even at the level of one-and two-equation models the closure of the mean scalar equation is done by prescribing the scalar diffusivity, or more often, the turbulent Prandtl number.

(c) Stress and Flux Transport Models

At all the levels of closure mentioned before, the shear stress is expressed by way of the Boussinesq expression (1.11), where the shear stress is made to respond at once to changes in the mean strain field. This is not correct in most fluid flow situations. Thus the need for a model which is capable of predicting a non-equilibrium flow arises. Reynolds stress models in which transport equations for the Reynolds stress tensor components are solved is the simplest model which is capable of doing this. The solution of partial differential equations for the Reynolds stress components has been suggested by CHOU [3], ROTTA [4] and later by many others. The partial differential equation for the Reynolds stress tensor can be obtained by differentiating and then manipulating the equation for the fluctuating component u_i of the velocity vector. The resultant transport equation for $\overline{u_i u_j}$ contains contributions from various physical processes; if these are modelled correctly then all components of the stress tensor $\overline{u_i u_j}$ can be estimated. This will allow the determination of the mean velocity field without recourse to the notion of an effective viscosity.

Parallel to the Reynolds stress equations it is possible to formulate partial differential equation for the scalar flux tensor, thus obviating the need for an effective diffusivity model. The partial differential equation for the scalar flux tensor can be derived starting from transport equations for the fluctuating velocity u_i and the fluctuating component of sealar c.

1.3.3 Higher Order Closures

In the transport equation for the components of the Reynolds stress tensor there appears the triple correletion $\overline{u_i u_j u_l}$ which represents the contribution of the transport by the fluctuating velocity of $\overline{u_i u_j}$ in direction x_l. One may either approximate this quantity in terms of the Reynolds stress and mean velocity field (as in a second-order closure), or alternatively one may obtain from the solution of transport equation for $\overline{u_i u_j u_l}$. Models which incorporate solution of partial differential equations for this correlation are called third-order closures. Correspondingly, it is possible to formulate the partial differential equation for the components of the correlation $\overline{u_i u_j c}$ whose gradients appear in the transport equations for the scalar fluxes.

Likewise, it is possible to generate transport equations for higher and higher order correlations but the modelling of the contributing terms become more and more abstract due to lack of experimental evidence to understand their behaviour.

1.3.4 Other Closures

At least one method which needs mention here is the three-dimensional time-dependent numerical computation of the large scale turbulence. Here only the small scale turbulence is modelled, the large scale turbulence being obtained from the time-dependent numerical solutions.

1.4 Evaluation of Available Models

In this section the capabilities and limitations of available hydrodynamic and scalar transport models described in the previous section are evaluated. This is done by comparing expected performance of a given model with corresponding evidence from experiments.

1.4.1 Eddy Viscosity Models

In local-equilibrium flows the generation and destruction of the components of the Reynolds stress tensor are nearly equal, the mean and turbulent transport being negligible. In self preserving shear flows these two quantities, although not equal to each other, are proportional; the constant of proportionality being a function of non-dimensional cross-stream distance only. In these flows it is possible to obtain simple relations between Reynolds stress components and the components of the mean-rate-of-strain tensor. The eddy viscosity model is a generalisation of this possibility. Thus in local-equilibrium regions and in self preserving flows, the eddy viscosity models with correctly chosen empirical constants can be expected to perform satisfactorily. Indeed in the calculation of wall boundary layers where the near-wall region outside of the viscous layer is in local equilibrium, the eddy viscosity formulation with empirical corrections is known to give satisfactory results for a variety of physical and boundary conditions. (see Ref [5], Chapter 6)

Similarly, in the calculation of self preserving flows, for example the plane or radial jet, Prandtl mixing length formula can be employed to obtain satisfactory agreement with experimental observations. The relationship between the mixing length and the width of the respective flow, however, needs to be adjusted if the rate of spread of the flow is to be predicted correctly. This heavy reliance on empirical formulae

is one of the major weaknesses in the mixing length models even in predicting equilibrium or self preserving flows.

The one-equation models have some capability of representing the dependence of shear stress on flow history. Although it is a major step towards the true representation of the flow bahaviour, the need to prescribe a turbulence length scale, in order to model the dissipation term, greatly reduces its usefulness in flow calculations. Since accurate prior knowledge of the turbulence length scale is not always available the empiricism associated with the mixing length models becomes apparent in these schemes as well. Further, due to the neglect of transport effects on the length scale itself, the advantages of a one-equation model over a mixing length model are limited.

Two-equation models incorporate the transport effects of length scale (often a length-scale-related quantity of the form $k^a l^b$) into the turbulence model. Thus, they may be expected to perform satisfactorily in both developing as well as developed flows. RODI and SPALDING [6] reported that with a single set of constants it is possible to make satisfactory predictions of the spreading rates of plane mixing layer, plane jet and radial jet. The predictions of LAUNDER et al. [7] show satisfactory agreement in a large variety of free shear flows, in many cases significant improvements over predictions from the mixing length hypothesis are obtained.

It appears however, that the effective viscosity concept is inadequate for describing some turbulent flow situations. In these situations often the transport effects on the Reynolds stresses are dominant. For example in flow through an annulus or in an asymmetric duct or in a wall jet, the maximum velocity surfaces do not coincide with the zero shear stress surfaces. This pheomenon can not be accounted for with an effective viscosity formulation. The secondary motion that

develops in corners of straight axis ducts due to cross stream gradients of Reynolds stresses is another class of flow where isotropic eddy viscosity models are inadequate. The concept also fails to allow satisfactory prediction of flows with influential body forces; gravitational effects on turbulence is an example. The direct effect of the mean velocity tensor on the stress tensor diminishes with increasing influence of the body forces on the turbulent structure; hence the eddy viscosity model becomes less relevant in representing the turbulent stresses.

1.4.2 Eddy Diffusivity Models and Turbulent Prandtl (or Schmidt) Number

The eddy diffusivity models have widely been applied in parallel with eddy viscosity models, in calculating scalar transfer problems. Again the eddy diffusivity formulation is a generalisation of the possibility that in local-equilibrium regions and in self preserving flows there exist some simple relation between the scalar flux tensor and the gradients of the mean scalar tensor. In flow regions where both hydrodynamic and scalar fields are in local equilibrium, i.e. when the transport effects are negligible in both shear stress equations as well as in scalar flux equations, the effective diffusivity and simple formulations for turbulent Prandtl number can be expected to give satisfactory agreement with experiments. The velocity and scalar fields close to the wall (the so-called "semi-logarithmic region") is one where one may assume local-equilibrium structure and where an eddy diffusivity formulation should perform satisfactorily. The review paper by KADER and YAGLOM [8] clearly indicate that in the semi-logarithmic regions of a variety of wall flow geometries under a large range of Reynolds numbers and molecular Prandtl (or Schmidt) numbers, the implied turbulent Prandtl (or Schmidt) number is indeed a constant in the range of 0.9. The predictions of PATANKAR and SPALDING [9] and others, of wall boundary

layers with prescribed turbulent Prandtl number of 0.9 show good agreement with experiments.

There are numerous engineering applications, however, where the scalar field is far from fully developed or self preserved. Correspondingly, several experimental investigations aimed at examining the diffusivity in developing flows has shown considerable disagreement with the idea of constant Pr_t (or Sc_t).

BLOM's [10] investigation of wall boundary layer with a step in wall temperature indicated clearly that the turbulent Prandtl number is a function of both streamwise and lateral distances. His temperature profiles show that an assumption of Pr_t of 0.9 would substantially in error at least in the developing region of the boundary layer.

QUARMBY and QUIRK's [11] measurements of temperature and concentration profiles downstream of a short heated (or porous) section in a pipe, again imply that the turbulent Prandtl number is far from constant across the flow. In their flow situations the transport effects play a significant role in determining the scalar field.

The eddy diffusivity models which incorporate prescribed Pr_t (or Sc_t) variations across the flow can not be expected to give satisfactory agreement in predicting flows such as that of Quarmby and Quirk or that of Blom, where the transport effects are important.

The turbulent flow situations where the effect of buoyancy on the turbulent structure is significant, the eddy diffusivity model becomes less relavant. In such situations the turbulent Prandtl number is known to vary considerably with relative effect of the buoyancy forces. For example in stably stratified flows the turbulent Prandtl number increases sharply with increase in Richardson number (which is a measure of the negative of the production of turbulent kinetic energy due to buoyancy as a fraction of production due to mean shear). Thus,

satisfactory predictions of buoyancy influenced flows with the use of eddy diffusivity models will certainly require some ad-hoc corrections.

In asymmetrically heated shear flows, the zero heat flux plane may not coincide with the plane of zero temperature gradient. For example, the study of slightly heated two-dimensional jet expanding into a plane mixing layer by FULACHIER et al. [12] indicate the presence of a region where the temperature gradient and the lateral heat flux are of the same sign. In this region, the production of temperature fluctuations is negative. Their spectral analysis of lateral heat flux in the negative production region confirm the fact, that the high frequency components are related to the local gradient, whereas, the low frequency components are related to the larger eddies. An eddy viscosity/diffusivity hypothesis which assume a simple relation between local properties can not accommodate these complex effects.

In three-dimensional scalar transport, diffusivities need not be isotropic. Certainly the measurements of three-dimensional heat transfer in pipes by QUARMBY and QUIRK [11], indicate that the tangential diffusivity of heat is much larger than the radial diffusivity in regions close to the tube wall. Similar experiments by BLACK and SPARROW [13] suggest the same. An eddy diffusivity model, if employed, needs considerable empiricism in order to predict this behaviour.

1.4.3 Reynolds Stress Models

Unlike eddy viscosity models, in Reynolds stress models the transport effects of the Reynolds stress tensor are incorporated directly. Thus, this model in principle, can be expected to give a satisfactory representation of the turbulence in flows with and without influential transport effects. Of course there is an additional task of modelling several unknown correlations which appear in the transport equation for $\overline{u_i u_j}$. Since the solution of the partial differential equations produce the stress components explicitly their incorporation in the mean velocity equation is now directly possible. Therefore, in principle, none of the restrictions associated with the eddy viscosity formulation apply to Reynolds stress model. For example, the effects of buoyancy, effects of asymmetry, the secondary flow generation due to gradients in stresses in three-dimensional ducts etc. are all within the capabilities of a Reynolds stress model.

Among the applications of this type of model, HANJALIĆ and LAUNDER [14] obtained satisfactory predictions of several shear flows including a strongly asymmetric channel flow, using a three-equation (Reynolds shear stress-turbulent kinetic energy-and its dissipation rate) model of turbulence. LAUNDER et al. [15] showed further capabilities of Reynolds stress models by solving for all non-zero stress components in several two-dimensional shear flow situations.

1.4.4 Scalar-Flux Models

Corresponding to the capabilities of Reynolds stress models, the scalar-flux level of closure appears capable of giving satisfactory representation of several flow situations where the eddy diffusivity formulation is inadequate. Often transport effects of scalar transfer are even more predominant than those on the flow field. Therefore the use of a scalar-flux model may be required even when the hydrodynamic field is in local equilibrium. In modelling scalar flux equations, however, accurate knowledge of the stress tensor, particularly the normal stresses are required. Therefore the scalar-flux models are often associated with Reynolds stress models which are capable of determining the normal stress components accurately.

1.5 Present Contribution

1.5.1 Theoretical Contribution

The aim of the present theoretical investigation is to devise and verify a model of turbulence capable of predicting convective heat and mass transport in three-dimensional temperature and concentration fields. Emphasis will be placed in obtaining a closure simple enough for practical calculations yet with least amount of empiricism.

1.5.2 Choice of Turbulence Model

The most crucial feature of the flow that this investigation attempts to understand and formulate is the non-isotropic diffusivity in three-dimensional scalar transfer. The experimental evidence of BLACK and SPARROW [13] and QUARMBY and QUIRK [11] clearly indicates that the anisotropy of the diffusivity is quite significant and increases as the wall is approached. The data of [11] suggest that in fully developed turbulent pipe flow the circumferential diffusivity near the wall is more than three times as large as the radial one. As mentioned in Section (1.4.2) the experimental findings of BLOM [10] and QUARMBY and QUIRK [11] suggest that the diffusivity in two-dimensional flow is not constant in either the streamwise or lateral directions. So in three-dimensional flows the diffusivity of a scalar can be expected to vary in all three directions.

If an eddy diffusivity model is to be used in this investigation without any ad-hoc modifications, it would produce only an isotropic diffusivity effect. On the other hand if the directional bias of the diffusivity is to be incorporated in some way, far too much information from the same experimental situation that the investigation is trying to simulate, will have to be given as an input to the model. Even though this could lead to satisfactory prediction of the flows concerned, it would not amount to more than a sophisticated curve fit. The contribution

of such an investigation towards the understanding of convective turbulence transport would be very small.

The scalar flux transport model, however, solves for the component fluxes in all three directions and the anisotropy of the scalar diffusivity will be an output rather than an input as in the eddy diffusivity model. Further the model would ideally be a general one, applicable in two-and three-dimensional free shear flows as well as those affected by a wall and would not contain ad-hoc modifications. A scalar flux model has therefore been chosen for the closure of the mean scalar equation.

For the hydrodynamic closure the Reynolds stress models have shown a greater range of applicability than eddy viscosity models. Even though an eddy viscosity model with suitably chosen empirical constants is adequate to predict the mean flow features of the flow situations considered, the component of the stress tensor which are required in the scalar transport modelling can not be obtained with sufficient accuracy from that model. Therefore the Reynolds stress model was chosen as the mean flow closure model. This would enable the proposed numerical scheme to be extended to solve fully three-dimensional hydrodynamic as well as scalar fields where the eddy viscosity models have had only modest success.

1.5.3 Path for Verification of the turbulence Model

For the purpose of establishing the validity of the turbulence model it is necessary to make systematic computations in flow geometries where accurate experimental data are available. First the flow geometries should be identified with their known physical characteristics. It is well known that the structure in near-wall turbulence is vastly different from that away from a wall. Large gradients in mean velocity and large anisotropies in the turbulent stress tensor are the main characteristics

in flows affected by walls, whereas free shear flows are characterised by only moderate gradients and anisotropies. Further, in near-wall regions, the length scales associated with turbulence increase in size with increase in distance to the wall. In regions remote from the influence of walls, on the other hand, the turbulence length scale is more or less constant in size. It will be seen in the following chapter that present modelling directions clearly distinguish the wall effects in simulating pressure interaction correlations in the stress and scalar flux equations.

Thus, the turbulence model is first tested in free shear flows. In the present investigation the plane mixing layer, the plane jet and the plane wake are simulated and predictions obtained of their hydrodynamic and scalar fields. Even though they are all self-preserving flows they cover a large range of turbulent production/dissipation rates. Thus, a model capable of satisfactorily predicting all these flow situations can be expected to perform well in many more free shear flows.

The turbulent model is next applied to wall affected flows such as boundary layers, channel and pipe flows. Here the near-wall-effect parts of the pressure interaction correlations are included in the model. All other terms and coefficients in modelled terms are kept unchanged from the forms employed in predicting free shear flows. In the near-wall regions it is these additional terms that are under test, whereas away from the walls where turbulent transport is influential, it is mainly the diffusion models that are being scrutinized.

As for investigating three-dimensional scalar transport problems the turbulence model is virtually unchanged from the above.

1.5.4 Numerical Contribution

The present numerical investigation has been aimed at providing numerical schemes for solving problems of two-and three-dimensional turbulent scalar transport in two-dimensional boundary layer type flow field, using second-order closure models.

As the first step in verifying the turbulence model, calculations were made in two-dimensional situations with the use of numerical procedure of PATANKAR and SPALDING [9] modified so as to facilitate efficient calculation of second order turbulence variables. After a considerable amount of testing it was decided to incorporate a staggered grid arrangament for turbulence variables so as to remove some numerical instabilities found in the conventional finite difference grid arrangement. All free shear flow calculations and flat plate boundary layer calculations were performed with this numerical scheme.

Development, testing and use of a numerical scheme capable of solving variables in a three-dimensional marching fashion forms the remainder of the present numerical contribution. This basic solving scheme is a three-dimensional marching numerical scheme used by others (SYED [16] and BRYANT [17]) in simulating free shear flows. The contributions by the writer are the following.

(a) Modification of the three-dimensional numerical scheme so as to allow economical calculation of two-dimensional situations. This was an obvious step as the present calculations considered only two-dimensional flow fields. The modifications were made to facilitate the solution of both two-and three-dimensional situations with only a small number of modifications.

(b) The simplification described later in Section (3.3.5), valid for two-dimensional internal flow calculation was incorporated. For example, in a laminar flow situation, this requires only

a single partial differential equation (instead of three equations) to be solved to obtain the velocity field.

(c) Incorporation of second-order closure model set out in a staggered grid scheme (in place of the two-equation model in the original program). As pointed out later in Section (3.5) for two-dimensional flow problems, it is convenient and sufficient to calculate all turbulence variables in a grid shifted only in the cross-stream direction.

(d) Calculation of channel and pipe flow hydrodynamic and scalar transport problems in two-dimensional form.

(e) Solution of three-dimensional scalar transport problems. Here the solution of corresponding two-dimensional hydrodynamic flow fields were obtained first and then frozen, before making three-dimensional calculations. Simultaneous calculation of hydrodynamic and scalar fields can however be made with little modifications to the computer code.

(f) Finally, in order to allow proper account to be taken of circumferential conduction in thick-walled tubes subjected to three-dimensional heat-transfer, the numerical scheme was extended to include the tube wall as well the flow in the tube. This facilitates simulation of experimental situations where the heat source is applied externally.

1.5.5 Experimental Contribution

The present experimental program has aimed at providing a set of data for the circumferentially non symmetric heat transfer problem. With the limited facilities and time available for exploration, measurements were made only of the outer surface of the tube wall. In three-dimensional heat transfer situations, circumferential conduction is unavoidable. In the present investigation it was minimised by chosing a glass tube. Thus this experiment should closely resemble a three-dimensional mass transfer situation where circumferential conduction is absent. Further it should provide the turbulence model a stringent test than other available three-dimensional heat transfer situations (e.g. BLACK and SPARROW [13]).

CHAPTER 2

TURBULENCE MODEL

2.1 Introduction

It was decided in the previous chapter that the Reynolds stresses and the turbulent scalar fluxes needed for the closure of mean velocity and mean scalar equations in the present investigation could best be obtained by solving transport equations for those variables. In this chapter those transport equations are presented. As there are several unknown terms in those equations they have to be modelled in terms of other known variables. In Section (2.2) a model for the Reynolds stress transport equation in formulated. The transport equation for the isotropic dissipation

$$\varepsilon = \nu \left(\overline{u_{i,j} u_{j,i}} \right) \tag{2.1}$$

is presented in Section (2.3) and its modelling discussed. Section (2.4) contains the modelling of the scalar flux equation and Section (2.5) deals with the scalar fluctuation equation. The chapter concludes by presenting in Sections (2.6) and (2.7), a summary of the models and the transport equations in modelled form.

2.2 Reynolds Stress Equation and its Trace

An exact equation for the transport of the components of the Reynolds stress tensor can be derived from the Navior-Stokes equations, equation (1.3). By multiplying equation (1.3) by u_j and adding the same equation with suffixes i and j interchanged and time averaging the sum, one obtains,

$$\overline{u_i u_j}_{,t} + U_k \overline{u_i u_j}_{,k} = - (\overline{u_i u_k} U_{j,k} + \overline{u_j u_k} U_{i,k})$$

Convection (a) Production

$$- 2\nu \overline{u_{i,k} u_{j,k}}$$

(b) Dissipation

$$- (\overline{u_i u_j u_k} - \nu \overline{u_i u_j}_{,k} + \overline{\frac{p}{\rho} (\delta_{kj} u_i + \delta_{ki} u_j)})_{,k}$$

(c) Diffusion

$$+ \overline{\frac{p}{\rho} (u_{i,j} + u_{j,i})} \qquad (2.2)$$

(d) Redistribution

In deriving equation (2.2) fluctuations in body forces are omitted. This limits the equation (2.2) to flows unaffected by the gravitational forces. Gravitational effects on turbulence transport is discussed in LAUNDER [18].

The equation (2.2) contains mainly two types of terms, those expressible as spatial gradient terms always represent transport of the conserved quantity from one place to the other, as such their integrals over the whole flow volume are zero; whereas the integrals of other terms over the whole flow volumes are generally non-zero.

The trace of the equation (2.2) may be written

$$k_{,t} + U_k k_{,k} = - \overline{u_i u_k} U_{i,k} - \nu \overline{u_{i,k} u_{i,k}}$$

(a) Production (b) Dissipation

$$- (\overline{k u_k} - \nu k_{,k} + \overline{\frac{p}{\rho} k_i u_i})_{,k} \qquad (2.3)$$

(c) Diffusion

where

$$k = \frac{1}{2}\overline{u_i u_i} \tag{2.4}$$

is the turbulent kinetic energy. Terms in equations (2.2) and (2.3) represent the contributions from different physical effects to the maintenance of the corresponding transported quantity. The redistribution term (d) in equation (2.2) does not have a corresponding term in (2.3) because it vanishes by continuity. Thus, it represents only an exchange between the components of turbulent kinetic energy.

The left hand side of (2.2) and (2.3) represent the transport due to mean motion of $\overline{u_i u_j}$ and k respectively. The time derivative terms are zero in statistically stationary flows. In the present investigation these time derivatives are neglected though their inclusion when necessary would not require any further approximations in the turbulence model.

The term (a) of equation (2.2) whose integral over the whole flow volume is non-zero will generally have the same sign as $\overline{u_i u_j}$; it represents the generation of $\overline{u_i u_j}$ by interactions of the turbulent motion with the mean-rate-of-strain field. In equation (2.3), the production term (i.e. term(a)) represents the rate at which turbulence is generated by shear interaction which equals the amount of energy transfered from the mean flow to turbulence. The flow regions where the $\overline{u_i u_j}$ and its production are of opposite sign such as velocity maximum region in a wall jet are often marked by large transport effects.

The term (b) of equation (2.2) represents the destruction of $\overline{u_i u_j}$ due to viscous action. In the normal stress terms, they are negative definite and provide mechanism of turbulent kinetic energy dissipation, (b) in equation (2.3).

Term (c) in equations (2.2) and (2.3) represent the transport of $\overline{u_i u_j}$ and k due to three distinct actions. They are transport by velocity fluctuations in the direction x_k, transport due to fluctuations in pressure field and transport by viscous action.

Term (d) in equation (2.2) is the mean product of fluctuating pressure and the fluctuating strain fields, and is called the pressure-strain term. It's effect on normal stress components is clearly to diminish the differences between them. In the shear stress equation this term acts as a sink term.

In the present form, the equation (2.2), contains a number of turbulence correlations whose determination is necessary prior to it's employment in a closure model. Those terms, namely the destruction, diffusion and pressure-strain terms are modelled as described in the following sections.

2.2.1 The Viscous Destruction Term

It is a well established experimental fact that the turbulence is dissipated by small scale eddies i.e. at high wave numbers. Further, spectral measurements of turbulent components clearly indicate (see for example LAWN [19] or HANJALIĆ and LAUNDER [20]) that at high wave numbers the turbulence is isotropic. Thus, at high Reynolds numbers where the dissipating wave number range is remote from that of the energy-producing wave number range, the dissipation process can be considered isotropic, i.e.

$$\varepsilon_{ij} = \frac{2}{3} \delta_{ij} \varepsilon \tag{2.5}$$

where ε is the dissipation rate of turbulent kinetic energy given by (2.1).

The transport equation for ε can be derived starting from the equation for velocity fluctuations. This is done in Section (2.3).

2.2.2 The Diffusion Term

The diffusion term in equation (2.2) is

$$T_{ij} = -\left(\overline{u_i u_j u_k} - \nu\, \overline{u_i u_j} + \overline{\frac{p}{\rho}\left(\delta_{kj} u_i + \delta_{ki} u_j\right)}\right)_{,k} .$$

The first term is the triple velocity correlation which has to be found algebraically or via a partial differential equation for its transport equation. Some components of $\overline{u_i u_j u_k}$ are measurable and their gradients are found to be significant. The second term of T_{ij} represents the transport of $\overline{u_i u_j}$ due to viscous action. At high Reynolds numbers this term is small and hence generally neglected but it's inclusion if needed is straight forward. Little is known about the diffusion due to pressure fluctuation interaction. LUMLEY [21] has pointed out that the separation of transport and redistribution parts of the pressure interaction in the Reynolds stress equation is not unique. He argues that the correct form of the redistribution term is

$$-\frac{1}{\rho}\left(\overline{p_{,i} u_j} + \overline{p_{,j} u_i}\right) + \frac{2}{3}\frac{1}{\rho}\,\delta_{ij}\left(\overline{p u_k}\right)_{,k}$$

and the corresponding transport part is

$$-\frac{2}{3}\frac{1}{\rho}\,\delta_{ij}\left(\overline{p u_k}\right)_{,k} .$$

Thus, there is no pressure transport of shear stress. Anyway, the measurements by HANJALIĆ and LAUNDER [20] in asymmetric plane channel indicated that the term $\frac{d}{dx_2}\left(\overline{p u_2}\right)$ in the turbulent kinetic energy equation is small compared to other terms appearing in that equation. Due to lack of any other experimental evidence, the transport term due to pressure interaction is neglected here.

This leaves the triple correlation to be modelled in order to determine T_{ij}. A transport equation for $\overline{u_i u_j u_k}$ had been proposed by CHOU [3], KOLOVANDIN and VATUTIN [22] and others. This equation contains quadruple velocity correlation and pressure-stress correlations. As the turbulent transport terms in the stress equations are of relatively minor importance in most of the flows considered, it is found inappropriate to adopt such an elaborate treatment of $\overline{u_i u_j u_k}$. Thus, an algebraic formulation of $\overline{u_i u_j u_k}$ is attempted by direct referance to the terms in the transport equation for $\overline{u_i u_j u_k}$. HANJALIĆ and LAUNDER [14] obtained the following formulation for $\overline{u_i u_j u_k}$.

$$- \overline{u_i u_j u_k} = C_s \frac{k}{\varepsilon} (\overline{u_i u_l} \cdot \overline{u_j u_k}_{,l} + \overline{u_j u_l} \cdot \overline{u_k u_i}_{,l} + \overline{u_k u_l} \cdot \overline{u_i u_j}_{,l}) \tag{2.6}$$

The assumptions made in obtaining the above formulation are:

(a) flow is at high Reynolds number - viscous terms are negligible,

(b) the triple correlations are small and have Gaussian properties and thus following MILLIONSHTCHKOV [23]:

$$\overline{u_i u_j u_k u_l} = \overline{u_i u_j} \cdot \overline{u_k u_l} + \overline{u_i u_k} \cdot \overline{u_j u_l} + \overline{u_i u_l} \cdot \overline{u_j u_k} \tag{2.7}$$

(c) the terms of the form $\overline{u_i u_j u_l}\, U_{k,l}$ are comparatively small and hence neglected,

(d) the pressure stress correlation can be modelled as proportional to $- \frac{\varepsilon}{k} \overline{u_i u_j u_k}$.

and (e) convective transport of $\overline{u_i u_j u_k}$ is neglected.

All except assumption (c) are either asymptotically exact or are necessary for closure at this level. At least in two-dimensional boundary layer flows, assumption (c) is not necessary although its employment greatly simplifies the algebra. The measurements of HANJALIĆ and LAUNDER [20] in asymmetric plane channel indicated that assumption (c) was reasonable

in their flows. Therefore equation (2.6) in chosen as the model for $\overline{u_i u_j u_k}$ in the present study. The coefficient C_s has to be found by reference to established experimental data.

An alternative model is that suggested by DALY and HARLOW [24] where the first two terms of equation (2.6) are omitted. Thus

$$- \overline{u_i u_j u_k} = C_s' \frac{k}{\varepsilon} (\overline{u_k u_l} \cdot \overline{u_i u_{j,l}}) \tag{2.8}$$

Equation (2.8) is not compatible in its symmetry properties, only the left side being independent of the order of the indicies i,j and k. LAUNDER et al. [15] employed the equation (2.8) in predicting several free shear flows and found satisfactory behaviour. REECE [25] made prediction of plane wall flows using both (2.7) and (2.8) and found no advantage to employing the more numerically complicated form (2.7). It can be seen from the diffusion transport term of turbulent kinetic energy, that for consistency, the coefficent C_s' should be about 1.8 C_s. The computer optimised values of C_s = 0.11 and C_s' = 0.20 obtained by Reece quite closely tally with the above.

In the present investigation forms (2.7) and (2.8) are compared in axisymmetric wall flows..

2.2.3 The Pressure-Strain Term

The main characteristic feature of the pressure-strain term $\overline{\frac{p}{\rho}(u_{i,j} + u_{j,i})}$ is its redistributive effect on normal stresses (see HINZE (Ref. [26], pp 323-328)).

The appearence of pressure in the pressure-strain term can be eliminated following CHOU [3], by first formulating a Poisson equation for the fluctuating pressure and multiplying by the fluctuating strain. On averaging, there results

$$\overline{\frac{p}{\rho}(u_{i,j})} = \frac{1}{4\pi}\int_{Vol}\left(\overline{(u'_l u'_m)_{,lm} u_{i,j}} + 2\,\overline{U'_{l,m} u'_{m,l} u_{i,j}}\right)\frac{dVol}{(X-Y)} + S_{ij} \tag{2.9}$$

$$\phi_{ij} = \phi_{ij1} + \phi_{ij2} + S_{ij} \tag{2.10}$$

where, terms with and without a prime relate to values at X and Y respectively. The term S_{ij} is a surface integral having significance only in flows affected by the presence of rigid walls. Equation (2.9) suggests that the pressure-strain correlation originates, apart from wall effects, from two distinct effects. The first part ϕ_{ij1} is generated purely from turbulence interactions, whereas the second part ϕ_{ij2} relates to interactions between turbulence and mean rate of strain.

In non-isotropic homogeneous flows with negligible mean strain the turbulence decays towards an isotropic state. The process ϕ_{ij1} is the only one in (2.9) that can promote an equalising of the normal stress components and a diminishing of shear stress components. With this in mind ROTTA [4] proposed the following plausible form:

$$(\phi_{ij} + \phi_{ji})_1 = -C_{s1}\frac{\varepsilon}{k}\left(\overline{u_i u_j} - \frac{2}{3}\delta_{ij}k\right) \tag{2.11}$$

where C_{s1} is assumed to be a constant which determines the rate of return to isotropy and the quotient $\frac{k}{\varepsilon}$ is the characteristic dacay time of the turbulence. If isotropy is to be established the constant C_{s1} should

take a value greater than unity. It is the form (2.11) that is adopted in the present investigation.

Though some workers, for example DALY and HARLOW [24], have neglected the part ϕ_{ij2} in their modelling of the pressure-strain term, CROW [27] has pointed out that the effects of ϕ_{ij2} may even be larger than ϕ_{ij1} under conditions of rapid distortion. Following ROTTA [4] ϕ_{ij2} is expressed as

$$\phi_{ij2} = U_{l,m}\, a_{lj}^{mi} \tag{2.12}$$

where

$$a_{lj}^{mi} = -\frac{1}{2\pi}\int_{Vol} \overline{\frac{\partial u'_m u_i}{\partial \xi_l \partial \xi_j}}\, \frac{dVol}{(X-Y)} \tag{2.13}$$

and the ξs are the Cartesian components of the position vector $(X-Y)$. Equation (2.12) is a rigorous consequence of (2.9) when the inhomogeneities of the turbulence are only minor and the second and higher order derivatives of the mean velocity are negligible. Rotta pointed out that the fourth-order tensor a_{lj}^{mi} should satisfy certain symmetry and mass conservation constraints. The most general fourth-order tensor satisfying these constraints and comprising only linear combination of Reynolds stresses is given in LAUNDER et at. [15]. With that tensor form, the mean strain part of the pressure-strain correlation can be written

$$\begin{aligned}(\phi_{ij} + \phi_{ji})_2 = & -\alpha\,(P_{ij} - \tfrac{2}{3}\delta_{ij} P) \\ & - \beta\, k\,(U_{i,j} + U_{j,i}) \\ & - \eta\,(D_{ij} - \tfrac{2}{3}\delta_{ij} P)\end{aligned} \tag{2.14}$$

where

$$P_{ij} \equiv -(\overline{u_i u_k}\, U_{j,k} + \overline{u_j u_k}\, U_{i,k}) \tag{2.15}$$

and

$$D_{ij} \equiv -(\overline{u_i u_k}\, U_{k,j} + \overline{u_j u_k}\, U_{k,l}) \tag{2.16}$$

and

$$P \equiv \frac{1}{2} P_{kk}$$

is the production of kinetic energy. The coefficients α, β and η can be expressed by relations containing a single constant C_{s2} as

$$\alpha = \frac{1}{11}(C_{s2} + 8)$$

$$\beta = \frac{1}{55}(30\, C_{s2} - 2)$$

$$\eta = \frac{1}{11}(8\, C_{s2} - 2) \tag{2.17}$$

This is the form of ϕ_{ij2} that will be used in the present investigation. The following inferences are useful to note:

(a) in isotropic turbulence subjected to sudden distortion, equation (2.14) reduces to

$$(\phi_{ij} + \phi_{ji})_2 = 0.4\, k\, (U_{i,j} + U_{j,i}) \tag{2.18}$$

which is same as derived by CROW's [27] detailed analysis

(b) the degenerate form,

$$(\phi_{ij} + \phi_{ji})_2 = -\gamma\, (P_{ij} - \frac{2}{3}\delta_{ij} P) \tag{2.19}$$

of the equation (2.14) can be considered as a parallel of equation (2.11). Here the action of mean strain is to isotropize the production tensor P_{ij} whereas the action of ϕ_{ij1} was to isotropize the stress tensor. NAOT et al. [28] proposed the form (2.19) as a replacement for ϕ_{ij1}, whereas here it is considered in addition to the ϕ_{ij1} term. Here again for sudden distortion in isotropic turbulence requires γ to take a value 0.6.

In the present investigation both forms, i.e. equation (2.14) and equation (2.19), are employed as the model for ϕ_{ij2} and compared.

The present model for ϕ_{ij} is exactly the same as that used by LAUNDER et al. [15] in predicting a variety of wall and free shear flows. Previous to that HANJALIĆ and LAUNDER [14] modelled the mean strain part ϕ_{ij2} in terms of non-linear combinations of Reynolds stress. Through their choice for C_{s1} of 2.8 they had found it necessary to include non-linear terms in ϕ_{ij2} in order to predict correctly the stress levels of nearly homogeneous shear flow data of CHAMPAGNE et el. [29].

The model of ϕ_{ij} given here still has two coefficients to be determined. C_{s1} and C_{s2} (or C_{s1} and γ). The ideal information to evaluate these coefficients are that of CHAMPAGNE et al. [29], where the transport effects are negligible in the stress equations. Further, the production and dissipation of kinetic energy are in equilibrium leading to simple algebraic relations for the relative magnitudes of the Reynolds stresses. Noting the inability of the "redistribution of production" model (equation (2.19)) to predict the difference between the magnitudes of lateral and transverse normal stresses, for best possible agreement with the data of CHAMPAGNE et al. the coefficients of ϕ_{ij} models can be obtained as,

(a) C_{s1} = 1.5 in equation (2.11) and C_{s2} = 0.4 in equation (2.14)

or (b) C_{s1} = 1.8 in equation (2.11) and γ = 0.6 in equation (2.19).

2.2.4 Wall Effects in the Pressure-Strain Term

In modelling the ϕ_{ij} term in flows unaffected by walls the surface integral S_{ij} in equation (2.9) was neglected. The influence of this term on ϕ_{ij} must be included in modelling the wall region. When ϕ_{ij} is affected by a single flat wall the surface integral can be eliminated from equation (2.9) and the resultant equation expressed as:

$$u_{i,j} = \frac{1}{4\pi}\int_V \left[\overline{(u_l u_{m,lm})' u_{i,j}} + 2(U'_{1,2})\overline{(u'_{2,1} u_{i,j})}\right] \cdot \left[\frac{1}{X-Y} + \frac{1}{X-Y^*}\right] dV \tag{2.20}$$

where suffixes 1 and 2 stand for streamwise and lateral flow directions and Y^* is the image of point Y with respect to the wall. As with equation (2.9), it can be inferred from equation (2.20) that the near-wall effect of ϕ_{ij} also arises from two effects, one due to turbulent interactions and the other due to mean velocity gradients. Thus, as a framework for divising a model of the near-wall effects, one is led to write

$$(\phi_{ij} + \phi_{ji})_w = \left[C_{s1w}\frac{\varepsilon}{k}\left(\overline{u_i u_j} - \frac{2}{3}\delta_{ij}k\right) + U_{l,m}\left(b^{mi}_{lj} + b^{mj}_{li}\right)\right] f\left(\frac{l_\varepsilon}{x_2}\right) \tag{2.21}$$

where the function $f\left(\frac{l_\varepsilon}{x_2}\right)$ has the effect of diminishing $(\phi_{ij} + \phi_{ji})_w$ with increasing distance from the wall. The fourth order tensor should have the following properties.

(a) In order to be redistributive, $b^{mi}_{li} = 0$.

(b) Since the relative levels of the transverse component (i.e. the component parallel to the wall and normal to the flow direction) of the Reynolds stress in free flows and in wall flows are more or less equal, the component b^{23}_{13} should be small. In fact it is assumed zero.

Applying those properties, LAUNDER et al. [15] obtained the ϕ_{ijw} as

$$(\phi_{ij} + \phi_{ji})_w = C_{s1w} \frac{\varepsilon}{k} (\overline{u_i u_j} - \frac{2}{3} \delta_{ij} k)$$
$$+ C_{s2w} (P_{ij} - D_{ij})$$
$$+ \zeta_w k (U_{i,j} + U_{j,i}) f(\frac{l_\varepsilon}{x_2}) . \qquad (2.22)$$

In order to obtain the numerical values for the coefficients C_{s1w}, C_{s2w} and ζ_w reference is made to near-wall flows. There the transport terms in the stress equations are again negligible. Therefore it is possible to obtain algebraic expressions for the relative stress levels in that region. Further, if the near wall effect function $f(\frac{l_\varepsilon}{x_2})$ is defined so that it takes a numerical value of unity in near-wall region, then the numerical values for the coefficients in equation (2.22) can be obtained as $C_{s1w} = 0.5$, $C_{s2w} = 0.06$ and $\zeta_w = 0$.

An alternative model was suggested by DALY and HARLOW [24] who were the first to recognise the need for a separate near-wall contribution in pressure-strain modelling. They proposed that ϕ_{ijw} be modelled as

$$\phi_{ijw} \propto (\overline{u_l u_j} \beta_{il} + \overline{u_i u_l} \beta_{jl} - \frac{2}{3} \overline{u_l u_m} \beta_{lm} \delta_{ij}) \qquad (2.23)$$

where the wall-effect tensor β_{ab} is of importance for the enhancement of anisotropy near a wall. The last term of equation (2.23) ensures the redistributive property of ϕ_{ijw}. In this form equal amounts of energy is transferred from the turbulent stress component normal to the wall, to streamwise and transverse components.

An integral formulation of the near-wall effect tensor β_{ab} for a flat plate takes the form:

$$\beta_{yy} \propto \frac{1}{y} \tag{2.24}$$

and

$$\beta_{xx} = \beta_{zz} = 0$$

where y is the normal distance to the wall. SHIR [30] considered the Daly-Harlow model and incorporated unit normal vectors to represent the wall effect tensor, as

$$\beta_{ab} = n_a n_b \psi \tag{2.25}$$

where ψ is a decay function which accounts for the diminishing effects away from the wall.

In a recent investigation of ground effects on pressure fluctuations in the atmospheric boundary layer, GIBSON and LAUNDER [31] extended the formulation of DALY and HARLOW [24] to cover the mean strain part ϕ_{ij2w} and gravitational effects of ϕ_{ijw}. (In the Daly-Harlow proposal no near-wall influence on ϕ_{ij2} was present and the gravitational influence was omitted altogether.) In the Gibson-Launder model the near-wall effect of ϕ_{ij2} was considered to be the redistribution of ϕ_{ij2} itself with respect to the wall orientation i.e.

$$\phi_{ij,1w} = C_{s1w} \frac{\varepsilon}{k} \left(\overline{u_k u_m}\, n_k n_m\, \delta_{ij} - \frac{3}{2}\, \overline{u_k u_i}\, n_k n_j - \frac{3}{2}\, \overline{u_k u_j}\, n_k n_i\right) \times f\left(\frac{l_\varepsilon}{n_l x_l}\right) \tag{2.26}$$

and

$$\phi_{ij,2w} = C_{s2w} \left(\phi_{km,2}\, n_k n_m\, \delta_{ij} - \frac{3}{2}\, \phi_{ki,2}\, n_k n_j - \frac{3}{2}\, \phi_{kj,2}\, n_k n_i\right) \times f\left(\frac{l_\varepsilon}{n_l x_l}\right) \tag{2.27}$$

The effect of the mean strain part ϕ_{ij2w} is also to redistribute energy from the component normal to the wall, equally between longitudinal and transverse parts. The experimental data of well documented wall flows however do not support this behaviour. There it seems that the energy transfer is essentially from the normal to the longitudinal component only, and that the transverse component is more or less uneffected. The attractiveness of this model is that it is possible to extend the basic idea to cover other effects in pressure redistribution (e.g. gravitational effects). Further, its extension to the case of pressure-scalar gradient distribution term is clear. In the present investigation the Launder et al. model (equation (2.22)) is compared with the Gibson-Launder model (equations (2.26) and (2.27)) in plane and axi-symmetric flows.

The form of the dacay factor f in (2.21), (2.26), (2.27) (or β_{ab} in (2.23)) determines the effectiveness of ϕ_{ijw} terms for positions away from the wall. REECE [25] has shown by examining the HANJALIĆ and LAUNDER [20] asymmetric channel and KLEBANOFF's [32] flat plate boundary layer data that ϕ_{ijw} terms as a whole should decrease as the inverse of normal distance to the wall. Since the production P_{11} or P decreases inversely with the distance from the wall, l should be more or less constant in the near-wall region. The results of LAUNDER et el. [15] suggest that

$$f \propto \frac{l_\varepsilon}{y} \tag{2.28}$$

is an appropriate non-dimensional decay form for a single wall, where l_ε is the length scale of energy containing eddies. The length scale l_ε can be considered either as $\frac{k^{3/2}}{\varepsilon}$ or as $\frac{|\overline{uv}|^{3/2}}{\varepsilon}$, though of course they produce slightly different decay functions. If there are two walls present (e.g. channel flow), the effects are assumed to be additive, so that the

factor is revised to read

$$f_{channel} \propto \left(\frac{l_\varepsilon}{y} + \frac{l_\varepsilon}{D - y} \right) \tag{2.29}$$

where D is the width of the channel. The above form could account for the slow decay of near wall effects felt in the HANJALIĆ and LAUNDER [20] flow and in the symmetric channel flow of COMTE-BELLOT [33].

In the case of a round pipe, the effect of near wall terms should be even more pronounced in positions away from the wall. From geometrical consideration (see Appendix A) of equation (2.28), extended to the case of a circular pipe, the following form emerges:

$$f_{pipe} \propto \frac{l_\varepsilon}{y_o} \tag{2.30}$$

where

$$y_o = \frac{R}{\int_0^\pi \frac{1 - b\cos\theta}{(1 + b^2 - 2b\cos\theta)^{3/2}} d\theta} \tag{2.31}$$

where $b = r/R$ is the dimensional radius.

LAUFER's [34] pipe flow data however does not show any stress anisotropy near the axis which would suggests that the near wall terms are very small near the axis. More recent measurements by LAWN [19] in pipe flow, on the other hand, suggest substantial anisotropy in stresses which may be either due to wall effects or due to some turbulent transport effects.

2.3 The Transport Equation for Isotropic Dissipation Rate

The exact transport equation for $\varepsilon \equiv \nu \overline{u_{i,l} u_{i,l}}$ has been presented by many workers (see for e.g. HARLOW and NAKAYAMA [35]) and it takes the form:

$$
\begin{aligned}
\underset{A}{\varepsilon_{,t} + U_k \varepsilon_{,k}} = & \underset{B}{- 2\nu \; U_{i,k} (\overline{u_{i,l} u_{k,l}} + \overline{u_{l,i} u_{l,k}})} \\
& \underset{C}{- 2\nu \; (\overline{u_{i,l} u_{k,l} u_{i,k}})} \underset{D}{- 2 \nu^2 \; (\overline{u_{i,kk} u_{i,ll}})} \\
& \underset{E}{- 2\nu \; (\overline{u_{i,l} u_k}) \; U_{i,lk}} \\
& \underset{F}{- \overline{u_k \varepsilon'_{,k}}} \underset{G}{- \frac{2\nu}{\rho} \; (\overline{p_{,l} u_{k,l}})_{,k}} \underset{H}{+ \tfrac{1}{2} \nu \; \varepsilon_{,kk}}
\end{aligned}
\qquad (2.32)
$$

Terms F, G and H represent the transport of ε in direction x_k due to turbulent interaction, pressure fluctuation and viscous action respectively. Term E is negligible in the fully turbulent region. The terms B, C and D represent the sources and sinks of dissipation rate ε.

HANJALIĆ and LAUNDER [14] considered the term B as the generation term in (2.32) and C and D as the sink terms. LUMLEY and KHAJEH-NOURI [36] on the other hand argued that the term B is negligible and that the terms C and D together represent the generation minus destruction of ε. The final forms of generation minus destruction of ε, arrived by [14] and [36] however are similar. It is

$$\frac{\varepsilon}{k} \left(- C_{\varepsilon 1} \; \overline{u_i u_j} \; U_{i,j} - C_{\varepsilon 2} \; \varepsilon \right) . \qquad (2.33)$$

In formulating the diffusive term in (2.32) the following considerations are applied:

(a) the viscous transport term, H is negligible at high Reynolds numbers

(b) at the present level of closure the term G should be neglected (consistant with the practice in closing the $\overline{u_i u_j}$ equation)

(c) an algebraic expression for the term F should be obtained with reference to the transport equation for $\overline{u_k \varepsilon'}$.

The transport equation for the correlation $\overline{u_k \varepsilon'}$ at high Reynolds numbers can be simplified to an algebraic form by neglecting convective transport of $\overline{u_k \varepsilon'}$. HANJALIĆ and LAUNDER [14] proposed that for boundary layer flows the algebraic relation can further be simplified to obtain

$$\overline{u_k \varepsilon'} = - C_\varepsilon \frac{k}{\varepsilon} \overline{u_k u_l} \, \varepsilon_{,l} \quad . \tag{2.34}$$

Thus, the modelled form of equation (2.32) is

$$\varepsilon_{,t} + U_k \, \varepsilon_{,k} = - C_{\varepsilon 1} \frac{\varepsilon}{k} \overline{u_i u_j} \, U_{i,j} - C_{\varepsilon 2} \frac{\varepsilon^2}{k} - C_\varepsilon \left(\frac{k \, \overline{u_k u_l}}{\varepsilon} \varepsilon_{,l} \right)_{,k} \quad . \tag{2.35}$$

The equation (2.35) contains three coefficients which need to be determined.

The exponent of the decay of turbulent kinetic energy in isotropic turbulence is about - 1.1 (see for example COMTE-BELLOT and CORRSIN [37]). For this condition equation (2.35) and the kinetic energy equation (2.3) can be rearranged to the form

$$C_{\varepsilon 2} = 1 - \frac{1}{n} \tag{2.36}$$

where n is the decay exponent. Therefore $C_{\varepsilon 2}$ takes a value 1.90 .

A further relationship between the coefficients in equation (2.35) can be obtained by reference to the constant stress layer adjacent to a wall. There

(a) the convective transport of ε is negligible

and (b) production and dissipation of turbulent kinetic energy are equal.

Equation (2.35) then may be reduced to:

$$C_\varepsilon = \frac{(C_{\varepsilon 2} - C_{\varepsilon 1}) \, U_\tau^6}{\kappa^2 \, k^2 \, \overline{u_2^2}} \tag{2.37}$$

where κ is the von Kármán constant and U_τ the friction velocity. The most suitable numerical magnitude for C_ε and hence $C_{\varepsilon 1}$ via equation (2.37) can only be obtained by computer optimisation with reference to a variety of flow data. LAUNDER et al. [15] arrived at $C_{\varepsilon 1} = 1.44$ and hence $C_\varepsilon = 0.15$ by computer optimising the ε equation in several free and wall boundary layers.

Thus, in the present investigation equation (2.35) with $C_{\varepsilon 1} = 1.44$, $C_{\varepsilon 2} = 1.90$ and $C_\varepsilon = 0.15$ will be used as the model for determining the isotropic dissipation rate ε.

An alternative form of dissipation model has been suggested by LUMLEY and KHAJEH-NOURI [36]. They argue that the source of ε due to strain applied to the flow cannot come purely from the term B of equation (2.32). Instead they argue that the source of ε by strain should be modelled in terms of anisotropy, b_{ij} of the Reynolds stress tensor, where

$$b_{ij} \equiv \left(\frac{\overline{u_i u_j}}{k} - \frac{2}{3}\delta_{ij} \right) \tag{2.38}$$

Then they propose

$$\text{(Source - Sink) of } \varepsilon = \left(C'_{\varepsilon 2} - C'_{\varepsilon 1}\, b^2 \right) \frac{\varepsilon^2}{k} \tag{2.39}$$

where

$$b^2 = b_{ij} b_{ij}$$

Reynolds [38] has shown that in the case of a two-equation model of turbulence, where b^2 should be found from the constitutive relation (1.11), equation (2.29) may be re-expressed as:

$$\text{(Source - Sink) of } \varepsilon = \left(C'_{\varepsilon 2} - C^*_{\varepsilon 1} \frac{P}{\varepsilon} \right) \frac{\varepsilon^2}{k} \tag{2.40}$$

which is the same as the form (2.33) obtained by many others e.g. LAUNDER et al. [15].

OWEN [39] treated terms C and D in equation (2.32) as the (source, sink) terms and modelled the difference between them with reference to the decay of grid turbulence. His equation for isotropic dissipation rate, therefore lacked a positive source term but satisfied equation (2.37) to obtain a large diffusion coefficent (C_ε = 0.64). He made numerical predictions of pipe flows with this model for ε using a near-wall boundary condition of dissipation rate equal to the production of kinetic energy. The absence of a positive source term here was compensated by large diffusive leakage of ε . His model would have been completely unsatisfactory for free flows without a generation term in ε equation.

2.4 The Scalar Flux Equation

The correlation $\overline{u_i c}$ represents the rate of transport in direction x_i of the scalar C by turbulent velocity fluctuations. The exact transport equation for $\overline{u_i c}$ can be obtained by multiplying the instantaneous scalar, $(C+c)$ equation (1.4) by u_i component and adding it to the x_i component of the Navier-Stokes equation (1.3) multiplied by c. The time averaged form of the sum is

$$\overline{u_i c}_{,t} + U_k \overline{u_i c}_{,k} = - (\overline{u_i u_k}\, C_{,k} + \overline{u_k c}\, U_{i,k}) + \frac{\overline{\rho' c}}{\rho} g_i$$

Convection (a) Generation

$$- (\Gamma + \nu)\, \overline{c_{,k} u_{i,k}}$$

(b) Dissipation

$$- (\overline{u_i u_k c} - \Gamma\, \overline{u_i c}_{,k} - \nu\, \overline{c u_{i,k}} + \frac{\overline{pc}}{\rho} \delta_{ik})_{,k}$$

(c) Diffusion

$$+ \frac{\overline{p}}{\rho} c_{,i} \qquad (2.41)$$

(d) Pressure interaction

This equation is valid for incompressible flows with small gradients in mean scalar C so that the fluctuation in the molecular viscosity and molecular conductivity are negligible. The fluctuations in density of the fluid too is assumed negligible in all terms except the gravitational term i.e. the second term on the right hand side of equation (2.41). A more general form of the exact equation for the transport of $\overline{u_i c}$ can be found in RUBESIN and ROSE [40].

In the present investigation only the transport of passive scalars is considered i.e. a hydrodynamic field completely unaffected by the scalar field. Under this condition the gravitational term in (2.41) will be neglected. LAUNDER [18] deals with the modelling of the gravitational terms in the Reynolds stress and scalar flux equations for active scalar transport situation.

Term (a) represents the generation of $\overline{u_i c}$ due to the interaction of turbulence with mean gradients. It is interesting to note that gradients of mean velocity contribute to the generation of scalar fluxes. The widely adopted Boussinesq type formula does not contain this contribution of the mean velocity field. It must be noted that, however, in two dimensional boundary layer flows the contribution of the production due to mean velocity is negligibly small. In the case of developing flows where the streamwise scalar fluxes are important, the presence of these production terms may be significant.

An order of magnitude analysis of the dissipation correlations, as presented by TENNEKES and LUMLEY [41], yields

$$\nu \left(\overline{c_{,k} u_{i,k}} \right) \sim O \left(Re_{turb}^{-\frac{1}{2}} \right) \tag{2.42}$$

and

$$\Gamma \left(\overline{c_{,k} u_{i,k}} \right) \sim O \left(Pe_{turb}^{-\frac{1}{2}} \right) \tag{2.43}$$

In the present study the turbulent Reynolds number is assumed to be high. If the analysis is confined to fluids with close to unity Prandtl numbers, the dissipation terms (b) can be considered negligible. If the Prandtl number of the fluid differs markedly from unity then one of the above terms will become significant and should be retained in the analysis. OWEN [39] concluded that inclusion of these dissipation terms are necessary only for low Reynolds number flows of fluids with Prandtl number differing substantially from unity.

Apart from the above, (2.41) contains the pressure-scalar gradient correlation (d) and the diffusive transport term (c) which need to be modelled in terms of known variables before (2.41) can be used in a closure model for the mean scalar equation. In the following subsection models for these terms will be presented.

2.4.1 The Diffusion Term

The diffusion term in equation (2.41) is

$$T_i \equiv -\left(\overline{u_i u_k c} - \Gamma \overline{u_i c}_{,k} - \nu \overline{c u_{i,k}} + \frac{\overline{pc}}{\rho} \delta_{ik} \right)_{,k} , \quad (2.44)$$

The first term of the right hand side of (2.44) represents the diffusive transport of $\overline{u_i c}$ due to fluctuations in velocity. The experimental measurements of some of the components can be found in the literature and their gradients are found to be significant. The second and third terms represent diffusion of $\overline{u_i c}$ due to molecular action and these terms are generally neglected along with dissipative correlations mentioned in Section (2.4). There is no information available about the magnitude of the diffusion term due to pressure fluctuations. So, parallel to the neglect of the pressure diffusion term in the Reynolds stress equation, pressure diffusion is neglected in the $\overline{u_i c}$ equation too.

This leaves the triple correlation $\overline{u_i u_k c}$ to be modelled. In order to obtain an algebraic relation for $\overline{u_i u_k c}$, reference is made to the transport equation of $\overline{u_i u_k c}$ given for example in KOLOVANDIN and VATUTIN [22]. In appendix (B) it is shown that with some simplifying assumptions the correlation $\overline{u_i u_k c}$ can be written as,

$$-\overline{u_i u_k c} = C_c \frac{k}{\varepsilon} \left(\overline{u_k u_l}\, \overline{u_i c}_{,l} + \overline{u_i u_l}\, \overline{u_k c}_{,l} + \overline{u_l c}\, \overline{u_i u_k}_{,l} + \overline{u_i u_k u_l}\, C_{,l} \right) . \quad (2.45)$$

As OWEN [39] and LAUNDER [42] have done, in the present investigation only the first two terms of (2.45) will be included as the model for $\overline{u_i u_k c}$.

The coefficient C_c in (2.45) can only be determined by computer optimisation. Its value is expected to be around 0.11 , which is the magnitude of computer optimised diffusion coefficient in the stress model.

The diffusion models suggested by other workers are often simplified versions of (2.45). WYNGAARD and COTE [43] retained only the first of the terms in (2.45) with a coefficient of 0.15, whereas DONALDSON et al. [44] effectively expressed the stress components in terms of turbulent kinetic energy to suppose that

$$-\overline{u_i u_k c} \propto \frac{k^2}{\varepsilon}\left(\overline{u_k c}_{,i} + \overline{u_i c}_{,k}\right) \tag{2.46}$$

LUMLEY and KHAJEH-NOURI [36] suggest that when gravitational effects are present the buoyant transport term is an order of magnitude larger than that due to scalar flux gradients. Further for unstratified conditions their model will have a term $\frac{k^2}{\varepsilon}\delta_{ik}\overline{u_l c}_{,l}$, in addition to the form suggested by LAUNDER [42] and OWEN [39].

In LUMLEY [45], a suggestion is made for the incorporation of a term like $\overline{u_i c}(k^2/\varepsilon)_{,k}$ in order to account for the spatial variation in the transport coefficient. The third term in (2.45) has more or less this effect.

2.4.2 The Pressure-Scalar Gradient Correlation

The pressure-scalar gradient correlation $\overline{\frac{p}{\rho} c_{,i}}$ is the counterpart of the pressure-strain correlation in the stress equation. This term provides the mechanism which limits the growth of the scalar fluxes. The exact equation for the correlation can be obtained by multiplying the Poisson equation for fluctuating pressure by the gradient of scalar fluctuations. On averaging the product one obtains (see Appendix (C) for details):

$$\overline{\frac{p}{\rho} c_{,i}} = \frac{1}{4\pi}\int_V \overline{(u'_m u'_n)_{,nm} c_{,i}} \frac{dVol}{(X-Y)} + \frac{1}{2\pi} U'_{n,m} \overline{(u'_{n,m} c_{,i})} \frac{dVol}{(X-Y)} + S_{ci}$$

$$\phi_{ic} = \phi_{ic1} + \phi_{ic2} + S_{ci} \tag{2.47}$$

where the prime superscripts on the right hand side of (2,47) refers to quantities evaluated at Y .

Following CHOU [3] who showed that the surface integrals in the velocity correlations are negligible in positions away from free boundaries, the surface integral S_{ci} is included for further examination in near-wall situations only. Equation (2.47) would contain an additional term, if gravitational effects were included in the velocity equations. The first two terms on the right hand side of (2.47) fall on two categories, one dependent only on fluctuating quantities ϕ_{ic1} and the other ϕ_{ic2} dependent on the interactions of the mean strain field.

The most widely used form of the turbulent part ϕ_{ic1} is based on Rotta's linear-return-to-isotropy approximation of the pressure-strain correlation. Here the effect is expressed as a linear function of the component scalar flux, i.e.

$$\phi_{ic1} = - C_{c1} \frac{\varepsilon}{k} \overline{u_i c} \quad . \tag{2.48}$$

Strictly the time scales for this process should depend on both hydrodynamic turbulence time scale $\frac{k}{\varepsilon}$ and the scalar turbulence time scale $\frac{\overline{c^2}}{2\varepsilon_c}$. At least in local equilibrium flows these two time scales can be assumed proportional, hence the use of $\frac{k}{\varepsilon}$ is preferred over inclusion of two yet unknown quantities $\overline{c^2}$ and ε_c . This form of ϕ_{ic1} was suggested by MONIN [46] and then by LAUNDER [18], LUMLEY [47], DONALDSON et al. [44] and others. Equation (2.48) is the model for ϕ_{ic1} used in the present investigation.

In modelling the mean strain part of the pressure-scalar gradient correlation ϕ_{ic2} , the same steps taken in modelling ϕ_{ij2} are followed. It is assumed that any inhomogeneities in the flow do not make a major contribution to the integral ϕ_{ic2} . Therefore ϕ_{ic2} can be expressed as,

$$\phi_{ic2} = U_{n,m} \, c^m_{ni} \tag{2.50}$$

where

$$c^m_{ni} = -\frac{1}{2\pi}\int_{Vol} \frac{\overline{\partial^2 u'_m c}}{\partial\xi_n \, \partial\xi_i} \frac{dVol}{(X-Y)} \tag{2.51}$$

where ξ's are the Cartesian components of the position vector $(X-Y)$. The third order tensor c^m_{ni} should satisfy the symmetry constraint,

$$c^m_{ni} = c^m_{in} \quad . \tag{2.52}$$

Further, in order to satisfy the conservation of mass principle, equation (2.47) indicates that,

$$c^m_{mi} = 0 \quad . \tag{2.53}$$

Also, applying Green's theorem to the integral in (2.51), away from boundaries,

$$c^m_{ii} = 2\,\overline{u_m c} \quad . \tag{2.54}$$

Equation (2.54) suggests that a linear combination of scalar fluxes may be suitable for expressing c^m_{ni}. Thus the form

$$c^m_{ni} = \alpha_c\,\delta_{ni}\,\overline{u_m c} + \beta_c\,\delta_{mi}\,\overline{u_n c} + \nu_c\,\delta_{mn}\,\overline{u_i c} \tag{2.55}$$

should satisfy the relations

$$\begin{aligned} \beta_c &= \nu_c \\ 0 &= \alpha_c + \beta_c + 3\nu_c \\ 2 &= 3\alpha_c + \beta_c + \nu_c \end{aligned} \tag{2.56}$$

implied by equations (2.52) - (2.54). Therefore the mean strain part of ϕ_{ic} can be written as

$$\phi_{ic2} = 0.8\,\overline{u_m c}\,U_{i,m} - 0.2\,\overline{u_m c}\,U_{m,i} \tag{2.57}$$

LAUNDER [42] and later LUMLEY [47] arrived at these expressions following more or less similar arguments as given here.

An alternative formulation has been proposed by LAUNDER [18] in which the sole effect of ϕ_{ic2} was considered to be to reduce the effect of generation of $\overline{u_i c}$ by mean gradients. This is parallel to the idea of redistribution of stress production as given in (2.19). Here,

$$\phi_{ic2} = C_{c2}\, \overline{u_m c}\, U_{i,m} \quad . \tag{2.58}$$

Note that in two-dimensional boundary layer flows (2.58) does not contribute to the equation for lateral scalar flux, whereas (2.58) has a contribution of $-\,0.2\,\overline{uc}\,\frac{\partial U}{\partial y}$. OWEN [39] adopted this model for his calculation of scalar transport in pipe flows. In the present investigation, equation(2.58) is employed as the model for ϕ_{ic2}. Equation (2.57) will also be used as a comparison model in free shear flows.

An alternative form of a model has been suggested by LUMLEY and KHAJEH-NOURI [36], where the explicit appearence of mean strain terms were excluded from the analysis. Briefly, their method was, first to consider the $\overline{\frac{c}{\rho} p_{,i}}$ (consideration of $\overline{\frac{p}{\rho} c_{,i}}$ would lead to the same result) as a function of the form

$$-\overline{\frac{c}{\rho} p_{,i}} = F \left\{ \overline{u_i c}\,,\ \overline{u_i u_j}\,,\ \varepsilon\,,\ \text{gravitational terms} \right\} \tag{2.59}$$

and then to make a Taylor series expansion to obtain

$$-\overline{\frac{c}{\rho} p_{,i}} = -\left(a_1 + a_2 b_{ij} + a_3 \Pi + a_4 b_{ij}^2 + \text{gravitational terms} \right) \times \frac{\overline{u_i c}}{\tau} \tag{2.60}$$

where

$$\tau \propto \frac{k}{\varepsilon}\ ; \qquad b_{ij} = \frac{\overline{u_i u_j}}{k} - \frac{2}{3}\delta_{ij}\ ;$$

$$b_{ij} = b_{ik}\, b_{ik} \quad \text{and} \quad \Pi = b_{ij}\, b_{ji} \quad .$$

In the present investigation a model consisting of only the first two terms in (2.60) is considered as an addition to ϕ_{ic2} form (2.57) and not as Lumley and Khajeh-Nouri proposed as a replacement for ϕ_{ic2} i.e.

$$\phi_{ic1} = - C_{c1} \frac{\varepsilon}{k} \overline{u_i c} - C'_{c1} \frac{\varepsilon}{k} b_{il} \overline{u_l c} \quad . \tag{2.61}$$

Now in order to find the numerical values for the coefficients in the models of ϕ_{ic} described above, the local equilibrium forms of the scalar flux equations in free shear flows are considered. In these flows one should aim to get a Prandtl number of about 0.6 - 0.7 and a ratio of the scalar fluxes in streamwise to the lateral direction of about 1.2. (WEBSTER's [48] data indicate a value of 1.1 for this ratio; however, his measured levels of $\frac{\overline{u^2}}{\overline{v^2}}$ are about 25% lower than the accepted level and hence his $\frac{\overline{uc}}{\overline{vc}}$ is likely to be rather too low.)

(a) Redistribution Model, i.e. Equations (2.48) and (2.58)

Under local equilibrium conditions in a two-dimensional flow one obtains

$$C_{c1} = \frac{\overline{v^2}}{k} \left(\frac{k}{\overline{uv}} \right)^2 \sigma_t . \tag{2.62}$$

With stress levels from the nearly homogeneous shear data of CHAMPAGNE et al. [29], and with $\sigma_t = 0.65$, C_{c1} is obtained as equal to 2.9.

The streamwise scalar flux equation in local equilibrium conditions reduces to

$$\frac{\overline{uc}}{\overline{vc}} = \frac{1}{C_{c1}} \left(\frac{k}{\overline{uv}} \right) \left(\sigma_t + 1 - C_{c2} \right) \quad . \tag{2.63}$$

With a scalar flux ratio of 1.2 this implies that C_{c2} should be about 0.5, which is the value used by OWEN [39].

(b) Quasi-Isotropic Model

If the equation (2.48) is used for ϕ_{ic1}, along with the given quasi-isotropic model (2.57), clearly incompatible magnitudes for C_{c1} will be obtained from the two flux equations. Therefore in adopting the quasi-isotropic relation the non-linear form (2.61) for ϕ_{ic1} will have to be used. The resulting flux equations in local equilibrium form are

$$0 = \sigma_t \left(\frac{\overline{v^2}}{k}\right)\left(\frac{k}{\overline{uv}}\right)^2 - C_{c1} - C'_{c1}\, b_{12}\left(\frac{\overline{uc}}{\overline{vc}}\right) - C'_{c1}\, b_{22} + 0.2\left(\frac{\overline{uc}}{\overline{vc}}\right)\left(\frac{k}{\overline{uv}}\right) \tag{2.64}$$

and

$$0 = \sigma_t \left(\frac{k}{\overline{uv}}\right) + 0.2\left(\frac{k}{\overline{uv}}\right) - C_{c1}\left(\frac{\overline{uc}}{\overline{vc}}\right) - C'_{c1}\, b_{11}\left(\frac{\overline{uc}}{\overline{vc}}\right) - C'_{c1}\, b_{12}\,. \tag{2.65}$$

On substituting numerical values for σ_t, $\frac{\overline{uc}}{\overline{vc}}$ and stress levels the coefficients C_{c1} and C'_{c1} can be obtained as 4.3 and - 3.2 respectively.

2.4.3 Wall Effects on the Pressure-Scalar Gradient Term

The surface integral term neglected in the analysis subsequent to equation (2.47) can be expected to have a considerable effect in near-wall flows. As in Section (2.2.4), this surface integral can be eliminated by manipulating the equation (2.47). The resultant form is

$$\overline{\frac{p}{\rho}\, c_{,i}} = \frac{1}{4\pi}\int_V \left(\overline{(u'u')_{mn}\, c_{,mn}}_{,i} + 2\, U'_{1,2}\, \overline{u'_{2,1}\, c}_{,i}\right)\left(\frac{1}{X-Y} + \frac{1}{X-Y^*}\right) dV \tag{2.66}$$

where, suffices *1* and *2* stand for the streamwise and lateral directions respectively. Further, Y^* is the image of Y with respect to the wall.

Here again, the turbulent and mean strain parts can be identified and modelled in a manner exactly parallel to that of the wall effects on the pressure-strain correlation. In a general form this can be written as,

$$\phi_{icw} = \left(- C_{c1w} \frac{\varepsilon}{k} \overline{u_i c} + U_{l,m} d^m_{li} \right) f \left\{ \frac{l_\varepsilon}{x_2} \right\} . \tag{2.67}$$

The function f has the effect of diminishing ϕ_{icw} with increasing distance away from the wall. The general third-order tensor d^m_{li} comprising linear combination of scalar fluxes is

$$d^m_{li} = \alpha'_c \, \delta_{li} \, \overline{u_m c} + \beta'_c \, \delta_{mi} \, \overline{u_l c} + \nu'_c \, \delta_{ml} \, \overline{u_i c} \quad . \tag{2.68}$$

This tensor should satisfy the symmetry requirement $d^m_{li} = d^m_{il}$ and the mass conservation constraint $d^m_{mi} = 0$. They lead to

$$\beta'_c = \nu'_c \qquad \text{and} \qquad 0 = \alpha'_c + 4\beta'_c \quad . \tag{2.69}$$

Thus the resultant form for the wall effect on pressure-scalar gradient correlation is

$$\phi_{icw} = \left(- C_{c1w} \frac{\varepsilon}{k} \overline{u_i c} - 4\beta'_c \delta_{li} \overline{u_m c} \, U_{l,m} + \beta'_c \delta_{mi} \overline{u_l c} \, U_{l,m} \right) f \left\{ \frac{l_\varepsilon}{x_2} \right\} . \tag{2.70}$$

An alternative near-wall model has been suggested by GIBSON and LAUNDER [31] which parallels their near-wall pressure-strain model. The turbulent and mean strain parts of their model are

$$\phi_{ic1w} = C_{ciw} \frac{\varepsilon}{k} \overline{u_k c} \, n_k n_i \, f \left\{ \frac{l_\varepsilon}{n_j x_j} \right\} \tag{2.71}$$

and

$$\phi_{ic2w} = C_{c2w}\, \phi_{kc2}\, n_k n_i\, f\left\{\frac{l_\varepsilon}{n_j x_j}\right\} . \tag{2.72}$$

In the present investigation this near-wall model is used along with equations (2.48) and (2.58). The form in equation (2.70) is employed as a comparison model.

Now, in order to find the numerical values for the unknown coefficients (two in each model) in these near-wall forms attention is turned to turbulent scalar characteristics in wall flows. As will be seen later in Chapter (4), the turbulent Prandtl number and the ratio of levels of scalar fluxes in the streamwise direction to that of lateral flow direction in two-dimensional flows are about 0.9 and 2.0 - 2.5 respectively.

(a) Gibson- Launder Model

Equations (2.58) and hence (2.72) do not contribute to the lateral scalar flux equation in two-dimensional boundary layers, thus the coefficient C_{c1w} in (2.71) must be chosen in order to get a turbulent Prandtl number of 0.9. With near-wall stress levels, the local equilibrium form of $\overline{vc}$ equation imply a C_{c1w} of 0.75. Equation (2.71) and (2.72) do not contribute to the streamwise scalar flux equation, therefore C_{c2w} in (2.70) can not be found in two-dimensional flows. Further it means that the streamwise scalar flux equation is unchanged in the near-wall region. This implies a ratio $\overline{uc}/\overline{vc}$ of about 2.0 which agrees reasonably well with the experimental data though is perhaps a little low.

(b) Isotropic Model

When equation (2.70) is employed in the local equilibrium regions, the scalar flux equations for the lateral and streamwise directions can be written in algebraic forms as,

$$0 = -\frac{\overline{v^2}}{\overline{uv}}\sigma_t + (C_{c1} + C_{c1w})\frac{\overline{uv}}{k} + \beta'_c\frac{\overline{uc}}{\overline{vc}} \tag{2.73}$$

and

$$0 = -\sigma_t - (1-C_{c2}) + (C_{c1} + C_{c1w})\frac{\overline{uv}}{k}\frac{\overline{uc}}{\overline{vc}} - 4\beta'_c \quad . \tag{2.74}$$

With the above mentioned near-wall stress levels and scalar characteristics, these two equations can be solved to obtain $C_{c1w} = 0.25$ and $\beta'_c \simeq 0.06$.

2.5 The Transport Equation for Scalar Fluctuations

The variable representing the level of scalar fluctuation is taken as $\frac{1}{2}\overline{c^2}$, which corresponds to the turbulent kinetic energy $k = \frac{1}{2}\overline{u_i^2}$. The transport equation for $\frac{1}{2}\overline{c^2}$ can be obtained by multiplying the instantaneous scalar $(C+c)$ equation by the fluctuation $\frac{1}{2}c$. On time averaging the result yields

$$(\tfrac{1}{2}\overline{c^2})_{,t} + U_k\,(\tfrac{1}{2}\overline{c^2})_{,k} = \overline{u_j c}\,C_{,j} - \Gamma\,\overline{c_{,j}c_{,j}} - (\overline{u_j \tfrac{1}{2}c^2} - \Gamma\,\tfrac{1}{2}\overline{c^2}_{,j})_{,j} \tag{2.75}$$

Convection = Generation - Dissipation - Diffusion .

In order to solve (2.75) models have to be supplied for the dissipation and diffusion terms in this equation.

The time scale of turbulence associated with the scalar turbulence is $\frac{1}{2}\overline{c^2}/\varepsilon_c$ where $\varepsilon_c = \Gamma\,\overline{c_{,j}c_{,j}}$. The assumption that there is a constant ratio between the time scales of the scalar field and the hydrodynamic field yields

$$\varepsilon_c = \frac{\varepsilon\,\frac{1}{2}\overline{c^2}}{k\,R} \tag{2.76}$$

where R is the time scale ratio. The magnitude of R , if it is a constant, should be evident from the dacay of turbulence behind a heated grid as the ratio of decay exponents is equal to the ratio of time scales. The survey of scalar fluctuation decay data compiled by LIN and LIN [112] however show a large variation in dacay exponents. They imply time scale ratio between the extremes 1.26 to 0.35 .

In computer modelling SPALDING [49] used a value of 0.5 whereas LAUNDER [18] used a value of 0.8 in predicting buoyant free shear flows. In the present study a value of 0.5 is used for the time scale ratio in (2.76).

The more appropiate method of course is to solve for ε_c via its

transport equation, an attempt similar to solving ε the dissipation of turbulent kinetic energy. Current modelling ideas have followed lines similar to that used in closing the ε equation. Here however the presence of two time scales k/ε and $\frac{1}{2}\overline{c^2}/\varepsilon_c$ complicates the modelling a great deal. OWEN [39] has suggested a model for ε_c , but his equation containing no positive source term is clearly incorrect.

As for the modelling of diffusive transport of $\frac{1}{2}\overline{c^2}$ reference is made to the transport equation for $\overline{u_j c^2}$. The algebraic expression obtainable with the level of assumptions used in modelling $\overline{u_i u_j u_k}$ of $\overline{u_i u_j c}$, is,

$$- \tfrac{1}{2}\,\overline{u_j c^2} = C_g \frac{k}{\varepsilon}\left(\overline{u_k u_j}\,(\tfrac{1}{2}\overline{c^2})_{,k} + \overline{u_k c}\;\overline{u_j c}_{,k} + \overline{u_j u_k c}\;C_{,k} \right) . \tag{2.77}$$

WYNGAARD [43] omitted the last terms in (2.77) thus retaining the usual gradient diffusion form. In the present investigation too only the gradient form is retained

$$- \tfrac{1}{2}\,\overline{u_j c^2} = C_g \frac{k}{\varepsilon}\left(\overline{u_k u_j}\,(\tfrac{1}{2}\overline{c^2})_{,k} \right) . \tag{2.78}$$

0 0 0 0 4 9 0 2 0 2 3

2.6 A Summary of the Models to be Investigated

The turbulence models discussed in previous sections of this chapter are summarised here. Table (2.1) corresponds to the hydrodynamic closure models whereas Table (2.2) refers to the scalar transport models. The different models are identified here with different code names and the methods used in obtaining unknown coefficients that appear in modelled terms are mentioned.

Term	Model				How Determined
	Name	Description	Equation of its First Mention	Coefficient and Value Used	
Pressure -velocity gradient correlation ϕ_{ij}	R_{s1}	LAUNDER et al. [15] isotropic model	(2.11) and (2.14)	C_{s1} = 1.5 and C_{s2} = 0.4	Normal stress levels in nearly homogeneous shear flow
	R_{s2}	LAUNDER et al. [15] simple model;	(2.11) and (2.19)	C_{s1} = 1.5 and C_{s2} = 0.6	
		also in [31]	(2.11) and (2.19)	C_{s1} = 1.8 and C_{s2} = 0.55	
Near-wall effects on ϕ_{ij}	R_{sw1}	LAUNDER et al. [15] model	(2.22)	C_{s1w} = 0.5 and C_{s2w} = 0.06	Near-wall stress levels
	R_{sw2}	GIBSON-LAUNDER [31] model	(2.26) and (2.27)	C_{s1w} = 0.5 and C_{s2w} = 0.3	
Turbulent diffusion	D_{s1}	Tensor invariant model	(2.6)	C_s = 0.11	Computer optimisation
	D_{s2}	Gradient diffusion model	(2.8)	C'_s = 0.2	

Table 2.1 Hydrodynamic Models Used in the Present Study

(contd.)

Term	Model				How Determined
	Name	Description	Equation of its First Mention	Coefficient and Value Used	
Energy dissipation rate equation		LAUNDER et al. [15] model	(2.33)	$C_{\varepsilon 1} = 1.44$	Computer optimisation
			(2.33)	$C_{\varepsilon 2} = 1.90$	Decay of grid turbulence
			(2.34)	$C_{\varepsilon} = 0.15$	Consistency with Von Kármán constant and near-wall stress levels

Table 2.1 Hydrodynamic Models Used in the Present Study

Term	Model				How Determined
	Name	Description	Equation of its First Mention	Coefficient and a Tentative Value	
Pressure -scalar gradient correlation in flux equation ϕ_{ic}	R_{c1}	1) Linear destruction	(2.48)	$C_{c1} = 2.9$	Prandtl number of 0.65 in free flows
		2) Redistribution of production (due to mean velocity gradients) tensor	(2.58)	$C_{c2} = 0.4$	Flux ratio of 1.2 in free flows
	R_{c2}	1) Non-linear destruction	(2.61)	$C_{c1} = 4.0$ and $C'_{c1} = -3.2$	
		2) Quasi-isotropic model	(2.57)	exact term known	
Near-wall effects on ϕ_{ic}	R_{cw1}	Isotropic model	(2.70)	$C_{c1w} = 0.25$ and $\beta'_c = 0.06$	Prandtl number of 0.885 in near-wall flows
	R_{cw2}	1) A modified linear destruction term	(2.71)	$C_{c1w} = 0.75$	Flux ratio of 2.05 in near-wall flows
		2) Modified linear destruction term	(2.72)	C_{c2w} = not applicable in two-dimensional boundary layers	

Table 2.2 Scalar Transport Models Investigated in the present Study

(contd.)

Term	Model				How Determined
	Name	Description	Equation of its First Mention	Coefficient and a Tentative Value	
Diffusive transport of fluxes	D_{c1} D_{c2} D_{c3}	Gradient diffusion Gradient diffusion Tensor invariant type	(2.45)	$C_c = 0.20$ $C_c = 0.11$ $C_c = 0.11$	Similarity with existing stress model coefficients
Diffusive transport of $\overline{c^2}$		Gradient diffusion	(2.78)	$C_g = 0.11$	Similarity with kinetic energy equation
Destruction of of scalar fluctuations		Constant time scale ratio type	(2.76)	$C_{g2} = \frac{1}{R} = 1.3 \rightarrow 2.0$	Levels of scalar fluctuations Computer optimisation

Table 2.2 Scalar Transport Models Investigated in the Present Study

0 0 1 0 4 9 0 1 8 9 - 0 2 5

2.7 Modelled Equations in Cartesian Tensor Form

2.7.1 Reynolds Stress Equations

The conservation equations for the Reynolds stresses are

$$\frac{D}{Dt}\left(\overline{u_i u_j} \right) = P_{ij} + \phi_{ij} - \varepsilon_{ij} + D\left(\overline{u_i u_j} \right) \tag{2.79}$$

where,

(a) the convection,

$$\frac{D}{Dt}\left(\overline{u_i u_j} \right) = \left(\frac{\partial}{\partial t} + U_k \frac{\partial}{\partial x_k} \right) \overline{u_i u_j}$$

(b) the production,

$$P_{ij} = - \left(\overline{u_i u_k} \frac{\partial U_j}{\partial x_k} + \overline{u_j u_k} \frac{\partial U_i}{\partial x_k} \right)$$

(c) the pressure-strain correlation,

for free flows,

$$\phi_{ij} = \phi_{ij1} + \phi_{ij2}$$

and for wall flows,

$$\phi_{ij} = \phi_{ij1} + \phi_{ij2} + \phi_{ij1w} + \phi_{ij2w}$$

where

$$\phi_{ij1} = - C_{s1} \frac{\varepsilon}{k} \left(\overline{u_i u_j} - \frac{2}{3} \delta_{ij} k \right) \qquad \text{Models } R_{s1} \text{ and } R_{s2}$$

$$\phi_{ij2} = - \left(\alpha \left(P_{ij} - \frac{2}{3} P \delta_{ij} \right) + \beta k \left(\frac{\partial U_i}{\partial x_j} + \frac{\partial U_j}{\partial x_i} \right) + \eta \left(D_{ij} - \frac{2}{3} P \delta_{ij} \right) \right) \qquad \text{Model } R_{s1}$$

or

$$\phi_{ij2} = - \gamma \left(P_{ij} - \frac{2}{3} P \delta_{ij} \right) \qquad \text{Model } R_{s2}$$

$$\phi_{ij1w} = C_{s1w} \frac{\varepsilon}{k} \left(\overline{u_i u_j} - \frac{2}{3} k \delta_{ij} \right) f \left(\frac{l_\varepsilon}{x_2} \right) \qquad \text{Model } R_{sw1}$$

or

$$\phi_{ij1w} = C_{s1w} \frac{\varepsilon}{k} \left(\overline{u_k u_m} n_k n_m \delta_{ij} - \frac{3}{2} \overline{u_k u_i} n_k n_j - \frac{3}{2} \overline{u_k u_j} n_k n_i \right) f \left(\frac{l_\varepsilon}{x_2} \right) \qquad \text{Model } R_{sw2}$$

$$\phi_{ij2w} = C_{s2w} \left(P_{ij} - D_{ij} \right) f \left(\frac{l_\varepsilon}{x_2} \right) \qquad \text{Model } R_{sw1}$$

or

$$\phi_{ij2w} = C_{s2w} \left(\phi_{km2} \, n_k \, n_m \, \delta_{ij} - \frac{3}{2} \phi_{ki2} \, n_k \, n_j - \frac{3}{2} \phi_{kj2} \, n_k \, n_l \right) \times f \left(\frac{l_\varepsilon}{x_2} \right) \qquad \text{Model } R_{sw2}$$

with

$$P = \tfrac{1}{2} P_{mm}$$

and

$$D_{ij} = - \left(\overline{u_i u_k} \frac{\partial U_k}{\partial x_j} + \overline{u_j u_k} \frac{\partial U_k}{\partial x_i} \right)$$

(d) the dissipation,

$$\varepsilon_{ij} = \frac{2}{3} \varepsilon \, \delta_{ij}$$

(e) the diffusion,

$$D \left(\overline{u_i u_j} \right) = \frac{\partial}{\partial x_k} C_s \frac{k}{\varepsilon} \left(\overline{u_k u_m} \frac{\partial \overline{u_i u_j}}{\partial x_m} + \overline{u_i u_m} \frac{\partial \overline{u_j u_k}}{\partial x_m} + \overline{u_j u_m} \frac{\partial \overline{u_i u_k}}{\partial x_m} \right) \qquad \text{Model } D_{s1}$$

or

$$D \left(\overline{u_i u_j} \right) = \frac{\partial}{\partial x_k} C_s' \frac{k}{\varepsilon} \left(\overline{u_k u_m} \frac{\partial \overline{u_i u_j}}{\partial x_m} \right) . \qquad \text{Model } D_{s2}$$

2.7.2 Isotropic dissipation rate equation

The conservation equation for the dissipation rate is

$$\frac{D}{Dt}(\varepsilon) = C_{\varepsilon 1} \frac{\varepsilon}{k} P - C_{\varepsilon 2} \frac{\varepsilon^2}{k} + D(\varepsilon) \tag{2.80}$$

where

(a) the convection,

$$\frac{D}{Dt}(\varepsilon) = \left(\frac{\partial}{\partial t} + U_k \frac{\partial}{\partial x_k} \right) \varepsilon$$

and

(b) the diffusion,

$$D(\varepsilon) = \frac{\partial}{\partial x_k} C_\varepsilon \frac{\varepsilon}{k} \left(\overline{u_k u_l} \frac{\partial \varepsilon}{\partial x_l} \right) .$$

2.7.3 Scalar Flux Equations

The conservation equation for scalar fluxes are

$$\frac{D}{Dt}(\overline{u_i c}) = P_{ic} + \phi_{ic} + D(\overline{u_i c}) \tag{2.81}$$

where

(a) the convection,

$$\frac{D}{Dt}(\overline{u_i c}) = \left(\frac{\partial}{\partial t} + U_k \frac{\partial}{\partial x_k}\right)\overline{u_i c}$$

(b) the production,

$$P_{ic} = -\left(\overline{u_k c}\frac{\partial U_i}{\partial x_k} + \overline{u_k u_i}\frac{\partial C}{\partial x_k}\right)$$

(c) the pressure-scalar gradient correlation,

for free flows

$$\phi_{ic} = \phi_{ic1} + \phi_{ic2}$$

and for wall flows

$$\phi_{ic} = \phi_{ic1} + \phi_{ic2} + \phi_{ic1w} + \phi_{ic2w}$$

where

$$\phi_{ic1} = -C_{c1}\frac{\varepsilon}{k}\overline{u_i c} \qquad \text{Model } R_{c1}$$

or

$$\phi_{ic1} = -C_{c1}\frac{\varepsilon}{k}\overline{u_i c} - C'_{c1}\frac{\varepsilon}{k}b_{il}\overline{u_l c} \qquad \text{Model } R_{c2}$$

$$\phi_{ic2} = C_{c2}\overline{u_k c}\frac{\partial U_i}{\partial x_k} \qquad \text{Model } R_{c1}$$

or

$$\phi_{ic2} = 0.8\,\overline{u_k c}\frac{\partial U_i}{\partial x_k} - 0.2\,\overline{u_k c}\frac{\partial U_k}{\partial x_i} \qquad \text{Model } R_{c2}$$

$$\phi_{ic1w} = -C_{c1w}\frac{\varepsilon}{k}\overline{u_i c}\, f + \frac{l_\varepsilon}{x_2} + \qquad \text{Model } R_{cw1}$$

or

$$\phi_{ic1w} = -C_{c1w}\frac{\varepsilon}{k}\overline{u_m c}\, n_m n_i\, f + \frac{l_\varepsilon}{x_2} + \qquad \text{Model } R_{cw2}$$

$$\phi_{ic2w} = \left(- 4\beta'_c \, \delta_{li} \, \overline{u_m c} \, \frac{\partial U_l}{\partial x_m} + \beta'_c \, \delta_{mi} \, \overline{u_l c} \, \frac{\partial U_l}{\partial x_m} \right) f \left\{ \frac{l_\varepsilon}{x_2} \right\}$$

Model R_{cw1}

or

$$\phi_{ic2w} = - C_{c2w} \, \phi_{mc2} \, n_m \, n_i \, f \left\{ \frac{l_\varepsilon}{x_2} \right\}$$

Model R_{cw2}

(d) the diffusion,

$$D \left(\overline{u_i c} \right) = \frac{\partial}{\partial x_k} C_c \frac{k}{\varepsilon} \left(\overline{u_k u_l} \, \frac{\partial \, \overline{u_i c}}{\partial x_l} \right)$$

Model D_{c1}

or

$$D \left(\overline{u_i c} \right) = \frac{\partial}{\partial x_k} C_c \frac{k}{\varepsilon} \left(\overline{u_k u_l} \, \frac{\partial \, \overline{u_i c}}{\partial x_l} + \overline{u_i u_l} \, \frac{\partial \, \overline{u_k c}}{\partial x_l} \right)$$

Model D_{c2}

or

$$D \left(\overline{u_i c} \right) = \frac{\partial}{\partial x_k} C_c \frac{k}{\varepsilon} \left(\overline{u_k u_l} \, \frac{\partial \, \overline{u_i c}}{\partial x_l} + \overline{u_i u_l} \, \frac{\partial \, \overline{u_k c}}{\partial x_l} + \overline{u_l c} \, \frac{\partial \, \overline{u_i u_k}}{\partial x_l} \right) .$$

Model D_{c3}

2.7.4 Scalar Fluctuation Equation

The conservation equation for mean square scalar fluctuations is

$$\frac{D}{Dt} \left(\frac{\overline{c^2}}{2} \right) = P_c - \varepsilon_c + D \left(\frac{\overline{c^2}}{2} \right) \tag{2.82}$$

where

(a) the convection,

$$\frac{D}{Dt} \left(\frac{\overline{c^2}}{2} \right) = \left(\frac{\partial}{\partial t} + U_k \frac{\partial}{\partial x_k} \right) \frac{\overline{c^2}}{2}$$

(b) the production,

$$P_c = - \overline{u_k c} \, \frac{\partial C}{\partial x_k}$$

(c) the dissipation,

$$\varepsilon_c = C_{g2} \frac{\varepsilon}{k} \frac{\overline{c^2}}{2}$$

(d) the diffusion,

$$D \left(\frac{\overline{c^2}}{2} \right) = \frac{\partial}{\partial x_k} C_g \frac{\varepsilon}{k} \left(\overline{u_l u_k} \, \frac{\partial \, \overline{c^2}/2}{\partial x_l} \right) .$$

CHAPTER 3

NUMERICAL PROCEDURES

3.1 Introduction

The conservation equations for mean and turbulent quantities presented in the previous chapter can be solved using finite difference numerical methods. In general those equations are three-dimensional, unsteady and elliptic. In engineering practice, however, there are many statistically stationary or steady flows which are of interest. Further there are many important situations where the flow is of boundary layer type, i.e. with at least one direction having negligible diffusive fluxes. In the present analysis the attention is limited to steady flows of boundary layer type. Although the present calculations are limited to incompressible constant property flows, the numerical procedures to be discussed can be generalised easily to variable-property flows.

PATANKAR and SPALDING [9] presented a numerical procedure for the solution of partial differential conservation equations for steady two-dimensional, axi-symmetric boundary layer flows. This procedure is probably the most widely tested numerical scheme, designed to solve the above equations, available to date. In Section (3.2), the main features of this procedure and its application to the solution of mean and turbulent conservation equations are presented. The problems encountered, e.g. instabilities, their possible causes and cures are discussed there.

The procedure used to predict three-dimensional boundary layers is an outgrowth of the two-dimensional elliptic numerical method of GOSMAN and PUN [50]. This procedure incorporates displaced grids for velocity and pressure, employed by HARLOW and WELCH [51]. Here, as in CARETTO et al. [52], a guess-and-correct procedure is used for the

velocity field. The correction of the velocity field is obtained through a linearised pressure-velocity relation which in turn satisfies continuity. This procedure with an obvious simplification to the case of two-dimensional internal flows is discussed in Section (3.3).

The remainder of the chapter is concerned with adaptations to the basic structure of the codes that the writer has introduced to facilitate the introduction of a second-order closure.

In Section (3.4), a finite difference staggered grid suitable for the application of a second order closure-model in a fully three-dimensional flow situation is described. The aim here has been to stagger the variables so that when they appear in the mean equations, requires a minimum of interpolation. This is expected to eliminate the instabilities encounted in using numerical procedures outlined in previous sections.

The idealised grid arrangement described in Section (3.4) is simplified in the Section (3.5), so that, it is economically applied to the solution of three-dimensional scalar transport problem in two-dimensional boundary layer flow situation. It is seen here that this modified grid arrangement simplifies the calculation of generally more predominant terms in the mean as well as in the turbulence equations.

In Section(3.6) the limitations of cell layout and the application of the boundary conditions are discussed. The inclusion of a solid wall into the domain of the three-dimensional calculation procedure is discussed in Section (3.7). This allows circumferential conduction to be taken into account in instances where it is necessary.

3.2 The Patankar-Spalding Procedure for Two-Dimensional Boundary Layers

3.2.1 Main Features

The Patankar-Spalding procedure for the solution of conservation equations for two-dimensional boundary layer flows is widely used by research workers and in industry and is well documented in [9]. Accordingly only the main features will be mentioned here.

(a) The Coordinate System:

In this procedure the boundary-layer equations are transformed to x-ω coordinate system, where x is the displacement coordinate in the main flow direction and ω is the dimensionless stream function, given by

$$\omega = \frac{\Psi - \Psi_I}{\Psi_E - \Psi_I} . \tag{3.1}$$

The stream function is defined so that Ψ is a constant along a stream line and

$$d\Psi = \rho \, U \, r \, dy \tag{3.2}$$

The edge stream functions Ψ_I and Ψ_E are chosen as functions of x , so that all the important variations in the dependent variables takes place within their limits, i.e. ω values between zero and unity; this practice assures an efficient and flexible grid layout.

(b) The Difference Equation:

The finite difference forms of the conservation equations are obtained by integrating the partial differential equations over control volumes. (see Fig. 3.1) Being a boundary layer procedure, the control volumes at a given x-level are defined so as to cover only upto the immediate forward x-level. In ω-space, the control volumes are defined by known discrete

ω-levels, so that a given number of control volumes occupy the ω-space between I and E boundaries. For the purpose of integration it is assumed that in the ω-direction, the dependent variable Φ varies linearly with ω between grid points. For convenience it is assumed that, in the x-direction, the variation of Φ is stepwise and it is the downstream level that is prevailing over the control volume.

The individual terms of the conservation equation are integrated over the control volumes so as to obtain difference equations for each control volume. The resulting equations are of the form

$$\Phi_d = A\,\Phi_{d+} + B\,\Phi_{d-} + C \tag{3.3}$$

where Φ_{d+} and Φ_{d-} are the values of Φ_d's at adjacent control volumes in ω-space. (The suffix d stands for the downstream level.) The coefficients A, B and C are explicitly evaluated with known Φ's at upstream x-level.

(c) Treatment of Diffusion Terms:

In the published version of the numerical procedure the diffusion terms of the momentum and heat transport equation are arranged to suit gradient diffusion models. Thus the incorporation of an "eddy diffusivity" model of turbulent transport is straight forward. In order to incorporate a Reynolds stress-Scalar flux closure, modifications are needed. The following sub section outlines alternative approaches.

3.2.2 Treatment of Turbulent Shear Stress and Scalar Flux

Consider a control volume whose edge values of ω are $\omega_{-\frac{1}{2}}$ and $\omega_{+\frac{1}{2}}$ (see Fig. (3.1)). The total shear stress at the edge $\omega_{+\frac{1}{2}}$ is given by

$$\tau_{\frac{1}{2}} = \left[\mu \left(\frac{\partial U}{\partial y} \right)_d - \rho \, \overline{uv} \right]_{+\frac{1}{2}} . \tag{3.4}$$

With a gradient diffusion model, this is expressed as,

$$\tau_{\frac{1}{2}} = \left[\mu_{eff} \left(\frac{\partial U}{\partial y} \right)_d \right]_{+\frac{1}{2}} \tag{3.5}$$

where μ_{eff} is the effective viscosity obtained by

$$\mu_{eff} = \mu + \mu_{turb} \tag{3.6}$$

and the turbulent viscosity μ_{turb} is obtained via a constitutive relation.

With a Reynolds stress closure, however, equation (3.4) can be evaluated directly. Thus the turbulent shear stress term can be incorporated either,

(a) by constructing a pseudo-viscosity and applying equation (3.5)

or (b) as a source term in the momentum equation.

If the effective viscosity method is to be pursued, the turbulent viscosity μ_{turb} is calculated by

$$\mu_{turb,+\frac{1}{2}} = - \frac{(\rho \, \overline{uv})_{+\frac{1}{2}} \cdot (y_{+1} - y)}{(U_{+1} - U)_u} \tag{3.7}$$

Equation (3.7) is not satisfactory in regions of small velocity gradient unless measures are introduced to counteract instabilities. Alternatively the net diffusion due to turbulent shear stress can be written as,

$$\left(\frac{\partial \tau_{turb}}{\partial y} \right) = - \frac{(\rho \, \overline{uv})_{+\frac{1}{2}} - (\rho \, \overline{uv})_{-\frac{1}{2}}}{y_{+\frac{1}{2}} - y_{-\frac{1}{2}}} . \tag{3.8}$$

unlike equation (3.7), this equation can be incorporated unconditionally, even in regions where the mean gradient is negligibly small. Especially in flows with regions where the eddy diffusivity concept is not valid, e.g. maximum velocity region is a wall jet, equation (3.8) is satisfactory, whereas equation (3.7) is not.

3.2.3 Instability in Solution and A Possible Remedy

Several workers (e.g. REECE [25], MORSE [53]) making numerical computations of boundary layer flows using second-order closure models employed the Patankar-Spalding procedure for their calculations. In those investigations, the turbulent variables were evaluated at the same grid points as those of mean variables. In the present investigation as well, a large number of calculations were performed with that grid arrangement. It was sometimes seen however that numerical instability occured and that, when it did, the numerical scheme seemed apparently contained no mechanism for damping it. The following hypothetical situation will clarify how this happens.

Consider a mean velocity profile as shown in Fig. (3.2) and suppose there is a peturbation in this profile at grid point (I) (dash lines), so that the velocity is now $U_{(I)} + \delta U_{(I)}$. Since the shear stresses are calculated at points $(I-1)$, (I) , $(I+1)$ etc., velocity gradients have to be interpolated in order to calculate production and other terms due to mean gradients. Thus, the velocity gradient across the cell (I) is in fact unchanged whereas gradients across cells $(I+1)$ and $(I-1)$ are changed slightly. Thus, the resultant shear stress at (I) is unchanged whereas at $(I+1)$ and $(I-1)$ the shear stress will have changed in the right direction. Now since the interpolated values of shear stresses are needed for inclusion in mean velocity equation the net effect would be to change the velocity profile towards the stable solution but at a too low response level.

In order to ensure full exchange of information between mean velocity and shear stress equations, which are interlinked via their gradients, the scheme must be able to feel correct gradients created by the pertubation. POPE and WHITELAW [54] and ANDRÉ [55] proposed schemes which had staggered grid arrangements where the shear stress nodes are shifted by a half a grid node spacing from the mean velocity nodes. This idea has previously being used by CHORIN [56] and in PATANKAR and SPALDING [57] numerical procedures, with respect to the velocity and pressure nodes.

In a staggered grid arrangement the shear stress values are calculated at points $(I-\frac{1}{2})$, $(I+\frac{1}{2})$etc., shifted half a grid spacing away from $(I-1)$, (I) , $(I+1)$ etc.. Now the production type terms of difference equations at $(I-\frac{1}{2})$ and $(I+\frac{1}{2})$ directly feel the total perturbation. The shear stress at $(I+\frac{1}{2})$ will be rapidly raised while that at $(I-\frac{1}{2})$ will fall. The velocity cell at (I) , therefore, will experience a restorative force which will cause the perturbation to diminish.

The above argument is satisfactory in regions of flows where the mean velocity (or scalar) and the corresponding flux are strongly linked to one another, i.e. having a predominant production due to mean shear term in the shear stress equation. In a weakly linked flow, for example a flow region with dominant diffusion effects, any instabilities in the mean profile will not be strongly felt by the corresponding flux equation so that the instability would vanish only very slowly. Even in such regions, however, the staggered grid can be helpful although to a lesser extent.

3.3 Description and Application of the Three-Dimensional (θ, r, z) Boundary Layer Procedure

The general form of the conservation equations written out in Section (2.7) can be reexpressed here as

$$\frac{\partial}{r\partial\theta}\left(\rho U_\theta \Phi\right) + \frac{\partial}{r\partial r}\left(r\rho U_r \Phi\right) + \frac{\partial}{\partial z}\left(\rho U_z \Phi\right)$$

$$= \frac{\partial}{r\partial\theta}\left(\Gamma_\theta^\Phi \frac{\partial\Phi}{r\partial\theta}\right) + \frac{\partial}{r\partial r}\left(r\Gamma_r^\Phi \frac{\partial\Phi}{\partial r}\right) + \frac{\partial}{\partial z}\left(\Gamma_z^\Phi \frac{\partial\Phi}{\partial z}\right) + S^\Phi \qquad (3.9)$$

where Φ stands for any of the dependent variables U_θ, U_r, U_z, k, ε, $\overline{u_i u_j}$ (with i = 1,3 and j = 1,3), C, $\overline{u_i c}$ (with i = 1,3) and $\overline{c^2}$. Here Γ_i^Φ stands for the diffusion coefficient of Φ in the direction-i and S^Φ stands for the net generation of Φ per unit volume.

Equation (3.9) can be interpreted in Cartesian coordinates by transforming (θ, r, z) to (x, y, z) using

$$\frac{\partial}{\partial x} = \frac{\partial}{r\partial\theta} \; ; \; \frac{\partial}{\partial y} = \frac{\partial}{\partial r} \; ; \; \frac{\partial}{\partial z} = \frac{\partial}{\partial z} \; ; \; r = 1 \, . \qquad (3.10)$$

The following discussion, however is made with respect to the (θ, r, z) form and the Cartesian equivalent is always implied.

For the case of a three-dimensional boundary layer with the main flow in the z direction, the diffusion in that direction is so small compared with convective processes that the term

$$\frac{\partial}{\partial z}\left(\Gamma_z^\Phi \frac{\partial\Phi}{\partial z}\right) ,$$

is discarded. Equation (3.9) thus becomes first order (parabolic) in the z coordinate, permitting evaluation of all variables progressively in planes normal to direction-z, with the knowledge of upstream and boundary conditions. It is this form that is solved in this numerical procedure.

3.3.1 Finite Difference Grid

The finite difference grid for this procedure consists of three orthogonal sets of lines of constant θ, r and z. The (θ,r) plane covers the cross-stream and the direction-z coincides with the main flow direction. The control volumes are centered around the grid nodes which are the intersection points of given (θ, r, z) lines. These control volumes cover the whole domain of interset. The general equation being parabolic in the z direction, at a given moment in the calculation, attention is given only to a single z-spacing.

In general, a compromise is sought, between the cost of computation and accuracy of results, in deciding the optimum number of lines to be used in grid formation. Some further limitations apply, under turbulent flow conditions, in laying out of the grid near walls and this is discussed later.

The control volumes defined above are centered around the grid nodes where the pressure is calculated. As in the numerical schemes of HARLOW and WELCH [51] and GOSMAN and PUN [50] the velocity components are evaluated at grid points shifted by half a node-spacing from the pressure grid. This allows a direct estimation of pressure gradients relevant to the velocity component equations. The positions of the dependent variables are denoted by their corresponding grid node numbers. For example $\Phi_{(I,J)}$ refers to the variable Φ at the position where grid lines I (in the θ-direction) and J (in the r-direction) intersect. (see Fig. (3.3))

3.3.2 Derivation of Finite Difference Equations

Only a brief discussion is made here on the derivation of the finite difference equations. Datailed discussion of the topic has been provided by others, see for example SYED [16], BERGELES [58].

The finite difference equations are derived by integrating the partial differential equation (3.8) for Φ, over the control volume centering the point where Φ is required to be calculated. The net total of convection and diffusive fluxes of Φ leaving the control volume is equated to the net generation of Φ within the control volume. For the calculation of total flux of Φ across any surface of the control volume, the value of Φ at that surface has to be approximated. This can be done by weighting the values of Φ at neighbouring locations according to the local flow Peclet number. The one-dimensional analytical solution to the flux equation yields

$$\Phi = \xi \, \Phi_{(I+1)} + (1-\xi) \, \Phi_{(I)} \tag{3.11}$$

where $\Phi_{(I)}$ and $\Phi_{(I+1)}$ are Φ's at grid points at either side of the surface $(I+\frac{1}{2})$ and ξ, the weighting factor is given by

$$\xi = \frac{e^{Pe} - 1}{e^{Pe_{(I+1)}} - 1} \tag{3.12}$$

where

$$Pe_{(I+1)} = (\rho U)_{(I+\frac{1}{2})} \cdot (X_{(I+1)} - X_{(I)}) \, / \, \Gamma^{\Phi}_{(I+\frac{1}{2})}$$

and

$$Pe = Pe_{(I+1)} \frac{X - X_{(I)}}{X_{(I+1)} - X_{(I)}}$$

The net total flux of Φ in direction I, can now be written as

$$\Pi_I = (\alpha\rho U)_{(I+\frac{1}{2})} \left[\zeta_{(I+\frac{1}{2})} \Phi_{(I)} + (1 - \zeta_{(I+\frac{1}{2})}) \Phi_{(I+1)} \right]$$

$$- (\alpha\rho U)_{(I-\frac{1}{2})} \left[\zeta_{(I-\frac{1}{2})} \Phi_{(I-1)} + (1 - \zeta_{(I-\frac{1}{2})}) \Phi_{(I)} \right] \tag{3.13}$$

where

$$\zeta_{(I+\frac{1}{2})} = 1 - \xi_{(I+\frac{1}{2})} + \frac{1}{Pe_{(I+1)}}$$

and

$$\zeta_{(I-\frac{1}{2})} = 1 - \xi_{(I-\frac{1}{2})} + \frac{1}{Pe_{(I-1)}}$$

Here $\alpha_{(I+\frac{1}{2})}$ and $\alpha_{(I-\frac{1}{2})}$ denote the areas of surfaces normal to the direction (I).

Use of (3.13) would require evaluation of ξ's which contain exponentials, which are expensive to compute. An alternative form of ζ's, suggested in [50], is used with little loss of accuracy.

For,

$$Pe > 2 \quad , \quad \zeta = 1 \quad ;$$

$$Pe < -2 \quad , \quad \zeta = 0 \quad ;$$

$$|Pe| < 2 \quad , \quad \zeta = \tfrac{1}{2}\left(1 + \frac{2}{Pe}\right) . \tag{3.14}$$

The first two expressions mean that when $|Pe|$ is high the flux of Φ across a surface depends solely upon the upwind value. It is the exact solution for $|Pe| \to \infty$. In the third expression the surface value is taken as the central-difference, arithmetic mean value of the neighbouring Φ's. It is the exact solution for $Pe = 0$.

The net generation term S^{Φ} is the only term in equation (3.9) remaining to be considered. The integral of S^{Φ} is expressed in the following linearised form

$$\int_{Vol(I,J)} S^{\Phi} \, dVol = b^{\Phi}_{(I,J)} \, \Phi_{(I,J)} + C^{\Phi}_{(I,J)} \tag{3.15}$$

where $b^{\Phi}_{(I,J)}$ and $C^{\Phi}_{(I,J)}$ may be functions of $\Phi_{(I,J)}$. Values $b^{\Phi}_{(I,J)}$ and $C^{\Phi}_{(I,J)}$ are not unique, they can be chosen to enhance the stability of the procedure. It will be seen later in (3.33) that $b^{\Phi}_{(I,J)}$ should in fact be negative, or small and positive, in order to achieve a stable solution.

3.3.3 Assembly of Finite Difference Terms

The finite difference forms of total flux expressions and net generation term derived in Section (3.3.2), when assembled gives

$$\left(\sum A^{\Phi}_{(I,J)} - b^{\Phi}_{(I,J)} \right) \Phi_{(I,J)} = A^{\Phi}_{(I+1,J)} \Phi_{(I+1,J)} + A^{\Phi}_{(I-1,J)} \Phi_{(I-1,J)} + A^{\Phi}_{(I,J+1)} \Phi_{(I,J+1)} + A^{\Phi}_{(I,J-1)} \Phi_{(I,J-1)} + A^{\Phi}_{(I,J,u)} \Phi_{(I,J,u)} + A^{\Phi}_{(I,J,d)} \Phi_{(I,J,d)} + C^{\Phi}_{(I,J)} \qquad (3.16)$$

where

$$A^{\Phi}_{(I+1,J)} = (a\rho U)_{(I+\frac{1}{2})} (\zeta_{(I+\frac{1}{2})} - 1)$$

$$A^{\Phi}_{(I-1,J)} = (a\rho U)_{(I-\frac{1}{2})} (\zeta_{(I-\frac{1}{2})}) \qquad \text{etc.}$$

and

$$\sum A^{\Phi}_{(I,J)} = A^{\Phi}_{(I+1,J)} + A^{\Phi}_{(I-1,J)} + A^{\Phi}_{(I,J+1)} + A^{\Phi}_{(I,J-1)} + A^{\Phi}_{(I,J,u)} + A^{\Phi}_{(I,J,d)}$$

The finite difference equation for neighbouring control volumes are kept implicitly connected by taking $\Phi_{(I+1,J)}$ etc. in the right hand side of (3.16) as equal to $\Phi_{(I+1,J,d)}$ etc..

3.3.4 Finite Difference Equation for Velocity Components and SIMPLE Algorithm

Assembled finite difference equation for velocity compontnts U_θ, U_r, U_z can be obtained by replacing Φ in (3.14) by these respective components. Here the pressure gradient terms will appear as part or whole of C^{U_i} terms. Due to the shifted control volume layout,

$$C^{U_\theta} \sim -\left(p_{(I,J)} - p_{(I-1,J)} \right) \Delta X_J \, \Delta X_K$$

$$C^{U_r} \sim -\left(p_{(I,J)} - p_{(I,J-1)} \right) \Delta X_I \, \Delta X_K$$

$$C^{U_z} \sim -\left(p_{(I,J,d)} - p_{(I,J,u)} \right) \Delta X_I \, \Delta X_J \qquad (3.17)$$

As given in equation (3.8), the gradients of turbulent stresses appearing in U_i equation can too be expressed as a source term. The C^{U_i} may contain a part or whole of that as well. Assuming that those stress terms are known, there still remains the pressure field to be found separately.

In the SIMPLE algorithm of PATANKAR and SPALDING [57], the continuity equation is consulted in order to guess the correct pressure field. The supposition is made that the velocity component is a linear function of the pressure gradient in that direction. Thus

$$U_z = U_z^* + \frac{\partial U_z}{\partial(\Delta p^*)} \left(\Delta p^* \right)' \qquad \text{etc.} \qquad (3.18)$$

where U_z^* is the velocity component in the direction z corresponding to the pressure difference field Δp^*, and $(\Delta p^*)'$ an increment in (Δp^*) which will produce a new value U_z. On examining (3.16) and (3.17) it can be seen that,

$$\frac{\partial U_z}{\partial(\Delta p^*)} = -\frac{\Delta X_I \, \Delta X_J}{\left(A^{U_z}_{(I,J)} - b^{U_z}_{(I,J)} \right)} \quad \text{etc..} \qquad (3.19)$$

Suppose the corrected velocity field U_θ, U_r and U_z in (3.18) satisfies the continuity equation, then it can be shown that the increment in pressure at the point (I,J), necessary to cause this effect, is governed by the equation

$$\begin{aligned} A^p_{(I,J)}\, p'_{(I,J)} = {} & A^p_{(I+1,J)}\, p'_{(I+1,J)} + A^p_{(I-1,J)}\, p'_{(I-1,J)} \\ & + A^p_{(I,J+1)}\, p'_{(I,J+1)} + A^p_{(I,J-1)}\, p'_{(I,J-1)} \\ & + A^p_{(I,J,u)}\, p'_{(I,J,u)} + A^p_{(I,J,d)}\, p'_{(I,J,d)} \\ & + m^*_{(I,J)} \end{aligned} \tag{3.20}$$

where

$$A^p_{(I+1,J)} = \rho_{(I+\frac{1}{2})} \left(\frac{\partial U_\theta}{\partial(\Delta p^*)} \right)_{(I+\frac{1}{2})} (\Delta X_J \, \Delta X_K)$$

and

$$\begin{aligned} m^*_{(I,J)} = \Big(& (\rho U^*_\theta)_{(I+\frac{1}{2},J)} (\Delta X_J \, \Delta X_K)_{(I+\frac{1}{2})} \\ & + (\rho U^*_\theta)_{(I-\frac{1}{2},J)} (\Delta X_J \, \Delta X_K)_{(I-\frac{1}{2})} \\ & + (\rho U^*_r)_{(I,J+\frac{1}{2})} (\Delta X_I \, \Delta X_K)_{(J+\frac{1}{2})} \\ & + (\rho U^*_r)_{(I,J-\frac{1}{2})} (\Delta X_I \, \Delta X_K)_{(J-\frac{1}{2})} \\ & + (\rho U^*_z)_{(I,J,d)} (\Delta X_I \, \Delta X_J)_{(K,d)} \\ & + (\rho U^*_z)_{(I,J,u)} (\Delta X_I \, \Delta X_J)_{(K,u)} \Big) \; . \end{aligned}$$

$m^*_{(I,J)}$ is the net imbalance for the control volume (I,J) as evaluated by the U^*_θ, U^*_r, U^*_z flow field which resulted from the solution of the finite difference momentum equations.

The pressure correction equation (3.20) is fully elliptic in character, $A^{p}_{(I,J,d)}$ being non zero. Thus an iterative procedure, which will require a larger computational capability is needed for its solution. If there is a means of correctly guessing the variations in the pressure field in z-direction (so that $p'_{(I,J,d)} = 0$), the pressure correction equation too can be treated as parabolic in the direction-z.

In the shear layers the mean momentum equation in the lateral direction can be written as

$$0 = -\frac{1}{\rho}\frac{\partial p}{\partial r} + F_r \quad . \tag{3.21}$$

So, in the absence of body forces F_r in r-direction, the pressure gradient in z-direction is given by

$$\left(\frac{dp}{dz}\right) = \left(\frac{dp}{dz}\right)_{\infty} . \tag{3.21a}$$

As a boundary condition the right hand side of (3.21a) in known. Therefore correct pressure gradient can be incorporated in the U_z equation, so that the pressure correction $p'_{(I,J,d)}$ is zero. This makes the equation (3.20) parabolic in z-direction for thin shear layers.

For confined flows, the prior knowledge of the total mass flow rate enables one to estimate the error in the assumed streamwise pressure gradient. Linearising the z-direction momentum equation with respect to the pressure gradient $\frac{dp}{dz}$, one obtains,

$$\left(A^{U_z}_{(I,J)} - b^{U_z}_{(I,J)} \right) U_{z(I,J)} = A^{U_z}_{(I+1,J)} U_{z(I+1,J)} + \cdots - \frac{dp}{dz} (\Delta X_1 \Delta X_2 \Delta z) \quad . \tag{3.22}$$

Usually $b^{U_z}_{(I,J)}$ is zero, giving

$$U_{z_{(I,J)}} = -\frac{dp}{dz}\frac{\Delta X_1 \Delta X_2 \Delta z}{A^{U_z}_{(I,J)}} + constant_1 \quad . \tag{3.23}$$

Thus the mass flow rate across the control volume at (I,J), in z-direction is

$$m_z = \rho_{(I,J)}\, U_{z_{(I,J)}}\, \Delta X_1\, \Delta X_2$$

$$= -\left(\frac{dp}{dz}\right)\frac{\Delta X_1 \Delta X_2 \Delta z \Delta X_1 \Delta X_2}{A^{U_z}_{(I,J)}} + constant_2$$

giving

$$\frac{\partial m_z}{\partial\left(\frac{dp}{dz}\right)} = -\frac{\Delta X_1 \Delta X_2 \Delta z \Delta X_1 \Delta X_2}{A^{U_z}_{(I,J)}} \quad . \tag{3.24}$$

Now,

$$m_{z_{(I,J)}} = m^*_{z_{(I,J)}} + \frac{\partial m^*_{z_{(I,J)}}}{\partial\left(\frac{dp}{dz}\right)^*}\,\Delta\left(\frac{dp}{dz}\right) \tag{3.25}$$

where $m^*_{z_{(I,J)}}$ correspond to the pressure gradient $\left(\frac{dp}{dz}\right)^*$. Now summing up equation (3.25) over the whole cross-stream plane.

$$\sum m_{z_{(I,J)}} = \sum m^*_{z_{(I,J)}} + \Delta\left(\frac{dp}{dz}\right)\sum \frac{\partial m^*_{z_{(I,J)}}}{\partial\left(\frac{dp}{dz}\right)^*}$$

therefore

$$\Delta\left(\frac{dp}{dz}\right) = \frac{\sum m_{z_{(I,J)}} - \sum m^*_{z_{(I,J)}}}{\sum\left(-\frac{\Delta X_1 \Delta X_2 \Delta z \Delta X_1 \Delta X_2}{A^{U_z}_{(I,J)}}\right)} \tag{3.26}$$

giving

$$\left(\frac{dp}{dz}\right)_{corrected} = \left(\frac{dp}{dz}\right)^* + \Delta\left(\frac{dp}{dz}\right) \tag{3.27}$$

Equation (3.25) and (3.27) form a consistent set of corrections to the U_z component and pressure gradient fields. The corrected $U_z$field from (3.25) will satisfy continuity exactly and $\left(\frac{dp}{dz}\right)_{corrected}$ from (3.27) will be a good assumption for the next calculation step in the z-direction.

3.3.5 The Case of Axi-Symmetric (or Plane- Symmetric) confined Flow

In the previous subsection it was seen that it is possible to obtain a U_z-velocity field (equation (3.25)) which satisfies the overall mass conservation requirement. In a symmetric flow there will be no transverse gradients of any of the variables. Thus, consideration of individual control volume mass-balance with the knowledge of U_z-fields in consecutive z-planes will give expressions for velocities in the lateral direction, (see Fig. (3.4)) such as

$$0 = (a\rho U_z)_{(I,J,d)} - (a\rho U_z)_{(I,J,d)} + (a\rho U_r)_{(I,J-\frac{1}{2})} - (a\rho U_r)_{(I,J+\frac{1}{2})} \quad . \tag{3.28}$$

At the symmetric boundary, however, the U_r velocity is zero. Therefore, the equation (3.28) can be successively applied in control volumes away from the axis to obtain the complete lateral velocity field.

Thus, in the case of two-dimensional confined flows, the solution of finite difference equations for the lateral velocity U_r and that for the pressure-correction p' is unnecessary.

3.4 An Ideal Grid

The numerical procedure is employed to calculate, in the order of importance, the mean variables U_i and C, their respective fluxes $\overline{u_i u_j}$ and $\overline{u_j c}$, and other quantities e.g. ε etc.. The inevitable errors associated in using interpolation formulae in calculations can be minimised by choosing a grid system where the individual terms in all equations are calculable without extensive interpolations. In fact it is not possible to avoid interpolations entirely. The staggered grid system shown in Fig. (3.5) does allow one to obtain all terms (except the convective terms which require interpolations in any grid system) in the mean equations without interpolation. The variable locations for this grid system is given in Table (3.1).

In this arrangement, however, interpolations are required in calculating terms in all the turbulent equations. Now, in boundary layer flow situations, where, the gradients in main flow direction are much smaller than those in lateral directions, this grid system can be modified to advantage with little loss of accuracy.

Variable		Location
Pressure	p	I , J , K
Mean Velocity Components	U_θ	$I-\frac{1}{2}$, J , K
	U_r	I , $J-\frac{1}{2}$, K
	U_z	I , J , $K-\frac{1}{2}$
Shear Stresses	$\overline{u_r u_z}$	I , $J-\frac{1}{2}$, $K-\frac{1}{2}$
	$\overline{u_\theta u_z}$	$I-\frac{1}{2}$, J , $K-\frac{1}{2}$
	$\overline{u_\theta u_r}$	$I-\frac{1}{2}$, $J-\frac{1}{2}$, K
Mean Scalar	C	I , J , K
Scalar Fluxes	$\overline{u_\theta c}$	$I-\frac{1}{2}$, J , K
	$\overline{u_r c}$	I , $J-\frac{1}{2}$, K
	$\overline{u_z c}$	I , J , $K-\frac{1}{2}$
Normal Stress Components	$\overline{u_\theta^2}$	I , J , K
	$\overline{u_r^2}$	I , J , K
	$\overline{u_z^2}$	I , J , K
All Other Scalar Variables e.g. ε, k, $\overline{c^2}$		I , J , K

Table 3.1 Variable Lacations in an Ideal Grid

3.5 Staggered Grid Arrangement for (θ-r-z) Procedure for Three-and Two-Dimensional Scalar Transport in a Two-dimensional Hydrodynamic Field

All equations under consideration in the present investigation are parabolic in z-direction. This enables one to refrain from considering a grid system displaced in z-direction. In such a grid system the variables can be located as shown in Fig. (3.6). Here all variables are known in a given plane-u and the finite difference equation can be formulated to obtain new values for the variables at the downstream plane, d.

Further simplification to the grid system is now made by noting that only two-dimensional flow fields without a swirl component in velocity are treated. Consequently, U_θ, $\overline{u_\theta u_z}$, $\overline{u_\theta u_r}$ are all zero. Therefore all mean and turbulent flow variables can be located in a single $(r$-$z)$ plane.

In the present flow situation the gradients of the shear stress $\overline{u_r u_z}$ are the most important in the U_z equation. The streamwise gradients of normal stresses have only a secondary effect in the U_z equation (through their effect on $\overline{u_r u_z}$). Therefore the location of normal stress control volumes can be made so as to facilitate easier calculation of their source terms. Now it is obvious that, $(I,J-\frac{1}{2})$ point, where the non-zero shear stress $\overline{u_r u_z}$ is located, is the best place for the normal stresses to be located. At this point the major velocity gradient $\frac{\partial U_z}{\partial r}$ can be evaluated without interpolation. Further, the dissipation rate ε can also be evaluated at $(I,J-\frac{1}{2})$, so that the calculation of source terms in the ε equation as well as those containing ε in the stress equations can be made without interpolation.

The scalar field (temperature or concentration etc.) however, being three-dimensional, its important flux variables should be located as in the idealised grid. The streamwise scalar flux whose streamwise gradients

have only an indirect effect however, is located along with shear stress etc. so that calculation of its source terms becomes straight forward. The variable locations thus displaced to suit the present flow and scalar transport situation are shown in Fig. (3.7) (only non-zero variables are shown).

3.5.1 Staggered Grid Arrangement for (x-Ψ) procedure

Being a two-dimensional boundary layer precedure, the control volumes can be displaced only in direction-Ψ. It can be seen by reasoning similar to that of the previous subsection, that it is useful to shift the control volume for all turbulent quantities in the Ψ-direction by half a grid spacing. The derivation of the general finite difference equation in a shifted (x-Ψ) coordinate system is presented in Appendix (E).

3.6 Cell layout and Boundary Conditions

In both (x-Ψ) and (θ-r-z) numerical precedures cells are generally distributed in order to cover the full domain of interest and in particular, capable of giving closer attention to areas where important variations occur. Since the turbulence model described in Chapter (2) is valid only for high Reynolds number turbulence, it can not be applied in regions very close to the wall where the Reynolds number is small. Therefore limitations do apply in laying out the grid in near-wall regions.

In Fig. (3.8), a typical grid distribution in a near-wall region is presented. Here, A is the node nearest to the wall where mean variables (i.e.U_z and C) are evaluated. As a criterion the distance between the node A and the wall is chosen so that,

$$y_A^+ > 30 \quad .$$

Thus A lies outside of the viscous sublayer and the mean variables at A satisfies the logarithmic laws to be described in the next sub section. Since the lateral velocity gradients in the near-wall region varies inversely with the distance to the wall more grid points should be concentrated in this area. In order to achieve this a non-uniform grid distribution should be employed in the near-wall regions.

The method of applying boundary conditions in the (x-Ψ) procedure is given in [9]. The same method can be employed for the variables evaluated in a staggered grid as well.

In applying boundary conditions in the (θ-r-z) procedure, the false-source technique of GOSMAN and PUN [50] is employed (see Fig. (3.9)). Here, the flux of Φ implied by the boundary condition is first explicitly evaluated. Then this flux, $\dot{J}''$, is supplied to the control volume closest to the boundary in a linearised source form given in (3.15), and further, the finite difference coefficient which connects the boundary value Φ_b to the control volume value Φ is set to zero.

The flux through the boundary $\dot{J}''$ can be calculated with the knowledge of prevailing physical conditions. These are discussed in the following subsections.

3.6.1 Wall Boundary Condition

(a) Mean Velocity Equation

The total stress, τ_{tot}, opposing the turbulent flow of fluid parallel to a rigid wall is used in defining the friction velocity U_τ with

$$U_\tau = \left(\frac{\tau_{tot}}{\rho} \right)^{\frac{1}{2}} \tag{3.29}$$

This friction velocity is supposed to satisfy the logarithmic "law of the wall",

$$\frac{U_z}{U_\tau} = \frac{1}{\kappa} \ln \left(\frac{yU_\tau}{\nu} E \right) \tag{3.30}$$

where U_z is the velocity component parallel to the wall, at a distance y away from the wall. The von Kármán constant κ is taken as equal to 0.42 and the constant E is taken as 9.85. In the numerical precedures employed here, the friction velocity U_τ is evaluated from (3.30) and the corresponding total stress at the wall is enforced as the boundary condition.

(b) Mean Scalar Equation

Generally as a boundary condition, the wall scalar flux, $\dot{q}''$ or the wall value of the scalar itself C_{wall} is known. In either case it is the wall scalar flux that is enforced as the boundary condition for the scalar equation. When C_{wall} is known, the implied total scalar flux through the wall is calculated

using the logarithmic law for scalar i.e.

$$\frac{C_{wall} - C}{C_\tau} = \frac{1}{\kappa_c} \ln \left(\frac{yU_\tau}{\nu} E_c \right) . \tag{3.31}$$

Here C is the magnitude of the scalar at a distance y away from the wall. The constant κ_c is taken as 0.46, and the coefficient E_c, which is a function of molecular Prandtl (or Schmidt) number of the fluid, is chosen from equation (4.18) which represents a consensus of wall flow data. The total scalar flux through the wall

$$\dot{q}''_i = \rho c_p U_\tau C_\tau \tag{3.32}$$

can now be calculated with U_τ and C_τ obtained from (3.30) and (3.31) respectively.

(c) Shear Stress and Lateral Scalar Flux Equations

The control volume for $\overline{u_r u_z}$ (or $\overline{u_r c}$) closest to the wall is centered at B (see Fig. (3.8)). It is the diffusive flux of $\overline{u_r u_z}$ (or $\overline{u_r c}$) across the surface at A that is required as the boundary condition. Now in order to evaluate the diffusive flux across A, the value of $\overline{u_r u_z}$ (or $\overline{u_r c}$) at A needs to be known. This value is estimated with reference to the relevant mean equation. By integrating the mean momentum U_z equation between the limits $r = r_b$ (i.e. at A) and $r = R$ (i.e. at the wall) one obtains

$$\left(r \, \overline{u_r u_z} \right)_{r=r_b} = - \left(U_z \frac{\partial U_z}{\partial z} + U_r \frac{\partial U_z}{\partial r} + \frac{1}{\rho} \frac{\partial p}{\partial z} \right) \int_{r_b}^{R} r \, dr$$

$$+ \left(r \, \nu \frac{\partial U_z}{\partial r} \right)_{r=R} - \left(r \, \nu \frac{\partial U_z}{\partial r} \right)_{r=r_b} \tag{3.33}$$

where

$$\left[r \, \nu \frac{\partial U_z}{\partial r} \right]_{r=R} = \tau_{tot} = - R \, U_\tau^2 \, .$$

Similarly, the integration of the scalar equation yields,

$$\left[r \, \overline{u_r c} \right]_{r=r_b} = - \left[U_z \frac{\partial C}{\partial z} + U_r \frac{\partial C}{\partial r} \right] \int_{r_b}^{R} r \, dr$$

$$+ \left[r \frac{\Gamma}{\rho c_p} \frac{\partial C}{\partial r} \right]_{r=R} - \left[r \frac{\Gamma}{\rho c_p} \frac{\partial C}{\partial r} \right]_{r=r_b} \qquad (3.34)$$

where

$$\left[r \, \Gamma \frac{\partial C}{\partial r} \right]_{r=R} = \frac{R \, \dot{q}_i''}{\rho c_p} \, .$$

The right hand side of (3.33) and (3.34) can be explicitly evaluated. The diffusion coefficient in the equations for turbulence quantities are of the form,

$$constant \times \frac{k \, \overline{u_r^2}}{\varepsilon}$$

which increases linearly with y, in the local equilibrium region since $\varepsilon \propto y^{-1}$ and the stresses are constant. Thus the diffusion of $\overline{u_r u_z}$ and $\overline{u_r c}$ through the surface A (see Fig. (3.8)) can be written as

$$\text{flux of } \overline{u_r u_z} \text{ through } A = constant \left(\frac{k \, \overline{u_r^2}}{\varepsilon} \right)_B \frac{y_A}{y_B} \frac{(\overline{u_r u_z})_A - (\overline{u_r u_z})_B}{y_A - y_B}$$

and

$$\text{flux of } \overline{u_r c} \text{ through } A = constant \left(\frac{k \, \overline{u_r^2}}{\varepsilon} \right)_B \frac{y_A}{y_B} \frac{(\overline{u_r c})_A - (\overline{u_r c})_B}{y_A - y_B} \, . \qquad (3.35)$$

The value of the constant is determined from the diffusion model employed.

(d) All Other Turbulence Equations

In all other turbulence equations, expressions similar to (3.35) are employed in calculating the diffusion fluxes through the surface at A. For all normal stresses and remaining scalar fluxes, their magnitudes at A are taken as simply related to $\overline{u_r u_z}$ and $\overline{u_r c}$ values obtained by equations (3.33) and (3.34) respectively, constants of proportionality are obtained from consensus of near wall data, as discussed later in Section (4.6). The value of dissipation rate at A i.e. ε_A is chosen in order to get the diffusive flux as implied by the relation

$$\varepsilon = \left| \overline{u_r u_z} \frac{U_\tau}{\kappa y} \right| \tag{3.36}$$

3.6.2 Symmetry Axis (or Plane) Boundary Conditions

For all variables except the shear stress $\overline{u_r u_z}$ and the scalar flux $\overline{u_r c}$, the boundary condition at $r = 0$ is that of zero gradient, i.e. zero flux through the boundary. The values of $\overline{u_r u_z}$ and $\overline{u_r c}$ at $r = 0$ is in fact zero by definition. In the three-dimensional problems the θ-boundary condition too should be given. In a general problem a gradient of C in the θ-direction can be enforced by supplying the implied scalar flux. In the present investigation, however, two $(r\text{-}z)$ planes of symmetry could always be identified. In these cases the transverse scalar flux is zero at the boundary.

3.6.3 Free-Stream Boundary Condition

The $(\theta\text{-}r\text{-}z)$ procedure in its present form has a $(r\text{-}\theta)$ grid which is invariant in the z-direction. In flows with free boundaries, however, due to the spread of the layer, it is undesirable to employ such a grid

in calculation. For such flows it is useful to have a grid which expands, along with the flow, in the main flow direction. Therefore problems with one or two free stream boundaries are tackled by Patankar-Spalding procedure which has an expanding grid facility. (Problems with free stream boundary were successfully solved with slightly different $(\theta\text{-}r\text{-}z)$ procedure by SYED [16].) The free stream values of all variables can be evaluated with reference to their respective differential equation by assuming zero lateral gradients for all variables. This will yield equations of the form

$$U \frac{\partial \Phi}{\partial x} = S^{\Phi} \quad , \tag{3.37}$$

which can be rearranged to an explicit form as,

$$\Phi_d = \frac{S^{\Phi} \, \Delta X}{U} + \Phi_u \tag{3.38}$$

where Φ_d and Φ_u are the downstream and upstream values of Φ respectively. The value Φ_d obtained from (3.38) can be incorporated in the procedure as given in [9].

3.7 Treatment of Conducting Wall in the Numerical Procedure

Investigation of scalar diffusion in internal flows e.g. pipes, under laboratory conditions is common and practically very relevant. BLACK and SPARROW [13], QUARMBY and ANAND [59], CHAN et al. [60], and the present experimental investigation (see Chapter 5) considered three-dimensional scalar diffusion with a variety of wall boundary conditions. While the attainment of a perfectly impermeable wall in a mass transfer experiment presents no difficulties the same is not the case in a heat transfer study. Heat conduction in the pipe wall may significantly modify the idealized boundary conditions particularly when the heat source is applied externally (an arrangement that simplifies the experimental task). Though conduction effects can be minimized by correct choice of materials, in three-dimensional scalar transport investigations they can not completely be neglected. In making predictions of such cases it was thus necessary that the mean scalar transport equation (which is the only variable relevant in the wall scalar transfer) be solved in an area covering both the wall and the inside of tube.

Inclusion of a wall, with finite thickness, does not pose any additional problems in the numerical procedure, because the heat conduction is just a much simplified version of the convection equation. For generality, consider a tube heated by a flux $q_o''(\theta)$ through its outer surface (as in the present experimental investigation) and heated internally, by say an electric current (as in BLACK and SPARROW's [13] experiment) at the rate of $S^C_{(r,\theta)}$ per unit volume. Due to the circumferential conduction effects in the tube wall the heat flux through the inner wall can not be directly evaluated. The solution of the partial differential equation for C however require following additional relations,

(a) Total heat from outer surface = $q_o''(\theta)\ R_o \Delta\theta\ \Delta z$ (3.39)

(b) Generation of heat in wall control volumes

$$= S^C(r,\theta)\ r^2\ \Delta\theta\ \Delta z \tag{3.40}$$

and

(c) Total heat diffused from the tube to the fluid

$$= \dot{q}''_i\ (\theta)\ R_i\ \Delta\theta\ \Delta z \tag{3.41}$$

where

$$\dot{q}''_i\ (\theta) = \left[\Gamma_{wall} \frac{\partial C}{\partial r} \right]_{r=R_i} \tag{3.42}$$

and

$$\dot{q}''_i\ (\theta) = \frac{(C_b - C_A)\ \rho\ c_p\ U_\tau\ \kappa_c}{ln\ (\ y^+_A E_c\ )} \quad . \tag{3.43}$$

These relations of heat flow can be incorporated into the numerical procedure in the following manner. The equation (3.39) is the boundary condition applied to the outermost control volumes, E (see Fig. (3.10)). The heat generation (3.40) is included in the source form for all wall control volumes. The heat flow relations (3.41) - (3.43) can be incorporated implicitly by expressing them in the finite difference forms, i.e. (3.41) and (3.42) written as

$$Q_i = \Gamma_{wall} \frac{R_i\ \Delta\theta\ \Delta z}{\Delta r_{Db}} (\ C_D - C_b\ ) \tag{3.44}$$

$$= A^C_{(I,J-1)}\ (\ C_D - C_b\ ) \quad .$$

The relevant coefficient $A^C_{(I,J-1)}$ of the control volume at D can be modified as

$$A^C_{(I,J-1)} = \Gamma_{wall} \frac{R_i\ \Delta\theta\ \Delta z}{\Delta r_{Db}} \quad . \tag{3.45}$$

Similarly the coefficient $A^C_{(I,J+1)}$ of the control volume A, can be modified to read

$$A^C_{(I,J+1)} = \frac{\rho\ c_p\ U_\tau\ \kappa_c}{ln\ (\ y^+_A E_c\ )} R_i\ \Delta\theta\ \Delta z \quad . \tag{3.46}$$

In the present computational code, however, there is a grid node at b , having zero volume. Therefore its $A^{C}_{(I,J+1)}$ and $A^{C}_{(I,J-1)}$ coefficients should be adjusted so that they are equal to the right hand side of (3.45) and (3.46) respectively. This has the effect of solving (3.42) and (3.43) to obtain C_b.

CHAPTER 4

REVIEW OF EXPERIMENTAL DATA

4.1 Introduction

Accurate experimental data are essential for the development turbulence models. It is these which direct the initial modelling ideas; mathematics follow next. Again, since the turbulence models are not fully analytic, determination of any unknown coefficients can be done only with reference to experimental data. Then in order to check the validity and generality more and more accurate experimental findings are necessary.

Measurements of scalar fields are not as extensively available as those for hydrodynamic fields. Even among those available there are few which are relevant for this Thesis. Moreover, judgement have to be made in order to establish their reliability. An extensive review of free shear flow hydrodynamic data are given by RODI [61]. Here in this chapter, attempt is made to survey free shear flow and wall flow scalar field data in situations covered by this Thesis.

Section (4.2) identifies the kind of data which are useful to have in order to formulate and validate second-order closure models in scalar transport. The basic criteria for assessment of these data are presented next.

Characteristics of free shear flows, mainly with respect to self similarity, are presented in Section (4.3). The expressions for scalar flux in terms of mean scalar and local flow characteristics are obtained for the shear flows under consideration. This further enables one to obtain expressions of the eddy diffusivity ratio between momentum and scalar transport in terms of local characteristics. In Section (4.4) these relationships are used in checking the consistency of available data.

Characteristics and review of two-dimensional wall flows are presented in Section (4.5) - (4.6). This covers the hydrodynamic and scalar transport aspects of the flat plate boundary layer and the circular pipe. The discussion is centered around the logarithmic laws for mean velocity and mean scalar.

The three-dimensional scalar field data are discussed next. The different geometrical arrangements used by experimenters in obtaining three-dimensional scalar fields are given here. The comments made by them on the thermal or mass diffusivity, especially the anisotropy in the near wall region, are mentioned here.

4.2 Data Required and Criteria for Assessment

In order to understand the scalar transport problem in turbulent flows it is useful to have accurate information on the individual terms in both hydrodynamic and scalar equations. Focusing attention solely on the scalar transport equations, Table (4.1) sets out the quantities whose measurements are desirable for better understanding and guidance to the solution of the problem. They are categorised in their order of importance.

Mean scalar field measurements are the most important in understanding the flow situation. They are directly relevant in practical usage and reliability of these measurements is greater than for other quantities. In some flows the scalar flux field is directly expressible in terms of the main scalar field: Section (4.3). Hence these measurements can be used in checking the accuracy of the flux field measurements.

The second-order correlations i.e. the turbulent fluxes $\overline{u_i c}$ and scalar fluctuations $\overline{c^2}$ are very desirable to have, since it is these quantities that a second-order closure will solve for. Direct comparison of predicted correlations is possible only when accurate measurements of these quantities are available. The knowledge of other correlations are useful in modelling terms in the flux and scalar fluctuation equations.

Category	Mean Scalar	Second-Order Correlations				Other Correlations										
Quantity	C	$\overline{vc}$	$\overline{uc}$	$\overline{c^2}$	$\overline{wc}$	ε_c	$\overline{v^2c}$	$\overline{uvc}$	$\overline{vc^2}$	$\overline{vwc}$	$\overline{uwc}$	$\overline{wc^2}$	$\overline{w^2c}$	$\overline{p\frac{\partial c}{\partial y}}$	$\overline{p\frac{\partial c}{\partial x}}$	$\overline{p\frac{\partial c}{\partial z}}$
Equations in which they appear	C	**	*		**											
	**	$\overline{vc}$	*				*			*				*		
	**		$\overline{uc}$					*			*				*	
	**	**		$\overline{c^2}$		**			*			*				
	**				$\overline{wc}$					*			*			*
Remarks				†	In 3-D only					In 3-D only	In 3-D only	In 3-D only	In 3-D only			In 3-D only

† $\overline{c^2}$ interlinks with other equations only when buoyancy is present

Table 4.1 Data Required and Their Relative Importance

4.2.1. Criteria for Assessment of Data

Turbulence measurements of properties of the scalar field are rare in the literature. Often it is only the mean scalar field that is measured, sometimes scalar fluxes and scalar fluctuation correlation are reported and seldom any higher-order correlations. Thus the following criteria will be used mainly for the purpose of establishing credibility of data and understanding their applicability to the present investigation, and not necessarily for making any form of selection between them.

Criterion (a) Hydrodynamic field measurements, if reported, should have high credibility. In the case of free shear flows, reference is made to RODI [61] where an extensive review is given. In the absence of any analytical forms for the turbulent field, data will be assessed in the light of measurements by other workers.

Creterion (b) The mean scalar should be conserved.

NOTE: Most data in the literature are found in non-dimensional forms, often implying satisfaction of this criterion.

Criterion (c) The directly measured scalar flux field should agree with the corresponding fluxes obtained from mean scalar equations.

4.3 Characteristics of Free Shear Flows

4.3.1 Integral Forms of Mean Equations

The general behaviour of a free shear flow depends primarily on the total excess or deficit of momentum and that of scalar present in the layer relative to the external streams. Integrating the momentum equation (1.8) over the whole cross-section of the layer defined by boundaries I and E , for plane flows results in the following equation

$$\frac{\partial}{\partial x}\int_0^{y_E}\left[U\,(U - U_E) + \overline{u^2} - \overline{v^2}\right] dy + \frac{dU_E}{dx}\int_0^{y_E}(U - U_E)\,dy$$

$$+ \left[V\,(U - U_E)\right]_I^E = 0 \quad . \tag{4.1}$$

In symmetric flows I is the plane of symmetry; therefore the last term in (4.1) vanishes in those flows. In the present investigation only free shear flows in zero pressure gradient are considered. Hence equation (4.1) reduces to

$$\frac{\partial}{\partial x}\int_0^{y_E}\left[U\,(U - U_E) + \overline{u^2} - \overline{v^2}\right] dy - V_I\,(U_I - U_E) = 0 \quad . \tag{4.2}$$

Similarly, by integrating the mean scalar equation between boundaries I and E and applying the boundary condition that the external-stream value of the mean scalar, C_E , is constant,

$$\frac{\partial}{\partial x}\int_0^{y_E}\left[U\,(C - C_E) + \overline{uc}\right] dy - V_I\,(C_I - C_E) = 0 \tag{4.3}$$

The experimental data for the present investigation should satisfy equations (4.2) and (4.3).

In fully turbulent flow there exists a region of flow over which the direct action of viscosity on the mean flow is negligible. Within this region the mean and turbulent motion are determined by the boundary conditions alone. So that all terms in the mean and turbulent equations vary at the same rate in the streamwise direction. Sometimes there are features in a flow which prevent the occurence of a self similar form or allowing only an asymptotic self preserving form. In order to find out the relevant form for a given flow condition equations (4.2) and (4.3) should be checked in that flow condition.

4.3.2 Definition of Self Similarity and Decay Laws

Definition of self similarity as given in TOWNSEND [62] is,

> "For a particular flow to be self preserving, it is necessary that the variation of any quantity over any plane, x = constant should be expressible non-dimensionally through suitable scales of length and velocity, δ and U_o , as a universal function of y/δ . The scales of length and velocity are functions of x only."

In order to cover the scalar transport problem this definition is extended by prescribing a mean scalar scale C_o which is a function of x only. It is often the maximum deficits in velocity and mean scalar at a given section that are used as characteristics of that section. As for characteristic length however, one can make a choice to suit the situation. In the present investigation the representative length scales are chosen so that they are easily comparable with available experimental data and that they are easily obtainable from numerical calculation. The Fig. (4.1) shows the characteristic lengths chosen. They are,

(a) For plane jet and plane wake,

δ = distance between centre line and $\frac{U_o}{2}$ plane.

(b) For plane mixing layer,

δ = distance between $0.1U_o$ and $0.9U_o$ planes .

Often in literature the scalar field measurements are presented with respect to another characteristic length δ_c , given by

(a) For plane jet and plane wake,

δ_c = distance between centre line and $\frac{C_o}{2}$ plane.

(b) For plane mixing layer,

δ_c = distance between $0.1C_o$ and $0.9C_o$ planes.

Here too δ_c is chosen as the characteristic length for the scalar field, noting that δ_c is directly proportional to δ in all flows.

The self similar forms of variable profiles in the cross-stream can now be expressed as

$$U = U_E + U_o f\{\eta\}$$
$$V = U_o g\{\eta\}$$
$$\overline{uv} = U_o^2 h\{\eta\}$$
$$\overline{u^2} - \overline{v^2} = U_o^2 q\{\eta\} \qquad \text{etc.}$$

and

$$C = C_E + C_o m\{\eta_c\}$$
$$\overline{vc} = U_o C_o n\{\eta_c\}$$
$$\overline{uc} = U_o C_o p\{\eta_c\} \qquad \text{etc..}$$

where functions f , g etc. are the non-dimensional variable profiles. For symmetric flows,

$$\eta = \frac{y}{\delta} \qquad \text{and} \qquad \eta_c = \frac{y}{\delta_c} \ . \tag{4.4}$$

For plane mixing layer,

$$\eta = \frac{(y - y_I)}{\delta} \qquad \text{and} \qquad \eta_c = \frac{(y - y_I)}{\delta_c} \ .$$

The conditions for exact self similarity can be obtained by substituting (4.4) into the mean momentum and mean scalar equations. They are:

$$\frac{d\delta}{dx} = constant$$

$$\frac{U_E}{U_O} = constant$$

$$\frac{\delta}{U_O}\frac{dU_O}{dx} = constant$$

$$\frac{d\delta_c}{dx} = constant$$

$$\frac{\delta_c}{C_O}\frac{dC_O}{dx} = constant \quad . \qquad (4.5)$$

The flows under consideration, if and when self similar, should satisfy equation (4.5). Of the three flow situations under consideration experimental data (see Section (4.4)) suggest that the plane jet and the plane mixing layer satisfy (4.5). The plane wake does not satisfy $\frac{U_E}{U_O} = constant$, exactly, but found to achieve an approximately self similar form when $\frac{U_E}{U_O} >> 1$.

Table (4.2) gives the decay laws which can be derived from equation (4.5). To be exact, the power laws given in Table (4.2) should have $(X + X_O)$ as the basis, where X_O is the virtual origin of the flow This origin is found to depend on the exact conditions of flow generation and is generally estimated by back extrapolating data at known x-locations.

Flow	U_E	δ	U_o	C_o	δ_c
Plane Jet	0	$\propto x$	$\propto x^{-\frac{1}{2}}$	$\propto x^{-\frac{1}{2}}$	$\propto x$
Plane Mixing Layer	0	$\propto x$	*constant*	*constant*	$\propto x$
	constant	$\propto x$	*constant*	*constant*	$\propto x$
Plane Wake	$\frac{U_E}{U_o} >> 1$	$\propto x^{\frac{1}{2}}$	$\propto x^{-\frac{1}{2}}$	$\propto x^{-\frac{1}{2}}$	$\propto x^{\frac{1}{2}}$

Table 4.2 Decay Laws

4.3.3 Expressions for Shear Stress and Scalar Flux for Self Similar Flows

The shear stress and scalar flux at the free edge is zero and at a plane of symmetry they change sign. Hence shear stress or scalar flux at any point in the layer can be calculated by integrating their respective mean equations. The expressions thus obtained are tabulated in (4.3). The shear stress relations were taken from RODI [63].

The expressions for scalar fluxes can readily be transformed to incorporate the characteristic length of the scalar field δ_c and its associated parameter η_c where

$$\delta_c \, \eta_c = \delta\eta \tag{4.6}$$

Flow	Shear Stress Relation (RODI [63])	Scalar Flux Relation (Present Work)
Plane Jet $U_E = 0$	$h = \frac{d\delta}{dx}\left(\frac{1}{2} f \int_0^\eta f \, d\eta + \eta q \right)$ (4.6)	$n = \frac{d\delta}{dx}\left(\frac{1}{2} m \int_0^\eta f \, d\eta + \eta p \right)$ (4.7)
Plane Mixing Layer $\frac{U_E}{U_I} = \lambda$	$h = \frac{d\delta}{dx}\left(\left(\frac{\lambda}{1-\lambda} \right)\left(\eta f - \int_0^\eta f \, d\eta \right) - \int_0^\eta f^2 \, d\eta - (f - 1) \left(\left(\frac{\lambda}{1-\lambda} \right) \int_0^\eta f \, d\eta + \int_0^\eta f^2 \, d\eta + \int_0^\eta q \, d\eta \right) + m \int_0^\eta f \, d\eta - \int_0^\eta q \, d\eta + (\eta + \eta_I) q \right)$ (4.8)	$n = \frac{d\delta}{dx}\left(\left(\frac{\lambda}{1-\lambda} \right)\left(\eta m - \int_0^\eta m \, d\eta \right) - \int_0^\eta fm \, d\eta - (m - 1) \left(\left(\frac{\lambda}{1-\lambda} \right) \int_0^\eta m \, d\eta + \int_0^\eta fm \, d\eta + \int_0^\eta p \, d\eta \right) + m \int_0^\eta f \, d\eta - \int_0^\eta p \, d\eta + (\eta + \eta_I) p \right)$ (4.9)
Plane Wake $\frac{U_E}{U_O} >> 1$	$h = \frac{U_E}{2 U_O} \frac{d\delta^2}{dx} \eta f$ (4.10)	$n = \frac{U_E}{2 U_O} \frac{d\delta^2}{dx} \eta m$ (4.11)

Table 4.3 Self Similar Shear Stress and Scalar Flux Relations

4.4 Review of Data for Free Shear Flows

In this section scalar transport data for free shear flows are discussed. The analytical, self similar scalar flux relations derived in the previous section are used here to calculate the shear stress and flux profiles implied by the mean equations. They are compared with measured profiles of $\overline{uv}$ and $\overline{vc}$.

4.4.1 Plane Jet

Table (4.4) shows important flow parameters for some scalar measurements of plane jet. NEWMAN's [64] review suggest a value of 0.11 for the rate of spread $\frac{d\delta}{dx}$ of plane jets. RODI's [61] review show values ranging from 0.102 to 0.11 for the same. Rodi's recommended target velocity profile of a plane jet is that of ROBINS [65] and it has a spreading rate of 0.103. In passively heated jets the value given in DAVIES et al. [66] comes closest to the above. Jet of VAN DER HEGGE ZIJNEN [67] can not possibly be considered passive because of its high temperature difference.

Unfortunately there are no measured cross-stream scalar flux data available for comparison here. The maximas of calculated $\overline{vc}$ profiles show good agreement with each other. The ratio of the spreading rate of scalar field to that of velocity field has a value of 1.40 to 1.46 in all cases except that of Davies et al., JENKINS and GOLDSCHMIDT [68] quote values of 1.41 and 1.40 for this ratio from experiments of REICHARDT [69] and SINGH and UBEROI [70]. The spreading rate ratio found by Davies et al. is even smaller than the value 1.25 generally quoted for round jets. This may imply that the low aspect ratio of 6 in Davies et al.'s experiment is not sufficient to give a fully plane symmetric jet.

Davies et al. made conditionally sampled measurements of mean velocity and temperature fields and found that turbulent fractions of these fields spread at more or less similar rates, 0.155 and 0.140. They

Experimenter	Geometry	Flow Range	Reported Variables; Technique	$\frac{d\delta}{dx}$	$\frac{d\delta_c}{dx}$	$\frac{\overline{vc}_m}{U_o C_o}$ meas.	$\frac{\overline{vc}_m}{U_o C_o}$ calc. †	$\frac{(\overline{c^2})^{\frac{1}{2}}_m}{\Delta C}$
VAN DER HEGGE ZIJNEN [67]	D = 0.5cm L = 10 cm and D = 1 cm L = 25 cm	ΔC_{jet} = 107°C	U , C , hot-wire anemometer	0.096	0.141		0.0295	
JENKINS and GOLDSCHMIDT [68]	D = 1.27cm L = 30.4cm	$Re = 1.43 \times 10^4$ ΔC_{jet} = a) 1.11°C b) 20.7°C c) 35.0°C	U , C , pitot-static tube and hot wire anemometer	a) 0.088 b) 0.091 c) 0.096	a) 0.123 b) 0.128 c) 0.137		0.0273	
DAVIES et al. [66]	D = 5.1 cm L = 30.5cm	$Re \simeq 4.6\times10^4$ ΔC_{jet} 14.6°C $\frac{x}{\delta} = 10 \rightarrow 25$	U , $\overline{u^2}$, C , $\overline{c^2}$, hot wire anemometer	0.109	0.125		0.0271	0.18

† see Table (4.3)

Table 4.4 Scalar Measurements in Plane Jets

0 0 0 4 9 9 0 -139-4 7

concluded that the spread of the heated turbulent jet is better represented by a variable associated uniquely with the turbulent fluid and chose the half intermittancy point of U and C fields for comparison. The variation in U and C fields were coincidental. LAUNDER [71] reports that conditionally sampled measurements of JENKINS and GOLDSCHMIDT [68] indicate that for turbulent fluid in plane jet a Prandtl number of 0.40 , virtualy uniform across the jet. This is much lower than the implied value of 0.80 in the experiments of Davies et al..

Thus it seems that there is considerable disagreement between experiments as regards to the relative spreading rates of scalar and velocity fields. Since a value of 1.40 - 1.46 from unconditional (conventional) measurements seem more consistent, that value is chosen as the representative one suitable for comparison with numerical predictions.

As for the hydrodynamic field, on the recommendation of RODI [61], ROBINS' [65] velocity profile and BRADBURY's [72] turbulent stresses are considered for comparison with numerical predictions.

4.4.2 Plane Mixing Layer

Table (4.5) lists the experimental conditions and some important flow parameters of scalar field measurements found in literature.

RODI [61] pointed out that the agreement in the spreading rates of the mixing layers he considered with given velocity ratio is rather poor. WATT's [73] velocity field spreading rate lies along the average value for that velocity ratio whereas SUNYACH and MATHIEU's [74] spreading rate is slightly higher than the average level for $\frac{U_E}{U_I} = 0$.

The spreading rates of the scalar field again depends on the ratio between the free stream velocities. The overall Prandtl number of the flow is inversely proportional to the ratios of the squares of spreading rates. Thus Watt's data imply an overall Prandtl number of 0.78 whereas Sunyach and Mathieu's data imply a Prandtl number of 0.5 .

Experimenter	Flow Conditions	Reported Variables and Technique used	$\frac{d\delta}{dx}$	$\frac{d\delta_c}{dx}$	meas. $\frac{\overline{uv}_m}{U_o^2}$	calc. $\frac{\overline{uv}_m}{U_o^2}$	meas. $\frac{\overline{vc}_m}{U_oC_o}$	calc. $\frac{\overline{vc}_m}{U_oC_o}$	$\frac{\sqrt{\overline{c^2}_m}}{C_o}$
WATT [73]	$\frac{U_E}{U_I} = 0.50$	U , $\overline{uv}$, $\overline{u^2}$, $\overline{v^2}$, $\overline{w^2}$, C ; $\overline{c^2}$,	0.045	0.051	.0091	.0105	†	.0120	0.112
SUNYACH and MATHIEU [74]	Half plane jet, 4cm × 4.8cm $\frac{U_E}{U_I} = 0$ $\frac{X}{D} = 1.0 \rightarrow 3.0$ $Re_{jet} = 5.25 \times 10^4$ $\Delta T = 54^oc$	U , $\overline{uv}$, $\overline{u^2}$, $\overline{v^2}$, $\overline{w^2}$, C , $\overline{c^2}$,	0.18	0.249	.0140	.0132		.0203	0.135
FIEDLER [75]	Half plane jet, $\Delta T = 26^oc$	C , $\overline{c^2}$,							0.210
BROWN and ROSHKO [76]	$\frac{\rho_I}{\rho_E} = \frac{1}{7}$, 1 and 7 $\frac{U_I}{U_E} = \sqrt{7}$ and 7	U , ρ , Pilot + hot wire							

† normalised with respect to maximum value

Table 4.5 Scalar Measurements in Plane Mixing Layers

Again there are no reported heat flux profiles in plane mixing layer found in the literature. Watt has given a heat flux profile normalised with respect to the value at the centre of the layer. The heat flux $\overline{vc}$ calculated from his profiles of correlation coefficient $\overline{vc}/(\overline{v^2}\ \overline{c^2})^{\frac{1}{2}}$, $\overline{v^2}$ and $\overline{c^2}$ has a maximum of about $0.003U_oC_o$, which is only one quarter of what is implied form his temperature profiles. This raises serious doubts about the accuracy of other variable measurements.

The hydrodynamic field measurements of SUNYACH and MATHIEU [74] are not in good agreement with more consistent data of others (for e.g. BRADSHAW et al. [75]). The measured shear stress has a maximum which is about 40% higher than that of Bradshaw et al. and also the kinetic energy is about double that found in measurements reviewed by RODI [61]. This appears due to the flow being still not fully self similar in turbulent producing central region of the mixing layer.

The temperature fluctuation profiles of SUNYACH and MATHIEU [74] and those of FIEDLER [76] show remarkably similar uniform level over the central 50% of the layer. Fiedler pointed out that the corresponding mean temperature profiles has three inflection points and they in fact coincide with the two maximas and one minimum found near the mid regions of $\overline{c^2}$ profile.

BROWN and ROSHKO [77] studied mixing between different velocity streams with different densities. Mixtures of Nitrogen and Helium were employed to obtain density ratio up to 1:7 and measurements were made of mean velocity and density. In this case density can be treated as the scalar. Their deduced value of the turbulent Schmidt number was only 0.16 in the central regions of the mixing layer which is far lower than values reported for any other turbulent free shear flow.

For comparison with numerical predictions, Watt's data will be used for the case $\frac{U_E}{U_I} \neq 0$ and SUNYACH and MATHIEU [74] and WYGNANSKI and FIEDLER's [78] data for the case $\frac{U_E}{U_I} = 0$.

4.4.3 Plane Wake

Plane wake can become approximately self similar for large values of $\frac{U_E}{U_O}$. TOWNSEND [79] appears to be the first one to have conducted detailed measurements in heated and unheated wakes. His results indicate that both mean quantities as well as turbulent structure become nearly self preserving for $(X - X_O)/D > 500$, the former achieving similarity earlier than the latter. Experimental findings of others given in Table (4.6) indicate that self preserving region for the mean variables can start as early as $100D$.

RODI's [61] review recommend Townsend's measurements of the hydrodynamic field as the best in consistency. The spreading parameter for a plane wake,

$$S = \tfrac{1}{2} \frac{d}{dx} \left(\frac{U_E}{U_O} \delta \right) \tag{4.12}$$

in Townsend's case has a value 0.114,† and is 10-15% higher than other reported wake data. The spreading parameters of other measurement sets are in good agreement with data sets presented in Rodi's review.

The relative rate of spreads of scalar and velocity fields seem to be in reasonably good agreement with each other. In all cases, the implied overall Prandtl number, which is the inverse of the square of the relative rate of spreads, indicate values in the range 0.6 - 0.7 .

Although TOWNSEND's [79] lateral hear flux data have large scatter, agreement with level of flux implied by the mean temperature profile is reasonably good. The measured level of heat flux maximum in FREYMUTH and UBEROI's [80] data and that of FABRIS [81] are too small by 40% and 45%

---

† Rodi has obtained a value of 0.098 from Townsend's data and correspondingly his calculated value of non dimensional shear stress maximum is 0.051 . This is in good agreement with Townsend's measured $(\overline{uv}/v_O^2)_{max}$.

Experimenter	Flow Range; Geometry	Reported Variables; Technique	$\frac{U_o}{U_E}$	S	$\frac{\delta_c}{\delta}$	meas. $\frac{\overline{uv}_m}{U^2}$	calc. $\frac{\overline{uv}_m}{U^2}$	meas. $\frac{\overline{vc}_m}{U_oC_o}$	calc. $\frac{\overline{vc}_m}{U_oC_o}$	$\frac{(\overline{c^2})^{\frac{1}{2}}_m}{C_o}$
TOWNSEND [79]	Re = 1360 circular cylinder $\frac{X}{D}$ = 80 - 950	U, $\overline{uv}$, $\overline{u^2}$, $\overline{v^2}$, $\overline{w^2}$, C, $\overline{vc}$,	0.093 - 0.031	0.114	1.30	0.049	0.059	0.073-0.086	0.078	
FREYMUTH and UBEROI [80]	Re = 960 circular cylinder $\frac{X}{D}$ = 25 → 1140 $\frac{X_o}{D}$ = 40	U, C, $\overline{vc}$, $\overline{c^2}$, $\overline{vc^2}$, ε_c,	0.0344 at $\frac{X}{D}$ = 1140	0.0934	1.22			0.035	0.056	0.403
LA RUE and LIBBY [82]	Re = 2800 circular cylinder $\frac{X}{D}$ = 400, 500 $\frac{X_o}{D}$ = 40	C, $\overline{c^2}$,								
FABRIS [81]	Re = 2400 circular cylinder $\frac{X}{D}$ = 200, 400	U, V, C, $\overline{vc}$, $\overline{uc}$, $\overline{c^2}$, $\overline{vc^2}$, $\overline{uc^2}$, $\overline{uvc}$, $\overline{v^2c}$ Hot wire	0.057 at $\frac{X}{D}$ = 400	0.0958	1.26		0.050	0.034	0.061	0.351

Table 4.6 Scalar Measurements in Plane Wakes

respectively. The reason for such a large discrepancy is not clear, at least in FREYMUTH and UBEROI's [80] measurements it is not due to lack of self similarity because their final measuring station is 1140 diameters from the cylinder.

Fabris measured the streamwise heat flux $\overline{uc}$ and in the area of maximum lateral heat flux, the ratio $\frac{\overline{uc}}{\overline{vc}}$ is about 1.4 . At the plane of symmetry the value of $\overline{uc}$ is about half the maximum $\overline{uc}$.

The levels of temperature fluctuations in wakes reported here seem to agree resonably well with each other. LA RUE and LIBBY's [82] $\sqrt{\overline{c^2}}$ profile normalized with respect to the value at the axis coincide over most parts of the wake with profiles of Freymuth and Uberoi. The maximum value of $\sqrt{\overline{c^2}}$ is 40% higher than the value at the axis.

FREYMUTH and UBEROI's [80] measurements of temperature gradient fluctuations indicate local isotropy over the bulk of the wake. Although they have shown that the terms in temperature fluctuation equation are in balance, the overall accuracy may be rather suspect with the large discrepancy between measured and calculated heat flux profiles.

The measurements of heated wake behind a flat plate made by KOVASZNAY and ALI [83] show some effects of buoyancy. Even though their mean velocity and mean temperature profiles are hardly affected, the shear stress and heat flux profiles across the wake show considerable asymmetry.

For comparison with numerical predictions, TOWNSEND's [62], [79] data will be used. The data of others too will be presented for further comparison.

4.5 Characteristics of Flows Affected by Walls

In flows which are affected by one or more walls, there exist thin layers adjacent to the walls where the viscous stresses are more significant than turbulent stresses. The principle of Reynolds number similarity can only be applied to the fully turbulent region where these viscous effects are negligible. The similarity and dimensional arguments show that (see for example TOWNSEND [62], page 200), in the region of overlap between this viscous layer and the fully turbulent region, the mean velocity takes a universal distribution of the form,

$$U = \frac{U_\tau}{\kappa} \ln \frac{U_\tau y}{\nu} + B \tag{4.13}$$

where

$$U_\tau = \frac{1}{\rho} \tau_{wall}^{\frac{1}{2}} \tag{4.14}$$

κ is the Von Kármán constant and has a value about 0.41 . (Different workers have obtained values between 0.35 and 0.43 from their experiments.) B too is constant and has a value equal to about 5 , again determined from experiments. This is probably the most extensively used expression in wall flows. It has limited validity in adverse pressure gradient flows, while in strong favourable pressure gradient flows considerable deviations occur.

Now, when the mean scalar equation is examined with the similarity and dimensional arguments parallel to previous considerations it can be seen (see for example KADER and YAGLOM [8]) that the mean scalar takes the form

$$(C_w - C) = \frac{C_\tau}{\kappa_c} \ln \frac{y U_\tau}{\nu} + B_c \{Pr\} \tag{4.15}$$

where C_w is the wall value of C , and C_τ is given by

$$C_\tau = \frac{\dot{q}''_w}{\rho \, c_p \, U_\tau} \tag{4.16}$$

$\dot{q}''_w$ is the total flux of C through the wall. Here again κ_c is a constant and B_c a function of the molecular Prandtl number of the fluid. The turbulent Prandtl number of the flow in the region where the above logarithmic laws are valid can be obtained as

$$Pr_t = \frac{\kappa}{\kappa_c} \quad . \tag{4.17}$$

4.5.1 Turbulent Prandtl Number in the Near Wall Logarithmic Region

In the absence of any analytical forms for the mean velocity and mean scalar profiles, the turbulent Prandtl number can be found with known Reynolds stress and scalar flux only. Like in free shear flows, the stress and flux profiles implied by the mean velocity and scalar profiles can be obtained by integration. A knowledge of streamwise variation of mean variables and the values of wall stress and flux are however needed for the integrations.

In the review paper by KESTIN and RICHARDSON [84], the Prandtl numbers were obtained by the above method. The numerical value of Pr_t close to the wall seems to lie in the region of 0.9 - 0.7 , however the dependence of Pr_t on the distance from the wall did not seem to follow any particular pattern. It is clear that if the mean velocity and passive scalar obey some universal logarithmic laws in the near wall region, then in that region the turbulent Prandtl number will come out to be a constant. KADER and YAGLOM [8] compiled heat and mass transfer data in boundary layer, circular pipe and channels and reploted them in semi-logarithmic coordinates in order to obtain Pr_t as from (4.17). Their findings clearly show that Pr_t in the logarithmic region is independent of the flow geometry and molecular Prandtl number of the fluid. Out of twenty one data sets only five were found to give Pr_t outside the range 0.8 - 0.9 . Also they

noted that the constant B_c in equation (4.15) is a strong function of the molecular Prandtl number. Some curvefit expressions for B_c are given in [8], for example

$$
\begin{aligned}
B_c\ (\ air\ ,\ Pr = 0.7\ ) &= 3.0 - 4.0 \\
B_c\ (\ water\ ,\ Pr \simeq 6.0\ ) &= 30.0 - 40.0 \\
B_c\ (\ mercury\ ,\ Pr \simeq 0.026\ ) &= -8.0 - -10.0\ ,
\end{aligned}
\tag{4.18}
$$

It is important to note here that a range of 0.8 - 0.9 for Pr_t is representative only in regions where both mean velocity and scalar satisfy respective logarithmic regions, if at all present, can be very thin and will depend on the main stream distance in both the streamwise and cross-stream directions.

Several workers have investigated the effect of molecular Prandtl number on the turbulent Prandtl number. QUARMBY and QUIRK's [11] pipe flow diffusion studies covering a Schmidt number range of 0.7 to 1200 show no detectable effect of Pr on Pr_t .

4.6 Review of Data for Wall Flows

In the external wall flows, the characteristic Reynolds number of the flow does not generally stay constant. Therefore evaluation of shear stresses and scalar fluxes from corresponding mean profiles is possible only if they are known at two or more streamwise locations. Since this evaluation can not be done very accurately using published mean velocity and scalar profiles, no attempt will be made to do so here.

For fully-developed internal flows analytical evaluation of shear stress and scalar flux for fully developed flows can easily be obtained from:

$$\rho \overline{uv} = \tau_w \left(\frac{r}{R} \right) + \mu \frac{\partial U}{\partial r} \tag{4.19}$$

and

$$\overline{vc} = - q_w \frac{R}{r} \frac{1}{\rho c_p} \frac{\int_0^R U r \, dr}{\int_0^R U r \, dr} + \frac{\Gamma}{\rho c_p} \frac{\partial C}{\partial r} \quad . \tag{4.20}$$

For the developing flows to which attention is given in this thesis, the scalar flux can be evaluated only if the streamwise development of mean scalar profile is fully documented. Here again no attempt will be made to calculate $\overline{vc}$ from previously reported C profiles.

4.6.1 Flat Plate Boundary Layer

As mentioned in Section (4.5.1) there are several investigations of turbulent heat transfer from flat plate boundary layers to be found in the literature. Extensive measurements of mean temperature fields with a variety of wall boundary conditions was reported by REYNOLDS et al. [85]. Following them measurements of turbulent scalar correlations started to appear. Table (4.7) gives some details of such available data for smooth

Experimenter	Boundary Condition	Re_δ	Reported Variables	Near- Wall Pr_t	$\overline{uc}$	$\frac{\overline{uc}}{\overline{vc}}$	$\overline{c^2}$	Remarks
JOHNSON [88] and [89]	step in wall temperature		U , $\overline{u^2}$, $\overline{v^2}$, $\overline{w^2}$, $\overline{uv}$, C , $\overline{uc}$, $\overline{vc}$, $\overline{c^2}$, $\overline{uv^2}$, $\overline{v^3}$, $\overline{vw^2}$, $\overline{vc^2}$,	1.0-1.1	$\frac{\overline{uc}_{max}}{U_o \Delta C_o}$ = 5.5×10^{-3}	3.0	$\frac{\overline{c^2}_{max}}{(\Delta C_o)^2}$ = 1.0×10^{-2}	Measurements made at only two locations
BLOM [10] see also [86]	step in wall temperature	$Re_{\delta,max}$ = 2870	U , $\overline{u^2}$, $\overline{uv}$, C , $\overline{c^2}$, $\overline{vc}$,	≃ 0.92				Several measuring locations
ANTONIA et al. [90]	step in wall heat flux	$Re_{\delta,0}$ = 3070	C , $\overline{c^2}$, $\overline{vc}$, $\overline{uc}$,	1.0-1.1	$\frac{\overline{uc}_{max}}{U_\tau C_\tau}$ = 2.1	$\left(\frac{\overline{uc}}{\overline{vc}}\right)_{max}$ = 2.1	$\frac{\overline{c^2}_{max}}{C_\tau^2}$ = 4.6	U profile not reported

Table 4.7 Scalar Measurements in Smooth Flat Plate Boundary Layers

wall boundary layers. Also the works of FULACHIER and his collegues (see for example [87]) have presented considerable amount of data for boundary layers with heat and mass transfer.

JOHNSON [88] presented a complete set of second order correlation data in a thin thermal boundary layer growing inside a thick velocity boundary layer. From measurements at two streamwise locations he could calculate the shear stress and heat flux profiles implied by mean profiles. Though his measured $\overline{uv}$ is about 30% less than the values implied by velocity profile, the measured heat flux $\overline{vc}$ is in good agreement with calculated $\overline{vc}$. Because of rather short heating length the temperature profie is probably not fully developed and the turbulent Prandtl number seems rather high at about 1.0 - 1.1 .

BLOM [10] made measurements effectively under similar conditions to that of JOHNSON [88]. However he concentrated on fewer variables over a larger heating length. Mean quantities were presented in semi-logarithmic scale. In the semi-logarithmic region the Pr_t had a value of about 0.92.

ANTONIA et al. [90] presented conditionally sampled measurements of scalar correlations in a thin thermal boundary layer created by a step in wall heat flux. They obtained a value of 0.41 for constant κ_c in equation (4.15), implying a Prandtl number of about 1.0 . Their wall heat flux calculated from the enthalpy integral equation was about 20% higher than the actual wall flux.

Johnson's value of 3.0 for the ratio of streamwise to lateral heat flux in the near wall region is higher than the values found by others. ANTONIA et al. [90] indicated $\frac{\overline{uc}}{\overline{vc}}$ of 2.1 similar to the value obtained in the rough surface boundary layer experiments of PIMENTA et al. [91]. As seen later this value is consistent with the near wall value of $\frac{\overline{uc}}{\overline{vc}}$ in pipe flows. The correlation coefficient of the streamwise heat flux obtained in Johnson's tests was about 0.75 near the wall and this value is the same as that obtained by Pimenta in his experiments.

For comparison with numerical predictions of heat transfer in the flat plate boundary layer, the data of ANTONIA et al. [90] is employed. They have reported measurements of mean and turbulent scalar variables for several locations along the plate and prediction of this development should be a testing task for the turbulence models.

4.6.2 Pipe Flow

Measured second order turbulent correlations of scalar fields in pipes are so few that some data sets with only mean flow measurements are considered here for comparison with numerical predictions.

The investigation of BREMHORST and BULLOCK's [92] and that of BOURKE and PULLING [93] are the only two known attempts at measuring second order scalar correlations in pipe flows. Both investigations were for fully developed thermal boundary layer inside a pipe. The first presented the mean scalar C , $\overline{c^2}$, $\overline{u^2}$ and $\overline{uc}$ whereas Bourke and Pulling reported radial heat flux, $\overline{c^2}$, C and U . Bourke and Pullings measurements were confined to the inner 70% radius of the pipe and hence its use as a guide for numerical solutions is limited. The non-dimensional streamwise scalar flux $\frac{\overline{uc}}{U_\tau C_\tau}$ reported in [90] has a value of about 2.1 in the near-wall region. This is the same as the values found in flat plate boundary layers. The normalised scalar fluctuations $\frac{\overline{c^2}}{C_\tau^2}$ has a near wall value of 2.5 in [92] whereas flat plate boundary layer investigation of ANTONIA et al. [90] indicated a value of about 4.6 .

Quarmby and his colleagues presented several non axi-symmetric scalar transfer measurements in pipes which are discussed in the following section. In order to suppliment these works QUARMBY and ANAND [94] presented axi-symmetric mass transfer measurements in fully developed pipe flow. Their experimental investigation was to make measurements of mean concentration at several axial locations downstream of two types of mass

sources. In the first type, Nitrous Oxide gas was made to diffuse through a permeable ring of 1.5 diameters length fitted to the wall of the pipe. The second mass source was a "point" source of Nitrous Oxide at the centre of the pipe so that it diffused towards the wall due to turbulent and viscous action. In all cases the passive scalar was conserved.

A rather suprising aspect of their investigation was that they could satisfactorily predict the concentration profiles at downstream locations by making an assumption of unity turbulent Schmidt number throughout the flow. In the description of the velocity profiles using a mixing length hypothesis, however, they used a von Kármán constant of 0.36, a rather low value. Further their expression for eddy diffusivity made by combining Van Driest expression and a Reichardt formulation is not consistent with the mean velocity profile except in the viscous sublayer. Thus their theoretical calculations, even with a very good final agreement with experiment can not be considered very useful. Moreover on reanalysing the data of [94], QUARMBY and QUIRK [11] found that indeed the variation of turbulent Schmidt number inside the pipe can best be fitted by

$$Pr_{t(z)}^{-1} = 1 + 400^{z-1} \tag{4.21}$$

where z is the non-dimensional radius. This is quite at variance with their previous assumption of unity Sc_t throughout the pipe.

4.7 Review of Data in Three-dimensional Scalar Transport

Several experiments have been reported in which the hydrodynamic field was a two-dimensional thin shear flow type and the scalar field was three-dimensional, although again, boundary layer type. Thus the scalar field had significant scalar fluxes in both directions normal to the mean velocity vector. The aim of these experiments was to find out the extent of anisotropy in the diffusivities of these fluxes. All experiments on this topic reported here were performed in circular pipes with a fully developed velocity field. The only measurements reported are the mean temperature or concentration and wall fluxes; no turbulent correlation measurements appear to have been reported yet. All authors chose to compare their results with theoretical expectations based on assumed diffusivity models.

Table (4.8) summarises the methods employed in order to create and measure the three-dimensional scalar fields. QUARMBY and ANAND's [59] case-b was for diffusion of nitrous oxide from a dimetric line source. In all other experiments the three-dimensional fields were created by circumferentially non-symmetric wall scalar fluxes.

Quarmby and his collegues chose to investigate three-dimensional scalar transfer from a short length (for example, 1½D in [59]) of non-zero wall scalar flux. This will create situations where the three-dimensionality of the scalar field is decreasing. Since the asymmetric scalar field at the end of the short section is not fully developed, the scalar transfer situation inside the pipe may be highly influenced by the transport effects. The experimental situation investigated by others [13], however were on situations where the three-dimensionality is maintained. Over large length of such boundary conditions fully developed three-dimensional scalar profiles can be expected to attain. Due to the limited facilities available the works of CHAN et al. [60] and indeed the present experimental investigation were focussed on wall properties only. Still they present challanging data for development of variation in Nusselt numbers.

Experimenter; Type of Scalar Transfer and Fluid	Scalar Input	Re_D	Range of C	Measurements Made and Techniques Used	Conclusions (made by the respective authors) on Diffusivity	Remarks
BLACK and SPARROW [13], also BLACK [95]; Heat transfer; air, $Pr = 0.7$	Self heating, long stainless steel tube with sinusoidal variation in thickness; giving sinusiodal heat flux along the circumference, period = 2π .	7500 - 58000	$\Delta C_{wall,max} < 70^{o}F$ $\Delta C_{bulk,max} = 43^{o}F$.	1) Outside wall temperature by Chromel-Alumel thermocouples. 2) Total power supply by ammeter × voltmeter. 3) Air flow by ASME orifice. 4) Air temperature by thermocouples as in (1).	Diffusivity ratio of 10 near wall decreasing to unity beyond $y^+ = 20$.	
QUARMBY and ANAND [59]; Mass transfer; nitrous oxide to air, $Sc = 0.77$.	a) Four porous segments in the wall, period = $\frac{\pi}{2}$ length ≃ 1½ Dia. width = $\pi/4$. b) Diametric line source, period = π .	20000 -120000		1) Concentration measurements in flow by infra-red gas analyser. 2) Total contaminent input by rotameter gauges. 3) Flow velocity by pilot tubes.	Diffusivity ratio i.e. Sc_t , unity through the flow domain	

Table 4.8 Three-Dimensional Scalar Experiments in Fully Developed Pipe Flows

(contd)

Experimenter; Type of Scalar Transfer and Fluid	Scalar Input	Re_D	Range of C	Measurements Made and Techniques Used	Conclusions (made by the respective authors) on Diffusivity	Remarks
QUARMBY and QUIRK [11]; a) Heat transfer; air, $Pr = 0.7$	Electrically heated stainless steel strip, period = 2π length $\simeq$ 3 Dia. width $\simeq \pi/16$.	10000-100000	Surface temperature up to 70°C.	1) Temperature by Chromel-Alumel thermocouple probe. 2) Flow of air by pilot tube.	Pr_t in radial direction is about 0.5 near wall varies smoothly to unity at the axis. Tangential diffusivity is larger than the radial diffusivity near wall. This ratio is unity over most other parts of the flow.	Large heat loss through the wall apparent in C profiles. Apparent effect of buoyancy in C profiles.
b) Mass transfer; nitrous oxide to air, $Sc = 0.77$.	Short porous slot in the wall, period = 2π length = ½ Dia. width $\simeq \pi/25$.	6000-170000		1) same as in [59].		
QUARMBY and QUIRK [96]; Mass transfer; brine to air, Sc = 760-1200	Porous segment in the wall period = π length = (not reported) width = $\pi/2$	5230 - 21780		1) Concentration measurement by electrical conductivity probe.	The high Schmidt number has no effect on diffusivity ratios.	

Table 4.8 Three-Dimensional Scalar Experiments in Fully Developed Pipe Flows

(contd)

Experimenter; Type of Scalar Transfer and fluid	Scalar Input	Re_D	Range of C	Measurements Made and Techniques Used	Conclusions (made by the respective authors) on Diffusivity	Remarks
CHAN et al. [60]; Heat transfer; water, $Pr \simeq 6.0$.	Stainless steel tube segmentally heated from outside heaters, period = 2π width = π .	10000–100000	ΔC_{bulk} $< 1^{o}C$.	1) Outside wall temperature by Chromel-Alumel thermocouples 2) Wall heat flux by microfoil sensors 3) Flow measurements by ASME orifice and by rotameter.		
Present experimental investigation; Heat transfer; air, $Pr = 0.7$	Glass tube segmentally heated from outside by an electrically conducting coating, period = 2π width = π .	20000–90000	$\Delta C_{wall,max}$ $= 10^{o}C$ ΔC_{bulk} $< 1^{o}C$.	1) Outside wall temperature by Chromel-Alumel thermocouples. 2) Total power input by ammeter × voltmeter. 3) Air flow by pilot tube.	see Chapter 7.	For details see Chapter 5.

Table 4.8 Three-Dimensional Scalar Experiments in Fully Developed Pipe Flows

0 0 0 5 4 9 0 - 155 - 5 6

One other aspect which is of interest is the shape of the wall flux profiles. In mass transfer experiments it is possible to create (or assume) rectangular wave shape wall fluxes whereas, in heat transfer experiments, due to circumferential conduction within the tube material the wall flux profiles display an S-shape variation. Thus profiles of the wall meterial and goemetry become important in the numerical predictions of these situations. In the present experiment (see Chapter 5) the three-dimensional heat transfer in a segmentally heated thin glass tube was investigated. Here the objective was to design a three-dimensional heat transfer situation where the circumferential variation of wall heat flux is close to a square wave profile.

CHAPTER 5

EXPERIMENTAL INVESTIGATION

5.1 Preliminary Considerations

5.1.1 Aim of the Experimental Investigation

The aim of this experimental investigation was to obtain data for the case of transversely non-symmetric heat transport situation in a wall-affected two-dimensional shear flow. Previous workers e.g. BLACK and SPARROW [13], QUARMBY and ANAND [59], have made measurements in non-symmetrical scalar situations in tubes. Flow in circular tubes has been used for these studies because of its wide practical application. Further, it is a convenient and a simple geometry to investigate under laboratory conditions. For this reason it was adopted as the geometry understudy in the present investigation.

In mass transfer experiments it is possible to establish boundary conditions of square-wave form in the circumferential direction. In heat transfer experiments due to circumferential conduction in the tube wall such a situation can not be exactly achieved. However, the present heat transfer experiments were designed to minimise the circumferential conduction in the tube wall. Thus the three-dimensionality of the scalar field obtained is far stronger than that of [13]. It was hoped that this will provide a rather stringent test for the turbulence model employed in numerical calculations. Further the present experiments were carried out at low temperature difference levels (maximum of 1.5^{o}K in bulk temperature rise) and hence can be assumed to be void of any significant property variation.

5.1.2 Facilities Available and the Level of Measurements

As the present investigation was mainly aimed at the theoretical and numerical aspects of the solution of three-dimensional scalar transport situations, only a short, limited period was available for the experimental investigation. At the time of this investigation, the laboratory facilities at the writer's disposal required the exploration be limited to the study of wall heat transfer characteristics for the case of non-symmetric heating of a circular tube. A regulated supply of water and compressed air was available for use as the fluid medium. Previously, CHAN et al. [60] had made investigations using these facilities. Their experimental investigation was conducted to determine the heat transfer characteristics of turbulent flow of water in a circular stainless steel tube with non-uniform boundary conditions.

5.1.3 Methods of Obtaining Circumferentially Non-Uniform Heating Rates

Circumferentially non-symmetric heating is common in practical engineering applications. Under laboratory conditions, however, one has the additional task of quantifying the non-uniformity i.e. one should be able to make measurements of heat fluxes and temperatures around the inner surface of the tube. As in the present investigation, if the measurements are to be made at the outer surface of the tube, then one would like to keep the temperature drop across the tube wall to a minimum. The methods of obtaining and making measurements of non-symmetrical heating, as adopted by previous workers, are the following:

(a) Heat generated by an electrically conducting tube having a non uniform thickness (as in BLACK and SPARROW's [13] experiment). Here the heat flux profile through the inner surface of the tube depends on the geometry of the tube, circumferential conduction

and the fluid heat transfer characteristics. As [13] points out, accurate construction of a tube with given non-uniformity in thickness is really a difficult task.

(b) A tube segmentally heated by an outside source as in CHAN et al. [60]. Here the outside source is placed at a given distance away from the tube. The uniformity of heat flux within the segment, however depends on the uniformity in the gap distance between the tube and the heater. Accurate and reliable measurement of the outer surface temperature of the tube is quite difficult, as found by [60], under these circumstances.

Recently GIESBRECHT [97] explored methods of achieving a constant heat flux boundary condition on long tube lengths. He considered methods of obtaining thin metallic film deposits on tubes. If the tube is of an electrically non-conducting material then the conducting film can be heated by supplying a voltage along its length. The uniformity of the heat flux in this case depends on the uniformity of the metallic film. Thin and uniform coatings of metallic substance can be obtained for example, by vacuum deposition, chemical deposition or by metallic painting. As for getting such deposit on long tubes, Giesbrecht pointed out that metallic painting is the most convenient. His investigation of heat transfer from a yawed cylinder to air with a constant heat flux wall boundary condition seems to indicate the reliability of the method of obtaining metallic film deposit on non conducting (electrically) cylinders. His results for cross-flow tests are in good agreement with previous experiments and his new data for yawed cylinder show excellent self consistency. In the present investigation this method is extended to obtain thin uniform metallic film segments on the tube. It can be expected to give square-wave profiles of heat flux to the cylinder.

5.1.4 Choice of Tube Material

When choosing the tube material for the present experiment, the following criteria were used.

(a) Once it was decided that the tube be heated at its outer surface by passing a current through the matallic film, the tube had to be made of electrically non-conducting material.

(b) A one-dimensional consideration of the heat flow in the circumferential direction shows that, the extent of circumferential conduction is proportional to $K_w \frac{t}{R}$, where K_w is the thermal conductivity of the tube material and t the thickness of the tube of mean radius R . So that, if circumferential conduction is to be minimised, the thickness of the chosen tube should be a minimum. The thermal conductivity should also be low to reduce the circumferential conduction

(c) Since the measurement of temperature is to be made at the outer surface of the tube, it would be best to have only a small temperature drop across the tube material. Again, one-dimensional consideration of the heat flow to the fluid shows that,

$$\frac{C_i - \overline{C}}{C_o - C_i} = 2 \frac{K_w}{K_f} \frac{1}{Nu} \frac{1}{ln\left(\frac{R_o}{R_i}\right)} \tag{5.1}$$

where K_w , K_f and Nu are the thermal conductivity of the wall material, that of the fluid and the Nusselt number (assumed constant) of the flow situation respectively. Here $\overline{C}$ is the bulk temperature and suffixes i and o stand for inner and outer surfaces respectively. Equation (5.1) suggests that for a given fluid flowing inside a thin tube at a given Reynolds number the temperature drop across the tube material is inversely proportional to $K_w \frac{R}{t}$. Thus, the thermal conductivity of the wall material should be as high as possible.

The first requirement rules out commonly used stainless steel tubing. Commonly available electrically insulating tube materials are glass, plastic and some synthetic compounds. The thermal conductivity of plastic and other synthetics depends of their composition; however, on average it is about one-fifth that of glass. Although it is possible to obtain rather thin synthetic tubing, consideration of the quantity $K_w \frac{R}{t}$ suggest that a glass tube of 1.92 cm diameter is more suitable than available plastic tubes of nominally similar size.

5.1.5 Choice of Fluid

The choice could be made between the laboratory supplies of air and water to suit the aims and limitations of the experiment. As one would like to minimise temperature drop across the tube wall, again, reference is made to equation (5.1) in deciding the fluid be used in this experiment. For a given Reynolds number, the heat transfer characteristics of a given fluid can be obtained empirically by using, for example the Petukhov-Pepov equation along with an expression for the friction factors (e.g. the Filinenko equation (see for example KARLEKAR and DESMOND [98] page 300)). At a Reynolds number of 20000, the equation (5.1) gives

for air,

$$\frac{C_w - \overline{C}}{C_o - C_i} = 11.75$$

and for water,

$$\frac{C_w - \overline{C}}{C_o - C_i} = 0.1695 \quad .$$

This shows that as far as the temperature drop across the tube wall is concerned air is seventy times better than water. Therefore in the present investigation air was selected as the working fluid.

5.2 Experimental Equipment

5.2.1 Design of the Tube

The glass tube used in the present investigation is a commonly available T6-type fluorescent tube with a nominal diameter of 3/4 in.. The inner and outer diameters of the tube are 1.715 cm and 1.920 cm respectivily. In preparing the tube for mettalic spraying the steps taken are the following;

(a) Carefully remove the aluminium caps and electrodes from an already used fluorescent tube. This was done in a suitably protected surrounding. Once one end is broken open, the tube is kept in a well ventilated place for a short period so that its gas can diffuse out.

(b) The two ends of the tube are now cut off using a glass cutting machine. The tube is then washed well so as to remove the phosphorous dust. The micrometer measurements of inner and outer diameters were made next. Then half an inch thick plexi-glass flanges were fitted to the two ends of the tube using a self drying adhesive.

(c) The spraying technique used here provides a satisfactorily uniform coating [97]. In the present werk, however, a method of obtaining two-segments of conducting strips has to be developed. After considering several methods, it was decided to stick two very thin (about 1 mm in width) strips of adhesive tape (sellotape) along the length of the tube spaced 180° apart (see Fig. (5.1)). In a tube of 1.92 cm outer diameter, each piece of tape covers roughly a 6° arc.

(d) The electroconducting paint used in the present investigation (as in GIESBRECHT [97]) is the "Flexible silver No. 16" manufactured by Englehard of New Jersey. This paint cures at room temperatures and can be thinned for spraying. The spraying was done on a lathe

bed where a precision spray gun was mounted to get a transverse motion at a constant speed. The spray paint was then applied in very thin coats on the rotating glass tube. The rotation speed was several times larger than the transversing speed. Several passes were made until the desired coating resistance was achieved. A period of about two minutes between the passes was allocated for the spray to dry out. A rough check on the resistance along the length of the sprayed section was made using an ohmmeter, this was used as the guide in deciding the total film to be applied.

Safety requirements (with regard to the lathe), made it necessary to spray the tube in two sections each about 30 - 40 D. One section was masked while the other was being sprayed. Our original intention was to get the tube sprayed over its whole length and then to supply a suitably adjusted electrical inputs to the two sections so as to get the same heat flux in both sections. The resistance measurements, to be discussed later, ruled out this possibility and only a length of 26.5 D was chosen as the heating length of the present work.

(e) Now, the two adhesive strips were carefully removed from the tube so as to get two segments of sprayed silver. The width of a segment can be considered as about 174° arc at the outer surface (see Fig. (5.2)).

(f) The initial testing of the tube for uniformity of the coating in the longitudinal direction was done at this stage. (described in Subsection (5.3.1)). The circumferential uniformity within a segment was not measured as there is no conveniently simple method of doing so.

(g) Four copper strips each of width 5 mm were clamped to the silver coated glass tube, two at each end of selected length, so that each segment of the coating made contact at its end with a given pair of strips (see Fig. (5.3)). This allowed the heating of the two silver segments independently.

5.2.2 Thermocouple Installation

The thermocouple installation was made with the aim of obtaining as much information as possible of the circumferential and longitudinal development of the temperature distribution of asymmetrically heated situations. Thermocouples were installed at five axial locations: 5 , 10 , 15 , 20 and 25 (internal) diameters from the start of the copper strip.

The thermocouple used in this installation were of 3 mil (0.003 in diameter) teflon covered Chromel-Constantan wire which is the most sensitive commonly used type suitable for low temperature measurements. The conversion factor as given by the manufacturers of these thermocouples is 0.060 mV/^{o}K . The wires were drawn from the same pair of spools to minimise any difference in quality between thermocouples.

At each axial location six thermocouples were installed, as shown in Fig. (5.4) spaced 36° apart. Since the silver coating was rather fragile, extreme care was taken in installing these thermocouples. The method adopted, was the following. First the thermocouples were placed on the adhesive side of a sellotape so that their beads just stuck out of the strip and the distance between the beads was equal to $\frac{\pi}{12} D_o$. Then another strip was placed on top of the former so that non-adhesive sides were at the outer sides. This strip was then carefully positioned on the glass tube without damaging the silver coating.

The cold junction was installed in front of the heating region and thus the thermocouples could be used in a differential manner. The potentiometer used had an accuracy of 0.02 mV and the thermocouple readings were in the range 0 - 1.0 mV . The thermocouple circuit is shown in Fig. (5.5).

5.2.3 Power Measurement

As the two segments were to be heated independently, the measurement of their power inputs were likewise made separately. The resistances of the segments were of the order of 1 ohm and, for the highest Reynolds number flow investigated (Re = 90000), the total power requirement was about 20 watts to get a bulk temperature rise of 1.0 - 1.5 ^{o}K . Thus the experiment could be conducted at very low voltages and currents. The electrical circuit simply consisted of a stepdown variac and an ammeter in series with each segment. This is schematicaly shown in Fig (5.6) . The ammeter used could be read to the nearest 0.05 amp . The voltage drop across each segment was measured using a digital voltmeter with an accuracy of ± 0.5% . With this system it was possible to adjust the variacs so as to obtain a predetermined total power input to a given segment.

5.2.4 Flow Measurement

The air supply to the experiment was from the laboratory compressed air unit. The regulator valve could be adjusted in order to get the required manomatric height which represent the difference between total and static heads as read by a Pitot tube. The Pitot tube was mounted at the end of the glass tube so that it was lacated on the tube axis. After passing through the regulator air enters a long stainless steel tube of nominally the same diameter as the glass tube. The length of the stainless steel tube is about 80 diameters. The glass tube is rigidly attached to this stainless steel tube and there is 35 diameters of glass tube length preceding the heated section. Thus it can be conveniently assumed that the air flow is fully developed by the time it reaches the heating section. For the range 0 - 8 cm (0 - 3 in) an inclined water manometer which could be read to the nearest 1/8 cm (0.05 in) was used. At Reynolds numbers of 40000 and 90000 a vertical

manometer which could be read to the nearest 1/4 cm (0.1 in) was used. In calculating the total flow rate it was assumed that the velocity on the axis was 1.20 times the average velocity.

5.3 Preliminary Measurements

5.3.1 Verification of Uniformity of the Silver Coating

The verification of the uniformity of the coating is a necessary step prior to any other measurement. This was done before installing the thermocouples. After segmenting the silver coating the tube was allowed to dry overnight and then the total resistances of the two segments were 5.8 ohm and 6.0 ohm . After considerable heat curing this resistances decreased to a steady level of about 1.5 ohm each.

In order to evaluate the uniformity of the coating the voltage drop along the tube was measured at 2 cm intervals. Over a length of 45 diameters, the root mean square deviation was 9.6% . This unsatisfactorily large value was due to a small section in the tube (between l = 28 D and 32 D) which had large irregularities. It was decided at this point that the glass tube be heated only in the first 26½ D length where the root mean square deviation was less than 5% . The resistances of the segments for a length of 26½ D were,

(a) for top half, Resistance = 0.99 - 1.00 ohm

(b) for bottom half, Resistance = 0.91 - 0.92 ohm .

The discrepancy between the resistances in top and bottom segments gives some indication of the level of non-uniformity in the circumferential direction. Even though the resistances were different, since the voltage supply to each segment could be adjusted so as to get the required volt-ampere (V × I) rate, the total heat production in each segment could be controlled as desired.

5.3.2 Uncertainties in Measurements

The largest uncertainity in this experiment concerns uniformity of the coating. The silver spraying was done in order to get best uniformity in the longtudinal direction. Since the tube was rotated at a higher circumferential speed as compared to the transverse speed of the spray gun it could be assumed that the circumferential uniformity was satisfactory as well. Initial measurements of resistance variation along the tube suggest that there could be variations upto 5% in longtudinal direction. This was considered satisfactory as GIESBRECHT [97] obtained considerable reproducibility in his experiment with similar variation in resistace of his tube. The circumferential variation of resistance could not however be exactly quantified. Ideally, one would expect a heat flux variation as shown in Fig. (5.7). In the region of the groove (where sellotape strip was removed), however, it is possible that the adhesion of the silver coating to the surface was weakened. Even though extreme care was taken while removing these tapes, it was found that there was minute damage to the paint. This would of course increase the local resistance and consequently the heat flux profile may look like that in Fig. (5.8). By heating both segments and observing the resultant circumferential temperature profile one could hope to quantify the modification to the circumferential heat-flux profile before studying the fully asymmetric situation.

There are some other uncertainties which can be considered to have only minor effect. They are

(a) Possible inequality in the size of the two segments; This can come about due to the difficulty in laying out the adhesive tape strips along the length of the pipe. Although it is easy to lay one strip along the length, it is not easy to position the other exactly 180° apart from the first. The error associated with this is about $\pm 2^{o}$.

(b) The voltage drop across the contacts to the silver coating; Since the silver coating was fragile it was not advisable to press the prong of the voltmeter on the coating. Thus the voltage drop across the length of the tube was measured as that between one copper strip and the other. The voltage drop across the copper strip is very small and hence neglected. The copper strip fits the shape of the tube and further it was hand painted with the flexible silver at the contacts. It is possible however that due to the stress in clamping, the contact is not uniform. This may cause a distorted voltage drop pattern. Its effect however is confined to areas very close to the contact points.

5.4 Experimental Results

Only the different conditions for which the tests were carried out are mentioned here. The wall temperature obtained in these tests are presented along with the numerical predictions of the same.

Heating Condition: Two heating conditions were investigated. In the first the voltage applied to each segment was adjusted to give equal volt-ampere inputs to the segments. If the gap between the segments was negligibly small, in a uniformly coated tube, this would be equivalent to a uniform heat flux boundary condition. All measurements were repeated several times over a period of about two hours until the readings showed complete steadiness. The other boundary condition used was that where only the top segment was heated. This condition creates a strongly three-dimensional temperature field.

Reynolds Number: Tests were carried out at three different Reynolds numbers: 20000 , 40000 and 90000 . The air supply valve was manually adjusted several times during a test so as to counter any fluctuations in the supply system.

Temperature Range: The total power supplied to the tube was predetermined so as to get a total bulk temperature rise of only 1.0 - 1.5 ^{o}K over a length of 26½ diameters of heating. The maximum wall temperature rise was in the range of 12°K . For this temperature difference the percentage variation of thermal conductivity, specific heat and density of air are 3.52 , 0.085 and 3.60 respectively. Thus the heat transfer situation under study could be satisfactorily assumed as a passive scalar transfer.

CHAPTER 6

PREDICTION OF TWO-DIMENSIONAL SCALAR TRANSPORT

6.1 Introduction

Turbulence models described in Chapter (2) are examined here by applying them in flow geometries where consistent experimental measurements exist. The numerical schemes employed for this purpose have been described in Chapter (3). As the scalar transport precesses are heavily dependent on the hydrodynamics, a considerable number of explorations were made of flow field predictions. When comparing the predictive performance of models, as far as possible, a single aspect or effect of the models were chosen, so that it was possible to draw definite conclusions. As for the basic hydrodynamic turbulence model, the following models as in LAUNDER et al. [15] was chosen.

(a) Pressure-velocity gradient correlation by the complete Launder et al. model (equations (2.11) and (2.14)) - denoted by R_{s1} ,

(b) Turbulent diffusion of stress by the tensor invariant form, equation (2.6) - denoted by D_{s1} ,

and (c) Near-wall effects of (a) by Launder et al. model, equation (2.22) - denoted by R_{sw1} .

When comparing the scalar transport models, the above hydrodynamic model is employed along with the following basic scalar transport model.

(a) Pressure-scalar gradient correlation by linear destruction of flux (equation (2.48)) and redistribution of generation of flux (equation (2.58)) model - denoted by R_{c1} ,

(b) Turbulent diffusion of scalar fluxes by gradient diffusion model (equation (2.45), see Table (2.2)) - denoted by D_{c2} ,

and (c) Near-wall effects of pressure-scalar gradient correlation by equation (2.70) - denoted by R_{cw1} .

6.2 Prediction of Free Shear Flows

The aim here is to compare the performance of the pressure-strain and pressure-scalar gradient models with experimental data. The basic pressure strain models, (described in the previous section) is compared with the redistribution of production model (equation (2.19)) denoted by R_{s2} . In both models, the turbulent part (ϕ_{ij1}) is represented by the linear-return-to-isotropy model (equation (2.11)) with different coefficients (see Table (2.1)). For scalar transport, the performance of the quasi-isotropic model (equation (2.61) and (2.57) denoted by R_{c2}) is compared with the basic model described in the previous section. Models D_{s1} and D_{c2} were employed to simulate the diffusion of stresses and scalar fluxes respectively.

6.2.1 The Plane Jet

The plane jet in stagnant surroundings is considered first. RODI [61] has concluded that the plane jet measurements of ROBINS [65] and BRADBURY [72] display the best internal consistency and it is these data that were employed for comparison with predictions. Figures (6.1) and (6.2) show the measured and predicted mean velocity and shear stress profiles across the jet cross section. The agreement is quite satisfactory in the bulk of the cross section, but tends to be poor as the free stream is approached. The spreading rates obtained by the two models are 0.116 and 0.107 for models R_{s1} and R_{s2} respectively. The mean experimental value for the spreading rate quoted by Rodi is 0.11 . The difference between the predicted maximum shear stresses can be directly attributed to the above difference in spreading rates. The predicted turbulence intensity profiles are given against the data of Bradbury in Fig. (6.3). RODI [61] has pointed out that the rather implausible result of $\overline{v^2} > \overline{u^2}$

at the centre of the jet is unique to Bradbury's data. The turbulence energy production rate (all of which enters via the $\overline{u^2}$ equation) has its maximum around 0.8 of the half width of the jet; the mechanism which makes any turbulent component very much larger away from this region is not clear. Certainly no linear effect could produce such behaviour. Over the whole of the jet cross-section, the predicted levels of $\overline{u^2}$ are about 15% larger than data, whereas the corresponding difference between predicted and measured levels in $\overline{w^2}$ is slightly smaller. Although this discrepancy is large, being a free shear layer they may be within the uncertainty of the measurements. The difference between $\overline{v^2}$ and $\overline{w^2}$ profiles obtained from the simple pressure-strain model R_{s2} is purely due to diffusion coefficient for $\overline{v^2}$ being about three times as large as that for $\overline{w^2}$. With a simple gradient diffusion model for stresses, on the other hand, model R_{s2} would predict identical profiles for $\overline{v^2}$ and $\overline{w^2}$. The turbulent intensities closer to the free stream indicate that the use of the same coefficient C_s in the diffusion model for both ϕ_{ij} models is inappropiate. It seems that the simple pressure-strain model requires a lower value for C_s than the other model. This aspect, which has not been pursued further in the present investigation, indicates that one can not identify with certainty between effects due to diffusion or to pressure-strain effects unless one has directly available measurements of the magnitudes of the processes themselves.

The scalar transport predictions of plane jets are shown in Fig. (6.4) to (6.7). The predicted mean temperature profiles seem to agree quite well with data of JENKINS and GOLDSCHMIDT [68] and those of VAN DER HEGGE ZIJNEN [67]. Note here that the same hydrodynamic model is employed with both scalar transport models R_{c1} and R_{c2} , thus any difference between their performance is due purely to differences in the scalar transport models. Model R_{c1} produces a better mean temperature profile

than model R_{c2} . The spreading rates of the temperature field from models R_{c1} and R_{c2} are 0.145 and 0.134 respectively, which are 25% and 15% higher than the spreading rate of the velocity field; experiments suggest an increase of about 25% in agreement with model R_{c1} . As there are no measurements available on cross-stream heat flux profiles, the predictions are compared with $\overline{vc}$ profiles obtained by applying a mean enthalpy balance to the measured temperature with the assumption of self similar profiles. This is obtained with the help of the expressions given in Table (4.3). The agreement is quite satisfactory in this comparison. The Figures (6.6) and (6.7) show the predictions of the ratio of the heat fluxes (streamwise to cross-stream) and turbulent Prandtl number of the plane jet. Over the bulk of the flow the streamwise flux is about 1.2 - 1.3 times larger than the cross-stream flux. At the plane of symmetry, the cross-stream heat flux drops to zero but the streamwise flux stays up thus giving a large $\frac{\overline{uc}}{\overline{vc}}$. The Prandtl numbers as predicted by the two models show a considerable difference. The profile from model R_{c1} can be considered satisfactory as the average level predicted by that model is about 0.70 . The non-linear model R_{c2} produces too high Prandtl numbers near the centre of the jet. Although this effect could have been reduced by adjusting the coefficients of model R_{c2} , with non-linear terms it will always produce higher Prandtl numbers near the centre than over the other parts of the flow. Thus any adjustments in the coefficients will change the levels of Pr and $\frac{\overline{uc}}{\overline{vc}}$ over larger regions of flow. It can be seen that if the effects of the non-linear terms in the model R_{c2} are to be small near the symmetry axis (which is necessary to produce a more plausible variation in turbulent Prandtl number) then the normal stress field should be closer to isotropy than predicted by present hydrodynamic models. This possibility is, however, not supported by the experimental data shown in Fig. (6.3).

6.2.2 The Plane Wake

In Figures (6.8) to (6.10) the flow predictions of a far plane wake are compared with the measurements of TOWNSEND [62] and FABRIS [81]. The calculations were carried out until the velocity deficit was only about 5% of the main stream velocity, for which level self similarity is achieved with certainty. In the selected data positions of Townsend and Fabris, the velocity defects are 3.1% and 5.7% respectively. The agreement of predictions with models R_{s1} and R_{s2} with above data are not satisfactory; the level of maximum shear stress being 22% lower than the experimental value. This in turn is seen in the predicted spreading parameter S being 0.074 and 0.071 with the models R_{s1} and R_{s2} respectively, as compared to the average level of 0.098 reported by RODI [61]. The predicted spread of the half width of the layer is lower than in data. This is responsible for rather poor agreement of all components of turbulence kinetic energy in regions near the free stream. At the plane of symmetry, Townsends $\frac{\overline{u^2}}{U_o^2}$ is only 0.072, whereas that from prediction, by both models R_{s1} and R_{s2}, is about 0.095 . It must be noted however that this predicted level of $\overline{u^2}$ agrees well with data of ALEXOPOULOS and KEFFER [99] and that of UBEROI and FREYMUTH [100]. The level of $\overline{w^2}$ predicted by model R_{s1} agrees well with data over the inner half of the layer, whereas in the outer half, along with other components this too falls far too rapidly to the free stream levels. As in Bradbury's plane jet data, Townsend's measurements of $\overline{v^2}$ show a maximum at the plane of symmetry; a feature not obvious from the stress equations.

Considering the large discrepancy between predicted and measured spreading rates of the flow field, it is unwise to expect to obtain correct behaviour in the predicted scalar fields; relative magnitudes can however be compared. The predicted temperature field given in Fig. (6.11) show considerable departure from data, especially for the linear model R_{c1} .

The measured cross-stream heat fluxes from Townsends experiment are consistent with his self similar mean profiles. The measured levels of $\overline{vc}$ of Fabris, however, are about 45% lower than what is implied by self similar analysis of his mean velocity and mean temperature profiles. Present predictions - with a rather low spreading parameter - agrees well with data of Fabris. The predicted ratio of half-widths of the temperature and velocity field are 1.17 and 1.09 for the linear (R_{c1}) and non-linear (R_{c2}) models respectively. Corresponding ratio from the experiments are in the range of 1.20 to 1.30 . The predicted levels of ratio of streamwise to cross-stream heat fluxes and of turbulent Prandtl number are quite similar to those obtained from the plane jet predictions. Again, the implausible Prandtl number levels near the central plane obtained from the non-linear model R_{c2} can be attributed to the anisotropy of stresses in that region. In Figures (6.15) and (6.16) the prediction of streamwise heat flux and the temperature fluctuation are compared with the experimental data of FABRIS [81]. Although in the view of discrepancy between measured C and $\overline{vc}$, even the streamwise heat flux is to be expected too low, the ratio $\frac{\overline{uc}}{\overline{vc}}$ from the experiment is suitable for comparison. The predicted level of 1.30 to 1.40 in the bulk of the layer compares well with the range 1.40 to 1.50 obtained by measurements of Fabris.

6.2.3. The Plane Mixing Layer

First attention is given to the prediction of a mixing layer between two moving streams. Fig. (6.17) shows the predictions by models R_{s1} and R_{s2} compared with the data of WATT [73]. The ratio of the velocities at the two streams is 0.5 . The prediction of mean velocity profile by models R_{s1} and R_{s2} are indistinguishable and are in quite good agreement with the measured profile. The spreading rates of the mixing layer predicted by the models R_{s1} and R_{s2} are 0.0486 and 0.0462 respectively and they can

be considered satisfactorily close to Watt's reported spreading rate of 0.045 . The predicted level of shear stress is about 15% too high when compared with the measured level; however, the shear stress calculated from Watt's mean velocity profile is much closer to the present predicted levels, the maximum of $\frac{\overline{uv}}{U_o^2}$ being about 0.105 . Over the bulk of the layer, the predicted levels of turbulence intensity profiles, shown in Fig. (6.19), are in good agreement with measurements. At the centre of the layer, the relative levels of the turbulent components predicted by model R_{s1} are in excellent agreement with data, whereas, model R_{s2} predicted the $\overline{u^2}$ component (r.m.s. value) about 5% too high; moreover, the difference between $\overline{w^2}$ and $\overline{v^2}$ at the centre of the layer is reduced by half. (As remarked above, any difference between $\overline{w^2}$ and $\overline{v^2}$ in predictions by model R_{s2} is purely due to the non-isotropic diffusion model D_{s1}.) Near the free streams the agreement of the predictions with measurements deteriorates, the prediction being consistently lower than the measurement.

The mean temperature profiles predicted from models R_{c1} and R_{c2} are again identical and they compare satisfactorily with the measurements of Watt. The predicted spreading rates of the temperature layer are 0.0547 and 0.0554 for models R_{c1} and R_{c2} respectively and they compare well with the Watt's measured level of 0.051 . Certainly the ratios of spreading rates of temperature and velocity layers are in good agreement. Watt's measurements of cross-stream heat flux are in serious error by a factor of four. Thus the $\overline{vc}$ profiles as deduced from measured mean velocity and temperature fields under self similar conditions are employed for comparison with present predictions. Except near the faster moving edge the agreement is within 10%; a large fraction of this discrepancy is due to the disagreement in spreading rate of the velocity mixing layer. There is a considerable difference between the predicted and calculated heat flux profiles near the faster moving edge. This aspect is similar to the

behaviour noticed in predicting the plane wake, Figures (6.22) and (6.23) show the predicted $\frac{\overline{uc}}{\overline{vc}}$ and the turbulent Prandtl number variation across the layer. The two models show a similar overall variation eventhough the levels of $\frac{\overline{uc}}{\overline{vc}}$ are different in the two cases.

Considered next is a mixing layer formed in the initial region of a jet. RODI [61] recommended data of BRADSHAW et al. [75] as the most consistent with respect to compliance with self similar velocity - shear stress relation. The predicted variations of the mean velocity profile obtained with models, R_{s1} and R_{s2} are identical except at the faster moving edge. The predicted profiles are in good agreement with data except in that region. The predicted spreading rates are 0.158 and 0.152 respectively, for models R_{s1} and R_{s2} . As there is considerable scatter in the spreading rates among experimental data these predicted spreading rates can probably be considered satisfactory in comparison with Bradshaw's value of 0.165 . The predicted shear stress profiles agree well with measurements of Bradshaw et al.. It Should be noted however, that the discrepancy of about 10% between calculated and measured levels of shear stress (see [61]) in Bradshaw's data is hidden in the present predictions by a similar discrepancy in the rate of spread.

Shown in Fig. (6.26) is the predicted variation of mean temperature across the layer compared with the data of SUNYACH and MATHIEU [74]. The predictions from models R_{c1} and R_{c2} are not distinguishable. Again the largest discrepancy between predictions and measurements lies in the faster moving edge. The spreading rates of the temperature layer predicted by models R_{c1} and R_{c2} are 0.198 and 0.201 respectively. The spreading rate of the velocity field as measured by Sunyach and Mathieu is 0.18 which is the highest value reported in Rodi's review, thus this reported spreading rate of 0.249 for temperature field can likewise be considered too high. Predicted profiles of cross-stream heat flux are shown in Fig. (6.27). The maximum

level of $\frac{\overline{vc}}{U_o C_o}$ implied by Sunyach and Mathieu's mean data is about 60% higher than the predicted levels. The average level in the ratios of spreading rates between temperature and velocity mixing layers are 1.37 and 1.28 from measurements and predictions respectively. The $\frac{\overline{uc}}{\overline{vc}}$ and σ_t profiles predicted by models R_{c1} and R_{c2} are shown in Figures (6.28) and (6.29). They are quite similar to those obtained for the case of mixing between two moving streams.

6.2.4 Conclusions

The hydrodynamic predictions of the three free shear flows discussed above show on average satisfactory agreement with corresponding experimental data. Predictions with both pressure-strain models R_{s1} and R_{s2} show similar behaviour, model R_{s2} gives slightly smaller spreading rates than model R_{s1}. In predictions reported in LAUNDER et al [15], the simple pressure-strain model with C_{s1} = 1.5 was employed along with the gradient diffusion model. Present predictions by the simple model with C_{s1} = 1.7 along with the tensor invariant diffusion model D_{c1} , show on average, improvements over the above predictions of Launder et al.. As far as the measurements employed are concerned, the largest uncertainity lies in the normal stress levels at the planes of symmetry in the palne wake and the jet. Even though the data of Bradbury and Townsend show considerably larger values for the $\overline{v^2}$ component than other components, measurements by PATEL [101] and by CHEVRAY and KOVASZNAY [102] do not show such effect. Thus no attempt had been made to improve the predictions in this regard. As far as the numerical predictions are concerned, the largest discrepancy was seen near the fast moving boundaries in plane wake and in mixing layers. Consistently the predictions show more abrupt approach to free stream conditions than do the measurements. The numerical predictions were thoroughly checked to make sure that this behaviour is not a numerical shortcoming.

The linear and non-linear models (R_{c1} and R_{c2}) for the pressure-scalar gradient correlation show similar mean temperature predictions. The prediction of large turbulent Prandtl numbers near the symmetry plane by the non-linear model R_{c2} however, is quite unacceptable. As seen before, model R_{c2} can be expected to give a more acceptable Pr_t profile only if applied with a hydrodynamic model which predicts near isotropy in regions closer to the planes of symmerty. For this reason this model is not considered for further investigation. The scalar field predictions to be reported in the remainder of the Thesis with thus be made only with model R_{c1} .

6.3 Flat Plate Boundary Layer

The flat plate boundary layer in a zero pressure gradient with no mass transfer through the wall provides excellent conditions for the verification of the models for near-wall effect terms of the pressure-velocity gradient correlation. Similarly the models for the pressure-scalar gradient correlation can be verified with flat plate boundary layer heat and mass transfer data. Here the near-wall models discussed in Chapter (2) are employed with corresponding ϕ_{ij} models as follows:

(a) The LAUNDER et al. [15] near-wall model given in equation (2.22) is employed with the complete pressure-strain model given in equation (2.14) and is denoted by R_{sw1} ,

(b) The GIBSON-LAUNDER [31] near-wall model given in equations (2.26) - (2.27) is employed along with the simpler version of ϕ_{ij} (equation (2.19)) and is denoted by R_{sw2} ,

(c) The isotropic near-wall model for ϕ_{ic} given in equation (2.70) is employed along with the linear model R_{c1} (equations (2.48) and (2.58)) and is denoted by R_{cw1} ,

(d) The Gibson-Launder model for near-wall effects of ϕ_{ic} (equations (2.71) and (2.72)) is employed along with model R_{c1} and is denoted by R_{cw2} .

Model R_{cw1} is employed in conjunction with model R_{sw1} while model R_{cw2} is used along with R_{sw2} .

6.3.1 Hydrodynamic Predictions

As data of KLEBANOFF [32] relate to turbulence measurements in zero-pressure gradient, smooth flat plate boundary layer, they are very suitable for the verification of

(a) different models for wall effects on the pressure-strain correlation

and (b) different decay functions (controlling how fast wall effects disappear at distances away form the wall).

The predictions with near-wall effect models R_{sw1} and R_{sw2} are compared with Klebanoff's data in Figures (6.30) to (6.32). For this test, the near-wall effect function of $f \propto \frac{k^{3/2}}{\varepsilon y}$ and the tensor invariant form (equation (2.6)) of the stress diffusion model were employed. The distance from the wall to the point where $U = 0.995U_E$, where U_E is the free stream velocity, was taken as the boundary layer thickness δ . The mean velocity profiles predicted by models R_{sw1} and R_{sw2} are in moderately good agreement with data. The predicted friction coefficients by models R_{sw1} and R_{sw2} are larger by 6.0% and 2.7% respectively than the value implied by the power law formula given by HINZE [26], p.638 . The predicted shear stress profiles are however indistinguishable from each other with these two models. Fig. (6.32) show the predicted normal stress profiles against data of Klebanoff. Model R_{sw1} shows considerably better agreement with data than model R_{sw2} . Model R_{sw1} correctly predicts the increasing trends in magnitudes of $\overline{u^2}$ and $\overline{w^2}$ components, as the wall is approached. The difference between the models in predicting the $\overline{u^2}$ component is appreciable where that of $\overline{w^2}$ components is purely due to different boundary conditions applied in order to be consistent with the extents of redistribution expected by near-wall-effect models.

The next test to be reported here is the effect of the near-wall-effect function on the predictions of turbulence intensities. Two functions

were tested, $f \propto \frac{k^{3/2}}{\varepsilon y}$ and $f \propto \frac{|\overline{uv}|^{3/2}}{\varepsilon y}$. The proportionality constants were chosen so that, with boundary values of near-wall stress levels, f takes a value of unity. The models R_{sw1} and D_{s1} were employed along with above functions and predicted behaviour was compared. The mean velocity profile and the shear stress profile were identical in the two cases; the normal-stress profile shown in Fig. (6.33), however, were considerably affected. As the shear stress is practically constant in the near-wall region, with the dissipation rate being inversely proportional to the distance from the wall, function $f \propto \frac{|\overline{uv}|^{3/2}}{\varepsilon y}$ is rather flat over a considerable distance away from the wall. On the other hand the turbulent kinetic energy is roughly proportional to y^{-n} where n is about 0.20 - 0.25 and therefore $f \propto \frac{k^{3/2}}{\varepsilon y}$ decreases considerably with distance from wall. Comparison between turbulence intensities predicted by these two functions with Klebanoff's data indicate that $f \propto \frac{k^{3/2}}{\varepsilon y}$ represents the correct decay in effects of ϕ_{ijw} terms whereas $f \propto \frac{|\overline{uv}|^{3/2}}{\varepsilon y}$ provides excessive levels of $\overline{u^2}$ due to near-wall actions.

Fig. (6.34) shows the effects of turbulent diffusion models D_{s1}, the tensor invariant form and D_{s2}, the gradient diffusion model. The coefficient C_s in these two models was given values 0.11 and 0.20 respectively. Model R_{sw2} was used here as the model for ϕ_{ij}. The mean velocity and shear stress profiles are again identical for the two models. The gradient diffusion model produces excessive diffusion in stress components $\overline{u^2}$ and $\overline{w^2}$ and has negligible effect on the $\overline{v^2}$ component. Fig. (6.35) shows a rather interesting effect that was seen in the shear correlation coefficient. In Klebanoff's reported data, the correlation coefficient is constant at 0.5 upto 80% of the boundary layer thickness and then drops linearly to zero at $1.2\,\delta$. The predicted shear correlation coefficient with model D_{s2} shows a similar behaviour but with sudden drop to zero at $1.1\,\delta$, whereas model D_{s1} produces an implausible increase. This however can not be considered a serious defect as the shear stress in this region is anyway rather small.

6.3.2 Scalar Transport Predictions

The investigation of a developing thermal boundary layer within a thick velocity boundary layer provides an interesting problem for prediction methods. ANTONIA et al. [90] have reported datailed temeprature field measurements of such a flow (the velocity field measurements were not reported in datail). The momentum thickness Reynolds number at the upstream edge of the heated section was about 3070 . The velocity and thermal boundary layer thickness δ and δ_c were defined as the distances to the wall from positions $U = 0.995U_E$ and $(C - C_\infty) = 0.01\ (C_w - C_\infty)$ respectively. Two major discrepancies were reported in their measurements: the skin friction coefficients obtained from the growth rate of the momentum thickness were about 25% larger than those obtained from measured velocity profiles (using a "Clauser" chart), and the wall heat flux implied by the mean enthalpy integral equation is about 20% higher than the measured levels. These discrepancies suggest a slight convergence of their streamlines, possibly due to the growth of boundary layers on the side walls.

The predictions by models R_{cw1} and R_{cw2} of this flow are shown in Figures (6.36) to (6.40). The agreement of the predictions with the mean temperature data as shown in Fig. (6.36) is rather poor. The discrepancies can be explained by looking more closely at the numerical treatment of the near wall region. Boundary conditions applied to the mean temperature and cross-stream heat flux equations are that of a given wall flux which is exactly known. There are no other relations feeding the numerical scheme†. Thus the discrepancy seen in Fig. (6.36) is due to

(a) the logarithmic law of the wall for temperature used in evaluating wall temperature,

---

† For the case of known temperature wall boundary however, some auxiliary relation (generally the logarithmic law for temperature) will have to be used for the estimation of wall flux.

and (b) the turbulence model coefficients which expect a near-wall Prandtl number of about 0.9 .

The logarithmic law of the wall used in evaluation the wall temperature is

$$C^+ = \frac{1}{\kappa_c} \ln y^+ E_c \tag{6.1}$$

where κ_c and E_c were taken as 0.46 and 4.5 respectively, which were obtained from a consensus of near-wall data (see KARDAR and YAGLOM [8]). The value of 0.46 for κ_c is consistent with a Prandtl number of 0.9 , whereas the coefficient E_c which represent the resistance by viscous sublayer to heat transfer, was given a value which is consistent with values quoted by JAYATILLEKE [103] in his extensive review of near-wall data (a slightly different nomenclature was used in [103]).

The discrepancy between predicted and measured levels of Prandtl number can be isolated by looking at the temperature profiles in defect coordinates. This is done in Fig. (6.37). The near-wall Prandtl numbers implied by data at all experimental stations are in the range 1.0 - 1.3 , whereas predictions show a value of about 0.85 . The reason for rather high levels of Prandtl number obtained by Antonia et al. is not clear. The values of σ_t obtained by other workers who examined the problem of developing thermal layer however fall much closer to present predictions. For example, the constant-wall-temperature experiments of FULACHIER [104] and that of BLOM [86] and constant wall flux experiments of BRADSHAW and FERRISS [105] all indicate values of σ_t = 0.90 - 0.92 in the near-wall regions.

The data on Fig. (6.36) indicate that the additive constant E_c should in fact be a function of the streamwise distance, whose asymptotic value seems to have reached by $\frac{X}{\delta_o}$ of 11.4 . The review paper by JAYATILLEKE [103] however does not document such an effect. As there are no such correlations, in the present predictions, E_c was kept at a constant value which is consistent with reviews by [8] and [103].

The variation of Prandtl number across the thermal layer as calculated by ANTONIA et al. [90] has a large scatter and does not seem to approach a regular pattern at downstream locations. Self preserving analysis however suggets an asymptotic behaviour for all variations. This data is another piece of evidence on the unreliability of measurements of Prandtl number. The predicted Prandtl numbers, shown in Fig. (6.38) against data of Antonia et al., indicate a near-wall value of about 0.9 decreasing smoothly away from the wall. The agreement of predicted Prandtl number variation with the data of FULACHIER [104] and BLOM [86] in the inner 40% of the thermal boundary layer is satisfactory. In the outer regions of the layer, where estimation of mean gradients in data are less reliable, the variations in σ_t in data of

- ANTONIA et al. [90] do not show a clear pattern,
- FULACHIER [104] show an increase,
- BLOM [86], by turbulence measurements, show a decrease,
- BLOM [86], by mean profiles, show an increase†,
- JOHNSON [89] show a decrease.

The present predictions show a decrease.

Antonia et al. report that the thermal layer thickness at the last measuring station (i.e. at $\frac{X}{\delta_o} = 42.9$) was 66% of the velocity boundary layer thickness at the same point. The corresponding predicted spreads of the thermal layers are 81% and 82% from models R_{cw1} and R_{cw2} respectively. This high rate of spread indicated by the predictions is consistent with difference between measured and predicted levels of Prandtl numbers.

---

† The Prandtl number variation across the boundary layer given by Blom in his Thesis [10] does not agree with his earlier reported version [86]. In [10], the Prandtl number profile across the layer calculated by turbulent variables as well as by mean profiles show a decrease away from a maximum of about 0.90 at $y^+ \simeq 50$.

Predicted turbulent heat flux and temperature fluctuation profiles are compared with data in Figures (6.39) to (6.41). The cross-stream heat flux profiles show satisfactory agreement with measurements at all but first two measuring stations. Predicted streamwise heat flux profiles shown against data in Fig. (6.40) indicate that the boundary value of $\overline{uc}$ in the prediction is too low. The near-wall effect model R_{cw1} does not seem to give sufficient level of $\overline{uc}$. Model R_{cw2} , except very near to the wall, shows the correct decrease in $\overline{uc}$ away from the wall. The temperature fluctuation predictions shown in Fig. (6.41) suggest insufficient diffusion of $\overline{c^2}$ in the outer parts of the layer. A value of 0.13 used for the gradient diffusion coefficient C_g is however not an optimised value. Predictions of the far plane wake also indicated an insufficient diffusion indicating that a higher level of C_g , to about 0.18 - 0.20,would probably produce an overall improvement.

6.4 Pipe Flow

6.4.1 Hydrodynamic Predictions

The mean and turbulence measurements by LAUFER [34] in smooth-walled pipes are a complete set of data suitable for comparison, Laufer made measurements at two Reynolds numbers Re = 50000 and Re = 500000 , and found considerable Reynolds number dependence in mean and turbulence profiles. More recently LAWN [19] made measurements of turbulence quantities essentially for the same flow with more advanced electronics. He concluded that for the range of Reynolds numbers 36000 - 250000 , the turbulence intensities suitably non-dimensionalised with the friction velocity are independent of Reynolds number. Shown in Fig. (6.42) are the fully developed velocity profiles obtained from predictions with models R_{sw1} and R_{sw2} . They agree reasonably well with data of Laufer. The shear stress variation across the pipe radius as shown in Fig. (6.43) is mainly a check on the numerical procedure and on the fully developed character of the predictions. As shown here, the viscous effects are significant only very close to the wall at this high Reynolds number and for all other positions the shear stress profile is essentially linear.

In Fig. (6.44) the turbulence intensity profiles predicted from models R_{sw1} and R_{sw2} are compared with data of Laufer. The agreement of the predictions with data are not very satisfactory; it is noted however that the streamwise component of stress measured by Lawn is in good agreement with predictions. The other components of normal stress obtained by Lawn lie rather close to Laufer's data for Re = 500000 . While, as remarked above Laufer's data indicate turbulence intensities which are highly dependent on Reynolds number influence. In the near-wall region, even though the predicted $\overline{u^2}$ and $\overline{w^2}$ are within the scatter, the $\overline{v^2}$ component seems to be too low. As a boundary condition the level of $\overline{v^2}$ at the grid point closest to the wall is indirectly imposed as equal in magnitude to the local shear stress. Laufer's data for Re = 500000 however imply a 20% larger level for $\overline{v^2}$ in

this region, a behaviour inconsistent with most other near-wall data (e.g. KLEBANOFF [32]).

Near the axis of the pipe the components $\overline{v^2}$ and $\overline{w^2}$ are predicted too low. Higher levels for these two components can be obtained by increasing the diffusion coefficient C_s , which however will increase the near axis levels of $\overline{u^2}$ as well, thus worsening the agreement of this component with experiment. The turbulent diffusion models D_{s1} and D_{s2} are compared in Fig. (6.45). Model D_{s2} , with a coefficient of $C_s' = 0.20$, seems to have rather too high diffusion rate. When C_s' was reduced to 0.15 model D_{s2} provides more acceptable stress levels near the axis; however no overall improvement over model D_{s1} was seen.

6.4.2 Scalar Transport Predictions

The predictions in the models R_{cw1} and R_{cw2} for the case of fully-developed temperature fields in pipes are shown in Figures (6.46) to (6.49). The predicted behaviour is compared with data of BREMHORST and BULLOCK [92] for a Reynolds number of 34200 . Model R_{cw1} predicts a flatter mean temperature profile than R_{cw2} ; the agreement with data is satisfactory. The radial heat flux profiles given by the two models are identical. The streamwise heat flux profile shown in Fig. (6.48) is in excellent agreement with data of [92]. Considering the slight scatter in the experimental values it is not possible to choose which one of the near-wall models is more acceptable. The turbulent Prandtl number profile shown in Fig. (6.49) is that obtained for fully developed pipe flow.

Shown in Fig. (6.50) is the prediction of concentration profiles downstream of a small mass transfer region in the pipe wall, a configuration studied experimentally by QUARMBY and ANAND [94]. The first set of experimental data is given for the position where the porous region ends. There the agreement of the predicted profiles with data is quite satisfactory.

Under adiabatic wall conditions, the concentration profile will develop towards the asymptotic state of constant concentration across the cross-section. The prediction of this development is only in moderately satisfactory agreement with data.

At this point it is useful to look back at the modelling ideas and assumptions employed in the scalar flux model. In modelling the pressure-scalar gradient term in the scalar flux equation it was assumed that the time scales of hydrodynamic and thermal turbulence fields, i.e. $\frac{k}{\varepsilon}$ and $\frac{\overline{c^2}}{2\varepsilon_c}$ respectively, are proportional. This assumption is likely to be satisfactory when

(i) mean velocity and mean scalar equations are nearly similar i.e. having similar boundary conditions etc.,

(ii) the different contributing turbulence processes to the maintenance of the turbulent kinetic energy and the scalar fluctuations have the same relative magnitude, i.e. at any given region of flow,

$$\frac{P}{\varepsilon} \simeq \frac{P_c}{\varepsilon_c} \quad .$$

In situations where these conditions are not satisfied, the time scales $\frac{k}{\varepsilon}$ and $\frac{\overline{c^2}}{2\varepsilon_c}$ can not be expected to be proportional; then the use of one scale will not be sufficient to describe a process where both time scales are influential. One of the limitations of the present model is that it assumes proportionality of velocity and scalar time scales and we may there expect anomalies to show up if the above conditions are not satisfied. The QUARMBY and ANAND [94] experiment is one situation where the boundary conditions for mean velocity and mean scalar are quite dissimilar. The mean velocity field is characterised by large gradients near the wall (i.e. non-zero wall friction) while the mean concentration profile downstream of the porous region has zero gradient at the (impermeable) wall. Thus while the

hydrodynamic turbulence field is in local equilibrium, (i.e. $\frac{P}{\varepsilon} \rightarrow 1.0$), in the near-wall regions, the concentration fluctuation field is one of decaying strength; the production of $\overline{c^2}$ being nearly zero in regions close to the wall, i.e. $\frac{P_c}{\varepsilon_c} \rightarrow 0$. With less production, in the near-wall region, $\overline{c^2}$ is likely to decrease faster than ε_c . Thus the effect of the time scale $\frac{\overline{c^2}}{2\varepsilon_c}$ on the characteristic time scale (previously expressed as proportional to $\frac{k}{\varepsilon}$) is to decrease its magnitude. If this process was to be accounted for, in an ad-hoc manner, within the framework of the present model, one would need to increase the coefficient C_{c1} near the wall, thus decreasing the effective thermal conductivity and raising the Prandtl number. This is certainly the direction of change needed to procure agreement with the measurements. In fact in the theoretical work of QUARMBY and ANAND [94] it was assumed that the turbulent Schmidt number was unity, compared with values much less than unity obtained in present predictions (see Fig. (6.51)) throughout the flow, and satisfactorily predicted the development of the concentration field. Due to above mentioned dissimilarity between velocity and scalar fields some assumptions made in modelling turbulent diffusion of scalar fluxes too become less relevant. Their implications however are not very clear (see Appendix (B)).

6.4.3 Conclusions

The prediction of flat plate boundary layer data of KLEBANOFF [32] suggests that model R_{sw1} is superior to model R_{sw2} and that the near-wall effect function $f \propto \frac{k^{3/2}}{\varepsilon y}$ is more suitable than the function $f \propto \frac{\overline{uv}^{3/2}}{\varepsilon y}$. The models for near-wall effect of pressure-scalar gradient correlation do not show any large differences in their predictions. Therefore model R_{cw1} which parallel the near-wall model R_{sw1} is chosen for further work. The

tensor invariant diffusion model D_{s1} shows superiority over the model D_{s2} in pipe flow predictions. Therefore it is the model D_{s1} that is employed in further applications. Models D_{c1} and D_{c2} could not be distinguished when predicting Quarmby and Anand's flow. The model D_{c2} is thus chosen for further applications.

CHAPTER 7

PREDICTION OF THREE-DIMENSIONAL SCALAR TRANSPORT

7.1 Introduction

Prediction of three-dimensional scalar transport provides a searching test for the turbulence model chosen in the previous chapter. For the first time all components of scalar fluxes become influential in the predictions here. The main feature that is under test here is the relative magnitude of the tangential scalar diffusivity with respect to the radial one. Ad-hoc assumptions, made by previous workers, on the ratio of tangential to radial scalar diffusivity, $\Gamma_\theta^C / \Gamma_r^C$, are briefly,

(a) REYNOLDS' [106] assumption of unity throughout the flow,

(b) SPARROW and LIN's [107] assumption of a diffusivity ratio varing with radial position (for flow in pipes),

(c) QUARMBY and ANAND's [59] assumption of an isotropic diffusivity in predicting concentration profiles behind a short mass transfer section in a pipe,

and (d) Consideration made by BERGELES et al. [108] where diffusivity ratio was taken as equal to the ratio of transverse to cross-stream normal stress levels.

Out of these assumptions it is the last one (Bergeles et al.), that is closer to generality. This relation is the form to which the present model reduces when convective and diffusive transport effects and near-wall effects are neglected. In the present investigation, where transport equations for the turbulent fluxes are being solved, the diffusivities are an <u>outcome</u> of the calculation rather than an input. It will be seen later, that the ratio of diffusivities in the tangential to radial directions is not a well-behaved two-dimensional function as assumed by previous workers,

but a complex three-dimensional function strongly dependent on the boundary conditions.

Section (7.2) reports preliminary testing of the three-dimensional calculation procedure. The aim here was to ensure that,

(a) there were no asymmetries induced by the three-dimensional procedure, (caused by the chosen sweep direction, etc.)

(b) the mean scalar was conserved,

and (c) the solutions were independent of the finite difference grid chosen.

In Section (7.3) predicted results of three-dimensional scalar transport situations are compared with experimental data.
They are the simulations of,

(a) QUARMBY and ANAND's [59] experiment, where the three-dimensionality is rather weak,

(b) BLACK and SPARROW's [13] experiment, where the three-dimensionality is moderate and persisting,

and (c) Present experimental situation (see Chapter (5)), where the three-dimensionality is strong and persisting.

Section (7.4) concludes the chapter by summarising the inferences made on the three-dimensional calculations.

7.2 Verification of the Three-Dimensional Solution Procedure

The $(\theta-r-z)$ numerical procedure described in Chapter (3) was utilised previously in Chapter (6) in predicting two-dimensional scalar transport situation. There the calculations were confined to a single $(\theta-z)$ plane. All three-dimensional scalar transport situations considered in this Thesis had two-dimensional fully developed flow fields. Thus the flow field calculations were performed on two-dimensional basis and the results were transfered to the three-dimensional procedure and then made to spread over all $(\theta-z)$ planes. The three-dimensional scalar field was then calculated with a frozen hydrodynamic field. The numerical solutions were checked to ensure that they correctly represented the solutions of the finite difference transport equations.

7.2.1 Check for Numerically Induced Asymmerty in Scalar Field

As the hydrodynamic field was obtained for a single θ-line in the cross-section of flow and then all other θ-lines were assigned, the flow field can be considered exactly symmetric. In the finite difference solution of the scalar transport equations however, even under symmetric boundary conditions, asymmetry can enter the calculations via

(i) the method of imposing boundary conditions, which may make the finite difference equation of a variable Φ at any control volume remote from a boundary different from one adjacent to a boundary,

and (ii) incorrect interpolation practices.

In order to check that the computer code is free from these deficiencies, a pseudo-three-dimensional calculation of heat transfer in a circumferentially uniformly heated pipe was made. The mean temperature field showed no asymmetry in the result. Also the diffusivity of scalar in the radial direction,

$$\Gamma_r^C = -\frac{\overline{u_r c}}{\frac{\partial C}{\partial r}} \tag{7.1}$$

showed prefect symmetry; the tangential diffusivity,

$$\Gamma_\theta^C = -\frac{\overline{u_\theta c}}{\frac{\partial C}{r\partial\theta}} \tag{7.2}$$

however, showed asymmetry, less than 3% at any point. It should be noted here that both $\overline{u_\theta c}$ and $\frac{\partial C}{\partial\theta}$ should be zero under these boundary conditions and thus above accuracy is remarkably good. This makes it possible to proceed in the knowledge that the asymmetries predicted with three-dimensional boundary conditions are in fact real.

7.2.2 Check for the Conservation of Mean Scalar

In making calculations of scalar transport inside tubes (without considering the conduction through the tube material), the wall scalar fluxes are given as the boundary condition to the fluid medium. Conservation of enthalpy or concentration is thus always achieved. The solution of problems where tube-wall conduction is present, however, presents an additional requirement. Since the axial conduction is to be neglected, here one must make sure that under steady state conditions, the heat generated (or supplied through the outer surface of the tube) in a given length of pipe wall is exactly equal to the net gain in heat by the fluid passing along the same length. Thus, for example, if the heat input per unit length is constant along the pipe, the bulk temperature rise should be exactly linear. As the general form of the finite difference equations for control volumes within the pipe wall (no turbulent transport) is strikingly different from those for control volumes in the fluid, these equations are not expected to converge to the solution at the same rate. In calculations where the grid was confined to the fluid inside the pipe it was found that at a given cross

section it was sufficient to make two sweeps each, in the radial and tangential directions, of the line-by-line solution of the finite difference equations. In cases where tube conduction was considered, however, a large number of sweeps was necessary to make sure that the fluid had absorbed all the heat that was supplied under steady conditions. During the first few steps of the calculation i.e. in the region close to start of the heating, the mean temperature equation was swept eight times, whereas, as the calculation proceeded downstream the number of sweeps were gradually reduced to four. This practice made sure that the total deficit in the bulk temperature was less that 0.1% of the exact value at all positions along the tube. As all turbulent variables were confined to the fluid, as before two sweeps were sufficient for their convergence.

7.2.3 Check for Grid Independence of the solution

It is necessary to make sure that the final solution of the equations was, for practical purposes, independent of the finite difference grid employed. Apart from limitations in grid placement in near-wall regions, as discussed in Section (3.6), one can generally expect to achieve higher accuracy by increasing the number of grid nodes across the region of interest, however, with added cost in computing. In two-dimensional calculations 22 grid nodes were used in the radial direction. Number of grid nodes necessary in the transverse direction were checked in three-dimensional calculations and 8 grid nodes were found to be sufficient to give mean field results with 1% of what is obtained with 14 grid nodes. As the computational time nearly doubled in the latter case it was felt that the accuracy with (8 × 22) grid was sufficient for the present investigation.

7.3 Comparison of Predicted Results with Experimental Data

Three sets of experiments in three-dimensional scalar transport (weak, moderate and strong in three-dimensionality) are compared here with the predicted behaviour.

The first situation considered is QUARMBY and ANAND's [59] measurements of concentration profiles downstream of a short mass transfer section. This work followed their two-dimensional explorations [93] made with the same apparatus and all details of the measurement technique and measuring stations etc. were given then. The presentation of the results in [59] however is rather misleading. The location $x^+ = 0$ in the first (axisymmetric) paper was at the downstream end of the mass transfer patch on the wall. In the second paper no statement as to the whereabouts of the origin was made. It was evident, however that it could not refer to a position in the porous patch since the reported near-wall radial gradients of concentration were low (indicationg an impermeable wall). The experimenter reported that the stations were the same as for the axisymmetric tests however. It was eventually discovered that by interpreting $x^+ = 0$ as corresponding to the next position downstream the values of x^+ reported in the two studies were indeed the same (see Table (7.1)).

Present Notation $X^+ = \frac{X}{D}$	Notation in QUARMBY and ANAND's [59] Two-Dimensional Experiment, $x^+ = \frac{x}{R}$	Notation in QUARMBY and ANAND's [93] Three-Dimensional Experiment, $x^+ = \frac{x}{R}$
0	(Start of Porous Region)	
1.493	0 (End of Porous Region)	
3.558	4.13	0
8.208	13.43	-
12.858	22.73	18.60
19.058	35.13	31.00
29.388	55.79	51.66

Table 7.1 Measuring Stations for Quarmby and Anand's Experiments

Now the predicted concentration profiles are compared with data of [59]. Shown in Fig. (7.1) is the variation of concentration at position (a) and (b) (which are the maximum and minimum of concentrations close to the wall). The agreement between the predicted variation and experimental data is poor. Some useful inferences can however be drawn.

(i) Data at $\frac{X}{D} = 3.558$ indicate that the circumferential diffusion of matter is much larger than what is implied in the predictions (otherwise the concentration at (b) would not be so high).

(ii) Data at locations further downstream indicate that circumferential diffusion is considerably smaller than that implied in the predictions (otherwise difference between the concentrations at (a) and (b) should decrease faster).

(iii) The variation of the near-wall concentration (denoted as C_{2D}) profile in QUARMBY and ANAND's [93] two-dimensional investigation for the same Reynolds number (Re = 20800) is given in Fig. (7.1). Their three-dimensional mass source was obtained by blocking 50% of the porous ring used in two-dimensional investigation. Therefore, for the purpose of comparison, the intensity of mass source in three-dimensional case; q_{3D} , can be considered double as that for two-dimensional case; q_{2D} , i.e.

$$q_{3D} = 2\, q_{2D}$$

In regions where diffusive effects are not predominant, concentration is likely to be proportional to the local mass flux. Therefore in regions close to the porous ring C_a should be roughly $2C_{2D}$. Quarmby and Anand's three-dimensional measurements, however, does not support this, indicating a clear discrepancy between their measurements. It is most likely that their three-dimensional measurements at $X^+ = 3.558$ are grossly in error.

The above discussion indicates that QUARMBY and ANAND's [59] data are neither consistent nor reliable. The fact remains however that the circumferential diffusion of matter as indicated by their data is substantially smaller than that implied in the present predictions. This fact in the light of other experimental data is discussed later.

It is worth mentioning here that QUARMBY and ANAND [59] came out with a set of assumptions which made it possible for them to predict their flow satisfactorily. They assumed that the diffusivities of mass and momentum are equal and that diffusivities of mass in radial and circumferential directions are equal. They assumed profiles for mean velocity and effective viscosity and then solved the concentration equation with the use of above assumptions. As initial conditions they took the experimental results at $\frac{X}{D} = 3.558$. Their predicted profiles at downstream locations were in excellent agreement with the experiment. It was seen earlier that data at $\frac{X}{D} = 3.558$ however are inconsistent with above assumptions. Thus with these assumptions, if their calculation started at $\frac{X}{D} = 0$, it would not have been possible for them to satisfactorily predict their data.

The next three-dimensional scalar transport situation to be considered is the investigation of BLACK and SPARROW [13] (see also BLACK [95]). Here the fluid is subjected to a circumferentially varing heat flux boundary condition obtained by resistance heating of a stainless steel tube of varing thickness. This boundary condition is applied to a length of 60 diameters of tube and temperature measurements were reported at the position $\frac{X}{D} = 52$. The ratio of maximum to minimum heat flux as implied by the variation in thickness is 2.92:1.00; however, due to circumferential conduction in the pipe wall this ratio of heat fluxes at the surface was reduced to a mere 1.31:1.00 at a Reynolds number of 7500 . Thus their situation can be considered only moderately three-dimensional. Results were published for several Reynolds numbers in the range 7500 - 58000 . For the present

investigation two Reynolds numbers were chosen, 40500 and 16800 , for which complete sets of wall and flow measurements are available. (Wall data for Re = 17200 are taken as that would prevail for Re = 16800). The temperature and heat flux distribution at the inner wall (calculated by BLACK [95] by solving† the tube conduction problem) and the implied local Nusselt number variation were reported at $\frac{X}{D} = 52.0$. The predicted behaviour of

(a) the wall heat flux through the inner surface of the wall

(b) the wall temperature at the inner surface of wall

and (c) the implied local nusselt number calculated as

$$Nu \left(\omega , \frac{X}{D} \right) = \frac{q_i \left(\omega , \frac{X}{D} \right)}{C_i \left(\omega , \frac{X}{D} \right) - C_b \left(\frac{X}{D} \right)} \cdot \frac{D_i}{K_w} \tag{7.3}$$

at the two Reynolds numbers, are compared with calculated profiles of BLACK and SPARROW [13] in Fig. (7.2) and (7.3). There are discrepancies of 4% and 2.6% between the predicted and measured circumferential heat flux vatiations at Re = 40500 and 16800 respectively. The predicted variation in the inner surface temperature however agree well with data. It should be noted that as Black did not apply an inner wall boundary condition in his calculations, but relied on two boundary conditions at the outer surface, the results of his calculation are liable to be rather sensitive to any errors in those boundary conditions. The maximum discrepancies in $Nu \left(\omega , \frac{X}{D} \right)$ are 6% and 2.8% for Re = 40500 and 16800 respectively. It is thus clear that a major portion of the difference between the calculated (by BLACK [95]) and predicted Nusselt numbers is due to difference in q-profiles which in their case is probably in error.

---

† The boundary conditions used in solving the conduction problem are,
(i) Symmetry at $\omega = 0°$ and $\omega = 180°$
(ii) Known temperature at the outer surface (measured values)
and (iii) Assumed adiabatic outer surface, (heat generation rate calculated from measured enthalpy rise in air).

The non dimensional temperature contours drawn from the data of [95] and present predictions are compared in Figures (7.4) and (7.5). The agreement of the calculated and measured behaviour is very satisfactory. The radial diffusivity of heat implied in the predictions seems to be slightly too low whereas the circumferential diffusivity seems just correct shown in Fig. (7.6(a) and (b)) are the measured temperature profiles and predictions at $\frac{X}{D} = 52$. The dashed lines indicate calculations made by Black using SPARROW and LIN's [107] analysis which assumed unity Prandtl number and isotropic diffusivity for heat. Since the agreement of the present predictions with measured levels is far better than with the isotropic assumption, it is possible to conclude that the notion of isotropy is not in accord with experiment.

The development of the local Nusselt number in the streamwise direction is shown in Figures (7.8) and (7.9). Five angular locations 45° apart in the tube were chosen for representation. The following inferences can be drawn

(a) The thermal flow has not become fully developed even at $\frac{X}{D} = 60$,

(b) The Nusselt numbers in the hotter areas seem to be close to fully developed levels than do the others.

The final three-dimensional scalar transport situation to be considered is that of the experiment described in Chapter (5). Here the three-dimensionality is obtained by heating only the top half of a glass tube. Due to conduction through glass, however, a small fraction of heat found its way through the non heated half. As the heat flux variation around the circumference was not measured one had to make an assumption as to how it varied in that direction. Preliminary calculation with a square-wave heat flux distribution in the θ-direction showed that the measured temperature variations were by no means compatible with this distribution. To find a more probable q-profile around the circumference measurements

were made with both sides heated. Figures (7.9) to (7.12) show the results of these explorations. The aim here was to obtain a $q_o \langle \omega \rangle$ profile which would give best agreement with wall temperature measurements made for the Reynolds numbers 20000 , 40000 and 90000 . The profile of $q_o \langle \omega \rangle$ chosen after considerable exploration is given in Fig. (7.9). The $q_i \langle \omega \rangle$ profiles refer to the heat flux variation entering the fluid. As expected the wall conduction effects are more dominant at lower Reynolds numbers.

It should be noted here that the temperature profiles shown in Figures (7.10) to (7.12) are obtained without modifications to the turbulence model. It was hoped that any shortcomings in the turbulence model would still be evident with the adjusted q_o profiles. On average predicted temperature profiles indicate slightly lower values than that obtained from measurements. This may be inferred as an effect of slightly high radial diffusivity in near wall regions.

Shown in Fig. (7.13) is the streamwise development of local Nusselt number (non dimensionalised with respect to the fully developed value for the axi-symmetric case) at three different angular positions. The wall fluxes corresponding to this case are those at Fig. (7.9(a)). The Nusselt number profile at $\omega = 45°$ for which point $\frac{q_i}{q_i}$ is very nearly unity falls along with that obtained in the axi-symmetric calculation described in Subsection (7.2.1). The data of entrance region Nusselt number by MILLS [109] for the case of uniformly heated tube (long calming section entrance) are shown here for comparison. Considering the scatter in data the predicted variation for the axi-symmetric case can be considered satisfactory. The non dimensional temperature contours at axial locations $\frac{X}{D} = 5$, 10 , 15 , 20 , 25 for the case of $Re \simeq 40000$ are shown in Fig. (7.14). The slight asymmetry created by the weakly three-dimensional wall boundary condition is evident here.

The simulation of the situation where only one half of the tube was heated will be discussed next. The outer wall heat flux distribution $\frac{q_o}{\overline{q_o}}$ profile is that given in Fig. (7.15(a)). Again measurements and predictions were made for three Reynolds numbers 20000 , 40000 and 90000 . The results of these tests are given in Figures (7.15) to (7.20), two figures for each Reynolds number. The first of these show the given q_o $\langle \omega \rangle$ profile along with predicted q_i $\langle \omega \rangle$ profile (q_i $\langle \omega \rangle$ varies in the axial direction as well, however this variation is quite small). Again, larger influence of conduction at lower Reynolds number is evident. The ratio of maximum to minimum heat fluxes (predicted, inner surface of tube) was 51.5 , 131 , 405 respectively for Reynolds numbers 20000 , 40000 and 90000 . (cf. Black and Sparrow experiment where this ratio was 1.67 for Re = 40500) The predicted temperature profiles around the circumference suitably non-dimensionalised with respect to the local bulk temperature show satisfactory agreement with measurements .The discrepancy at $\frac{X}{D}$ = 5 could arise from two possibilities; one, as mentioned before, a high radial diffusivity in the prediction and the other a possibly low heat flux in the initial region of the experimented tube. The Nusselt number profiles shown here indicates negative values over most of the half where the heat flux is very low. (The local Nusselt number becomes negative when the wall temperature is smaller than the bulk temperature at that axial location.) Non-dimensional temperature contours at five axial locations for Re = 40000 are given in Fig. (7.21). The rather strong three-dimensionality obtained with present boundary conditions is clear. The temperature measurements in the fluid, had they been available, would have provided an invaluable test for the detailed turbulence modelling.

The ratio of diffusivities in tangential to radial direction for two representative cases are shown in Figures (7.22) and (7.23). The first refers to the Black and Sparrow's experimental situation at Re = 40500 . Here the three-dimensionality of the scalar field being only moderate, the transport effects in the scalar flux equations are never dominant. This can be seen in these contours which indicate values for ratio of diffusivities in two directions quite close to ratio in respective normal stresses. Fig. (6.23) which relate to the case of Re = 40000 in the present experiment indicate that for strongly three-dimensional scalar situations the ratio of tangential to radial diffusivities of heat is indeed clearly three-dimensional.

7.4 Conclusions

It was shown that the measurements of concentrations behind a short mass transfer section in a pipe made by QUARMBY and ANAND [11] are not reliable. Their data however indicate that the near-wall diffusivities are predicted too high. As noted before, similar impression was given by predictions of their data for the two-dimensional problem as well. Other two situations which the predictions were attempting to simulate were for the cases where there were non-zero heat fluxes at all cross-sections of the flow. The three-dimensionality of the scalar field in these cases were much stronger and the predictions were in very good agreement with data certainly far superior to the calculations with the assumption of unity for the ratio between diffusivities in tangential and radial directions. It was shown at the end that this ratio is in fact a three-dimensional function very much dependent on boundary conditions and is far from well-behaved ad-hoc assumptions found in the literature.

CHAPTER 8

CONCLUDING REMARKS

8.1 Achievements and Limitations of Present Work

The main theoretical contribution of this Thesis has been in the area of extension and application of existing second-order closure models. The Reynolds stress closure models employed have previously being tested by others e.g. LAUNDER et al [15], in the same or similar experimental situations. In the present work, the main concern was to apply the scalar transport models in situations where reliable experimental data exist. Models for two terms, the pressure-scalar gradient term and the turbulent diffusion term, that appear in the scalar flux equation were tested. Attention was given to the modelling of influence of a rigid wall on the pressure-scalar gradient term, and a new model based on ideas exactly parallel to the modelling of near-wall effects of pressure-strain term is presented.

Two existing numerical schemes, Patankar-Spalding $(x\text{-}\Psi)$ procedure and $(\theta\text{-}r\text{-}z)$ procedure developed by Gosman and his colleagues, were extensively modified so as to facilitate the study of hydrodynamic and scalar transport problems with second-order closure models. New set of nodes, staggered with respect to those at which the mean flow variables were stored, were introduced for the calculation of turbulence variables. In the $(x\text{-}\Psi)$ procedure, for two-dimensional boundary layer flows, turbulent variables were calculated in positions shifted half a grid node in the Ψ-direciion. In $(\theta\text{-}r\text{-}z)$ procedure the displacements of the turbulent grid were chosen with due regard to the appearance of these variables in the mean equations. This technique clearly stabilized the numerical calculations by keeping the correct degree of tightness between mean and turbulent equations. Within the framework of the above numerical schemes, this idea

of staggered grid for turbulent variables provided a much improved arrangement for the solution of conservation equations in the second-order closure models.

The final version of the $(\theta\text{-}r\text{-}z)$ computer code contains a facility that permit the solution of the mean temperature equation both within the flow and in the wall of the containing pipe. This enables one to take a correct account of the effects of conduction in the tube wall under circumferentially non-symmetric boundary conditions.

The present work has provided measurements in strongly three-dimensional heat transfer situations in a pipe. The technique of obtaining uniform heat flux boundaries in long pipes using metallic spray deposition has been extended to obtain segments of uniform heat flux regions. Experiments which were performed for three Reynolds numbers (20000 , 40000 and 90000) provide a useful set of data for the verification of turbulence model.

Several free as well as wall-affected two-dimensional flow and scalar transport situations were numerically predicted using the second-order turbulence models. The level of agreement obtained in the hydrodynamic predictions is similar to that obtained by previous workes. Even though the predictions of the plane jet and of the mixing layer between two moving streams is quite satisfactory, the plane wake and the mixing layer with $\frac{U_I}{U_E} \simeq 0$ show too low spreading rates. The weak point there seems to lie in the modelling of the dissipation rate of turbulent kinetic energy. The level of agreement obtained in scalar transport predictions is satisfactory, however, it is always limited by the corresponding success in the hydrodynamic predictions. The present pressure-scalar gradient model predicts about the correct level of turbulent Prandtl numbers in free shear flows. The effects of considerably different production to dissipation rates on the level of turbulent Prandtl number, while in the correct direction, however seem to be underpredicted.

One of the major limitations of the present scalar transport model is that it assumes proportionality between the turbulent velocity and scalar time scales. When the boundary conditions for velocity and mean scalar are nearly similar this assumption is found to be satisfactory. The computations of mass diffusion downstream from a wall source has shown however that the supposition is inadequate when the boundary conditions are dissimilar.

The major physical phenomenon under study was the anisotropy of diffusivities in three-dimensional scalar transport situations. The present numerical predictions clearly confirm that the distribution of the diffusivities in the circumferential and radial direction is in fact quite complex and three-dimensional and certainly far from isotropy. When the three-dimensionality is only moderate the transport effects never being dominant, the ratio of tangential to radial diffusivity seems to be close to the ratio of corresponding normal stress levels. Under conditions of strong three-dimensionality, there are considerably larger regions where transport effects are dominant and hence the ratio of the diffusivities of scalar is a strongly three-dimensional function.

8.2 Suggestions for Future Work

(a) The experimental technique employed in the present investigation can be improved in a number of ways. As the first step towards perfecting methods of achieving a more square-wave-like heat flux variation around the tube, the present tests should be repeated with larger diameter tube. (A commonly available T12 fluorescence tube of nominal diameter 1.5 in., if employed, should reduce the conduction effects by a factor of three and the damage in peeling the strip of silver off from the tube would be confined to a much smaller angular region).

Over a slightly longer time scale, attempts should be made to make mean temperature and temperature fluctuation measurements in the flow. It is only such detailed measurements that can provide the depth of information needed for improving the turbulence models.

(b) A complete rethinking in modelling of turbulent kinetic energy dissipation rate equation is necessary. It is rather sad to note that even though the stress and flux modelling have progressed considerably during last dacade, the modelling of dissipation rate equation has not changed very much. In this regard, more recent ideas of multiple length scale models which take into account the transfer of energy between adjacent wave number regions should be pursued.

(c) As discussed in Sub section (6.4.2) the present assumption of proportional time scales for the velocity and scalar fields needs to be replaced. The way forward would be to provide a model for the dissipation rate of scalar fluctuations, ε_c .

As the measurement of terms in the ε_c equation is relatively easy (compared with terms in the ε equation), the model of ε_c may end up being a better representation of scalar dissipation than does the model for ε .

REFERENCES

1. REYNOLDS, W.C. and CEBECI, T. : Calculation of turbulent flows, in: Turbulence - Topics in Applied Physics; Vol. 12 (editor- P. Bradshaw). Springer-Verlag, Berlin, Heidelberg, New York (1976)

2. LAUNDER, B.E. and SPALDING, D.B. : Mathematical models of turbulence. Academic Press, London and New York (1972)

3. CHOU, P.Y. : On velocity correlations and the solutions of the equations of turbulent fluctuation. Quart. Appl. Math. 3, 38 (1945)

4. ROTTA, J.C. : Statistische theorie nichthomogener turbulenz. Z. Phys. 129, 547 and 131, 51 (1951) (Translation to english by W. Rodi, Rep. Nos. TWF/TN/38 and TWF/TN/39, Dept. Mech. Eng., Imperial College, London. (1968)

5. CEBECI, T. and SMITH, A.M.O. : Analysis of turbulent boundary layers. Academic Press, New York (1974)

6. RODI, W. and SPALDING, D.B. : A two-parameter model of turbulence and its application to free jets. Rep. No. HTS/69/20, Dept. Mech. Eng., Imperial College, London (1969)

7. LAUNDER,B.E., MORSE, A., RODI, W. and SPALDING, D.B. : Prediction of free shear flows - A comparison of the performance of six turbulence models. NASA - SP321, Free Turbulent Shear Flows Vol. I, 361 (1972)

8. KADER, B.A. and YAGLOM, A.M. : Heat and mass transfer laws for fully turbulent wall flows. Intern. J. Heat Mass Transf. 15, 2329 (1972)

9. PATANKAR, S.V. and SPALDING, D.B. : Heat and mass transfer in boundary layers (2nd edition). Intertext Books, London. (1970)

10. BLOM, J. : An experimental determination of the turbulent Prandtl number in a developing temperature boundary layer. PhD Thesis, The Technological University, Eindhoven, Holland. (1970)

11. QUARMBY, A. and QUIRK, R. : Measurements of the radial and tangential eddy diffusivities of heat and mass in turbulent flow in a plain tube. Intern. J. Heat Mass Transf. 15, 2309 (1972)

12. FULACHIER, L., BEGUIER, C. and KEFFER, J.F. : Interpretation of negative production of temperature fluctuations by spectral analysis. Symposium on Turbulent Shear Flows (The Pennsylvania State University), 15 (1977)

13. BLACK, A.W. and SPARROW, E.M. : Experiments on turbulent heat transfer in a tube with circumferentially varing boundary conditions. J. Heat Mass Transf., Trans ASME 89, 258 (1967)

14. HANJALIĆ, K. and LAUNDER, B.E. : A Reynolds stress model of turbulence and its application to thin shear flows. J. Fluid Mech. 52(4), 609 (1972)

15. LAUNDER, B.E., REECE, G.J. and RODI, W. : Progress in the development of a Reynolds-stress turbulence closure. J. Fluid Mech. 68(3), 537 (1975)

16. SYED, S.A. : Experimental and theoretical investigation of a horizontal free turbulent diffusion flame. PhD Thesis, University of London. (1977)

17. BRYANT, D. : PhD Thesis (to be published), University of London. (1978)

18. LAUNDER, B.E. : On the effects of a gravitational field on the turbulent transport of heat and momentum. J. Fluid Mech. 67(3), 569 (1975)

19. LAWN, C.J. : The determination of the rate of dissipation in turbulent pipe flow. J. Fluid Mech. 48(3), 477 (1971)

20. HANJALIĆ, K. and LAUNDER, B.E. : Fully developed asymmetric flow in a plane channel. J. Fluid Mech. 51(2), 301 (1972)

21. LUMLEY, J.L. : Pressure-strain correlation. Phys. Fluids 18(6), 750 (1975)

22. KOLOVANDIN, B.A. and VATUTIN, I.A. : Statistical transfer theory in non-homogeneous turbulence. Intern. J. Heat Mass Transf. 15, 2371 (1972)

23. MILLIONSHTCHIKOV, M.D. : On the theory of homogeneous isotropic turbulence. C.R. Acad. Sci. S.S.S.R. 32, 615 (1941)

24 DALY, B.J. and HARLOW, F.H. : Transport Equations in turbulence. Phys. Fluids 13(11), 2634 (1970)

25. REECE, G.J. : Development and application of a generalized Reynolds-stress model of turbulence. PhD Thesis, University of London (1977)

26. HINZE, J.O. : Turbulence (2nd edition). McGraw-hill, New York. (1975)

27. CROW, S.C. : Viscoelastic properties of fine grained incompressible turbulence. J. Fluid Mech. 33(1), 1 (1968)

28. NAOT, D., SHAVIT, A. and WOLFSHTEIN, M. : Two-point correlation model and the redistribution of Reynolds stress. Phys. Fluids 16(6), 738 (1973)

29. CHAMPAGNE, F.H., HARRIS, V.G. and CORRSIN, S. : Experiments on nearly homogeneous turbulent shear flow, J. Fluid Mech. 41(1), 81 (1970)

30. SHIR, C.C. : A preliminary numerical study of atmospheric turbulent flows in the idealized planetary boundary layer. J. Atmos. Sci. 30, 1327 (1972)

31 GIBSON, M.M. and LAUNDER, B.E. : Ground effects on pressure fluctuations in the atmospheric boundary layer. J. Fluid Mech. (to be published) (1978)

32. KLEBANOFF, P.S. : Characteristics of turbulence in a boundary layer with zero pressure gradient. NACA TN 3178, (1954)

33. COMTE-BELLOT, G. : Ecoulement turbulent entre deux parois parallèles. Publ. Sci. Tech. Ministère de l'Air, No. 419 (1965)

34. LAUFER, J. : The structure of turbulence in fully developed pipe flow. NACA Rep. 1174, (1954)

35. HARLOW, F.H. and NAKAYAMA, P.I. : Turbulent transport equations. Phys. Fluids 10(11), 2323 (1967)

36. LUMLEY, J.L. and KHAJEH-NOURI, B. : Computational modelling of turbulent transport. Adv. Geophysics 18A, 169 (1974)

37. COMTE-BELLOT, G. and CORRSIN, S. : The use of a contraction to improve the isotropy of grid-generated turbulence. J. Fluid Mech. 25(4), 657 (1966)

38. REYNOLDS, W.C. : Computation of turbulent flows. Ann. Rev. Fluid Mech. 8, 183 (1976)

39. OWEN, R.G. : An analytical turbulent transport model applied to non-isothermal fully-developed duct flows. PhD Thesis, The Pennsylvania State University. (1973)

40. RUBESIN, M.W. and ROSE, W.C. : The turbulent mean flow, Reynolds stress and heat flux equations in mass averaged dependent variables. NASA TM-X-62248, (1973)

41. TENNEKES, H. and LUMLEY, J.L. : A first course in turbulence, MIT Press, Cambridge. (1972)

42. LAUNDER, B.E. : Scalar property transport by turbulence. Rep. No. HTS/73/26 Dept. Mech. Eng., Imperial College, London. (1973)

43. WYNGAARD, J.C. and COTE, O.R. : The evolution of a convective planetary boundary layer - A higher order closure model study. Boundary-Layer Meteorology 7, 289 (1974)

44. DONALDSON, C du P., SULLIVAN, R.D. and ROSENBAUM, H. : A theoretical study of the generation of Atmospheric-clear air turbulence. AIAA J. 10(2), 162 (1972)

45. LUMLEY, J.L. : Modelling turbulent flux of passive scalar quantity in inhomogeneous flows. Phys. Fluids 18(6), 619 (1975)

46. MONIN, A.S. : On the symmetry properties of turbulence in the surface layer of air. Izvestiya, Atmos. Oceanic Phys. 1, 45 (1965)

47. LUMLEY, J.L. : Lecture series No. 76, von Kármán Institute, Belgium. (1975)

48. WEBSTER, C.A.G. : An experimental study of turbulence in a density - stratified shear flow. J. Fluid Mech. 19(2), 221 (1964)

49. SPALDING, D.B. : Concentration fluctuations in a round turbulent free jet. Chem. Eng. Sci. 26, 95 (1971)

50. GOSMAN, A.D. and PUN, W.M. : Lecture notes for course entitled "Calculation of recirculating flows". Rep. No. HTS/74/2, Dept. Mech. Eng., Imperial College, London. (1974)

51. HARLOW, F.H. and WELCH, J.E. : Numerical calculation of time-dependent viscous incompressible flow of fluid with free surface. Phys. Fluids 8(12), 2182 (1965)

52. CARETTO, L.S., GOSMAN, A.D. PATANKAR, S.V. and SPALDING, D.B. : Two calculation procedures for steady, three-dimensional flows with recirculation. Proc. 3rd Intern. conference on numerical methods in Fluid Dynamics, Springer-Verlag. (1972)

53. MORSE, A. : PhD Thesis (to be published), University of London (1978)

54. POPE, S.B. and WHITELAW, J.H. : The calculation of near-wake flows. J. Fluid Mech. 73(1), 9 (1976)

55. ANDRÉ, J.C., DE MOOR, G., LACARRÈRE, P. and DU VACHAT, R. : Turbulence approximation for inhomogeneous flows. Part I: The clipping approximation. Part II: The numerical simulation of a penetrative convection experiment. J. Atmos. Sci. 33, 482 (1976)

56. CHORIN, A.J. : Numerical solution of the Navier-Stokes equations. Maths. Comput. 22, 745 (1968)

57. PATANKAR, S.V. and SPALDING, D.B. : A calculation procedure for heat, mass and momentum transfer in three-dimensional parabolic flows. Intern. J. Heat Mass Transf. 15, 1787 (1972)

58. BERGELES, G. : Three-dimensional discrete-hole cooling processes. An experimental and theoretical study. PhD Thesis, University of London. (1976)

59. QUARMBY, A. and ANAND, R.K. : Non-axisymmetric turbulent mass transfer in a circular tube. J. Fluid Mech. 38(3), 457 (1969)

60. CHAN, A.L., BAUGHN, J.W. and HOFFMAN, M.A. : Non uniform circumferential heat flux experiments in a circular tube. ASME 75-WA/HT-52 (1976)

61. RODI, W. : A review of experimental data of uniform density free turbulent boundary layers, in: Studies in Convection - Theory, measurements and applications; Vol. 1 (editor-B.E. Launder) Academic Press, London, New York (1975)

62. TOWNSEND, A.A. : The structure of turbulent shear flow. Cambridge University Press (1956)

63. RODI, W. : The prediction of free turbulent boundary layers by use of a two-equation model of turbulence. PhD. Thesis, University of London. (1972)

64. NEWMAN, B.G. : Turbulent jets and wakes in a pressure gradient, in: Proc. Symposium on Fluid Mechanics of Internal Flow, (editor-G. Sovran). (1967)

65. ROBINS, A. : The structure and development of a plane turbulent free jet. PhD Thesis, University of London. (1971)

66. DAVIES, A.E., KEFFER, J.F. and BAINES, W.D. : Spread of a heated plane turbulent jet. Phys. Fluids 18(7), 770 (1975)

67. VAN DER HEGGE ZIJNEN, B.G. : Measurements of turbulence in a plane jet of air by the diffusion method and by the hot-wire method. Appl. Sci. Res. 7A, 293 (1958)

68. JENKINS, P.E. and GOLDSCHMIDT, V.W. : Mean temperature and velocity in a plane turbulent jet. J. Fluids Eng., Trans ASME 95, 581 (1973)

69. REICHARDT, H. : Gesetzmässigkeiten der freien turbulenz. VDI - Forschungsheft, 414 (1942)

70. SINGH, P.I. and UBEROI, M.S. : Instantaneous measurements of turbulent-nonturbulent interface and temperature in a two-dimensional jet. American Phys. Soc., Fluid Dynamics Div., Boulder, Colorado. (1972)

71. LAUNDER, B.E. : Heat and mass transport, in; Turbulence - Topics in Applied Physics; Vol. 12 (editor-P. Bradshaw) Springer-Verlag, Berlin, Heidelberg, New York (1976)

72. BRADBURY, L.J.S. : The structure of a self-preserving turbulent plane jet. J. Fluid Mech. 23(1), (1965)

73. WATT, W.E. : The velocity-temperature mixing layer. Rep. No. TP 6705, Dept. Mech. Eng., University of Toronto. (1967)

74. SUNYACH, M. and MATHIEU, J. : Zone de melange D'un jet plan fluctuations induites dans le cone a potentiel-intermittence. Intern. J. Heat Mass Transf. 12, 1679 (1969)

75. BRADSHAW, P., FERRISS, D.H. and JOHNSON, R.F. : Turbulence in the noise producing region of a circular jet. J. Fluid Mech. 19, 591 (1964)

76. FIEDLER, H.E. : Transport of heat across a plane turbulent mixing layer. Adv. Geophysics 18A, 93 (1974)

77. BROWN, G.L. and ROSHKO, A. : On density effects and large structure in turbulent mixing layers. J. Fluid Mech. 64(4), 775 (1974)

78. WYGNANSKI, I. and FIEDLER, H.E. : The two-dimensional mixing region. J. Fluid Mech. 41(2), 327 (1970)

79. TOWNSEND, A.A. : The fully developed turbulent wake of a circular cylinder. Australian Inst. Sci. Res. 2A, 451 (1949)

80. FREYMUTH, P. and UBEROI, M.S. : Structure of temperature fluctuations in the turbulent wake behind a heated cylinder. Phys. Fluids 14(12), 2574 (1971)

81. FABRIS, G. : Turbulent temperature and thermal flux characteristics in the wake of a cylinder. Symposium on Turbulent Shear Flows (The Pennsylvania State University), 15.11 (1977)

82. LARUE, J.C. and LIBBY, P.A. : Temperature fluctuations in the plane turbulent wake. Phys. Fluids 17(11), 1956 (1974)

83. KOVASZNAY, L.S.G. and ALI, S.F. : Structure of the turbulence in the wake of a heated flat plate, Paper FC 3.2. Proc. 5th Intern. Heat Transf. Conf. (Vol. 4) Tokyo. (1975)

84. KESTIN , J. and RICHARDSON, P.D. : Heat trasnfer across turbulent, incompressible boundary layers. Intern. J. Heat Mass Transf. 6, 147 (1963)

85. REYNOLDS, W.C., KAYS, W.M. and KLINE, S.J. : Heat transfer in the turbulent incompressible boundary layer
(i) Constant wall temperature
(ii) Step wall-temperature distribution
(iii) Arbitrary wall temperature and heat flux
and (iv) Effects of location of transition and prediction of heat transfer in a known transition region.
NASA Memo 12-1-58W to 12-4-58W, (1958)

86. BLOM. J. : Experimental determination of the turbulent Prandtl number in a developing temperature boundary layer, Paper FC 2.2. 4th Intern. Heat Transf. Conf.. Paris. (1970)

87. FULACHIER, L., VEROLLET, E. and DEKEYSER, I. : Resultats experimentaux concernant une couche limite turbulente avec aspiration et chauffage a la paroi. Intern. J. Heat Mass Transf. 20, 731 (1977)

88. JOHNSON, D.S. : Velocity and temperature fluctuation measurements in a turbulent boundary layer downstream of a stepwise discontinuity in wall temperature. J. Appl. Mech., Trans ASME 81, 325 (1959)

89. JOHNSON, D.S. : Velocity, temperature and heat-transfer measurements in a turbulent boundary layer downstream of a stepwise discontinuity in wall temperature. J. Appl. Mech., Trans ASME 79, 2 (1958)

90. ANTONIA, R.A., DANH, H.Q. and PRABHU, A. : Response of a turbulent boundary layer to a step change in surface heat flux. J. Fluid Mech. 80(1), 153 (1977)

91. PIMENTA, M.M., MOFFAT, R.J. and KAYS, W.M. : The turbulent boundary layer: an experimental study of the transport of momentum and heat with the effect of roughness. Rep. No. HMT-21, Mech. Eng. Dept., Stanford University, (1975)

92. BREMHORST, K. and BULLOCK, K.J. : Spectral measurements of temperature and longitudinal velocity fluctuations in fully developed pipe flow. Intern. J. Heat Mass Transf. 13, 1313 (1970)

93. BOURKE, P.J. and PULLING, D.J. : A turbulent heat flux meter and some measurements of turbulence in air flow through a heated pipe. Intern. J. Heat Mass Transf. 13, 1331 (1970)

94. QUARMBY, A. and ANAND, R.K. : Axisymmetric turbulent mass transfer in a circular tube. J. Fluid Mech. 38(3), 433 (1969)

95. BLACK, A.W. : The effect of circumferentially-varing boundary conditions on turbulent heat transfer in a tube. PhD Thesis, University of Minnesota. (1966)

96. QUARMBY, A. and QUIRK, R. : Axisymmetric and non-axisymmetric turbulent diffusion in a plain circular tube at high Schmidt number. Intern. J. Heat Mass Transf. 17, 143 (1974)

97. GIESBRECHT, A.J. : Heat transfer from a yawed cylinder to air with a constant heat flux thermal boundary condition. M.S. Thesis, University of California, Davis. (1978)

98. KARLEKAR, B.V. and DESMOND, R.M. : Engineering heat transfer. West Publishing Company, New York. (1977)

99. ALEXOPOLOUS, C.C. and KEFFER, J.F. : Turbulent wake in a passively stratified fluid. Phys. Fluids 14(2), 216 (1971)

100. UBEROI, M.S. and FREYMUTH, P. : Spectra of turbulence in wakes behind circular cylinders. Phys. Fluids 12(7), 1359 (1969)

101. PATEL, R.P. : A study of two-dimensional symmetric and asymmetric turbulent shear flows. PhD Thesis, McGill University. (1970)

102. CHEVRAY, R. and KOVASZNAY, L.S.G. : Turbulent measurements in the wake of thin flat plate. AIAA J. 7, 1641 (1969)

103. JAYATILLEKE, C.L.V. : The influence of Prandtl number and surface roughness on the resistance of the laminar sub-layer to momentum and heat transfer. Prog. Heat Mass Transf. 1, 193 (1959)

0 0 0 0 4 9 0 2 0 8 8

104. FULACHIER, L. : Contribution à l'étude des analogies des champs dynamique et thermique dans une couche limite turbulente. Effect de l'aspiration. Thèse Docteur ès Sciences, Université de Provence. (1972)

105. BRADSHAW P. and FERRISS, D.H. : Calculation of boundary layer development using the turbulent energy equation. (IV) Heat transfer with small temperature difference. N.P.L. Aero. Rep. 1271, (1968)

106. REYNOLDS. W.C. : Turbulent heat transfer in a circular tube with variable circumferential heat flux. Intern. J. Heat Mass Transf. 6, 445 (1963)

107. SPARROW, E.M. and LIN, S.H. : Turbulent heat transfer in a tube with circumferentially varing temperature or heat flux. Intern. J. Heat Mass Transf. 6, 866 (1963)

108. BERGELES, G., GOSMAN, A.D. and LAUNDER, B.E. : The turbulent jet in a cross-stream at finite injection rates: A three-dimensional numerical treatment. (to be published)

109. MILLS, A.F. : Experimental investigation of turbulent heat transfer in the entrance region of a circular conduit. J. Mech Eng. Sci. 4(1), 63 (1962)

110. BIERNES DE HANN : Nouvelles tables d'intégrales définies. Hafner Publishing Company, New York. (1957)

111. ARIS, R. : Vectors, tensors and the basic equations of fluid mechanics. Prentice-Hall, N.J.. (1962)

112. LIN, S.C. and LIN, S.C. : Study of strong temperature mixing in subsonic grid turbulence. Phys. Fluids 16(10), 1587 (1973)

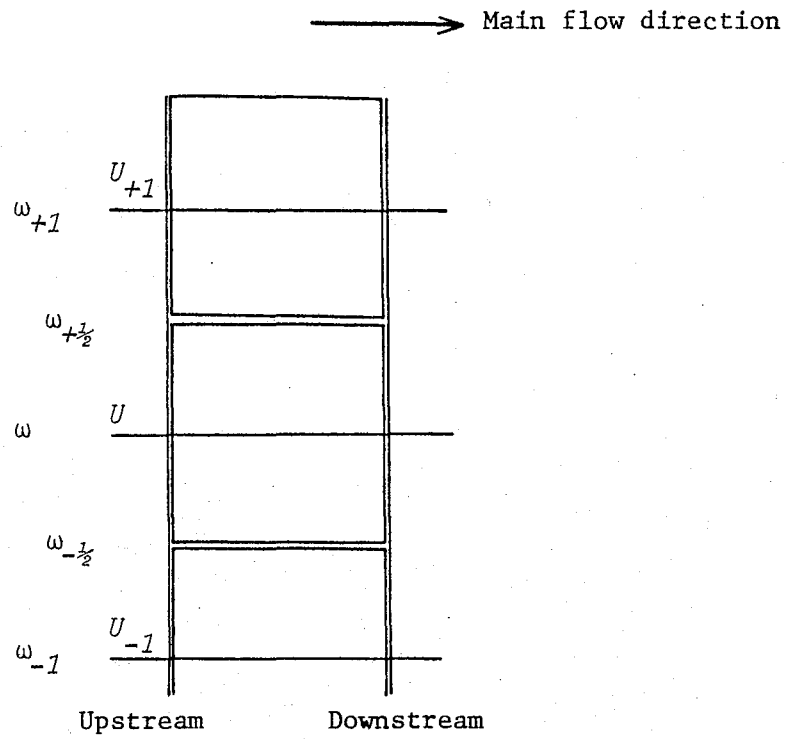

Fig. 3.1 Control Volumes in Patankar-Spalding Method

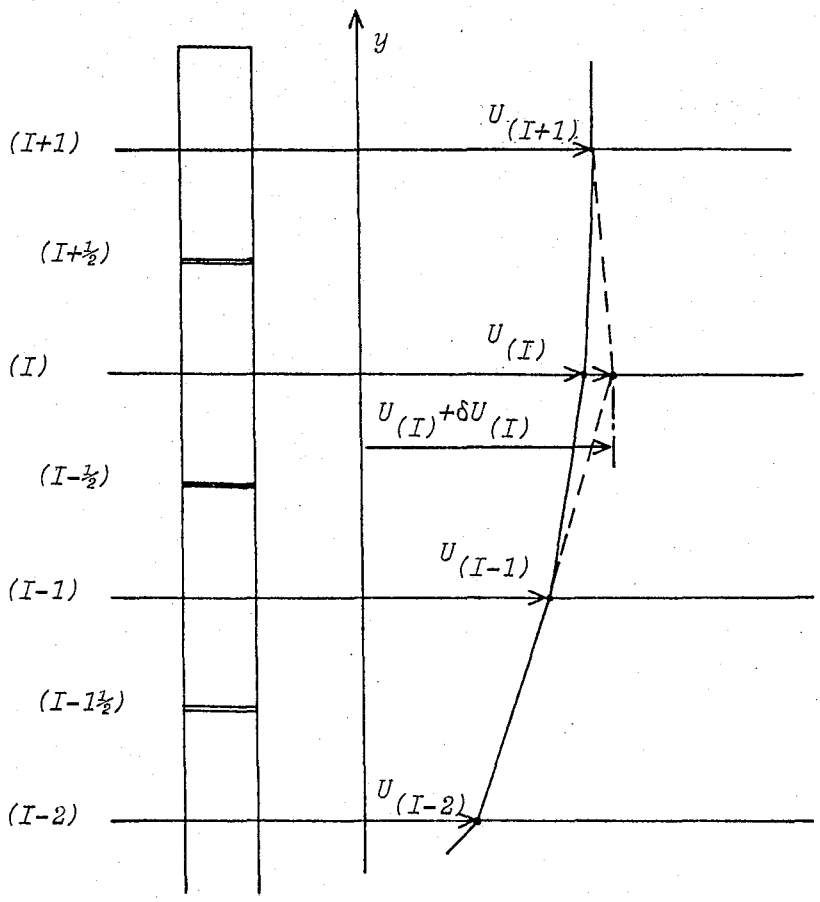

Fig. 3.2 Conventional Grid Arrangement

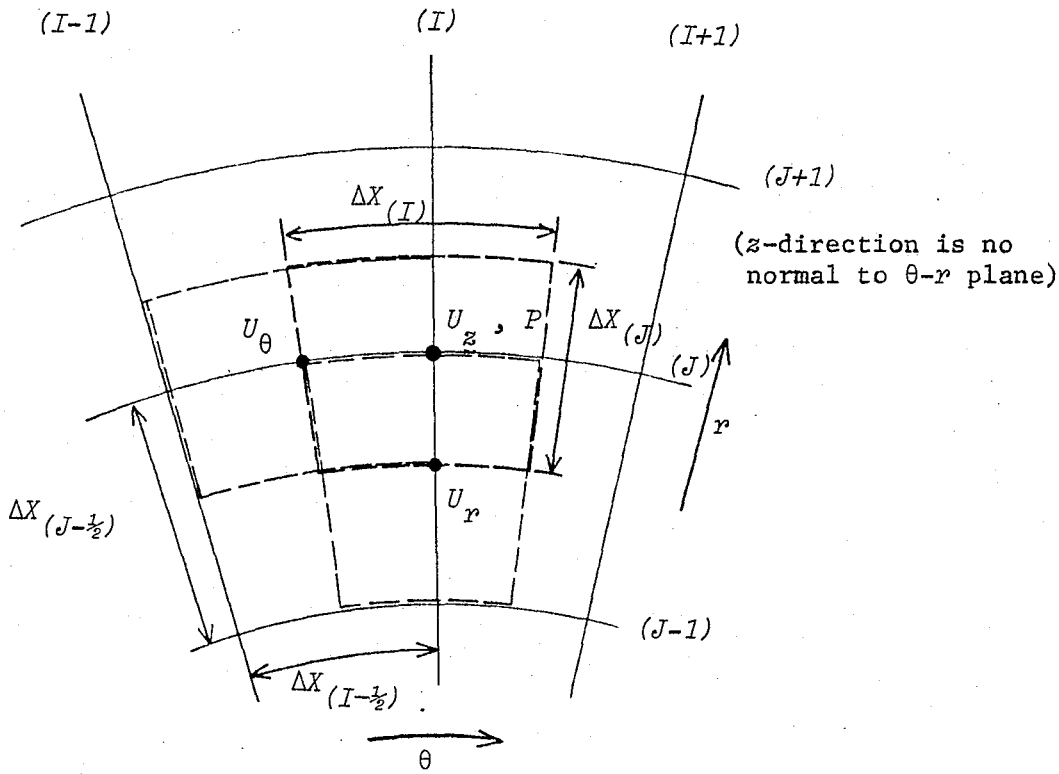

Fig. 3.3 Grid Layout in the Cross-Stream

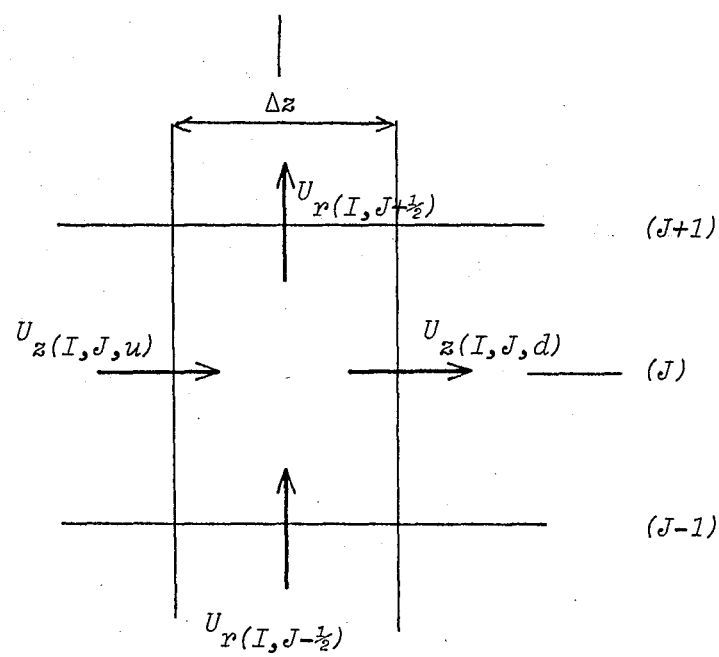

(Plane-I)

Fig. 3.4 Cell Mass Balance

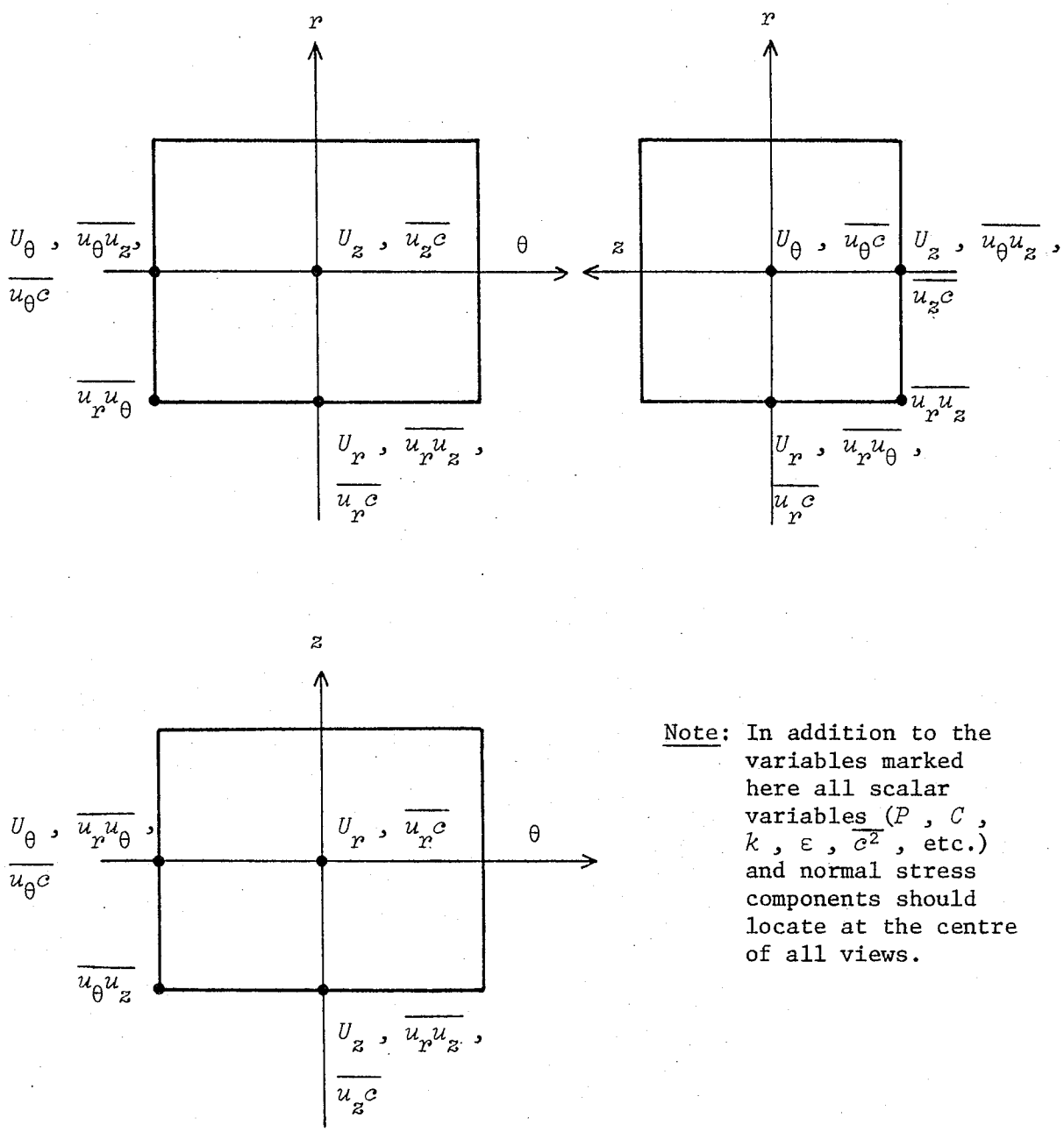

Note: In addition to the variables marked here all scalar variables (P , C , k , ε , $\overline{c^2}$, etc.) and normal stress components should locate at the centre of all views.

Fig. 3.5 Three orthogonal views of control volume with ideal orientation of stresses and fluxes. (A Cartesian, non expanding grid is shown here for clarity)

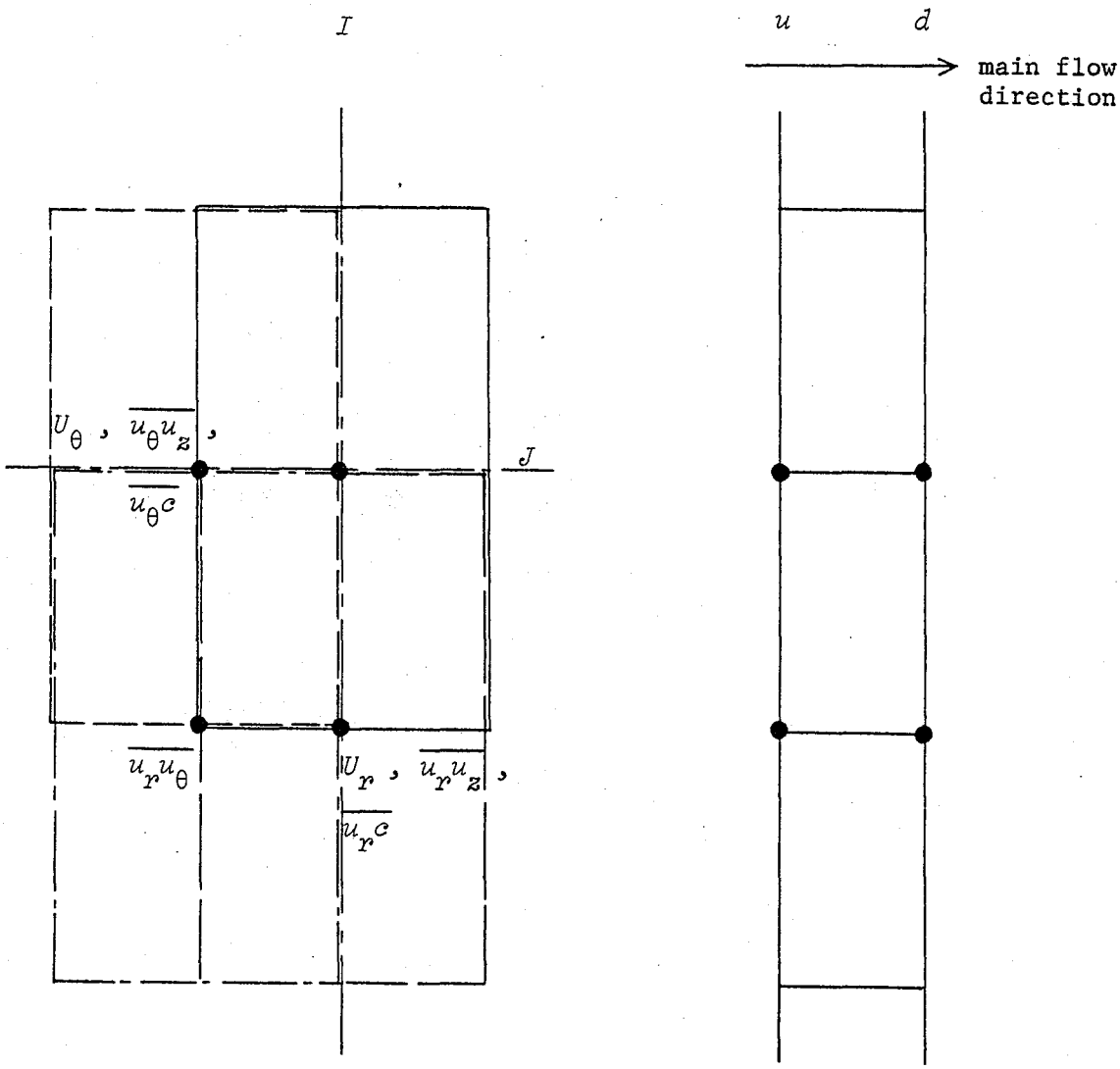

Note: All scalar variables and z components of all first-order vectors are located at (I,J)

Fig. 3.6 Idealised Grid System for Three-Dimensional Boundary Layer Flows

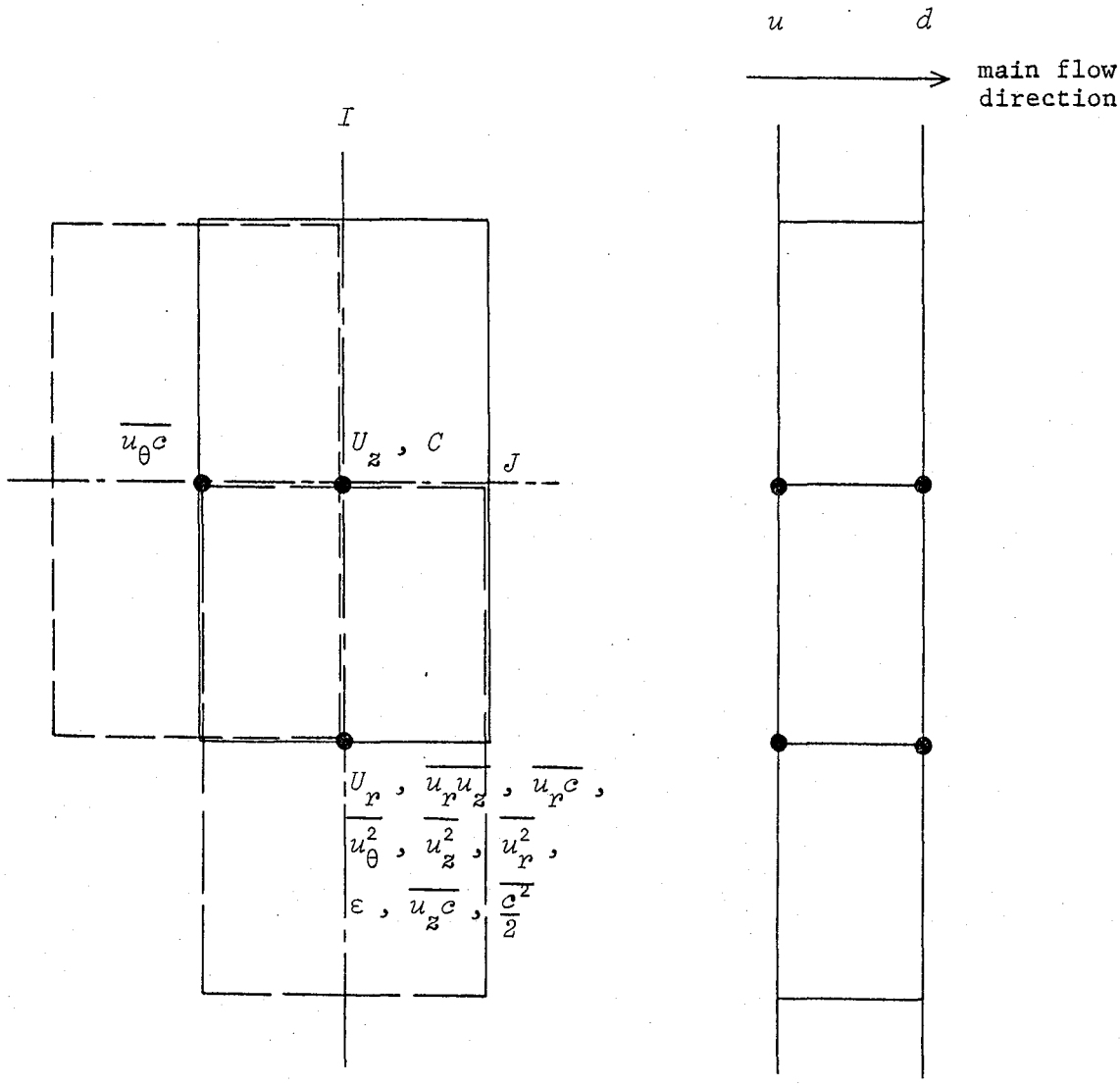

Fig. 3.7 Modified Grid System for the Present Problem

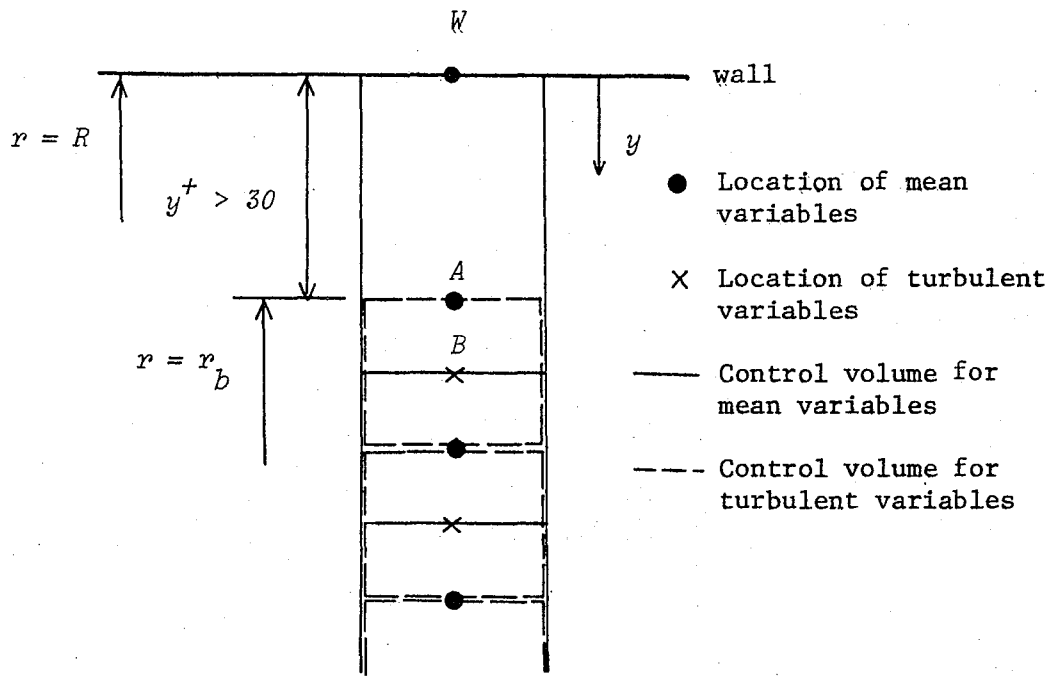

Fig. 3.8 Typical Grid Pattern in the Near-wall Region

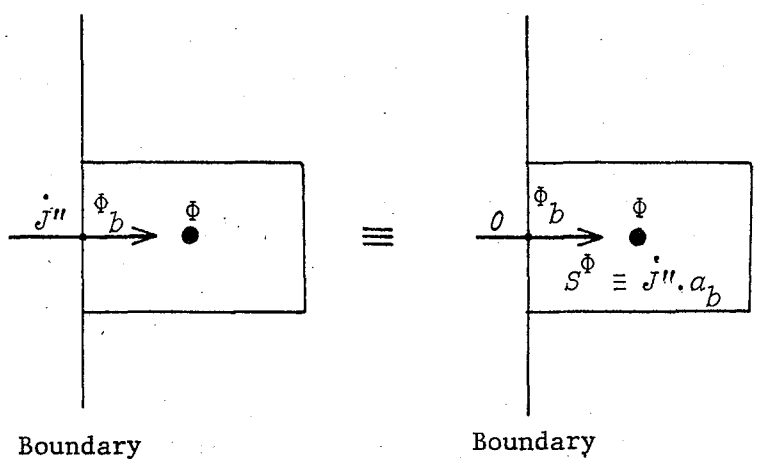

Fig. 3.9 False-Source Term Technique

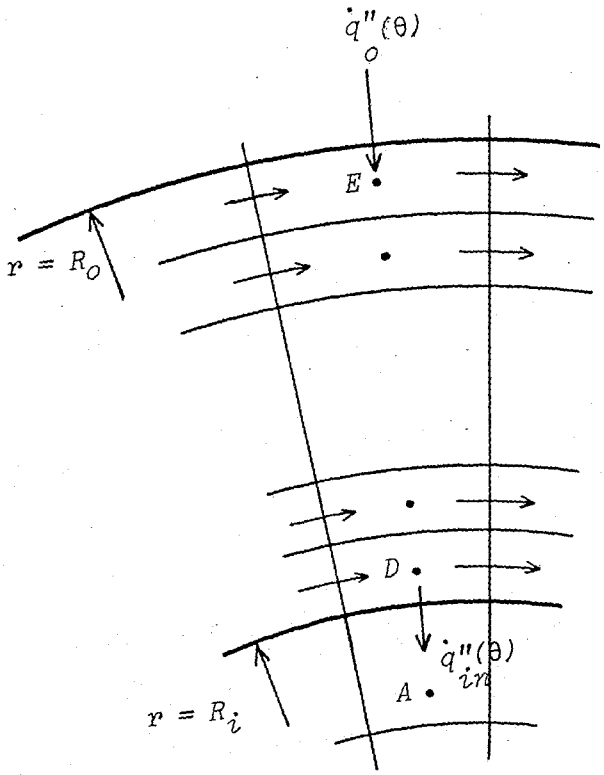

Fig. 3.10 Treatment of a Conducting Thick Wall

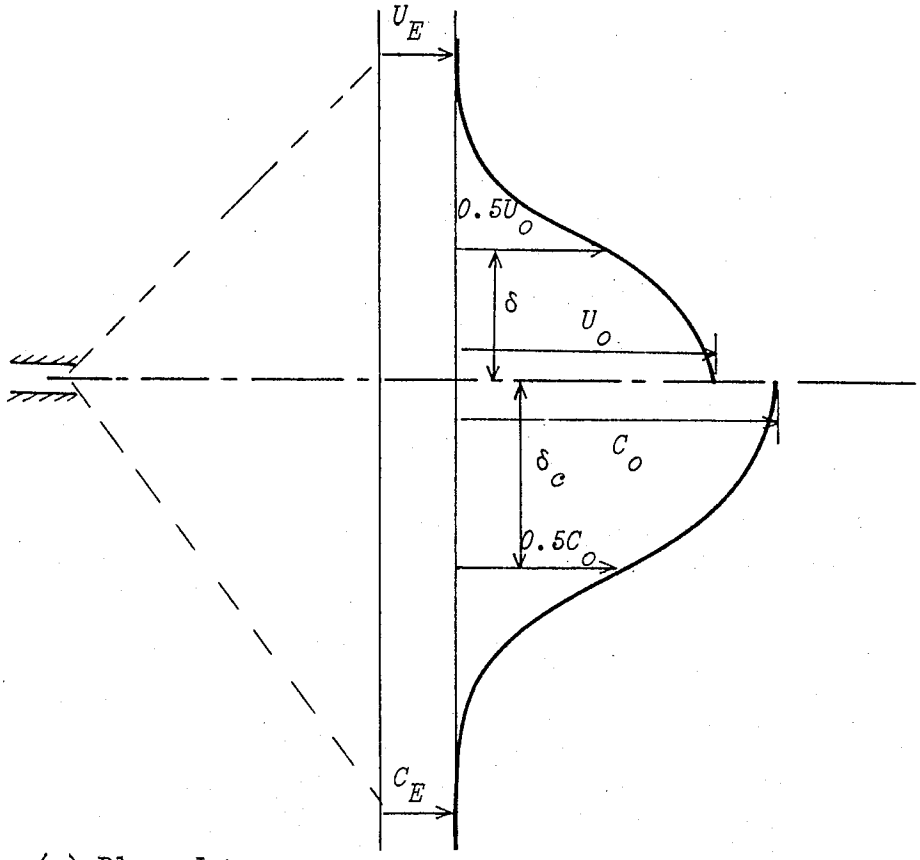

(a) Plane Jet

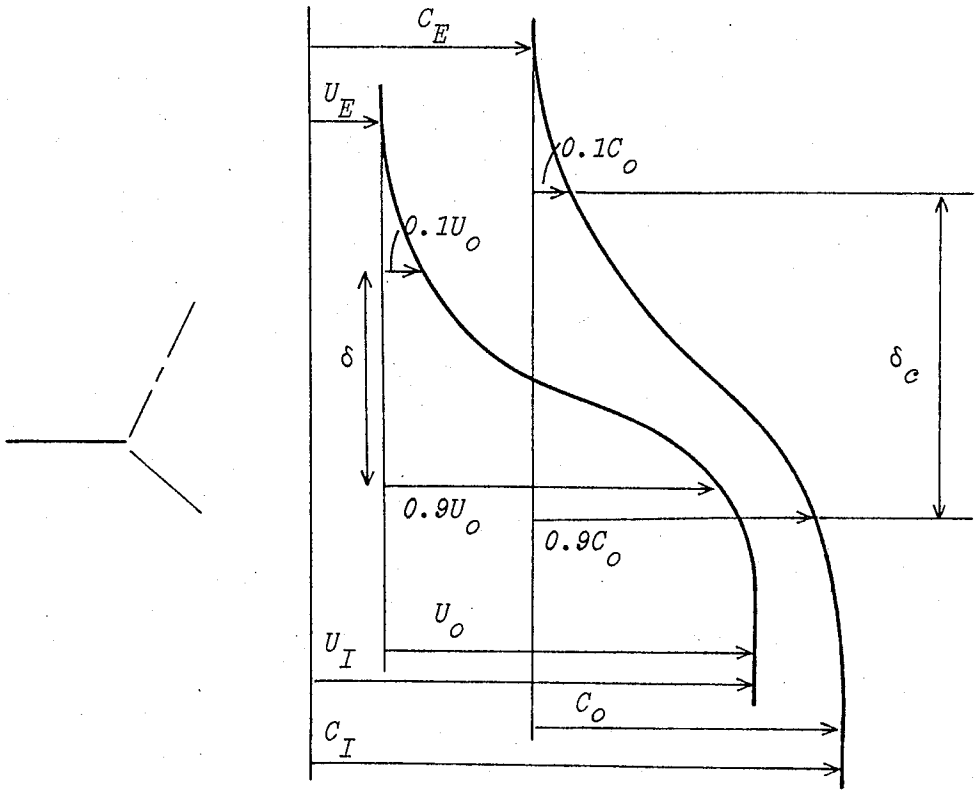

(b) Plane Mixing Layer

Fig. 4.1 (a) and (b)

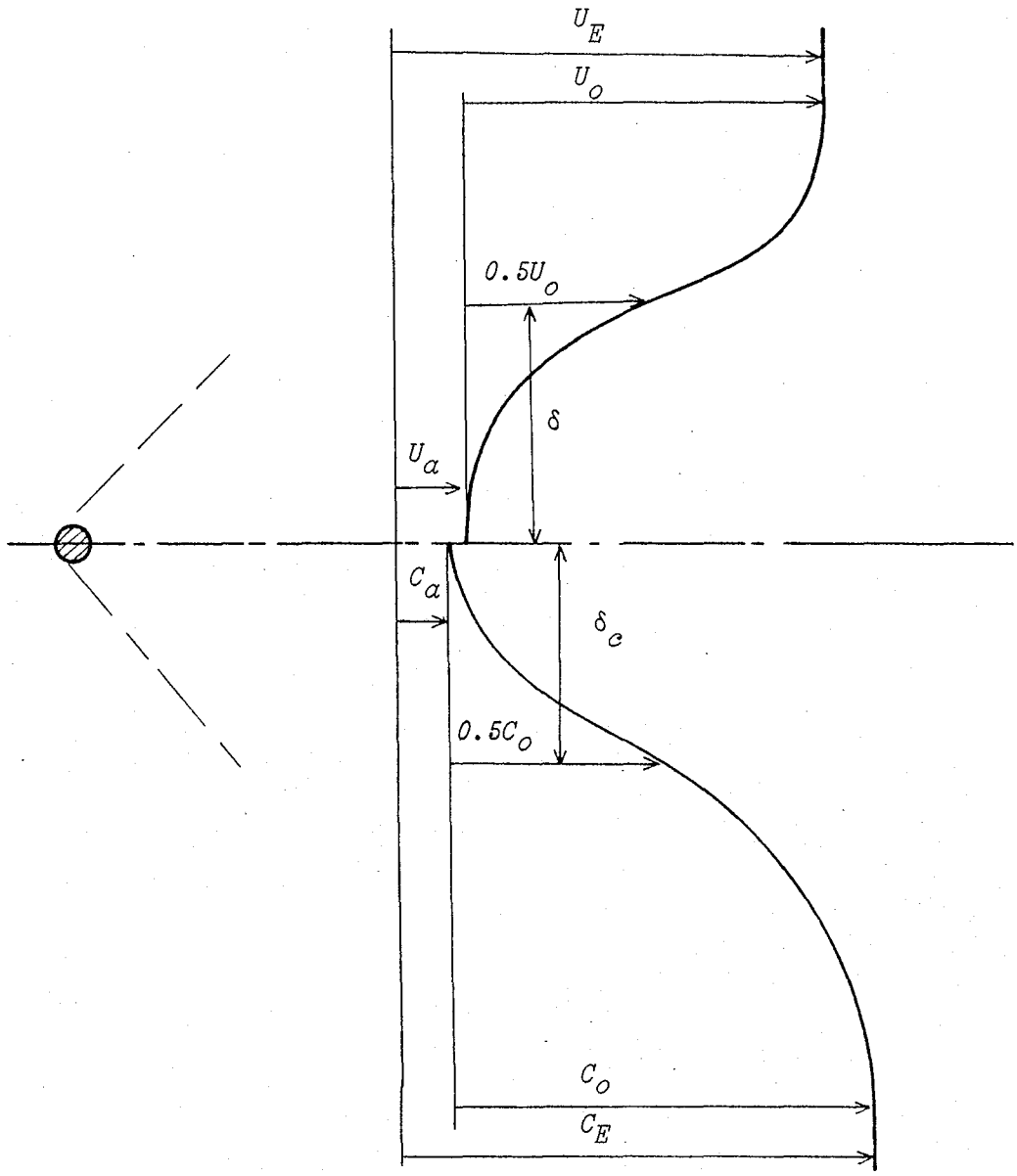

(c) Plane Wake

Fig. 4.1 Notation for Velocity and Scalar Field Configurations

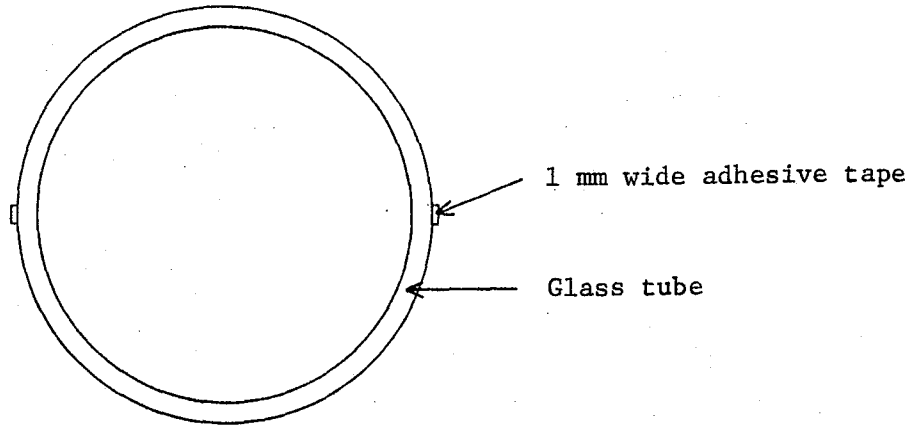

Fig. 5.1 Adhesive Tape Strips

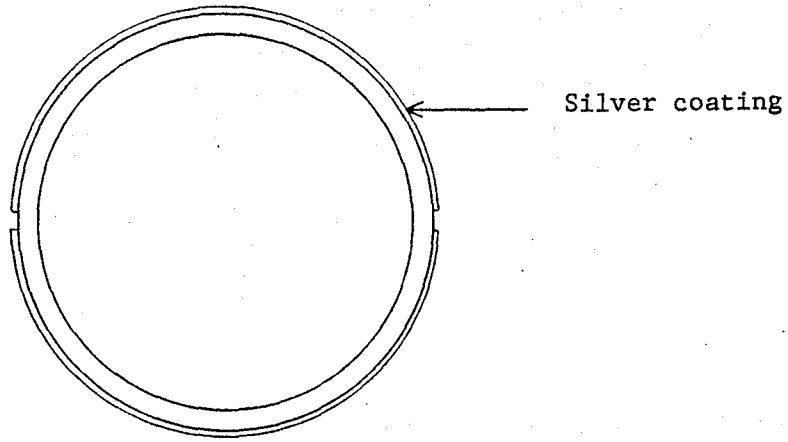

Fig. 5.2 Silver Coating on the Tube

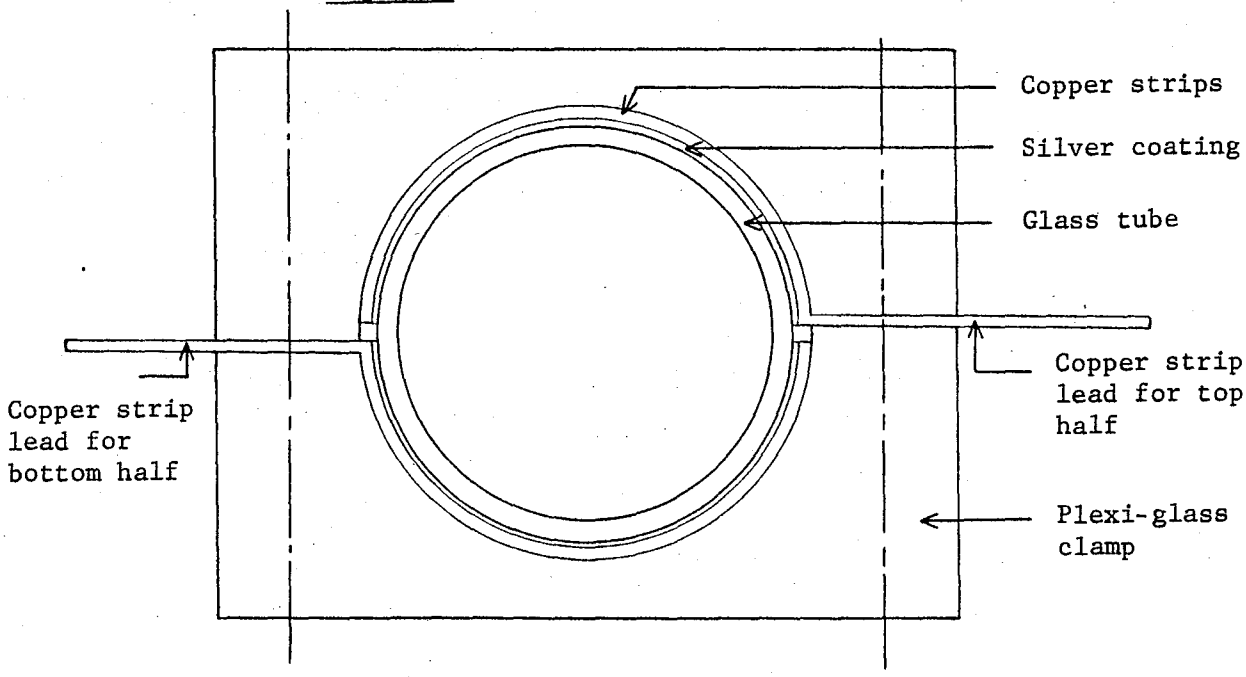

Fig. 5.3 Electrical Connections to the Silver Coating

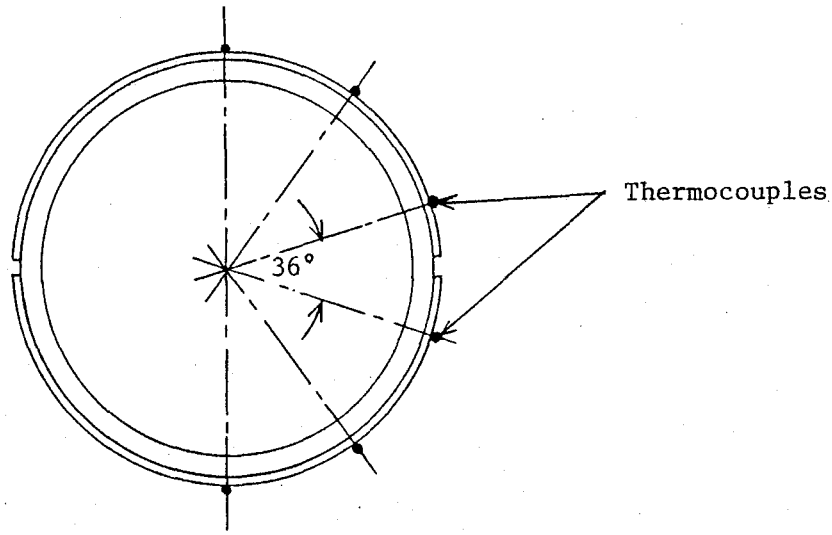

Fig. 5.4 Thermocouple Arrangement Around the Tube

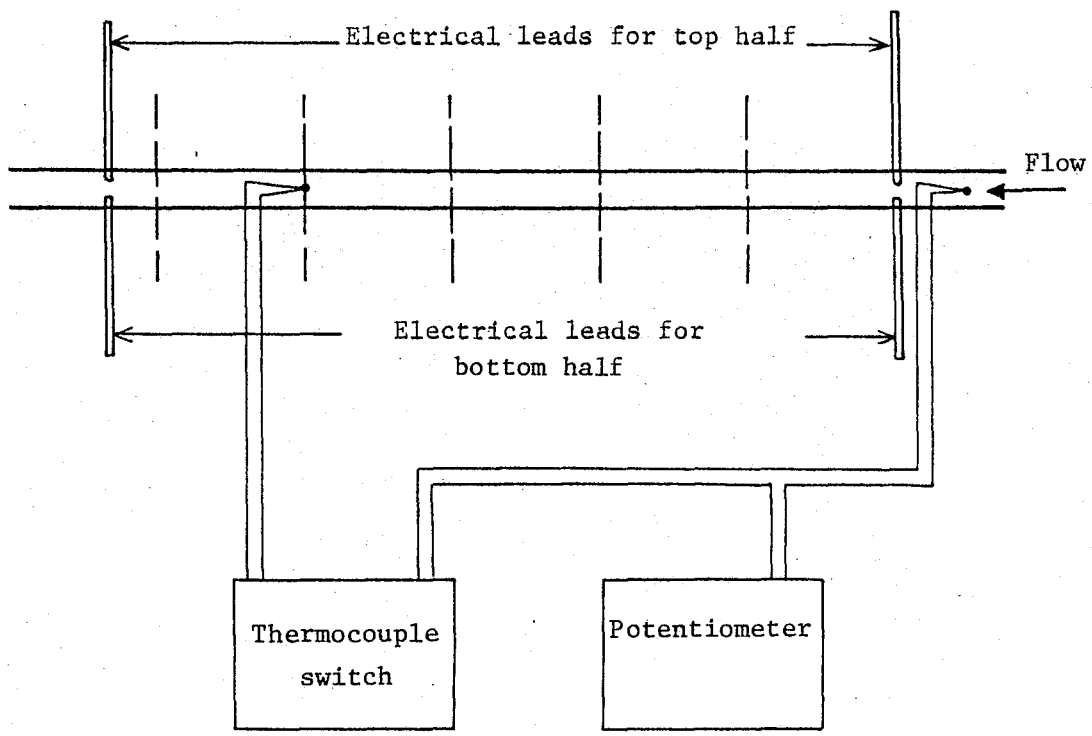

Fig. 5.5 Thermocouple Circuit

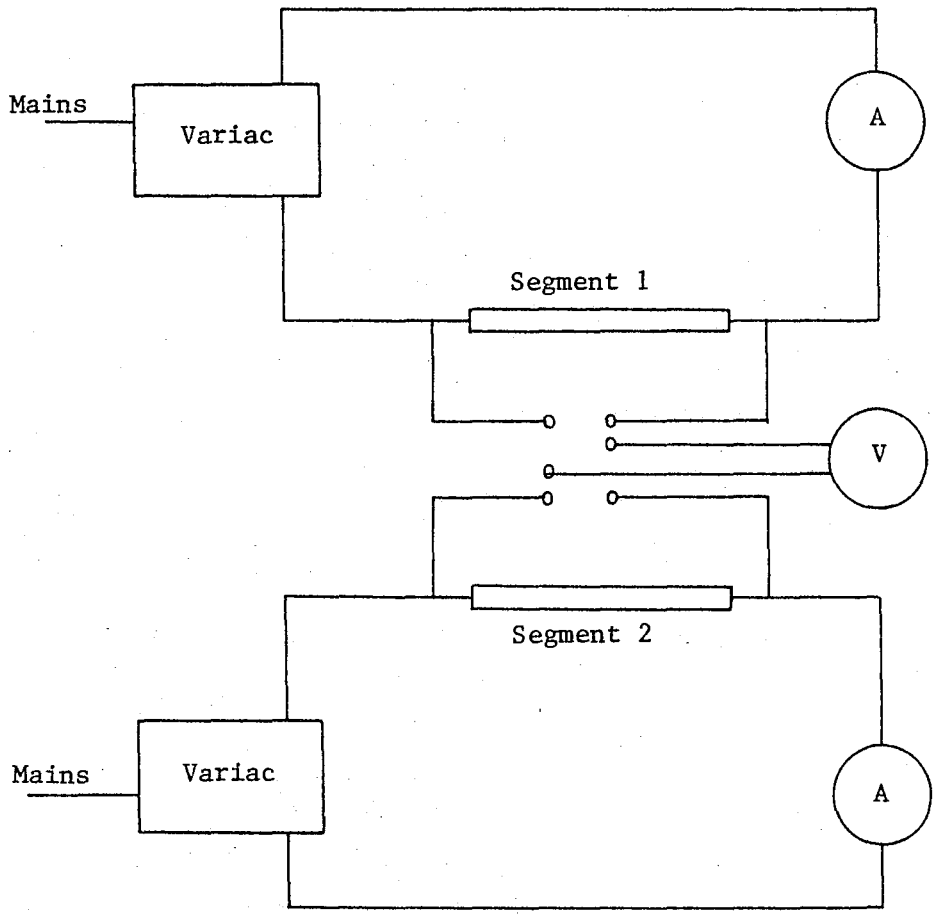

Fig. 5.6 Electrical Power Circuit

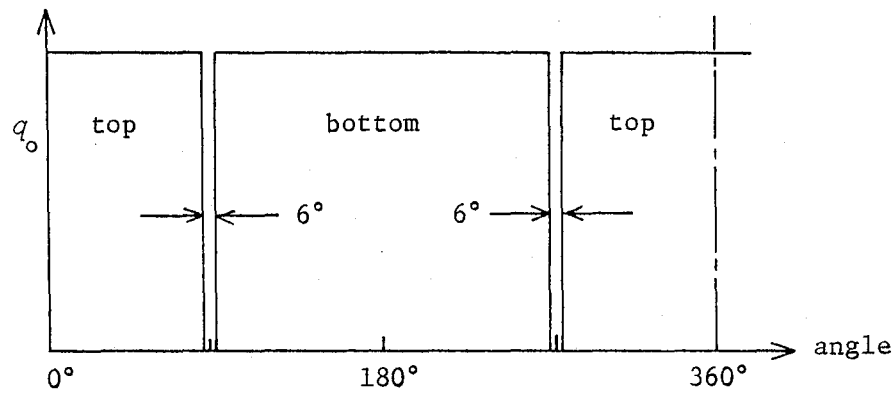

(a) Heat Flux Variation if Both Segments were Heated

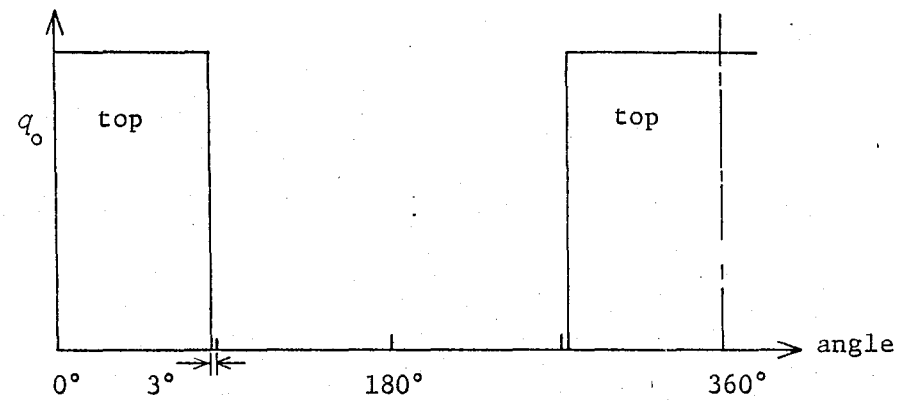

(b) Heat Flux Variation if Only Top Segment Heated

Fig. 5.7 Heat Flux Variation (Ideal)

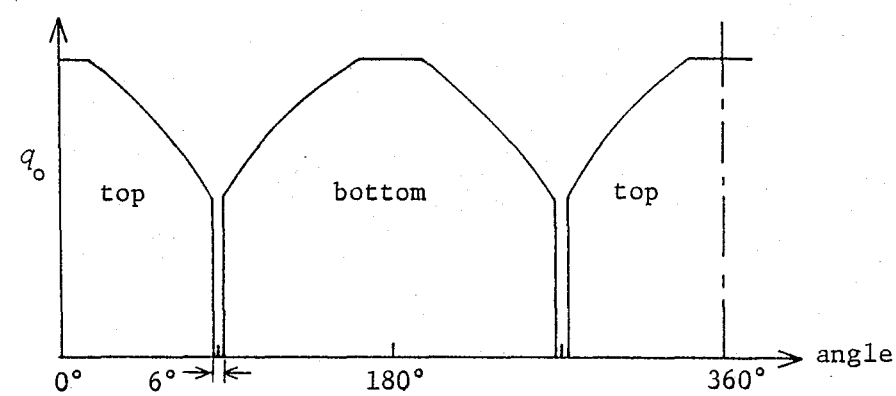

(a) Heat Flux Variation if Both Segments were Heated

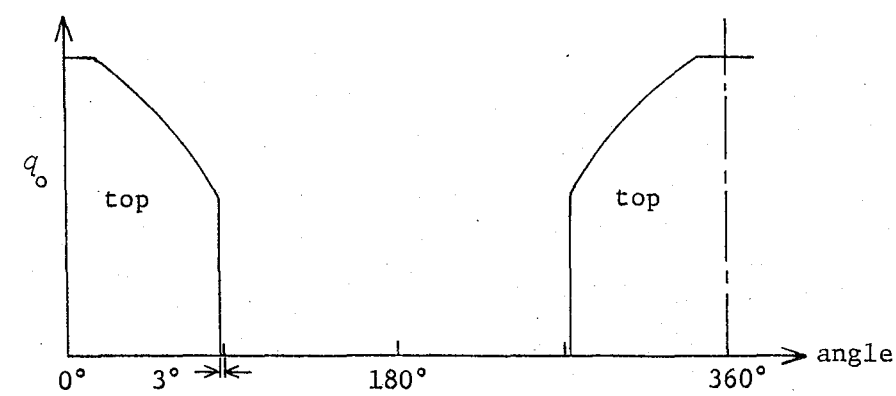

(b) Heat Flux Variation if Only Top Segment Heated

Fig. 5.8 A More Plausible Heat Flux Variation

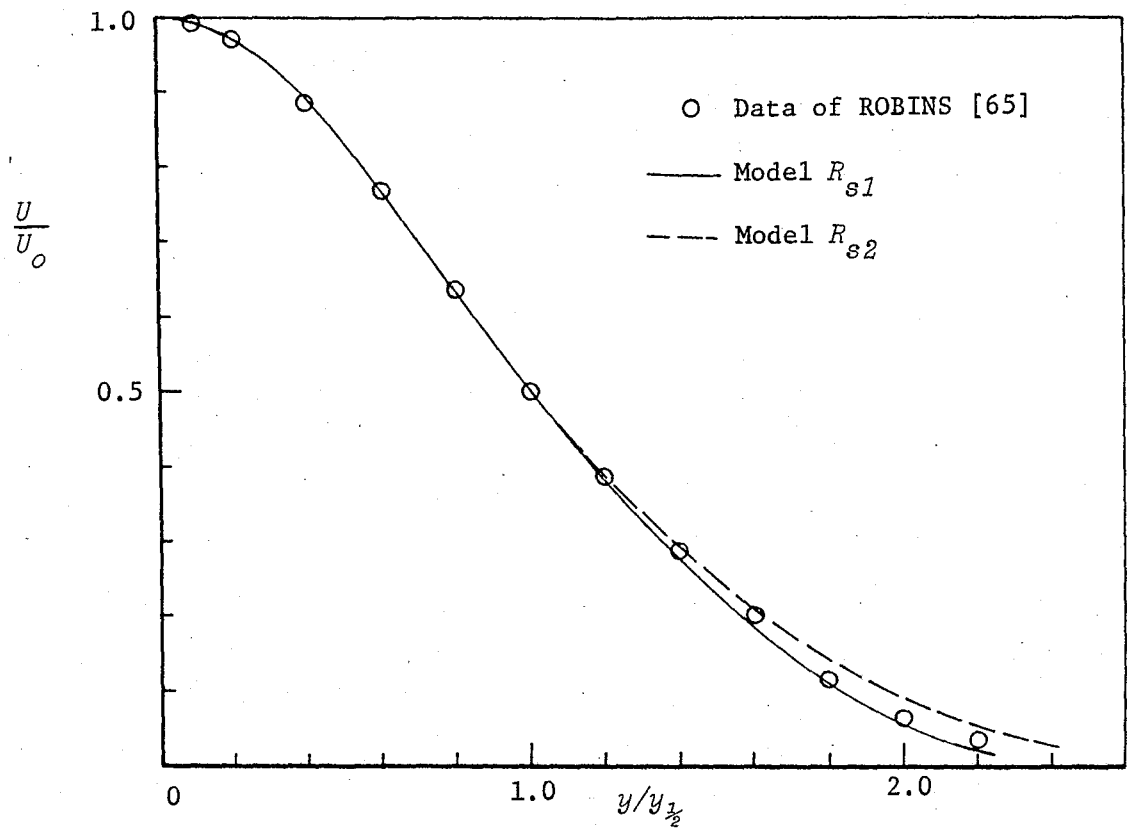

Fig. 6.1 The Plane Jet in Stagnant Surroundings : Mean Velocity Profiles

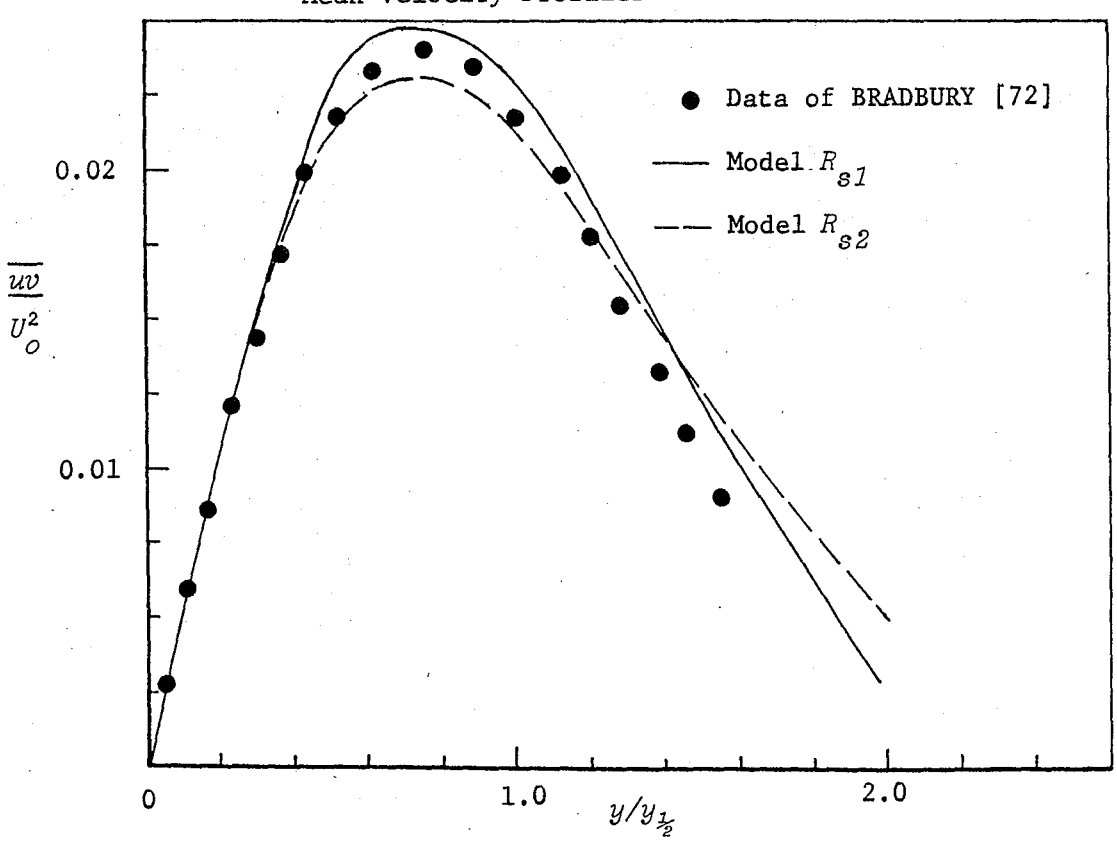

Fig. 6.2 The Plane Jet in Stagnant Surroundings : Shear Stress Profiles

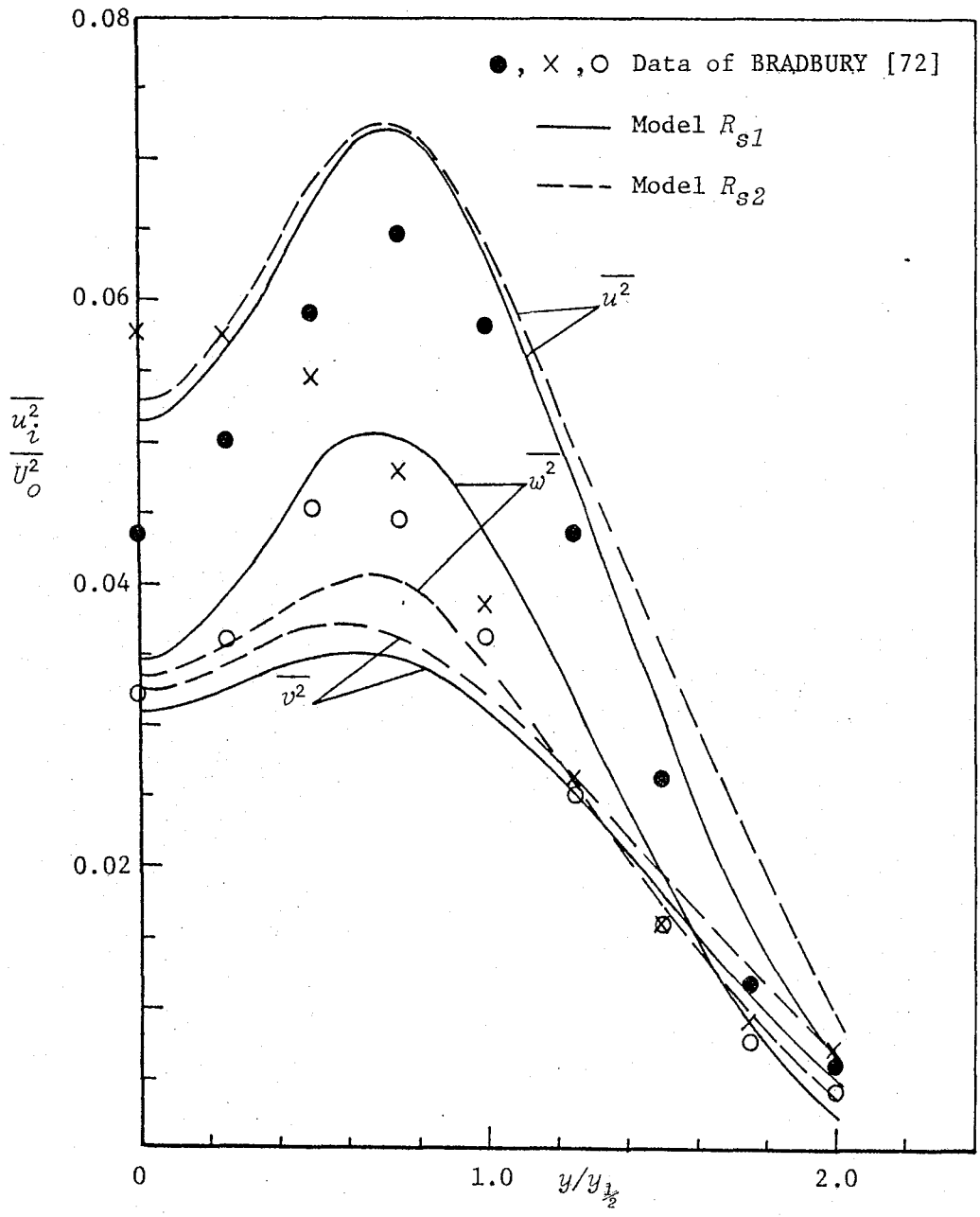

Fig. 6.3 The Plane Jet in Stagnant Surroundings : Turbulence Intensity Profiles

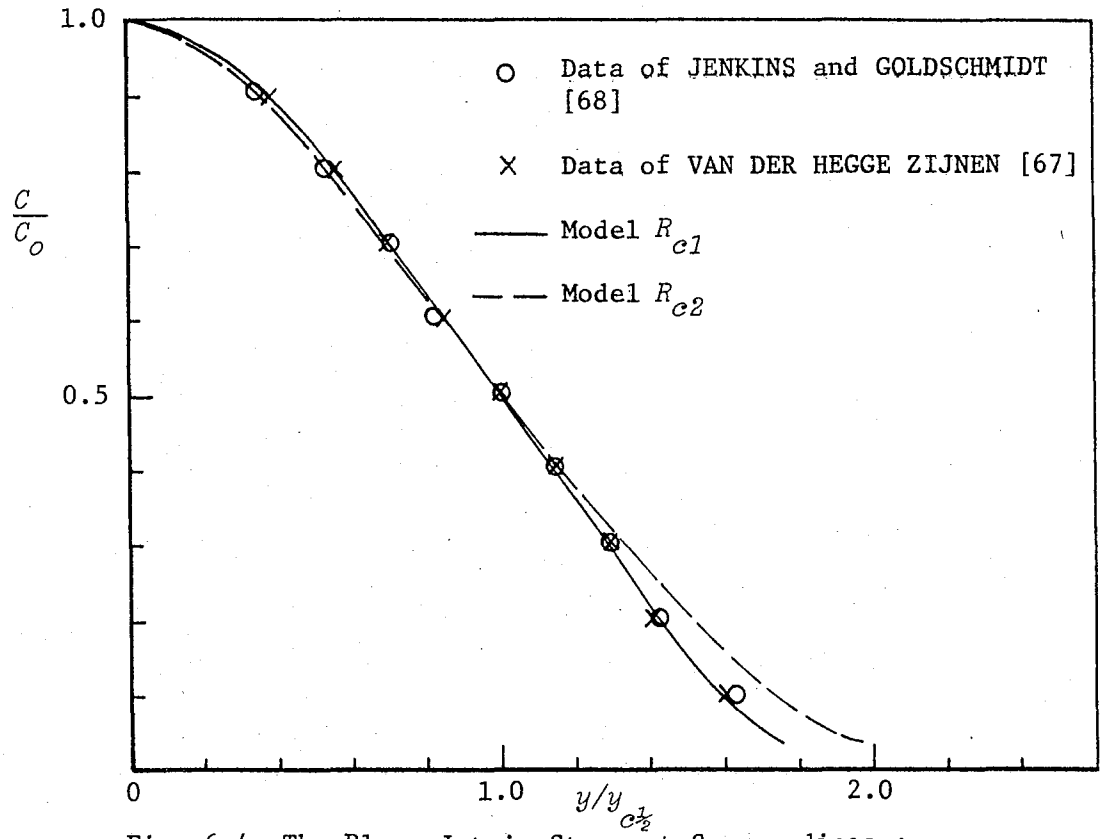

Fig. 6.4 The Plane Jet in Stagnant Surroundings : Mean Temperature Profiles

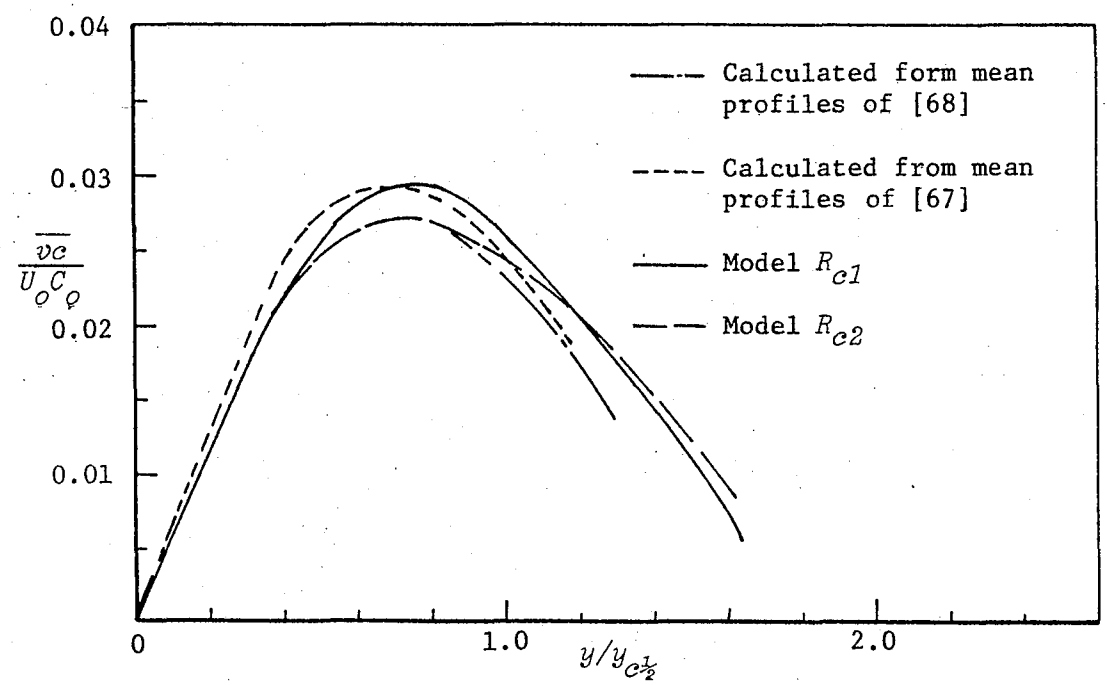

Fig. 6.5 The Plane Jet in Stagnant Surroundings : Cross-stream Heat Flux Profiles

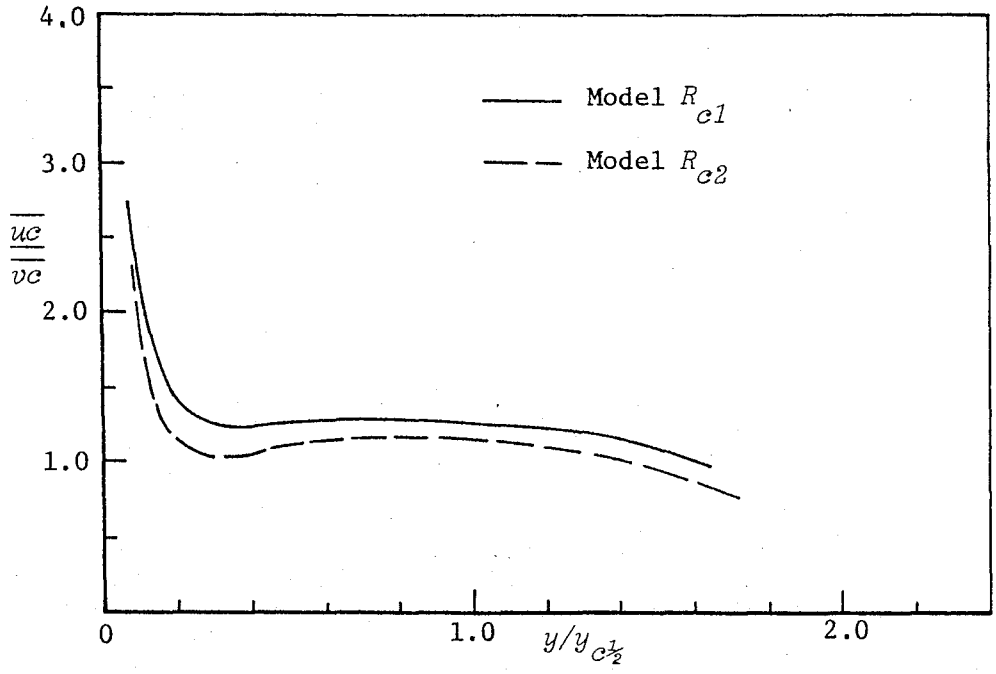

Fig. 6.6 The Plane Jet in Stagnant Surroundings : The Ratio of Streamwise to Cross-stream Scalar Flux Profiles

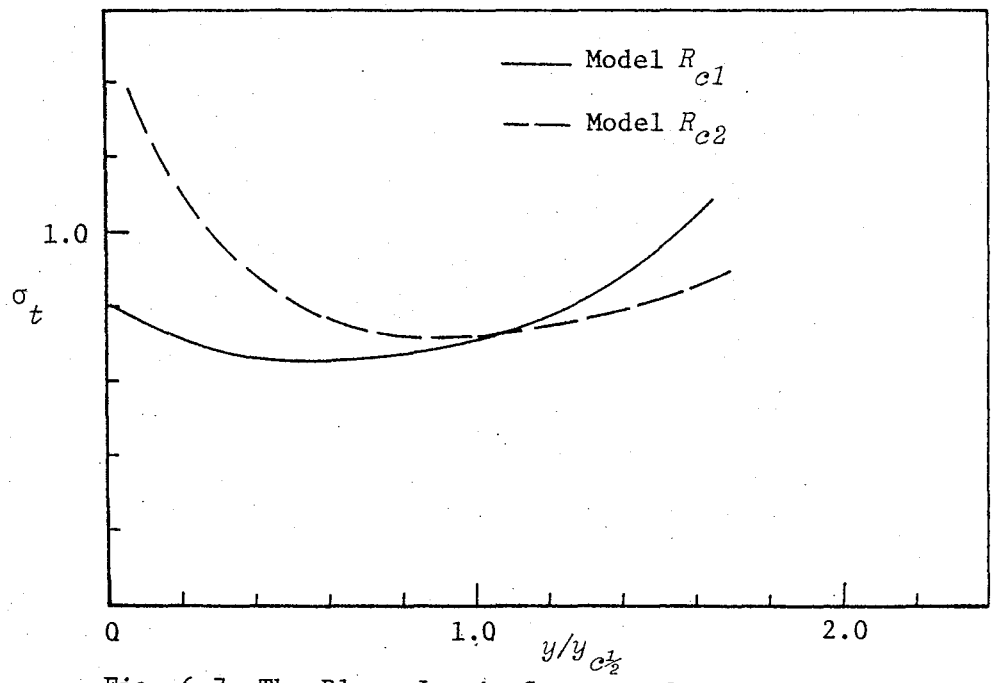

Fig. 6.7 The Plane Jet in Stagnant Surroundings : Turbulent Prandtl Number Profiles

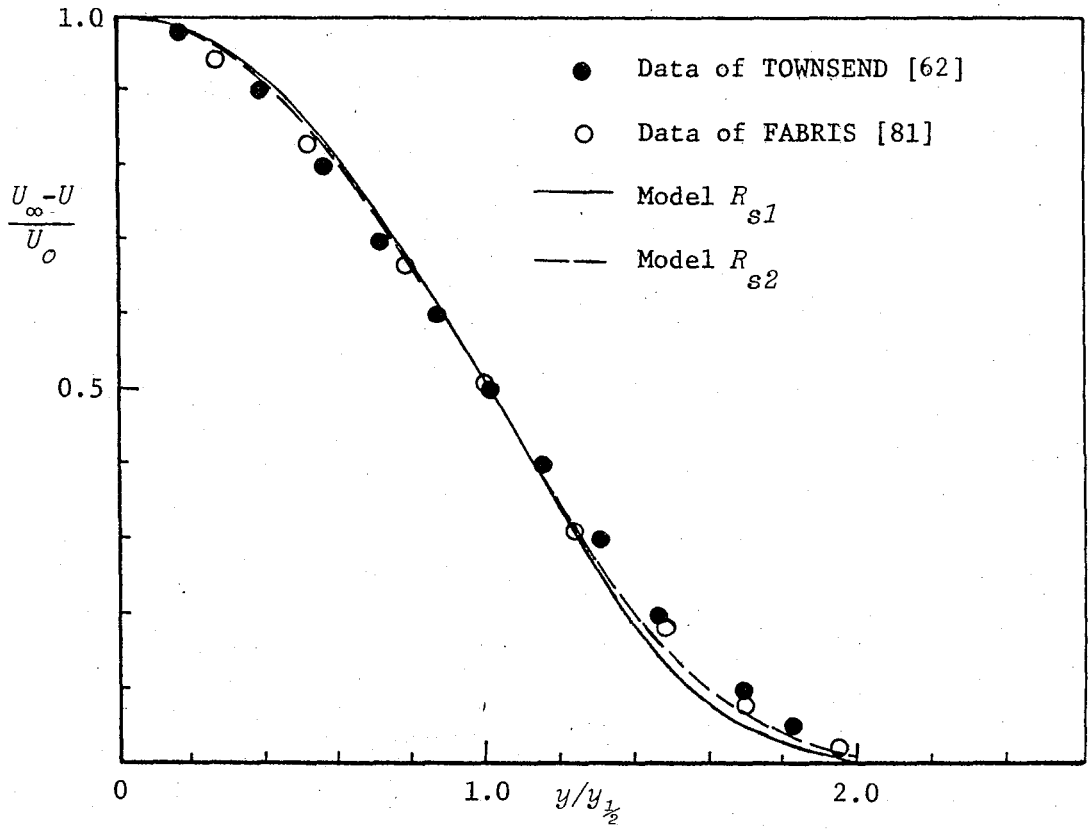

Fig. 6.8 The Plane Wake : Mean Velocity Profiles

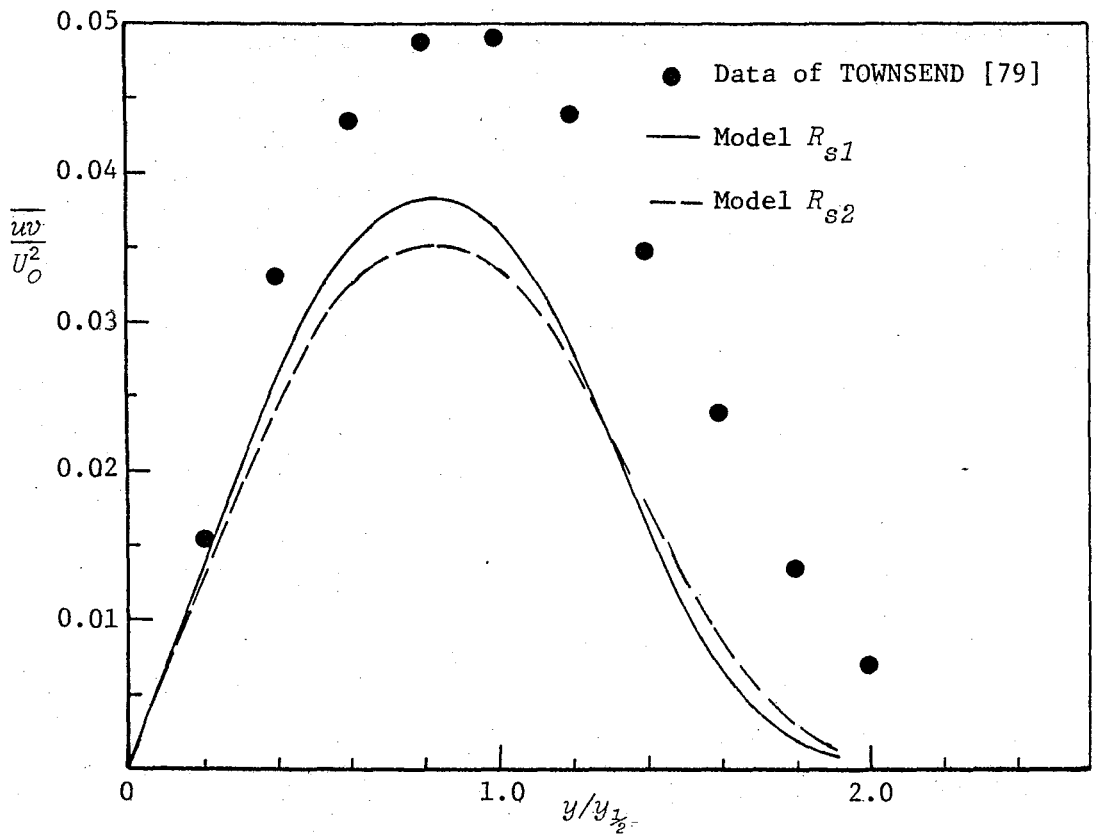

Fig. 6.9 The Plane Wake : Shear Stress Profiles

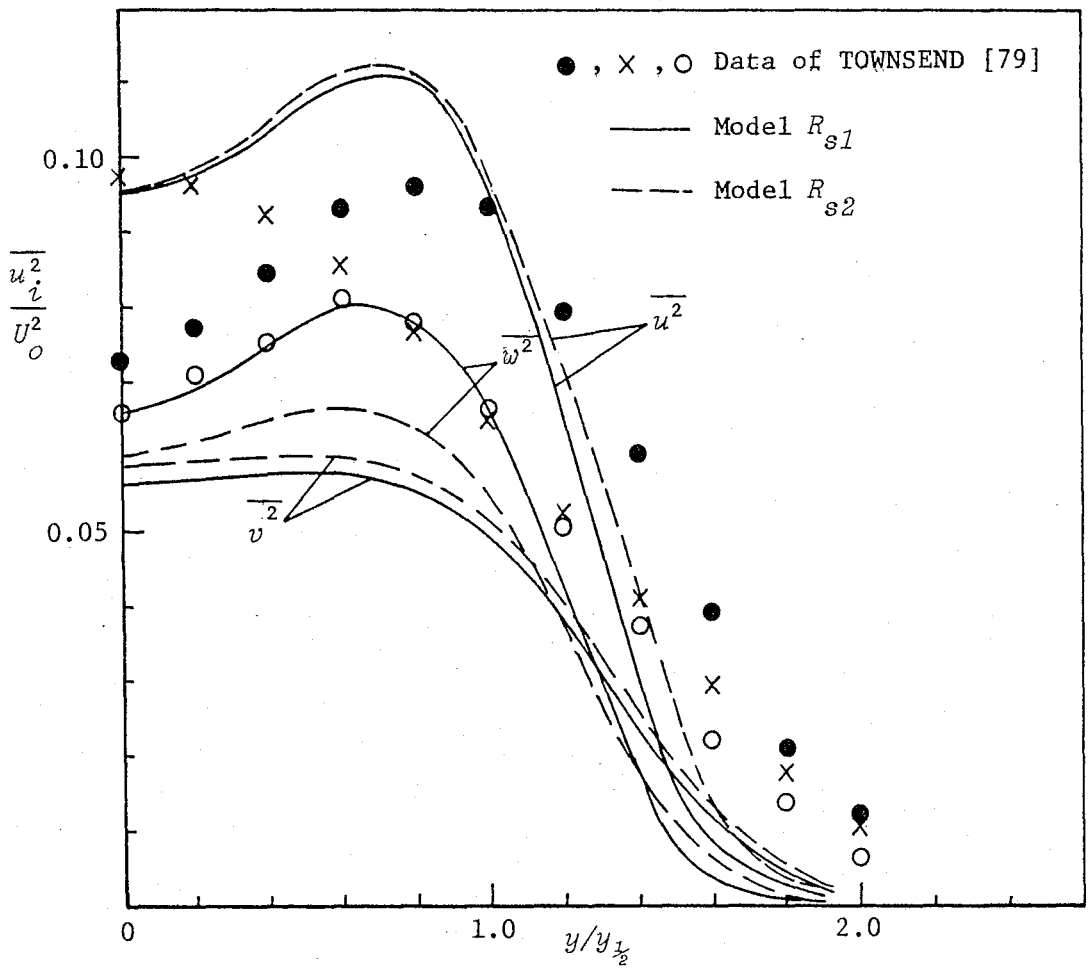

Fig. 6.10 The Plane Wake : Turbulence Intensity Profiles

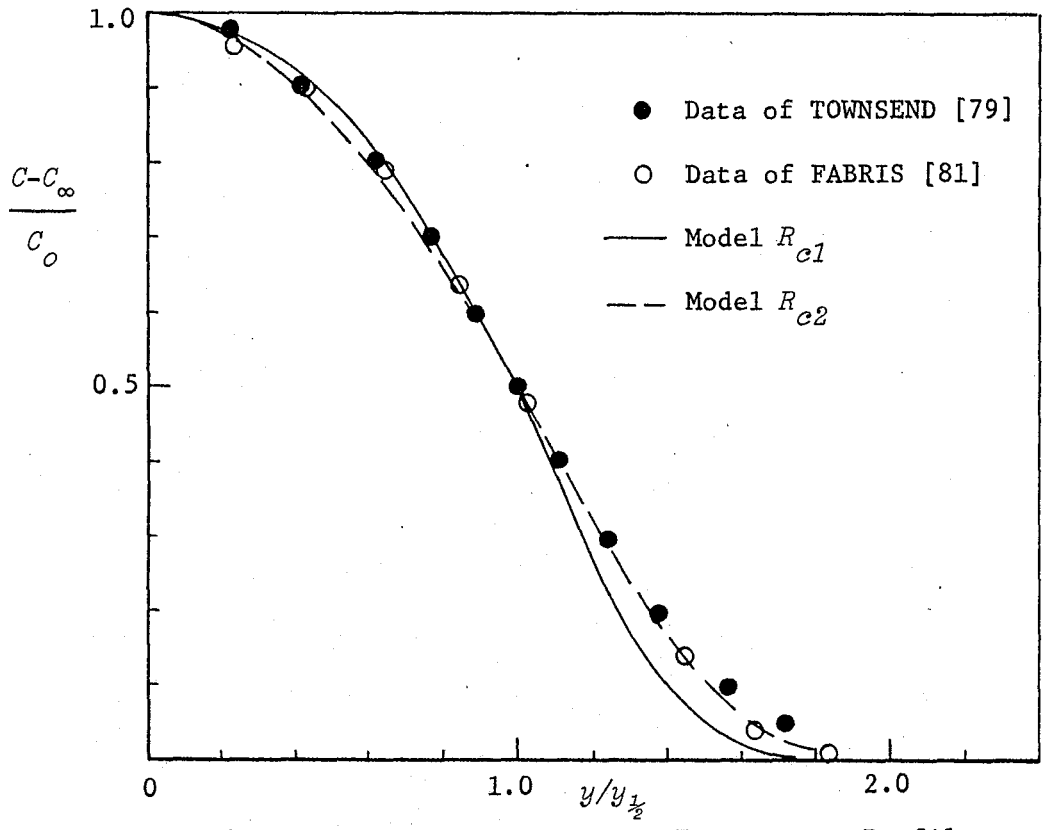

Fig. 6.11 The Plane Wake : Mean Temperature Profiles

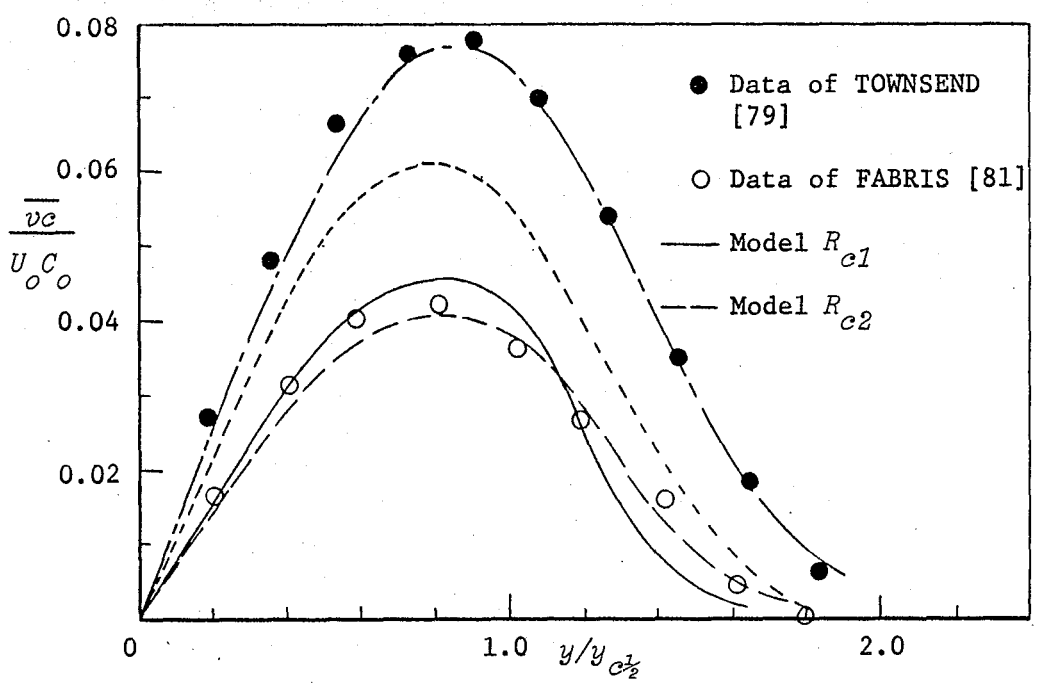

Fig. 6.12 The Plane Wake : Cross-stream Heat Flux Profiles,
—·— Calculated profiles from Townsend's mean data,
------- Calculated profiles from Fabris' mean data

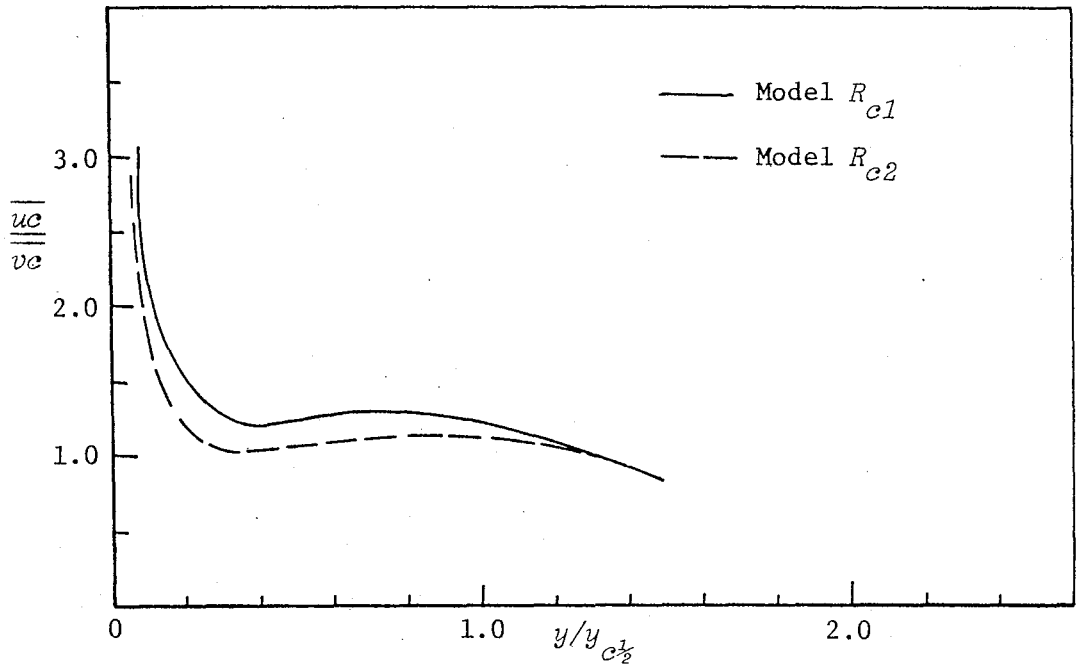

Fig. 6.13 The Plane Wake : Ratio of Streamwise to Cross-stream Scalar Flux Profiles

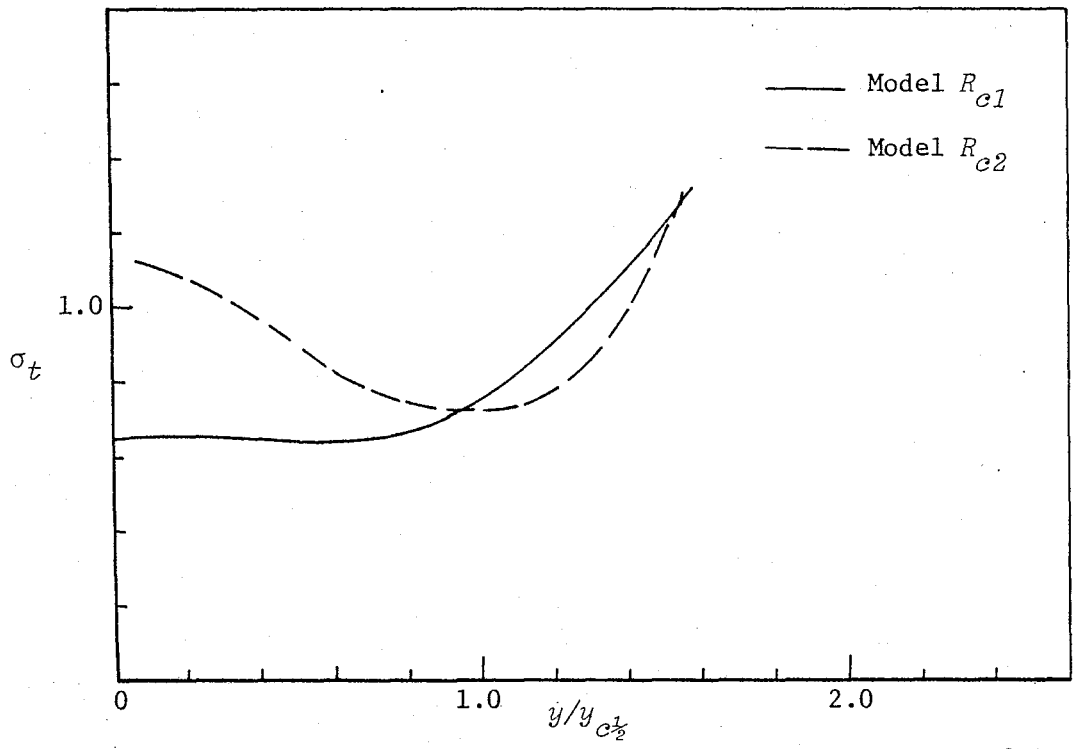

Fig. 6.14 The Plane Wake : Turbulent Prandtl Number Profiles

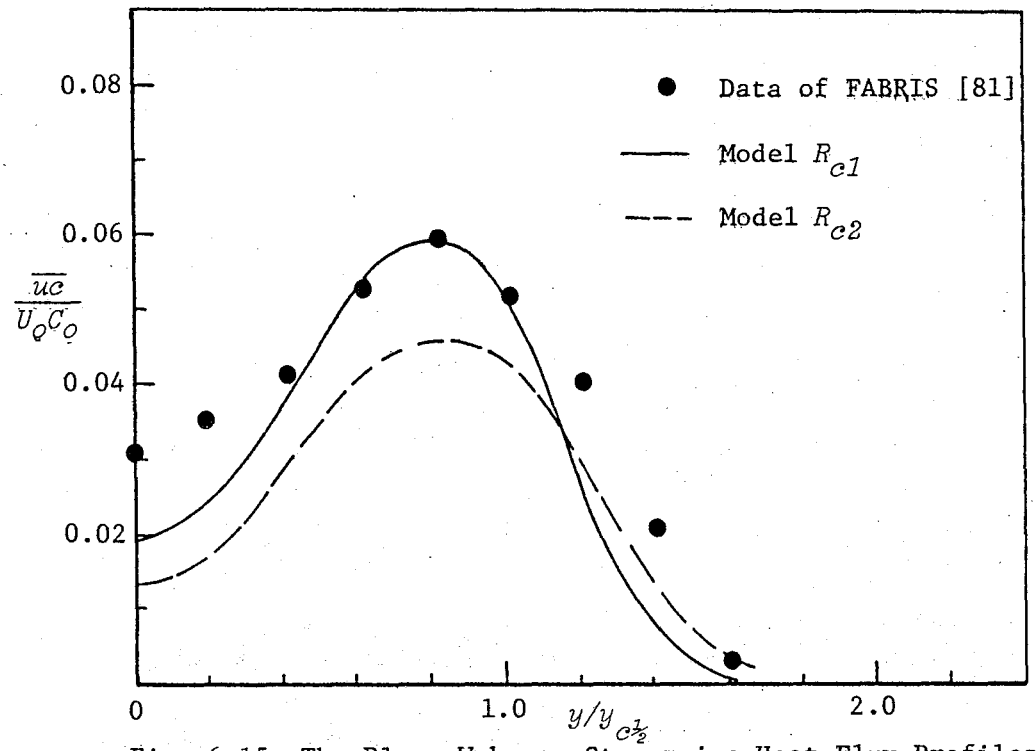

Fig. 6.15 The Plane Wake : Streamwise Heat Flux Profiles

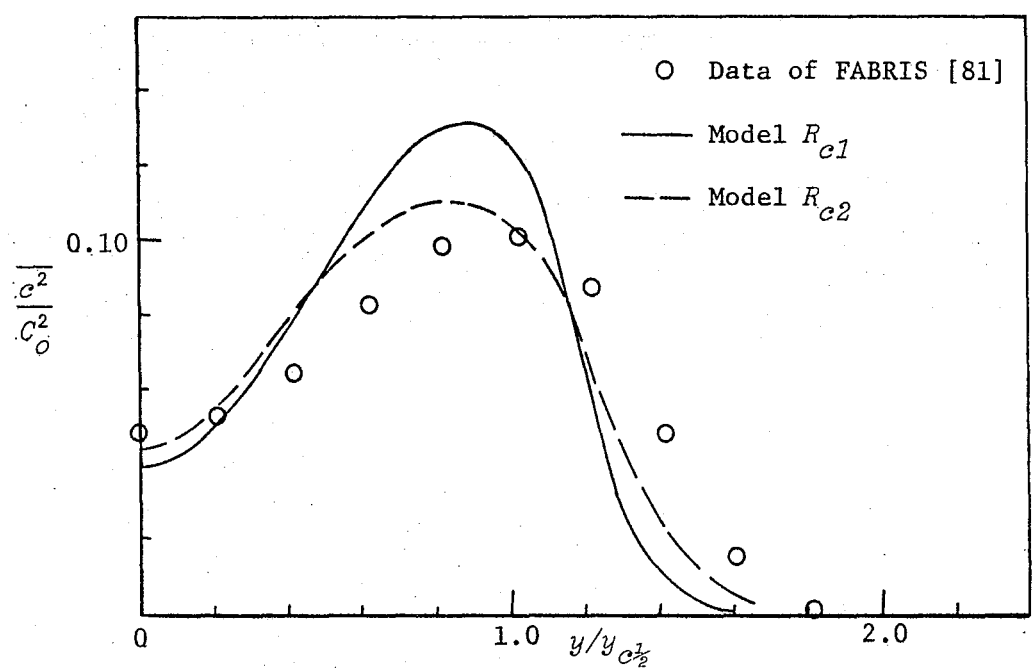

Fig. 6.16 The Plane Wake : Temperature Fluctuations Profiles

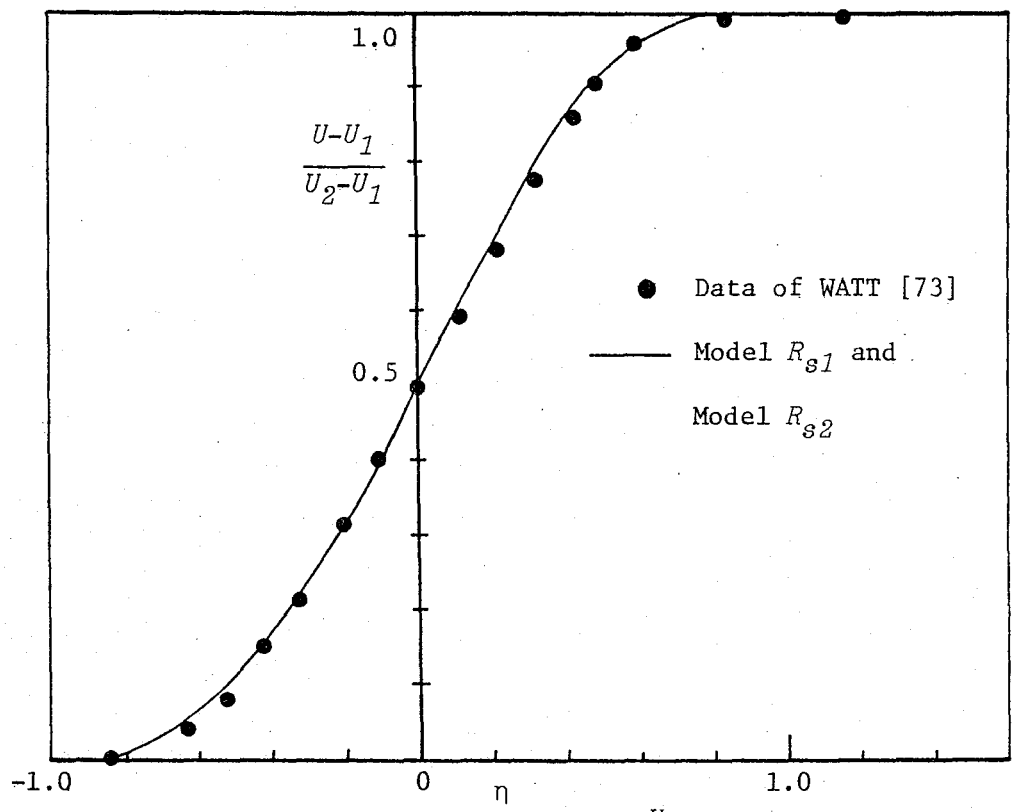

Fig. 6.17 The Plane Mixing Layer with $\frac{U_1}{U_2} = 0.5$:

Mean Velocity Profiles

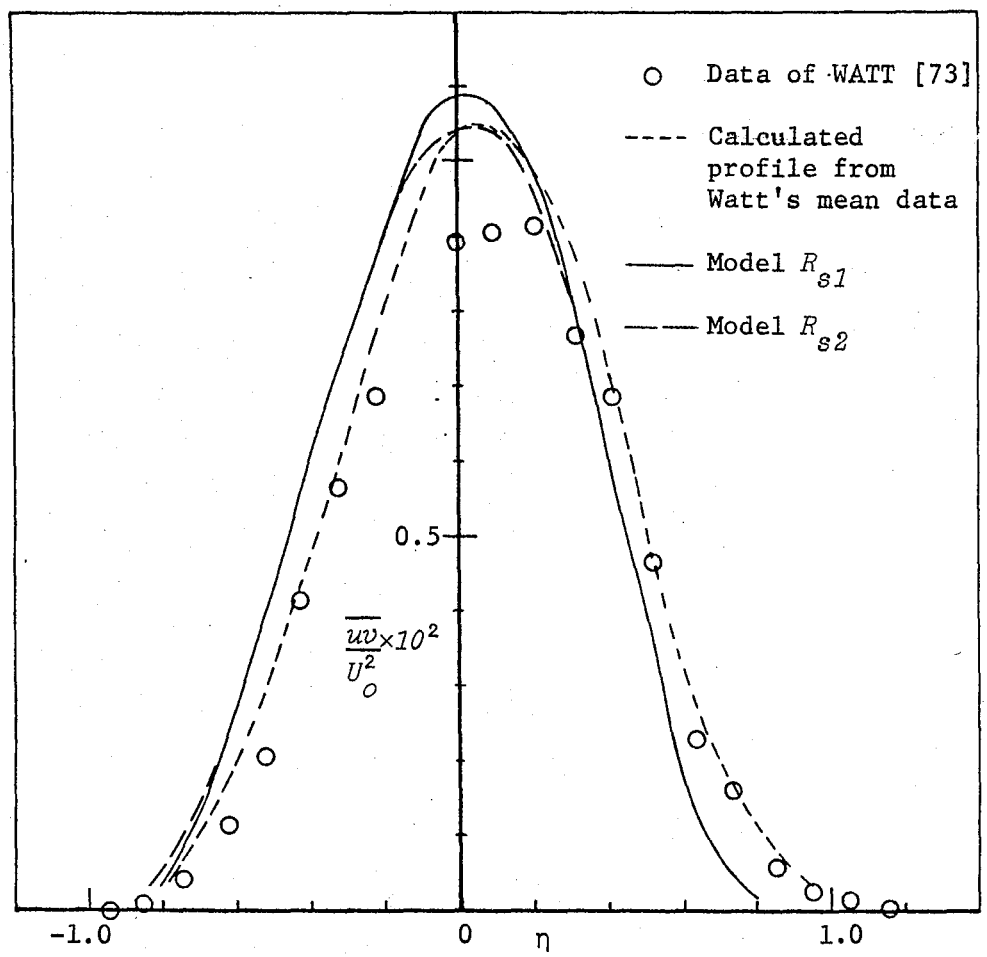

Fig. 6.18 The Plane Mixing Layer with $\frac{U_1}{U_2} = 0.5$:

Shear Stress Profiles

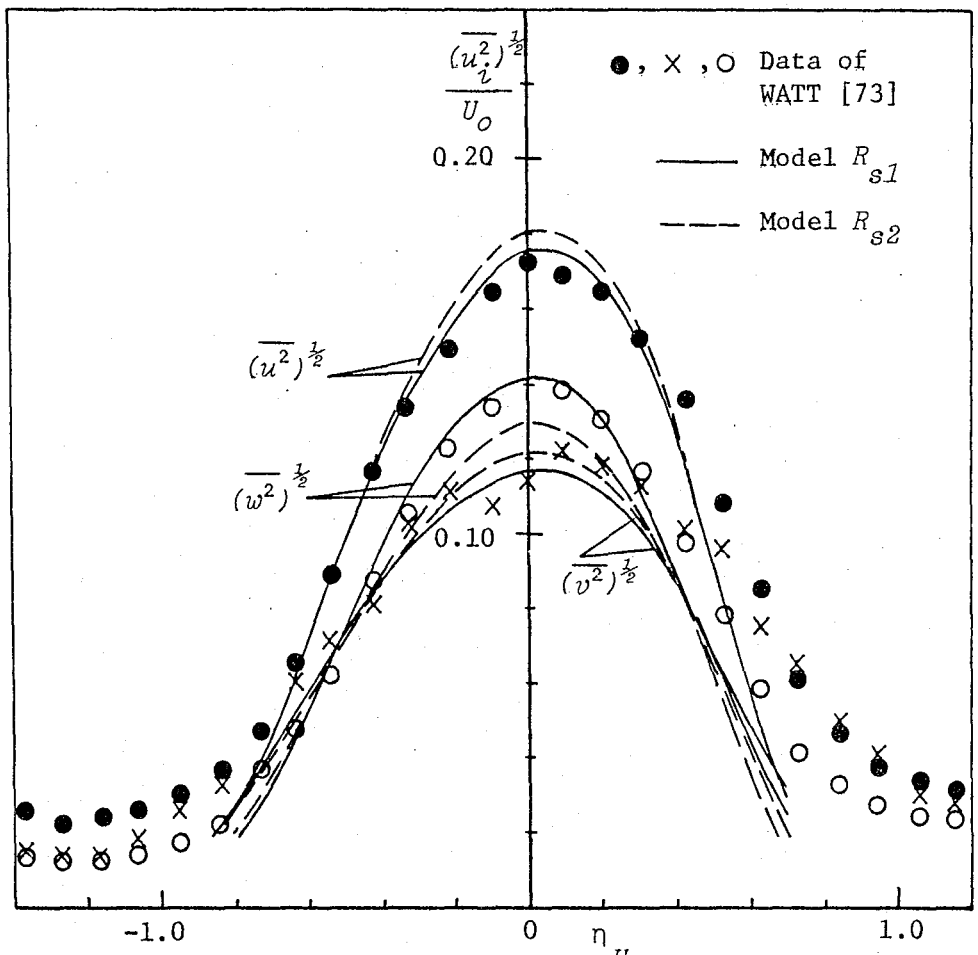

Fig. 6.19 The Plane Mixing Layer with $\frac{U_1}{U_2} = 0.5$;

Turbulence Intensity Profiles

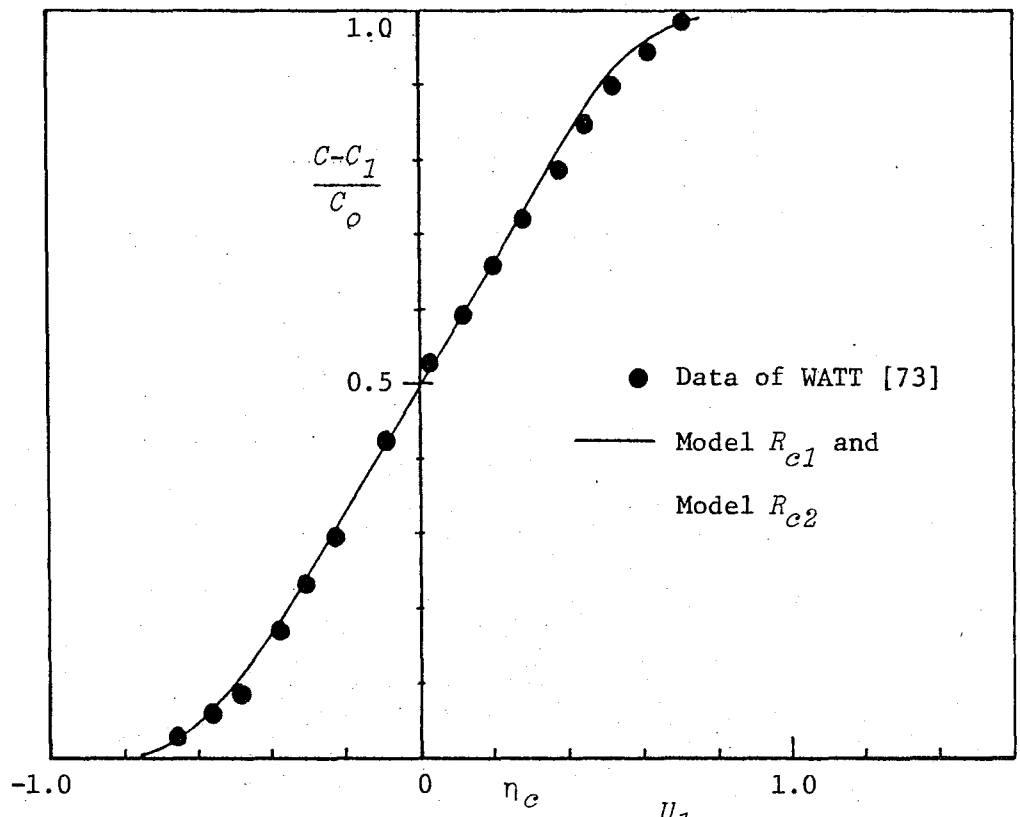

Fig. 6.20 The Plane Mixing Layer with $\frac{U_1}{U_2} = 0.5$:

Mean Temperature Profiles

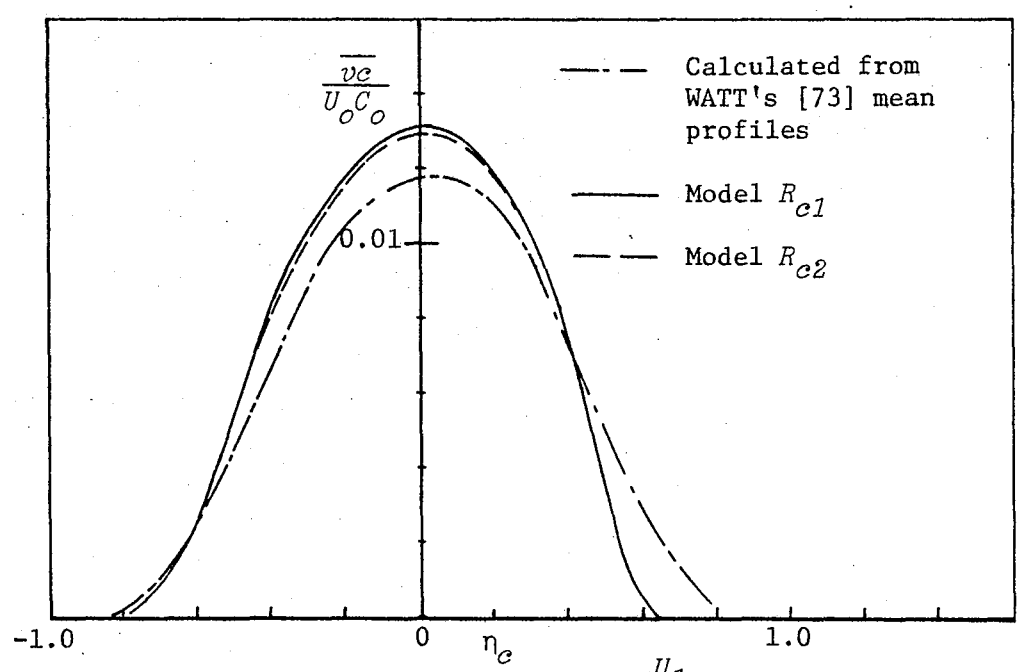

Fig. 6.21 The Plane Mixing Layer with $\frac{U_1}{U_2} = 0.5$:

Cross-stream Scalar Flux Profiles

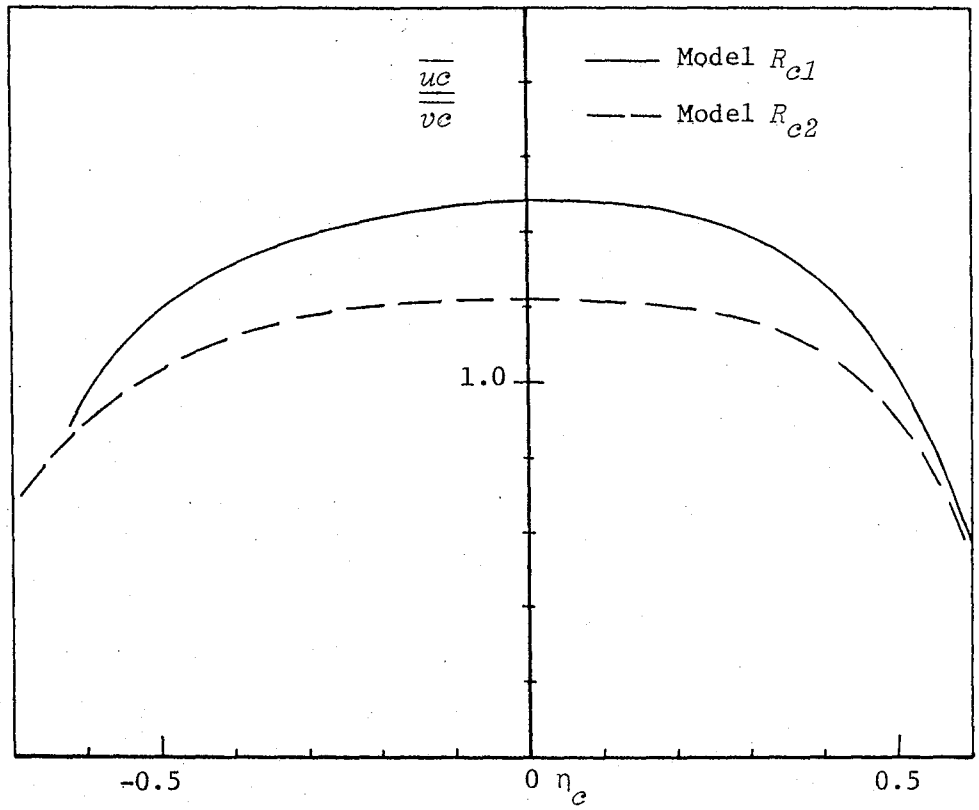

Fig. 6.22 The Plane Mixing Layer with $\frac{U_1}{U_2} = 0.5$:

Ratio of Streamwise to Cross-stream Scalar Flux Profiles

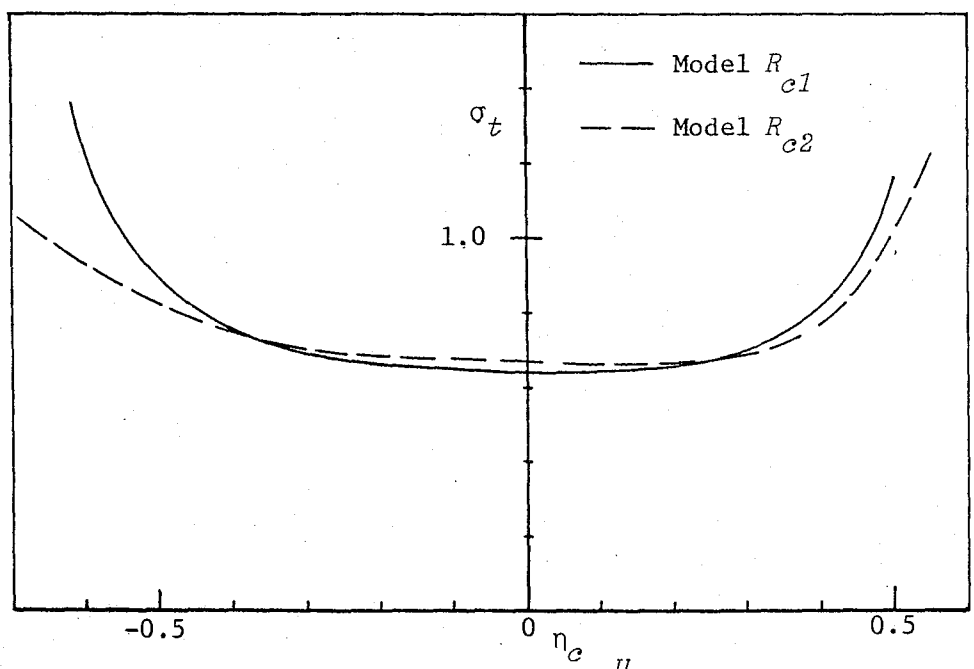

Fig. 6.23 The Plane Mixing Layer with $\frac{U_1}{U_2} = 0.5$:

Turbulent Prandtl Number Profiles

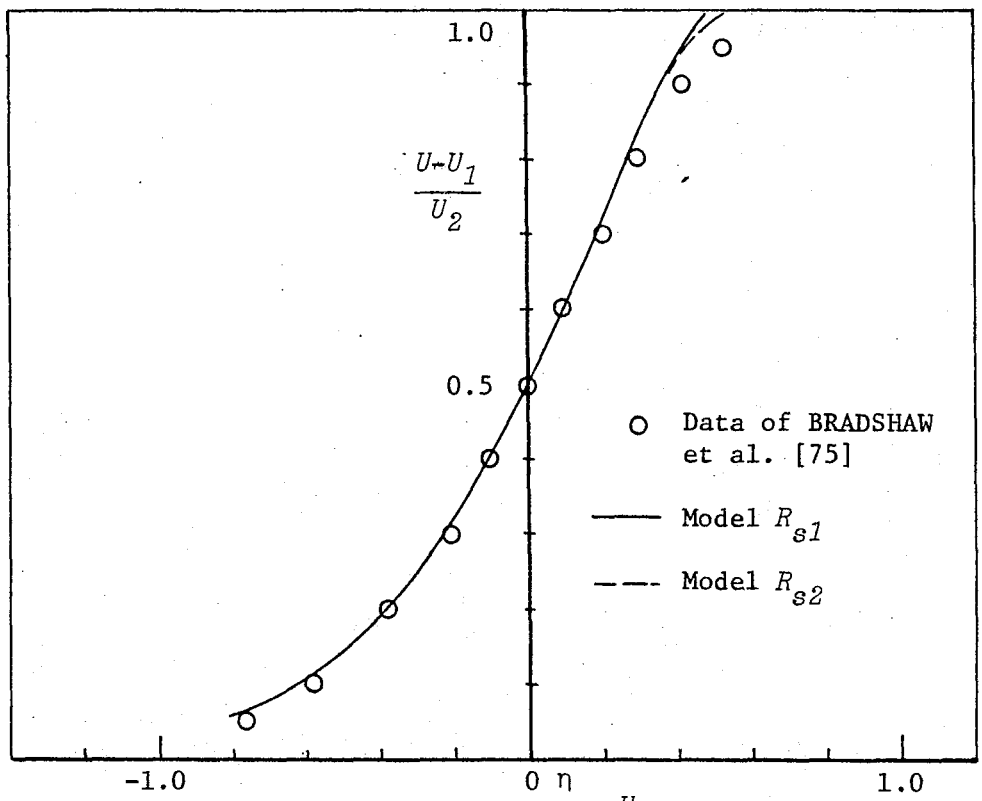

Fig. 6.24 The Plane Mixing Layer with $\frac{U_1}{U_2} \simeq 0$: Mean Velocity Profiles

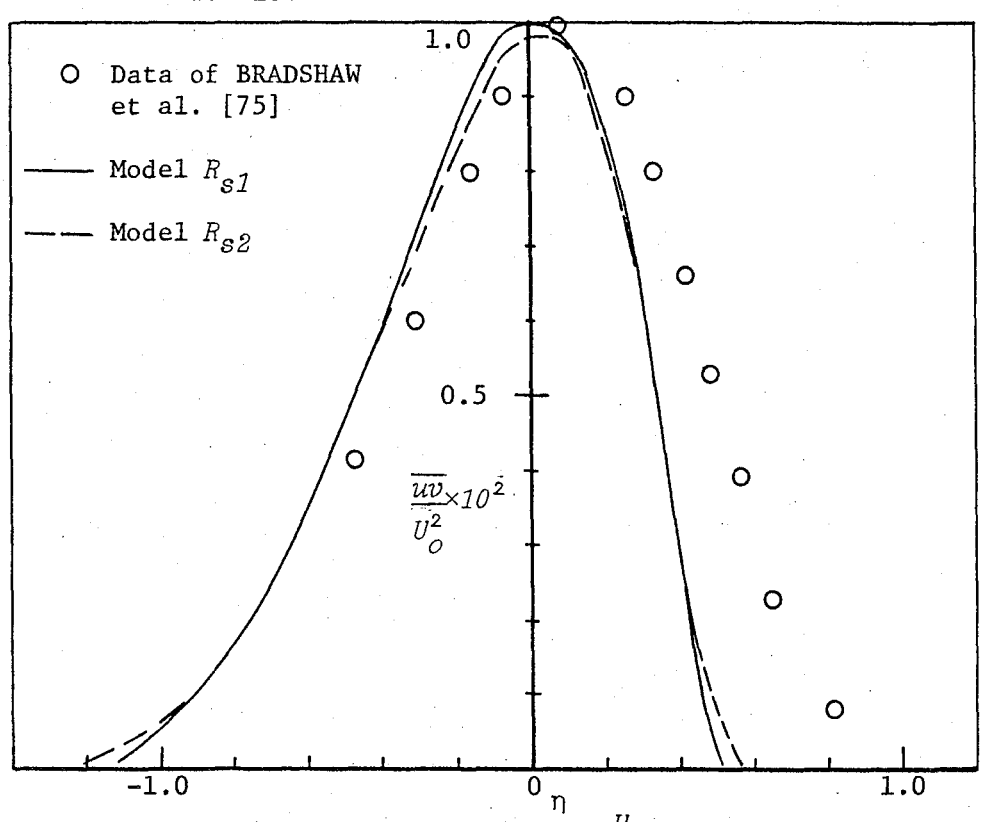

Fig. 6.25 The Plane Mixing Layer with $\frac{U_1}{U_2} \simeq 0$: Shear Stress Profiles

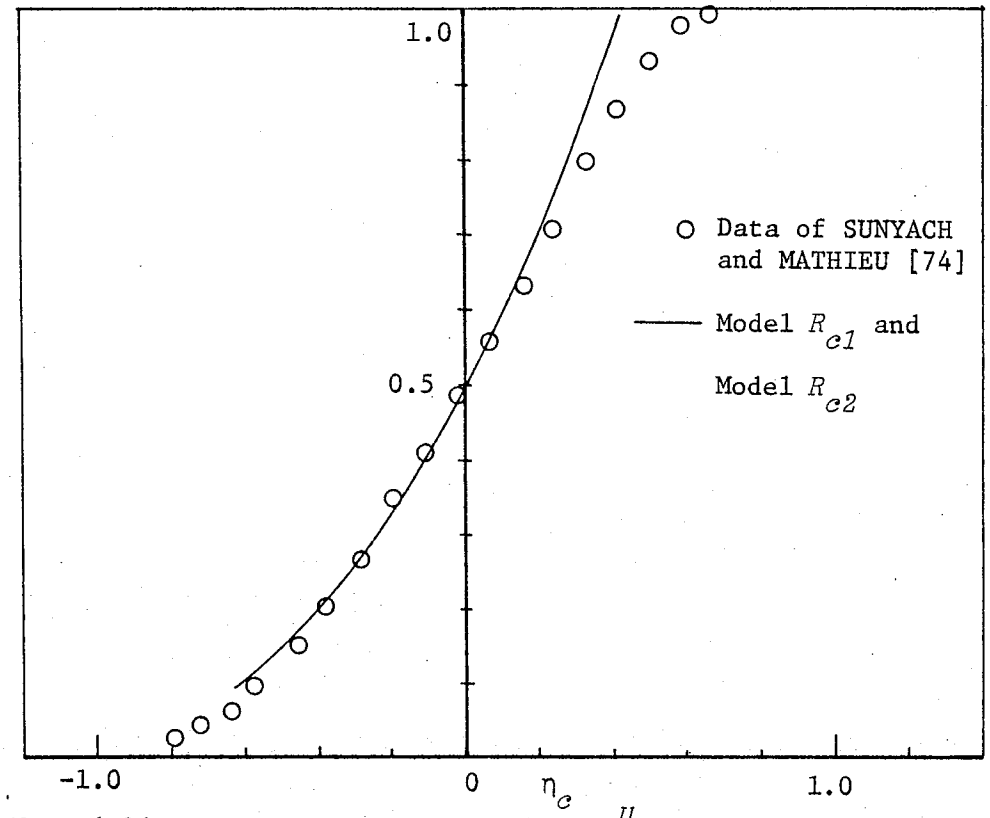

Fig. 6.26 The Plane Mixing Layer with $\frac{U_1}{U_2} \simeq 0$:

Mean Temperature Profiles

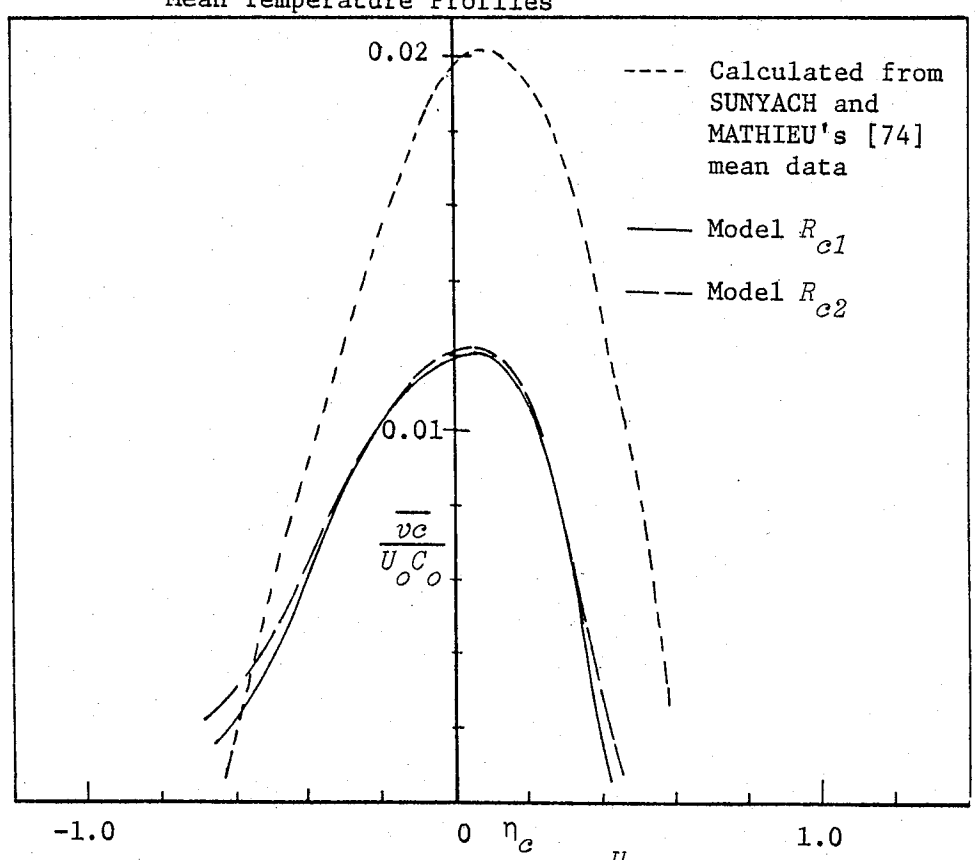

Fig. 6.27 The Plane Mixing Layer with $\frac{U_1}{U_2} \simeq 0$:

Cross-stream Heat Flux Profiles

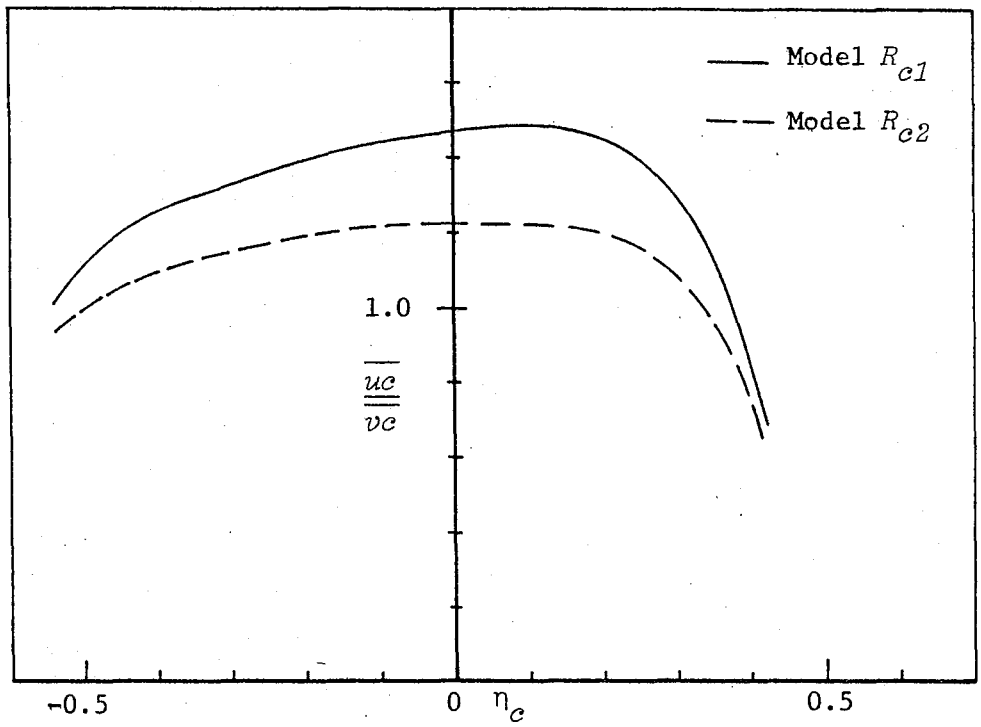

Fig. 6.28 The Plane Mixing Layer with $\frac{U_1}{U_2} \simeq 0$:

Ratio of Streamwise to Cross-stream Scalar Flux Profiles

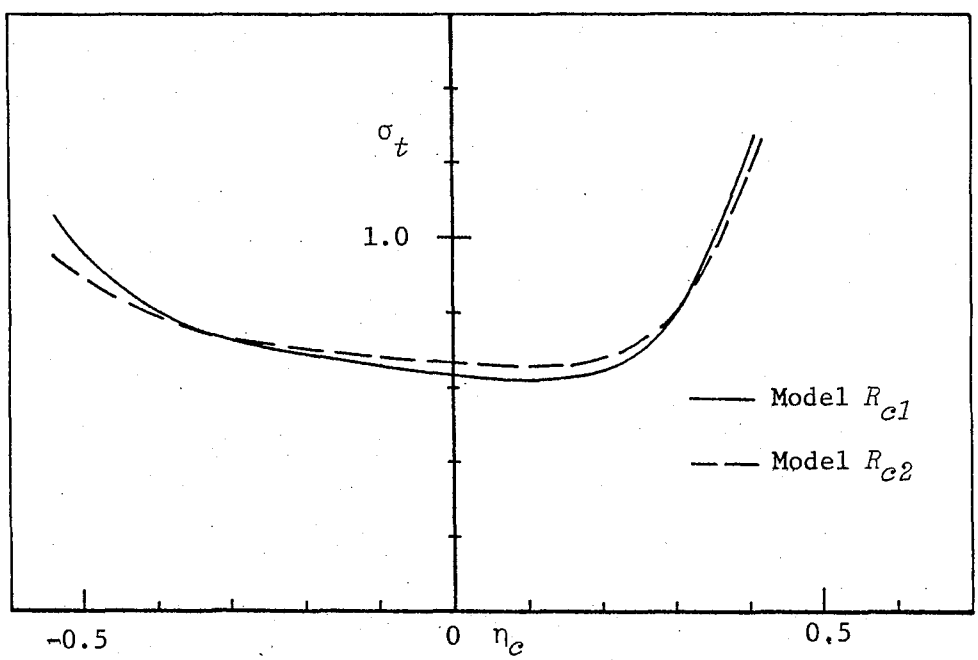

Fig. 6.29 The Plane Mixing Layer with $\frac{U_1}{U_2} \simeq 0$:

Turbulent Prandtl Number Profiles

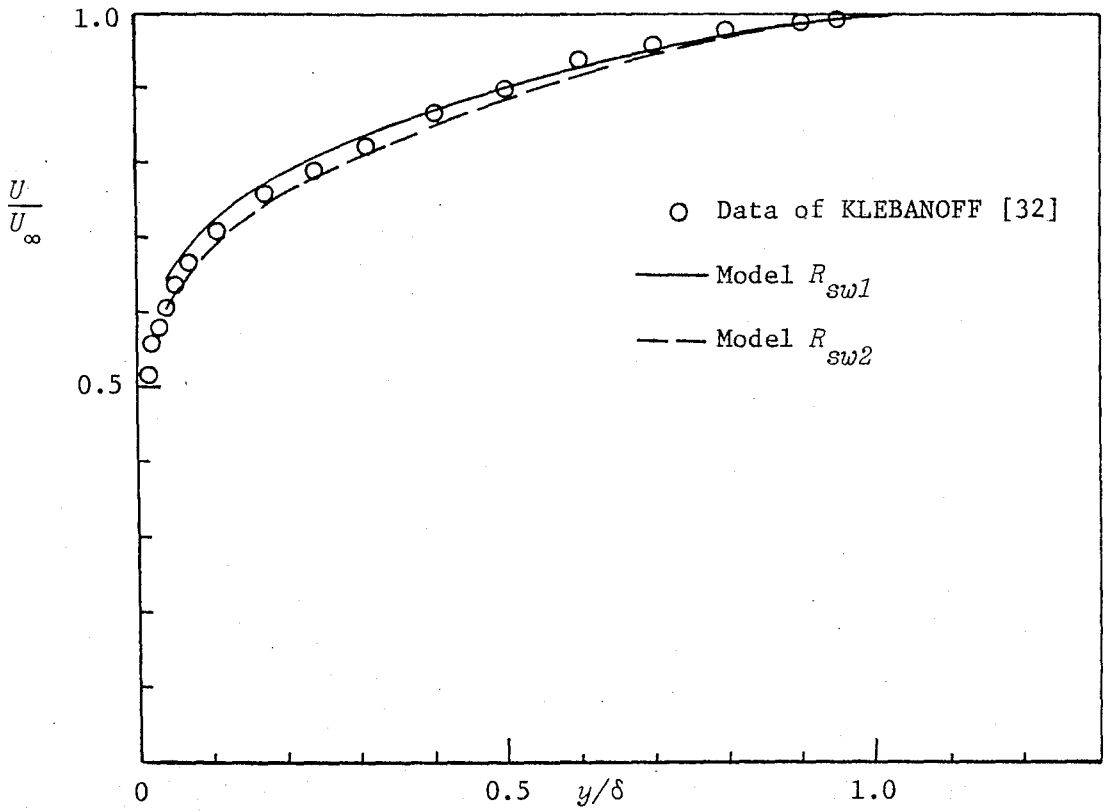

Fig. 6.30 Flat Plate Boundary Layer : Mean Velocity Profiles

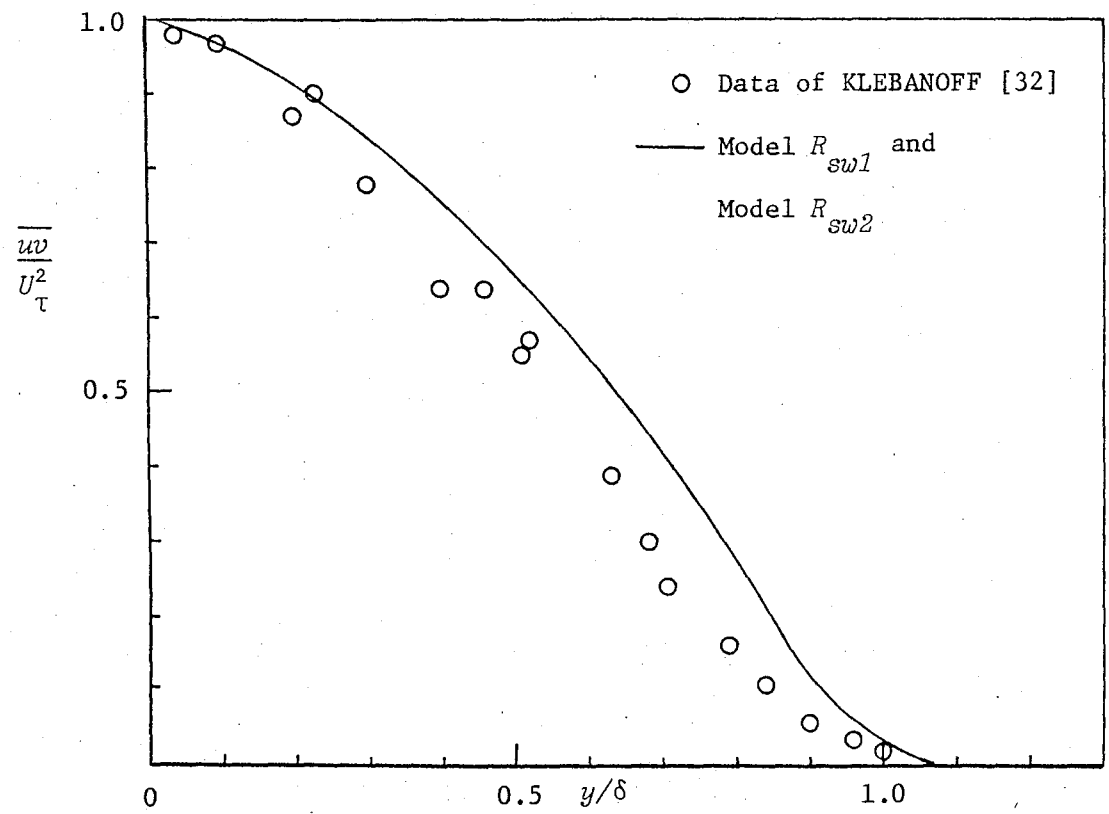

Fig 6.31 Flat Plate Boundary Layer : Shear Stress Profiles

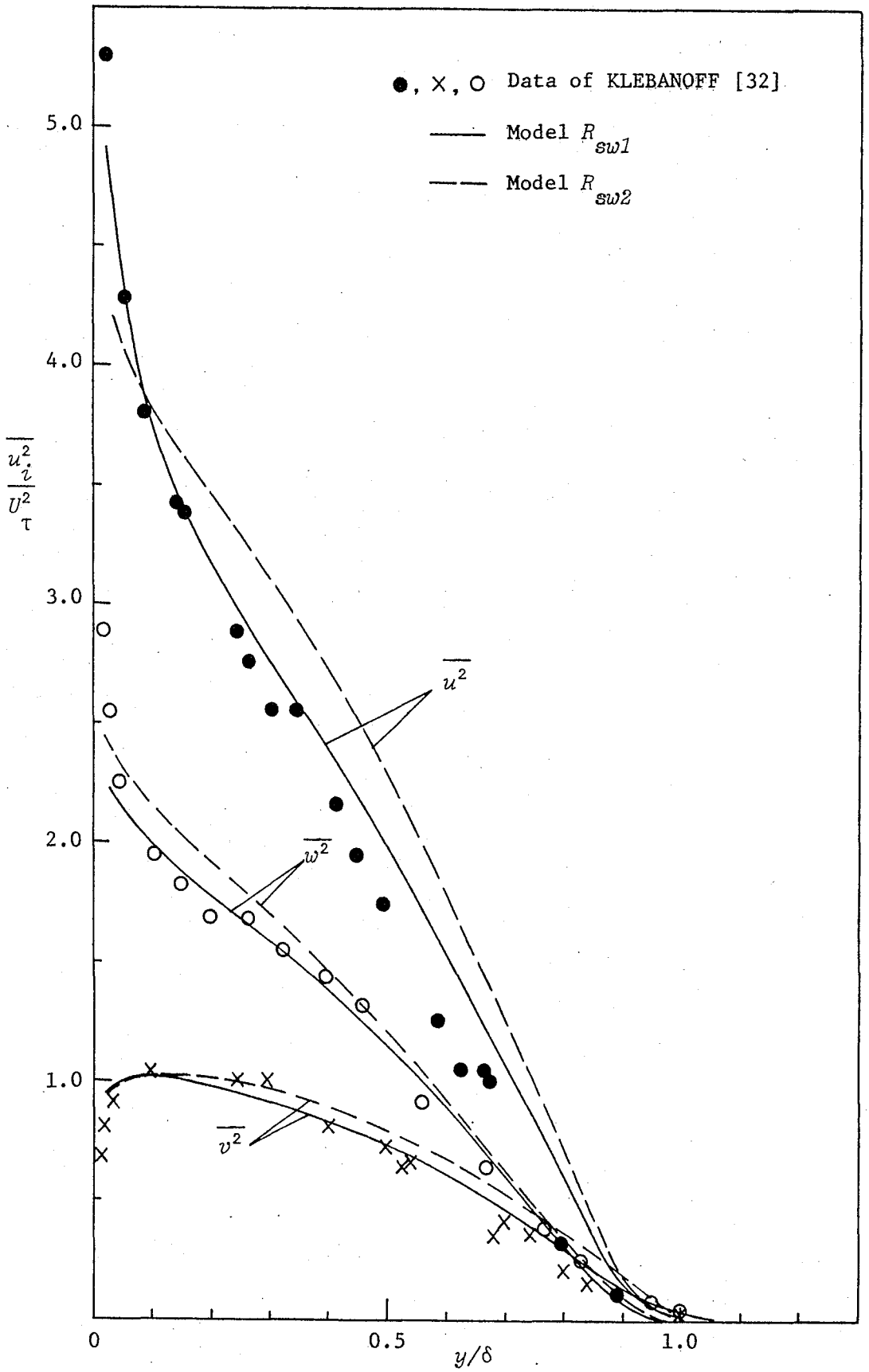

Fig. 6.32 Flat Plate Boundary Layer : Turbulence Intensity Profiles - Comparison of Two Near-wall Effect Models

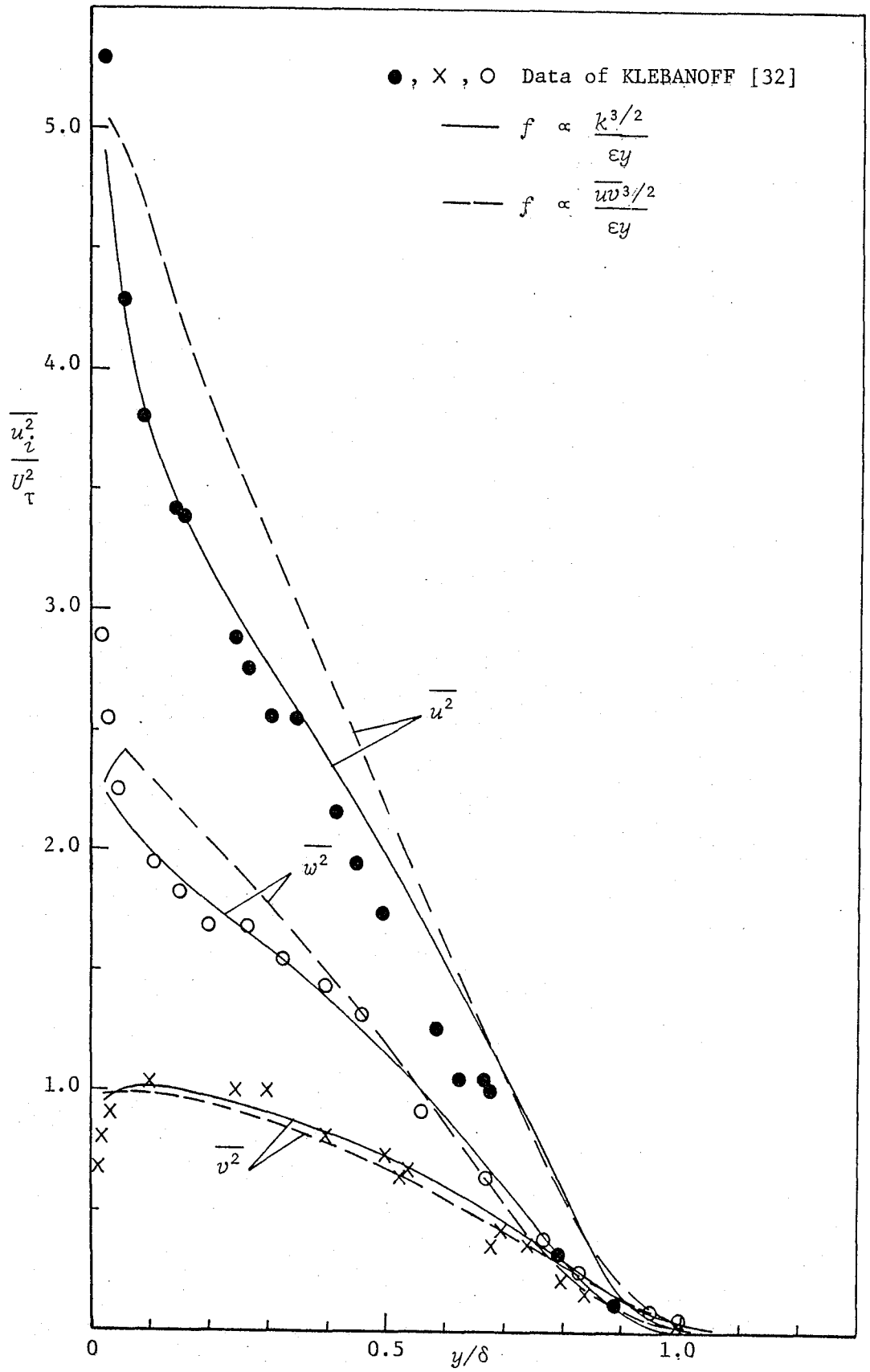

Fig. 6.33 Flat Plate Boundary Layer : Turbulence Intensity Profiles - Comparison of Two Near-wall Effect Functions

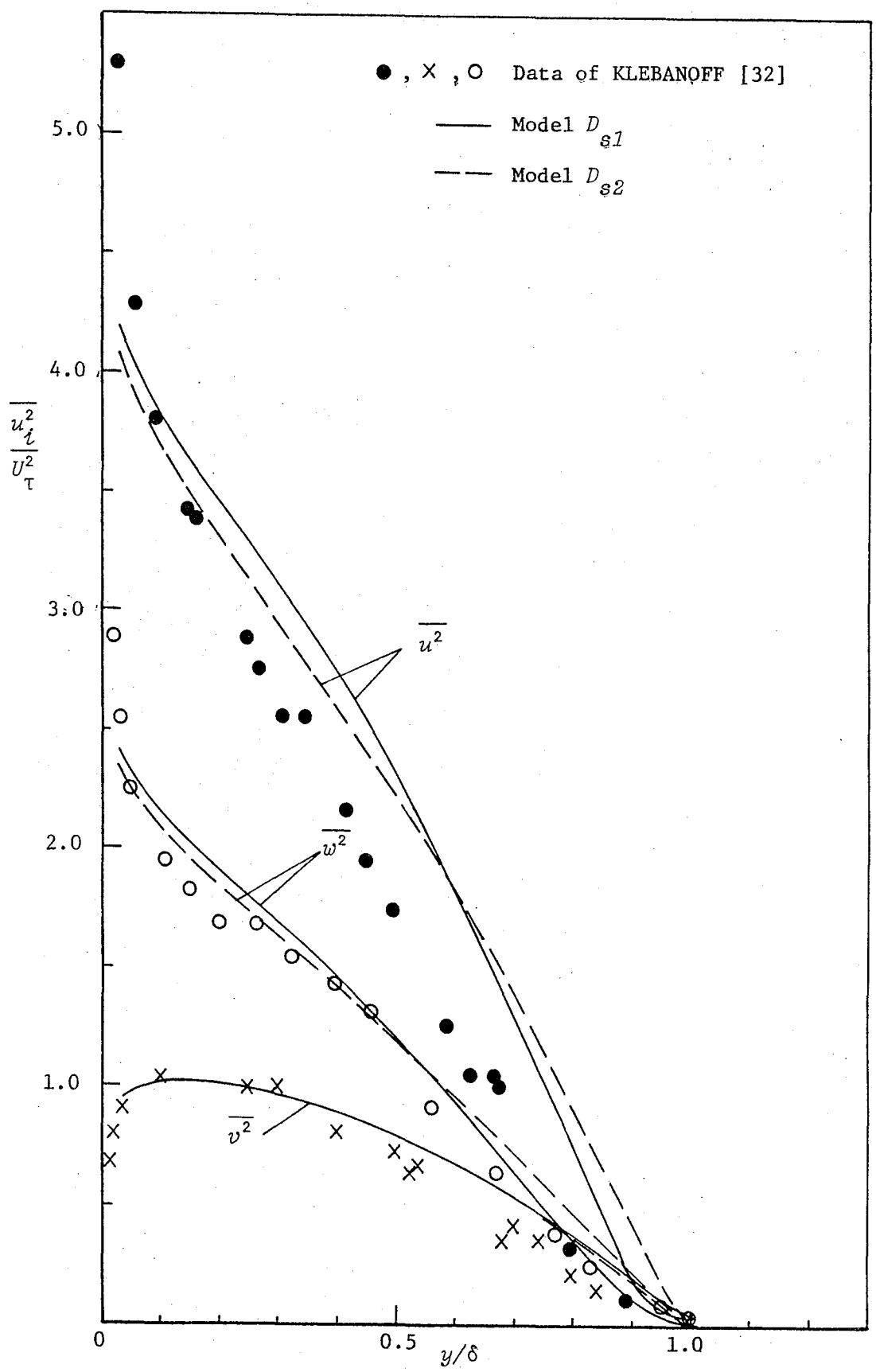

Fig. 6.34 Flat Plate Boundary Layer : Turbulence Intensity Profiles - Comparison of Two Diffusion Models

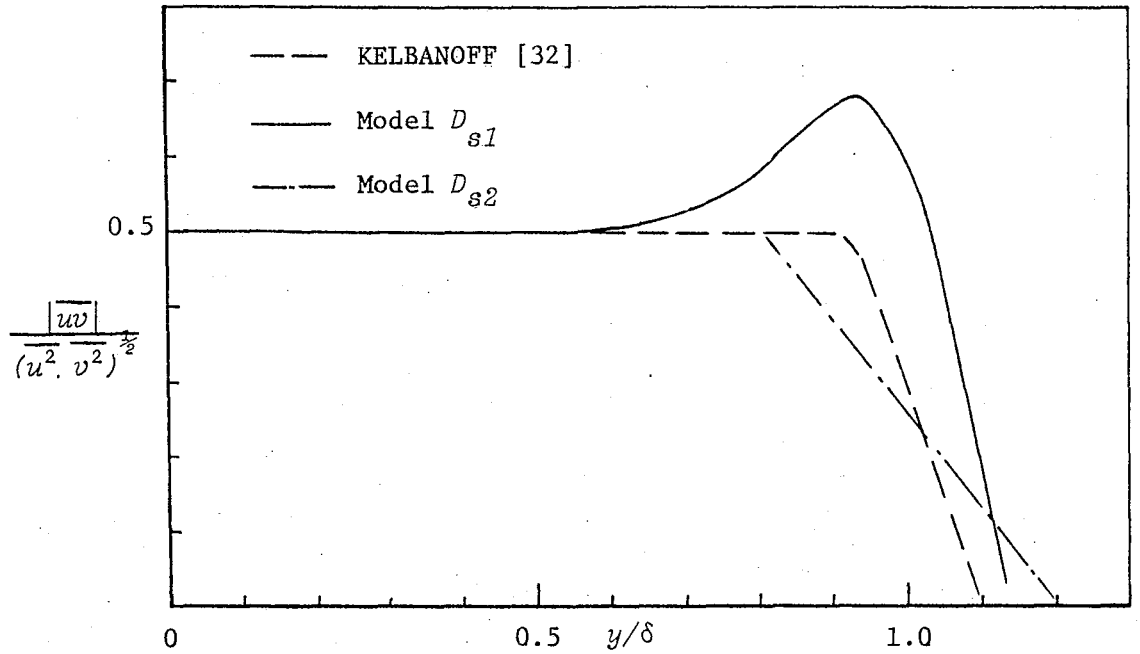

Fig. 6.35 Flat Plate Boundary Layer : Shear Correlation Coefficient - Comparison of Two Diffusion Models

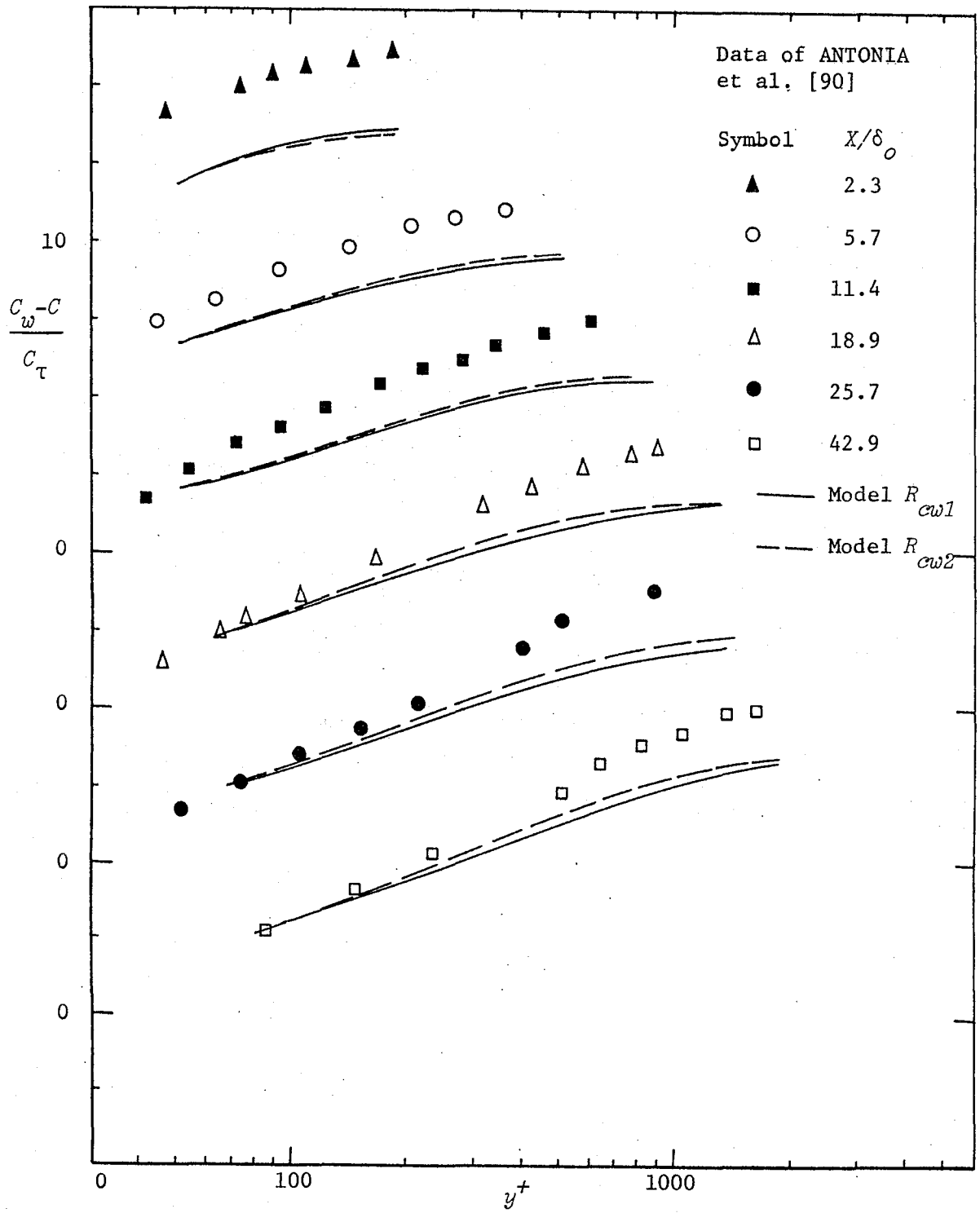

Fig. 6.36 Flat Plate Boundary Layer - Step in Wall Heat Flux : Mean Temperature Profiles

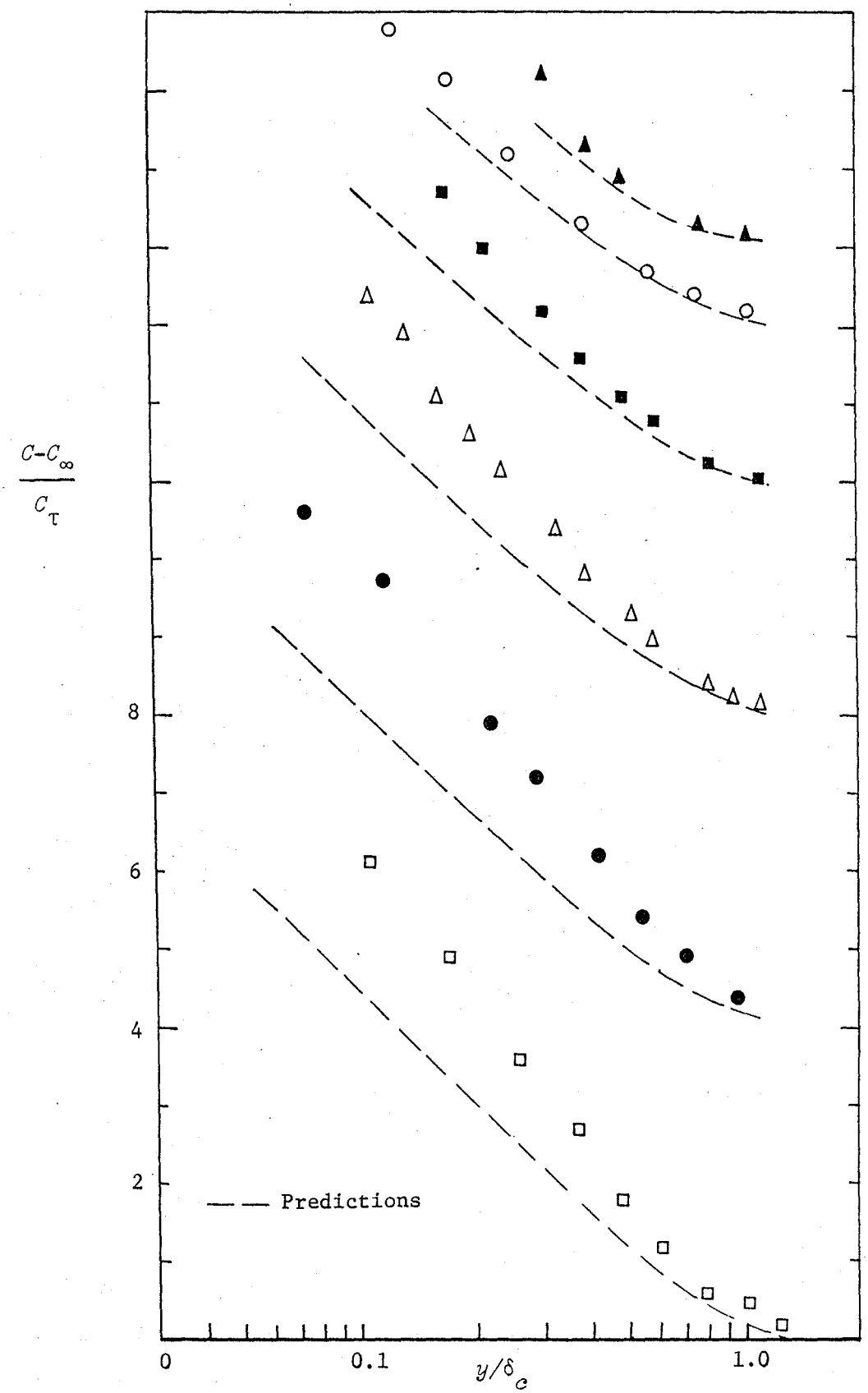

Fig. 6.37 Flat Plate Boundary Layer - Step in Wall Heat Flux : Temperature Defect Profiles; Symbols as in Fig. (6.36)

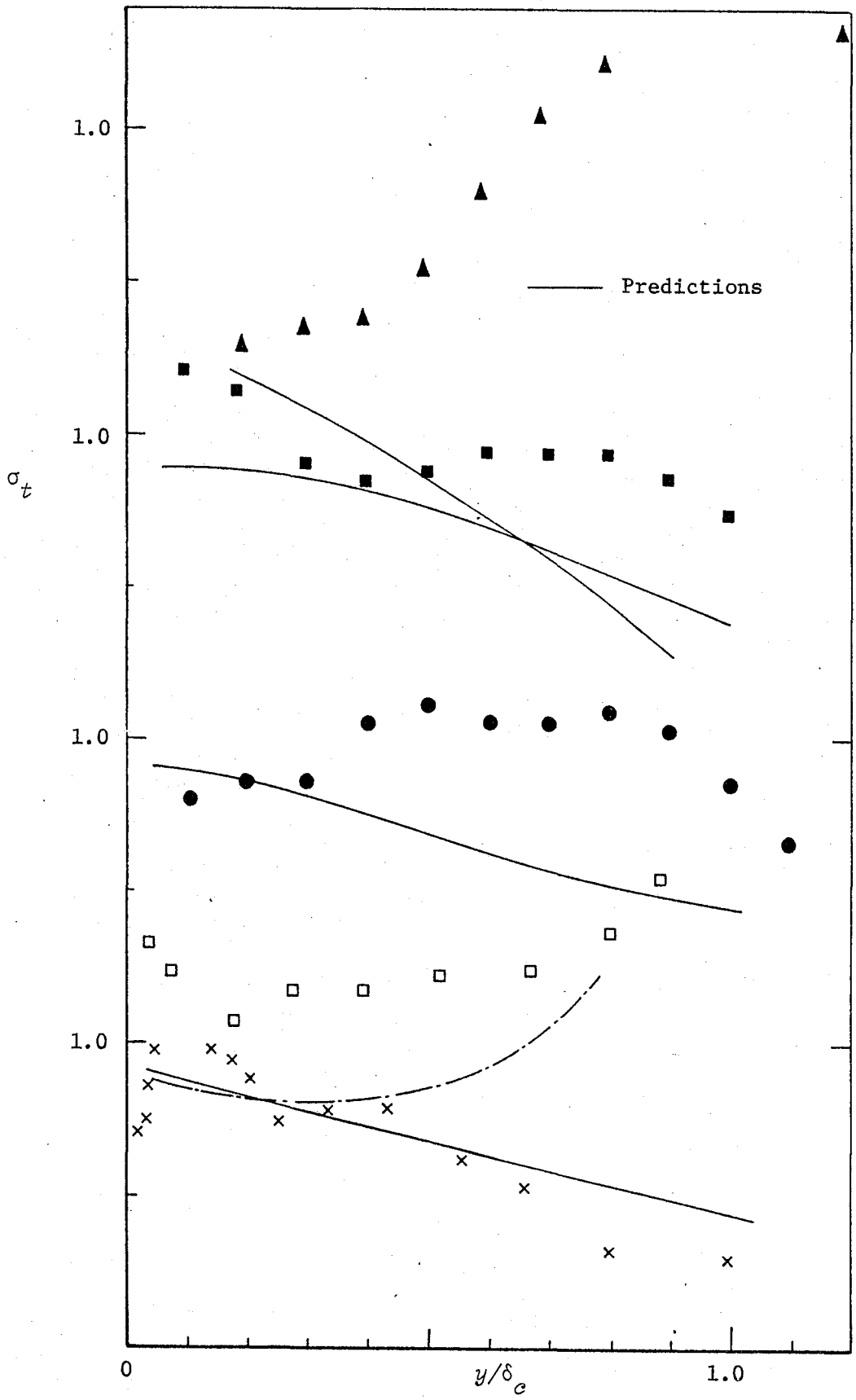

Fig. 6.38 Flat Plate Boundary Layer - Step in Wall Heat Flux : Turbulent Prandtl Number Profiles; Symbols as in Fig. (6.36), × Data of BLOM [86] , ——— Data of FULACHIER [104]

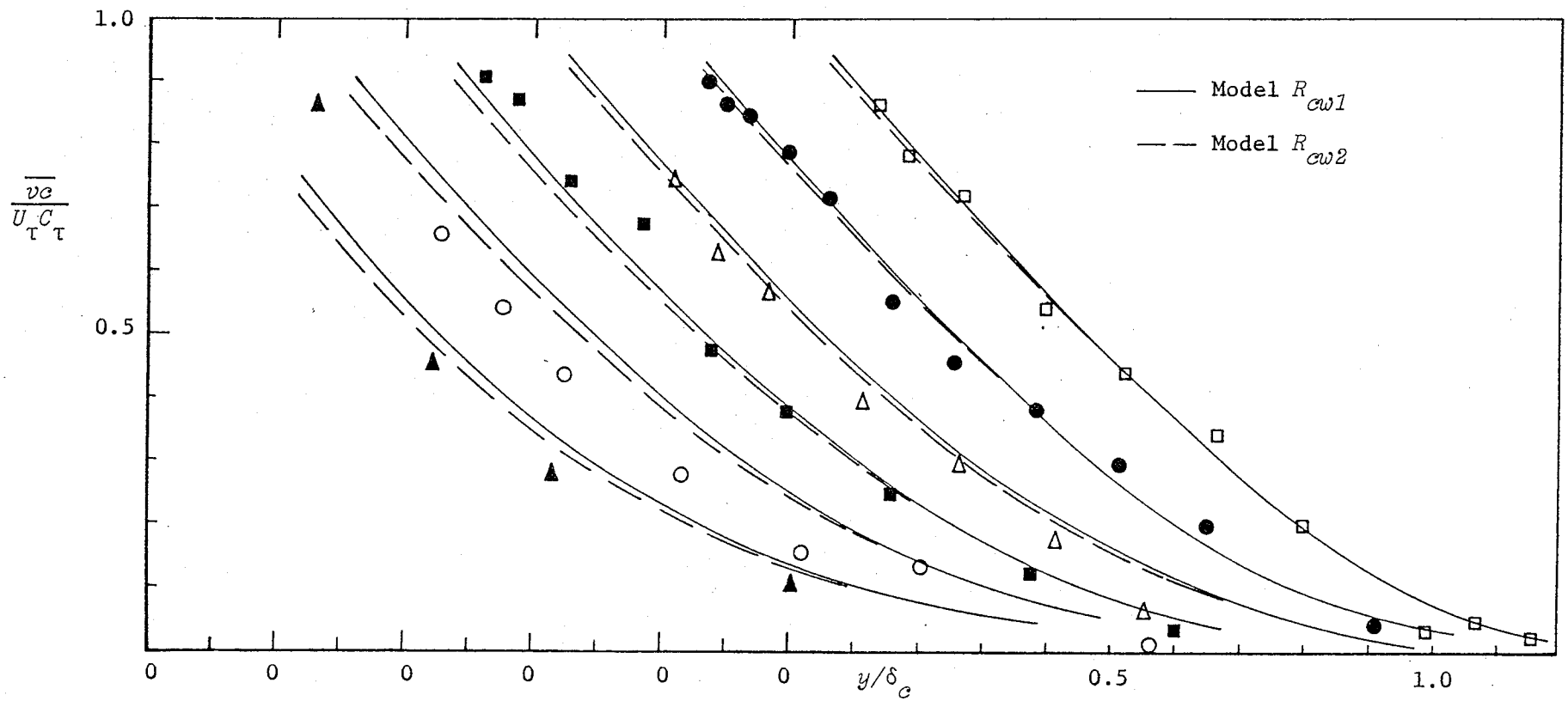

Fig. 6.39 Flat Plate Boundary Layer - Step in Wall Heat Flux : Cross-streas Heat Flux Profiles
Symbols as in Fig. (6.36)

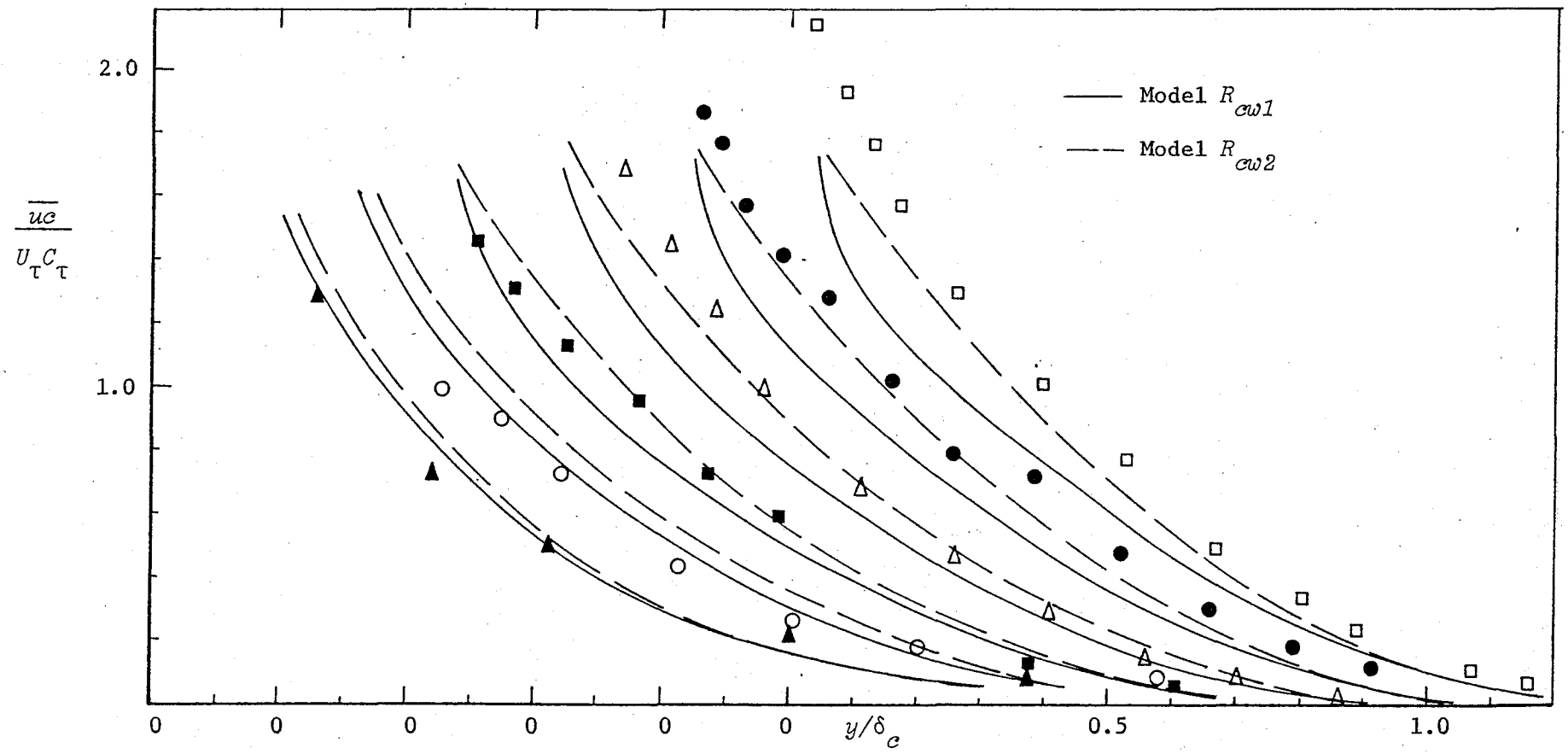

Fig. 6.40 Flat Plate Boundary Layer - Step in Wall Heat Flux : Streamwise Heat Flux Profiles
Symbols as in Fig. (6.36)

0 0 0 0 4 9 0 1 - 259 1 0 8

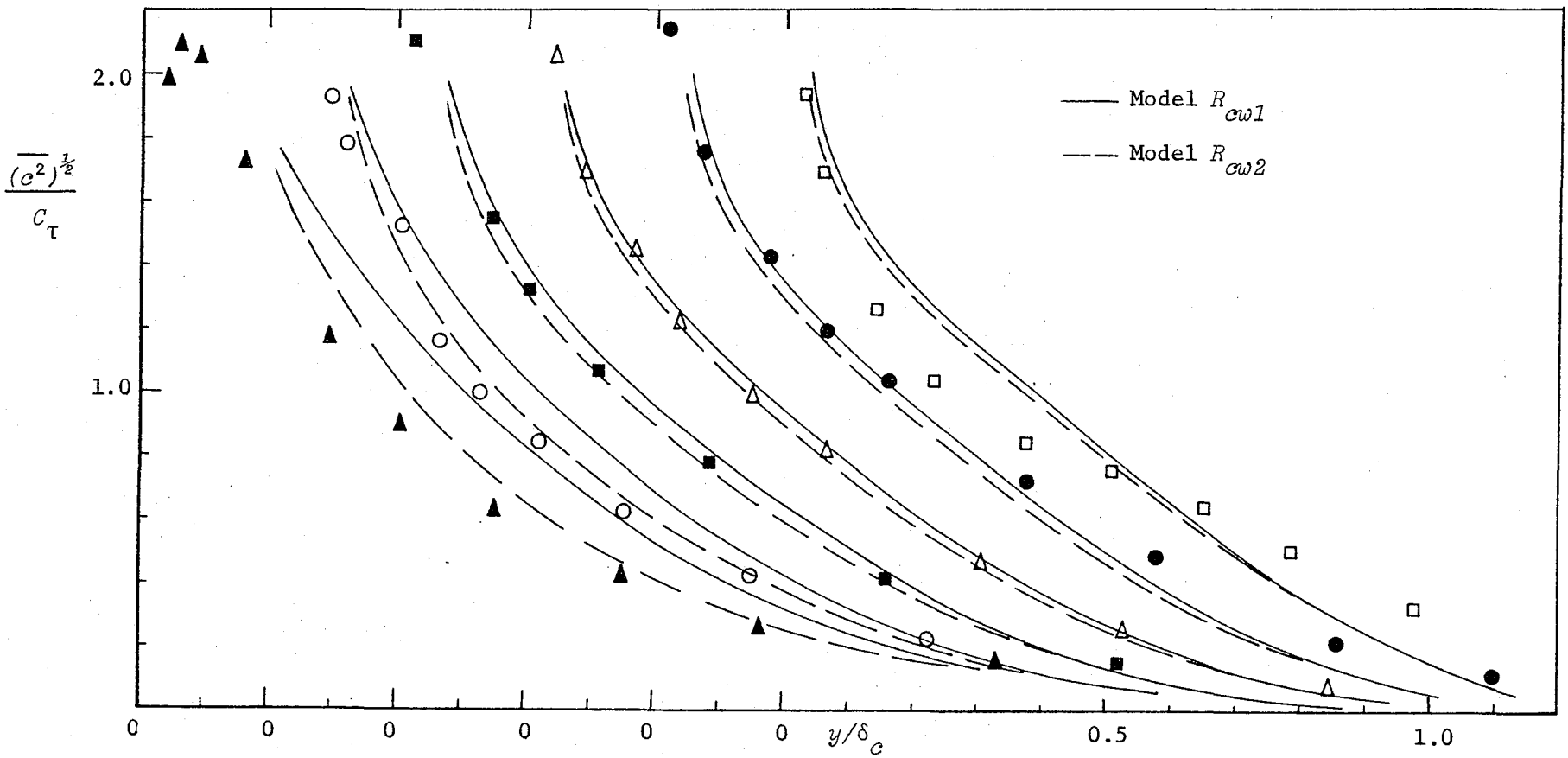

Fig. 6.41 Flat Plate Boundary Layer - Step in Wall Heat Flux : Temperature Fluctuations Profiles
Symbols as in Fig. (6.36)

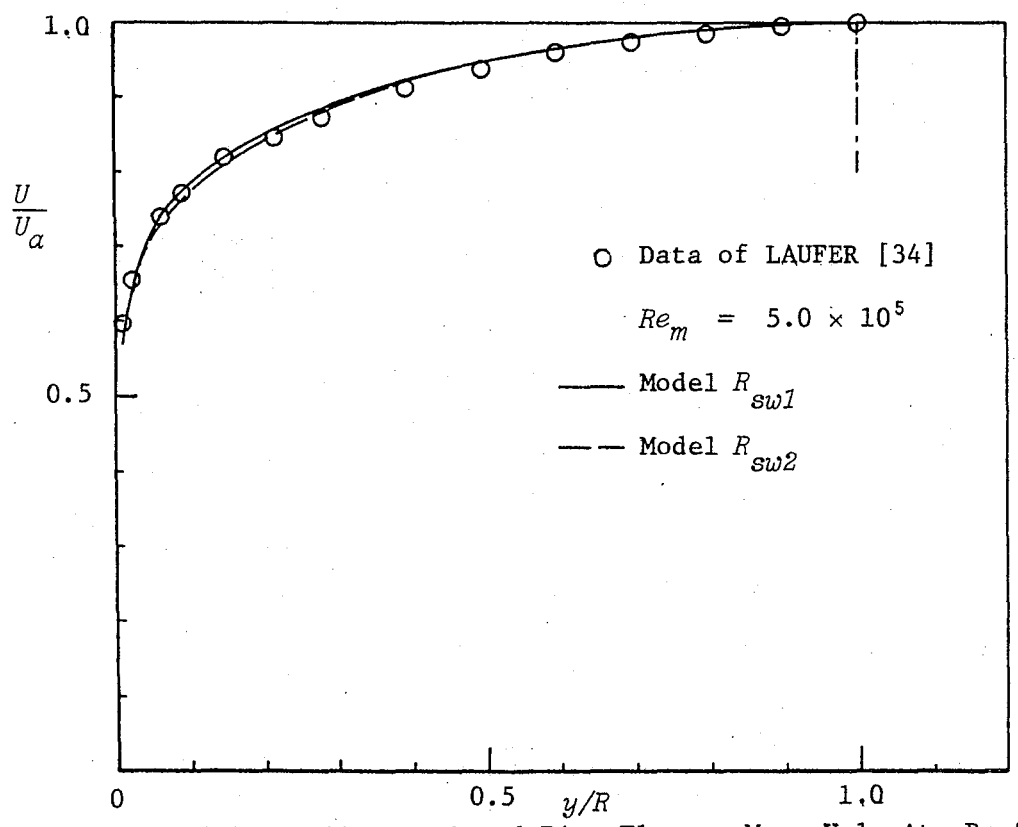

Fig. 6.42 Fully Developed Pipe Flow : Mean Velocity Profiles

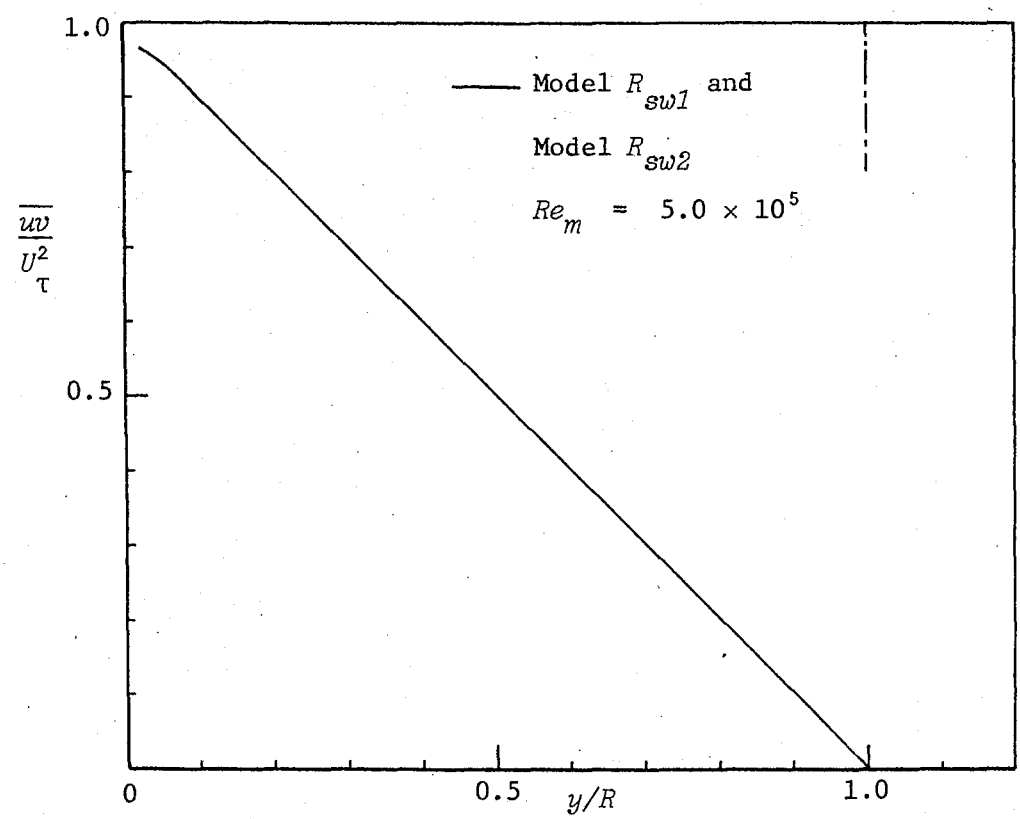

Fig. 6.43 Fully Developed Pipe Flow : Shear Stress Profiles

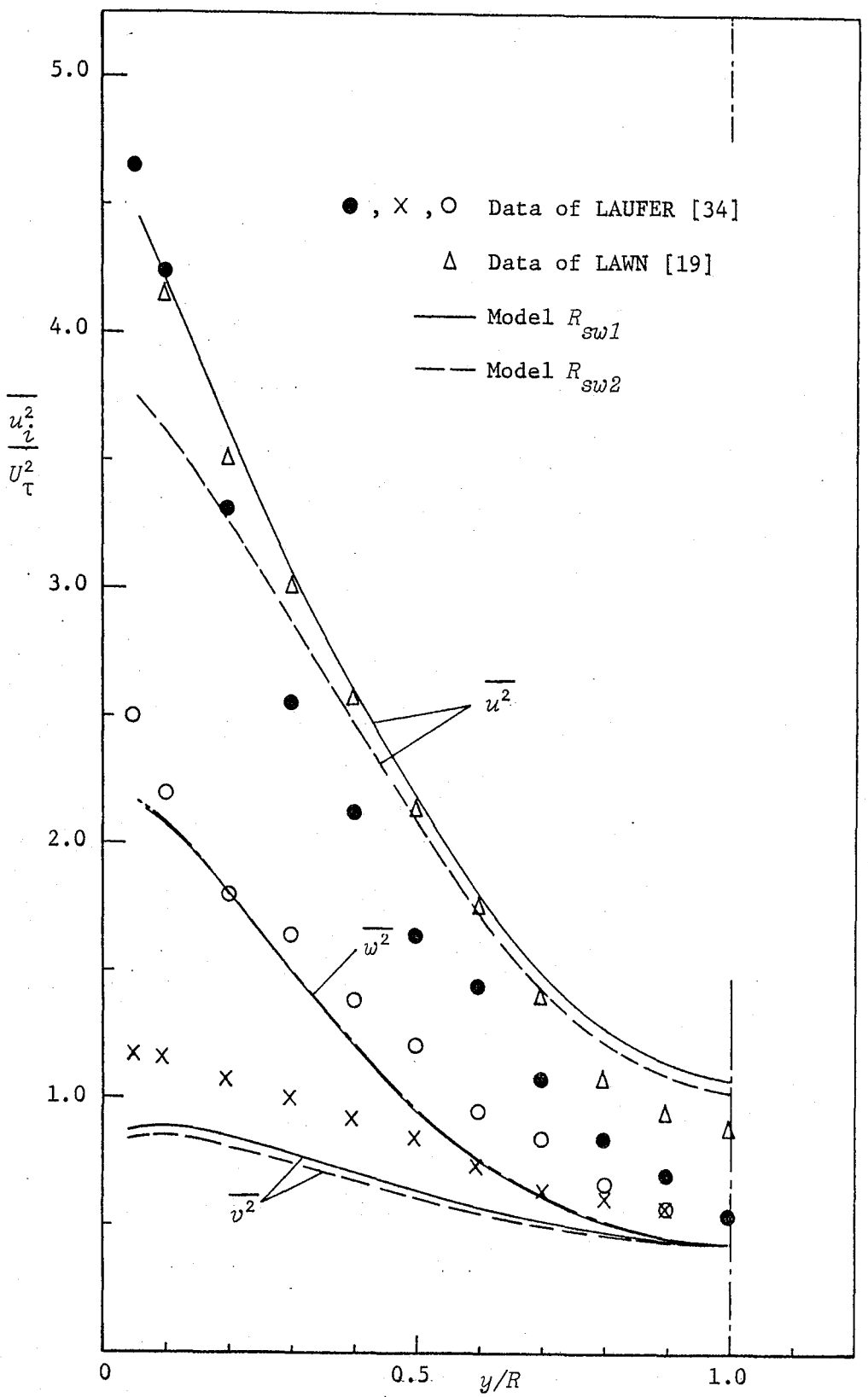

Fig. 6.44 Fully Developed Pipe Flow : Turbulence Intensity Profiles - Comparison of Two Near-wall Effect Models

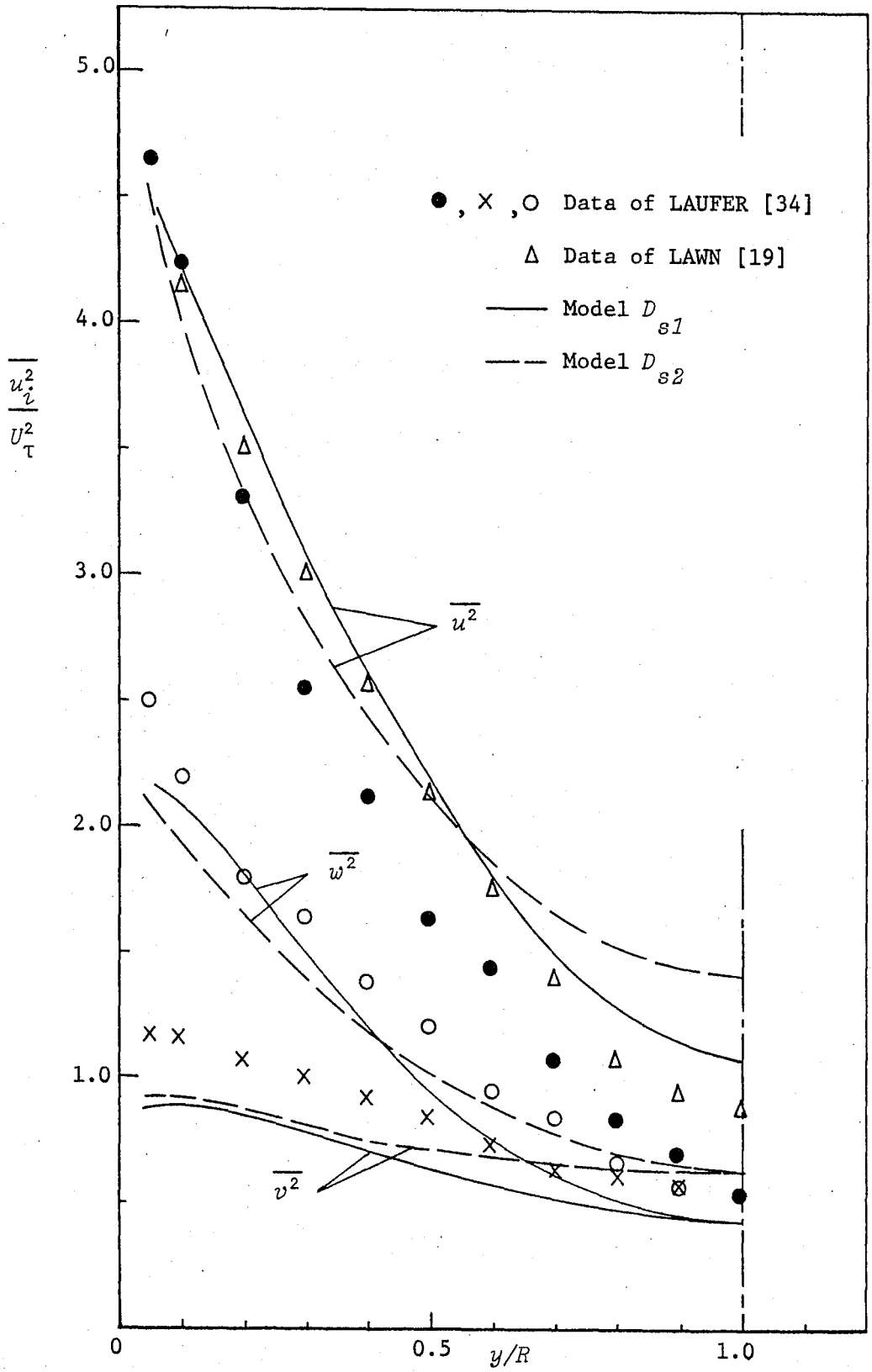

Fig. 6.45 Fully Developed Pipe Flow : Turbulence Intensity Profiles - Comparison of Two Diffusion Models

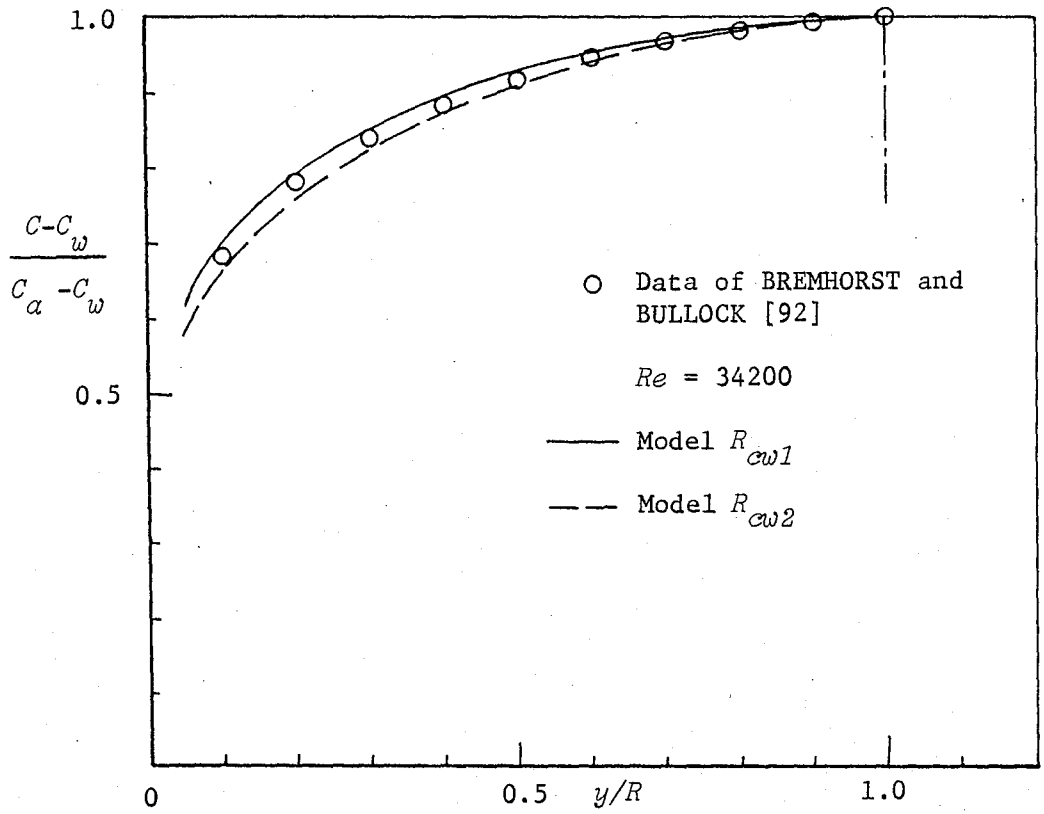

Fig. 6.46 Fully Developed Pipe Flow : Mean Temperature Profiles

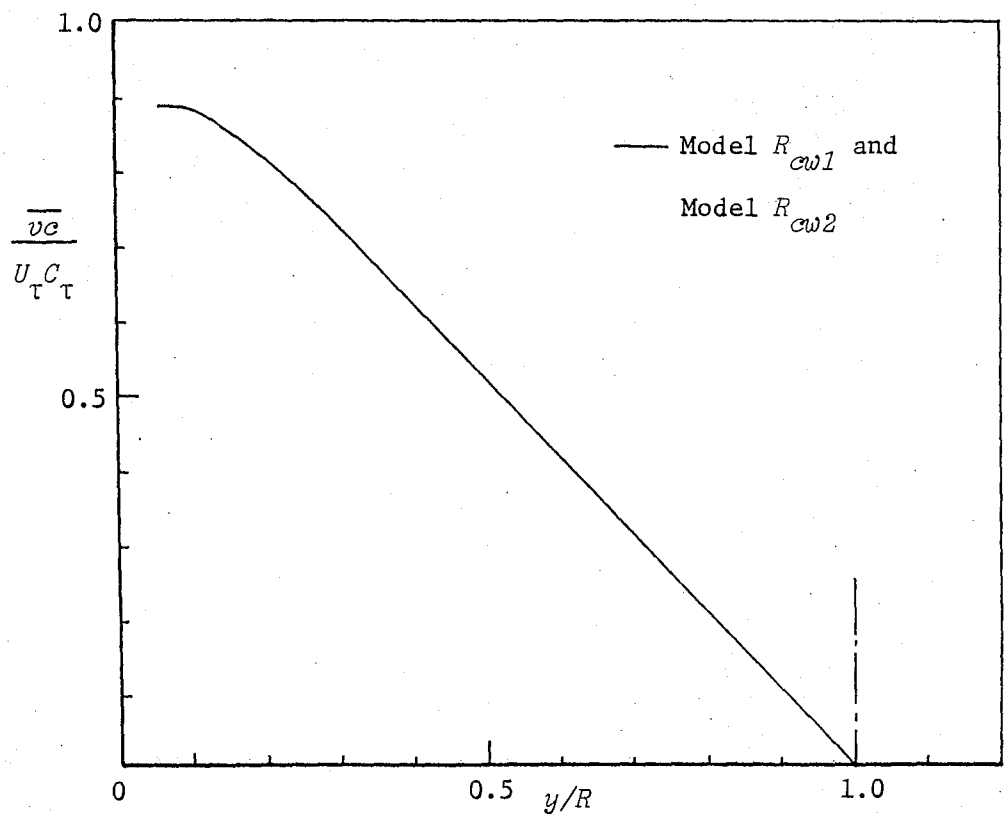

Fig. 6.47 Fully Developed Pipe Flow : Cross-stream Heat Flux Profiles

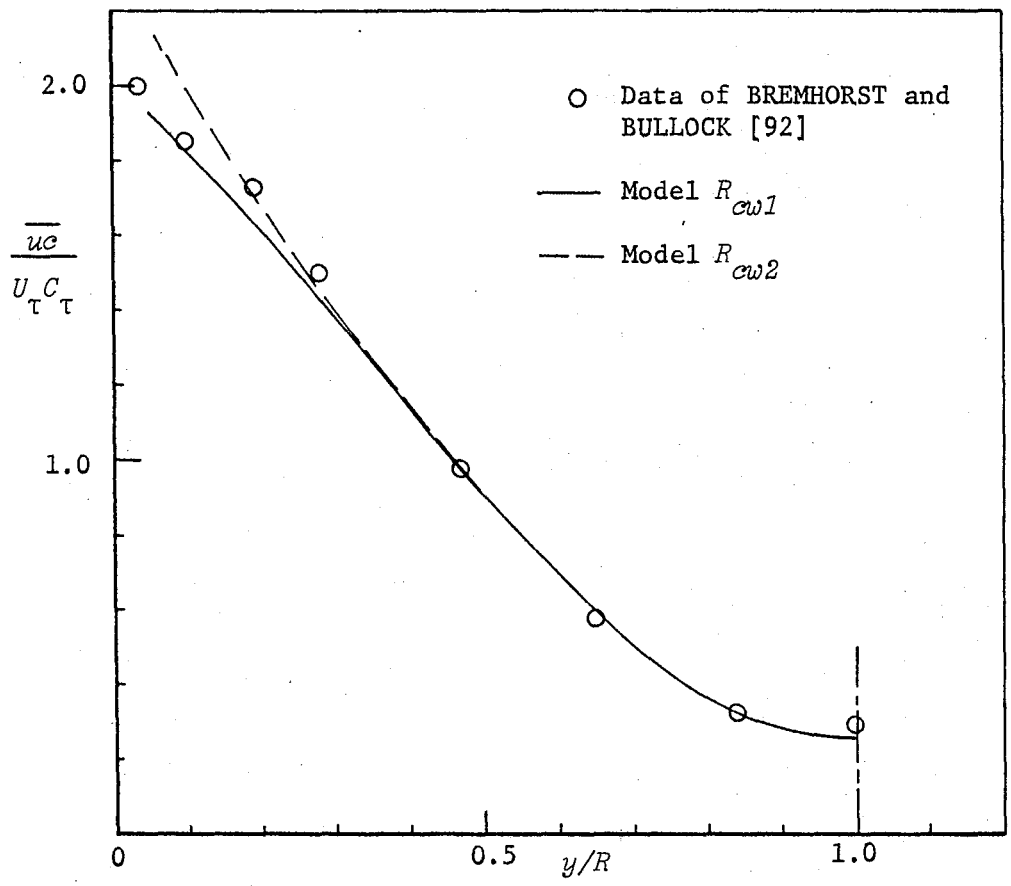

Fig. 6.48 Fully Developed Pipe Flow : Streamwise Heat Flux Profiles

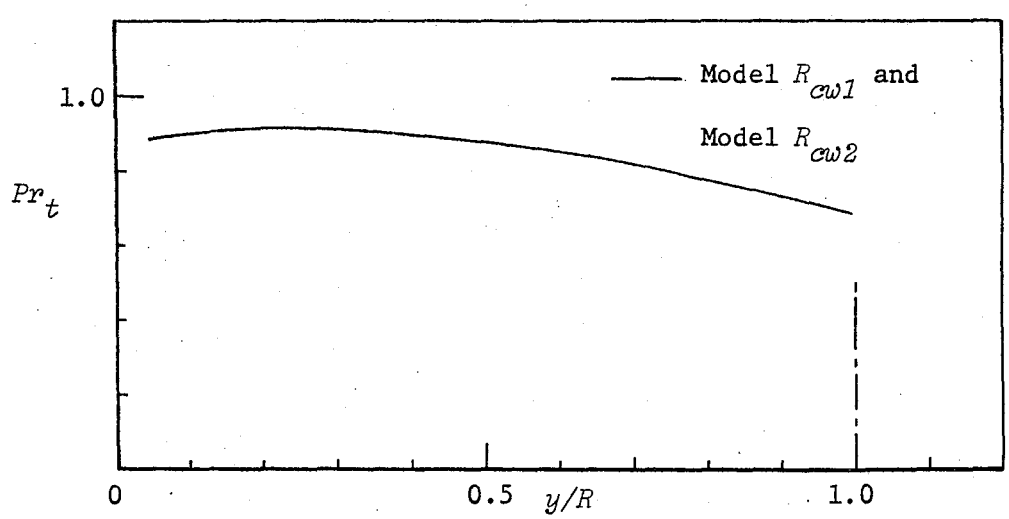

Fig. 6.49 Fully Developed Pipe Flow : Turbulent Prandtl Number Profiles

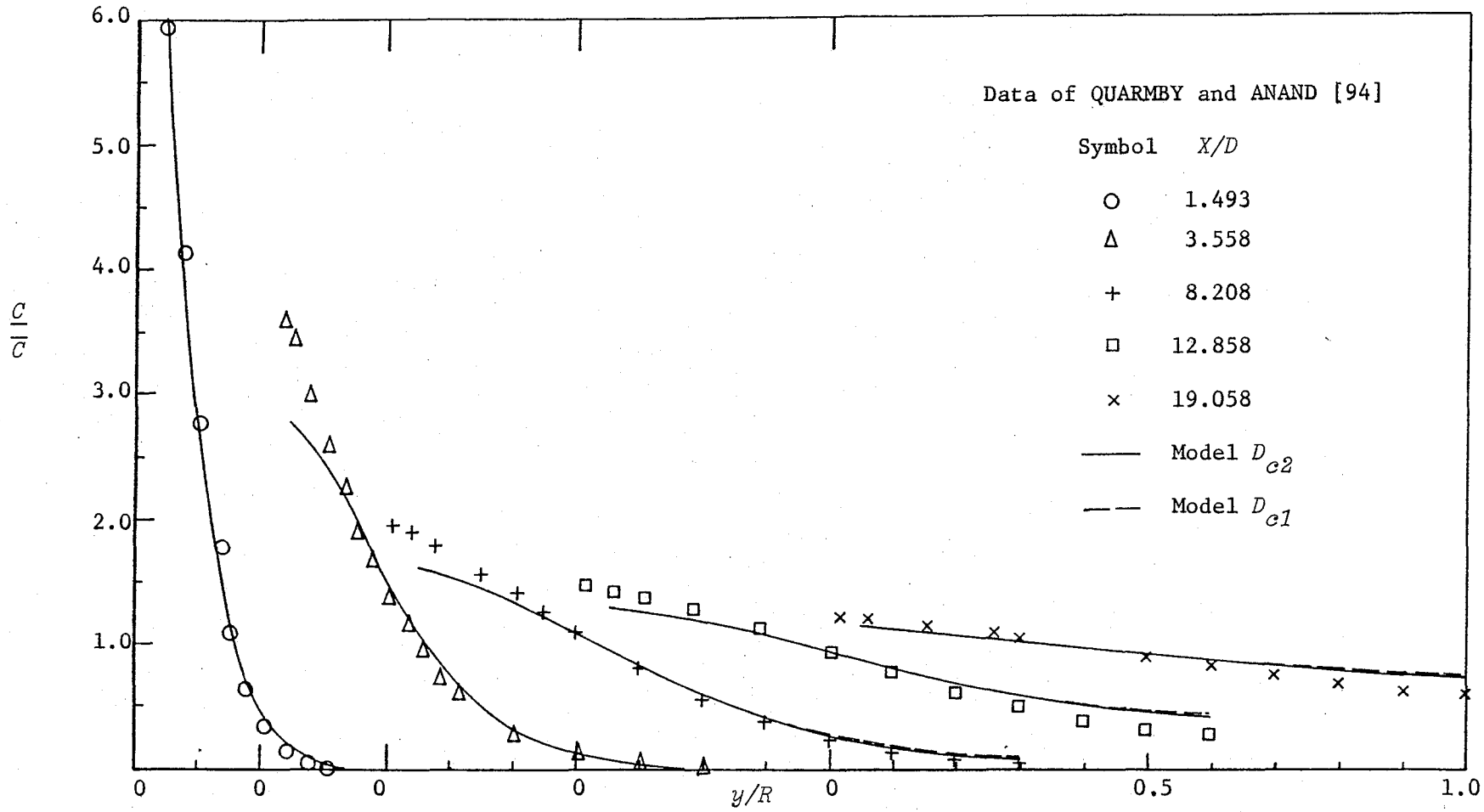

Fig. 6.50 Fully Developed Pipe Flow : Concentration Profiles Downstream of a Short Mass Transfer Region

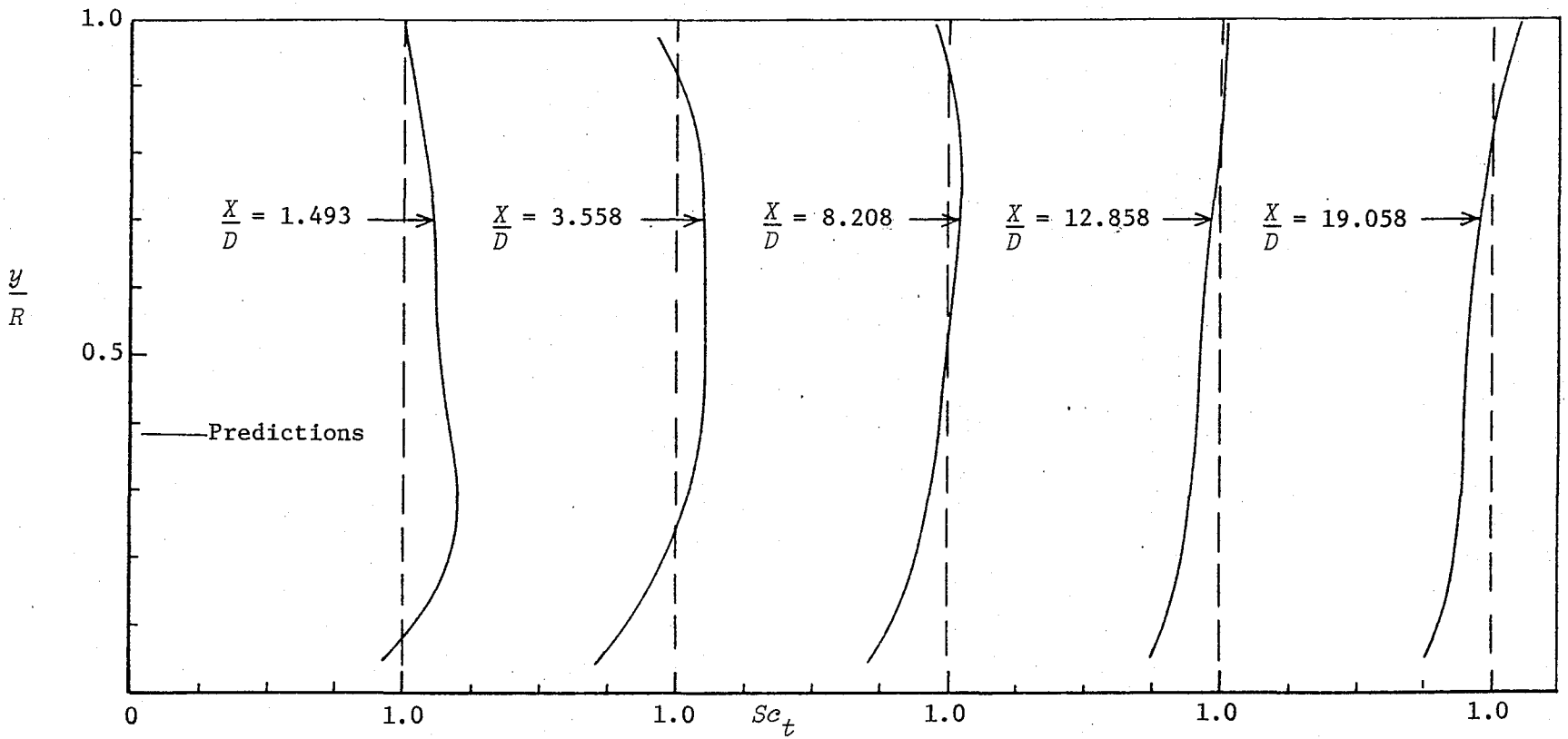

Fig. 6.51 Turbulent Schmidt Number Profiles Downstream of a Short Mass Transfer Section in the Wall-Pipe Flow

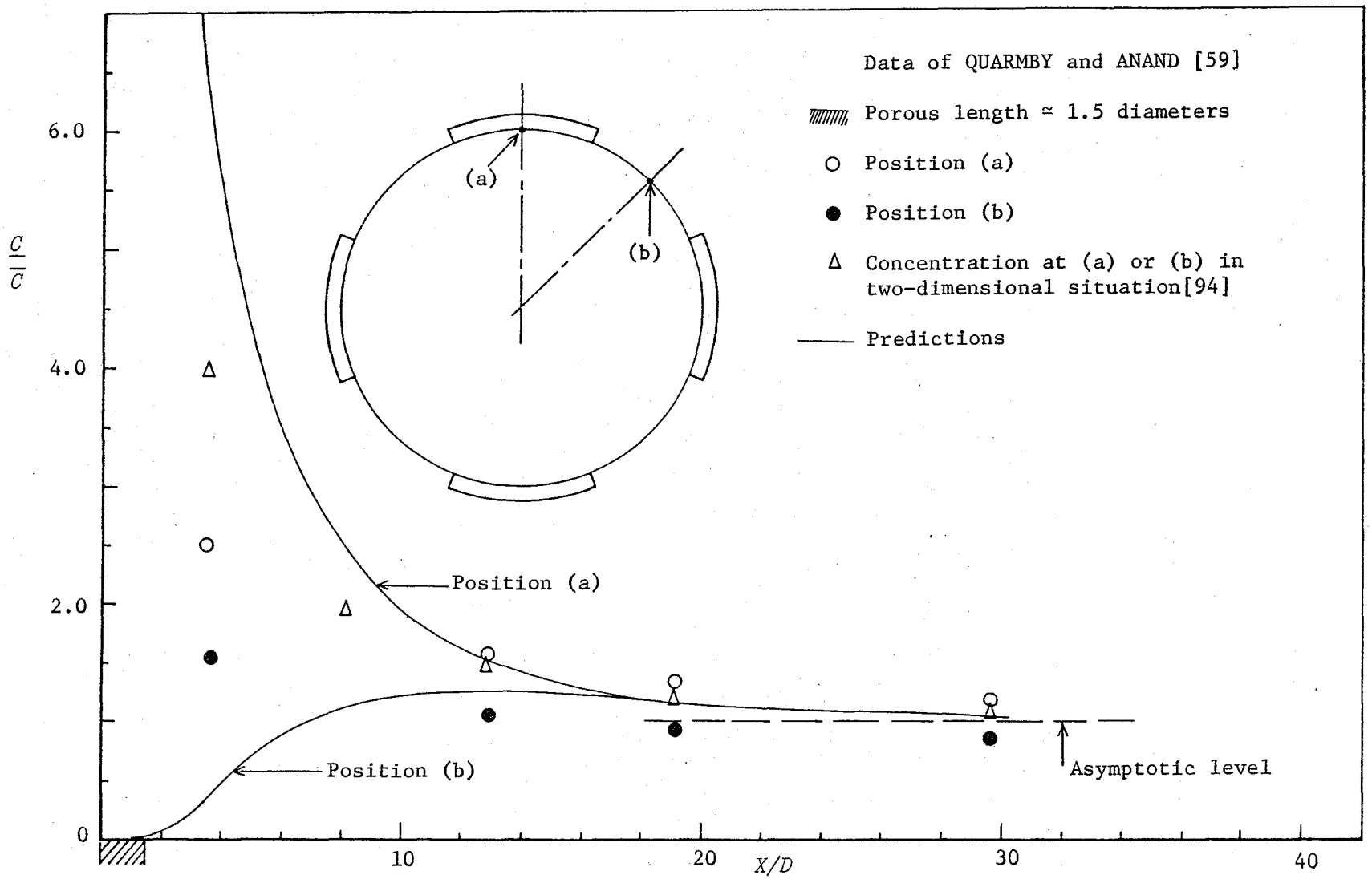

Fig. 7.1 Comparison of Streamwise Development of Near-wall Concentration Levels in QUARMBY and ANAND's [59] Experiment

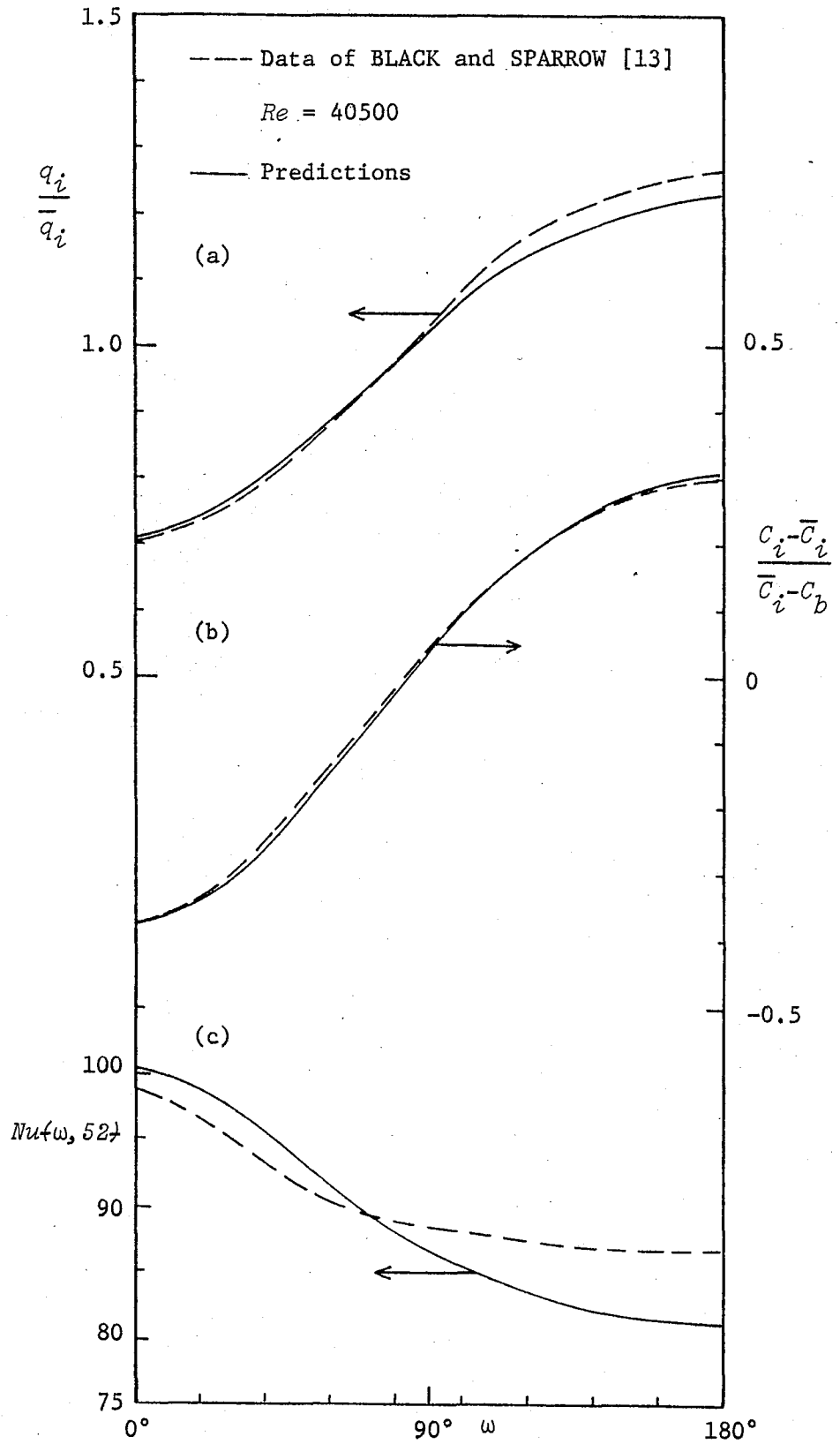

Fig. 7.2 The Angular Variation of (a) Wall Heat Flux, (b) Wall Temperature and (c) Nusselt Number $Nu\{\omega, X/D\}$, BLACK and SPARROW's [13] Experiment, Re = 40500.

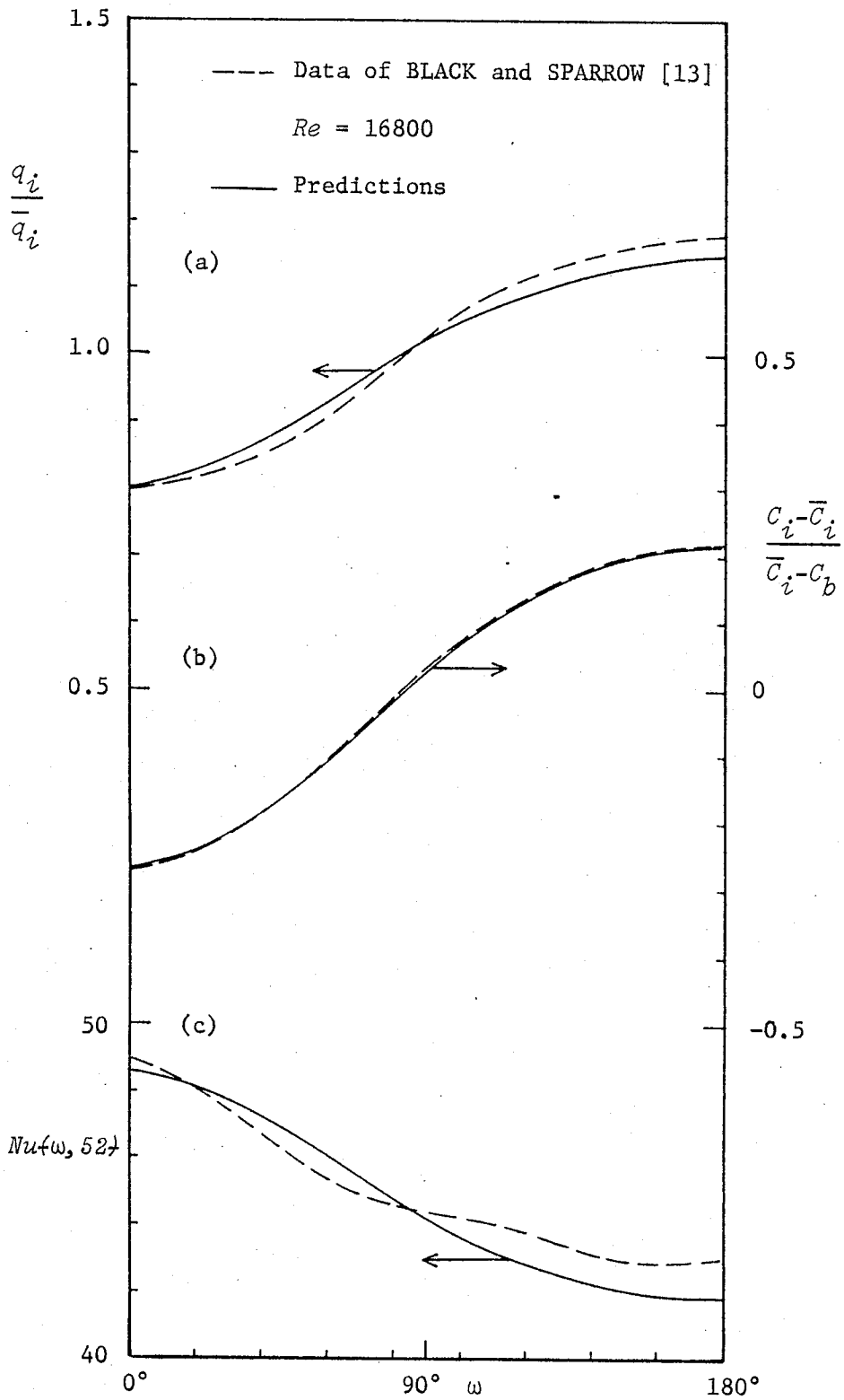

Fig. 7.3 The Angular Variation of (a) Wall Heat Flux, (b) Wall Temperature and (c) Nusselt Number $Nu(\omega, X/D)$, BLACK and SPARROW's [13] Experiment. Re = 16800

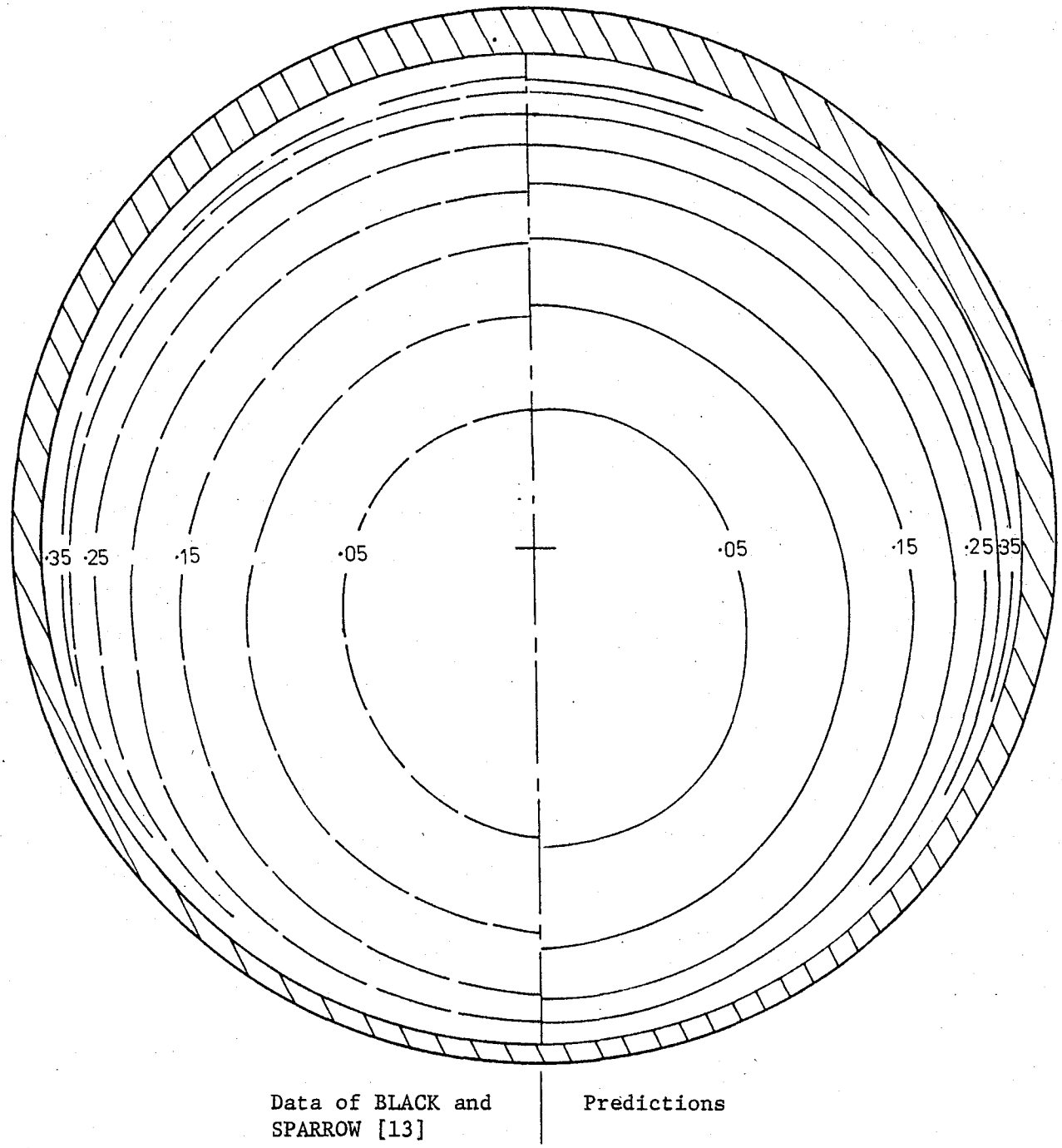

Note the variation in thickness of the tube wall through which heat is supplied.

Fig. 7.4 Non Dimensional Temperature $\frac{C - C_{min}}{C_{max} - C_{min}}$ contours : Black and Sparrow's Experiment, Re = 40500.

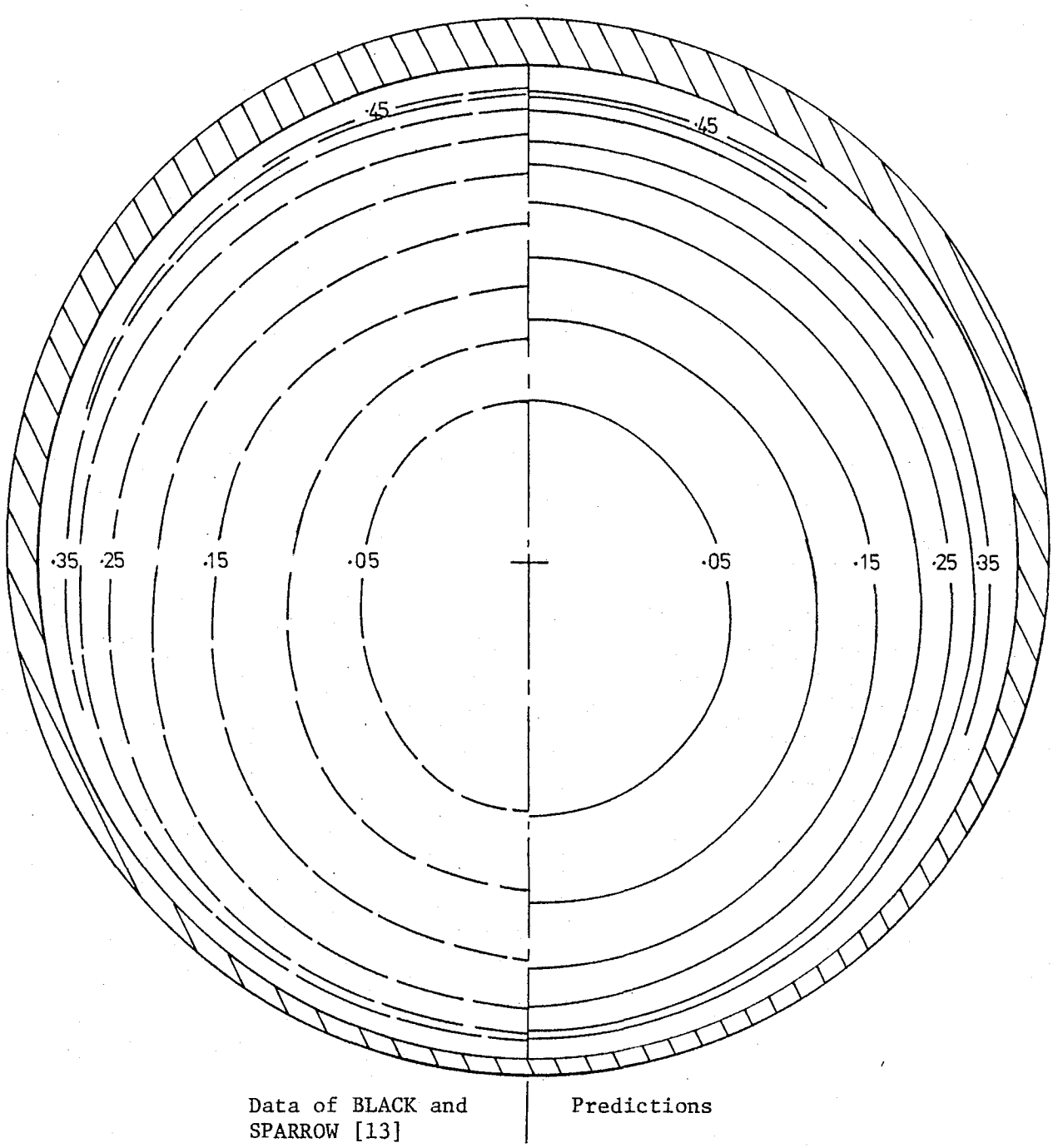

Note the variation in thickness of the tube wall through which heat is supplied.

Fig. 7.5 Non Dimensional Temperature $\frac{C - C_{min}}{C_{max} - C_{min}}$ contours : Black and Sparrow's Experiment, Re = 16800 .

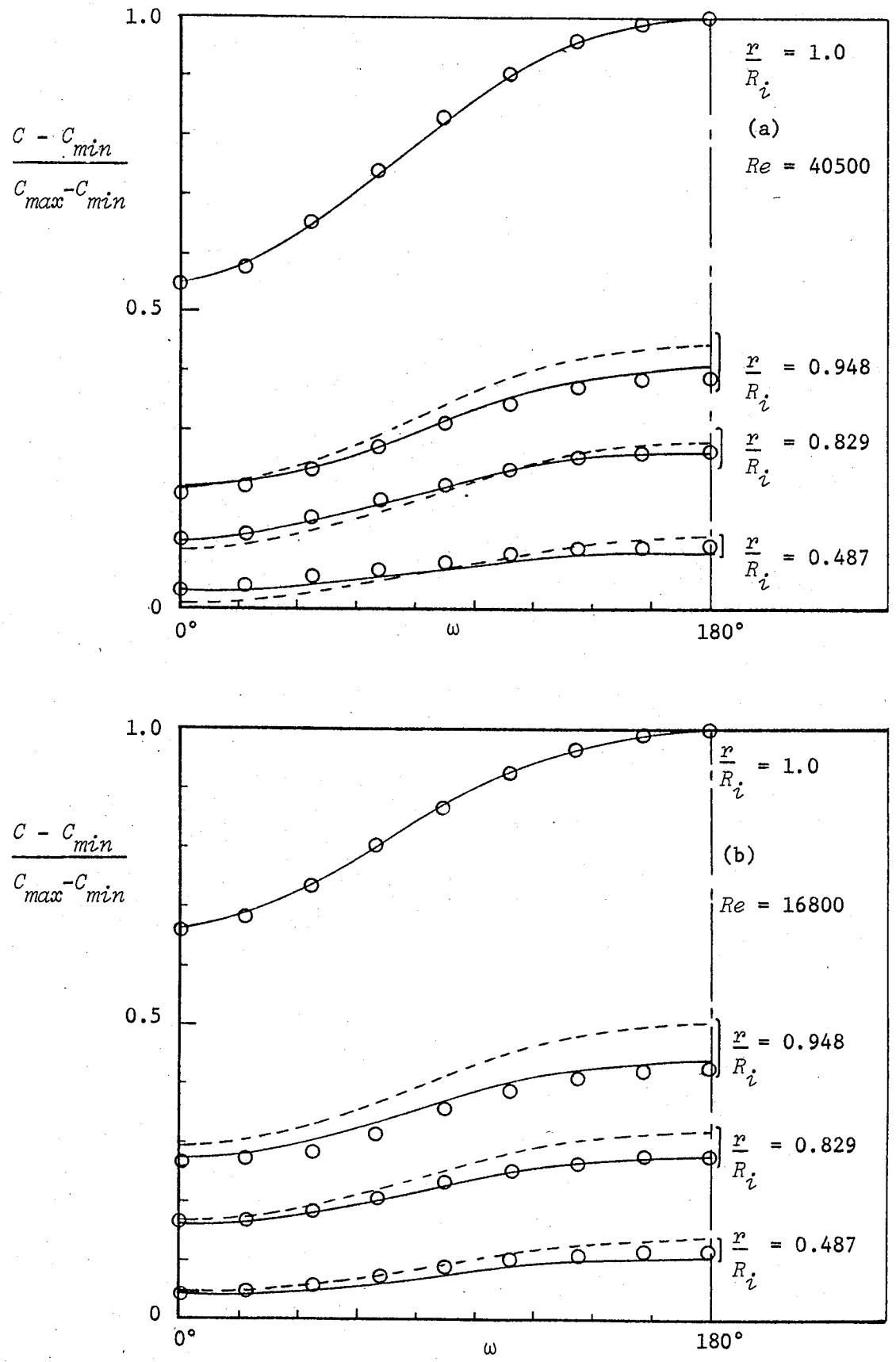

Fig. 7.6 Non-Dimensional Temperature Profiles in BLACK and SPARROW's [13] Experiment, X/D = 52 ;
O Data of [13], ——— Present Predictions,
--- Calculated Profiles Assuming Isotropic Diffusivity [13]

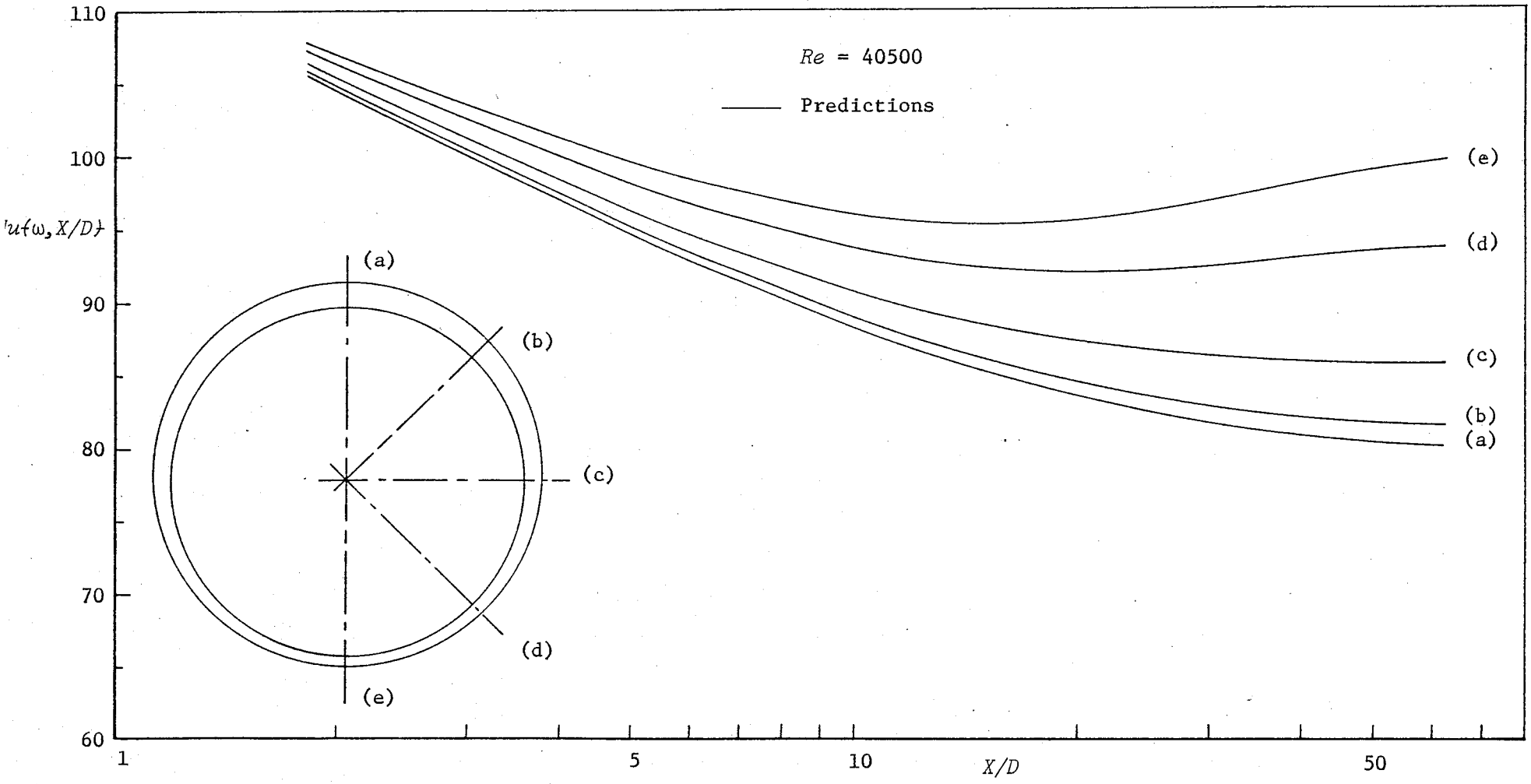

Fig. 7.7 Streamwise Development of Nusselt Numbers at Several Angular Locations - BLACK and SPARROW's [13] Experiment , Re = 40500 .

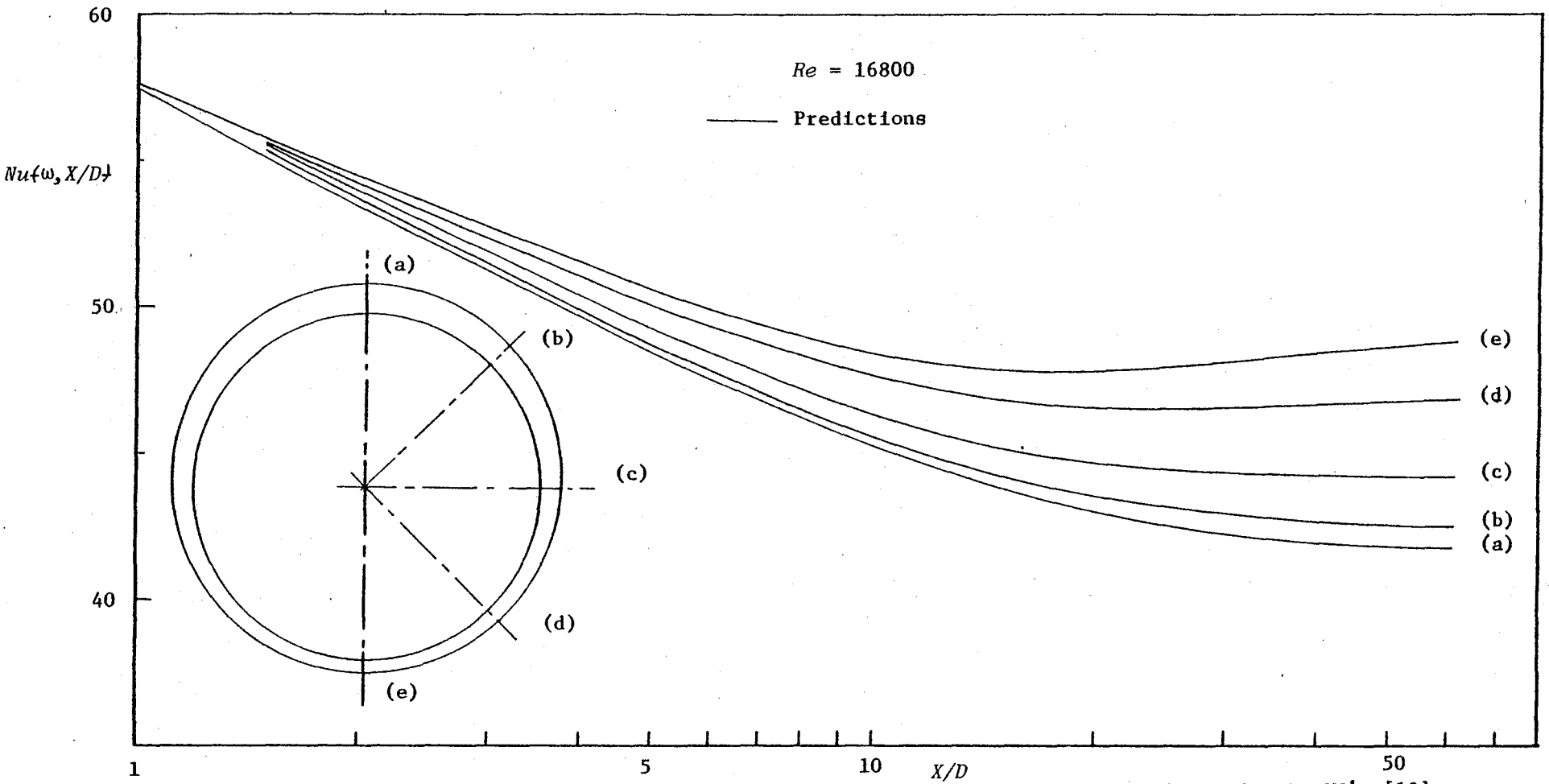

Fig. 7.8 Streamwise Development of Nusselt Numbers at Several Angular Locations - BLACK and SPARROW's [13] Experiment , Re = 16800 .

0 0 0 0 0 9 0 - 2751 - 1 6

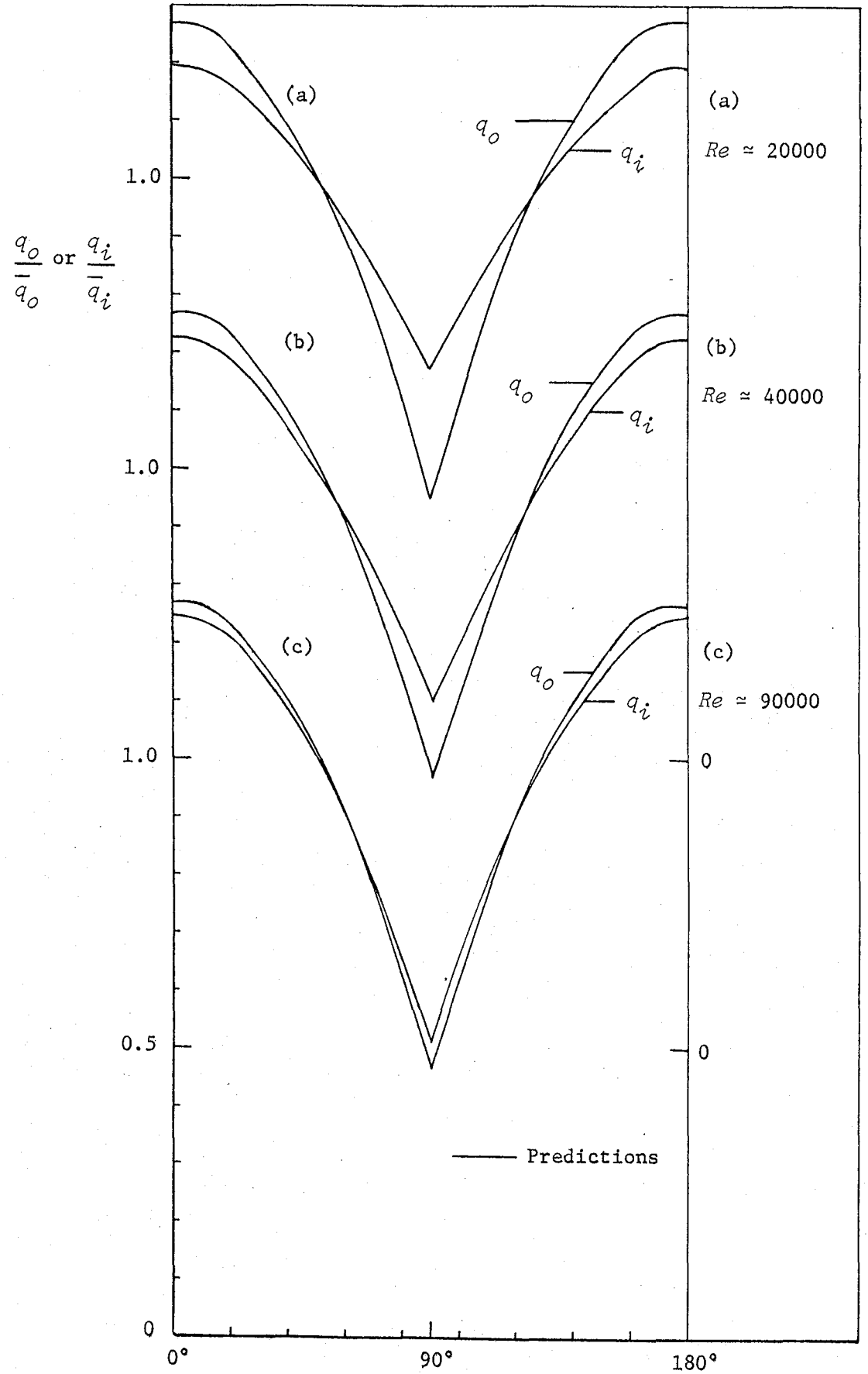

Fig. 7.9 Heat flux Through the Outer and Inner Surface of the Tube, (a) $Re \simeq 20000$, (b) $Re \simeq 40000$, (c) $Re \simeq 90000$.

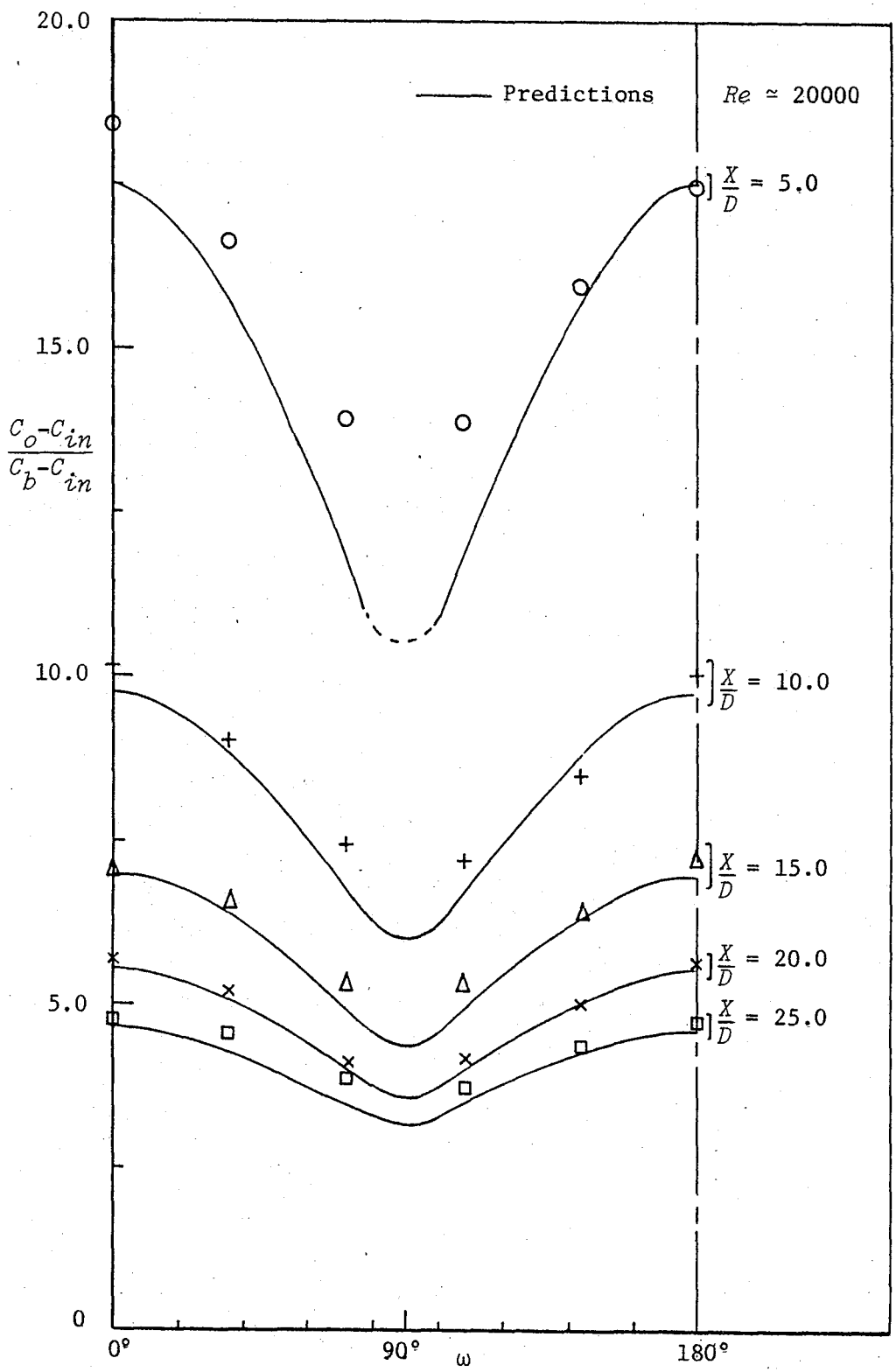

Fig. 7.10 Temperature Profiles at the Outer Surface of the Tube Wall : Present Experimental Situation; Both Halves Heating, $Re \simeq 20000$.

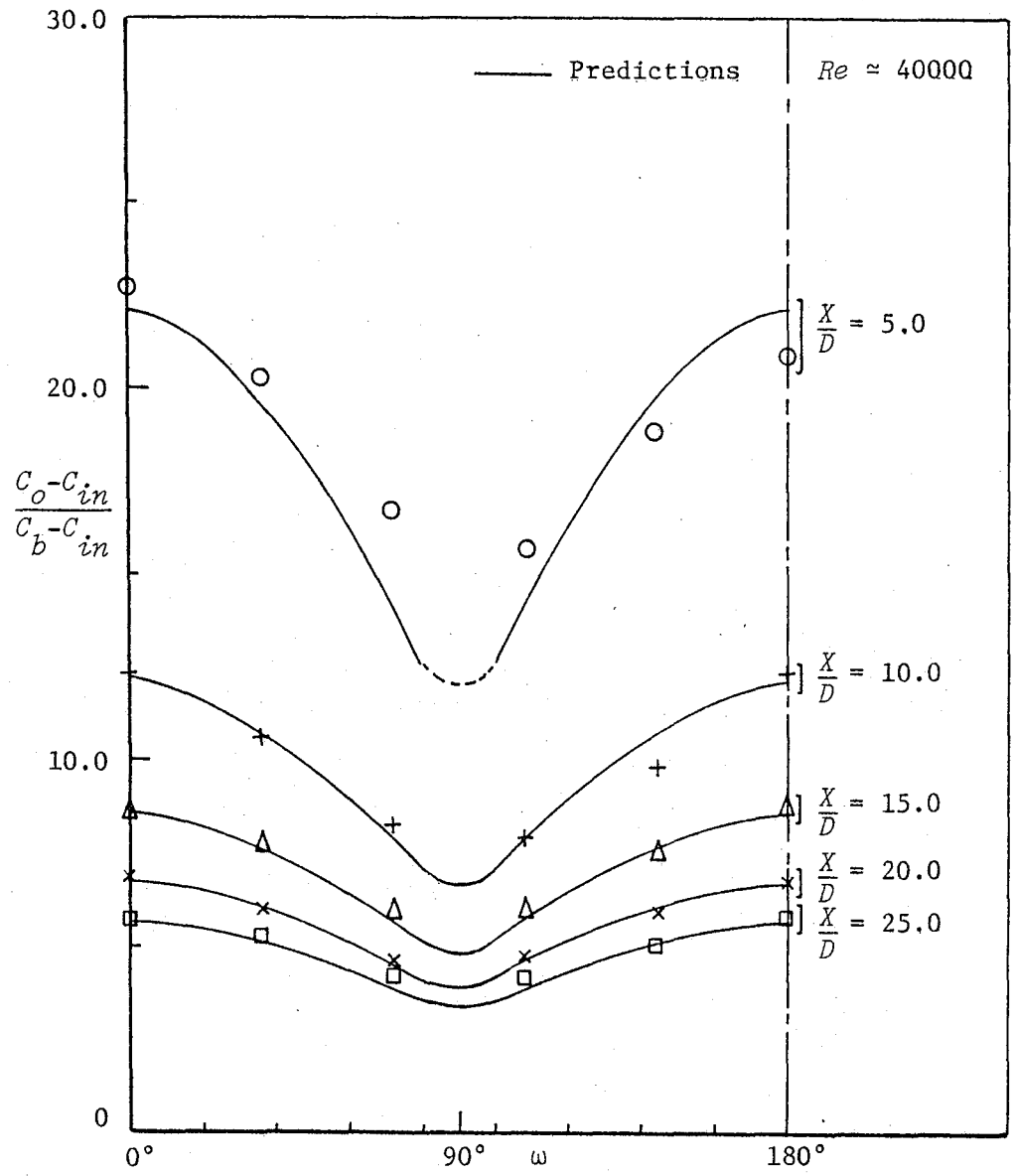

Fig. 7.11 Temperature Profiles at the Outer Surface of the Tube Wall : Present Experimental Situation; Both Halves Heating, $Re \simeq 40000$.

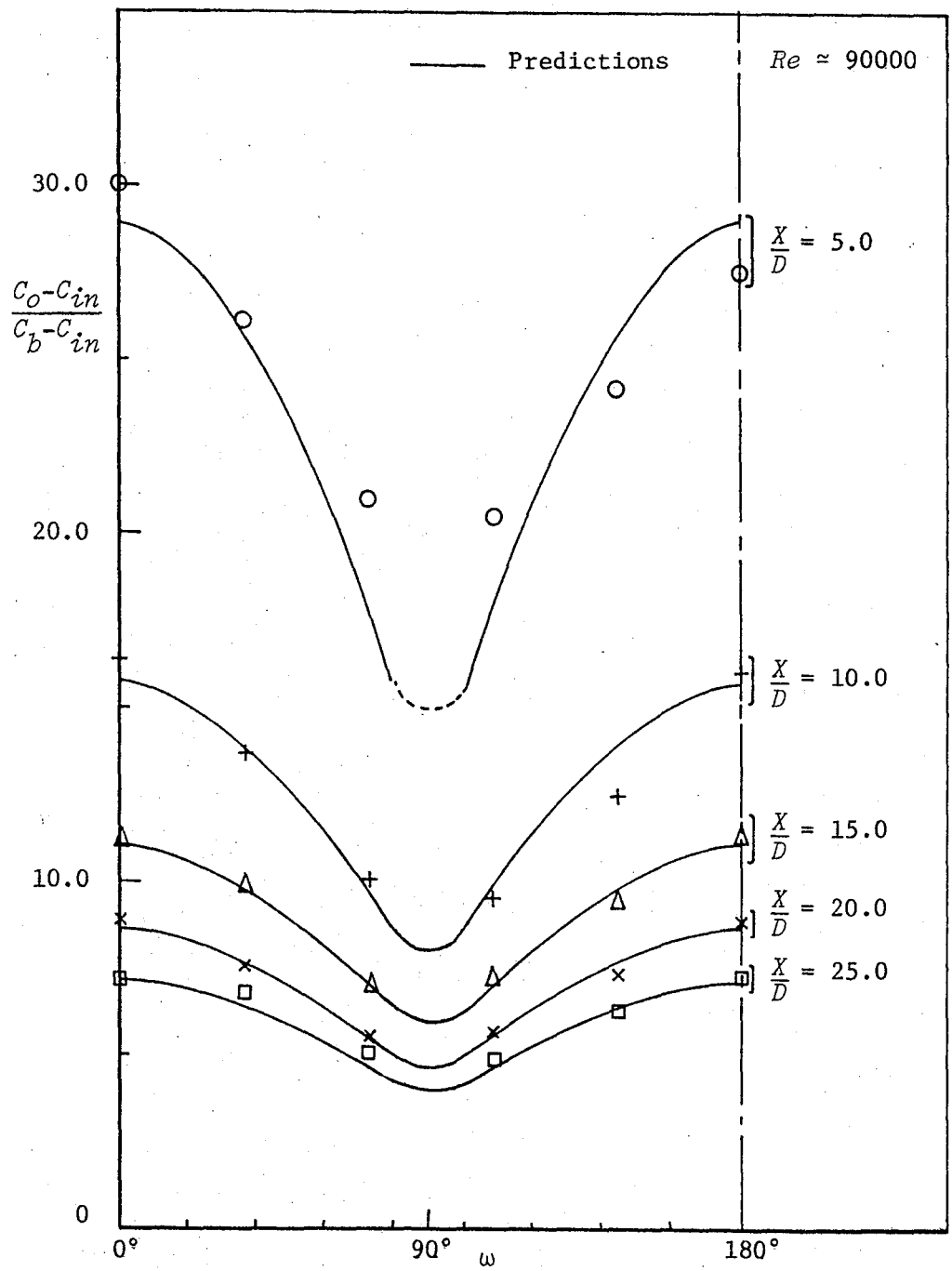

Fig. 7.12 Temperature Profiles at the Outer Surface of the Tube Wall : Present Experimental Situation; Both Halves Heating, $Re \simeq 90000$.

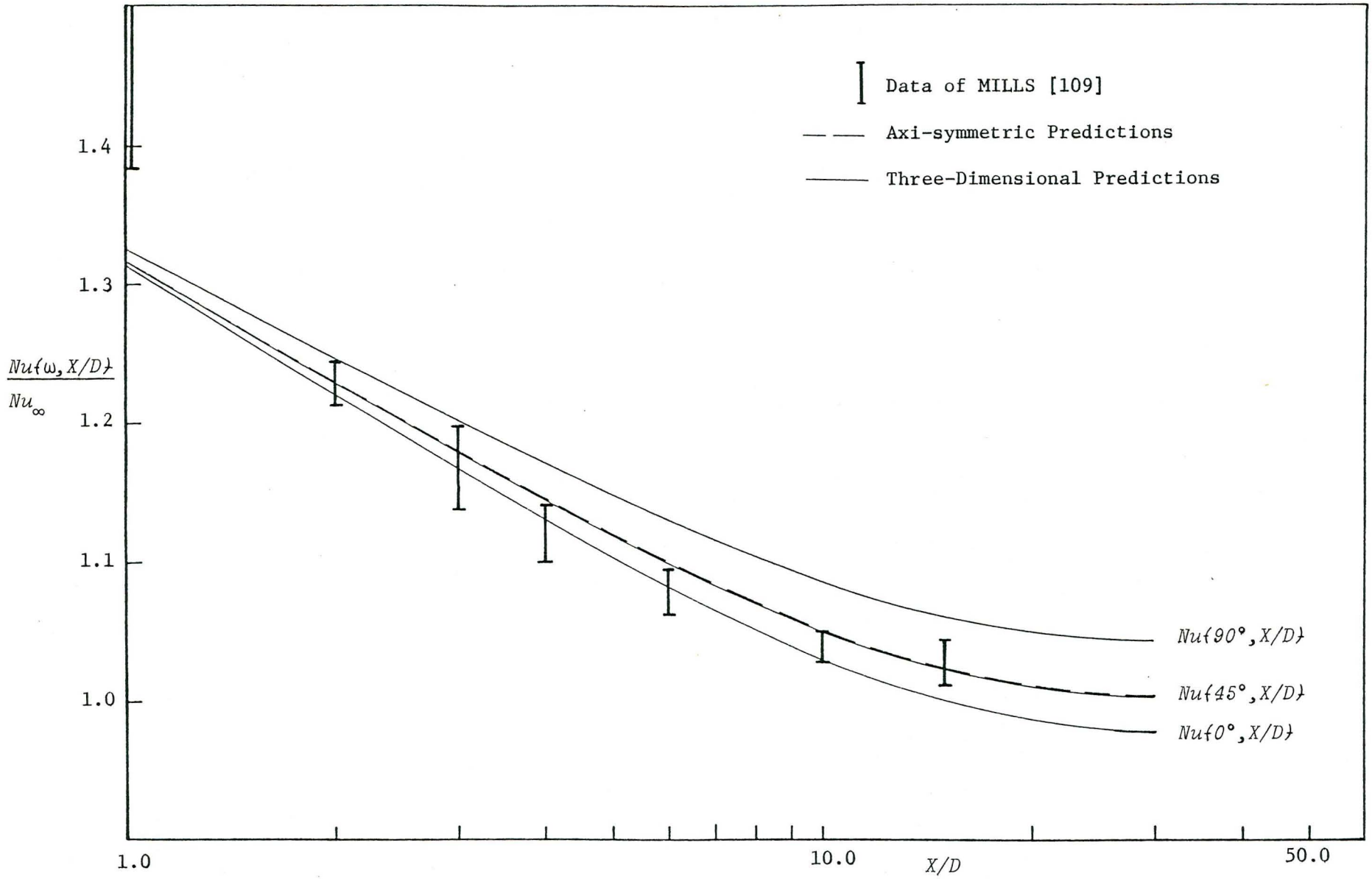

Fig. 7.13 Streamwise Variation of Nusselt Number : Present Experimental Investigation, Both Halves Heating, $Re \simeq 20000$.

(a)

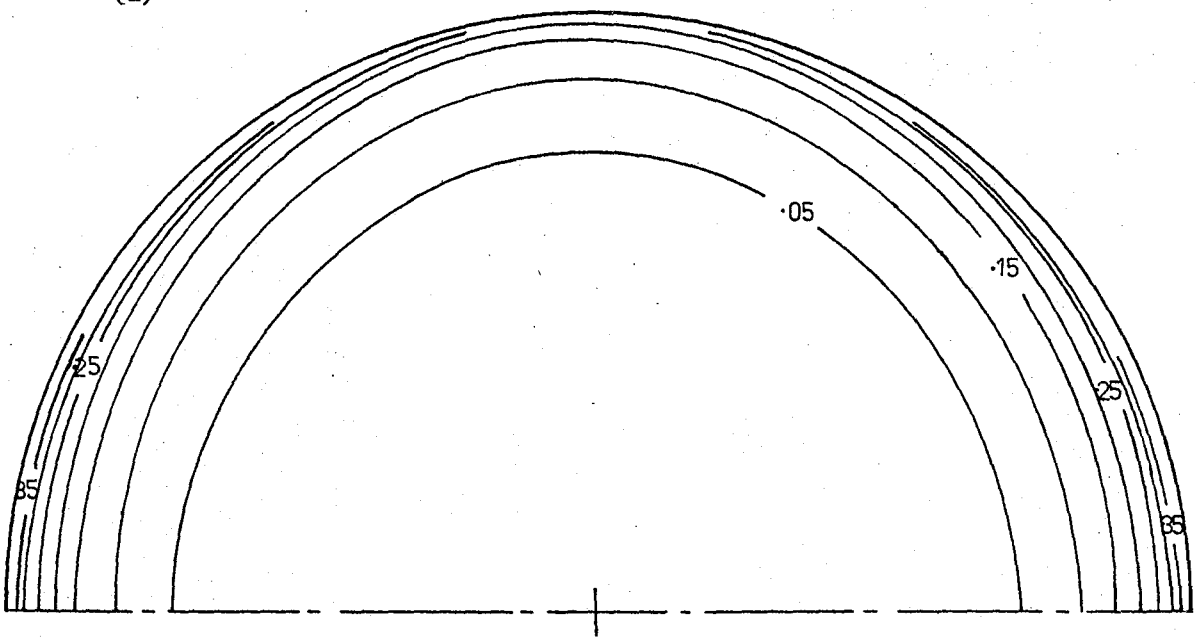

(b)

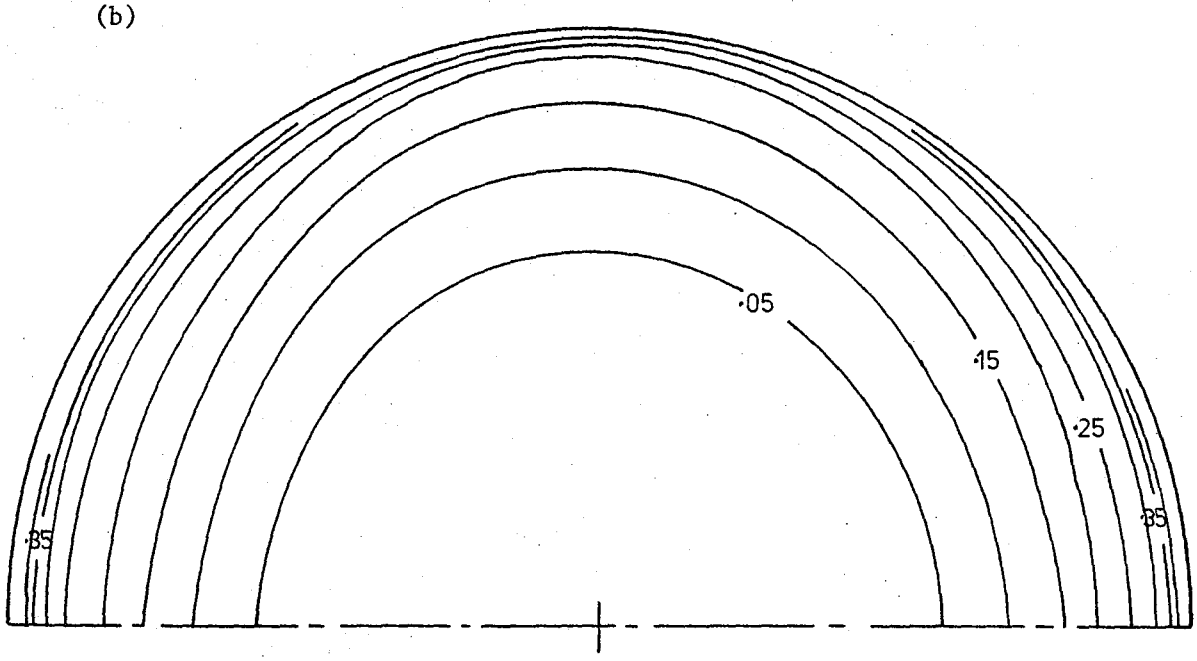

Fig. 7.14 (a) and (b)

(c)

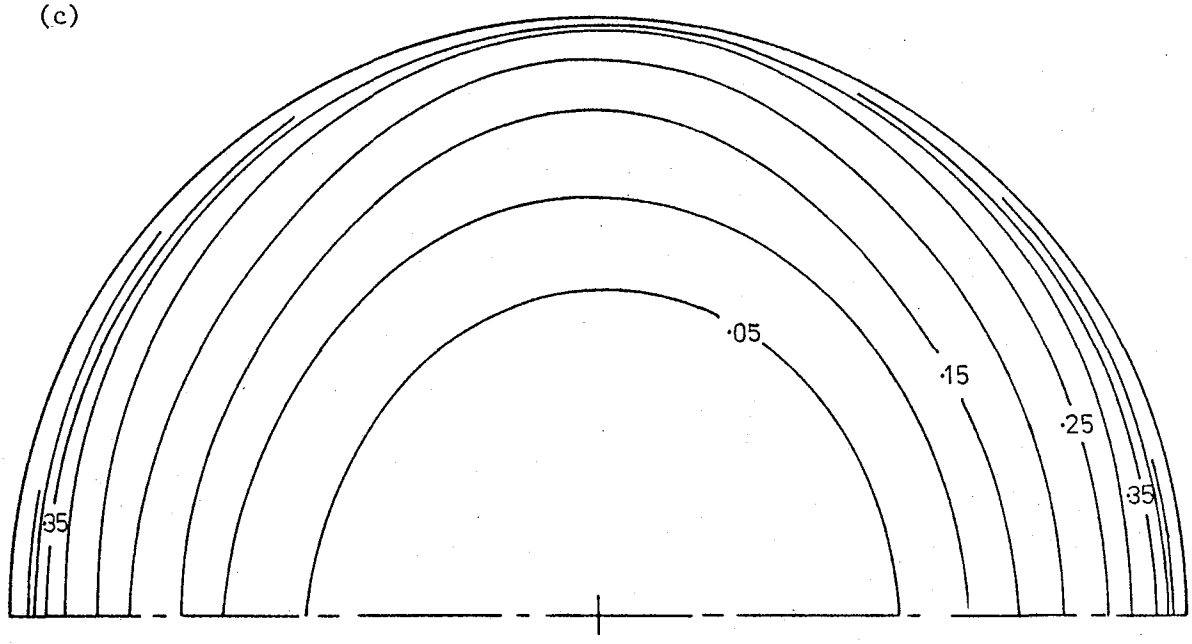

(d)

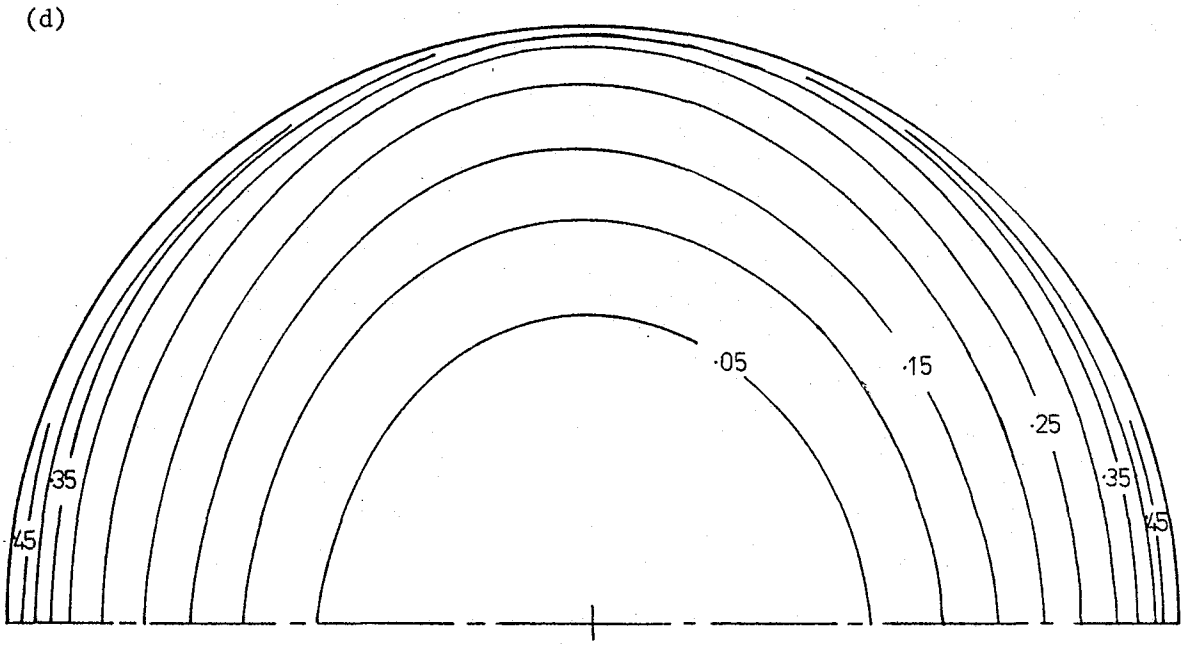

Fig. 7.14 (c) and (d)

(e)

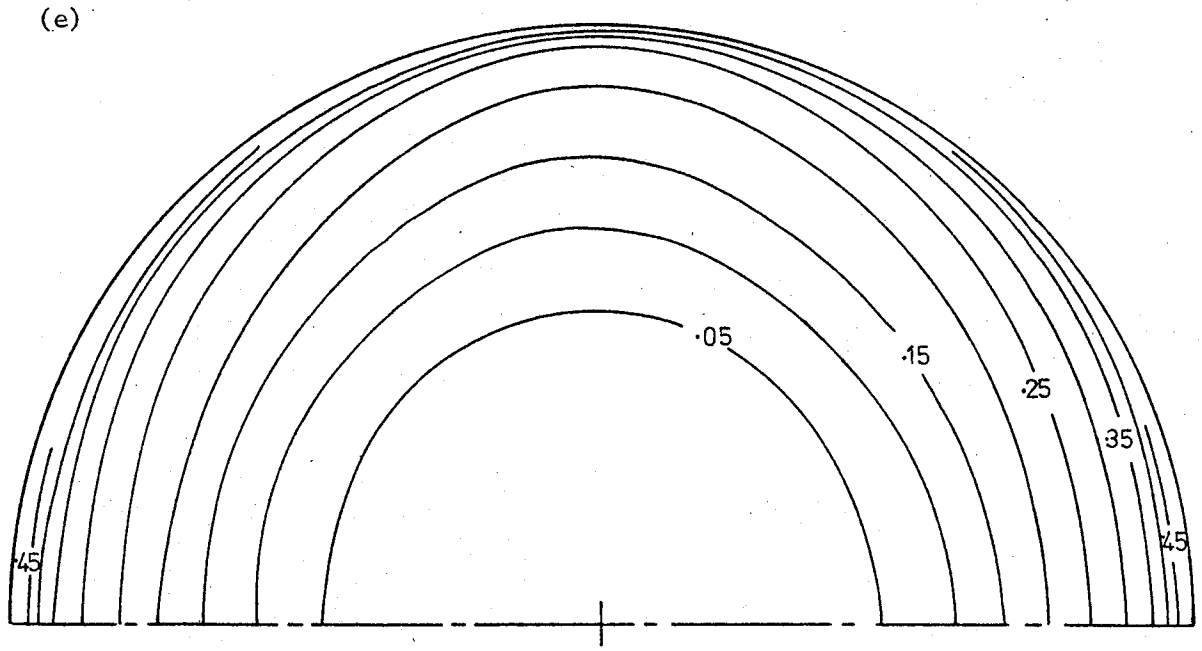

Fig. 7.14 Predicted Non-Dimensional Temperature $\frac{C - C_{min}}{C_{max} - C_{min}}$ contours : Present Experimental Situation; Both Halves Heating, $Re \simeq 40000$.

(a) $\frac{X}{D} = 5.0$, (b) $\frac{X}{D} = 10.0$, (c) $\frac{X}{D} = 15.0$,
(d) $\frac{X}{D} = 20.0$, (e) $\frac{X}{D} = 25.0$

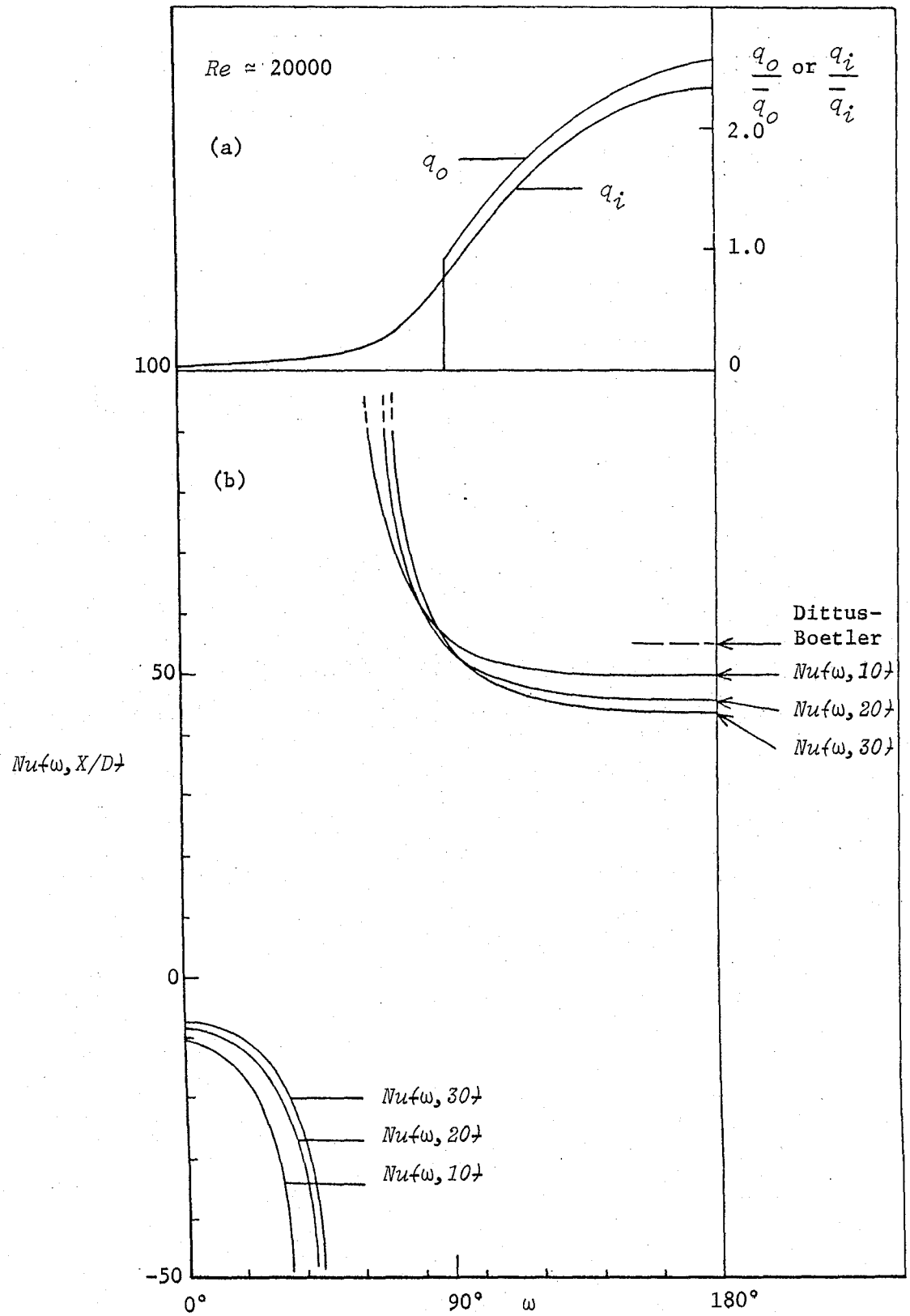

Fig. 7.15 Variation of (a) Heat Fluxes and (b) Local Nusselt Number, Around the Tube Wall .
$Re \simeq 20000$

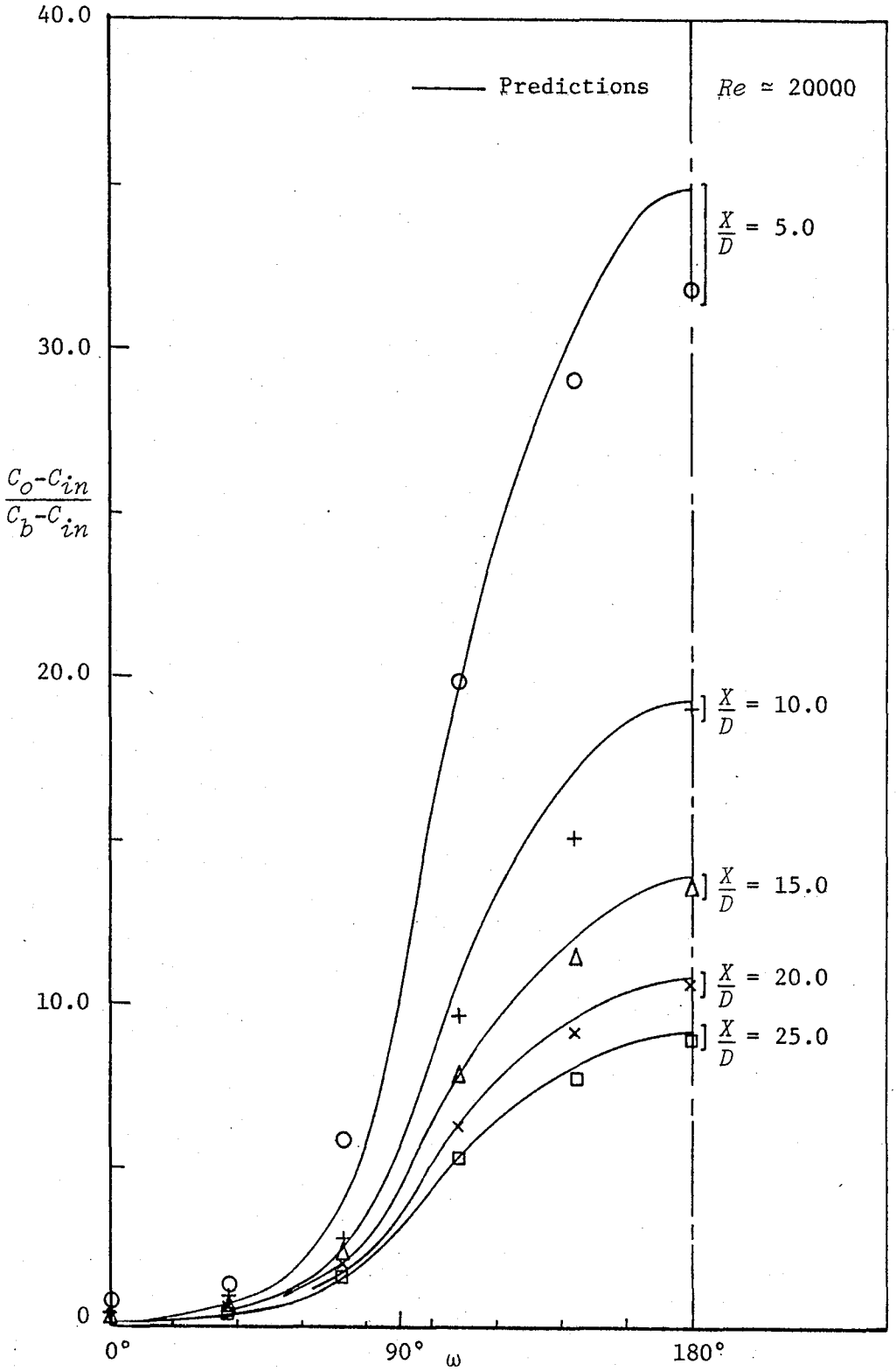

Fig. 7.16 Temperature Profiles at the Outer Surface of the Tube Wall : Present Experimental Situation (Heat Flux Profiles as in Fig. (7.15(a))) $Re \simeq 20000$

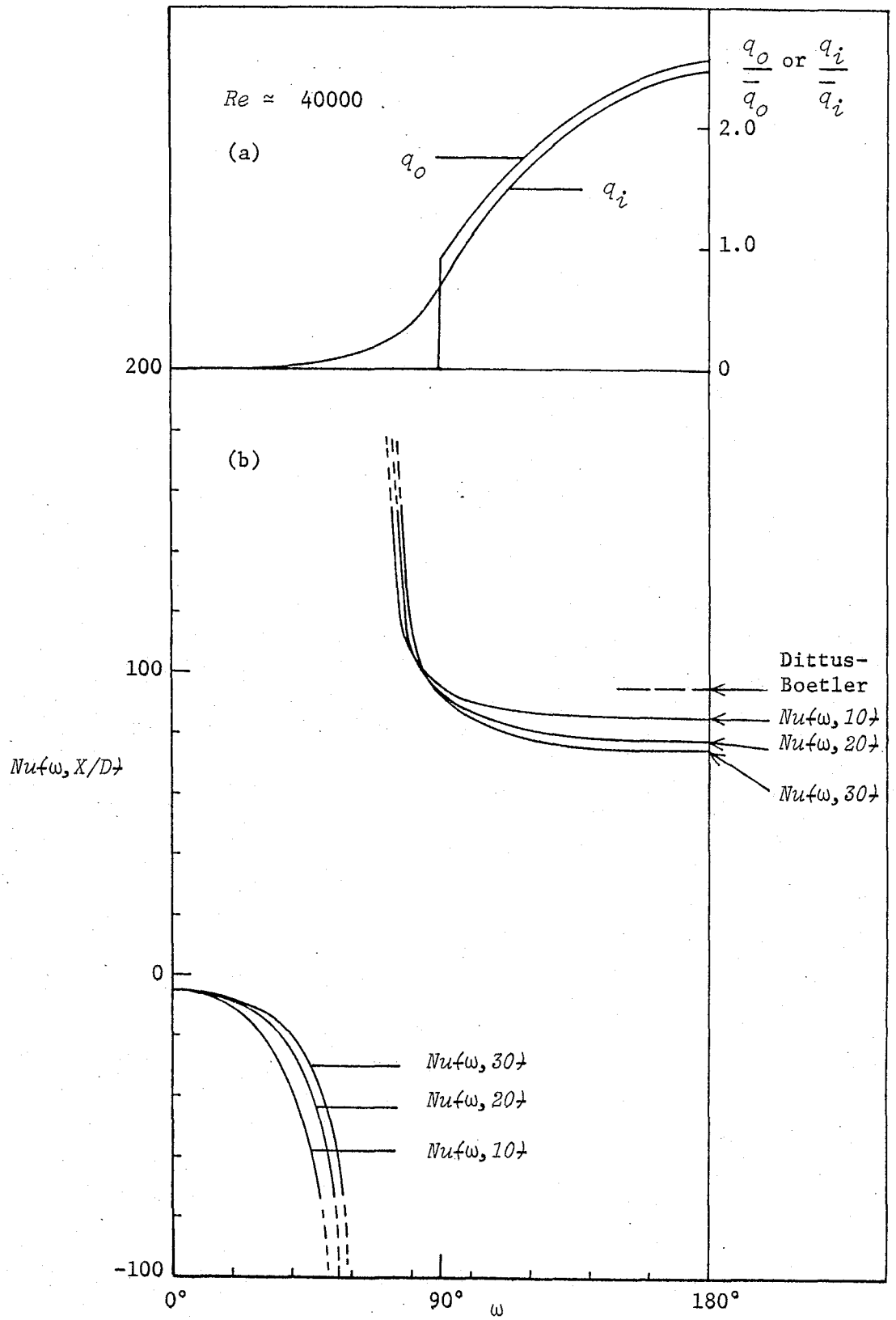

Fig. 7.17 Variation of (a) Heat Fluxes and (b) Local Nusselt Number, Around the Tube Wall .
Re ≃ 40000

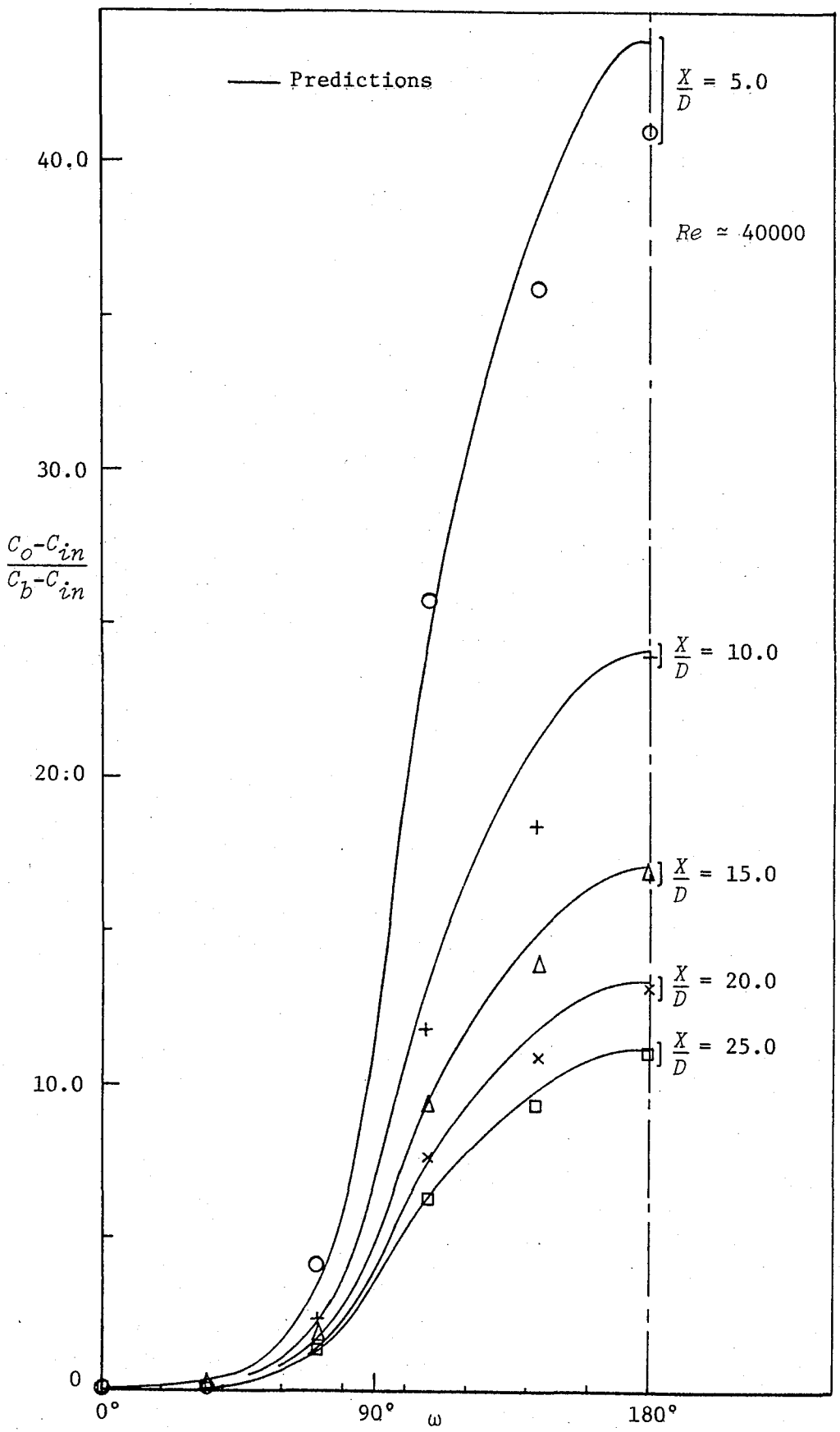

Fig. 7.18 Temperature Profiles at the Outer Surface of the Tube Wall : Present Experimental Situation (Heat Flux Profiles as in Fig. (7.17(a))) $Re \simeq 40000$

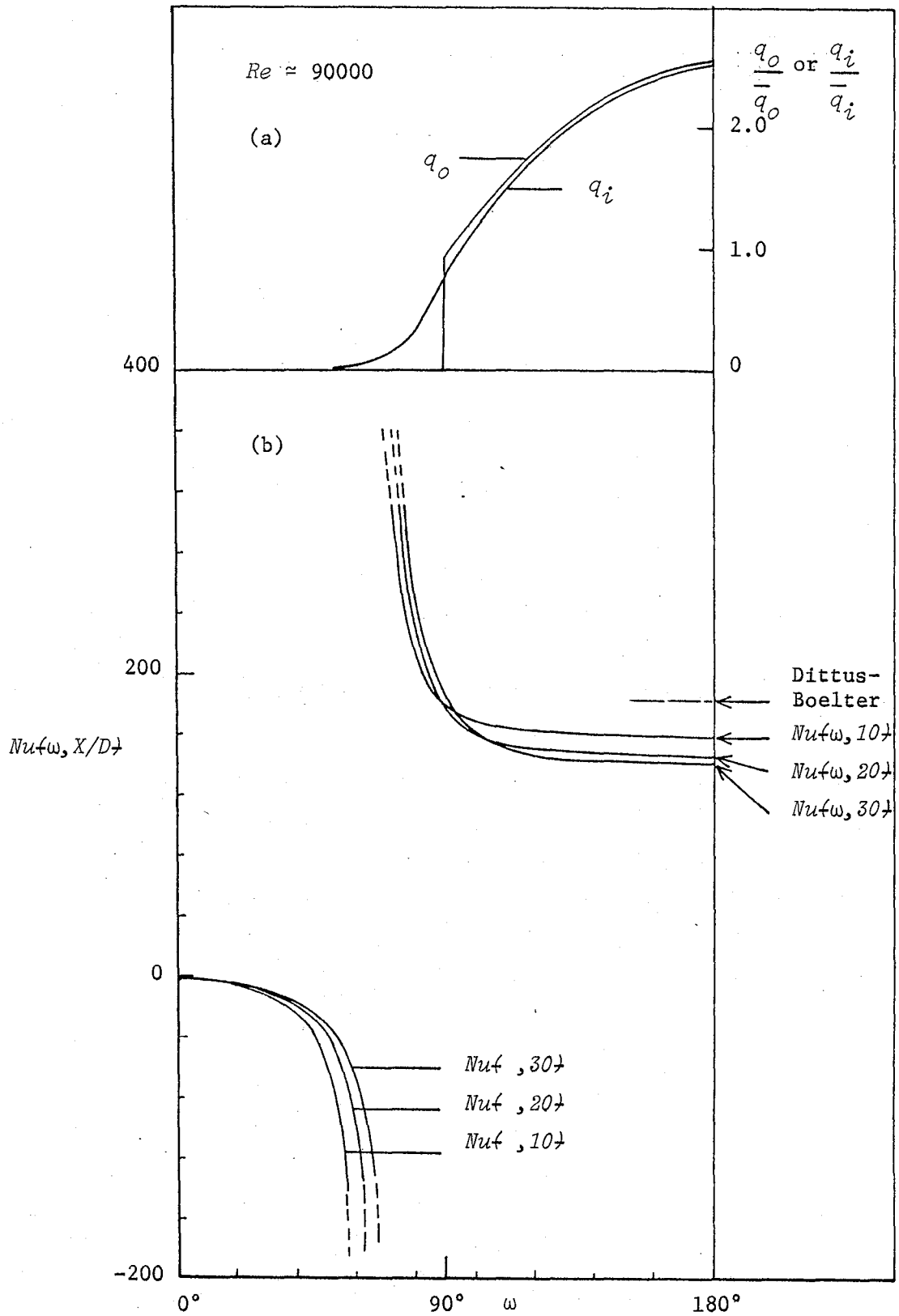

Fig. 7.19 Variation of (a) Heat Fluxes and (b) Local Nusselt Number, Around the Tube Wall .
Re ≃ 90000

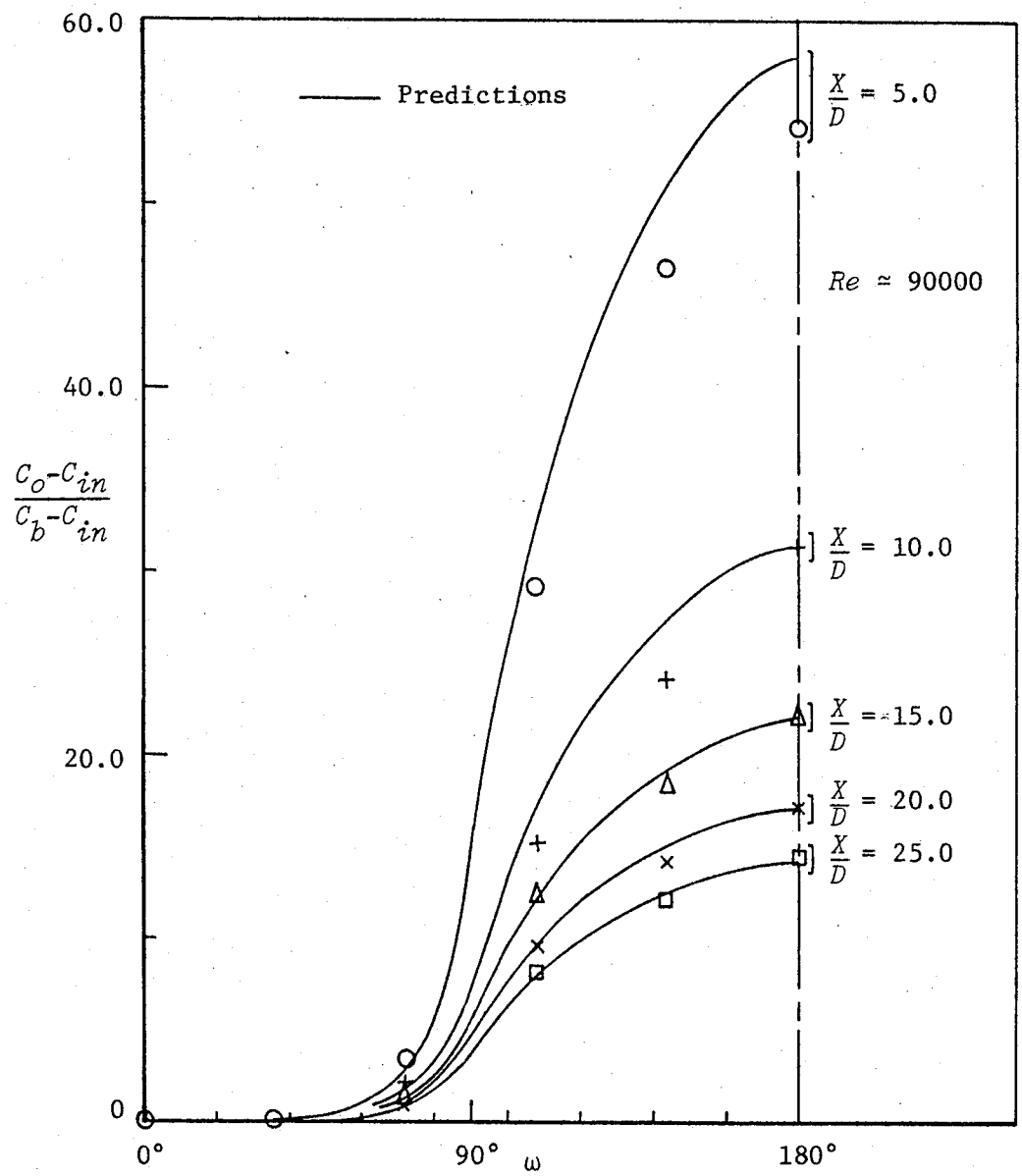

Fig. 7.20 Temperature Profiles at the Outer Surface of the Tube Wall : Present Experimental Situation (Heat Flux Profiles as in Fig. (7.10(a))) $Re \simeq 90000$

(a)

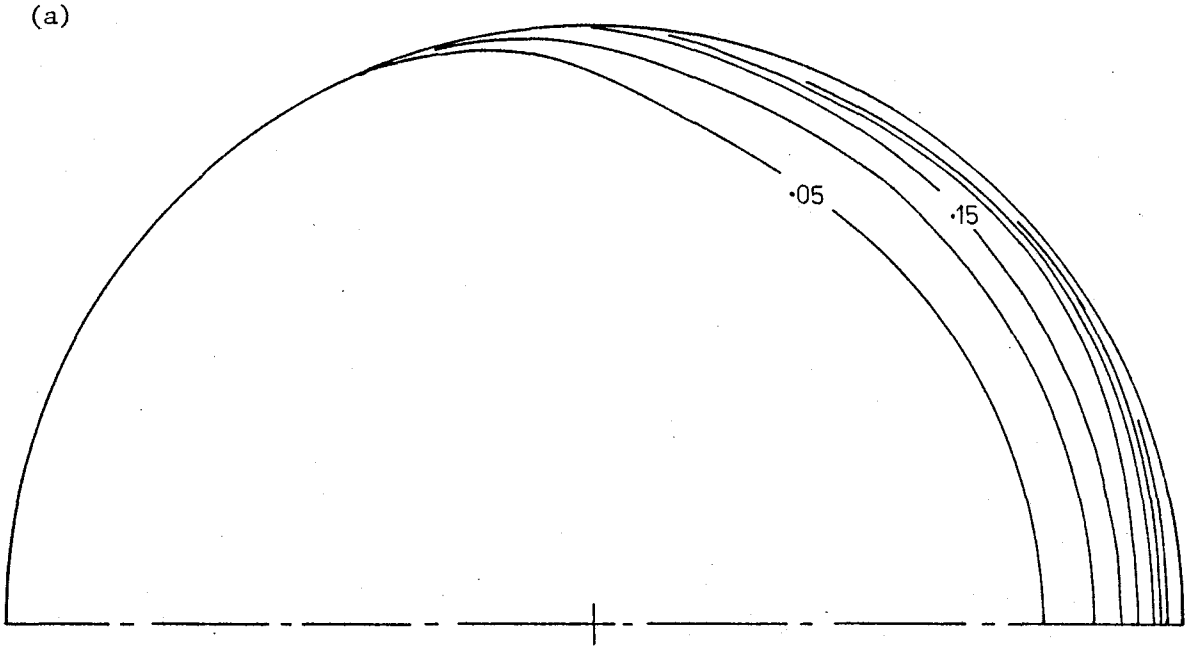

(b)

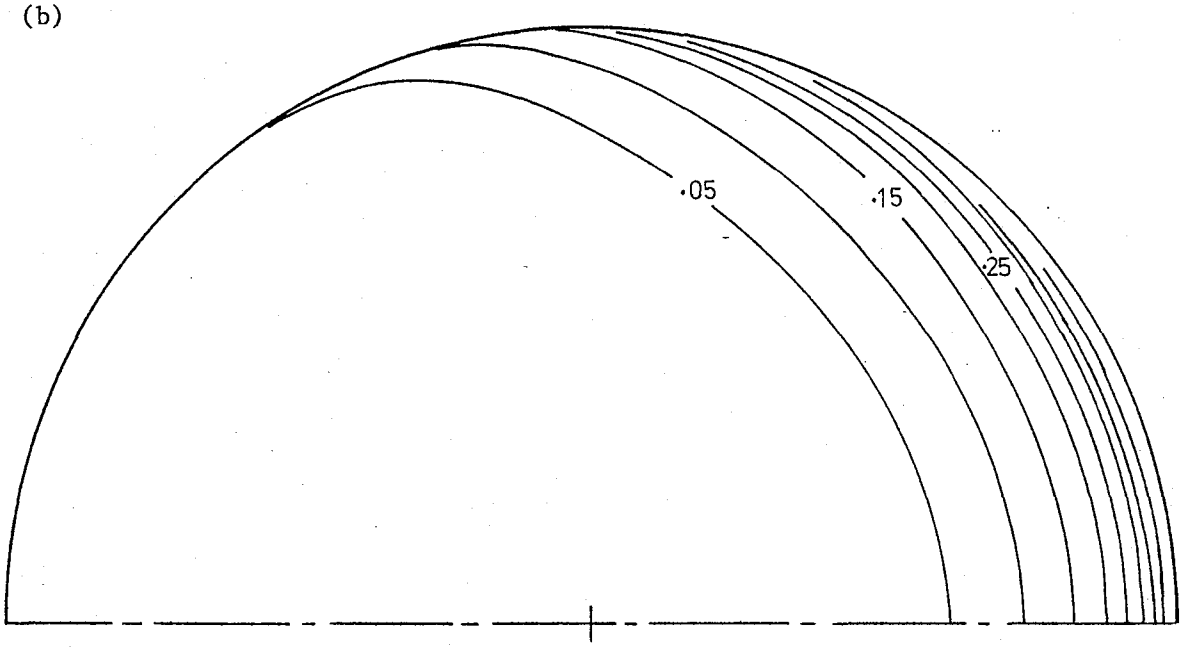

Fig. 7.21 (a) and (b)

(c)

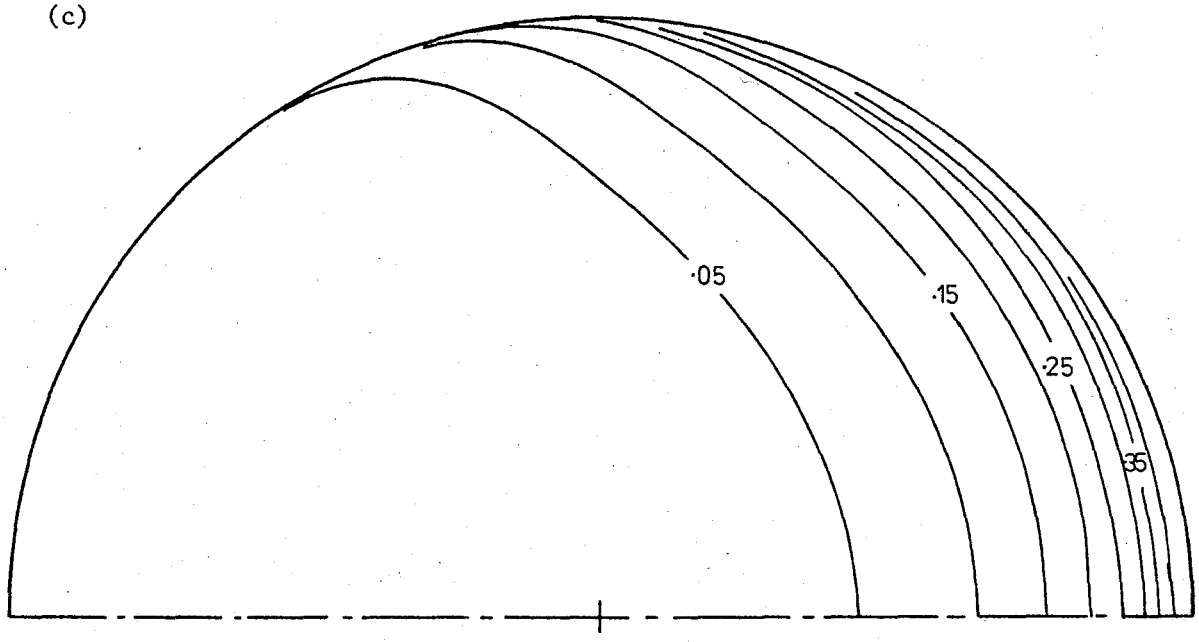

(d)

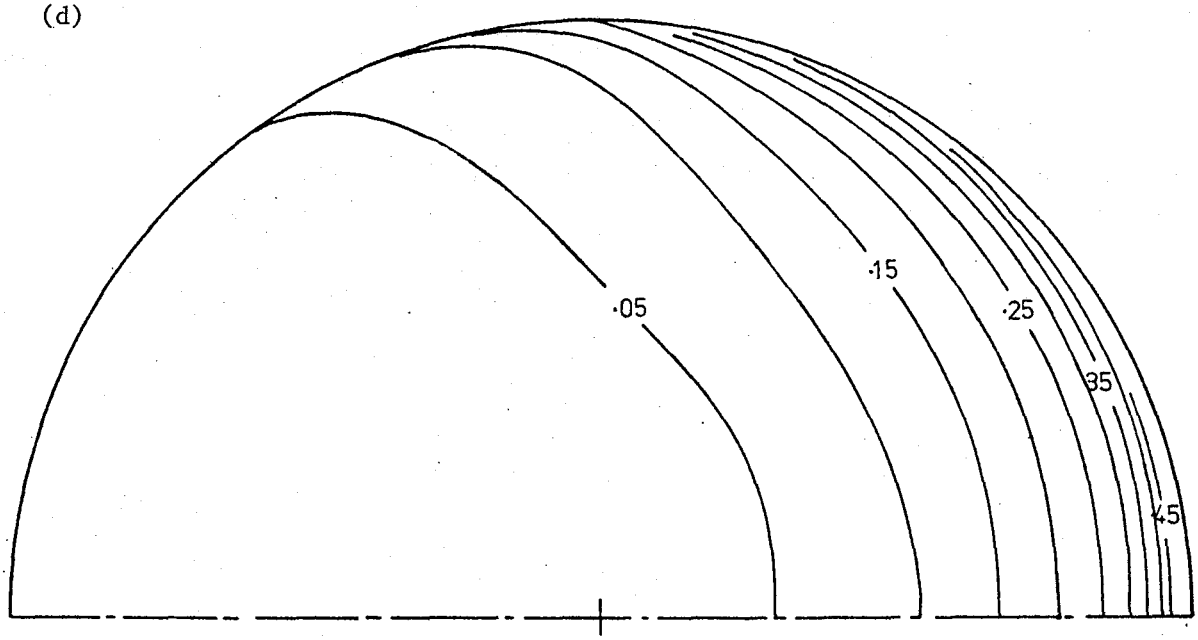

Fig. 7.21 (c) and (d)

(e)

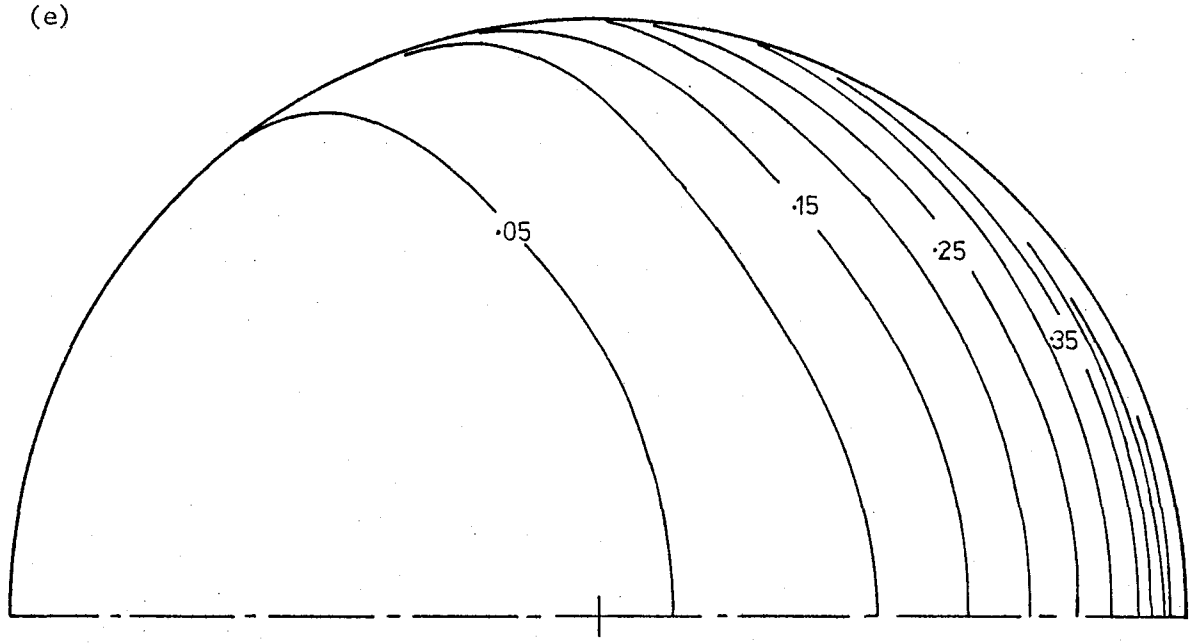

Fig. 7.21 Predicted Non-Dimensional Temperature $\frac{C - C_{min}}{C_{max} - C_{min}}$ contours : Present Experimental Situation; Only Right Half Heating, $Re \simeq 40000$.

(a) $\frac{X}{D} = 5.0$, (b) $\frac{X}{D} = 10.0$, (c) $\frac{X}{D} = 15.0$
(d) $\frac{X}{D} = 20.0$, (e) $\frac{X}{D} = 25.0$

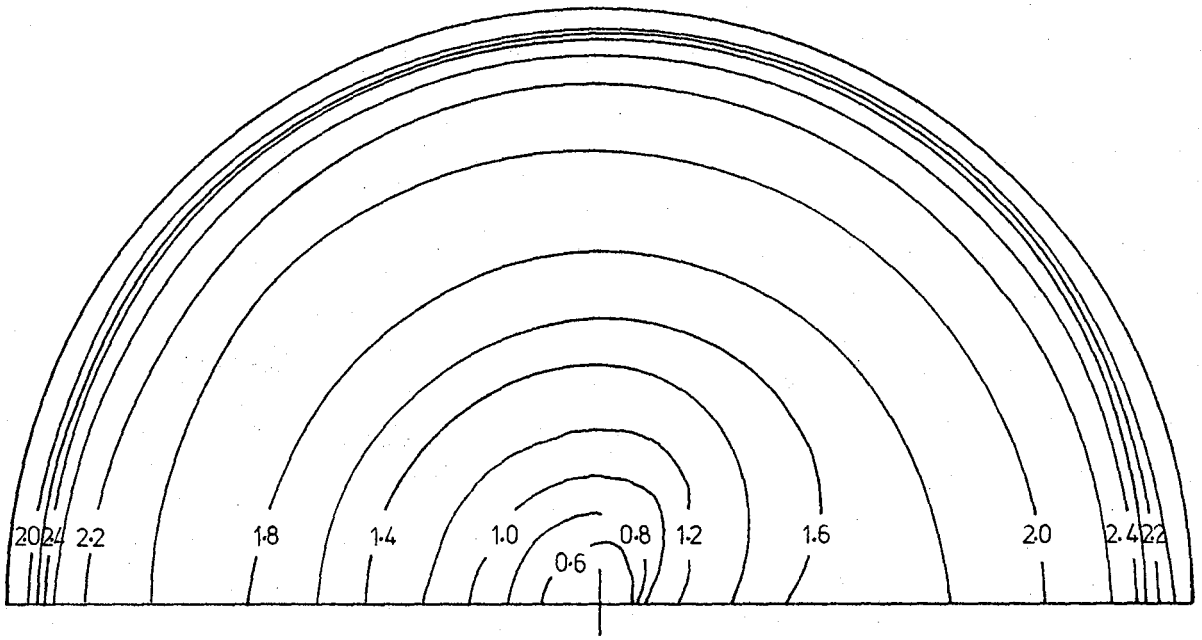

Fig. 7.22 Ratio of Diffusivity of Heat in Tangential to Radial Direction : Prediction of Black and Sparrow's Flow, Re = 40500 .

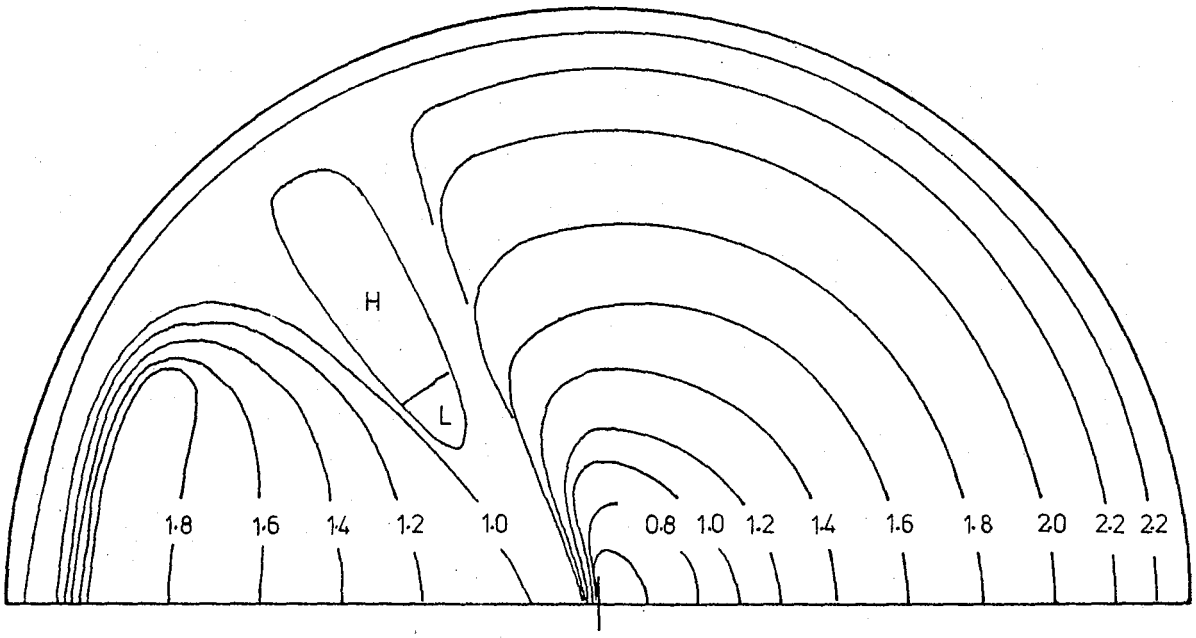

Fig. 7.23 Ratio of Diffusivity of Heat in Tangential to Radial Direction : Prediction of Present Experiment , $Re \simeq$ 40000 (Only Right Half Heated).

APPENDIX (A)

A Form for the Near-Wall Effect Function in Cylindrical Geometry

A form for the near-wall function can be obtained by considering the respective geometric configurations. The Fig. (A.1) considers the following situations

(a) flow affected by a single plane wall,

(b) flow affected by two parallel plane walls,

and (c) flow inside a circular tube.

If the near-wall function,

$$f = f\left(\frac{l_\varepsilon}{y_o}\right) \tag{A.1}$$

is to depict the effective influence of the wall, then for a point at a given distance, a , from the wall,

$$f_{(a)} < f_{(b)} < f_{(c)} \quad . \tag{A.2}$$

Out of several plausible forms the following is chosen to represent the effective distance to the wall.

$$\frac{1}{y_o} \propto \left| \int_{-\infty}^{+\infty} \frac{\cos \alpha}{l^2} \, dx \right| \quad . \tag{A.3}$$

Thus for case (a),

$$\frac{1}{y_o} = \left| 2 \int_0^{\pi/2} \frac{a \cos \theta \sec^2 \theta \, d\theta}{a^2 \sec^2 \theta} \right| = \frac{2}{a} \tag{A.4}$$

i.e.

$$y_o = K_o \, a \quad . \tag{A.5}$$

The constant of proportionality in (A.3) is thus equal to ½ . For the case of two plane walls (A.3) can be applied to both walls to obtain,

$$y_o = K_o \left(\frac{1}{\left(\frac{1}{a}\right) + \left(\frac{1}{h-a}\right)} \right) \quad . \tag{A.6}$$

For the case of a cylindrical geometry, case (c),

$$\frac{1}{y_o} \propto \left| 2 \int \frac{R \cos(\theta - \beta)}{R^2 (1 + b^2 - 2 b \cos \beta)} d\beta \right| \tag{A.7}$$

where $b = \frac{R - a}{R}$

i.e.

$$y_o = K_o \left(\frac{R}{\int_0^{\pi} \frac{(1 - b \cos \theta)\, d\theta}{(1 + b^2 - 2 b \cos \theta)^{3/2}}} \right) \quad . \tag{A.8}$$

Though the exact solution of the definite integral in (A.8) can be obtained (see Table 67, BIERNES DE HANN [110]) its inclusion in a calculation may be rather expensive. A fourth order polynomial equivalent of the integral can however be easily obtained as

$$y_o = k_o R g$$

where,

$$g = q - 1.4955 q^2 + 1.2673 q^3 - 0.4535 q^4 \tag{A.9}$$

and,

$$q = 1 - b \quad .$$

APPENDIX (B)

Simulation of the Diffusive Transport of $\overline{u_i c}$ and $\overline{c^2}$

The transport equation for the triple correlation $\overline{u_i u_k c}$ for high Reynolds and Peclet numbers can be written as

$$\overline{u_i u_k c}_{,t} + U_l \, \overline{u_i u_k c}_{,l} = - (\underbrace{\overline{u_i u_l c} \, U_{k,l} + \overline{u_i u_k u_l} \, C_{,l} + \overline{u_l u_k c} \, U_{i,l}}_{(a)})$$

$$- \underbrace{\overline{u_i u_k u_l c}_{,l}}_{(b)} - (\underbrace{\overline{u_i c \, p_{,k}} + \overline{u_k c \, p_{,i}}}_{(c)})$$

$$+ (\underbrace{\overline{u_i c} \cdot \overline{u_k u_l}_{,l} + \overline{u_i u_k} \cdot \overline{u_l c}_{,l} + \overline{u_k c} \cdot \overline{u_i u_l}_{,l}}_{(d)}) \, . \tag{B.1}$$

The quadruple correlation $\overline{u_i u_k u_l c}$ can be simplified with reference to MILLIONSHTCHIKOV's [23] hypothesis,

$$\overline{u_i u_k u_l c} = \overline{u_i u_k} \cdot \overline{u_l c} + \overline{u_i u_l} \cdot \overline{u_k c} + \overline{u_i c} \cdot \overline{u_k u_l} \tag{B.2}$$

which is strictly valid only in random fields with Gaussian probability density distributions but approximately satisfied even in non-homogeneous turbulence fields [22]. Therefore

$$(b) + (d) = - (\overline{u_k u_l} \cdot \overline{u_i c}_{,l} + \overline{u_l c} \cdot \overline{u_i u_k}_{,l} + \overline{u_i u_l} \cdot \overline{u_k c}_{,l}) \, . \tag{B.3}$$

The exact expression for the pressure-scalar flux correlation can be obtained as,

$$\frac{1}{\rho} \overline{u_i c \, p_{,k}} = \frac{1}{2\pi} \int_V \frac{1}{r'} \left(U'_{m,n} \, \overline{u'_n u_i c}_{,m} \right)_{,k} dVol$$

$$+ \frac{1}{4\pi} \int_V \frac{1}{r'} \left(\overline{u'_m u'_n u_i c}_{,mnk} \right) dVol + S \tag{B.4}$$

This expression clearly has two distinct types, one expressing the influence of the mean-rate-of-strain and the other involving only turbulent quantities. The first process can be modelled, following the pattern of pressure-strain modelling, by terms of the form $\overline{u_p u_q c}\, U_{m,n}$. The second term can be modelled following the approximation of ϕ_{ijl} as $-\frac{\varepsilon}{k}(\overline{u_i u_k c})$.

The parts of term (a) with mean velocity gradients are now neglected following a similar action by HANJALIĆ and LAUNDER [14] in deriving the algebraic model of $\overline{u_i u_j u_k}$. Consistent with that step the mean strain terms in the pressure-scalar flux correlation can be neglected too.

Finally, on neglect of the convective transport term in (B.1) and on substitution of the above formulations an algebraic expression for $\overline{u_i u_k c}$ emerges. That is,

$$\overline{u_i u_k c} = -C_c \frac{k}{\varepsilon}\left(\overline{u_k u_l}\cdot\overline{u_i c}_{,l} + \overline{u_l c}\cdot\overline{u_i u_k}_{,l} + \overline{u_i u_l}\cdot\overline{u_k c}_{,l} + \overline{u_i u_k u_l}\, C_{,l} \right) \quad . \tag{B.5}$$

In order to derive the corresponding algebraic expression for $\overline{u_k c^2}$, which appears in the diffusion term of $\overline{c^2}$, again reference is made to its transport equation. As given for example in KOLOVANDIN and VATUTIN [22], for high Reynolds and Peclet numbers,

$$\overline{u_k c^2}_{,t} + U_l\, \overline{u_k c^2}_{,l} = \underbrace{-\left(\overline{u_l c^2}\, U_{k,l} + 2\, \overline{u_k u_l c}\, C_{,l} \right)}_{(a)} \underbrace{- \overline{u_k u_l c^2}_{,l}}_{(b)} \underbrace{- \frac{1}{\rho}\, \overline{c^2 p_{,k}}}_{(c)} + \underbrace{\left(\overline{c^2}\, \overline{u_k u_l}_{,l} + 2\, \overline{u_k c}\cdot\overline{u_l c}_{,l} \right)}_{(d)} \quad . \tag{B.6}$$

Now following arguments and assumptions similar to those made in deriving the algebraic form for $\overline{u_i u_k c}$ one obtains,

$$\overline{u_k c^2} = -C_g \frac{k}{\varepsilon}\left(\overline{u_k u_l}\, \overline{c^2}_{,l} + 2\, \overline{u_l c}\cdot\overline{u_k c}_{,l} + 2\, \overline{u_k u_l c}\, C_{,l} \right) \quad . \tag{B.7}$$

Inherent in the above formulations for $\overline{u_i u_k c}$ and $\overline{u_k c^2}$ is the assumption that the velocity and scalar time scales are proportional. Under circumstances of dissimilar hydrodynamic and scalar fields however,(for example QUARMBY and ANAND's [94] experiment where the velocity field has large gradients in near-wall region (due to wall friction) and scalar field has zero gradients (impermeable wall)), the time scales are not likely to be proportional. The second term in (B.4) was expressed as proportional to $\frac{\overline{u_i u_k c}}{\tau}$ where τ was taken as equal to $\frac{k}{\varepsilon}$. More accurately τ should be a mixture of $\frac{k}{\varepsilon}$ and $\frac{\overline{c^2}}{\varepsilon}$.

Moreover, in modelling the $\overline{u_i u_k c}$ term, the effects of the production term due to mean strain

$$- (\overline{u_i u_l c}\, U_{k,l} + \overline{u_i u_k c}\, U_{i,l})$$

as well as mean strain contributions to $\frac{1}{\rho}\, \overline{u_i c\, p_{,k}}$ were neglected. It was hoped that the effect of these terms would be small and conveniently be absorbed in the coefficient C_c . Eventhough it is likely that this is possible in situations where the scalar and hydrodynamic fields nearly similar, under circumstances where $\frac{\partial U}{\partial y}$ is large and $\frac{\partial C}{\partial y}$ is small, the above terms may even be the dominant.

These shortcomings may show up in predicting scalar transport situations where strong dissimilarities between velocity and scalar fields exist.

APPENDIX (C)

Derivation of the Exact Equation for Pressure-Scalar Gradient Correlation

In order to obtain correlations of the type pressure-scalar gradient $\overline{\frac{p}{\rho} c_{,i}}$, pressure gradient-scalar flux $\overline{\frac{u_i c}{\rho} p_{,k}}$ one should first derive the Poisson equation for p . Consider the equation for fluctuating component of velocity u_i obtained by substracting the mean velocity equation from the instantaneous velocity equation. It is

$$u_{i,t} + U_k u_{i,k} + u_k U_{i,k} + u_k u_{i,k} = -\frac{1}{\rho} p_{,i} + \nu u_{i,kk} + (\overline{u_i u_k})_{,k} \quad . \tag{C.1}$$

Taking the divergence with respect to x_i , and considering continuity,

$$u_{i,i} = 0 \tag{C.2}$$

one obtains,

$$U_{k,i} u_{i,k} + u_{k,i} U_{i,k} + u_{i,k} u_{k,i} = -\frac{1}{\rho} p_{,ii} + (\overline{u_i u_k})_{,ik} \quad . \tag{C.3}$$

Now

$$(u_i u_k)_{,ik} = (u_i u_{k,i})_{,k} = u_{i,k} u_{k,i} \quad .$$

Therefore

$$\frac{1}{\rho} p_{,ii} = -2 u_{i,k} U_{k,i} - (u_i u_k)_{,ik} + (\overline{u_i u_k})_{,ik} \tag{C.4}$$

or taking the derivative with respect to x_k

$$\frac{1}{\rho} (p_{,k})_{,ii} = -2 (u_{n,m} U_{m,n})_{,k} - (u_n u_m)_{,nmk} + (\overline{u_n u_m})_{,nmk} \quad . \tag{C.5}$$

The Green's theorem applied to a variable a is,

$$a = -\frac{1}{4\pi}\int_V \frac{\nabla^2 a}{r}\, dV + \textit{Surface integrals} \quad . \tag{C.6}$$

So that Green's theorem on fluctuating pressure p is

$$\frac{p}{\rho} = \frac{1}{2\pi}\int_V \frac{1}{r'}\, u'_{n,m}\, U'_{m,n}\, dV' + \frac{1}{4\pi}\int_V \frac{1}{r'}\left[u'_n u'_m \right]_{,mn} dV'$$

$$- \frac{1}{4\pi}\int_V \frac{1}{r'}\left[\overline{u'_n u'_m} \right]_{,nm} dV' + S \quad . \tag{C.7}$$

Here p is a function at (X_o , Y_o , Z_o) the point under consideration and the right hand side of (C.7) is evaluated at (X' , Y' , Z') points over the control volume V of surface s. Similarly,

$$\frac{1}{\rho} p_{,k} = \frac{1}{2\pi}\int_V \frac{1}{r'}\left[u'_{n,m}\, U'_{m,n} \right]_{,k} dV' + \frac{1}{4\pi}\int_V \frac{1}{r'}\left[u'_n u'_m \right]_{,mnk} dV'$$

$$- \frac{1}{4\pi}\int_V \frac{1}{r'}\left[\overline{u'_n u'_m} \right]_{,mnk} dV' + S \quad . \tag{C.8}$$

The equations (C.7) and (C.8) can be used in obtaining various correlations that appear as pressure related terms in turbulence equations.

In order to obtain the pressure-scalar gradient $\overline{\frac{p}{\rho} c_{,i}}$ correlation, (C.7) is multiplied by $c_{,i}$ and time averaged, thus

$$\overline{\frac{p}{\rho} c_{,i}} = \frac{1}{2\pi}\int \frac{1}{r'}\, U'_{m,n}\, \overline{u'_{n,m}\, c_{,i}}\, dV'$$

$$+ \frac{1}{4\pi}\int \frac{1}{r'}\, \overline{(u'_n u'_m)_{,mn}\, c_{,i}}\, dV' + S_i \quad . \tag{C.9}$$

This is same as the equation (2.47) used in Section (2.4.2). Similarly scalar flux-pressure gradient correlation is obtained by multiplying (C.8) by $\overline{u_i c}$ and time averaging the product,

$$\overline{\frac{u_i c}{\rho} p_{,k}} = \frac{1}{2\pi} \int_{V'} \frac{1}{r'} \left(U'_{m,n} \, \overline{u'_n u_i c}_{,m} \right)_{,k} dV'$$

$$+ \frac{1}{4\pi} \int_{V'} \frac{1}{r'} \left(\overline{u'_n u'_m u_i c}_{,mnk} \right) dV' + S_{ik} \quad . \qquad \text{(C.10)}$$

This equation is utilised in Appendix (B) in obtaining the algebraic expression for $\overline{u_i u_k c}$.

APPENDIX (D)

Modelled Reynolds Stress and Scalar Flux Equations in Cylindrical Polar Coordinates

Reynolds stress and scalar flux equations presented in Chapter (2) are in Cartesian tensor form. In order to transform them into any curvilinear coordinate system, the contravariant and covariant character of the tensors involved should be recognised. The covariant differentials appearing in exact and modelled terms of present set of equations can be reexpressed in partial differential forms using expressions involving Christoffel symbols of the second kind. A complete account of such tensorial manupulations, with particular reference to fluid mechanics, is given in ARIS [111]. In Table (D.1), the modelled forms of Reynolds stress equations as employed in the present study are displayed. They are valid for

- two-dimensional, non swirling i.e. $U_\theta = 0$, $\frac{\partial}{\partial\theta} = 0$
- steady i.e. $\frac{\partial}{\partial t} = 0$
- boundary layer, with negligible streamwise gradients i.e. $\frac{\partial}{\partial z} = 0$ (except for convection terms).

flow situations only.

These equations have previously being obtained by others, for e.g. MORSE [53].

Presented in Table (D.2) are the scalar flux equations in the forms utilized in the numerical prediction of situations covered by this Thesis. These equations are relevant only for the flow situations mentioned above. In addition the lateral velocity U_r is neglected too. The scalar field is

- three-dimensional
- boundary layer type i.e. $\frac{\partial}{\partial z} = 0$ except in convection terms.

Term; Model	Stress Component			
	$\overline{u_z^2}$	$\overline{u_r^2}$	$\overline{u_\theta^2}$	$\overline{u_r u_z}$
$\frac{D}{Dt}(\overline{u_i u_j})$	$U_z\frac{\partial\overline{u_z^2}}{\partial z}+U_r\frac{\partial\overline{u_z^2}}{\partial r}$	$U_z\frac{\partial\overline{u_r^2}}{\partial z}+U_r\frac{\partial\overline{u_r^2}}{\partial r}$	$U_z\frac{\partial\overline{u_\theta^2}}{\partial z}+U_r\frac{\partial\overline{u_\theta^2}}{\partial r}$	$U_z\frac{\partial\overline{u_r u_z}}{\partial z}+U_r\frac{\partial\overline{u_r u_z}}{\partial r}$
P_{ij}	$-2\overline{u_r u_z}\frac{\partial U_z}{\partial r}$	0	$-2\frac{U_r}{r}\overline{u_\theta^2}$	$-\overline{u_r^2}\frac{\partial U_z}{\partial r}$
$-\varepsilon_{ij}$	$-\frac{2}{3}\varepsilon$	$-\frac{2}{3}\varepsilon$	$-\frac{2}{3}\varepsilon$	0
ϕ_{ij1}	$-C_{s1}\frac{\varepsilon}{k}\left(\overline{u_z^2}-\frac{2}{3}k\right)$	$-C_{s1}\frac{\varepsilon}{k}\left(\overline{u_r^2}-\frac{2}{3}k\right)$	$-C_{s1}\frac{\varepsilon}{k}\left(\overline{u_\theta^2}-\frac{2}{3}k\right)$	$-C_{s1}\frac{\varepsilon}{k}\overline{u_r u_z}$

Table D.1 Modelled Reynolds Stress Equations in Cylindrical Polar Coordinates

0 0 0 0 4 9 0 - 303 T 3 0

(contd.)

Term; Model	Stress Component			
	$\overline{u_z^2}$	$\overline{u_r^2}$	$\overline{u_\theta^2}$	$\overline{u_r u_z}$
ϕ_{ij2}; • R_{s1}	$-\left\{-\frac{4}{3}\alpha\left(\overline{u_r u_z}\frac{\partial U_z}{\partial r}+\frac{U_r}{r}\overline{u_\theta^2}\right) -\beta 2k\frac{\partial U_z}{\partial z} +\frac{2}{3}\gamma\left(\overline{u_r u_z}\frac{\partial U_z}{\partial r}+\frac{U_r}{r}\overline{u_\theta^2}\right)\right\}$	$-\left\{\frac{2}{3}\alpha\left(\overline{u_r u_z}\frac{\partial U_z}{\partial r}+\frac{U_r}{r}\overline{u_\theta^2}\right) -\beta 2k\frac{\partial U_r}{\partial r} -\frac{4}{3}\gamma\left(\overline{u_r u_z}\frac{\partial U_z}{\partial r}+\frac{U_r}{r}\overline{u_\theta^2}\right)\right\}$	$-\left\{\frac{2}{3}\alpha\left(\overline{u_r u_z}\frac{\partial U_z}{\partial r}+\frac{U_r}{r}\overline{u_\theta^2}\right) -\beta 2k\frac{U_r}{r} +\frac{2}{3}\gamma\left(\overline{u_r u_z}\frac{\partial U_z}{\partial r}+\frac{U_r}{r}\overline{u_\theta^2}\right)\right\}$	$-\left\{-\alpha\left(\overline{u_r^2}\frac{\partial U_z}{\partial r}\right) -\beta k\frac{\partial U_z}{\partial r} -\gamma\left(\overline{u_z^2}\frac{\partial U_z}{\partial r}\right)\right\}$
• R_{s2}	same as R_{s1} with $\alpha = C_{s2}$, $\beta = \gamma = 0$			
ϕ_{ij1w} ; • R_{sw1}	$C_{s1w}\frac{\varepsilon}{k}\left(\overline{u_z^2}-\frac{2}{3}k\right)f$	$C_{s1w}\frac{\varepsilon}{k}\left(\overline{u_r^2}-\frac{2}{3}k\right)f$	$C_{s1w}\frac{\varepsilon}{k}\left(\overline{u_\theta^2}-\frac{2}{3}k\right)f$	$C_{s1w}\frac{\varepsilon}{k}\overline{u_r u_z}f$
• R_{sw2}	$C_{s1w}\frac{\varepsilon}{k}\overline{u_r^2}f$	$-2C_{s1w}\frac{\varepsilon}{k}\overline{u_r^2}f$	$C_{s1w}\frac{\varepsilon}{k}\overline{u_r^2}f$	$-\frac{3}{2}C_{s1w}\frac{\varepsilon}{k}\overline{u_r u_z}f$

Table D.1 Modelled Reynolds Stress Equations in Cylindrical Polar Coordinates

(contd.)

Term; Model	Stress Component			
	$\overline{u_z^2}$	$\overline{u_r^2}$	$\overline{u_\theta^2}$	$\overline{u_r u_z}$
ϕ_{ij2w}; • R_{sw1}	$-2C_{s2w}\left(\overline{u_r u_z}\frac{\partial U_z}{\partial r}+\frac{U_r}{r}\overline{u_\theta^2}\right)f$	$2C_{s2w}\left(\overline{u_r u_z}\frac{\partial U_z}{\partial r}+\frac{U_r}{r}\overline{u_\theta^2}\right)f$	0	$C_{s2w}\left((\overline{u_z^2}-\overline{u_r^2})\frac{\partial U_z}{\partial r}\right)f$
• R_{sw2}	$C_{s2w}\phi_{rr2}f$	$-2C_{s2w}\phi_{rr2}f$	$C_{s2w}\phi_{rr2}f$	$-\frac{3}{2}C_{s2w}\phi_{rz2}$
$D(\overline{u_i u_j})$; • D_{s1}	$\frac{\partial}{r\partial r}\left(r\Omega_s\overline{u_r^2}\frac{\partial\overline{u_z^2}}{\partial r}\right)$	$\frac{\partial}{r\partial r}\left(r\Omega_s\overline{u_r^2}\frac{\partial\overline{u_r^2}}{\partial r}\right)$ $-2\frac{\Omega_s}{r^2}\overline{u_\theta^2}(\overline{u_r^2}-\overline{u_\theta^2})$	$\frac{\partial}{r\partial r}\left(r\Omega_s\overline{u_r^2}\frac{\partial\overline{u_\theta^2}}{\partial r}\right)$ $+2\frac{\Omega_s}{r^2}\overline{u_\theta^2}(\overline{u_r^2}-\overline{u_\theta^2})$	$\frac{\partial}{r\partial r}\left(r\Omega_s\overline{u_r^2}\frac{\partial\overline{u_r u_z}}{\partial r}\right)$ $-\frac{\Omega_s}{r^2}\overline{u_\theta^2}\ \overline{u_r u_z}$
• D_{s2}	$\ldots+\frac{\partial}{r\partial r}\left(2r\Omega_s\overline{u_r u_z}\frac{\partial\overline{u_r u_z}}{\partial r}\right)$	$\ldots+\frac{\partial}{r\partial r}\left(2r\Omega_s\overline{u_r^2}\frac{\partial\overline{u_r^2}}{\partial r}\right)$ $-2\frac{\Omega_s}{r^2}\overline{u_\theta^2}(\overline{u_r^2}-\overline{u_\theta^2})$ $-2\frac{\Omega_s}{r}\overline{u_r^2}\frac{\partial\overline{u_\theta^2}}{\partial r}$	$\ldots+\frac{\partial}{r\partial r}\left(2\Omega_s\overline{u_\theta^2}(\overline{u_r^2}-\overline{u_\theta^2})\right)$ $+2\frac{\Omega_s}{r^2}\overline{u_\theta^2}(\overline{u_r^2}-\overline{u_\theta^2})$ $+2\frac{\Omega_s}{r}\overline{u_r^2}\frac{\partial\overline{u_\theta^2}}{\partial r}$	$\ldots+\frac{\partial}{r\partial r}\left(r\Omega_s\overline{u_r^2}\frac{\partial\overline{u_r u_z}}{\partial r}\right)$ $-\frac{\Omega_s}{r^2}\overline{u_\theta^2}\ \overline{u_r u_z}$ $+\frac{\partial}{r\partial r}\left(r\Omega_s\overline{u_r u_z}\frac{\partial\overline{u_r^2}}{\partial r}\right)$

Table D.1 Modelled Reynolds Stress Equations in Cylindrical Polar Coordinates

0 0 0 4 6 9 0 - 305 T 3 1

Term; Model	Flux Component		
	$\overline{u_z c}$	$\overline{u_r c}$	$\overline{u_\theta c}$
$\frac{D}{Dt}(\overline{u_i c})$	$U_z \frac{\partial \overline{u_z c}}{\partial z}$	$U_z \frac{\partial \overline{u_r c}}{\partial z}$	$U_z \frac{\partial \overline{u_\theta c}}{\partial z}$
P_{ic}	$-\overline{u_r c}\frac{\partial U_z}{\partial r} - \overline{u_r u_z}\frac{\partial C}{\partial r}$	$-\overline{u_r^2}\frac{\partial C}{\partial r}$	$-\overline{u_\theta^2}\frac{\partial C}{r\partial \theta}$
ϕ_{ic1}; • R_{c1}	$-C_{c1}\frac{\varepsilon}{k}\overline{u_z c}$	$-C_{c1}\frac{\varepsilon}{k}\overline{u_r c}$	$-C_{c1}\frac{\varepsilon}{k}\overline{u_\theta c}$
• R_{c2}	$\ldots -C'_{c1}\frac{\varepsilon}{k}\left((\overline{u_z^2}-\frac{2}{3}k)\overline{u_z c}+\overline{u_r u_z}.\overline{u_r c}\right)$	$\ldots -C'_{c1}\frac{\varepsilon}{k}\left((\overline{u_r^2}-\frac{2}{3}k)\overline{u_r c}+\overline{u_r u_z}.\overline{u_z c}\right)$	$\ldots -C'_{c1}\frac{\varepsilon}{k}(\overline{u_\theta^2}-\frac{2}{3}k)\overline{u_\theta c}$
ϕ_{ic2}; • R_{c1}	$C_{c2}\overline{u_r c}\frac{\partial U_z}{\partial r}$	0	0
• R_{c2}	$0.8\overline{u_r c}\frac{\partial U_z}{\partial r}$	$-0.2\overline{u_z c}\frac{\partial U_z}{\partial r}$	0

Table D.2 Modelled Scalar Flux Equations in Cylindrical Polar Coordinates

(contd.)

Term; Model	Flux Components		
	$\overline{u_z c}$	$\overline{u_r c}$	$\overline{u_\theta c}$
ϕ_{ic1w}; • R_{cw1}	$-C_{c1w}\frac{\varepsilon}{k}\overline{u_z c}f$	$-C_{c1w}\frac{\varepsilon}{k}\overline{u_r c}f$	$-C_{c1w}\frac{\varepsilon}{k}\overline{u_\theta c}f$
• R_{cw2}	0	$-C_{c1w}\frac{\varepsilon}{k}\overline{u_r c}f$	0
ϕ_{ic2w}; • R_{cw1}	$-4\beta'_c\overline{u_r c}\frac{\partial U_z}{\partial r}f$	$\beta'_c\overline{u_z c}\frac{\partial U_z}{\partial r}f$	0
• R_{cw2}	0	0	0
$D(\overline{u_i c})$; • D_{c1}	$\frac{\partial}{r\partial r}\left(r\Omega_c\overline{u_r^2}\frac{\partial\overline{u_z c}}{\partial r}\right)+\frac{\partial}{r\partial\theta}\left(\Omega_c\overline{u_\theta^2}\frac{\partial\overline{u_z c}}{r\partial\theta}\right)$	$\frac{\partial}{r\partial r}\left(r\Omega_c\overline{u_r^2}\frac{\partial\overline{u_r c}}{\partial r}\right)-\frac{\Omega_c}{r}\overline{u_\theta^2}\left(\frac{\partial\overline{u_\theta c}}{r\partial\theta}+\frac{\overline{u_r c}}{r}\right)$ $+\frac{\partial}{r\partial\theta}\left(\Omega_c\overline{u_\theta^2}\left(\frac{\partial\overline{u_r c}}{r\partial\theta}-\frac{\overline{u_\theta c}}{r}\right)\right)$	$\frac{\partial}{r\partial r}\left(r\Omega_c\overline{u_r^2}\frac{\partial\overline{u_\theta c}}{\partial r}\right)+\frac{\Omega_c}{r}\overline{u_r^2}\frac{\partial\overline{u_\theta c}}{\partial r}$ $+\frac{\partial}{r\partial\theta}\left(\Omega_c\overline{u_\theta^2}\left(\frac{\partial\overline{u_\theta c}}{r\partial\theta}+\frac{\overline{u_r c}}{r}\right)\right)$

Table D.2 Modelled Scalar Flux Equations in Cylindrical Polar Coordinates

0 0 0 0 1 9 0 - 3 0 7 - 1 3 2

(contd.)

Term; Model	Flux Component		
	$\overline{u_z c}$	$\overline{u_r c}$	$\overline{u_\theta c}$
$D(\overline{u_i c})$; • D_{c2}	$\ldots + \frac{\partial}{r\partial r}\left(r\Omega_c \overline{u_r u_z}\frac{\partial \overline{u_r c}}{\partial r}\right)$ $+ \frac{\partial}{r\partial\theta}\left(\Omega_c \overline{u_r u_z}\frac{\partial \overline{u_\theta c}}{\partial r}\right)$	$\ldots + \frac{\partial}{r\partial r}\left(r\Omega_c \overline{u_r^2}\frac{\partial \overline{u_r c}}{\partial r}\right)$ $+ \frac{\partial}{r\partial\theta}\left(\Omega_c \overline{u_r^2}\frac{\partial \overline{u_\theta c}}{\partial r}\right)$ $- \frac{\Omega_c}{r}\overline{u_\theta^2}\left(\frac{\partial \overline{u_\theta c}}{r\partial\theta} + \frac{\overline{u_r c}}{r}\right)$	$\ldots + \frac{\partial}{r\partial r}\left(r\Omega_c \overline{u_\theta^2}\left(\frac{\partial \overline{u_r c}}{r\partial\theta} - \frac{\overline{u_\theta c}}{r}\right)\right)$ $+ \frac{\partial}{r\partial\theta}\left(\Omega_c \overline{u_\theta^2}\left(\frac{\partial \overline{u_\theta c}}{r\partial\theta} + \frac{\overline{u_r c}}{r}\right)\right)$ $+ \frac{\Omega_c}{r}\overline{u_\theta^2}\left(\frac{\partial \overline{u_r c}}{r\partial\theta} - \frac{\overline{u_\theta c}}{r}\right)$
• D_{c3}	$\ldots + \frac{\partial}{r\partial r}\left(r\Omega_c \overline{u_r c}\frac{\partial \overline{u_r u_z}}{\partial r}\right)$ $+ \frac{\partial}{r\partial\theta}\left(\Omega_c \overline{u_\theta c}\frac{\overline{u_r u_z}}{r}\right)$	$\ldots + \frac{\partial}{r\partial r}\left(r\Omega_c \overline{u_r c}\frac{\partial \overline{u_r^2}}{\partial r}\right)$ $+ \frac{\partial}{r\partial\theta}\left(\frac{\Omega_c}{r}\overline{u_\theta c}(\overline{u_r^2} - \overline{u_\theta^2})\right)$ $- \frac{\Omega_c}{r}\overline{u_r c}\frac{\partial \overline{u_\theta^2}}{\partial r}$	$\ldots + \frac{\partial}{r\partial r}\left(\Omega_c \overline{u_\theta c}(\overline{u_r^2} - \overline{u_\theta^2})\right)$ $+ \frac{\partial}{r\partial\theta}\left(\Omega_c \overline{u_r c}\frac{\partial \overline{u_\theta^2}}{\partial r}\right)$ $+ \Omega_c \frac{\overline{u_\theta c}}{r^2}(\overline{u_r^2} - \overline{u_\theta^2})$

Table D.2 Modelled Scalar Flux Equations in Cylindrical Polar Coordinates

APPENDIX (E)

Derivation of Finite Difference Equation for Variables Stored in Staggered (x-Ψ) Grid

The finite difference equation to be solved in a staggered grid (see Fig.(E.1)) is same as in conventional grid. It is

$$\frac{\partial \phi}{\partial x} + (a + b\omega) \frac{\partial \Phi}{\partial \omega} = \frac{\partial}{\partial \omega} (c \frac{\partial \Phi}{\partial \omega}) + d \qquad \text{(E.1)}$$

where,

$$a = - \frac{1}{\Psi_E - \Psi_I} \frac{d\Psi_I}{dx}$$

$$b = - \frac{1}{\Psi_E - \Psi_I} \frac{d}{dx} (\Psi_E - \Psi_I)$$

$$c = \frac{r^2 \rho U \Gamma_{eff}}{(\Psi_E - \Psi_I)^2}$$

$$d = \frac{1}{\rho U} S^{\Phi} \quad .$$

Here the notation is same as that in Chapter (3). The suffices I and E denote the interior and exterior boundaries of the layer, whereas (I) denotes the grid point. Here Φ is the variable to be stored in the staggered location. Note that the mean velocity is stored at regular grid points i.e. at (I) , $(I-1)$ etc.

Consider a control cell shifted half a grid node from (I) in the (minus) ω-direction, and denote the variable to be calculated at this point by $\Phi_{(I)}$.

Notation: Except for the variable Φ , suffix (I) stands for that quantity at (I) the regular node. $\Phi_{(I)}$ stands for the variable Φ stored at the shifted grid node and $\overline{\Phi}_{(I)}$ denotes the interpolated value of Φ at the regular grid point (I) . The suffixes d and u

stand for quantities evaluated at downstream and upstream locations respectively.

Now assume that the variation of Φ between the shifted nodes is linear. (The variation of mean velocity U between its nodes too is assumed to be linear.) In order to obtain the finite difference equation for $\Phi_{(I)}$ multiply (E.1) by $d\omega$ and integrate between the limits $(I-1)$ and (I) .

(a) $$\int_{(I-1)}^{(I)} \frac{\partial \Phi}{\partial x}\, d\omega = \frac{1}{\Delta x} \int_{(I-1)}^{(I)} \left(\Phi_{(I,d)} - \Phi_{(I,u)} \right) d\omega \qquad \text{(E.2)}$$

(b) $$\int_{(I-1)}^{(I)} \left(a + b\omega \right) \frac{\partial \Phi}{\partial \omega}\, d\omega = \underbrace{- b \int_{(I-1)}^{(I)} \Phi_{(I,m)}\, d\omega}_{\text{(b1)}} + \underbrace{\left[(a + b\omega)\, \Phi \right]_{(I-1)}^{(I)}}_{\text{(b2)}} \qquad \text{(E.3)}$$

(c) $$\int_{(I-1)}^{(I)} \left(\frac{\partial}{\partial \omega}\, c\, \frac{\partial \Phi}{\partial \omega} \right) d\omega = \left[c\, \frac{\partial \Phi}{\partial \omega} \right]_{(I-1)}^{(I)} \qquad \text{(E.4)}$$

(d) $$\int_{(I-1)}^{(I)} \frac{1}{\rho\, U}\, S^{\Phi}\, d\omega = \int_{(I-1)}^{(I)} d_m\, d\omega \quad . \qquad \text{(E.5)}$$

In order to evaluate the right hand sides of (E.2) to (E.5) values of Φ at some intermediate locations should be known. To facilitate that, define weighting factors $\Omega^{+}_{(I)}$ and $\Omega^{-}_{(I)}$ by

$$\Omega^{+}_{(I)} = 0.5\, \frac{(\omega_{(I)} - \omega_{(I-1)})}{(\omega_{(I+1)} - \omega_{(I-1)})} \qquad \text{(E.6)}$$

and

$$\Omega^{-}_{(I)} = 0.5\, \frac{(\omega_{(I)} - \omega_{(I-1)})}{(\omega_{(I)} - \omega_{(I-2)})} \quad , \qquad \text{(E.7)}$$

so that (see Fig. (E.1)),

$$\Phi_a = \Omega^+_{(I)} \Phi_{(I+1)} + (1 - \Omega^+_{(I)}) \Phi_{(I)} \tag{E.8}$$

and

$$\overline{\Phi}_{(I)} = 2 \Omega^+_{(I)} \Phi_{(I+1)} + (1 - 2 \Omega^+_{(I)}) \Phi_{(I)} \quad . \tag{E.9}$$

Further, in obtaining partial derivatives with respect to ω , the values of Φ at $x = x_d$ are chosen. This is same as the practice of [9] and is both unconditionally stable and convenient. i.e.

$$\Phi_m = \Phi_d \quad . \tag{E.10}$$

Therefore

$$\text{(a) + (b1)} = \frac{1}{\Delta x} \int_{(I-1)}^{(I)} \Phi_{(I,d)} \, d\omega - \frac{1}{\Delta x} \int_{(I-1)}^{(I)} \Phi_{(I,u)} \, d\omega + \frac{1}{(\Psi_E - \Psi_I)} \frac{(\Psi_E - \Psi_I)_d - (\Psi_E - \Psi_I)_u}{\Delta x} \int_{(I-1)}^{(I)} \Phi_{(I,d)} \, d\omega \quad . \tag{E.11}$$

Substituting

$$\frac{(\Psi_E - \Psi_I)_u}{\Delta x} = P$$

and

$$\frac{(\Psi_E - \Psi_I)_d - (\Psi_E - \Psi_I)_u}{\Delta x} = G$$

and with (E.8) substituted on two halves of the shifted cell at (I) ,

$$(a) + (b1) = \frac{1}{(\Psi_E - \Psi_I)_u} \frac{\omega_{(I)} - \omega_{(I-1)}}{2}$$

$$\times \left[(P + G) \left[\Phi_{(I+1,d)} \Omega^+_{(I)} + \Phi_{(I,d)} (2 - \Omega^+_{(I)} - \Omega^-_{(I)}) + \Phi_{(I-1,d)} \Omega^-_{(I)} \right] \right.$$

$$\left. - P \left[\Phi_{(I+1,u)} \Omega^+_{(I)} + \Phi_{(I,u)} (2 - \Omega^+_{(I)} - \Omega^+_{(I)}) + \Phi_{(I-1,u)} \Omega^-_{(I)} \right] \right] \quad . \tag{E.12}$$

Rearranging,

$$(a) + (b1) = \frac{(\omega_{(I)} - \omega_{(I-1)})}{8 (\Psi_E - \Psi_I)_u}$$

$$\times \left[4 (2 - \Omega^+_{(I)} - \Omega^-_{(I)}) \left[(P + G) \Phi_{(I,d)} - P \Phi_{(I,u)} \right] \right.$$

$$+ 4 (\Omega^+_{(I)}) \left[(P + G) \Phi_{(I+1,d)} - P \Phi_{(I+1,u)} \right]$$

$$\left. + 4 (\Omega^-_{(I)}) \left[(P + G) \Phi_{(I-1,d)} - P \Phi_{(I-1,u)} \right] \right] . \tag{E.13}$$

The balance of the term (b) is,

$$(b2) = (a + b\omega)_{(I)} \overline{\Phi}_{(I)} - (a + b\omega)_{(I-1)} \overline{\Phi}_{(I-1)} \tag{E.14}$$

but,

$$(a + b\omega) = - \frac{1}{(\Psi_E - \Psi_I)_u} \left[\frac{d\Psi_I}{dx} + \omega \left[\frac{d\Psi_E}{dx} - \frac{d\Psi_I}{dx} \right] \right] \quad .$$

Denoting

$$L^+_{(I)} = - \left[(1 - \omega_{(I)}) \frac{d\Psi_I}{dx} + \omega_{(I)} \frac{d\Psi_E}{dx} \right] \tag{E.15}$$

and

$$L^-_{(I)} = - \left[(1 - \omega_{(I-1)}) \frac{d\Psi_I}{dx} + \omega_{(I-1)} \frac{d\Psi_E}{dx} \right] \tag{E.16}$$

equation (E.14) reduces to

$$(b2) = \frac{1}{(\Psi_E - \Psi_I)_u} \left(L^+_{(I)} \overline{\Phi}_{(I,d)} - L^-_{(I)} \overline{\Phi}_{(I-1,d)} \right) .$$

Substituting $\overline{\Phi}_{(I,d)}$ etc. from (E.9), obtain

$$(b2) = \frac{1}{(\Psi_E - \Psi_I)_u} \left(\Phi_{(I,d)} \left[L^+_{(I)} (1 - 2\,\Omega^+_{(I)}) - L^-_{(I)} (1 - 2\,\Omega^-_{(I)}) \right] + \Phi_{(I+1,d)} L^+_{(I)}\, 2\,\Omega^+_{(I)} - \Phi_{(I-1,d)} L^-_{(I)}\, 2\,\Omega^-_{(I)} \right) . \tag{E.17}$$

Note here that $L^+_{(I)}$ and $L^-_{(I)}$ are different from L^+ and L^- of [9] .

$$(c) = \left(\overline{c \frac{\partial \Phi}{\partial \omega}} \right)_{(I)} - \left(\overline{c \frac{\partial \Phi}{\partial \omega}} \right)_{(I-1)} . \tag{E.18}$$

The ω-differences across the regular grid can be written as

$$\omega_{(I+\frac{1}{2})} - \omega_{(I-\frac{1}{2})} \simeq r\,\rho\, U_{(I)} \left(y_{(I+\frac{1}{2})} - y_{(I-\frac{1}{2})} \right) / (\Psi_E - \Psi_I)$$

and

$$\omega_{(I-\frac{1}{2})} - \omega_{(I-1\frac{1}{2})} \simeq r\,\rho\, U_{(I-1)} \left(y_{(I-\frac{1}{2})} - y_{(I-1\frac{1}{2})} \right) / (\Psi_E - \Psi_I) . \tag{E.19}$$

The transport coefficients at the edges of the cell are

$$T^+_{(I)} = (r\,\Gamma_{eff})_{(I)} / \left(y_{(I+\frac{1}{2})} - y_{(I-\frac{1}{2})} \right)$$

$$T^-_{(I)} = (r\,\Gamma_{eff})_{(I-1)} / \left(y_{(I-\frac{1}{2})} - y_{(I-1\frac{1}{2})} \right) . \tag{E.20}$$

Therefore (E.18) can be reexpressed as

$$(c) = \frac{1}{(\Psi_E - \Psi_I)_u} \left(- \Phi_{(I,d)} \left(T^+_{(I)} + T^-_{(I)} \right) + \Phi_{(I+1,d)} T^+_{(I)} + \Phi_{(I-1,d)} T^-_{(I)} \right) . \tag{E.21}$$

Lastly, the source term can be integrated so as to read

$$(d) = \frac{1}{(\Psi_E - \Psi_I)_u} \left[S_u + S_d \, \Phi_{(I,d)} \right] . \qquad (E.22)$$

Now summing up the terms is (E.13), (E.17), (E.21) and (E.22) and rearranging,

$$\begin{aligned} 0 = \; & \Phi_{(I,d)} \Big[(P + G)(\omega_{(I)} - \omega_{(I-1)})(2 - \Omega^+_{(I)} - \Omega^-_{(I)}) \\ & \quad + 2 L^+_{(I)} (1 - 2\Omega^+_{(I)}) - 2 L^-_{(I)} (1 - 2\Omega^-_{(I)}) \\ & \quad + 2 T^+_{(I)} + 2 T^-_{(I)} - 2 S_d \Big] \\ & + \Phi_{(I+1,d)} \Big[(P + G)(\omega_{(I)} - \omega_{(I-1)}) \Omega^+_{(I)} + 4 L^+_{(I)} \Omega^-_{(I)} - 2 T^+_{(I)} \Big] \\ & + \Phi_{(I-1,d)} \Big[(P + G)(\omega_{(I)} - \omega_{(I-1)}) \Omega^-_{(I)} + 4 L^-_{(I)} \Omega^-_{(I)} - 2 T^-_{(I)} \Big] \\ & - \Big[P \Big[\Phi_{(I,u)} (\omega_{(I)} - \omega_{(I-1)})(2 - \Omega^+_{(I)} - \Omega^-_{(I)}) \\ & \quad + \Phi_{(I+1,u)} (\omega_{(I)} - \omega_{(I-1)}) \Omega^+_{(I)} \\ & \quad + \Phi_{(I-1,u)} (\omega_{(I)} - \omega_{(I-1)}) \Omega^-_{(I)} \Big] + 2 S_u \Big] . \end{aligned}$$

(E.23)

This is the finite difference equation for the variable Φ at (I) . As in [9] , implausible effects of this equation due to the linearity assumption of the $\Phi \sim \omega$ relation in high lateral flux situations can be removed by modifying the transport terms as

$$T^* = \tfrac{1}{2} (T + | 2 L \Omega | + | T - | 2 L \Omega ||) . \qquad (E.24)$$

Consequences of this modification and the implausibility of the uncorrected form is discussed in [9] .

Thus (E.23) can be rearranged to the form,

$$D_{(I)}\,\Phi_{(I)} = A_{(I)}\,\Phi_{(I+1)} + B_{(I)}\,\Phi_{(I-1)} + C_{(I)} \tag{E.25}$$

where,

$$A_{(I)} = 2\,T^{*+}_{(I)} - 4\,L^{+}_{(I)}\Omega^{+}_{(I)} - (\,P + G\,)(\,\omega_{(I)} - \omega_{(I-1)}\,)\,\Omega^{+}_{(I)}$$

$$B_{(I)} = 2\,T^{*-}_{(I)} + 4\,L^{-}_{(I)}\Omega^{-}_{(I)} - (\,P + G\,)(\,\omega_{(I)} - \omega_{(I-1)}\,)\,\Omega^{-}_{(I)}$$

$$C_{(I)} = P\,(\,\omega_{(I)} - \omega_{(I-1)}\,)\Big[\,\Phi_{(I,u)}\,(\,2 - \Omega^{+}_{(I)} - \Omega^{-}_{(I)}\,) + \Phi_{(I+1,u)}\Omega^{+}_{(I)} + \Phi_{(I-1,u)}\Omega^{-}_{(I)}\Big] + 2\,S_u$$

and

$$D_{(I)} = A_{(I)} + B_{(I)} + 2\,P\,(\,\omega_{(I)} - \omega_{(I-1)}\,) - 2\,S_d \quad .$$

Simultaneous solution of equations of the type (E.25) can now be done in a marching fashion with known initial and boundary conditions.

APPENDIX (F)

Computer Program for the Solution of Two-and Three-Dimensional Scalar Transport Problem

F.1 Introduction

The computer code to be described is an outgrowth of the TEACHL program outlined in GOSMAN and PUN [50]. It incorporates the staggered grid arrangement as described in Section (3.5). The program is arranged to solve the flow and scalar transport equations described in Section(2.7). The flow considered is of two-dimensional boundary layer type, whereas the scalar transport problem can either be two-or three-dimensional in character. The three-dimensional situations were considered with frozen hydrodynamic field obtained from two-dimensional calculations made before hand. Simultaneous solution of all equations can however be easily arranged.

This computer code was developed in CDC 7600 and CDC 6600 computers in the "update" mode, however, it can easily be adopted for other machines. The program is written in FORTRAN IV language.

In the Subroutine SOURCE which evaluates the source terms of all equations of the second-order (stress and scalar-flux) closere model, it was attempted, to retain the tensorial character of the terms. This may enhance the clarity and facilitate understanding of the evaluation of the source terms.

The coordinate system in which the equations are written is the cylindrical polar (θ-r-z) and can be converted to Cartesian coordinates (x-y-z) by changing an index. The notation followed is, for directions,

$$x_\theta \equiv x_1 \quad ; \quad x_r \equiv x_2 \quad ; \quad x_z \equiv x_3 \quad ,$$

and for velocities, stress and flux components

$$U_\theta \equiv U \quad , \quad U_r \equiv V \quad , \quad U_z \equiv W$$

$$\overline{u_\theta^2} \equiv \overline{u^2} \quad , \quad \overline{u_r^2} \equiv \overline{v^2} \quad , \quad \overline{u_z^2} \equiv \overline{w^2} \quad \text{etc.}$$

$$\overline{u_\theta c} \equiv \overline{uc} \quad , \quad \overline{u_r c} \equiv \overline{vc} \quad , \quad \overline{u_z c} \equiv \overline{wc} \quad .$$

F.1.1 Base Case

The program is set for the solution of mean and turbulent equations in a cylindrical geometry. As described in Section (3.3), for this case the partial differential equations for U_θ , U_r and P' are redundant. Thus these equations have been excluded from consideration here. These equations can however be incorporated easily as in TEACHT program. (Relevant turbulent stresses in U_θ and U_r equations can be inserted in a manner parallel to that of $U_z \equiv W$ equation described here.)

The boundary condition for the scalar transport situation considered is that discussed in Section (3.7). Note here that all other cases under investigation can be generated from this base case.

F.1.2 The Grid System

Main calculation domain is a segment of a circular area of radius $R_{(NJ)}$. See Fig. (F.1). The enclosed angle of Θ can be chosen as desired. NI is the number of grid lines in the angular direction, whereas NJ is the number of lines covering the radius. This enables one to have (NI-2)×(NJ-2) grid nodes for solution of the equations. The region between NJ and NJO represent the thick wall where only the partial differential equation for mean temperature is solved.

Fig. (F.2) shows the control volumes around the point P . The control volume for $U_z \equiv W$ equation is centered at P whereas those for $U_r \equiv W$ and $U_\theta \equiv U$ are shifted in $-r$ and $-\theta$ direction respectively. All hydrodynamic turbulent variables, in the present base case are solved at the shifted grid point V . The scalar fluxes $\overline{u_r c}$ and $\overline{u_\theta c}$ are solved at V and U respectively. The dimensions of the main and shifted control volumes are shown in Fig. (F.2).

F.2 Listing of FORTRAN Symbols

Given below is the list of all the important FORTRAN symbols that are used in the program. Symbols that only have a local meaning in the subroutines are not listed here. Whenever possible the variables are grouped together to avoid an unnecessary long index.

FORTRAN Symbol	Description	Dimension
AD, AE, AN, AP, AS, AU, AW	Coefficients of the general finite difference equation	IT×JT
AREA	$\iint r\, dr\, d\theta$	
BVE, BVS, BVW, BWS	Weighting factors near boundaries	
C	Mean scalar variable	IT×JT×2
CAPPA	κ ; the von Kármán constant	
CAPPAC	κ_c ; Coefficient in log law for C	
CBULK	$\overline{C}$; Bulk temperature	
CC, CC1, CC2, CC1W, CC2W	C_c , C_{c1} , C_{c2} , C_{c1w} , C_{c2w} ; Coefficients in scalar flux model	
CEPS, CEPS1, CEPS2	C_ε , $C_{\varepsilon 1}$, $C_{\varepsilon 2}$; Coefficients in modelled ε-equation	
CG, CG2	C_g , C_{g2} ; Coefficients in $\overline{c^2}$ equation	
CMU	C_μ ; Coefficient in two-equation model of turbuelnce	
CRS, CR1, CR2, CR1W, CR2W	C_s , C_{s1} , C_{s2} , C_{s1w} , C_{s2w} ; Coefficients in stress model	
CT	C_τ : Friction scalar	IT
D	D_{ij} ; see equation (2.16)	3×3
DCDXJ	$\frac{\partial C}{\partial x_j}$; e.g. DCDXJ(2) $\equiv \frac{\partial C}{\partial r}$	3

Table F.1 Listing of FORTRAN Symbols

(contd.)

FORTRAN Symbol	Description	Dimension
DCDZB	$\left(\frac{\Delta C}{\Delta z}\right)$ in the near-wall cell	IJ
DEL	δ_{ij} : Kronecker delta	3×3
DEN	ρ ; Density of fluid	IT×JT×2
DENSIT	ρ ; Density of fluid	
DET, DETU, ET, ETU	Geometrical parameters denoting tube wall control volumes	IT
DIF	Γ^{Φ} ; Diffusion coefficient of Φ	IT×JT×2
DIS	ε_{ij} ; Component of dissipation tensor	3×3
DISCSQ	ε_c ; Scalar dissipation rate	
DPDZ	$\frac{dP}{dz}$; Streamwise pressure gradient	
DUIDXJ	$\frac{\partial U_i}{\partial x_j}$; e.g. DUIDXJ(3,2) $\equiv \frac{\partial W}{\partial r}$	3×3
DXEP, DXPW, DXEPU, DXPWU	Geometrical variables, see Fig. (F.2)	IT
DYNP, DYPS, DYNPV, DYPSV	Geometrical variables, see Fig. (F.2)	JT
DYW	Geometrical parameter in thick wall control volumes	
DZ	dz ; Step size in streamwise direction	
D1C	$-\overline{u_k c}\,\frac{\partial U_k}{\partial x_j}$	3
EC	ε_c ; Scalar dissipation rate	IT×JT
ECCEN	Eccentricity of the tube wall	
ED	ε ; Isotropic dissipation rate	IT×JT
ELOG	E ; Coefficient in log-law for velocity	
ELOGC	E_c ; Coefficient in log-law for scalar	
ENUSS	Nu ; Nusselt number	
ES	Power input per unit vloume of tube wall	

Table F.1 Listing of FORTRAN Symbols

(contd.)

FORTRAN Symbol	Description	Dimension
EXCHAT	K_f ; Thermal conductivity of fluid	
EXCHAW	K_w ; Thermal conductivuty of wall material	
FF	$(\overline{u_\theta^2} - \overline{u_r^2})$;	IT×JT
FLOWIN	$\iint \rho\, U_z\, r\, dr\, d\theta$;	
FRA	Step size controlling factor	
FU, FV	$\overline{u_\theta u_z}$, $\overline{u_r u_z}$ or $\overline{u_\theta c}$, $\overline{u_r c}$; Fluxes in θ and r directions	IT×JT
FWL	f ; Near wall effect function	
FWM1	f in near wall cell	
F1, F2, F3	Coefficients in ϕ_{ij2} model	
GAM	Γ^C ; Molecular diffusivity of C	IT×JT×2
GINLET	Total mass flux at the inlet	
GREAT	A large numerical value	
GSTAR	Total mass flux in the new step	
G1, G2	Coefficients in ϕ_{ic2} model	
HEDU → HEDVIS	Variable titles	4
ICON	= 0 ; Starting run = 1 ; Continuation run	
IDIF	= 1 ; Gradient diffusion model = 2 ; Tensor invariant model of diffusion	
IEND	Number of steps required for the calculation	
IHT	= 0 ; Scalar transfer problem not solved = 1 ; Two-dimensional scalar transport = 2 ; Three-dimensional scalar transport	

Table F.1 Listing of FORTRAN Symbols

(contd.)

FORTRAN Symbol	Description	Dimension
IJ	Array dimension in x ($\equiv\theta$) direction	
IJET	= 1 ; for jet flow (this should be set to zero)	
IJT	IJ×JT	
INCALU → INCALR	Logical variables denoting the equations to be solved	
INDCOS	= 1 ; Plane flow = 2 ; Round flow	
INDEX	= 0 ; At the starting step in calculation = 1 ; After the first step	
INDIFF	= FALSE ; Turbulent stresses or fluxes to be treated in source form = TRUE ; Same to be treated in diffusion form	
INDPRI	Limited print-out control	
INPRO	= FALSE ; Constant transport coefficients = TRUE ; Variable transport coefficients	
INTURB	= FALSE ; Laminar flow = TRUE ; Turbulent flow	
INUM	Number of points for which the initial conditions are given	
IPRO	Argument for ZDPRO	
IQUE	= 0 ; Prescribed wall scalar value boundary condition = 1 ; Prescribed wall flux	
IRUN	= 1 ; First run = 2 ; Two-dimensional scalar calculation = 3 ; Second and subsequent runs in three-dimensional scalar calculation	
ISTEP	Step number	

Table F.1 Listing of FORTRAN Symbols

(contd.)

FORTRAN Symbol	Description	Dimension
ISC	= 0 ; Mean scalar equation = 1 ; Mean velocity equation	
IT	Array dimension in θ-direction	
ITESC, ITESU	= 1; When the source balance of respective equations are needed in the output	
ITEST	An index used when details of finite difference coefficients are required	
IU	= 0 ; Hydrodynamic field not solved = 1 ; Two-dimensional flow field = 2 ; Three-dimensional flow field	
IVAR	= IU or IHT ; Depending on whether flow or scalar variables are under consideration	
IWALL	= 0 ; Wall control volumes ignored in calculations = 1 ; Wall control volumes considered	
JUU → JEC	Indices denoting turbulent variables	
JT	Array dimension in r-direction	
K	= 1 ; Upstream plane = 2 ; Downstream plane	
KT	= 2 ; In boundary layers	
MCW	= 1 ; Model R_{cw1} = 2 ; Model R_{cw2}	
MODEC	= 1 ; Model R_{c1} = 2 ; Model R_{c2}	
MODEL	= 1 ; Model R_{s1} = 2 ; Model R_{s2}	
MRW	= 1 ; Model R_{sw1} = 2 ; Model R_{sw2}	

Table F.1 Listing of FORTRAN Symbols

(contd.)

FORTRAN Symbol	Description	Dimension
NI	Number of grid nodes in x (or θ-direction) NIM1 = NI-1 , NIM2 = NI-2	
NJ	Number of grid nodes in r-direction	
NJO	Number of grid nodes in r-direction (including wall) NJOM1 = NJO-1	
NJP	Same as NJ , NJP1 = NJP+1 , NJPM1 = NJP-1	
NK	Number of grid nodes in z-direction = 2 ; in boundary layers	
NSWPU → NSWPR	Number of times a certain equation be solved at a given streamwise plane	
NUMPRI	Full printout controlling index	
OLDU → ODPDZ	Variables transferred from two-dimensional calculations	
P	P_{ij} ; Stress production tensor (see equation (2.15)	3×3
PC	P_c ; Flux production tensor (see equation (2.41)	3
PCSQ	Generation rate of scalar fluctuations	
PE	P : Pressure	IT×JT×2
PI	π	
PHI	Φ ; General dependent variable	IT×JT×2
PHI1, PHI2, PHIW1, PHIW2	ϕ_{ij1} , ϕ_{ij2} , ϕ_{ijw1} , ϕ_{ijw2} ; Pressure strain model	3×3
PP	P' ; Pressure correction	IT×JT
PRANDT	Pr ; Prandtl number	
PSI1, PSI2, PSIW1, PSIW2	ϕ_{ic1} , ϕ_{ic2} , ϕ_{icw1} , ϕ_{icw2} ; Terms in model of pressure-scalar gradient correlation	3

Table F.1 Listing of FORTRAN Symbols

(contd.)

FORTRAN Symbol	Description	Dimension
PT	Production of turbulent kinetic energy	
P1C	P_{1c} ; $-\overline{u_k c}\ \frac{\partial U_j}{\partial x_k}$	
QLENTH	Heating length	
QUE	Heating flux entering the fluid	IT
QUO	Heating flux at the outer wall of the tube	IT
R, RV, RCV	Radial positions of the grids (see Fig. (F.2))	JT
RINNER	R_i; Inner radius	
ROUTER	R_o; Outer radius	
RS	Dummy turbulent variable	IT×JT
RSWALL	Boundary condition of turbulent variables	14
SAVE	Array for saving contents of the common block COMALL	Depends on IT and JT
SEW , SEWU	Geometric variables, see Fig. (F.2)	IT
SNS, SNSV	Geometric variables, see Fig. (F.2)	JT
SDEX	Extra sources due to diffusion term	14
SEX	Extra sources due to polar grid	14
SMALL	Numerically small near-zero number	
SP, SU	Parts of linearised source term	IT×JT
SPS, SUS	Parts of linearised source term	IJT
SPHEAT	c_p ; Specific heat of fluid	
SPH	= 1.0 ; In momentum equation = SPHEAT ; In C-equation	
STAN	= St ; Stanton number	
S1, S2	Parts of source terms of turbulent variables	14×IJT

Table F.1 Listing of FORTRAN Symbols

(contd.)

FORTRAN Symbol	Description	Dimension
TE	$= k$; Turbulent kinetic energy	IT×JT
U	U_θ ; Transverse velocity	IT×JT×2
UC	$\overline{u_\theta c}$; Transverse scalar flux	IT×JT
UIUJ	$\overline{u_i u_j}$; e.g. UIUJ(2,3) = $\overline{u_r u_z}$	3×3
UT	U_τ ; Friction velocity	IT
UU, UV, UW	$\overline{u_\theta^2}$, $\overline{u_\theta u_r}$, $\overline{u_\theta u_z}$	IT×JT
UUMAX etc.	Maximum magnitudes of variables (input conditions)	
UU1 etc.	Array of dimensionless UU etc. (input conditions)	INUM
URFS	Under-relaxation factor for source terms near axis	
V	U_r ; Cross-stream velocity	IT×JT×2
VC	$\overline{u_r c}$; Cross-stream scalar flux	IT×JT
VIS	μ ; Molecular viscosity of fluid	IT×JT×2
VISCOS	μ ; Molecular viscosity of fluid	
VISUU	$\frac{k\ \overline{u_\theta^2}}{\varepsilon}$	IT×JT
VISVV	$\frac{k\ \overline{u_r^2}}{\varepsilon}$	IT×JT
VMEAN	U_b ; Bulk mean velocity	
VV	$\overline{u_r^2}$; Cross-stream components of Reynolds stress	IT×JT
VW	$\overline{u_r u_z}$; Reynolds shear stress	IT×JT
W	U_z ; Streamwise component of mean velocity	IT×JT×2
WC	$\overline{u_z c}$; Streamwise turbulent scalar flux	IT×JT
WCORR	Correction to the W velocity	

Table F.1 Listing of FORTRAN Symbols

(contd.)

FORTRAN Symbol	Description	Dimension
WFE, WFW	Weighting factors	IT
WFN, WFS	Weighting factors	JT
WW	$\overline{u_z^2}$; Streamwise component of Reynolds stress	IT×JT
X, XU	Transverse coordinates of grid (see Fig. (F.2))	IT
XTOT	Maximum value of X, i.e. total angle covered by the domain	
Y,YV	Cross-stream coordinate of grid (see Fig.(F.2))	JT
YTOT	Maximum value of Y, i.e. radius of tube	
YTOTO	Outer radius of tube	
YPLUS	$y^+ = \frac{yU_\tau}{\nu}$	
Y2	Dimensionless Y locations for which initial profiles are given	INUM
Z, ZW	Streamwise coordinate of grid	2
ZDPRO	Streamwise locations for which output is required, ZDPRO is in number of diameters	18

Table F.1 Listing of FORTRAN Symbols

F.3 Description of the Subroutines and Common Blocks

As the program listing given in the next Section is produced by "update" mode each line in it is identified by a name and a sequence number. If that name is same as that of the particular subroutine then it identifies a line that is common to both two-and three-dimensional versions. If the identifier is DIM3, then it corresponds to a line which should be present only in the three-dimensional version. The sequence numbers on these identifiers clearly indicate whether any statements were deleated during this modification. All such deletions are explained after the following subroutine descriptions.

Comdeck COMALL

This common block contains all the variables that are needed to be transferred between subroutines. In the present form it allows a maximum of 15 grid points in the transverse direction and 30 grid points in the radial direction.

The array SAVE is equivalent to the bulk of the commom block and it is used in saving contents (via TAPE 4) from one run so that it can be used as input (via TAPE 3) in the next. This is a convenient and economical facility specially during the program development stages. It ensures fast turnaround from the computer too. Similarly, the array TRANS transfers relevant information of the two-dimensional hydrodynamic variables obtained in a previous run. This facilitates one to carry out variety to three-dimensional scalar transport explorations (for example, grid dependency tests, various model testing) with an established hydrodynamic field.

Broadly the contents of the main common block can be described as follows.

Line No.	Contents
1	Location of main grid nodes
2	Description of main control volumes
3	Description of staggered control volumes
4	The radial location and weighting factors
5	Mean flow variables and mean scalar
6 - 8	Turbulent variables
9	Density, kinematic and turbulent transport coefficients
10 - 11	Coefficients of finite difference equation
12	Useful wall parameters
13	Fluid properties
14 - 15	Coefficients of the turbulent model and wall laws
16	Identifying integers for turbulent variables
17	Limits of the calculation domain and that of arrays
18	Headings for the output
19	Logical variables
20	Number of sweeps in the solution for tri-diagonal matrix algorithm
21	Choice of model and choice of output
22 - 23	Dimensionality and other details of the particular run
24	Flow conditions, boundary conditions for turbulent variables
25	Output manipulation parameter and some near boundary weighting factors

Table F.2 Contents of Comdeck COMALL

The next two lines carry the variables that are relevant to the thick wall calculations. The main common block ends here. The next common block contains the variables that need be transferred from previous two-dimensional flow calculation.

The comdeck COMALL appears in all subroutines except LISOLV and PRINT.

Subroutine MAIN

This is the main section of the program which does the management of the calculation scheme. Briefly its major actions are the following.

- Call the subroutine INDATA(1) for initial conditions of the problem.
- Supply the main grid to cover the domain of interest.
- Call INTIG to get the geometric variables ready.
- Call INITO to set variables to zero.
- Call INDATA(2) in order to get the dependent variable profiles.
- Print out the problem heading and fluid properties.
- Call OUTPUT in order to get a full output of the initial conditions.
- Then enter the calculation loop which is to be traversed as many times as the number of steps taken in z-direction.
- Calculate the forward step by calling STEP.
- Call PROPS to calculate the fluid properties and kinematic and turbulent transport coefficients at all nodes.
- Calculate the source terms for all turbulence equations by entering the SOURCE subroutine at CALSOR.
- Call CALCRS in order to calculate finite difference coefficients and then to solve the turbulence equations. This step is taken for all turbulence variables.
- Call CALCM in order to solve the W-momentum equation.
- Call CALCM in order to solve the mean scalar C equation.
- If any intermediate output is required, call OUTPUT.

- Check for conditions for termination of the calculation. If more calculations are to be performed return to the begining of the calculation loop.
- If to be terminated, then produce an output just before stopping.

In addition to these, one thing worth a mention is that when solving turbulence equations, it is the shear stress $\overline{u_r u_z} \equiv$ VW and the lateral scalar flux $\overline{u_r c} \equiv$ VC equation that are solved first. This was done because description of near-wall boundary condition of all other turbulence variables are specified in terms of these two.

Subroutine INDATA

This subroutine supplies the external input data to the program. It has two entry points.

At the first level,

- Identifying integers for turbulence equations are prescribed.
- If necessary, data is read from a previous run (via SAVE or TRANS).
- Supply choice of model, turbulence constants, necessary numerical constants and controlling indicies.
- Supply the wall properties.

At the second level,

- Dimensionless profiles and their multiplying factors for all dependent variables are read from data.
- The mean profiles are interpolated to obtain values corresponding to the regular grid.
- The turbulence profiles are interpolated to obtain values corresponding to the respective shifted grid.

Subroutine SOURCE

This subroutine calculate the source terms for all turbulent variables. It has three entry points SORCEI, CALSOR and SORCE. SORCEI is entered only once in a given run. Here some arrays are initialised and some coefficients relevant to the turbulence model are calculated. The section CALSOR in entered once in every calculation step. In this section the tensorial character of the source terms of the turbulence equation is attempted to be maintained. Since most of the turbulence variables are to be evaluated at the grid shifted half spacing in direction $-r$, here the node refers to that at V (see Fig. (F.2)). In the Section CALSOR, for every shifted control volume the following calculations were made.

- Perform necessary initialisations.
- Assign the Reynolds stress tensor at the node (i.e. at V).
- Obtain gradients of Reynolds stress that are required in evaluations to follow.
- Similarly assign the scalar fluxes and evaluate any necessary gradients.
- Calculate mean velocity gradients.
- Calculate mean scalar gradients.

With these prelimineries now one is in a position to evaluate the source terms, and they are done in the following order.

(a) Evaluate sources for Reynolds stress equations

- Calculate Production terms.
- Calculate modelled terms of pressure-strain and dissipation terms.
- Evaluate the near-wall-effect terms of pressure-strain relation.
- Evaluate sources due to tensor invariant diffusion model, and those additional terms due to cylindrical polar grid.
- Assemble the source terms.

(b) Evaluate source terms for turbulent kinetic energy equation (in a two-equation model of turbulence),

- Calculate the production and assign the dissipation term in source form.

(c) Evaluate source terms for the dissipation rate equation

(d) Evaluate sources in turbulent scalar flux equations

- Calculate production terms
- Calculate the pressure-scalar gradient correlation terms.
- Evaluate the near-wall effects of the same.
- Evaluate additional sources from the diffusion model.
- Assemble the source terms.

(e) Evaluate sources in $\frac{\overline{c^2}}{2}$ equation.

Now one has the option of taking an output of source balance in component stress equations and turbulent scalar equations.

For a given step the third section SORCE is entered as many times as there are dependent turbulence variables. Here the source terms calculated in CALSOR are picked up by each variable, in the linearised source form.

Subroutine INIT

This subroutine provides the initialisation of variable fields and calculation of geometric parameters. It has three entry points, namely, INITG, INITO and STEP. The INITG is for the evaluation of the geometric variables. If it is the first run this section is entered once and on continuation runs this is not entered at all. This section calculates the locations and relevant weighting factors, distances for regular as well staggered grid systems. For three-dimensional heat transfer problems, the wall goemetry is calculated here.

In the Section INITO, the variables are set to zero and a call is made to SORCEI where some arrays are initialised.

In two-dimensional problems calculation is made only for one radial plane. In STEP all such planes were filled with those calculated values. This is done merely for cosmatic reasons and obviously is skipped in three-dimensional situations. The forward step calculation is also made here.

Subroutine PROPS

This subroutine prescribes the material properties and turbulent diffusion transport coefficients for the problem. If the hydrodynamic field is kept frozen then PROPS is called only once in a run.

Subroutine CALCM

Calculation of the mean variables (W and C) are done in this subroutine. When calling for solution of W -momentum equation, specify ISC = 1, and for C-equation specify ISC = 0. Other arguments of the call statements can be easily recognised (see call statements in MAIN).

The first section of the subroutine calculate the finite difference coefficients. Note here that the turbulent stresses or fluxes can be expressed either as diffusion terms or (as will be seen next) as source terms. A call to the relevant section of PROMOD (i.e. MODW or MODC) is made now to obtain boundary conditions and other problem modifications. Next the coefficients are assembled and solved in LISOLV. Next the pressure gradient is calculated and corresponding velocity corrections are made. The lateral velocity field is obtained next by considereing the mass continuity in individual cells. Lastly the variable W or C at the boundaries are calculated.

Subroutine CALCRS

This subroutine calculate the turbulent variables, such as, Reynolds Stresses, scalar flux etc.. It is done in the relevant shifted grid described previously. First section of CALCRS calculates the finite difference coefficients, the second section will perform the problem modification and assembly of coefficients. The equations are solved in subroutine LISOLV next and then the boundary values are calculated.

Subroutine PROMOD

This subroutine supplies the relevant problem modifications to all dependent variable equations. MODW supplies the modifications for W-momentum equation. Here

- the logarithmic law of the wall is applied,
- the source term due to turbulent stresses are calculated,
- other boundary conditions for momentum equation supplied.

In the Section MODC, the modifications to the C-equation are made. For the sake of clarity the modifications for the case of a thick conducting wall is given seperately. Here

- the logarithmic law of the wall for C-equation is applied,
- the source term due to turbulent scalar fluxes are calculated,
- boundary conditions of C-equation supplied.

For the thick wall case in addition to these,

- finite difference coefficients for the wall control volumes are calculated,
- sources of heat (say, due to electrical heating) are integrated,
- sources of heat externally applied to the tube (as in the present experimental arrangement) are integrated,
- and other boundary conditions supplied.

The Section MODRS supplies necessary boundary information to all turbulent equations. The near-wall boundary conditions of shear stress VW and scalar flux VC are obtained with respect to their corresponding mean equations. The near-wall boundary condition for other turbulent variables are expressed in terms of the boundary values of VW and VC.

Subroutine OUTPUT

This subroutine supplies the main output of the calculations. The first section supplies the characteristic single variable outputs, e.g. skin friction coefficient, Nusselt numbers etc.. Outputs of mean and turbulent hydrodynamic variables and any necessary details of these are obtained next. Similarly outputs of mean and turbulent scalar fields are obtained next. For three-dimensional problems these variables are printed in block form by calling subroutine PRINT.

Subroutine LISOLV

A line by line solving procedure is utilised in solving the finite difference equations generated in CALCM and CALCRS, Here, the tri-diagonal matrix algorithm is employed in each line to be solved. In three-dimensional problems the domain is swept in both transverse (west-east) and radial (north-south) directions.

Subroutine PRINT

This subroutine printout two-dimensional arrays in block form.

A note on deleted lines (as can be seen by missing sequence numbers)

- The comdeck COMALL has replaced a line (e.g. MAIN.3) in each subroutine.
- DIM3.92 can well be same as INIT.123 .
- DIM3.94 has replaced "DO 710 J = 1,NJ" (as NJO is not defined in the two-dimensional case).
- DIM3.153 has replaced "DO 670 J = 2,NJ" for the same reason.
- DIM3.165 has replaced "I = 3" (in two-dimensional flows only one I-plane is solved.
- DIM3.226 has replaced "LISOLV.4 and 5" which had a smaller three-dimensional array.

F.4 Listing of the Computer Program

A listing of the computer program used in the present study in solving two-and three-dimensional scalar transport problems is given in the next few pages. This listing was obtained by running the program in update mode. The meanings of the identifiers were explained before in Section (F.3).

```
  1.  0000008        PROGRAM MAIN(INPUT,OUTPUT,TAPE3,TAPE4,TAPE5=INPUT,TAPE6=OUTPUT)          MAIN.2
                 C*********************************************************************      COMALL.2
                 C                          COMMON BLOCKS                                    COMALL.3
                 C*********************************************************************      COMALL.4
  2.  0022058        DIMENSION SAVE(20229)                                                    DIM3.1
  3.  0022058        DIMENSION TRANS(512)                                                     DIM3.2
  4.  0022058        COMMON                                                                   COMALL.6
                    1X(15),Y(30),Z(02),XU(15),YV(30),ZW(02),                                  DIM3.3
                    1DXEP(15),DXPW(15),DYNP(30),DYPS(30),SEW(15),SNS(30),                     DIM3.4
                    1DXEPU(15),DXPWU(15),SEWU(15),DYNPV(30),DYPSV(30),SNSV(30),               DIM3.5
                    1R(30),RV(30),RCV(30),WFN(30),WFS(30),WFE(15),WFW(15),                    DIM3.6
                    1U(15,30,2),V(15,30,2),W(15,30,2),PE(15,30,2),C(15,30,2),PP(15,30),       DIM3.7
                    1UU(15,30),UV(15,30),UW(15,30),VV(15,30),VW(15,30),WW(15,30),             DIM3.8
                    1ED(15,30),TE(15,30),FF(15,30),UC(15,30),VC(15,30),WC(15,30),             DIM3.9
                    1C2(15,30),EC(15,30),RS(15,30),                                           DIM3.10
                    1DEN(15,30,2),VIS(15,30,2),GAM(15,30,2),VISUU(15,30),VISVV(15,30),        DIM3.11
                    1AW(15,30),AE(15,30),AN(15,30),AS(15,30),AD(15,30),AU(15,30),             DIM3.12
                    1AP(15,30),SJ(15,30),SP(15,30),                                           DIM3.13
                    1JT(15),CF(15),QUE(15),DCDZB(15),QUD(15),                                 DIM3.14
                    1DENSIT,VISCOS,PRANDT,SPHEAT,EXCHAT,                                      COMALL.19
                    1CMJ,CR1,CR2,CRS,CR1W,CR2W,CEPS1,CEPS2,CEPS,CAPPA,ELOG,                   COMALL.20
                    1CC1,CC2,CC,CC1W,CC2W,CG2,CG,CAPPAC,ELOGC,                                COMALL.21
                    1JUJ,JUV,JUW,JVV,JVW,JWW,JED,JTE,JFF,JUC,JVC,JWC,JC2,JEC,                 COMALL.22
                    1NI,NIM1,NIM2,NJ,NJM1,NJM2,NK,NKM1,IT,JT,KT,IJT,                          COMALL.23
                    1HEDU(4),HEDV(4),HEDW(4),HEDP(4),HEDC(4),HEDR(4),HEDD(4),HEDVIS(4),       COMALL.24
                    1INCALU,INCALV,INCALW,INCALP,INCALC,INPRO,INCALR(14),INTURB,INDIFF,       COMALL.25
                    1NSWPU,NSWPV,NSWPW,NSWPP,NSWPC,NSWPR,                                     COMALL.26
                    1MODEL,MODEC,MRW,MCW,IQUE,IDIF,IJET,ITEST,ITESU,ITESC,ICON,               COMALL.27
                    1IRUN,IJ,IHT,IU1,IU2,IC1,IC2,I1,I2,INDCOS,FRA,                            COMALL.28
                    1K,DZ,ISTEP,ISTP1,NRS,INDEX,DPDZ,                                         COMALL.29
                    1FLOWIN,VMEAN,QLENTH,SMALL,GREAT,XTOT,YTOT,RSWALL(14),                    COMALL.30
                    1ZDPRO(18),IPRO,IEND,INDPRI,NUMPRI,BVE,BVW,BVS,BWS                        COMALL.31
  5.  0022058        COMMON                                                                   DIM3.15
                    1ET(15),ETJ(15),DET(15),DETU(15),DYW,NJP,NJP1,NJPM1,IWALL,                DIM3.16
                    1ROUTER,RINNER,ECCEN,ES,NJO,YTOTO,EXCHAW,NJOM1                            DIM3.17
  6.  0022058        COMMON  OLDJ(30),OLDV(30),OLDW(30),OLDP(30),                             DIM3.18
                    1        OLDUU(30),OLDUV(30),OLDUW(30),OLDVV(30),OLDVW(30),               DIM3.19
                    1        OLDWW(30),OLDTE(30),OLDED(30),OLDFF(30),                         DIM3.20
                    1        OLDDEN(30),OLDVIS(30),OVISUU(30),OVISVV(30),                     DIM3.21
                    1        OLDUTA,ODPDZ                                                     DIM3.22
  7.  0022058        LOGICAL INCALU,INCALV,INCALW,INCALP,INCALC,INPRO,                        COMALL.32
                    1        INCALR,INTURB,INDIFF                                             COMALL.33
  8.  0022058        EQUIVALENCE (X(1),SAVE(1))                                               COMALL.34
  9.  0022058        EQUIVALENCE (OLDU(1),TRANS(1))                                           DIM3.23
                 C*********************************************************************      MAIN.4
                 C                          RUN SPECIFICATIONS                                MAIN.5
                 C*********************************************************************      MAIN.6
 10.  0022058        CALL INDATA(1)                                                           MAIN.7
 11.  0022078        INDEX=0                                                                  MAIN.8
 12.  0022078        IF(IRUN.EQ.3) GO TO 10                                                   MAIN.9
 13.  0022118        ISTEP=0                                                                  MAIN.10
 14.  0022128        ICON=0                                                                   MAIN.11
 15.  0022128        IPRO=1                                                                   MAIN.12
 16.  0022138        Z(1)=0.0                                                                 MAIN.13
 17.  0022148     10 CONTINUE                                                                 MAIN.14
 18.  0022158        IF(IRUN.NE.1) CALL INITO                                                 MAIN.15
 19.  0022218        IF(IRUN.EQ.3) CALL OUTPUT                                                MAIN.16
```

```
 20.  0022258        IF(IRUN.NE.1) GO TO 200                                  MAIN.17
                 C*****************************************************************  MAIN.18
                 C                          GRID DIMENSIONS                      MAIN.19
                 C*****************************************************************  MAIN.20
 21.  0022268        PI=3.14159                                               MAIN.21
 22.  0022278        IF(INDCOS.EQ.2) XTOT=XTOT*PI                             MAIN.22
                 C-----GRID SPACING                                            MAIN.23
 23.  0022348        DO 100 I=1,NI                                            MAIN.24
 24.  0022368    100 X(I)=X(I)*XTOT                                           MAIN.25
 25.  0022408        DO 110 J=1,NJ                                            MAIN.26
 26.  0022438    110 Y(J)=Y(J)*YTOT                                           MAIN.27
 27.  0022458        Z(1)=0.0                                                 MAIN.28
 28.  0022468        Z(2)=Z(1)                                                MAIN.29
 29.  0022468        DZ=0.0                                                   MAIN.30
 30.  0022478        K=2                                                      MAIN.31
                 C*****************************************************************  MAIN.32
                 C                          INITIAL OPERATIONS                   MAIN.33
                 C*****************************************************************  MAIN.34
                 C-----CALCULATE GEOMETRICAL QUANTITIES AND SET VARIABLES TO ZERO  MAIN.35
                                                                              MAIN.36
 31.  0022508        CALL INITG                                               MAIN.37
 32.  0022538        CALL INITO                                               MAIN.38
                 C-----INITIALISE VARIABLE FIELDS                              MAIN.39
 33.  0022558    200 IF(IRUN.EQ.3) GO TO 400                                  MAIN.40
                 C-----READ IN INITIAL PROFILES . (ZERO DEFAULT VALUES SET IN INITO)  MAIN.41
 34.  0022568        CALL INDATA(2)                                           MAIN.42
                 C-----INFLOW CALCULATION                                      MAIN.43
 35.  0022618        FLOWIN=0.0                                               MAIN.44
 36.  0022618        AREA=0.                                                  MAIN.45
 37.  0022618        DO 205 J=2,NJM1                                          MAIN.46
 38.  0022648        DO 205 I=IU1,IU2                                         MAIN.47
 39.  0022678        AREA=AREA+RCV(J)*SNS(J)*SEW(I)                           MAIN.48
 40.  0022738    205 FLOWIN=FLOWIN+DEN(I,J,2)*RCV(J)*SNS(J)*SEW(I)*W(I,J,2)   MAIN.49
 41.  0023048        VMEAN=FLOWIN/AREA/DENSIT                                 MAIN.50
 42.  0023058        RE=VMEAN*DENSIT*2.0*Y(NJ)/VISCOS                         MAIN.51
                 C-----PROBLEM HEADING AND INFORMATION                         MAIN.52
 43.  0023108        WRITE(6,210)                                             MAIN.53
 44.  0023158        WRITE(6,220)                                             MAIN.54
 45.  0023208        WRITE(6,230) RE                                          MAIN.55
 46.  0023248        WRITE(6,240) VMEAN                                       MAIN.56
 47.  0023308        WRITE(6,250) PRANDT                                      MAIN.57
 48.  0023348        WRITE(6,260) SPHEAT                                      MAIN.58
 49.  0023408        WRITE(6,270) VISCOS                                      MAIN.59
 50.  0023448        WRITE(6,280) DENSIT                                      MAIN.60
 51.  0023508        WRITE(6,210)                                             MAIN.61
                 C-----INITIAL OUTPUT                                          MAIN.62
 52.  0023538        K=2                                                      MAIN.63
 53.  0023538        CALL OUTPUT                                              MAIN.64
                 C*****************************************************************  MAIN.65
                 C                          ITERATION LOOP                       MAIN.66
                 C*****************************************************************  MAIN.67
 54.  0023568    300 ISTEP=ISTEP+1                                            MAIN.68
 55.  0023578        ISTP1=ISTEP+1                                            MAIN.69
 56.  0023578        IF(ISTEP.LT.IEND) GO TO 400                              MAIN.70
 57.  0023628        WRITE(4) SAVE                                            MAIN.71
 58.  0023728        GO TO 600                                                MAIN.72
 59.  0023728    400 CONTINUE                                                 MAIN.73
                 C-----STEP FORWARD NOW.                                       MAIN.74
 60.  0023738        CALL  STEP                                               MAIN.74
```

```
 61.  0023758        IF(INPRJ) CALL PROPS                                          MAIN.75
                C*****************************************************************MAIN.76
                C-----CALCULATE SOURCE TERMS FOR ALL TURBULENT EQUATIONS.          MAIN.77
 62.  0024008        IF(INTURB) CALL CALSOR(DS,NRS,SU,SP,IJT,I1,I2)                MAIN.78
                C*****************************************************************MAIN.79
                C-----UPDATE MEAN VARIABLES.                                       MAIN.80
 63.  0024038        DO 410 I=1,NI                                                 MAIN.81
 64.  0024058        DO 410 J=1,NJ                                                 MAIN.82
 65.  0024108        W(I,J,1)=W(I,J,2)                                             MAIN.83
 66.  0024138    410 C(I,J,1)=C(I,J,2)                                             MAIN.84
                C-----CALCULATE VARIABLES AT THE NEW STEP.                         MAIN.85
 67.  0024208        IF(INCALR(JVW)) CALL CALCRS(VW,JVW,CRS ,IT,JT,IU ,IU1,IU2)    MAIN.86
 68.  0024238        IF(INCALR(JUU)) CALL CALCRS(UU,JUU,CRS ,IT,JT,IU ,IU1,IU2)    MAIN.87
 69.  0024268        IF(INCALR(JVV)) CALL CALCRS(VV,JVV,CRS ,IT,JT,IU ,IU1,IU2)    MAIN.88
 70.  0024318        IF(INCALR(JWW)) CALL CALCRS(WW,JWW,CRS ,IT,JT,IU ,IU1,IU2)    MAIN.89
 71.  0024348        IF(INCALR(JTE)) CALL CALCRS(TE,JTE,CRS ,IT,JT,IU ,IU1,IU2)    MAIN.90
 72.  0024378        IF(INCALR(JED)) CALL CALCRS(ED,JED,CEPS,IT,JT,IU ,IU1,IU2)    MAIN.91
 73.  0024428        IF(INCALR(JVC)) CALL CALCRS(VC,JVC,CC  ,IT,JT,IHT,IC1,IC2)    MAIN.92
 74.  0024458        IF(INCALR(JUC)) CALL CALCRS(UC,JUC,CC  ,IT,JT,IHT,IC1,IC2)    MAIN.93
 75.  0024508        IF(INCALR(JWC)) CALL CALCRS(WC,JWC,CC  ,IT,JT,IHT,IC1,IC2)    MAIN.94
 76.  0024538        IF(INCALR(JC2)) CALL CALCRS(C2,JC2,CC  ,IT,JT,IHT,IC1,IC2)    MAIN.95
 77.  0024568        IF(INCALW) CALL CALCM(W,VIS,UW,VW,1.0   ,IT,JT,IU ,1,         MAIN.96
                    1              IU1,IU2,NSWPW)                                 MAIN.97
 78.  0024618        IF(INCALC) CALL CALCM(C,GAM,UC,VC,SPHEAT,IT,JT,IHT,0,         MAIN.98
                    1              IC1,IC2,NSWPC)                                 MAIN.99
 79.  0024648        IF(IWALL.EQ.0) GO TO 445                                      DIM3.24
 80.  0024658        DO 440 I=1,NI                                                 DIM3.25
 81.  0024678        QUE(I)=EXCHAW*(C(I,NJP1,K)-C(I,NJ,K))/DET(I)*2.0              DIM3.26
 82.  0024678    440 CONTINUE                                                      DIM3.27
 83.  0025048    445 CONTINUE                                                      DIM3.28
                C*****************************************************************MAIN.100
                C-----INTERMEDIATE OUTPUT                                          MAIN.101
 84.  0025048        K=2                                                           MAIN.102
 85.  0025048        IF(MOD(ISTEP,INDPPI).EQ.0) CALL OUTPUT                        MAIN.103
 86.  0025138        ZD=Z(2)/YTOT/2.0                                              MAIN.104
 87.  0025148        IF(ZD.GT.ZDPRO(IPRO+1)) IPRO=IPRO+1                           MAIN.105
 88.  0025218        IF(ZD.LT.ZDPRO(IPRO)) GO TO 450                               MAIN.106
 89.  0025238        NUMP=NUMPRI                                                   MAIN.107
 90.  0025248        NUMPRI=ISTEP                                                  MAIN.108
 91.  0025258        CALL OUTPUT                                                   MAIN.109
 92.  0025308        IPRO=IPRO+1                                                   MAIN.110
 93.  0025318        NUMPRI=NUMP                                                   MAIN.111
 94.  0025328    450 CONTINUE                                                      MAIN.112
                C-----TERMINATION TESTS                                            MAIN.113
 95.  0025338        IF(ISTEP.GT.IEND) GO TO 600                                   MAIN.114
 96.  0025358        INDEX=1                                                       MAIN.115
 97.  0025368        GO TO 300                                                     MAIN.116
                C*****************************************************************MAIN.117
 98.  0025368    600 CONTINUE                                                      MAIN.118
                C-----FINAL OUTPUT.                                                MAIN.119
 99.  0025378        CALL OUTPUT                                                   MAIN.120
100.  0025418        STOP                                                          MAIN.121
                C*****************************************************************MAIN.122
                C                          FORMAT STATEMENTS                       MAIN.123
                C*****************************************************************MAIN.124
101.  0025428    210 FORMAT(///1H0,120(1H*)///)                                    MAIN.125
102.  0025428    220 FORMAT(1H0,40X,*            TURBULENT PIPE FLOW  *////)       MAIN.126
103.  0025428    230 FORMAT(1H0,15X,*REYNOLDS NUMBER*,T60,1H=,3X,1PE11.3)          MAIN.127
```

0 0 1 0 4 9 6 - 341 - 1 4 9

```
 104.   0025428    240 FORMAT(///1H0,15X,*MEAN INITIAL VELOCITY*,T60,1H=,3X,1PE11.3)          MAIN.128
 105.   0025428    250 FORMAT(1H0,15X,*PRANDTL NUMBER*,T60,1H=,3X,1PE11.3)                   MAIN.129
 106.   0025428    260 FORMAT(1H0,15X,*FLUID SPECIFIC HEAT*,T60,1H=,3X,1PE11.3)              MAIN.130
 107.   0025428    270 FORMAT(1H0,15X,*FLUID VISCOSITY*,T60,1H=,3X,1PE11.3)                  MAIN.131
 108.   0025428    280 FORMAT(1H0,15X,*FLUID DENSITY*,T60,1H=,3X,1PE11.3///)                 MAIN.132
 109.   0025428        END                                                                   MAIN.133
```

```
 1.   0000008        SUBROUTINE INDATA(LEVEL)                                          INDATA.2
                 C*********************************************************************COMALL.2
                 C                              COMMON BLOCKS                          COMALL.3
                 C*********************************************************************COMALL.4
 2.   0000008        DIMENSION SAVE(20229)                                             DIM3.1
 3.   0000008        DIMENSION TRANS(512)                                              DIM3.2
 4.   0000008        COMMON                                                            COMALL.6
                    1X(15),Y(30),Z(02),XU(15),YV(30),ZW(02),                           DIM3.3
                    1DXEP(15),DXPW(15),DYNP(30),DYPS(30),SEW(15),SNS(30),              DIM3.4
                    1DXEPU(15),DXPWU(15),SEWU(15),DYNPV(30),DYPSV(30),SNSV(30),        DIM3.5
                    1R(30),RV(30),RCV(30),WFN(30),WFS(30),WFE(15),WFW(15),             DIM3.6
                    1J(15,30,2),V(15,30,2),W(15,30,2),PE(15,30,2),C(15,30,2),PP(15,30), DIM3.7
                    1UU(15,30),UV(15,30),UW(15,30),VV(15,30),VW(15,30),WW(15,30),      DIM3.8
                    1ED(15,30),TE(15,30),FF(15,30),UC(15,30),VC(15,30),WC(15,30),      DIM3.9
                    1C2(15,30),EC(15,30),RS(15,30),                                    DIM3.10
                    1DEN(15,30,2),VIS(15,30,2),GAM(15,30,2),VISUU(15,30),VISVV(15,30), DIM3.11
                    1AW(15,30),AE(15,30),AN(15,30),AS(15,30),AD(15,30),AU(15,30),      DIM3.12
                    1AP(15,30),SU(15,30),SP(15,30),                                    DIM3.13
                    1JT(15),CT(15),QUE(15),DCDZB(15),QUD(15),                          DIM3.14
                    1DENSIT,VISCOS,PRANDT,SPHEAT,EXCHAT,                               COMALL.19
                    1CMU,CR1,CR2,CRS,CR1W,CR2W,CEPS1,CEPS2,CEPS,CAPPA,ELOG,            COMALL.20
                    1CC1,CC2,CC,CC1W,CC2W,CG2,CG,CAPPAC,ELOGC,                         COMALL.21
                    1JUU,JUV,JUW,JVV,JVW,JWW,JED,JTE,JFF,JUC,JVC,JWC,JC2,JEC,          COMALL.22
                    1NI,NIM1,NIM2,NJ,NJM1,NJM2,NK,NKM1,IT,JT,KT,IJT,                   COMALL.23
                    1HEDU(4),HEDV(4),HEDW(4),HEDP(4),HEDC(4),HEDR(4),HEDD(4),HEDVIS(4), COMALL.24
                    1INCALU,INCALV,INCALW,INCALP,INCALC,INPRO,INCALR(14),INTURB,INDIFF, COMALL.25
                    1NSWPU,NSWPV,NSWPW,NSWPP,NSWPC,NSWPR,                              COMALL.26
                    1MODEL,MODEC,MRW,MCW,IQUE,IDIF,IJET,ITEST,ITESU,ITESC,ICON,        COMALL.27
                    1IRUN,IU,IHT,IU1,IU2,IC1,IC2,I1,I2,INDCOS,FRA,                     COMALL.28
                    1K,DZ,ISTEP,ISTP1,NRS,INDEX,DPDZ,                                  COMALL.29
                    1FLOWIN,VMEAN,QLENTH,SMALL,GREAT,XTOT,YTOT,RSWALL(14),             COMALL.30
                    1ZDPRO(18),IPRO,IEND,INDPRI,NUMPRI,BVE,BVW,BVS,BWS                 COMALL.31
 5.   0000008        COMMON                                                            DIM3.15
                    1ET(15),ETU(15),DET(15),DETU(15),DYW,NJP,NJP1,NJPM1,IWALL,         DIM3.16
                    1ROUTER,RINNER,ECCEN,ES,NJO,YTOTO,EXCHAW,NJOM1                     DIM3.17
 6.   0000008        COMMON  OLDU(30),OLDV(30),OLDW(30),OLDP(30),                      DIM3.18
                    1       OLDUU(30),OLDUV(30),OLDUW(30),OLDVV(30),OLDVW(30),         DIM3.19
                    1       OLDWW(30),OLDTE(30),OLDED(30),OLDFF(30),                   DIM3.20
                    1       OLDDEN(30),OLDVIS(30),OVISUU(30),OVISVV(30),               DIM3.21
                    1       OLDUTA,ODPDZ                                               DIM3.22
 7.   0000008        LOGICAL INCALU,INCALV,INCALW,INCALP,INCALC,INPRO,                 COMALL.32
                    1       INCALR,INTURB,INDIFF                                       COMALL.33
 8.   0000008        EQUIVALENCE (X(1),SAVE(1))                                        COMALL.34
 9.   0000008        EQUIVALENCE (OLDU(1),TRANS(1))                                    DIM3.23
                 C*********************************************************************INDATA.4
10.   0000008        DIMENSION Y2(21),W1(21),UU1(21),VV1(21),WW1(21),VW1(21),UW1(21),   INDATA.5
                    1         ED1(21),C1(21),UC1(21),VC1(21),WC1(21),C21(21),EC1(21)   INDATA.6
                 C*********************************************************************INDATA.7
                 C                              MISCELLANEOUS DATA                     INDATA.8
                 C*********************************************************************INDATA.9
11.   0000008        GO TO (100,200),LEVEL                                             INDATA.10
12.   0004468    100 CONTINUE                                                          INDATA.11
13.   0004508        GREAT=1.0E+30                                                     INDATA.12
14.   0004508        SMALL=1.0E-40                                                     INDATA.13
15.   0004528        JUU=1                                                             INDATA.14
16.   0004538        JUV=2                                                             INDATA.15
17.   0004548        JUW=3                                                             INDATA.16
```

```
000455B        JVV=4                                                    INDATA.17
000456B        JVW=5                                                    INDATA.18
000457B        JWW=6                                                    INDATA.19
000460B        JED=7                                                    INDATA.20
000461B        JTE=8                                                    INDATA.21
000462B        JFF=9                                                    INDATA.22
000463B        JUC=10                                                   INDATA.23
000464B        JVC=11                                                   INDATA.24
000465B        JWC=12                                                   INDATA.25
000466B        JC2=13                                                   INDATA.26
000467B        JEC=14                                                   INDATA.27
000470B        READ(5,010) HEDU,HEDV,HEDW,HEDP,HEDC                     INDATA.28
000506B        READ(5,010) HEDR,HEDD,HEDVIS                             INDATA.29
000517B        DO 120 L=1,14                                            INDATA.30
000520B    120 INCALR(L)=.FALSE.                                        INDATA.31
000522B        READ(5,020) IRUN,IEND                                    INDATA.32
000527B        IENDNE=IEND                                              INDATA.33
000527B        IRUNEW=IRUN                                              INDATA.34
000531B        READ(5,020) NI,NJ,NK,IT,JT,KT                            INDATA.35
000543B        IJT=IT*JT                                                INDATA.36
000544B        NIM1=NI-1                                                INDATA.37
000545B        NIM2=NI-2                                                INDATA.38
000547B        NJM1=NJ-1                                                INDATA.39
000550B        NJM2=NJ-2                                                INDATA.40
000552B        NKM1=NK-1                                                INDATA.41
000553B        READ(5,035) (X(I),I=1,NI)                                INDATA.42
000565B        READ(5,035) (Y(J),J=1,NJ)                                INDATA.43
           C-----FOLLOWING CARD IS INACTIVE IN TWO-DIMENSIONAL PROBLEMS. INDATA.44
000575B        IF(IRUN.EQ.1) READ(3) TRANS                              DIM3.29
000606B        IF(IRUN.EQ.1) GO TO 130                                  INDATA.46
000607B        READ(3) SAVE                                             INDATA.47
000617B    130 CONTINUE                                                 INDATA.48
000617B        IEND=IENDNE                                              INDATA.49
000617B        IRUN=IRUNEW                                              INDATA.50
000621B        READ(5,015) INCALU,INCALV,INCALW,INCALP,INCALC           INDATA.51
000632B        READ(5,015) INTURB,INCALR(JTE),INCALR(JED),INPRO,INDIFF  INDATA.52
000644B        READ(5,015) INCALR(JUU),INCALR(JVV),INCALR(JWW),INCALR(JVW) INDATA.53
              1            ,INCALR(JUW)                                INDATA.54
000661B        READ(5,015) INCALR(JUC),INCALR(JVC),INCALR(JWC),INCALR(JC2), INDATA.55
              1            INCALR(JEC)                                 INDATA.56
000676B        READ(5,020) MODEL,MODEC,MRW,MCW,IDIF                     INDATA.57
000706B        READ(5,020) IJET,INDCOS,IU,IHT,IQUE                      INDATA.58
           C-----DIMENSIONAL LIMITS.                                    INDATA.59
000716B        IU1=3                                                    INDATA.60
000716B        IU2=3                                                    INDATA.61
000717B        IC1=3                                                    INDATA.62
000717B        IC2=3                                                    INDATA.63
000720B        IF(IU.EQ.2) IU1=2                                        INDATA.64
000724B        IF(IU.EQ.2) IU2=NIM1                                     INDATA.65
000727B        IF(IHT.EQ.2) IC1=2                                       INDATA.66
000732B        IF(IHT.EQ.2) IC2=NIM1                                    INDATA.67
000735B        I1=MIN0(IU1,IC1)                                         INDATA.68
000737B        I2=MAX0(IU2,IC2)                                         INDATA.69
000742B        READ(5,020) NSWPU,NSWPV,NSWPW,NSWPP,NSWPR,NSWPC          INDATA.70
000754B        READ(5,020) ITEST,ITESU,ITESC,INDPRI,NUMPRI              INDATA.71
000764B        READ(5,025) FRA                                          INDATA.72
000770B        READ(5,025) CMU,CEPS1  PS2,CEPS                          INDATA.7
000777B        READ(5,025) CR1,CR2,C:   R1W,CR2W                        INDATA.7
```

```
 72.  0010078        READ(5,025) CC1,CC2,CC,CC1W,CC2W                          INDATA.75
 73.  0010178        READ(5,025) CG2,CG                                        INDATA.76
 74.  0010248        READ(5,025) CAPPA,ELOG                                    INDATA.77
 75.  0010318        READ(5,025) CAPPAC,ELOGC                                  INDATA.78
 76.  0010368        READ(5,030) VISCOS,DENSIT,PRANDT,SPHEAT                   INDATA.79
 77.  0010458        READ(5,030) XTOT,YTOT,QLENTH                              INDATA.80
 78.  0010538        QLENTH=QLENTH*YTOT*2.0                                    INDATA.81
 79.  0010548        READ(5,030) RSWALL(1),RSWALL(3),RSWALL(4),RSWALL(5)       INDATA.82
 80.  0010648        READ(5,030) RSWALL(6),RSWALL(8)                           INDATA.83
 81.  0010718        READ(5,030) RSWALL(10),RSWALL(11),RSWALL(12),RSWALL(13)   INDATA.84
 82.  0011008        READ(5,035) (ZDPRO(I),I=1,18)                             INDATA.85
 83.  0011078        WRITE(6,050) INCALU,INCALV,INCALW,INCALP,INCALR(JTE),INCALR(JED),  INDATA.86
                    1             INCALR(JUU),INCALR(JVV),INCALR(JWW),INCALR(JVW),  INDATA.87
                    1             INCALR(JUW),INDIFF,INCALC,INCALR(JUC),INCALR(JVC),  INDATA.88
                    1             INCALR(JWC),INCALR(JC2),INCALR(JEC)                 INDATA.89
 84.  0011508        WRITE(6,055) IRUN,ICON,INDCOS,IU,IHT,IQUE,IU1,IU2,IC1,IC2,I1,I2  INDATA.90
 85.  0011678        WRITE(6,060) MODEL,MODEC,MRW,MCW,IDIF                     INDATA.91
 86.  0011778        WRITE(6,065) CMU,CEPS1,CEPS2,CEPS,CR1,CR2,CRS,CR1W,CR2W,  INDATA.92
                    1             CAPPA,ELOG,                                  INDATA.93
                    1             CC1,CC2,CC,CC1W,CC2W,CG2,CG,CAPPAC,ELOGC,    INDATA.94
                    1             DENSIT,VISCOS,PRANDT,SPHEAT                  INDATA.95
                C     *****CAUTION...ONLY UNIFORM Y-SPACING INSIDE TUBE WALL PROVIDED.  DIM3.30
                C     IF WE NEED M GRID NODES INSIDE TUBE WALL,SUPPLY NJO=NJ+M+1  DIM3.31
                C-----IF IWALL=0, SUPPLY NJO=NJ, ROUTER=RINNER, ECCEN=0, EXCHAW=0  DIM3.32
 87.  0012328        READ(5,040) IWALL,NJO,YTOTO,EXCHAW                        DIM3.33
 88.  0012418        WRITE(6,066) IWALL,NJO,YTOTO,EXCHAW                       DIM3.34
 89.  0012508        READ(5,045) ROUTER,RINNER,ECCEN,ES                        DIM3.35
 90.  0012578        WRITE(6,067) ROUTER,RINNER,ECCEN,ES                       DIM3.36
 91.  0012668        RETURN                                                    INDATA.96
                C*********************************************************** INDATA.97
                C                          INITIAL PROFILES                     INDATA.98
                C*********************************************************** INDATA.99
                                                                               INDATA.100
 92.  0012708    200 CONTINUE                                                  INDATA.101
 93.  0012708        IF(IHT.EQ.2) GO TO 205                                    INDATA.102
 94.  0012718        READ(5,030) WMAX,UUMAX,VVMAX,WWMAX                        INDATA.103
 95.  0013018        READ(5,030) VWMAX,UWMAX,EDMAX                             INDATA.104
 96.  0013078    205 READ(5,030) CMAX,UCMAX,VCMAX,WCMAX                        INDATA.105
 97.  0013168        READ(5,030) C2MAX,ECMAX                                   INDATA.106
                C-----INITIAL CONDITONS IN DIMENSIONLESS FORM                  INDATA.107
 98.  0013238        INUM=21                                                   INDATA.108
 99.  0013238        READ(5,070) (Y2(J),J=1,INUM)                              INDATA.109
100.  0013348        IF(IHT.EQ.2) GO TO 206                                    INDATA.110
101.  0013358        READ(5,070) (W1(J),J=1,INUM)                              INDATA.111
102.  0013468        READ(5,070) (UU1(J),J=1,INUM)                             INDATA.112
103.  0013568        READ(5,070) (VV1(J),J=1,INUM)                             INDATA.113
104.  0013668        READ(5,070) (WW1(J),J=1,INUM)                             INDATA.114
105.  0013768        READ(5,070) (VW1(J),J=1,INUM)                             INDATA.115
106.  0014068        READ(5,070) (UW1(J),J=1,INUM)                             INDATA.116
107.  0014168        READ(5,070) (ED1(J),J=1,INUM)                             INDATA.117
108.  0014268    206 READ(5,070) ( C1(J),J=1,INUM)                             INDATA.118
109.  0014368        READ(5,070) (UC1(J),J=1,INUM)                             INDATA.119
110.  0014468        READ(5,070) (VC1(J),J=1,INUM)                             INDATA.120
111.  0014568        READ(5,070) (WC1(J),J=1,INUM)                             INDATA.121
112.  0014668        READ(5,070) (C21(J),J=1,INUM)                             INDATA.122
113.  0014768        READ(5,070) (EC1(J),J=1,INUM)                             INDATA.123
114.  0015068        READ(5,070) (CT(I),I=1,NI)                                INDATA.124
115.  0015168        READ(5,070) (QUE(I),I=1,NI)                               INDATA.125
116.  0015268        IF(IHT.EQ.2) GO TO 210                                    INDATA.126
```

```
117.  0015278        IF(IRUN.NE.1) GO TO 210                                  INDATA.126
118.  0015318        READ(5,070) DPDZ                                         INDATA.127
119.  0015368        READ(5,070) (UT(I),I=1,NI)                               INDATA.128
120.  0015468    210 CONTINUE                                                 INDATA.129
121.  0015468        IF(IWALL.EQ.0) GO TO 212                                 DIM3.37
122.  0015478        DO 211 I=1,NI                                            DIM3.38
123.  0015518        QUO(I)=QUE(I)                                            DIM3.39
124.  0015518        QUE(I)=0.0                                               DIM3.40
125.  0015528    211 CONTINUE                                                 DIM3.41
126.  0015548    212 CONTINUE                                                 DIM3.42
             C*********************************************************************** INDATA.130
                                                                              INDATA.131
127.  0015548        IF(IHT.EQ.2) GO TO 215                                   INDATA.132
128.  0015558        WRITE(6,0075) (J,Y2(J),W1(J),UU1(J),VV1(J),WW1(J),VW1(J),UW1(J)  INDATA.133
                    1                ,ED1(J),J=1,INUM)                        INDATA.134
129.  0016078    215 WRITE(6,0080) (J,Y2(J),C1(J),UC1(J),VC1(J),WC1(J),        INDATA.135
                    1                C21(J),EC1(J),J=1,INUM)                  INDATA.136
             C*********************************************************************** INDATA.137
                                                                              INDATA.138
130.  0016368        INUM1=INUM-1                                             INDATA.139
131.  0016378        NJ1=NJ+1                                                 INDATA.140
             C-----INTERPOLATION OF MEAN PROFILES.                            INDATA.141
132.  0016408        J=1                                                      INDATA.142
133.  0016418        DO 220 JJ=2,INUM                                         INDATA.143
134.  0016438    220 Y2(JJ)=Y2(JJ)*YTOT                                       INDATA.144
135.  0016458        DO 250 JJ=1,INUM1                                        INDATA.145
136.  0016508        IF(Y(J).LT.Y2(JJ)) GO TO 250                             INDATA.146
137.  0016538    230 IF(Y(J).GT.Y2(JJ+1)) GO TO 250                           INDATA.147
138.  0016578        RATIO=(Y(J)-Y2(JJ))/(Y2(JJ+1)-Y2(JJ))                    INDATA.148
139.  0016638        IF(IHT.EQ.2) GO TO 240                                   INDATA.149
140.  0016658        IF(IRUN.NE.1) GO TO 240                                  INDATA.150
141.  0016678        W(NI,J,2)=W1(JJ)+RATIO*(W1(JJ+1)-W1(JJ))                 INDATA.151
142.  0016768    240 C(NI,J,2)=C1(JJ)+RATIO*(C1(JJ+1)-C1(JJ))                 INDATA.152
143.  0017058        J=J+1                                                    INDATA.153
144.  0017068        IF(J.EQ.NJ1) GO TO 250                                   INDATA.154
145.  0017108        GO TO 230                                                INDATA.155
146.  0017108    250 CONTINUE                                                 INDATA.156
147.  0017138        IF(IRUN.EQ.1) W(NI,NJ,2)=0.0                             INDATA.157
             C*********************************************************************** INDATA.158
             C-----INTERPOLATION OF TURBULENT PROFILES.                       INDATA.159
148.  0017218        J=2                                                      INDATA.160
149.  0017218        DO 280 JJ=1,INUM1                                        INDATA.161
150.  0017238        IF(YV(J).LT.Y2(JJ)) GO TO 280                            INDATA.162
151.  0017268    260 IF(YV(J).GT.Y2(JJ+1)) GO TO 280                          INDATA.163
152.  0017328        RATIO=(YV(J)-Y2(JJ))/(Y2(JJ+1)-Y2(JJ))                   INDATA.164
153.  0017368        IF(IHT.EQ.2) GO TO 270                                   INDATA.165
154.  0017408        IF(IRUN.NE.1) GO TO 270                                  INDATA.166
155.  0017428        UU(NI,J)=UU1(JJ)+RATIO*(UU1(JJ+1)-UU1(JJ))               INDATA.167
156.  0017518        VV(NI,J)=VV1(JJ)+RATIO*(VV1(JJ+1)-VV1(JJ))               INDATA.168
157.  0017578        WW(NI,J)=WW1(JJ)+RATIO*(WW1(JJ+1)-WW1(JJ))               INDATA.169
158.  0017658        VW(NI,J)=VW1(JJ)+RATIO*(VW1(JJ+1)-VW1(JJ))               INDATA.170
159.  0017748        UW(NI,J)=UW1(JJ)+RATIO*(UW1(JJ+1)-UW1(JJ))               INDATA.171
160.  0020028        ED(NI,J)=ED1(JJ)+RATIO*(ED1(JJ+1)-ED1(JJ))               INDATA.172
161.  0020118    270 UC(NI,J)=UC1(JJ)+RATIO*(UC1(JJ+1)-UC1(JJ))               INDATA.173
162.  0020208        VC(NI,J)=VC1(JJ)+RATIO*(VC1(JJ+1)-VC1(JJ))               INDATA.174
163.  0020268        WC(NI,J)=WC1(JJ)+RATIO*(WC1(JJ+1)-WC1(JJ))               INDATA.175
164.  0020348        C2(NI,J)=C21(JJ)+RATIO*(C21(JJ+1)-C21(JJ))               INDATA.176
165.  0020438        EC(NI,J)=EC1(JJ)+RATIO*(EC1(JJ+1)-EC1(JJ))               INDATA.177
166.  0020518        J=J+1                                                    INDATA.178
167.  0020538        IF(J.EQ.NJ1) GO TO 28                                    INDATA.1
```

```
168.  0020548        GO TO 260                                          INDATA.178
169.  0020548    280 CONTINUE                                           INDATA.179
              C******************************************************* INDATA.180
              C-----CALCULATE ACTUAL MAGNITUDES OF ALL VARIABLES.       INDATA.181
                                                                       INDATA.182
170.  0020608        DO 320 I=1,NI                                      INDATA.183
171.  0020628        DO 310 J=1,NJ                                      INDATA.184
172.  0020658        IF(IRUN.NE.1) GO TO 300                            INDATA.185
173.  0020678        IF(IHT.NE.2) GO TO 305                             DIM3.43
174.  0020718        U(I,J,1)=OLDU(J)                                   DIM3.44
175.  0020768        U(I,J,2)=OLDU(J)                                   DIM3.45
176.  0021018        V(I,J,1)=OLDV(J)                                   DIM3.46
177.  0021048        V(I,J,2)=OLDV(J)                                   DIM3.47
178.  0021078        W(I,J,1)=OLDW(J)                                   DIM3.48
179.  0021128        W(I,J,2)=OLDW(J)                                   DIM3.49
180.  0021158        PE(I,J,1)=OLDP(J)                                  DIM3.50
181.  0021208        PE(I,J,2)=OLDP(J)                                  DIM3.51
182.  0021238        UU(I,J)=OLDUU(J)                                   DIM3.52
183.  0021268        UV(I,J)=OLDUV(J)                                   DIM3.53
184.  0021328        UW(I,J)=OLDUW(J)                                   DIM3.54
185.  0021368        VV(I,J)=OLDVV(J)                                   DIM3.55
186.  0021428        VW(I,J)=OLDVW(J)                                   DIM3.56
187.  0021468        WW(I,J)=OLDWW(J)                                   DIM3.57
188.  0021528        TE(I,J)=OLDTE(J)                                   DIM3.58
189.  0021568        ED(I,J)=OLDED(J)                                   DIM3.59
190.  0021628        FF(I,J)=OLDFF(J)                                   DIM3.60
191.  0021668        DEN(I,J,1)=OLDDEN(J)                               DIM3.61
192.  0021728        DEN(I,J,2)=OLDDEN(J)                               DIM3.62
193.  0021768        VIS(I,J,1)=OLDVIS(J)                               DIM3.63
194.  0022028        VIS(I,J,2)=OLDVIS(J)                               DIM3.64
195.  0022068        VISUU(I,J)=OVISUU(J)                               DIM3.65
196.  0022128        VISVV(I,J)=OVISVV(J)                               DIM3.66
197.  0022168        UT(I)=OLDUTA                                       DIM3.67
198.  0022178        DPDZ=ODPDZ                                         INDATA.186
199.  0022218        GO TO 300                                          INDATA.187
200.  0022218    305 CONTINUE                                           INDATA.188
201.  0022238        W(I,J,1)=W(NI,J,2)*WMAX                            INDATA.189
202.  0022318        W(I,J,2)=W(NI,J,2)*WMAX                            INDATA.190
203.  0022378        UU(I,J)=UU(NI,J)*UUMAX                             INDATA.191
204.  0022458        VV(I,J)=VV(NI,J)*VVMAX                             INDATA.192
205.  0022538        WW(I,J)=WW(NI,J)*WWMAX                             INDATA.193
206.  0022618        VW(I,J)=VW(NI,J)*VWMAX                             INDATA.194
207.  0022678        UW(I,J)=UW(NI,J)*UWMAX                             INDATA.195
208.  0022758        ED(I,J)=ED(NI,J)*EDMAX                             INDATA.196
209.  0023038        TE(I,J)=(UU(I,J)+VV(I,J)+WW(I,J))*0.5              INDATA.197
210.  0023118        FF(I,J)=UU(I,J)-VV(I,J)                            INDATA.198
211.  0023168    300 C(I,J,2)=C(NI,J,2)*CMAX                            INDATA.199
212.  0023248        C(I,J,1)=C(NI,J,2)*CMAX                            INDATA.200
213.  0023328        UC(I,J)=UC(NI,J)*UCMAX                             INDATA.201
214.  0023408        VC(I,J)=VC(NI,J)*VCMAX                             INDATA.202
215.  0023468        WC(I,J)=WC(NI,J)*WCMAX                             INDATA.203
216.  0023548        C2(I,J)=C2(NI,J)*C2MAX                             INDATA.204
217.  0023628        EC(I,J)=EC(NI,J)*ECMAX                             INDATA.205
218.  0023708    310 CONTINUE                                           INDATA.206
219.  0023738    320 CONTINUE                                           INDATA.207
220.  0023768        I=3                                                INDATA.208
221.  0023778        WRITE(6,0085) (J,UU(I,J),VV(I,J),WW(I,J),VW(I,J),UW(I,J)  INDATA.209
                   1              ,FF(I,J),TE(I,J),ED(I,J),J=1,NJ)     INDATA.210
222.  0024618        WRITE(6,0090) (J,C(I,J,2),UC(I,J),VC(I,J),WC(I,J),C2(I,J),
```

```
                 1                EC(I,J),J=1,NJ)                                    INDATA.211
               C*********************************************************************INDATA.212
               C                          FORMAT STATEMENTS                          INDATA.213
               C*********************************************************************INDATA.214
                                                                                     INDATA.215
223.   0025308    10 FORMAT(9A10)                                                     INDATA.216
224.   0025308    15 FORMAT(5(4X,L1))                                                 INDATA.217
225.   0025308    20 FORMAT(7(7X,I4))                                                 INDATA.218
226.   0025308    25 FORMAT(5(6X,F6.3))                                               INDATA.219
227.   0025308    30 FORMAT(4(7X,1PE10.3))                                            INDATA.220
228.   0025308    35 FORMAT(4X,1P6E11.3)                                              DIM3.68
229.   0025308   040 FORMAT(7X,I4,7X,I4,2(7X,1PE11.3))                                DIM3.69
230.   0025308   045 FORMAT(4X,4(4X,1PE11.3))                                         INDATA.221
231.   0025308    50 FORMAT(1H1///,5X,*SELECTION OF VARIABLES*,/                      INDATA.222
                 1        10X,*  U=*,L1,*  V=*,L1,*  W=*,L1,*  P=*,L1,/               INDATA.223
                 1        10X,* TE=*,L1,* ED=*,L1,* UU=*,L1,* VV=*,L1,* WW=*,L1,      INDATA.224
                 1            * VW=*,L1,* UW=*,L1,*DIF=*,L1,/                         INDATA.225
                 1        10X,*  C=*,L1,* UC=*,L1,* VC=*,L1,* WC=*,L1,* C2=*,L1,      INDATA.226
                 1            * EC=*,L1)                                              INDATA.227
232.   0025308    55 FORMAT(1H ,5X,*RUN SPECIFICATIONS*,//                            INDATA.228
                 1        10X,*IRUN=*,I2,*ICON=*,I2,*INOCOS=*,I2,*IU=*,I2,*IHT=*,I2,  INDATA.229
                 1            *IQUE=*,I2,*IU1=*,I2,*IU2=*,I2,*IC1=*,I2,*IC2=*,I2,     INDATA.230
                 1            *I1=*,I2,*I2=*,I2)                                      INDATA.231
233.   0025308    60 FORMAT(1H ,5X,*TURBULENCE MODEL*,//                              INDATA.232
                 1        10X,*MODEL=*,I2,*MODEC=*,I2,*MRW=*,I2,*MCW=*,I2,*IDIF=*,I2) INDATA.233
234.   0025308    65 FORMAT(1H ,5X,*TURBULENCE CONSTANTS ETC.*,//                     INDATA.234
                 1        10X,*  CMU=*,F6.3,*CEPS1=*,F6.3,*CEPS2=*,F6.3,*CEPS=*,F6.3/ INDATA.235
                 1        10X,*  CR1=*,F6.3,*  CR2=*,F6.3,*  CRS=*,F6.3,              INDATA.236
                 1            * CR1W=*,F6.3,* CR2W=*,F6.3/                            INDATA.237
                 1        10X,*CAPPA=*,F6.3,*ELOG=*,F6.3/                             INDATA.238
                 1        10X,*  CC1=*,F6.3,*  CC2=*,F6.3,*   CC=*,F6.3,              INDATA.239
                 1        *  CC1W=*,F6.3,*  CC2W=*,F6.3/                             INDATA.240
                 1        10X,*  CG2=*,F6.3,*   CG=*,F6.3/                            INDATA.241
                 1        10X,*CAPAC=*,F6.3,*ELOGC=*,F6.3/                            INDATA.242
                 1        10X,*DENSITY=*,1PE11.3,*VISCOSITY=*,1PE11.3/                INDATA.243
                 1        10X,*PRANDTL=*,1PE11.3,*SP. HEAT=*,1PE11.3)                 INDATA.244
235.   0025308   066 FORMAT(////40H**** UNIFORM Y-SPACING INSIDE WALL  ****//,        DIM3.70
                 110X,6HIWALL=,I3,5X,4HNJO=,I3,5X,6HYTOTO=,1PE11.3,7HEXCHAW=,         DIM3.71
                 21PE11.3)                                                           DIM3.72
236.   0025308    67 FORMAT(//24HSPARROW AND BLACK S DATA,7HROUTER=,1PE11.3,          DIM3.73
                 1  7HRINNER=,1PE11.3,7HECCEN =,1PE11.3,11HPOWER RATE=,1PE11.3)       DIM3.74
237.   0025308    70 FORMAT(4X,1P6E11.3)                                              INDATA.245
238.   0025308    75 FORMAT(5X,I3,1P8E11.3)                                           INDATA.246
239.   0025308    80 FORMAT(5X,I3,1P7E11.3)                                           INDATA.247
240.   0025308    85 FORMAT(5X,I3,1P8E11.3)                                           INDATA.248
241.   0025308    90 FORMAT(5X,I3,1P6E11.3)                                           INDATA.249
242.   0025308       RETURN                                                           INDATA.250
243.   0025328       END
```

```
 1.   0000008        SUBROUTINE SOURCE(PHI,IRS,SUS,SPS,IJMAX,IM1,IM2)                  SOURCE.2
                C*********************************************************************COMALL.2
                C                              COMMON BLOCKS                          COMALL.3
                C*********************************************************************COMALL.4
 2.   0000008        DIMENSION SAVE(20229)                                             DIM3.1
 3.   0000008        DIMENSION TRANS(512)                                              DIM3.2
 4.   0000008        COMMON                                                            COMALL.6
                    1X(15),Y(30),Z(02),XU(15),YV(30),ZW(02),                           DIM3.3
                    1DXEP(15),DXPW(15),DYNP(30),DYPS(30),SEW(15),SNS(30),              DIM3.4
                    1DXEPU(15),DXPWU(15),SEWU(15),DYNPV(30),DYPSV(30),SNSV(30),        DIM3.5
                    1R(30),RV(30),RCV(30),WEN(30),WFS(30),WFE(15),WFW(15),             DIM3.6
                    1U(15,30,2),V(15,30,2),W(15,30,2),PE(15,30,2),C(15,30,2),PP(15,30), DIM3.7
                    1UU(15,30),UV(15,30),UW(15,30),VV(15,30),VW(15,30),WW(15,30),      DIM3.8
                    1ED(15,30),TE(15,30),FF(15,30),UC(15,30),VC(15,30),WC(15,30),      DIM3.9
                    1C2(15,30),EC(15,30),RS(15,30),                                    DIM3.10
                    1DEN(15,30,2),VIS(15,30,2),GAM(15,30,2),VISUU(15,30),VISVV(15,30), DIM3.11
                    1AW(15,30),AE(15,30),AN(15,30),AS(15,30),AD(15,30),AU(15,30),      DIM3.12
                    1AP(15,30),SJ(15,30),SP(15,30),                                    DIM3.13
                    1UT(15),CT(15),QUE(15),DCDZB(15),QUO(15),                          DIM3.14
                    1DENSIT,VISCOS,PRANDT,SPHEAT,EXCHAT,                               COMALL.19
                    1CMU,CR1,CR2,CRS,CR1W,CR2W,CEPS1,CEPS2,CEPS,CAPPA,ELOG,            COMALL.20
                    1CC1,CC2,CC,CC1W,CC2W,CG2,CG,CAPPAC,ELOGC,                         COMALL.21
                    1JUU,JUV,JUW,JVV,JVW,JWW,JED,JTE,JFF,JUC,JVC,JWC,JC2,JEC,          COMALL.22
                    1NI,NIM1,NIM2,NJ,NJM1,NJM2,NK,NKM1,IT,JT,KT,IJT,                   COMALL.23
                    1HEDU(4),HEDV(4),HEDW(4),HEDP(4),HEDC(4),HEDR(4),HEDD(4),HEDVIS(4), COMALL.24
                    1INCALU,INCALV,INCALW,INCALP,INCALC,INPRO,INCALR(14),INTURB,INDIFF, COMALL.25
                    1NSWPU,NSWPV,NSWPW,NSWPP,NSWPC,NSWPR,                              COMALL.26
                    1MODEL,MODEC,MRW,MCW,IQUE,IDIF,IJET,ITEST,ITESU,ITESC,ICON,        COMALL.27
                    1IRUN,IU,IHT,IU1,IU2,IC1,IC2,I1,I2,INDCOS,FRA,                     COMALL.28
                    1K,DZ,ISTEP,ISTP1,NRS,INDEX,DPDZ,                                  COMALL.29
                    1FLOWIN,VMEAN,QLENTH,SMALL,GREAT,XTOT,YTOT,RSWALL(14),             COMALL.30
                    1ZDPRO(18),IPRO,IEND,INDPRI,NUMPRI,BVE,BVW,BVS,BWS                 COMALL.31
 5.   0000008        COMMON                                                            DIM3.15
                    1ET(15),ETU(15),DET(15),DETU(15),DYW,NJP,NJP1,NJPM1,IWALL,         DIM3.16
                    1ROUTER,RINNER,ECCEN,ES,NJO,YTOTO,EXCHAW,NJOM1                     DIM3.17
 6.   0000008        COMMON  OLDU(30),OLDV(30),OLDW(30),OLDP(30),                      DIM3.18
                    1       OLDUU(30),OLDUV(30),OLDUW(30),OLDVV(30),OLDVW(30),         DIM3.19
                    1       OLDWW(30),OLDTE(30),OLDED(30),OLDFF(30),                   DIM3.20
                    1       OLDDEN(30),OLDVIS(30),OVISUU(30),OVISVV(30),               DIM3.21
                    1       OLDUTA,ODPDZ                                               DIM3.22
 7.   0000008        LOGICAL INCALU,INCALV,INCALW,INCALP,INCALC,INPRO,                 COMALL.32
                    1       INCALR,INTURB,INDIFF                                       COMALL.33
 8.   0000008        EQUIVALENCE (X(1),SAVE(1))                                        COMALL.34
 9.   0000008        EQUIVALENCE (OLDU(1),TRANS(1))                                    DIM3.23
                C                                                                     SOURCE.4
10.   0000008        DIMENSION UIUJ(3,3),DUIDXJ(3,3),P(3,3),D(3,3),PHI1(3,3),PHI2(3,3), SOURCE.5
                    1          DIS(3,3),PHIW1(3,3),PHIW2(3,3),DEL(3,3),                SOURCE.6
                    1          UJC(3),DCDXJ(3),PC(3),P1C(3),D1C(3),PSI1(3),PSI2(3),    SOURCE.7
                    1          PSIW1(3),PSIW2(3),                                      SOURCE.8
                    1          S1(14,450),S2(14,450),                                  DIM3.75
                    1          SEX(14),SDEX(14),SOLD(14),                              SOURCE.10
                    1          SUS(IJMAX),SPS(IJMAX),PHI(IJMAX)                        SOURCE.11
                C*********************************************************************SOURCE.12
                C                          INITIALISING SECTION                       SOURCE.13
                C*********************************************************************SOURCE.14
11.   0000008        ENTRY SOURCEI                                                     SOURCE.15
12.   0307358        CS2=CR2                                                           SOURCE.16
```

0 0 0 0 4 9 0 - 349 8 8

```
                **SUBROUTINE SOURCE(PHI,IRS,SUS,SPS,IJMAX,IM1,IM2)**
 13.  030735B        URFS=0.1
            C-----SET INTERNAL VARIABLES TO ZERO INITIALLY.
 14.  030737B        DO 10 IRS=1,14
 15.  030741B        DO 10 IJ=1,IJT
 16.  030744B        S1(IRS,IJ)=0.0
 17.  030746B     10 S2(IRS,IJ)=0.0
 18.  030753B        DO 20 I=1,3
 19.  030754B        DO 20 J=1,3
 20.  030756B        DEL(I,J)=0.0
 21.  030760B        IF(I.EQ.J) DEL(I,J)=1.0
 22.  030765B     20 CONTINUE
            C*****************************************************************
            C-----CALCULATE RELEVANT CONSTANTS.
            C-----REDISTRIBUTION OF PRODUCTION MODEL
 23.  030771B        F1=-CS2
 24.  030772B        F2=0.0
 25.  030773B        F3=0.0
 26.  030773B        IF(MODEL.EQ.2)GO TO 30
            C-----LAUNDER-REECE-RODI MODEL
 27.  030776B        F1=-(CS2+8.0)/11.0
 28.  031001B        F2=-(30.0*CS2-2.0)/55.0
 29.  031005B        F3=-(6.0*CS2-2.0)/11.0
 30.  031010B     30 IF(IHT.EQ.0) GO TO 40
            C-----REDISTRIBUTION OF PRODUCTION (BY MEAN STRAIN) MODEL
 31.  031013B        G1=-CS2
 32.  031014B        G2= 0.0
 33.  031014B        IF(MODEC.EQ.1) GO TO 40
            C-----QUASI-ISOTROPIC MODEL
 34.  031017B        G1=-0.8
 35.  031020B        G2= 0.2
 36.  031021B     40 CONTINUE
 37.  031023B        RETURN
 38.  031025B        ENTRY CALSOR
            C*****************************************************************
            C                          PRELIMINARIES
            C*****************************************************************
 39.  031033B        CS1=CR1
 40.  031033B        CS=CRS
 41.  031035B        CE1=CEPS1
 42.  031036B        CE2=CEPS2
            C-----DECAY FUNCTION AT THE NEAR WALL POINT.
 43.  031040B        FWM1=ABS(VW(3,NJM1)*SQRT(ABS(VW(3,NJM1))))/(ED(3,NJM1)+SMALL)/
                   1    (Y(NJ)*Y(NJ)-YV(NJM1)*YV(NJM1))*2.0*Y(NJ)
 44.  031062B        DO 1000 J=2,NJM1
 45.  031065B        DO 1000 I=IM1,IM2
 46.  031070B        IJ=I+IT*(J-1)
 47.  031072B        DO 110 IRS=1,14
 48.  031075B        SULD(IRS)=0.0
 49.  031075B        SEX(IRS)=0.0
 50.  031075B        SDEX(IRS)=0.0
 51.  031076B    110 CONTINUE
 52.  031100B        IF(I.GT.IM1) GO TO 140
            C*****************************************************************
            C*****REYNOLDS STRESS TENSOR AND NECESSARY GRADIENTS.
            C-----AT THE NODE.
 53.  031102B        UIUJ(1,1)=UU(I,J)
 54.  031105B        UIUJ(1,2)=UV(I,J)
 55.  031110B        UIUJ(2,1)=UV(I,J)
```

```
 56.  0311138        UIUJ(1,3)=UW(I,J)                                    SOURCE.75
 57.  0311168        UIUJ(3,1)=UW(I,J)                                    SOURCE.76
 58.  0311218        UIUJ(2,2)=VV(I,J)                                    SOURCE.77
 59.  0311248        UIUJ(2,3)=VW(I,J)                                    SOURCE.78
 60.  0311278        UIUJ(3,2)=VW(I,J)                                    SOURCE.79
 61.  0311328        UIUJ(3,3)=WW(I,J)                                    SOURCE.80
 62.  0311358        T=TE(I,J)+SMALL                                      SOURCE.81
 63.  0311418        E=ED(I,J)+SMALL                                      SOURCE.82
                  C-----AT THE NORTH SIDE.                                SOURCE.83
 64.  0311468        UUN=UU(I,J)*WFN(J)+UU(I,J+1)*(1.0-WFN(J))            SOURCE.84
 65.  0311558        VVN=VV(I,J)*WFN(J)+VV(I,J+1)*(1.0-WFN(J))            SOURCE.85
 66.  0311648        VWN=VW(I,J)*WFN(J)+VW(I,J+1)*(1.0-WFN(J))            SOURCE.86
 67.  0311728        TEN=TE(I,J)*WFN(J)+TE(I,J+1)*(1.0-WFN(J))            SOURCE.87
 68.  0312018        EDN=ED(I,J)*WFN(J)+ED(I,J+1)*(1.0-WFN(J))            SOURCE.88
 69.  0312078        DVVN=(VV(I,J+1)-VV(I,J))/(YV(J+1)-YV(J))             SOURCE.89
 70.  0312178        DVWN=(VW(I,J+1)-VW(I,J))/(YV(J+1)-YV(J))             SOURCE.90
                  C-----AT THE SOUTH SIDE.                                SOURCE.91
 71.  0312258        UUS=UU(I,J)*(1.0-WFN(J-1))+UU(I,J-1)*WFN(J-1)        SOURCE.92
 72.  0312348        VVS=VV(I,J)*(1.0-WFN(J-1))+VV(I,J-1)*WFN(J-1)        SOURCE.93
 73.  0312428        VWS=VW(I,J)*(1.0-WFN(J-1))+VW(I,J-1)*WFN(J-1)        SOURCE.94
 74.  0312508        TES=TE(I,J)*(1.0-WFN(J-1))+TE(I,J-1)*WFN(J-1)        SOURCE.95
 75.  0312568        EDS=ED(I,J)*(1.0-WFN(J-1))+ED(I,J-1)*WFN(J-1)        SOURCE.96
 76.  0312648        DVVS=(VV(I,J)-VV(I,J-1))/(YV(J)-YV(J-1))             SOURCE.97
 77.  0312728        DVWS=(VW(I,J)-VW(I,J-1))/(YV(J)-YV(J-1))             SOURCE.98
 78.  0313008    140 IF(IHT.EQ.0) GO TO 150                               SOURCE.99
                  C*****SCALAR FLUX TENSOR AND NECESSARY GRADIENTS        SOURCE.100
                  C-----AT THE NODE                                       SOURCE.101
 79.  0313028        UJC(1)=UC(I,J)                                       SOURCE.102
 80.  0313058        UJC(2)=VC(I,J)                                       SOURCE.103
 81.  0313108        UJC(3)=WC(I,J)                                       SOURCE.104
 82.  0313138        CSQ=C2(I,J)                                          SOURCE.105
                  C-----AT THE NORTH SIDE                                 SOURCE.106
 83.  0313168        DVCN=(VC(I,J+1)-VC(I,J))/(YV(J+1)-YV(J))             SOURCE.107
                  C-----AT THE SOUTH SIDE                                 SOURCE.108
 84.  0313258        DVCS=(VC(I,J)-VC(I,J-1))/(YV(J)-YV(J-1))             SOURCE.109
 85.  0313338    150 CONTINUE                                             SOURCE.110
 86.  0313348        IF(IHT.NE.2) GO TO 160                               SOURCE.111
 87.  0313358        UCW=0.5*(UC(I,J)+UC(I,J-1))                          SOURCE.112
 88.  0313428        UCE=0.5*(UC(I+1,J)+UC(I+1,J-1))                      SOURCE.113
 89.  0313478        VCN=VC(I,J)*WFN(J)+VC(I,J+1)*(1.0-WFN(J))            SOURCE.114
 90.  0313578        EDTP1=ED(I,J+1)/(TE(I,J+1)+SMALL)                    SOURCE.115
 91.  0313638        UU1=UU(I,J+1)                                        SOURCE.116
 92.  0313668        DVCWN=(VC(I,J+1)-VC(I-1,J+1))/(X(I)-X(I-1))          SOURCE.117
 93.  0313758        DVCWS=(VC(I,J)-VC(I-1,J))/(X(I)-X(I-1))              SOURCE.118
 94.  0314038        DUCE=(UC(I+1,J)-UC(I,J))/(XU(I+1)-XU(I))             SOURCE.119
 95.  0314128        DUCW=(UC(I,J)-UC(I-1,J))/(XU(I)-XU(I-1)+SMALL)       SOURCE.120
 96.  0314218        UCN=0.5*(UC(I,J+1)+UC(I,J))                          SOURCE.121
 97.  0314268        UCS=0.5*(UC(I,J)+UC(I,J-1))                          SOURCE.122
 98.  0314338        VCN1=VC(I-1,J)*WFN(J)+VC(I-1,J+1)*(1.0-WFN(J))       SOURCE.123
 99.  0314438        DUCSE=(UC(I+1,J)-UC(I+1,J-1))/(Y(J)-Y(J-1))          SOURCE.124
100.  0314528        DUCSW=(UC(I,J)-UC(I,J-1))/(Y(J)-Y(J-1))              SOURCE.125
101.  0314628    160 CONTINUE                                             SOURCE.126
102.  0314638        EDT=E/T                                              SOURCE.127
103.  0314648        FWL=ABS(UIUJ(2,3)*SQRT(ABS(UIUJ(2,3))))/(E+SMALL)/   SOURCE.128
                    1     (Y(NJ)*Y(NJ)-YV(J)*YV(J))*2.0*Y(NJ)/(FWM1+SMALL)  SOURCE.129
                  C******************************************************* SOURCE.130
                  C*****MEAN GRADIENTS                                    SOURCE.131
104.  0315068        IF(I.GT.IM1) GO TO 190                               SOURCE.132
```

```
                C-----VELOCITY GRADIENTS.                                          SOURCE.133
 105.   0315108       WP=W(I,J,K)                                                  SOURCE.134
 106.   0315158       WPP=W(I,J,1)                                                 SOURCE.135
 107.   0315208       UP=0.0                                                       SOURCE.136
 108.   0315218       VP=V(I,J,K)                                                  SOURCE.137
 109.   0315268       WS=W(I,J-1,K)                                                SOURCE.138
 110.   0315328       WSP=W(I,J-1,1)                                               SOURCE.139
 111.   0315358       DUIDXJ(1,1)=0.0                                              SOURCE.140
 112.   0315358       DUIDXJ(1,2)=0.0                                              SOURCE.141
 113.   0315368       DUIDXJ(1,3)=0.0                                              SOURCE.142
 114.   0315378       DUIDXJ(2,1)=0.0                                              SOURCE.143
 115.   0315378       DUIDXJ(2,2)=0.0                                              SOURCE.144
 116.   0315408       DUIDXJ(2,3)=0.0                                              SOURCE.145
 117.   0315408       DUIDXJ(3,1)=0.0                                              SOURCE.146
 118.   0315418       DUIDXJ(3,2)=(WP-WS)/(Y(J)-Y(J-1))                            SOURCE.147
 119.   0315468       DUIDXJ(3,3)=(WP+WS-WPP-WSP)*0.5/(Z(2)-Z(1))                  SOURCE.148
 120.   0315558   190 CONTINUE                                                     SOURCE.149
                C-----SCALAR GRADIENTS.                                            SOURCE.150
 121.   0315568       CP=C(I,J,K)                                                  SOURCE.151
 122.   0315628       CPP=C(I,J,1)                                                 SOURCE.152
 123.   0315658       CWE=C(I-1,J,K)                                               SOURCE.153
 124.   0315728       CSS=C(I,J-1,K)                                               SOURCE.154
 125.   0315768       CSP=C(I,J-1,1)                                               SOURCE.155
 126.   0316018       DCDXJ(1)=(CP-CWE)/(R(J)*(X(I)-X(I-1)))                       SOURCE.156
 127.   0316068       DCDXJ(2)=(CP-CSS)/(Y(J)-Y(J-1))                              SOURCE.157
 128.   0316138       DCDXJ(3)=(CP+CSS-CPP-CSP)*0.5/(Z(2)-Z(1))                    SOURCE.158
 129.   0316228       IF(MODEL.EQ.3)GO TO 300                                      SOURCE.159
 130.   0316258       IF(IU.EQ.0) GO TO 500                                        SOURCE.160
 131.   0316268       IF(J.EQ.2) GO TO 500                                         SOURCE.161
                C*****************************************************************SOURCE.162
                C                  SOURCES FOR REYNOLDS STRESS EQUATIONS           SOURCE.163
                C*****************************************************************SOURCE.164
                C*****************************************************************SOURCE.165
                C*****PRODUCTION TERMS                                             SOURCE.166
 132.   0316308       DO 200 II=1,3                                                SOURCE.167
 133.   0316328       DO 200 JJ=1,II                                               SOURCE.168
 134.   0316348       P(II,JJ)=0.0                                                 SOURCE.169
 135.   0316358       D(II,JJ)=0.0                                                 SOURCE.170
 136.   0316358       DO 200 KK=1,3                                                SOURCE.171
 137.   0316418       P(II,JJ)=P(II,JJ)-(UIUJ(JJ,KK)*DUIDXJ(II,KK)+                SOURCE.172
                     1                  UIUJ(II,KK)*DUIDXJ(JJ,KK))                SOURCE.173
 138.   0316528       D(II,JJ)=D(II,JJ)-(UIUJ(II,KK)*DUIDXJ(KK,JJ)+                SOURCE.174
                     1                  UIUJ(JJ,KK)*DUIDXJ(KK,II))                SOURCE.175
 139.   0316618   200 CONTINUE                                                     SOURCE.176
                C-----EXTRA TERMS FOR CYLINDRICAL GRID.                            SOURCE.177
 140.   0316678       IF(INDCDS.EQ.1)GO TO 210                                     SOURCE.178
 141.   0316718       UPR=UP/YV(J)                                                 SOURCE.179
 142.   0316738       VPR=VP/YV(J)                                                 SOURCE.180
 143.   0316748       P(1,1)=P(1,1)-2.0*VPR*UIUJ(1,1)                              SOURCE.181
 144.   0317008       P(2,1)=P(2,1)+UPR*UIUJ(1,1)-VPR*UIUJ(1,2)                    SOURCE.182
 145.   0317038       P(2,2)=P(2,2)+2.0*UPR*UIUJ(1,2)                              SOURCE.183
 146.   0317068       P(3,1)=P(3,1)-VPR*UIUJ(1,3)                                  SOURCE.184
 147.   0317118       P(3,2)=P(3,2)+UPR*UIUJ(1,3)                                  SOURCE.185
                C                                                                  SOURCE.186
 148.   0317138       D(1,1)=D(1,1)+2.0*UPR*UIUJ(1,2)-VPR*UIUJ(1,1)                SOURCE.187
 149.   0317208       D(2,1)=D(2,1)-VPR*UIUJ(1,2)+UPR*UIUJ(2,2)                    SOURCE.188
 150.   0317248       D(3,1)=D(3,1)-VPR*UIUJ(1,3)+UPR*UIUJ(2,3)                    SOURCE.189
                C-----CALCULATE PRODUCTION OF TURBULENT ENERGY.                    SOURCE.
```

```
151.  031731B   210 PT=(P(1,1)+P(2,2)+P(3,3))/2.                                  SOURCE.191
                C*****************************************************************  SOURCE.192
                C*****PRESSURE STRAIN AND DISSIPATION TERMS                        SOURCE.193
152.  031735B        DO 220 II=1,3                                                SOURCE.194
153.  031737B        DO 220 JJ=1,II                                               SOURCE.195
154.  031741B        PHI1(II,JJ)=-CS1*EDT*(UIUJ(II,JJ)-2.*DEL(II,JJ)*T/3.)        SOURCE.196
155.  031750B        PHI2(II,JJ)=F1*(P(II,JJ)-2.*DEL(II,JJ)*PT/3.)                SOURCE.197
                    1            +F2*T*(DUIDXJ(II,JJ)+DUIDXJ(JJ,II))             SOURCE.198
                    1            +F3*(D(II,JJ)-2.*DEL(II,JJ)*PT/3.)              SOURCE.199
156.  031770B        DIS(II,JJ)=-2.*DEL(II,JJ)*E/3.                               SOURCE.200
157.  031774B   220 CONTINUE                                                      SOURCE.201
                C                                                                 SOURCE.202
                C-----EXTRA TERMS FOR CYLINDRICAL POLAR COORDINATES.              SOURCE.203
158.  032000B        IF(INDCJS.EQ.1)GO TO 230                                     SOURCE.204
159.  032001B        PHI2(2,1)=PHI2(2,1)-F2*UPR*T                                 SOURCE.205
160.  032005B        PHI2(1,1)=PHI2(1,1)-F2*2.0*VPR*T                             SOURCE.206
161.  032007B   230 CONTINUE                                                      SOURCE.207
                C*****************************************************************  SOURCE.208
                C*****NEAR WALL EFFECT TERMS ON PRESSURE STRAIN                    SOURCE.209
162.  032010B        PHI2(2,3)=PHI2(3,2)                                          SOURCE.210
163.  032010B        FWL=ABS(UIUJ(2,3)*SQRT(ABS(UIUJ(2,3))))/(E+SMALL)/           SOURCE.211
                    1     (Y(NJ)*Y(NJ)-YV(J)*YV(J))*2.0*Y(NJ)/(FWM1+SMALL)       SOURCE.212
164.  032033B        DO 250 II=1,3                                                SOURCE.213
165.  032035B        DO 250 JJ=1,II                                               SOURCE.214
166.  032037B        IF(MRW.EQ.2) GO TO 240                                       SOURCE.215
                C-----LAUNDER-REECE-RODI MODEL                                    SOURCE.216
167.  032041B        PHIW1(II,JJ)=CR1W*EDT*(UIUJ(II,JJ)-2.*DEL(II,JJ)*T/3.)*FWL   SOURCE.217
168.  032053B        PHIW2(II,JJ)=CR2W*(P(II,JJ)-D(II,JJ))*FWL                    SOURCE.218
169.  032061B        GO TO 250                                                    SOURCE.219
                C-----GIBSON-LAUNDER MODEL                                        SOURCE.220
170.  032062B   240 PHIW1(II,JJ)=CR1W*EDT*(UIUJ(2,2)*DEL(II,JJ)                   SOURCE.221
                    1     -1.5*UIUJ(2,II)*DEL(2,JJ)-1.5*UIUJ(2,JJ)*DEL(2,II))*FWL SOURCE.222
171.  032100B        PHIW2(II,JJ)=CR2W*(PHI2(2,2)*DEL(II,JJ)-1.5*PHI2(2,II)*DEL(2,JJ)  SOURCE.223
                    1     -1.5*PHI2(2,JJ)*DEL(2,II))*FWL                         SOURCE.224
172.  032116B   250 CONTINUE                                                      SOURCE.225
                C*****************************************************************  SOURCE.226
                C*****ADDITIONAL SOURCES DUE TO DIFFUSION MODEL                    SOURCE.227
                C-----SOURCES FROM TENSOR INVARIANT DIFFUSION MODEL                SOURCE.228
173.  032123B        IF(IDIF.EQ.1) GO TO 260                                      SOURCE.229
174.  032125B        SDEX(1)=0.0                                                  SOURCE.230
175.  032125B        SDEX(4)=2.*CS/YV(J)*(Y(J)*TEN/EDN*VVN*DVVN-                  SOURCE.231
                    1     Y(J-1)*TES/EDS*VVS*DVVS)/(Y(J)-Y(J-1))                  SOURCE.232
176.  032144B        SDEX(5)=CS/YV(J)*(Y(J)*TEN/EDN*(VVN*DVWN+VWN*DVVN)-          SOURCE.233
                    1       Y(J-1)*TES/EDS*(VVS*DVWS+VWS*DVVS))/(Y(J)-Y(J-1))     SOURCE.234
177.  032166B        SDEX(6)=2.*CS/YV(J)*(Y(J)*TEN/EDN*VWN*DVWN-                  SOURCE.235
                    1     Y(J-1)*TES/EDS*VWS*DVWS)/(Y(J)-Y(J-1))                  SOURCE.236
                C-----EXTRA SOURCES DUE TO CYLNDRICAL POLAR COORDINATES            SOURCE.237
178.  032203B   260 IF(INDCJS.EQ.1) GO TO 270                                     SOURCE.238
179.  032205B        SEX(1)=CS/EDT*2./YV(J)/YV(J)*(UIUJ(2,2)-UIUJ(1,1))*UIUJ(1,1) SOURCE.239
180.  032213B        IF(J.EQ.3) SEX(1)=URFS*SEX(1)+(1.0-URFS)*SOLD(I)             SOURCE.240
181.  032223B        IF(J.EQ.3) SOLD(I)=SEX(1)                                    SOURCE.241
182.  032227B        SEX(4)=-SEX(1)                                               SOURCE.242
183.  032230B        SEX(5)=-CS/EDT*UIUJ(1,1)*UIUJ(2,3)/YV(J)/YV(J)               SOURCE.243
184.  032233B        IF(IDIF.EQ.1) GO TO 270                                      SOURCE.244
185.  032236B        SEX(1)=2.*SEX(1)                                             SOURCE.245
186.  032237B        SEX(4)=2.*SEX(4)                                             SOURCE.246
187.  032240B        SEX(5)=2.*SEX(5)                                             SOURCE.247
188.  032241B        SDEX(1)=SDEX(1)+2.*CS/YV(J)*(TEN*UUN/EDN*(VVN-UUN)-          SOURCE.248
```

```
                  1          TES*UUS/EDS*(VVS-UUS))/(Y(J)-Y(J-1))                SOURCE.249
                  1        +2.*CS/EDT/YV(J)*UIUJ(2,2)*(UUN-UUS)/(Y(J)-Y(J-1))    SOURCE.250
189.   032271B     SDEX(4)=SDEX(4)-2.*CS/EDT/YV(J)*UIUJ(2,2)*(UUN-UUS)/         SOURCE.251
                  1                                    (Y(J)-Y(J-1))            SOURCE.252
190.   032303B     SDEX(5)=SDEX(5)-CS/EDT/YV(J)*UIUJ(2,3)*(UUN-UUS)/            SOURCE.253
                  1                                    (Y(J)-Y(J-1))            SOURCE.254
191.   032315B   270 CONTINUE                                                   SOURCE.255
               C*********************************************************************SOURCE.256
               C*****ASSEMBLY OF SOURCE TERMS                                   SOURCE.257
192.   032316B       DO 280 II=1,3                                              SOURCE.258
193.   032317B       DO 280 JJ=1,II                                             SOURCE.259
194.   032321B       IRS=II+JJ                                                  SOURCE.260
195.   032321B       IF(JJ.EQ.1)IRS=IRS-1                                       SOURCE.261
196.   032326B       S1(IRS,IJ)=P(II,JJ)+PHI1(II,JJ)+PHI2(II,JJ)                SOURCE.262
                  1          +PHIW1(II,JJ)+PHIW2(II,JJ)+SEX(IRS)+SDEX(IRS)     SOURCE.263
197.   032341B       S2(IRS,IJ)=DIS(II,JJ)                                      SOURCE.264
198.   032346B   280 CONTINUE                                                   SOURCE.265
199.   032353B       GO TO 400                                                  SOURCE.266
               C*********************************************************************SOURCE.267
               C                    TWO-EQUATION MODEL OF TURBULENCE            SOURCE.268
               C*********************************************************************SOURCE.269
               C*********************************************************************SOURCE.270
               C*****TURBULENT KINETIC ENERGY EQUATION                          SOURCE.271
200.   032353B   300 CONTINUE                                                   SOURCE.272
201.   032354B       S1(1,IJ)=0.0                                               SOURCE.273
202.   032356B       S1(4,IJ)=0.0                                               SOURCE.274
203.   032360B       S1(6,IJ)=0.0                                               SOURCE.275
204.   032362B       S2(1,IJ)=0.0                                               SOURCE.276
205.   032364B       S2(4,IJ)=0.0                                               SOURCE.277
206.   032366B       S2(6,IJ)=0.0                                               SOURCE.278
207.   032370B       PT=0.                                                      SOURCE.279
208.   032370B       DO 310 II=1,3                                              SOURCE.280
209.   032372B       DO 310 JJ=1,3                                              SOURCE.281
210.   032374B   310 PT=PT+(DUIDXJ(II,JJ)+DUIDXJ(JJ,II))*DUIDXJ(II,JJ)          SOURCE.282
               C-----EXTRA TERMS FOR CYLINDRICAL GRID.                          SOURCE.283
211.   032406B       IF(INDCOS.EQ.1) GO TO 320                                  SOURCE.284
212.   032410B       TERM1=VP**2/R(J)**2                                        SOURCE.285
213.   032413B       TERM2=2.0*VP*DUIDXJ(1,1)/R(J)                              SOURCE.286
214.   032415B       TERM3=-UP*(DUIDXJ(1,2)+DUIDXJ(2,1))/R(J)                   SOURCE.287
215.   032420B       TERM4=UP**2/R(J)**2                                        SOURCE.288
216.   032421B       PT=PT+2.0*(TERM1+TERM2+TERM3)+TERM4                        SOURCE.289
               C                                                                SOURCE.290
217.   032427B   320 PT=CMU*T/(EDT+SMALL)*PT                                    SOURCE.291
               C-----NOTE.SOURCE TIMES TWO TO ALLOW FOR LATER DIVISION BY TWO.  SOURCE.292
218.   032434B       S1(1,IJ)=2.*PT                                             SOURCE.293
219.   032437B       S2(1,IJ)=-2.*E                                             SOURCE.294
               C*********************************************************************SOURCE.295
               C            SOURCES IN ISOTROPIC DISSIPATION RATE EQUATION      SOURCE.296
               C*********************************************************************SOURCE.297
220.   032442B   400 CONTINUE                                                   SOURCE.298
221.   032443B       S1(7,IJ)=CE1*EDT*PT                                        SOURCE.299
222.   032447B       S2(7,IJ)=-CE2*EDT*E                                        SOURCE.300
223.   032453B   500 IF(IHT.EQ.0) GO TO 700                                     SOURCE.301
               C*********************************************************************SOURCE.302
               C              SOURCES IN TURBULENT SCALAR FLUX EQUATION         SOURCE.303
               C*********************************************************************SOURCE.304
               C*****PRODUCTION TERMS                                           SOURCE.3[illegible]
224.   032455B       PCSQ=0.0                                                   SOURCE.3[illegible]
```

```
225.  0324558        DO 520 JJ=1,3                                          SOURCE.307
226.  0324578        PC(JJ)=0.0                                             SOURCE.308
227.  0324578        P1C(JJ)=0.0                                            SOURCE.309
228.  0324578        D1C(JJ)=0.0                                            SOURCE.310
229.  0324608        DO 520 KK=1,3                                          SOURCE.311
230.  0324638        PC(JJ)=PC(JJ)-UJC(KK)*DUIDXJ(JJ,KK)-UIUJ(JJ,KK)*DCDXJ(KK)  SOURCE.312
231.  0324718        D1C(JJ)=D1C(JJ)-UJC(KK)*DUIDXJ(KK,JJ)                  SOURCE.313
232.  0324758        P1C(JJ)=P1C(JJ)-UJC(KK)*DUIDXJ(JJ,KK)                  SOURCE.314
233.  0325008        IF (JJ-1) 520,510,520                                  SOURCE.315
234.  0325038    510 PCSQ=PCSQ-2.0*UJC(KK)*DCDXJ(KK)                        SOURCE.316
235.  0325078    520 CONTINUE                                               SOURCE.317
236.  0325148        PC(1)=-JJN*DCDXJ(1)                                    SOURCE.318
237.  0325168        IF(J.EQ.2) GO TO 530                                   SOURCE.319
238.  0325208        IF(INDCDS.EQ.1) GO TO 530                              SOURCE.320
                 C-----EXTRA TERMS FOR CYLINDRICAL GRID                     SOURCE.321
239.  0325228        UPR=UP/YV(J)                                           SOURCE.322
240.  0325248        VPR=VP/YV(J)                                           SOURCE.323
241.  0325268        STORE=-UPR*UJC(1)                                      SOURCE.324
242.  0325308        P1C(1)=P1C(1)+STORE                                    SOURCE.325
243.  0325328        PC(1)=PC(1)+STORE                                      SOURCE.326
244.  0325338        STORE=VPR*UJC(1)                                       SOURCE.327
245.  0325358        P1C(2)=P1C(2)+STORE                                    SOURCE.328
246.  0325378        PC(2)=PC(2)+STORE                                      SOURCE.329
247.  0325408        D1C(2)=D1C(2)-UPR*UJC(2)+VPR*UJC(1)                    SOURCE.330
248.  0325458    530 CONTINUE                                               SOURCE.331
                 C*********************************************************** SOURCE.332
                 C*****PRESSURE-SCALAR CORRELATION                          SOURCE.333
249.  0325468        DO 540 JJ=1,3                                          SOURCE.334
250.  0325478        PSI1(JJ)=-CC1*EDT*UJC(JJ)                              SOURCE.335
251.  0325518        PSI2(JJ)= G1*P1C(JJ)                                   SOURCE.336
                    1          +G2*D1C(JJ)                                  SOURCE.337
252.  0325558    540 CONTINUE                                               SOURCE.338
253.  0325578        DISCSQ=-CG2*EDT*CSQ                                    SOURCE.339
254.  0325618        PSI1(1)=-CC1*EDN/TEN*UJC(1)                            SOURCE.340
                 C*********************************************************** SOURCE.341
                 C*****NEAR WALL EFFECTS ON PRESSURE-SCALAR CORRELATION     SOURCE.342
255.  0325658        DO 560 JJ=1,3                                          SOURCE.343
256.  0325678        IF(MCW.EQ.2) GO TO 550                                 SOURCE.344
257.  0325718        PSIW1(JJ)=-CC1W*EDT*UJC(JJ)*FWL                        SOURCE.345
258.  0325768        PSIW2(JJ)=-CC2W*(D1C(JJ)*DEL(JJ,2)-4.0*P1C(JJ)*DEL(JJ,3))*FWL  SOURCE.346
259.  0326058        GO TO 560                                              SOURCE.347
260.  0326068    550 PSIW1(JJ)=-CC1W*EDT*UJC(JJ)*DEL(JJ,2)*FWL              SOURCE.348
261.  0326148        PSIW2(JJ)=CC2W*PSI2(JJ)*DEL(JJ,2)*FWL                  SOURCE.349
262.  0326168    560 CONTINUE                                               SOURCE.350
                 C*********************************************************** SOURCE.351
                 C*****ADDITIONAL SOURCES FROM DIFFUSION MODEL              SOURCE.352
263.  0326228        IF(J.EQ.2) GO TO 580                                   SOURCE.353
264.  0326248        IF(IDIF.EQ.1) GO TO 570                                SOURCE.354
                 C-----SOURCES FROM TENSOR INVARIANT DIFFUSION MODEL        SOURCE.355
265.  0326268        SDEX(11)=CC/YV(J)*(Y(J)*TEN/EDN*VVN*DVCN-Y(J-1)*TES/EDS*VVS*DVCS)/ SOURCE.356
                    1   (Y(J)-Y(J-1))                                      SOURCE.357
266.  0326448        SDEX(12)=CC/YV(J)*(Y(J)*TEN/EDN*VWN*DVCN-Y(J-1)*TES/EDS*VWS*DVCS)/ SOURCE.358
                    1          (Y(J)-Y(J-1))                               SOURCE.359
267.  0326608        IF(IHT.NE.2) GO TO 570                                 SOURCE.360
268.  0326638        SDEX(10)=CC/Y(J)*(UU1/EDTP1*DVCWN-UIUJ(1,1)/EDT*DVCWS)/ SOURCE.361
                    1        (YV(J+1)-YV(J))                               SOURCE.362
                    1                  +CC/Y(J)/Y(J)*TEN/EDN*UUN*(DUCE-DUCW)/ SOURCE.363
                    1         (X(I)-X(I-1))                                SOURCE.364
```

```
 269.  0327118        SDEX(11)=SDEX(11)+CC/YV(J)/EDT*UIUJ(2,2)*(DUCSE-DUCSW)/
                     1      (XU(I+1)-XU(I))
 270.  0327238        SDEX(12)=SDEX(12)+CC/YV(J)/EDT*UIUJ(2,3)*(DUCSE-DUCSW)/
                     1                  (XU(I+1)-XU(I))
                C-----EXTRA SOURCES DUE TO CYLINDRICAL POLAR COORDINATES
 271.  0327358    570 IF(INDCDS.EQ.1) GO TO 580
 272.  0327378        SEX(11)=-CC/EDT*UIUJ(1,1)*UJC(2)/YV(J)/YV(J)
 273.  0327458        IF(IHT.NE.2) GO TO 575
 274.  0327478        SDEX(10)=SDEX(10)+CC/Y(J)*TEN/EDN*UUN/Y(J)*(VCN-VCN1)/
                     1      (X(I)-X(I-1))
                     1                 +CC/Y(J)*TEN/EDN*VVN*(UCN-UCS)/
                     1      (YV(J+1)-YV(J))
 275.  0327758        SDEX(11)=SDEX(11)-CC/EDT*UIUJ(1,1)/YV(J)/YV(J)*(UCE-UCW)/
                     1      (XU(I+1)-XU(I))
                     1                 -CC/EDT*UIUJ(1,1)/YV(J)/YV(J)*(UCE-UCW)/
                     1       (XU(I+1)-XU(I))
 276.  0330158    575 IF(IDIF.EQ.1) GO TO 580
 277.  0330178        SEX(11)=2.0*SEX(11)
 278.  0330208        IF(IHT.NE.2) GO TO 580
 279.  0330238        SDEX(10)=SDEX(10)-CC/Y(J)*(UU1/EDTP1*UCN-UIUJ(1,1)/EDT*UCS)/
                     1       (YV(J+1)-YV(J))
                     1                 +CC/Y(J)*TEN/EDN*UUN/Y(J)*(VCN-VCN1)/
                     1      (X(I)-X(I-1))
                     1                 +CC/Y(J)/Y(J)*TEN/EDN*UUN*((VCN-VCN1)/
                     1      (X(I)-X(I-1))-UJC(1))
 280.  0330608        SDEX(11)=SDEX(11)-CC/EDT*UIUJ(1,1)/YV(J)/YV(J)*(UCE-UCW)/
                     1      (XU(I+1)-XU(I))
 281.  0330738    580 CONTINUE
                C*********************************************************************
                C*****ASSEMBLY OF SOURCE TERMS
 282.  0330748        DO 590 JJ=1,3
 283.  0330758        IHF=9+JJ
 284.  0330768        S1(IHF,IJ)=PC(JJ)+PSI1(JJ)+PSI2(JJ)+PSIW1(JJ)+PSIW2(JJ)
                     1          +SEX(IHF)+SDEX(IHF)
 285.  0331078    590 S2(IHF,JJ)=0.0
                C*********************************************************************
                C                  SOURCES IN SCALAR FLUCTUATION EQUATION
                C*********************************************************************
 286.  0331138        S1(13,IJ)=PCSQ+DISCSQ
 287.  0331178        S2(13,IJ)=0.0
                C*********************************************************************
                C                              OPTIONAL OUTPUT
                C*********************************************************************
 288.  0331228    700 CONTINUE
                C-----SOURCE BALANCE OF STRESS TENSOR COMPONENTS.
 289.  0331228        IF(IJ.EQ.0) GO TO 750
 290.  0331238        IF(ITESU.EQ.0) GO TO 750
 291.  0331248        IF(MOD(ISTEP,NUMPRI).NE.0) GO TO 750
 292.  0331278        WRITE(6,720) I,J,P(1,1),DIS(1,1),P(2,2),DIS(2,2),P(3,3),DIS(3,3)
                     1            ,P(3,2),DIS(3,2),P(3,1),DIS(3,1)
 293.  0331478        WRITE(6,730) PHI1(1,1),PHI1(2,2),PHI1(3,3),PHI1(3,2),PHI1(3,1)
 294.  0331578        WRITE(6,730) PHI2(1,1),PHI2(2,2),PHI2(3,3),PHI2(3,2),PHI2(3,1)
 295.  0331678        WRITE(6,730) PHIW1(1,1),PHIW1(2,2),PHIW1(3,3),PHIW1(3,2)
                     1            ,PHIW1(3,1)
 296.  0331778        WRITE(6,730) PHIW2(1,1),PHIW2(2,2),PHIW2(3,3),PHIW2(3,2)
                     1            ,PHIW2(3,1)
 297.  0332078        WRITE(6,730) SEX(1),SE    ,SEX(6),SEX(5),SEX(3)
 298.  0332178        WRITE(6,730) SDEX(1),SD    4),SDEX(6),SDEX(5),SDEX(3)
```

```
299.  0332278        WRITE(6,740) S1(1,IJ),S2(1,IJ),S1(4,IJ),S2(4,IJ),S1(6,IJ)          SOURCE.423
                    1            ,S2(6,IJ),S1(5,IJ),S2(5,IJ),S1(3,IJ),S2(3,IJ)         SOURCE.424
                    1            ,S1(7,IJ),S2(7,IJ)                                    SOURCE.425
300.  0333128    720 FORMAT(/2X,2I3,5(1P2E9.2,2X))                                     SOURCE.426
301.  0333128    730 FORMAT(8X,5(1PE9.2,11X))                                          SOURCE.427
302.  0333128    740 FORMAT(1X,7HSOURCE=,6(1P2E9.2,2X)/)                               SOURCE.428
303.  0333128    750 CONTINUE                                                          SOURCE.429
                C                                                                      SOURCE.430
                C                                                                      SOURCE.431
                C-----SOURCE BALANCE OF SCALAR FLUX TENSOR COMPONENTS.                 SOURCE.432
304.  0333128        IF(IHT.EQ.0) GO TO 800                                            SOURCE.433
305.  0333138        IF(ITESC.EQ.0) GO TO 800                                          SOURCE.434
306.  0333148        IF(MOD(ISTEP,NUMPRI).NE.0) GO TO 800                              SOURCE.435
307.  0333178        WRITE(6,760) I,J,PC(1),PC(2),PC(3),PCSQ                           SOURCE.436
308.  0333318        WRITE(6,770) PSI1(1),PSI1(2),PSI1(3),DISCSQ                       SOURCE.437
309.  0333408        WRITE(6,780) PSI2(1),PSI2(2),PSI2(3)                              SOURCE.438
310.  0333468        WRITE(6,780) PSIW1(1),PSIW1(2),PSIW1(3)                           SOURCE.439
311.  0333548        WRITE(6,780) PSIW2(1),PSIW2(2),PSIW2(3)                           SOURCE.440
312.  0333628        WRITE(6,780) SEX(10),SEX(11),SEX(12)                              SOURCE.441
313.  0333708        WRITE(6,780) SDEX(10),SDEX(11),SDEX(12)                           SOURCE.442
314.  0333768        WRITE(6,790) S1(10,IJ),S1(11,IJ),S1(12,IJ),S1(13,IJ)              SOURCE.443
315.  0334218    760 FORMAT(/2X,2I3,1P4E13.2)                                          SOURCE.444
316.  0334218    770 FORMAT(8X,1P4E13.2)                                               SOURCE.445
317.  0334218    780 FORMAT(8X,1P3E13.2)                                               SOURCE.446
318.  0334218    790 FORMAT(1X,7HSOURCE=,1P4E13.2)                                     SOURCE.447
319.  0334218    800 CONTINUE                                                          SOURCE.448
                C                                                                      SOURCE.449
320.  0334218   1000 CONTINUE                                                          SOURCE.450
321.  0334268        RETURN                                                            SOURCE.451
                C                                                                      SOURCE.452
                C**********************************************************************SOURCE.453
                C                          SOURCE TERMS PICK-UP LEVEL                  SOURCE.454
                C**********************************************************************SOURCE.455
322.  0334308        ENTRY SORCE                                                       SOURCE.456
323.  0334368        IF(IRS.EQ.8) GO TO 1120                                           SOURCE.457
324.  0334378        DO 1110 I=IM1,IM2                                                 SOURCE.458
325.  0334428        DO 1110 J=2,NJM1                                                  SOURCE.459
326.  0334458        IJ=I+IT*(J-1)                                                     SOURCE.460
327.  0334478        SUS(IJ)=S1(IRS,IJ)                                                SOURCE.461
328.  0334538   1110 SPS(IJ)=S2(IRS,IJ)/(PHI(IJ)+SMALL)                                SOURCE.462
329.  0334648        RETURN                                                            SOURCE.463
                C                                                                      SOURCE.464
                C-----SOURCES FOR KINETIC ENERGY.                                      SOURCE.465
330.  0334668   1120 CONTINUE                                                          SOURCE.466
331.  0334668        DO 1130 I=IM1,IM2                                                 SOURCE.467
332.  0334708        DO 1130 J=2,NJM1                                                  SOURCE.468
333.  0334738        IJ=I+IT*(J-1)                                                     SOURCE.469
334.  0334758        SUS(IJ)=(S1(1,IJ)+S1(4,IJ)+S1(6,IJ))/2.                           SOURCE.470
335.  0335038   1130 SPS(IJ)=(S2(1,IJ)+S2(4,IJ)+S2(6,IJ))/2./(PHI(IJ)+SMALL)           SOURCE.471
336.  0335178        RETURN                                                            SOURCE.472
                C                                                                      SOURCE.473
337.  0335218        END                                                               SOURCE.474
```

0 0 0 0 1 4 9 0 - 357 1 8 7

```
 1.  0000008        SUBROUTINE INIT                                                    INIT.2
                 C*********************************************************************COMALL.2
                 C                              COMMON BLOCKS                          COMALL.3
                 C*********************************************************************COMALL.4
 2.  0000008        DIMENSION SAVE(20229)                                              DIM3.1
 3.  0000008        DIMENSION TRANS(512)                                               DIM3.2
 4.  0000008        COMMON                                                             COMALL.6
                   1X(15),Y(30),Z(02),XU(15),YV(30),ZW(02),                            DIM3.3
                   1DXEP(15),DXPW(15),DYNP(30),DYPS(30),SEW(15),SNS(30),               DIM3.4
                   1DXEPU(15),DXPWU(15),SEWU(15),DYNPV(30),DYPSV(30),SNSV(30),         DIM3.5
                   1R(30),RV(30),RCV(30),WFN(30),WFS(30),WFE(15),WFW(15),              DIM3.6
                   1U(15,30,2),V(15,30,2),W(15,30,2),PE(15,30,2),C(15,30,2),PP(15,30), DIM3.7
                   1UU(15,30),UV(15,30),UW(15,30),VV(15,30),VW(15,30),WW(15,30),       DIM3.8
                   1ED(15,30),TE(15,30),FF(15,30),UC(15,30),VC(15,30),WC(15,30),       DIM3.9
                   1C2(15,30),EC(15,30),RS(15,30),                                     DIM3.10
                   1DEN(15,30,2),VIS(15,30,2),GAM(15,30,2),VISUU(15,30),VISVV(15,30),  DIM3.11
                   1AW(15,30),AE(15,30),AN(15,30),AS(15,30),AD(15,30),AU(15,30),       DIM3.12
                   1AP(15,30),SU(15,30),SP(15,30),                                     DIM3.13
                   1JT(15),CF(15),QUE(15),DCDZB(15),QUO(15),                           DIM3.14
                   1DENSIT,VISCOS,PRANDT,SPHEAT,EXCHAT,                                COMALL.19
                   1CMU,CR1,CR2,CRS,CR1W,CR2W,CEPS1,CEPS2,CEPS,CAPPA,ELOG,             COMALL.20
                   1CC1,CC2,CC,CC1W,CC2W,CG2,CG,CAPPAC,ELOGC,                          COMALL.21
                   1JUU,JUV,JUW,JVV,JVW,JWW,JED,JTE,JFF,JUC,JVC,JWC,JC2,JEC,           COMALL.22
                   1NI,NIM1,NIM2,NJ,NJM1,NJM2,NK,NKM1,IT,JT,KT,IJT,                    COMALL.23
                   1HEDU(4),HEDV(4),HEDW(4),HEDP(4),HEDC(4),HEDR(4),HEDD(4),HEDVIS(4), COMALL.24
                   1INCALJ,INCALV,INCALW,INCALP,INCALC,INPRO,INCALR(14),INTURB,INDIFF, COMALL.25
                   1NSWPU,NSWPV,NSWPW,NSWPP,NSWPC,NSWPR,                               COMALL.26
                   1MODEL,MODEC,MRW,MCW,IJUE,IDIF,IJET,ITEST,ITESU,ITESC,ICON,         COMALL.27
                   1IRUN,IU,IHT,IU1,IU2,IC1,IC2,I1,I2,INDCOS,FRA,                      COMALL.28
                   1K,DZ,ISTEP,ISTP1,NRS,INDEX,DPDZ,                                   COMALL.29
                   1FLOWIN,VMEAN,QLENTH,SMALL,GREAT,XTOT,YTOT,RSWALL(14),              COMALL.30
                   1ZDPRO(18),IPRO,IEND,INDPRI,NUMPRI,BVE,BVW,BVS,BWS                  COMALL.31
 5.  0000008        COMMON                                                             DIM3.15
                   1ET(15),ETU(15),DET(15),DETU(15),DYW,NJP,NJP1,NJPM1,IWALL,          DIM3.16
                   1ROUTER,RINNER,ECCEN,ES,NJO,YTOTO,EXCHAW,NJCM1                      DIM3.17
 6.  0000008        COMMON  OLDU(30),OLDV(30),OLDW(30),OLDP(30),                       DIM3.18
                   1        OLDUU(30),OLDUV(30),OLDUW(30),OLDVV(30),OLDVW(30),         DIM3.19
                   1        OLDWW(30),OLDTE(30),OLDED(30),OLDFF(30),                   DIM3.20
                   1        OLDDEN(30),OLDVIS(30),OVISUU(30),OVISVV(30),               DIM3.21
                   1        OLDUTA,DDPDZ                                               DIM3.22
 7.  0000008        LOGICAL INCALU,INCALV,INCALW,INCALP,INCALC,INPRO,                  COMALL.32
                   1        INCALR,INTURB,INDIFF                                       COMALL.33
 8.  0000008        EQUIVALENCE (X(1),SAVE(1))                                         COMALL.34
 9.  0000008        EQUIVALENCE (OLDU(1),TRANS(1))                                     DIM3.23
10.  0000008        REAL MAXC,MINC                                                     INIT.4
                 C*********************************************************************INIT.5
                 C                          GEOMETRICAL VARIABLES                      INIT.6
                 C*********************************************************************INIT.7
11.  0000008        ENTRY INITG                                                        INIT.8
                 C*********************************************************************INIT.9
                 C*****CALCULATION OF LOCATION AND DISTANCES FOR P-CELLS                INIT.10
12.  0000108        DXPW(1)=0.0                                                        INIT.11
13.  0000108        DXEP(NI)=0.0                                                       INIT.12
14.  0000108        DO 100 I=1,NIM1                                                    INIT.13
15.  0000148        DXEP(I)=X(I+1)-X(I)                                                INIT.14
16.  0000158    100 DXPW(I+1)=DXEP(I)                                                  INIT.15
17.  0000178        DYPS(1)=0.0                                                        INIT.16
```

```
 18.  0000178        DYNP(NJ)=0.0                                          INIT.17
 19.  0000208        DO 110 J=1,NJM1                                       INIT.18
 20.  0000238        DYNP(J)=Y(J+1)-Y(J)                                   INIT.19
 21.  0000248    110 DYPS(J+1)=DYNP(J)                                     INIT.20
                C-----P-CELL DIMENSIONS                                    INIT.21
 22.  0000268        SEW(1)=0.0                                            INIT.22
 23.  0000268        SEW(2)=DXPW(2)+0.5*DXEP(2)                            INIT.23
 24.  0000328        SEW(NIM1)=0.5*DXPW(NIM1)+DXEP(NIM1)                   INIT.24
 25.  0000358        SEW(NI)=0.0                                           INIT.25
 26.  0000368        NIM2=NIM1-1                                           INIT.26
 27.  0000408        DO 200 I=3,NIM2                                       INIT.27
 28.  0000428    200 SEW(I)=0.5*(DXEP(I)+DXPW(I))                          INIT.28
 29.  0000468        SNS(1)=0.0                                            INIT.29
 30.  0000468        SNS(2)=DYPS(2)+0.5*DYNP(2)                            INIT.30
 31.  0000518        SNS(NJM1)=DYNP(NJM1)+0.5*DYPS(NJM1)                   INIT.31
 32.  0000558        SNS(NJ)=0.0                                           INIT.32
 33.  0000568        NJM2=NJM1-1                                           INIT.33
 34.  0000578        DO 210 J=3,NJM2                                       INIT.34
 35.  0000628    210 SNS(J)=0.5*(DYNP(J)+DYPS(J))                          INIT.35
                C*********************************************************INIT.36
                C*****CALCULATION OF LOCATION AND DISTANCES FOR U-CELLS    INIT.37
 36.  0000668        XU(1)=X(1)                                            INIT.38
 37.  0000678        XU(2)=X(1)                                            INIT.39
 38.  0000708        XU(NI)=X(NI)                                          INIT.40
 39.  0000718        DO 300 I=3,NIM1                                       INIT.41
 40.  0000748    300 XU(I)=0.5*(X(I)+X(I-1))                               INIT.42
 41.  0001008        DXPWU(1)=0.0                                          INIT.43
 42.  0001008        DXPWU(2)=0.0                                          INIT.44
 43.  0001018        DXEPU(1)=0.0                                          INIT.45
 44.  0001028        DXEPU(NI)=0.0                                         INIT.46
 45.  0001028        DO 310 I=1,NIM1                                       INIT.47
 46.  0001048        DXEPU(I)=XU(I+1)-XU(I)                                INIT.48
 47.  0001058    310 DXPWU(I+1)=DXEPU(I)                                   INIT.49
                C-----U-CELL DIMENSIONS                                    INIT.50
 48.  0001078        SEWU(1)=0.0                                           INIT.51
 49.  0001078        DO 320 I=2,NI                                         INIT.52
 50.  0001128    320 SEWU(I)=X(I)-X(I-1)                                   INIT.53
                C-----WEIGHTING FACTORS IN X-DIRECTION                     INIT.54
 51.  0001158        DO 330 I=3,NIM1                                       INIT.55
 52.  0001208        WFW(I)=SEWU(I-1)/(SEWU(I-1)+SEWU(I))                  INIT.56
 53.  0001218        WFE(I)=SEWU(I+1)/(SEWU(I+1)+SEWU(I))                  INIT.57
 54.  0001238    330 CONTINUE                                              INIT.58
 55.  0001258        WFE(2)=SEWU(3)/(SEWU(3)+2.0*SEWU(2))                  INIT.59
 56.  0001278        WFW(3)=SEWU(2)/(SEWU(2)+0.5*SEWU(3))                  INIT.60
 57.  0001318        WFE(NIM1)=SEWU(NI)/(SEWU(NI)+0.5*SEWU(NIM1))          INIT.61
                C*********************************************************INIT.62
                C*****CALCULATION OF LOCATION AND DISTANCES FOR V-CELLS    INIT.63
 58.  0001348        YV(1)=Y(1)-SMALL                                      INIT.64
 59.  0001378        YV(2)=Y(1)                                            INIT.65
 60.  0001378        YV(NJ)=Y(NJ)                                          INIT.66
 61.  0001418        DO 400 J=3,NJM1                                       INIT.67
 62.  0001448    400 YV(J)=0.5*(Y(J)+Y(J-1))                               INIT.68
 63.  0001508        DYPSV(1)=0.0                                          INIT.69
 64.  0001508        DYPSV(2)=0.0                                          INIT.70
 65.  0001518        DYNPV(1)=0.0                                          INIT.71
 66.  0001528        DYNPV(NJ)=0.0                                         INIT.72
 67.  0001528        DO 410 J=1,NJM1                                       INIT.73
 68.  0001548        DYNPV(J)=YV(J+1)-YV(J)                                INIT.74
```

```
 69.  000155B    410 DYPSV(J+1)=DYNPV(J)                                          INIT.75
                C-----V-CELL DIMENSIONS                                           INIT.76
 70.  000157B        SNSV(1)=0.0                                                  INIT.77
 71.  000157B        DO 420 J=2,NJ                                                INIT.78
 72.  000162B    420 SNSV(J)=Y(J)-Y(J-1)                                          INIT.79
                C-----WEIGHTING FACTORS IN Y-DIRECTION                            INIT.80
 73.  000165B        DO 430 J=3,NJM1                                              INIT.81
 74.  000170B        WFS(J)=SNSV(J-1)/(SNSV(J-1)+SNSV(J))                         INIT.82
 75.  000171B        WFN(J)=SNSV(J+1)/(SNSV(J+1)+SNSV(J))                         INIT.83
 76.  000173B    430 CONTINUE                                                     INIT.84
 77.  000175B        WFN(1)=0.0                                                   INIT.85
 78.  000175B        WFN(2)=SNSV(3)/(SNSV(3)+2.0*SNSV(2))                         INIT.86
 79.  000200B        WFS(3)=SNSV(2)/(SNSV(2)+0.5*SNSV(3))                         INIT.87
 80.  000202B        WFN(NJM1)=SNSV(NJ)/(SNSV(NJ)+0.5*SNSV(NJM1))                 INIT.88
                C*****************************************************************INIT.89
                C*****EXTRA WEIGHTING FACTORS FOR APPROXIMATING BOUNDARY VALUES.  INIT.90
 81.  000205B        STORE=(DXEP(1)+DXEP(2))**2                                   INIT.91
 82.  000210B        BVW=STORE/(STORE-DXEP(1)**2)                                 INIT.92
 83.  000212B        STORE=(DXPW(NI)+DXPW(NIM1))**2                               INIT.93
 84.  000215B        BVE=STORE/(STORE-DXPW(NI)**2)                                INIT.94
 85.  000217B        STORE=(SNS(2)+SNS(3))**2                                     INIT.95
 86.  000221B        BVS=STORE/(STORE-SNS(2)**2)                                  INIT.96
 87.  000223B        STORE=(SNSV(3)+SNSV(2))**2                                   INIT.97
 88.  000224B        BWS=STORE/(STORE-SNSV(2)**2)                                 INIT.98
                C*****************************************************************INIT.99
                C*****EXTRA VARIABLES DEFINED FOR CYLINDRICAL COORDINATES          INIT.100
 89.  000226B        DO 600 J=1,NJ                                                INIT.101
 90.  000231B        R(J)=Y(J)                                                    INIT.102
 91.  000231B    600 IF(INDCOS.EQ.1)  R(J)=1.0                                    INIT.103
 92.  000237B        RV(1)=R(1)                                                   INIT.104
 93.  000237B        RV(2)=R(1)                                                   INIT.105
 94.  000240B        RV(NJ)=R(NJ)                                                 INIT.106
 95.  000242B        DO 610 J=3,NJM1                                              INIT.107
 96.  000245B    610 RV(J)=0.5*(R(J)+R(J-1))                                      INIT.108
 97.  000251B        RCV(1)=R(1)                                                  INIT.109
 98.  000252B        RCV(NJ)=R(NJ)                                                INIT.110
 99.  000254B        DO 620 J=2,NJM1                                              INIT.111
100.  000256B    620 RCV(J)=0.5*(RV(J+1)+RV(J))                                   INIT.112
                C-----THICKNESS OF THE TUBE AS A FUNCTION OF THE ANGLE X          DIM3.76
101.  000262B        JNC=NJ0-NJ-1                                                 DIM3.77
102.  000264B        NJ0M1=NJ0-1                                                  DIM3.78
103.  000265B        NJP=NJ                                                       DIM3.79
104.  000265B        NJP1=NJ+1                                                    DIM3.80
105.  000266B        NJPM1=NJ-1                                                   DIM3.81
106.  000267B        DO 665 I=1,NI                                                DIM3.82
107.  000272B        ET(I)=SQRT(ROUTER*ROUTER-ECCEN*ECCEN*SIN(X(I))*SIN(X(I)))    DIM3.83
                    1       -RINNER-ECCEN*COS(X(I))                               DIM3.84
108.  000311B        ETU(I)=SQRT(ROUTER*ROUTER-ECCEN*ECCEN*SIN(XU(I))*SIN(XU(I)))DIM3.85
                    1       -RINNER-ECCEN*COS(XU(I))                              DIM3.86
109.  000331B        DET(I)=ET(I)/FLOAT(JNC)                                      DIM3.87
110.  000335B        DETU(I)=ETU(I)/FLOAT(JNC)                                    DIM3.88
111.  000337B        WRITE(6,670) I,ET(I),ETU(I),DET(I),DETU(I)                   DIM3.89
112.  000354B    665 CONTINUE                                                     DIM3.90
113.  000356B    670 FORMAT(/10X,I3,1P4E13.3)                                     DIM3.91
114.  000356B        RETURN                                                       INIT.113
                C*****************************************************************INIT.114
                C              INITIALISATION    DEPENDENT VARIABLE FIELDS        INIT.115
                C*************************      ***************************************INIT.116
```

```
115.  0003608        ENTRY INITO                                          INIT.117
116.  0003668        IF(IRUN.NE.1) GO TO 720                              INIT.118
117.  0003678        IF(ISTEP.GT.0) GO TO 720                             INIT.119
                C-----SET VARIABLES TO ZERO                               INIT.120
118.  0003718        EXCHAT=VISCOS*SPHEAT/PRANDT                          INIT.121
119.  0003738        DO 700 K=1,2                                         INIT.122
120.  0003768        DO 700 J=1,JT                                        DIM3.92
121.  0004018        DO 700 I=1,NI                                        INIT.124
122.  0004048        U(I,J,K)=0.0                                         INIT.125
123.  0004078        V(I,J,K)=0.0                                         INIT.126
124.  0004108        W(I,J,K)=0.0                                         INIT.127
125.  0004118        PE(I,J,K)=0.0                                        INIT.128
126.  0004118        UU(I,J)=0.                                           INIT.129
127.  0004138        UV(I,J)=0.                                           INIT.130
128.  0004148        UW(I,J)=0.                                           INIT.131
129.  0004158        VV(I,J)=0.                                           INIT.132
130.  0004158        VW(I,J)=0.                                           INIT.133
131.  0004168        WW(I,J)=0.                                           INIT.134
132.  0004168        ED(I,J)=0.                                           INIT.135
133.  0004178        TE(I,J)=0.                                           INIT.136
134.  0004178        FF(I,J)=0.                                           INIT.137
135.  0004208        C(I,J,K)=0.0                                         INIT.138
136.  0004208        UC(I,J)=0.0                                          INIT.139
137.  0004218        VC(I,J)=0.0                                          INIT.140
138.  0004218        WC(I,J)=0.0                                          INIT.141
139.  0004228        C2(I,J)=0.0                                          INIT.142
140.  0004228        EC(I,J)=0.0                                          INIT.143
141.  0004238        VISUU(I,J)=0.                                        INIT.144
142.  0004238        VISVV(I,J)=0.0                                       INIT.145
143.  0004248        DEN(I,J,K)=DENSIT                                    INIT.146
144.  0004258        VIS(I,J,K)=VISCOS                                    INIT.147
145.  0004268        GAM(I,J,K)=EXCHAT                                    INIT.148
146.  0004308        IF(J.GT.NJ) GAM(I,J,K)=EXCHAW                        DIM3.93
147.  0004378    700 CONTINUE                                             INIT.149
148.  0004468        DO 710 J=1,NJO                                       DIM3.94
149.  0004508        DO 710 I=1,NI                                        INIT.151
150.  0004538        PP(I,J)=0.0                                          INIT.152
151.  0004558        AE(I,J)=0.0                                          INIT.153
152.  0004558        AW(I,J)=0.0                                          INIT.154
153.  0004568        AN(I,J)=0.0                                          INIT.155
154.  0004568        AS(I,J)=0.0                                          INIT.156
155.  0004578        AU(I,J)=0.0                                          INIT.157
156.  0004578        AP(I,J)=0.0                                          INIT.158
157.  0004608        AD(I,J)=0.0                                          INIT.159
158.  0004608        SU(I,J)=0.0                                          INIT.160
159.  0004618        SP(I,J)=0.0                                          INIT.161
160.  0004618    710 CONTINUE                                             INIT.162
161.  0004658    720 CONTINUE                                             INIT.163
162.  0004668        DO 730 I=1,NI                                        INIT.164
163.  0004708        DCDZB(I)=0.0                                         INIT.165
164.  0004708    730 CONTINUE                                             INIT.166
                C                                                         INIT.167
                C******************************************************* INIT.168
                C*****CALL INITIALISING SECTION OF SOURCE SUBROUTINE      INIT.169
165.  0004738        CALL SORCEI(RS,NRS,SU,SP,IJT,I1,I2)                  INIT.170
166.  0004758        RETURN                                               INIT.171
                C******************************************************* INIT.172
                C                                FORWARD STEP             INIT.173
```

```
C*********************************************************************
      ENTRY STEP
      IF(ISTEP.EQ.1) GO TO 900
      Z(1)=Z(2)
C*********************************************************************
C*****SYMMETRY OF HYDRODYNAMIC FIELD
      IF(IU.EQ.0.AND.IHT.EQ.2) GO TO 900
      DO 800 I=1,NI
      DO 800 J=1,NJ
      II=3
      IF(IU.EQ.2) II=I
      U(I,J,1)=U(II,J,2)
      U(I,J,2)=U(II,J,2)
      V(I,J,1)=V(II,J,2)
      V(I,J,2)=V(II,J,2)
      W(I,J,2)=W(II,J,2)
      PE(I,J,1)=PE(II,J,2)
      PE(I,J,2)=PE(II,J,2)
      PP(I,J)=PP(II,J)
      VW(I,J)=VW(II,J)
      UW(I,J)=UW(II,J)
      UV(I,J)=UV(II,J)
      FF(I,J)=FF(II,J)
      UU(I,J)=AMAX1(SMALL,UU(II,J))
      VV(I,J)=AMAX1(SMALL,VV(II,J))
      WW(I,J)=AMAX1(SMALL,WW(II,J))
      ED(I,J)=AMAX1(SMALL,ED(II,J))
      TE(I,J)=AMAX1(SMALL,TE(II,J))
      DEN(I,J,1)=DEN(II,J,2)
      DEN(I,J,2)=DEN(II,J,2)
      VIS(I,J,1)=VIS(II,J,2)
      VIS(I,J,2)=VIS(II,J,2)
      VISUU(I,J)=AMAX1(SMALL,VISUU(II,J))
      VISVV(I,J)=AMAX1(SMALL,VISVV(II,J))
      IF(IHT.NE.1) GO TO 800
      C(I,J,2)=C(II,J,2)
      VC(I,J)=VC(II,J)
      WC(I,J)=WC(II,J)
      UC(I,J)=UC(II,J)
      C2(I,J)=AMAX1(SMALL,C2(II,J))
      EC(I,J)=AMAX1(SMALL,EC(II,J))
  800 CONTINUE
  900 CONTINUE
C*********************************************************************
C*****FORWARD STEP SIZE
      DZ=FRA*YTOT
      Z(2)=Z(1)+DZ
      IF(IHT.EQ.0) RETURN
      MAXC=0.0
      MINC=GREAT
      DO 910 I=IC1,IC2
      DO 910 J=2,NJ
      MAXC=AMAX1(C(I,J,2),MAXC)
  910 MINC=AMIN1(C(I,J,2),MINC)
      DZ=FRA*0.05*YTOT
      Z(2)=Z(1)+DZ
      IF(Z(2).LT.QLENTH) GO     920
      IF(Z(1).GE.QLENTH) GO     920
```

```
220.  0010378        Z(2)=QLENTH                                INIT.232
221.  0010408        DZ=Z(2)-Z(1)                               INIT.233
222.  0010428    920 CONTINUE                                   INIT.234
223.  0010438        IF(Z(1).EQ.QLENTH) CALL OUTPUT             INIT.235
224.  0010478        DO 930 I=1,NI                              INIT.236
225.  0010518        IF(Z(1).GE.QLENTH) CT(I)=0.0               INIT.237
226.  0010558    930 IF(Z(1).GE.QLENTH) QUE(I)=0.0              INIT.238
227.  0010638        RETURN                                     INIT.239
228.  0010658        END                                        INIT.240
```

0 0 0 0 4 9 0 2 3 6 3 1 6 0

```
PROPS                 **SUBROUTINE PROPS**
  1.   000000B        SUBROUTINE PROPS                                                  PROPS.2
               C*****************************************************************       COMALL.2
               C                          COMMON BLOCKS                                 COMALL.3
               C*****************************************************************       COMALL.4
  2.   000000B        DIMENSION SAVE(20229)                                             DIM3.1
  3.   000000B        DIMENSION TRANS(512)                                              DIM3.2
  4.   000000B        COMMON                                                            COMALL.6
                     1X(15),Y(30),Z(02),XU(15),YV(30),ZW(02),                           DIM3.3
                     1DXEP(15),DXPW(15),DYNP(30),DYPS(30),SEW(15),SNS(30),              DIM3.4
                     1DXEPU(15),DXPWU(15),SEWU(15),DYNPV(30),DYPSV(30),SNSV(30),        DIM3.5
                     1R(30),RV(30),RCV(30),WFN(30),WFS(30),WFE(15),WFW(15),             DIM3.6
                     1U(15,30,2),V(15,30,2),W(15,30,2),PE(15,30,2),C(15,30,2),PP(15,30), DIM3.7
                     1JU(15,30),UV(15,30),UW(15,30),VV(15,30),VW(15,30),WW(15,30),      DIM3.8
                     1ED(15,30),TE(15,30),FF(15,30),UC(15,30),VC(15,30),WC(15,30),      DIM3.9
                     1C2(15,30),EC(15,30),RS(15,30),                                    DIM3.10
                     1DEN(15,30,2),VIS(15,30,2),GAM(15,30,2),VISUU(15,30),VISVV(15,30), DIM3.11
                     1AW(15,30),AE(15,30),AN(15,30),AS(15,30),AD(15,30),AU(15,30),      DIM3.12
                     1AP(15,30),SU(15,30),SP(15,30),                                    DIM3.13
                     1UT(15),CT(15),QUE(15),DCDZB(15),QUO(15),                          DIM3.14
                     1DENSIT,VISCOS,PRANDT,SPHEAT,EXCHAT,                               COMALL.19
                     1CMU,CR1,CR2,CRS,CR1W,CR2W,CEPS1,CEPS2,CEPS,CAPPA,ELOG,            COMALL.20
                     1CC1,CC2,CC,CC1W,CC2W,CG2,CG,CAPPAC,ELOGC,                         COMALL.21
                     1JUU,JUV,JUW,JVV,JVW,JWW,JED,JTE,JFF,JUC,JVC,JWC,JC2,JEC,          COMALL.22
                     1NI,NIM1,NIM2,NJ,NJM1,NJM2,NK,NKM1,IT,JT,KT,IJT,                   COMALL.23
                     1HEDU(4),HEDV(4),HEDW(4),HEDP(4),HEDC(4),HEDR(4),HEDD(4),HEDVIS(4), COMALL.24
                     1INCALU,INCALV,INCALW,INCALP,INCALC,INPRO,INCALR(14),INTURB,INDIFF, COMALL.25
                     1NSWPU,NSWPV,NSWPW,NSWPP,NSWPC,NSWPR,                              COMALL.26
                     1MODEL,MODEC,MRW,MCW,IQUE,IDIF,IJET,ITEST,ITESU,ITESC,ICON,        COMALL.27
                     1IRUN,IU,IHT,IU1,IU2,IC1,IC2,I1,I2,INDCOS,FRA,                     COMALL.28
                     1K,DZ,ISTEP,ISTP1,NRS,INDEX,DPDZ,                                  COMALL.29
                     1FLOWIN,VMEAN,QLENTH,SMALL,GREAT,XTOT,YTOT,RSWALL(14),             COMALL.30
                     1ZOPRO(18),IPRO,IEND,INDPRI,NUMPRI,BVE,BVW,BVS,BWS                 COMALL.31
  5.   000000B        COMMON                                                            DIM3.15
                     1ET(15),ETU(15),DET(15),DETU(15),DYW,NJP,NJP1,NJPM1,IWALL,         DIM3.16
                     1ROUTER,RINNER,ECCEN,ES,NJO,YTOTO,EXCHAW,NJOM1                     DIM3.17
  6.   000000B        COMMON  OLDU(30),OLDV(30),OLDW(30),OLDP(30),                      DIM3.18
                     1       OLDUU(30),OLDUV(30),OLDUW(30),OLDVV(30),OLDVW(30),         DIM3.19
                     1       OLDWW(30),OLDTE(30),OLDED(30),OLDFF(30),                   DIM3.20
                     1       OLDDEN(30),OLDVIS(30),OVISUU(30),OVISVV(30),               DIM3.21
                     1       OLDUTA,ODPDZ                                               DIM3.22
  7.   000000B        LOGICAL INCALU,INCALV,INCALW,INCALP,INCALC,INPRO,                  COMALL.32
                     1       INCALR,INTURB,INDIFF                                       COMALL.33
  8.   000000B        EQUIVALENCE (X(1),SAVE(1))                                        COMALL.34
  9.   000000B        EQUIVALENCE (OLDU(1),TRANS(1))                                    DIM3.23
               C                                                                        PROPS.4
               C*****************************************************************       PROPS.5
               C              DENSITY,VISCOSITY AND THERMAL EXCHANGE COEFFICIENT        PROPS.6
               C*****************************************************************       PROPS.7
               C-----PROPERTIES ARE UNIFORM FOR THIS PROBLEM                            PROPS.8
 10.   000000B        EXCHAT=VISCOS/PRANDT*SPHEAT                                       PROPS.9
 11.   000002B        DO 500 I=I1,I2                                                    PROPS.10
 12.   000004B        DO 500 J=2,NJ                                                     PROPS.11
 13.   000007B        DO 500 K=1,2                                                      PROPS.12
 14.   000011B        IF(INDEX.NE.0) GO TO 200                                          PROPS.13
 15.   000013B        DEN(I,J,K)=DENSIT                                                 PROPS.14
 16.   000020B        VIS(I,J,K)=VISCOS                                                 PROPS.15
 17.   000024B        GAM(I,J,K)=EXCHAT                                                 PROPS.16
```

```
 18.  0000308        IF(K.EQ.2) GO TO 500                                    PROPS.17
 19.  0000328    200 IF(.NOT.INTURB) GO TO 500                               PROPS.18
                C-----EXTRA TERMS REQUIRED IN CALCULATION PROCEDURE          PROPS.19
 20.  0000348        IF(MODEL.EQ.3)GO TO 400                                 PROPS.20
 21.  0000368        IF(.NOT.INCALR(JTE))TE(I,J)=(UU(I,J)+VV(I,J)+WW(I,J))/2.0 PROPS.21
                C                                                            PROPS.22
                C*************************************************************PROPS.23
                C              DIFFUSIVE TRANSPORT COEFFICIENTS FOR REYNOLDS STRESSES. PROPS.24
                C*************************************************************PROPS.25
 22.  0000478        TDE=TE(I,J)/ED(I,J)*DEN(I,J,2)                          PROPS.26
 23.  0000558        VISUU(I,J)=TDE*UU(I,J)                                  PROPS.27
 24.  0000618        VISVV(I,J)=TDE*VV(I,J)                                  PROPS.28
 25.  0000658        VISUU(I,J)=AMAX1(VISUU(I,J),VISCOS)                     PROPS.29
 26.  0000728        VISVV(I,J)=AMAX1(VISVV(I,J),VISCOS)                     PROPS.30
 27.  0000778        GO TO 300                                               PROPS.31
                C*************************************************************PROPS.32
                C                       TWO EQUATION MODEL VISCOSITIES.      PROPS.33
                C*************************************************************PROPS.34
 28.  0000778    400 CONTINUE                                                PROPS.35
 29.  0001008        IF(ED(I,J).EQ.0.)GO TO 410                              PROPS.36
 30.  0001058        VISUU(I,J)=DEN(I,J,K)*TE(I,J)**2*CMU/ED(I,J)            PROPS.37
 31.  0001178    410 VISUU(I,J)=VISCOS                                       PROPS.38
 32.  0001238    500 CONTINUE                                                PROPS.39
 33.  0001338        DO 510 I=1,NI                                           PROPS.40
 34.  0001358        VISVV(1,2)=VISVV(I,3)*BVS+VISVV(I,4)*(1.0-BVS)          PROPS.41
 35.  0001358    510 CONTINUE                                                PROPS.42
 36.  0001448        IF(IU.EQ.0) INPRO=.FALSE.                               PROPS.43
 37.  0001468        RETURN                                                  PROPS.44
 38.  0001508        END                                                     PROPS.45
```

0 0 0 0 4 9 0 0 365 1 9 1

```
CALCM                 **SUBROUTINE CALCM(PHI,DIF,FU,FV,SPH,IMAX,JMAX,IVAR,ISC,**
  1.   0000008         SUBROUTINE CALCM(PHI,DIF,FU,FV,SPH,IMAX,JMAX,IVAR,ISC,
                      1                 IM1,IM2,NSWPHI)
                 C*********************************************************************
                 C                          COMMON BLOCKS
                 C*********************************************************************
  2.   0000008         DIMENSION SAVE(20229)
  3.   0000008         DIMENSION TRANS(512)
  4.   0000008         COMMON
                      1X(15),Y(30),Z(02),XU(15),YV(30),ZW(02),
                      1DXEP(15),DXPW(15),DYNP(30),DYPS(30),SEW(15),SNS(30),
                      1DXEPU(15),DXPWU(15),SEWU(15),DYNPV(30),DYPSV(30),SNSV(30),
                      1R(30),RV(30),RCV(30),WFN(30),WFS(30),WFE(15),WFW(15),
                      1U(15,30,2),V(15,30,2),W(15,30,2),PE(15,30,2),C(15,30,2),PP(15,30),
                      1UU(15,30),UV(15,30),UW(15,30),VV(15,30),VW(15,30),WW(15,30),
                      1ED(15,30),TE(15,30),FF(15,30),UC(15,30),VC(15,30),WC(15,30),
                      1C2(15,30),EC(15,30),RS(15,30),
                      1DEN(15,30,2),VIS(15,30,2),GAM(15,30,2),VISUU(15,30),VISVV(15,30),
                      1AW(15,30),AE(15,30),AN(15,30),AS(15,30),AD(15,30),AU(15,30),
                      1AP(15,30),SU(15,30),SP(15,30),
                      1JT(15),CT(15),QUE(15),DCDZB(15),QUD(15),
                      1DENSIT,VISCOS,PRANDT,SPHEAT,EXCHAT,
                      1CMU,CR1,CR2,CRS,CR1W,CR2W,CEPS1,CEPS2,CEPS,CAPPA,ELOG,
                      1CC1,CC2,CC,CC1W,CC2W,CG2,CG,CAPPAC,ELOGC,
                      1JUU,JUV,JUW,JVV,JVW,JWW,JED,JTE,JFF,JUC,JVC,JWC,JC2,JEC,
                      1NI,NIM1,NIM2,NJ,NJM1,NJM2,NK,NKM1,IT,JT,KT,IJT,
                      1HEDU(4),HEDV(4),HEDW(4),HEDP(4),HEDC(4),HEDR(4),HEDD(4),HEDVIS(4),
                      1INCALU,INCALV,INCALW,INCALP,INCALC,INPRO,INCALR(14),INTURB,INDIFF,
                      1NSWPU,NSWPV,NSWPW,NSWPP,NSWPC,NSWPR,
                      1MODEL,MODEC,MRW,MCW,IQUE,IDIF,IJET,ITEST,ITESU,ITESC,ICON,
                      1IRUN,IU,IHT,IU1,IU2,IC1,IC2,I1,I2,INDCDS,FRA,
                      1K,DZ,ISTEP,ISTP1,NRS,INDEX,DPDZ,
                      1FLOWIN,VMEAN,QLENTH,SMALL,GREAT,XTOT,YTOT,RSWALL(14),
                      1ZDPRO(18),IPRO,IEND,INDPRI,NUMPRI,BVE,BVW,BVS,BWS
  5.   0000008         COMMON
                      1ET(15),ETU(15),DET(15),DETU(15),DYW,NJP,NJP1,NJPM1,IWALL,
                      1ROUTER,RINNER,ECCEN,ES,NJO,YTOTO,EXCHAW,NJOM1
  6.   0000008         COMMON  OLDU(30),OLDV(30),OLDW(30),OLDP(30),
                      1       OLDUU(30),OLDUV(30),OLDUW(30),OLDVV(30),OLDVW(30),
                      1       OLDWW(30),OLDTE(30),OLDED(30),OLDFF(30),
                      1       OLDDEN(30),OLDVIS(30),OVISUU(30),OVISVV(30),
                      1       OLDUTA,ODPDZ
  7.   0000008         LOGICAL INCALU,INCALV,INCALW,INCALP,INCALC,INPRO,
                      1       INCALR,INTURB,INDIFF
  8.   0000008         EQUIVALENCE (X(1),SAVE(1))
  9.   0000008         EQUIVALENCE (OLDU(1),TRANS(1))
 10.   0000008         DIMENSION PHI(IMAX,JMAX,2),DIF(IMAX,JMAX,2),FU(IMAX,JMAX),
                      1          FV(IMAX,JMAX)
                 C*********************************************************************
                 C                        ASSEMBLY OF COEFFICIENTS
                 C*********************************************************************
 11.   0000008         IF(ISTEP.LT.5) URF=0.05
 12.   0000048         II=0
 13.   0000048    1400 CONTINUE
                 C
 14.   0000058         K=1
 15.   0000058         DO 100 I=IM1,IM2
 16.   0000108         DO 100 J=2,NJM1
```

```
                 **SUBROUTINE CALCM(PHI,DIF,FU,FV,SPH,IMAX,JMAX,IVAR,ISC,**
                C-----COMPUTE AREAS AND VOLUME                                  CALCM.17
                      AREAN=SEW(I)*DZ*RV(J+1)                                   CALCM.18
 17.   0000138        AREAEW=DZ*SNS(J)                                          CALCM.19
 18.   0000158        AREAU=SEW(I)*RCV(J)*SNS(J)                                CALCM.20
 19.   0000178        VOL=RCV(J)*DZ*SNS(J)*SEW(I)                               CALCM.21
 20.   0000218       C-----CALCULATE CONVECTION COEFFICIENTS                    CALCM.22
                      CU=DEN(I,J,K)*W(I,J,K)*AREAU*SPH                          CALCM.23
 21.   0000228        CN=0.5*(DEN(I,J,K)+DEN(I,J+1,K))*V(I,J+1,K)*AREAN*SPH     CALCM.24
 22.   0000318        CE=0.5*(DEN(I,J,K)+DEN(I+1,J,K))*U(I+1,J,K)*AREAEW*SPH    CALCM.25
 23.   0000428       C-----CALCULATE DIFFUSION COEFFICIENTS                     CALCM.26
                      DIFE=0.5*(DIF(I,J,K)+DIF(I+1,J,K))                        CALCM.27
 24.   0000528        DIFN=0.5*(DIF(I,J,K)+DIF(I,J+1,K))                        CALCM.28
 25.   0000618        IF(MODEL.EQ.3.OR..NOT.INDIFF) GO TO 120                   CALCM.29
 26.   0000748        FVN=FV(I,J+1)                                             CALCM.30
 27.   0001018        FUE=FU(I+1,J)                                             CALCM.31
 28.   0001048        DIFN=DIFN-FVN/(PHI(I,J+1,K)-PHI(I,J,K)-SMALL)*DEN(I,J,K)*SPH*  CALCM.32
 29.   0001078       1          SNSV(J+1)                                      CALCM.33
 30.   0001338        DIFE=DIFE-FUE/(PHI(I+1,J,K)-PHI(I,J,K)-SMALL)*DEN(I,J,K)*SPH*  CALCM.34
                     1          RCV(J)*SEWU(I+1)                               CALCM.35
 31.   0001548    120 CONTINUE                                                  CALCM.36
 32.   0001558        DIN=DIFN*AREAN/DYNP(J)                                    CALCM.37
 33.   0001578        DIE=DIFE*AREAEW/(DXEP(I)*RCV(J))                          CALCM.38
                C-----ASSEMBLE MAIN COEFFICIENTS                                CALCM.39
 34.   0001658        AU(I,J)=CU                                                CALCM.40
 35.   0001718        AD(I,J)=0.0                                               CALCM.41
 36.   0001748        AN(I,J)=AMAX1(ABS(0.5*CN),DIN)-0.5*CN                     CALCM.42
 37.   0002058        AS(I,J)=AN(I,J-1)                                         CALCM.43
 38.   0002118        AE(I,J)=AMAX1(ABS(0.5*CE),DIE)-0.5*CE                     CALCM.44
 39.   0002228        AW(I,J)=AE(I-1,J)                                         CALCM.45
 40.   0002268        SU(I,J)=DPDZ*FLOAT(ISC)*VOL                               CALCM.46
 41.   0002348        SP(I,J)=0.0                                               CALCM.47
 42.   0002378    100 CONTINUE                                                  CALCM.48
                C*********************************************************      CALCM.49
                C*****PROBLEM MODIFICATIONS                                     CALCM.50
 43.   0002448        IF(ISC.EQ.0) CALL MODC(RS,NRS,IT,JT,IC1,IC2)              CALCM.51
 44.   0002478        IF(ISC.EQ.1) CALL MODW(RS,NRS,IT,JT,IU1,IU2)              CALCM.52
                C*****FINAL COEFFICIENT ASSEMBLY                                CALCM.53
 45.   0002538        IF(ISC.EQ.1) GO TO 210                                    DIM3.95
 46.   0002548        IF(IWALL.EQ.0) GO TO 210                                  DIM3.96
 47.   0002568        NJM1=NJOM1                                                DIM3.97
 48.   0002568        NJ=NJO                                                    DIM3.98
 49.   0002608    210 CONTINUE                                                  DIM3.99
 50.   0002618        DO 300 I=IM1,IM2                                          CALCM.54
 51.   0002638        DO 300 J=2,NJM1                                           CALCM.55
 52.   0002668        AP(I,J)=AD(I,J)+AU(I,J)+AN(I,J)+AS(I,J)                   CALCM.56
                     1+AE(I,J)+AW(I,J)-SP(I,J)                                  CALCM.57
 53.   0002668    300 CONTINUE                                                  CALCM.58
                C*********************************************************      CALCM.59
                C                   SOLUTION OF DIFFERENCE EQUATION             CALCM.60
                C*********************************************************      CALCM.61
 54.   0003058        K=2                                                       CALCM.62
 55.   0003068        DO 400 N=1,NSWPHI                                         CALCM.63
 56.   0003108    400 CALL LISOLV(2,2,PHI,N,2,IVAR,IM1,IM2)                     CALCM.64
 57.   0003218        IF(ISC.EQ.1) GO TO 450                                    DIM3.100
 58.   0003238        IF(IWALL.EQ.0) GO TO 450                                  DIM3.101
 59.   0003248        NJ=NJP                                                    DIM3.102
 60.   0003258        NJM1=NJPM1                                                DIM3.103
 61.   0003268    450 CONTINUE                                                  DIM3.104
```

```
 62.  0003308        IF(ISC.EQ.1) GO TO 910                                    CALCM.65
 63.  0003318        NJPM2=NJM1                                                CALCM.66
 64.  0003328        DO 905 I=1,NI                                             CALCM.67
 65.  0003358        DCDZB(I)=(C(I,NJPM2,2)-C(I,NJPM2,1))/(DZ+SMALL)           CALCM.68
 66.  0003358    905 CONTINUE                                                  CALCM.69
 67.  0003468        GO TO 1250                                                CALCM.70
 68.  0003468    910 CONTINUE                                                  CALCM.71
                C*****************************************************************CALCM.72
                C*****CALCULATION OF PRESSURE GRADIENT                          CALCM.73
 69.  0003478        GINLET=FLOWIN                                             CALCM.74
 70.  0003478        GSTAR=0.0                                                 CALCM.75
 71.  0003508        DSUM=0.0                                                  CALCM.76
 72.  0003518        DO 1100 I=IM1,IM2                                         CALCM.77
 73.  0003548        DO 1100 J=2,NJM1                                          CALCM.78
 74.  0003578        AREAD=SEW(I)*SNS(J)*RCV(J)                                CALCM.79
 75.  0003618        DSUM1=AREAD*AREAD*DZ*DEN(I,J,2)/AP(I,J)                   CALCM.80
 76.  0003708        DSUM=DSUM+DSUM1                                           CALCM.81
 77.  0003728        GSTAR1=AREAD*W(I,J,K)*DEN(I,J,2)                          CALCM.82
 78.  0004008   1100 GSTAR=GSTAR+GSTAR1                                        CALCM.83
 79.  0004058        DPDZ1=(GINLET-GSTAR)/DSUM                                 CALCM.84
 80.  0004078        DPDZ=DPDZ+DPDZ1*URF                                       CALCM.85
 81.  0004128        IF(DPDZ.LE.0) STOP                                        CALCM.86
 82.  0004158        DPCENT=ABS(DPDZ1/(DPDZ+SMALL))                            CALCM.87
 83.  0004178        II=II+1                                                   CALCM.88
 84.  0004218        IF(DPCENT.GT.0.01) GO TO 1400                             CALCM.89
 85.  0004248        URF=AMAX1(URF,1.0/FLOAT(II))                              CALCM.90
 86.  0004278        DO 1200 I=IM1,IM2                                         CALCM.91
 87.  0004328        DO 1200 J=2,NJM1                                          CALCM.92
 88.  0004358        AREAD=SEW(I)*SNS(J)*RCV(J)                                CALCM.93
 89.  0004378        WCORR=DPDZ1*AREAD*DZ/AP(I,J)                              CALCM.94
 90.  0004448   1200 W(I,J,K)=W(I,J,K)+WCORR                                   CALCM.95
                C*****************************************************************CALCM.96
                C*****ESTIMATION OF V-VELOCITY                                  CALCM.97
                C-----THIS SIMPLIFICATION IS APPLICABLE IN AXISYMMETRIC INTERNAL CALCM.98
                C     FLOWS ONLY                                                CALCM.99
 91.  0004568        NJM2=NJ-2                                                 CALCM.100
 92.  0004578        DO 410 I=IM1,IM2                                          CALCM.101
 93.  0004618        DO 410 J=2,NJM2                                           CALCM.102
 94.  0004648        V(I,J+1,K)=(1.0/(DZ*RV(J+1)*SEW(I)))*                     CALCM.103
                    1          (+W(I,J,1)*RCV(J)*SEW(I)*SNS(J)                 CALCM.104
                    1           -W(I,J,2)*RCV(J)*SEW(I)*SNS(J)                 CALCM.105
                    1           +V(I,J,K)*DZ*RV(J)*SEW(I))                     CALCM.106
 95.  0004648    410 CONTINUE                                                  CALCM.107
 96.  0005148   1250 CONTINUE                                                  CALCM.108
                C*****************************************************************CALCM.109
                C*****SET BOUNDARY CONDITIONS FOR USE IN GRADIENT CALCULATIONS. CALCM.110
                C         (ASSUME PARABOLIC PROFILES NEAR SYMMETRY AXES)      CALCM.111
 97.  0005158        DO 401 I=I1,I2                                            CALCM.112
 98.  0005178    401 PHI(I,1,K)=BWS*PHI(I,2,K)+(1.0-BWS)*PHI(I,3,K)            CALCM.113
 99.  0005368        NIM2=NIM1-1                                               CALCM.114
100.  0005378        DO 402 J=1,NJO                                            DIM3.105
101.  0005428        PHI(1,J,K)=BVW*PHI(2,J,K)+(1.0-BVW)*PHI(3,J,K)            CALCM.116
102.  0005528    402 PHI(NI,J,K)=BVE*PHI(NIM1,J,K)+(1.0-BVE)*PHI(NIM2,J,K)     CALCM.117
103.  0005748        RETURN                                                    CALCM.118
104.  0005768        END                                                       CALCM.119
```

```
 62.  000330B        IF(ISC.EQ.1) GO TO 910                                  CALCM.65
 63.  000331B        NJPM2=NJM1                                              CALCM.66
 64.  000332B        DO 905 I=1,NI                                           CALCM.67
 65.  000335B        DCDZB(I)=(C(I,NJPM2,2)-C(I,NJPM2,1))/(DZ+SMALL)         CALCM.68
 66.  000335B    905 CONTINUE                                                CALCM.69
 67.  000346B        GO TO 1250                                              CALCM.70
 68.  000346B    910 CONTINUE                                                CALCM.71
                C*********************************************************** CALCM.72
                C*****CALCULATION OF PRESSURE GRADIENT                       CALCM.73
 69.  000347B        GINLET=FLOWIN                                           CALCM.74
 70.  000347B        GSTAR=0.0                                               CALCM.75
 71.  000350B        DSUM=0.0                                                CALCM.76
 72.  000351B        DO 1100 I=IM1,IM2                                       CALCM.77
 73.  000354B        DO 1100 J=2,NJM1                                        CALCM.78
 74.  000357B        AREAD=SEW(I)*SNS(J)*RCV(J)                              CALCM.79
 75.  000361B        DSUM1=AREAD*AREAD*DZ*DEN(I,J,2)/AP(I,J)                 CALCM.80
 76.  000370B        DSUM=DSUM+DSUM1                                         CALCM.81
 77.  000372B        GSTAR1=AREAD*W(I,J,K)*DEN(I,J,2)                        CALCM.82
 78.  000400B   1100 GSTAR=GSTAR+GSTAR1                                      CALCM.83
 79.  000405B        DPDZ1=(GINLET-GSTAR)/DSUM                               CALCM.84
 80.  000407B        DPDZ=DPDZ+DPDZ1*URF                                     CALCM.85
 81.  000412B        IF(DPDZ.LE.0) STOP                                      CALCM.86
 82.  000415B        DPCENT=ABS(DPDZ1/(DPDZ+SMALL))                          CALCM.87
 83.  000417B        II=II+1                                                 CALCM.88
 84.  000421B        IF(DPCENT.GT.0.01) GO TO 1400                           CALCM.89
 85.  000424B        URF=AMAX1(URF,1.0/FLOAT(II))                            CALCM.90
 86.  000427B        DO 1200 I=IM1,IM2                                       CALCM.91
 87.  000432B        DO 1200 J=2,NJM1                                        CALCM.92
 88.  000435B        AREAD=SEW(I)*SNS(J)*RCV(J)                              CALCM.93
 89.  000437B        WCORR=DPDZ1*AREAD*DZ/AP(I,J)                            CALCM.94
 90.  000444B   1200 W(I,J,K)=W(I,J,K)+WCORR                                 CALCM.95
                C*********************************************************** CALCM.96
                C*****ESTIMATION OF V-VELOCITY                               CALCM.97
                C-----THIS SIMPLIFICATION IS APPLICABLE IN AXISYMMETRIC INTERNAL CALCM.98
                C     FLOWS ONLY                                             CALCM.99
 91.  000456B        NJM2=NJ-2                                               CALCM.100
 92.  000457B        DO 410 I=IM1,IM2                                        CALCM.101
 93.  000461B        DO 410 J=2,NJM2                                         CALCM.102
 94.  000464B        V(I,J+1,K)=(1.0/(DZ*RV(J+1)*SEW(I)))*                   CALCM.103
                    1          (+W(I,J,1)*RCV(J)*SEW(I)*SNS(J)               CALCM.104
                    1           -W(I,J,2)*RCV(J)*SEW(I)*SNS(J)               CALCM.105
                    1           +V(I,J,K)*DZ*RV(J)*SEW(I))                   CALCM.106
 95.  000464B    410 CONTINUE                                                CALCM.107
 96.  000514B   1250 CONTINUE                                                CALCM.108
                C*********************************************************** CALCM.109
                C*****SET BOUNDARY CONDITIONS FOR USE IN GRADIENT CALCULATIONS. CALCM.110
                C        (ASSUME PARABOLIC PROFILES NEAR SYMMETRY AXES)     CALCM.111
 97.  000515B        DO 401 I=I1,I2                                          CALCM.112
 98.  000517B    401 PHI(I,1,K)=BWS*PHI(I,2,K)+(1.0-BWS)*PHI(I,3,K)          CALCM.113
 99.  000536B        NIM2=NIM1-1                                             CALCM.114
100.  000537B        DO 402 J=1,NJO                                          DIM3.105
101.  000542B        PHI(1,J,K)=BVW*PHI(2,J,K)+(1.0-BVW)*PHI(3,J,K)          CALCM.116
102.  000552B    402 PHI(NI,J,K)=BVE*PHI(NIM1,J,K)+(1.0-BVE)*PHI(NIM2,J,K)   CALCM.117
103.  000574B        RETURN                                                  CALCM.118
104.  000576B        END                                                     CALCM.119
```

0 0 0 4 9 0 6 - 3691 - 6 3

```
  1.  000000B        SUBROUTINE CALCRS(PHI,IRS,CO,IMAX,JMAX,IVAR,IM1,IM2)                CALCRS.2
              C*********************************************************************** COMALL.2
              C                              COMMON BLOCKS                                COMALL.3
              C*********************************************************************** COMALL.4
  2.  000000B        DIMENSION SAVE(20229)                                               DIM3.1
  3.  000000B        DIMENSION TRANS(512)                                                DIM3.2
  4.  000000B        COMMON                                                              COMALL.6
                    1X(15),Y(30),Z(02),XU(15),YV(30),ZW(02),                             DIM3.3
                    1DXEP(15),DXPW(15),DYNP(30),DYPS(30),SEW(15),SNS(30),                DIM3.4
                    1DXEPU(15),DXPWU(15),SEWU(15),DYNPV(30),DYPSV(30),SNSV(30),          DIM3.5
                    1R(30),RV(30),RCV(30),WFN(30),WFS(30),WFE(15),WFW(15),               DIM3.6
                    1J(15,30,2),V(15,30,2),W(15,30,2),PE(15,30,2),C(15,30,2),PP(15,30),  DIM3.7
                    1UU(15,30),UV(15,30),UW(15,30),VV(15,30),VW(15,30),WW(15,30),        DIM3.8
                    1ED(15,30),FE(15,30),FF(15,30),UC(15,30),VC(15,30),WC(15,30),        DIM3.9
                    1C2(15,30),EC(15,30),RS(15,30),                                      DIM3.10
                    1DEN(15,30,2),VIS(15,30,2),GAM(15,30,2),VISUU(15,30),VISVV(15,30),   DIM3.11
                    1AW(15,30),AE(15,30),AN(15,30),AS(15,30),AD(15,30),AU(15,30),        DIM3.12
                    1AP(15,30),SU(15,30),SP(15,30),                                      DIM3.13
                    1DT(15),CT(15),QUE(15),DCDZB(15),QUD(15),                            DIM3.14
                    1DENSIT,VISCOS,PRANDT,SPHEAT,EXCHAT,                                 COMALL.19
                    1CMU,CR1,CR2,CRS,CR1W,CR2W,CEPS1,CEPS2,CEPS,CAPPA,ELOG,              COMALL.20
                    1CC1,CC2,CC,CC1W,CC2W,CG2,CG,CAPPAC,ELOGC,                           COMALL.21
                    1JUU,JUV,JUW,JVV,JVW,JWW,JED,JTE,JFF,JUC,JVC,JWC,JC2,JEC,            COMALL.22
                    1NI,NIM1,NIM2,NJ,NJM1,NJM2,NK,NKM1,IT,JT,KT,IJT,                     COMALL.23
                    1HEDU(4),HEDV(4),HEDW(4),HEDP(4),HEDC(4),HEDR(4),HEDD(4),HEDVIS(4),  COMALL.24
                    1INCALU,INCALV,INCALW,INCALP,INCALC,INPRO,INCALR(14),INTURB,INDIFF,  COMALL.25
                    1NSWPU,NSWPV,NSWPW,NSWPP,NSWPC,NSWPR,                                COMALL.26
                    1MODEL,MODEC,MRW,MCW,IQUE,IDIF,IJET,ITEST,ITESU,ITESC,ICON,          COMALL.27
                    1IRUN,IU,IHT,IU1,IU2,IC1,IC2,I1,I2,INDCOS,FRA,                       COMALL.28
                    1K,DZ,ISTEP,ISTP1,NRS,INDEX,DPDZ,                                    COMALL.29
                    1FLOWIN,VMEAN,QLENTH,SMALL,GREAT,XTOT,YTOT,RSWALL(14),               COMALL.30
                    1ZDPRU(18),IPRO,IEND,INDPRI,NUMPRI,BVE,BVW,BVS,BWS                   COMALL.31
  5.  000000B        COMMON                                                              DIM3.15
                    1ET(15),ETU(15),DET(15),DETU(15),DYW,NJP,NJP1,NJPM1,IWALL,           DIM3.16
                    1RDJTER,RINNER,ECCEN,ES,NJO,YTOTO,EXCHAW,NJOM1                       DIM3.17
  6.  000000B        COMMON  OLDU(30),OLDV(30),OLDW(30),OLDP(30),                        DIM3.18
                    1        OLDUU(30),OLDUV(30),OLDUW(30),OLDVV(30),OLDVW(30),          DIM3.19
                    1        OLDWW(30),OLDTE(30),OLDED(30),OLDFF(30),                    DIM3.20
                    1        OLDDEN(30),OLDVIS(30),OVISUU(30),OVISVV(30),                DIM3.21
                    1        OLDUTA,ODPDZ                                                DIM3.22
  7.  000000B        LOGICAL INCALU,INCALV,INCALW,INCALP,INCALC,INPRO,                   COMALL.32
                    1        INCALR,INTURB,INDIFF                                        COMALL.33
  8.  000000B        EQUIVALENCE (X(1),SAVE(1))                                          COMALL.34
  9.  000000B        EQUIVALENCE (OLDU(1),TRANS(1))                                      DIM3.23
 10.  000000B        DIMENSION PHI(IMAX,JMAX)                                            CALCRS.4
              C*********************************************************************** CALCRS.5
              C                          ASSEMBLY OF COEFFICIENTS                         CALCRS.6
              C*********************************************************************** CALCRS.7
 11.  000000B        NRS=IRS                                                             CALCRS.8
 12.  000000B        CALL SORCE(PHI,IRS,SU,SP,IJT,IM1,IM2)                               CALCRS.9
 13.  000007B        K=1                                                                 CALCRS.10
 14.  000007B        IS1=IM1                                                             CALCRS.11
 15.  000010B        JS1=3                                                               CALCRS.12
 16.  000012B        IF(IRS.EQ.JUC) IS1=3                                                CALCRS.13
 17.  000016B        IF(IRS.EQ.JUC) JS1=2                                                CALCRS.14
 18.  000020B        DO 100 I=IM1,IM2                                                    CALCRS.15
 19.  000021B        DO 100 J=JS1,NJM1                                                   CALCRS.1
```

```
 20.  0000248        IF(IRS.EQ.JUC) GO TO 110                                  CALCRS.17
                 C-----COMPUTE AREAS AND VOLUME                                 CALCRS.18
 21.  0000268        AREAN=SEW(I)*DZ*R(J)                                      CALCRS.19
 22.  0000328        AREAEW=DZ*SNSV(J)                                         CALCRS.20
 23.  0000338        AREAU=SEW(I)*RV(J)*SNSV(J)                                CALCRS.21
 24.  0000358        VOL=RV(J)*DZ*SNSV(J)*SEW(I)                               CALCRS.22
                 C-----CALCULATE CONVECTION COEFFICIENTS                        CALCRS.23
 25.  0000378        CU=0.5*(DEN(I,J,K)*W(I,J,K)+DEN(I,J-1,K)*W(I,J-1,K))*AREAU CALCRS.24
 26.  0000508        CN=DEN(I,J,K)*(V(I,J+1,K)*(1.0-WFN(J))+V(I,J,K)*WFN(J))*AREAN CALCRS.25
 27.  0000628        CE=0.5*(0.5*(DEN(I,J,K)+DEN(I+1,J,K))*U(I+1,J,K)+          CALCRS.26
                    1        0.5*(DEN(I,J-1,K)+DEN(I+1,J-1,K))*U(I+1,J-1,K))*AREAEW CALCRS.27
                 C-----CALCULATE DIFFUSION COEFFICIENTS                         CALCRS.28
 28.  0001008        GAME=0.5*(VISUU(I,J)+VISUU(I+1,J))*CO                     CALCRS.29
 29.  0001068        GAMN=(VISVV(I,J)*WFN(J)+VISVV(I,J+1)*(1.-WFN(J)))*CO      CALCRS.30
 30.  0001178        IF(J.EQ.NJM1) GAMN=VISVV(I,J)*CO*(Y(NJ)-Y(NJM1))/SNS(NJM1) CALCRS.31
 31.  0001328        DIN=GAMN*AREAN/DYNPV(J)                                   CALCRS.32
 32.  0001348        DIE=GAME*AREAEW/(DXEP(I)*RV(J))                           CALCRS.33
 33.  0001428        GO TO 120                                                 CALCRS.34
 34.  0001428    110 CONTINUE                                                  CALCRS.35
 35.  0001438        CU=DEN(I,J,K)*W(I,J,K)*SEWU(I)*RCV(J)*SNS(J)              CALCRS.36
 36.  0001538        CN=CE=0.0                                                 CALCRS.37
 37.  0001548        DIN=VISVV(I,J+1)*CO*SEWU(I)*RV(J+1)*DZ/DYNP(J)            CALCRS.38
 38.  0001638        DIE=(VISUU(I,J)*WFN(J)+VISUU(I,J+1)*(1.0-WFN(J)))*CO*SNS(J)*DZ/ CALCRS.39
                    1    (DXEPU(I)*RCV(J))                                     CALCRS.40
 39.  0001778        VOL=RCV(J)*SEWU(I)*SNS(J)*DZ                              CALCRS.41
 40.  0002028    120 CONTINUE                                                  CALCRS.42
                 C-----ASSEMBLE MAIN COEFFICIENTS                               CALCRS.43
 41.  0002048        AU(I,J)=CU                                                CALCRS.44
 42.  0002078        AD(I,J)=0.0                                               CALCRS.45
 43.  0002128        AN(I,J)=AMAX1(ABS(0.5*CN),DIN)-0.5*CN                     CALCRS.46
 44.  0002238        AS(I,J)=AN(I,J-1)                                         CALCRS.47
 45.  0002278        AE(I,J)=AMAX1(ABS(0.5*CE),DIE)-0.5*CE                     CALCRS.48
 46.  0002408        AW(I,J)=AE(I-1,J)                                         CALCRS.49
 47.  0002448        SU(I,J)=SU(I,J)*VOL                                       CALCRS.50
 48.  0002508        SP(I,J)=SP(I,J)*VOL                                       CALCRS.51
 49.  0002548    100 CONTINUE                                                  CALCRS.52
                 C*********************************************************** CALCRS.53
                 C*****PROBLEM MODIFICATIONS                                    CALCRS.54
 50.  0002618        CALL MODRS (PHI,IRS,IMAX,JMAX,IM1,IM2)                    CALCRS.55
 51.  0002718        IF(IRS.EQ.JUC) GO TO 200                                  CALCRS.56
 52.  0002728        DO 150 I=IM1,IM2                                          CALCRS.57
 53.  0002758        J=2                                                       CALCRS.58
 54.  0002758        CN=DEN(I,J,K)*(V(I,J+1,K)*(1.0-WFN(J))+V(I,J,K)*WFN(J))*  CALCRS.59
                    1        SEW(I)*DZ*R(J)                                    CALCRS.60
 55.  0003108        DIN=(VISVV(I,J)*WFN(J)+VISVV(I,J+1)*(1.0-WFN(J)))*CO*SEW(I)* CALCRS.61
                    1          DZ*R(J)/DYNPV(J)                                CALCRS.62
 56.  0003228        AS(I,3)=AMAX1(ABS(0.5*CN),DIN)-0.5*CN                     CALCRS.63
 57.  0003278    150 CONTINUE                                                  CALCRS.64
 58.  0003318    200 CONTINUE                                                  CALCRS.65
                 C*****FINAL COEFFICIENT ASSEMBLY                               CALCRS.66
 59.  0003328        DO 300 I=IS1,IM2                                          CALCRS.67
 60.  0003348        DO 300 J=JS1,NJM1                                         CALCRS.68
 61.  0003378        AP(I,J)=AD(I,J)+AU(I,J)+AN(I,J)+AS(I,J)                   CALCRS.69
                    1+AE(I,J)+AW(I,J)-SP(I,J)                                  CALCRS.70
 62.  0003378    300 CONTINUE                                                  CALCRS.71
                 C*********************************************************** CALCRS.72
                 C                    SOLUTION OF DIFFERENCE EQUATION           CALCRS.73
                 C*********************************************************** CALCRS.74
```

0 0 0 0 4 9 0 9 - 371 L 0 4

```
63.  0003568        K=2                                                    CALCRS.75
64.  0003578        DO 400 N=1,NSWPR                                       CALCRS.76
65.  0003618    400 CALL LISOLV(IS1,JS1,PHI,N,1,IVAR,IS1,IM2)              CALCRS.77
66.  0003718        IF(IRS.EQ.JUW.OR.IRS.EQ.JUC) RETURN                    CALCRS.78
67.  0003778        IF(IRS.EQ.JVW.OR.IRS.EQ.JVC) GO TO 410                 CALCRS.79
68.  0004028        DO 401 I=IM1,IM2                                       CALCRS.80
69.  0004048        PHI(I,2)=BVS*PHI(I,3)+(1.0-BVS)*PHI(I,4)               CALCRS.81
70.  0004048    401 CONTINUE                                               CALCRS.82
71.  0004178    410 CONTINUE                                               CALCRS.83
72.  0004178        IF(IVAR.EQ.1) GO TO 405                                CALCRS.84
73.  0004208        DO 402 J=2,NJM1                                        CALCRS.85
74.  0004238        PHI(1,J)=BVW*PHI(2,J)+(1.0-BVW)*PHI(3,J)               CALCRS.86
75.  0004308    402 PHI(NI,J)=BVE*PHI(NIM1,J)+(1.0-BVE)*PHI(NIM2,J)        CALCRS.87
76.  0004468    405 CONTINUE                                               CALCRS.88
77.  0004468        RETURN                                                 CALCRS.89
78.  0004508        END                                                    CALCRS.90
```

```
 1.   0000008        SUBROUTINE PROMOD(PHI,IRS,IMAX,JMAX,IM1,IM2)                          PROMOD.2
                 C***********************************************************************  COMALL.2
                 C                              COMMON BLOCKS                              COMALL.3
                 C***********************************************************************  COMALL.4
 2.   0000008        DIMENSION SAVE(20229)                                                 DIM3.1
 3.   0000008        DIMENSION TRANS(512)                                                  DIM3.2
 4.   0000008        COMMON                                                                COMALL.6
                    1X(15),Y(30),Z(02),XU(15),YV(30),ZW(02),                               DIM3.3
                    1DXEP(15),DXPW(15),DYNP(30),DYPS(30),SEW(15),SNS(30),                  DIM3.4
                    1DXEPU(15),DXPWU(15),SEWU(15),DYNPV(30),DYPSV(30),SNSV(30),            DIM3.5
                    1R(30),RV(30),RCV(30),WFN(30),WFS(30),WFE(15),WFW(15),                 DIM3.6
                    1U(15,30,2),V(15,30,2),W(15,30,2),PE(15,30,2),C(15,30,2),PP(15,30),    DIM3.7
                    1UU(15,30),UV(15,30),UW(15,30),VV(15,30),VW(15,30),WW(15,30),          DIM3.8
                    1ED(15,30),TE(15,30),FF(15,30),UC(15,30),VC(15,30),WC(15,30),          DIM3.9
                    1C2(15,30),EC(15,30),RS(15,30),                                        DIM3.10
                    1DEN(15,30,2),VIS(15,30,2),GAM(15,30,2),VISUU(15,30),VISVV(15,30),     DIM3.11
                    1AW(15,30),AE(15,30),AN(15,30),AS(15,30),AD(15,30),AU(15,30),          DIM3.12
                    1AP(15,30),SU(15,30),SP(15,30),                                        DIM3.13
                    1UT(15),CT(15),QUE(15),DCDZB(15),QUD(15),                              DIM3.14
                    1DENSIT,VISCOS,PRANDT,SPHEAT,EXCHAT,                                   COMALL.19
                    1CMU,CR1,CR2,CRS,CR1W,CR2W,CEPS1,CEPS2,CEPS,CAPPA,ELOG,                COMALL.20
                    1CC1,CC2,CC,CC1W,CC2W,CG2,CG,CAPPAC,ELOGC,                             COMALL.21
                    1JUU,JUV,JUW,JVV,JVW,JWW,JED,JTE,JFF,JUC,JVC,JWC,JC2,JEC,              COMALL.22
                    1NI,NIM1,NIM2,NJ,NJM1,NJM2,NK,NKM1,IT,JT,KT,IJT,                       COMALL.23
                    1HEDU(4),HEDV(4),HEDW(4),HEDP(4),HEDC(4),HEDR(4),HEDD(4),HEDVIS(4),    COMALL.24
                    1INCALU,INCALV,INCALW,INCALP,INCALC,INPRO,INCALR(14),INTURB,INDIFF,    COMALL.25
                    1NSWPU,NSWPV,NSWPW,NSWPP,NSWPC,NSWPR,                                  COMALL.26
                    1MODEL,MODEC,MRW,MCW,IQUE,IDIF,IJET,ITEST,ITESU,ITESC,ICON,            COMALL.27
                    1IRUN,IU,IHT,IU1,IU2,IC1,IC2,I1,I2,INDCOS,FRA,                         COMALL.28
                    1X,DZ,ISTEP,ISTP1,NRS,INDEX,DPDZ,                                      COMALL.29
                    1FLOWIN,VMEAN,QLENTH,SMALL,GREAT,XTOT,YTOT,RSWALL(14),                 COMALL.30
                    1ZDPRO(18),IPRO,IEND,INDPRI,NUMPRI,BVE,BVW,BVS,BWS                     COMALL.31
 5.   0000008        COMMON                                                                DIM3.15
                    1ET(15),ETU(15),DET(15),DETU(15),DYW,NJP,NJP1,NJPM1,IWALL,             DIM3.16
                    1ROUTER,RINNER,ECCEN,ES,NJO,YTOTO,EXCHAW,NJOM1                         DIM3.17
 6.   0000008        COMMON  OLDU(30),OLDV(30),OLDW(30),OLDP(30),                          DIM3.18
                    1       OLDUU(30),OLDUV(30),OLDUW(30),OLDVV(30),OLDVW(30),             DIM3.19
                    1       OLDWW(30),OLDTE(30),OLDED(30),OLDFF(30),                       DIM3.20
                    1       OLDDEN(30),OLDVIS(30),OVISUU(30),OVISVV(30),                   DIM3.21
                    1       OLDUTA,CDPDZ                                                   DIM3.22
 7.   0000008        LOGICAL INCALU,INCALV,INCALW,INCALP,INCALC,INPRO,                     COMALL.32
                    1       INCALR,INTURB,INDIFF                                           COMALL.33
 8.   0000008        EQUIVALENCE (X(1),SAVE(1))                                            COMALL.34
 9.   0000008        EQUIVALENCE (OLDU(1),TRANS(1))                                        DIM3.23
10.   0000008        DIMENSION WNEAR(15,14),                                               DIM3.106
                    1         PHI(IMAX,JMAX)                                              PROMOD.5
                 C***********************************************************************  PROMOD.6
                 C                                W MOMENTUM                                PROMOD.7
                 C***********************************************************************  PROMOD.8
11.   0000008        ENTRY MODW                                                            PROMOD.9
                 C      AN OUTER WALL                                                      PROMOD.10
12.   0003308        IF(.NOT.INTURB) GOTO 220                                              PROMOD.11
13.   0003318        DO 200 I=IM1,IM2                                                      PROMOD.12
14.   0003338        YREF=YV(NJ)-Y(NJM1)                                                   PROMOD.13
15.   0003358        VISREF=VISCOS                                                         PROMOD.14
16.   0003368        DENREF=DEN(I,NJM1,1)                                                  PROMOD.15
17.   0003418        UVEC=W(I,NJM1,1)                                                      PROMOD.16
```

```
PROMOD                  **SUBROUTINE PROMOD(PHI,IRS,IMAX,JMAX,IM1,IM2)**                PROMOD.17
 18.  0003448                YPLUS=UT(I)*DENREF*YREF/VISREF                              PROMOD.18
 19.  0003478                UT(I)=UVEC*CAPPA/ALOG(ELOG*YPLUS)                           PROMOD.19
 20.  0003578                VW(I,NJ)=UT(I)*UT(I)                                        PROMOD.20
 21.  0003628                IF(.NOT.INDIFF) GO TO 200                                   PROMOD.21
 22.  0003648                SP(I,NJM1)=SP(I,NJM1)-UT(I)*UT(I)*SEW(I)*R(NJ)*DZ/          PROMOD.22
                            1        W(I,NJM1,1)*DEN(I,NJM1,1)                           PROMOD.23
 23.  0004008                AN(I,NJM1)=0.0                                              PROMOD.24
 24.  0004038            200 CONTINUE                                                    PROMOD.25
 25.  0004068                IF(INDIFF) GO TO 220                                        PROMOD.26
 26.  0004078                DO 210 I=IM1,IM2                                            PROMOD.27
 27.  0004118                AN(I,NJM1)=0.0                                              PROMOD.28
 28.  0004138                DO 210 J=2,NJM1                                             PROMOD.29
 29.  0004168            210 SU(I,J)=SU(I,J)-(VW(I,J+1)*RV(J+1)-VW(I,J)*RV(J))*DEN(I,J,1)  PROMOD.30
                            1      *SEW(I)*DZ                                            PROMOD.31
 30.  0004368            220 CONTINUE                                                    PROMOD.32
 31.  0004368                DO 230 J=2,NJ                                               PROMOD.33
 32.  0004408                AW(IM1,J)=0.0                                               PROMOD.34
 33.  0004438                AE(IM2,J)=0.0                                               PROMOD.35
 34.  0004458            230 CONTINUE                                                    PROMOD.36
 35.  0004478                DO 240 I=IM1,IM2                                            PROMOD.37
 36.  0004508            240 AS(I,2)=0.0                                                 PROMOD.38
 37.  0004528                RETURN                                                      PROMOD.39
                    C*****************************************************************  PROMOD.40
                    C                          MEAN SCALAR                              PROMOD.41
                    C*****************************************************************  PROMOD.42
 38.  0004548                ENTRY MODC                                                  PROMOD.43
                    C       AN OUTER WALL                                                PROMOD.44
 39.  0004628                IF(.NOT.INTJRB) GO TO 660                                   DIM3.107
 40.  0004638                IF(IWALL.EQ.1) GO TO 660                                    PROMOD.45
 41.  0004658                DO 630 I=IM1,IM2                                            PROMOD.46
 42.  0004678                YREF=YV(NJ)-Y(NJM1)                                         PROMOD.47
 43.  0004718                VISREF=VISCOS                                               PROMOD.48
 44.  0004728                DENREF=DEN(I,NJM1,K)                                        PROMOD.49
 45.  0004778                YPLUS=UT(I)*DENREF*YREF/VISREF                              PROMOD.50
 46.  0005028                IF(QUE.EQ.0) GO TO 610                                      PROMOD.51
 47.  0005058                CT(I)=QUE(I)/(DEN(I,NJ,2)*UT(I)*SPHEAT)                     PROMOD.52
 48.  0005128                CDIF=CT(I)/CAPPAC*ALOG(YPLUS*ELOGC)                         PROMOD.53
 49.  0005218                C(I,NJ,2)=C(I,NJM1,1)+CDIF                                  PROMOD.54
 50.  0005308                GO TO 620                                                   PROMOD.55
 51.  0005308            610 CDIF=ABS(C(I,NJ,K)-C(I,NJM1,K))                             PROMOD.56
 52.  0005418                CT(I)=CDIF*CAPPAC/ALOG(ELOGC*YPLUS)                         PROMOD.57
 53.  0005508            620 VC(I,NJ)=-CT(I)*UT(I)                                       PROMOD.58
 54.  0005558                IF(.NOT.INDIFF) GO TO 630                                   PROMOD.59
 55.  0005578                SU(I,NJM1)=SU(I,NJM1)-VC(I,NJ)*DEN(I,NJM1,1)*SEW(I)*R(NJ)*DZ*  PROMOD.60
                            1                        SPHEAT                              PROMOD.61
 56.  0005758                AN(I,NJM1)=0.0                                              PROMOD.62
 57.  0006008            630 CONTINUE                                                    PROMOD.63
 58.  0006038                IF(INDIFF) GO TO 660                                        PROMOD.64
 59.  0006048                DO 650 I=IM1,IM2                                            PROMOD.65
 60.  0006068                AN(I,NJM1)=0.0                                              PROMOD.66
 61.  0006108                DO 650 J=2,NJM1                                             PROMOD.67
 62.  0006138            650 SU(I,J)=SU(I,J)-SPHEAT*DEN(I,J,1)*(SEW(I)*DZ*(VC(I,J+1)*RV(J+1)-  PROMOD.68
                            1        VC(I,J)*RV(J))+SNS(J)*DZ*(UC(I+1,J)-UC(I,J)))      PROMOD.69
 63.  0006418            660 CONTINUE                                                    DIM3.108
 64.  0006428                IF(IWALL.EQ.0) GO TO 669                                    DIM3.109
 65.  0006438                DO 661 I=IM1,IM2                                            DIM3.110
 66.  0006458                YREF=YV(NJP)-Y(NJPM1)                                       DIM3.111
 67.  0006478                VISREF=VIS(I,NJPM1,K)
```

```
 68.  0006548        DENREF=DEN(I,NJPM1,K)                                  DIM3.112
 69.  0006608        YPLUS=UT(I)*DENREF*YREF/VISREF                         DIM3.113
 70.  0006628        ARWALL=R(NJP)*SEW(I)*DZ                                DIM3.114
 71.  0006668        AN(I,NJP)=GAM(I,NJP1,K)/DET(I)*2.0*ARWALL              DIM3.115
 72.  0006758        AS(I,NJP1)=AN(I,NJP)                                   DIM3.116
 73.  0007028        AS(I,NJP)=CAPPAC*UT(I)*DEN(I,NJP,K)*ARWALL/            DIM3.117
                    1      ALOG(ELOGC*YPLUS)*SPHEAT                        DIM3.118
 74.  0007228        AN(I,NJPM1)=AS(I,NJP)                                  DIM3.119
 75.  0007308        VC(I,NJP)=0.0                                          DIM3.120
 76.  0007338        CT(I)=CAPPAC*(C(I,NJP,K)-C(I,NJPM1,K))/ALOG(ELOGC*YPLUS)  DIM3.121
 77.  0007508    661 CONTINUE                                               DIM3.122
               C---- ECCENTRIC CONDUCTING ANNULUS OF SPARROW AND BLACK S FLOW.  DIM3.123
                                                                            DIM3.124
 78.  0007548        MMAX=NJO-NJP-1                                         DIM3.125
 79.  0007558        DO 662 I=IM1,IM2                                       DIM3.126
 80.  0007578        DO 662 M=1,MMAX                                        DIM3.127
 81.  0007628        J=NJP+M                                                DIM3.128
 82.  0007638        EM=FLOAT(M)                                            DIM3.129
 83.  0007648        RAD=R(NJP)+DET(I)*(EM-0.5)                             DIM3.130
 84.  0007708        RAD1=R(NJP)+DET(I)*EM                                  DIM3.131
 85.  0007718        RADU1=R(NJP)+DETU(I+1)*(EM-0.5)                        DIM3.132
 86.  0007748        AW(I,J)=AE(I-1,J)                                      DIM3.133
 87.  0010008        AE(I,J)=GAM(I,J,2)/RADU1/SEWU(I+1)*DETU(I+1)*DZ        DIM3.134
 88.  0010118        AS(I,J)=AN(I,J-1)                                      DIM3.135
 89.  0010158        AN(I,J)=GAM(I,J,2)/DET(I)*RAD1*SEW(I)*DZ               DIM3.136
 90.  0010268        SU(I,J)=ES*RAD*SEW(I)*DET(I)*DZ                        DIM3.137
 91.  0010348        IF(ISTEP.EQ.1) WRITE(6,663) I,J,AE(I,J),AW(I,J),AN(I,J),AS(I,J),  DIM3.138
                    1      SU(I,J)                                         DIM3.139
 92.  0010768    663 FORMAT(10X,2I3,1P5E11.3)                               DIM3.140
 93.  0010768    662 CONTINUE                                               DIM3.141
 94.  0011038        IF(INDIFF) GO TO 664                                   DIM3.142
 95.  0011048        DO 666 I=IM1,IM2                                       DIM3.143
 96.  0011068        DO 666 J=2,NJM1                                        DIM3.144
 97.  0011118    666 SU(I,J)=SU(I,J)-SPHEAT*DEN(I,J,1)*(SEW(I)*DZ*(VC(I,J+1)*RV(J+1)-  DIM3.145
                    1        VC(I,J)*RV(J))+SNS(J)*DZ*(UC(I+1,J)-UC(I,J)))  DIM3.146
 98.  0011378    664 CONTINUE                                               DIM3.147
 99.  0011408        DO 665 I=IM1,IM2                                       DIM3.148
100.  0011428        SU(I,NJOM1)=SU(I,NJOM1)+QUO(I)*(R(NJP)+ET(I))*SEW(I)*DZ  DIM3.149
101.  0011528        AN(I,NJOM1)=0.0                                        DIM3.150
102.  0011548        VC(I,NJP)=-CT(I)*UT(I)                                 DIM3.151
103.  0011608    665 CONTINUE                                               DIM3.152
104.  0011628    669 CONTINUE                                               DIM3.153
105.  0011628        DO 670 J=2,NJO                                         PROMOD.71
106.  0011648        AW(IM1,J)=0.0                                          PROMOD.72
107.  0011678    670 AE(IM2,J)=0.0                                          PROMOD.73
108.  0011738        DO 680 I=IM1,IM2                                       PROMOD.74
109.  0011748    680 AS(I,2)=0.0                                            PROMOD.75
110.  0011768        RETURN                                                 PROMOD.76
               C*********************************************************** PROMOD.77
               C                    ALL TURBULENT VARIABLES                PROMOD.78
               C*********************************************************** PROMOD.79
111.  0012008        ENTRY MODRS                                            PROMOD.80
112.  0012068        DO 800 I=IM1,IM2                                       PROMOD.81
113.  0012108        GO TO (710,710,710,710,700,710,720,740,740,760,750,760,770)IRS  PROMOD.82
114.  0012248    700 RSWALL(JVW)=Y(NJM1)/Y(NJ)-VISCOS/DENSIT/UT(I)/CAPPA/DYNP(NJM1)  PROMOD.83
115.  0012338        WNEAR(I,JVW)=UT(I)*UT(I)*RSWALL(JVW)                   PROMOD.84
116.  0012378        GO TO 790                                              PROMOD.85
117.  0012408    710 WNEAR(I,IRS)=WNEAR(I,JVW)*RSWALL(IRS)                  PROMOD.86
118.  0012468        GO TO 790
```

```
119.  0012478      720 WNEAR(I,JED)=WNEAR(I,JVW)*UT(I)/CAPPA/DYNP(NJM1)                PROMOD.87
120.  0012578          GO TO 790                                                       PROMOD.88
121.  0012608      740 WNEAR(I,IRS)=0.0                                                PROMOD.89
122.  0012638          GO TO 790                                                       PROMOD.90
123.  0012638      750 CONTINUE                                                        PROMOD.91
124.  0012648          NJM2=NJM1-1                                                     PROMOD.92
125.  0012658          RDR=(R(NJ)*R(NJ)-R(NJM1)*R(NJM1))*0.5                           PROMOD.93
126.  0012718          QWF=QUE(I)*R(NJ)/DEN(I,NJ,2)/SPHEAT                             PROMOD.94
127.  0012768          IF(QUE(I).NE.0.0) DCDYB=(C(I,NJM1,2)-C(I,NJM2,2))/SNSV(NJM1)*   PROMOD.95
                      1     SNS(NJM1)/(Y(NJ)-Y(NJM1))                                 PROMOD.96
128.  0013168          IF(QUE(I).EQ.0.0) DCDYB=(C(I,NJM1,2)-C(I,NJM2,2))/SNSV(NJM1)*   PROMOD.97
                      1                          (Y(NJ)-Y(NJM1))/SNS(NJM1)            PROMOD.98
129.  0013348          QVIS=R(NJM1)*GAM(I,NJM1,2)*DCDYB/DEN(I,NJM1,2)/SPHEAT           PROMOD.99
130.  0013428          QAX=DCDZB(I)*W(I,NJM1,2)*RDR*0.8                                PROMOD.100
131.  0013508          CDXIP=(C(I+1,NJM1,2)-C(I,NJM1,2))/(RCV(NJM1)*SEWU(I+1))         DIM3.154
132.  0013578          CDXIM=(C(I,NJM1,2)-C(I-1,NJM1,2))/(RCV(NJM1)*SEWU(I))           DIM3.155
133.  0013668          IF(I.EQ.IM1) CDXIM=0.0                                          DIM3.156
134.  0013718          IF(I.EQ.IM2) CDXIP=0.0                                          DIM3.157
135.  0013748          QVISX=(CDXIP-CDXIM)/(RCV(NJM1)*SEW(I))*GAM(I,NJM1,2)*RDR/       DIM3.158
                      1      DEN(I,NJM1,2)/SPHEAT                                     DIM3.159
136.  0014048          QUC=(UC(I+1,NJM1)-UC(I,NJM1))/(RCV(NJM1)*SEW(I))*RDR            DIM3.160
137.  0014148                 VCB=(-QWF+QVIS+QAX-QVISX+QUC)/RCV(NJM1)                  DIM3.161
138.  0014228          WNEAR(I,JVC)=VCB                                                PROMOD.102
139.  0014268          GO TO 790                                                       PROMOD.103
140.  0014278      760 WNEAR(I,IRS)=WNEAR(I,JVC)*RSWALL(IRS)                           PROMOD.104
141.  0014358          GO TO 790                                                       PROMOD.105
142.  0014368      770 WNEAR(I,JC2)=CT(I)*CT(I)*RSWALL(JC2)                            PROMOD.106
143.  0014428      790 PHI(I,NJ)=(WNEAR(I,IRS)*SNS(NJM1)-PHI(I,NJM1)*DYNP(NJM1))/      PROMOD.107
                      1                    (Y(NJM1)-YV(NJM1))                          PROMOD.108
144.  0014618      800 CONTINUE                                                        PROMOD.109
145.  0014648          IF(NRS.EQ.JUW.OR.NRS.EQ.JUC) GO TO 910                          PROMOD.110
146.  0014678          DO 900 J=2,NJ                                                   PROMOD.111
147.  0014728          AW(IM1,J)=0.0                                                   PROMOD.112
148.  0014758      900 AE(IM2,J)=0.0                                                   PROMOD.113
149.  0015018      910 CONTINUE                                                        PROMOD.114
150.  0015018          IF(NRS.NE.JUW.AND.NRS.NE.JUC) GO TO 930                         PROMOD.115
151.  0015058          DO 920 I=IM1,IM2                                                PROMOD.116
152.  0015078      920 AS(I,2)=0.0                                                     PROMOD.117
153.  0015118      930 CONTINUE                                                        PROMOD.118
154.  0015128          RETURN                                                          PROMOD.119
155.  0015148          END                                                             PROMOD.120
```

```
119.  0012478      720 WNEAR(I,JED)=WNEAR(I,JVW)*UT(I)/CAPPA/DYNP(NJM1)                PROMOD.87
120.  0012578          GO TO 790                                                       PROMOD.88
121.  0012608      740 WNEAR(I,IRS)=0.0                                                PROMOD.89
122.  0012638          GO TO 790                                                       PROMOD.90
123.  0012638      750 CONTINUE                                                        PROMOD.91
124.  0012648          NJM2=NJM1-1                                                     PROMOD.92
125.  0012658          RDR=(R(NJ)*R(NJ)-R(NJM1)*R(NJM1))*0.5                           PROMOD.93
126.  0012718          QWF=QUE(I)*R(NJ)/DEN(I,NJ,2)/SPHEAT                             PROMOD.94
127.  0012768          IF(QUE(I).NE.0.0) DCDYB=(C(I,NJM1,2)-C(I,NJM2,2))/SNSV(NJM1)*   PROMOD.95
                     1      SNS(NJM1)/(Y(NJ)-Y(NJM1))                                 PROMOD.96
128.  0013168          IF(QUE(I).EQ.0.0) DCDYB=(C(I,NJM1,2)-C(I,NJM2,2))/SNSV(NJM1)*   PROMOD.97
                     1                    (Y(NJ)-Y(NJM1))/SNS(NJM1)                   PROMOD.98
129.  0013348          QVIS=R(NJM1)*GAM(I,NJM1,2)*DCDYB/DEN(I,NJM1,2)/SPHEAT           PROMOD.99
130.  0013428          QAX=DCDZB(I)*W(I,NJM1,2)*RDR*0.8                                PROMOD.100
131.  0013508          CDXIP=(C(I+1,NJM1,2)-C(I,NJM1,2))/(RCV(NJM1)*SEWU(I+1))         DIM3.154
132.  0013578          CDXIM=(C(I,NJM1,2)-C(I-1,NJM1,2))/(RCV(NJM1)*SEWU(I))           DIM3.155
133.  0013668          IF(I.EQ.IM1) CDXIM=0.0                                          DIM3.156
134.  0013718          IF(I.EQ.IM2) CDXIP=0.0                                          DIM3.157
135.  0013748          QVISX=(CDXIP-CDXIM)/(RCV(NJM1)*SEW(I))*GAM(I,NJM1,2)*RDR/       DIM3.158
                     1      DEN(I,NJM1,2)/SPHEAT                                      DIM3.159
136.  0014048          QUC=(UC(I+1,NJM1)-UC(I,NJM1))/(RCV(NJM1)*SEW(I))*RDR            DIM3.160
137.  0014148                VCB=(-QWF+QVIS+QAX-QVISX+QUC)/RCV(NJM1)                   DIM3.161
138.  0014228          WNEAR(I,JVC)=VCB                                                PROMOD.102
139.  0014268          GO TO 790                                                       PROMOD.103
140.  0014278      760 WNEAR(I,IRS)=WNEAR(I,JVC)*RSWALL(IRS)                           PROMOD.104
141.  0014358          GO TO 790                                                       PROMOD.105
142.  0014368      770 WNEAR(I,JC2)=CT(I)*CT(I)*RSWALL(JC2)                            PROMOD.106
143.  0014428      790 PHI(I,NJ)=(WNEAR(I,IRS)*SNS(NJM1)-PHI(I,NJM1)*DYNP(NJM1))/      PROMOD.107
                     1                    (Y(NJM1)-YV(NJM1))                          PROMOD.108
144.  0014618      800 CONTINUE                                                        PROMOD.109
145.  0014648          IF(NRS.EQ.JUW.OR.NRS.EQ.JUC) GO TO 910                          PROMOD.110
146.  0014678          DO 900 J=2,NJ                                                   PROMOD.111
147.  0014728          AW(IM1,J)=0.0                                                   PROMOD.112
148.  0014758      900 AE(IM2,J)=0.0                                                   PROMOD.113
149.  0015018      910 CONTINUE                                                        PROMOD.114
150.  0015018          IF(NRS.NE.JUW.AND.NRS.NE.JUC) GO TO 930                         PROMOD.115
151.  0015058          DO 920 I=IM1,IM2                                                PROMOD.116
152.  0015078      920 AS(I,2)=0.0                                                     PROMOD.117
153.  0015118      930 CONTINUE                                                        PROMOD.118
154.  0015128          RETURN                                                          PROMOD.119
155.  0015148          END                                                             PROMOD.120
```

0 0 0 0 4 9 0 1 3 7 4 6 7

```
 1.  0000008        SUBROUTINE OUTPUT                                                  OUTPUT.2
               C*********************************************************************  COMALL.2
               C                              COMMON BLOCKS                            COMALL.3
               C*********************************************************************  COMALL.4
 2.  0000008        DIMENSION SAVE(20229)                                              DIM3.1
 3.  0000008        DIMENSION TRANS(512)                                               DIM3.2
 4.  0000008        COMMON                                                             COMALL.6
                   1X(15),Y(30),Z(02),XU(15),YV(30),ZW(02),                            DIM3.3
                   1DXEP(15),DXPW(15),DYNP(30),DYPS(30),SEW(15),SNS(30),               DIM3.4
                   1DXEPU(15),DXPWU(15),SEWU(15),DYNPV(30),DYPSV(30),SNSV(30),         DIM3.5
                   1R(30),RV(30),RCV(30),WFN(30),WFS(30),WFE(15),WFW(15),              DIM3.6
                   1J(15,30,2),V(15,30,2),W(15,30,2),PE(15,30,2),C(15,30,2),PP(15,30), DIM3.7
                   1UU(15,30),UV(15,30),UW(15,30),VV(15,30),VW(15,30),WW(15,30),       DIM3.8
                   1ED(15,30),TE(15,30),FF(15,30),UC(15,30),VC(15,30),WC(15,30),       DIM3.9
                   1C2(15,30),EC(15,30),RS(15,30),                                     DIM3.10
                   1DEN(15,30,2),VIS(15,30,2),GAM(15,30,2),VISUU(15,30),VISVV(15,30),  DIM3.11
                   1AW(15,30),AE(15,30),AN(15,30),AS(15,30),AD(15,30),AU(15,30),       DIM3.12
                   1AP(15,30),SU(15,30),SP(15,30),                                     DIM3.13
                   1UT(15),CT(15),QUE(15),DCDZ8(15),QUD(15),                           DIM3.14
                   1DENSIT,VISCOS,PRANDT,SPHEAT,EXCHAT,                                COMALL.19
                   1CMU,CR1,CR2,CRS,CR1W,CR2W,CEPS1,CEPS2,CEPS,CAPPA,ELOG,             COMALL.20
                   1CC1,CC2,CC,CC1W,CC2W,CG2,CG,CAPPAC,ELOGC,                          COMALL.21
                   1JUU,JUV,JUW,JVV,JVW,JWW,JED,JTE,JFF,JUC,JVC,JWC,JC2,JEC,           COMALL.22
                   1NI,NIM1,NIM2,NJ,NJM1,NJM2,NK,NKM1,IT,JT,KT,IJT,                    COMALL.23
                   1HEDU(4),HEDV(4),HEDW(4),HEDP(4),HEDC(4),HEDR(4),HEDD(4),HEDVIS(4), COMALL.24
                   1INCALU,INCALV,INCALW,INCALP,INCALC,INPRO,INCALR(14),INTURB,INDIFF, COMALL.25
                   1NSWPU,NSWPV,NSWPW,NSWPP,NSWPC,NSWPR,                               COMALL.26
                   1MODEL,MODEC,MRW,MCW,IQUE,IDIF,IJET,ITEST,ITESU,ITESC,ICON,         COMALL.27
                   1IRUN,IU,IHT,IU1,IU2,IC1,IC2,I1,I2,INDCOS,FRA,                      COMALL.28
                   1K,DZ,ISTEP,ISTP1,NRS,INDEX,DPDZ,                                   COMALL.29
                   1FLOWIN,VMEAN,QLENTH,SMALL,GREAT,XTOT,YTOT,RSWALL(14),              COMALL.30
                   1ZDPRO(18),IPRO,IEND,INDPRI,NUMPRI,BVE,BVW,BVS,BWS                  COMALL.31
 5.  0000008        COMMON                                                             DIM3.15
                   1ET(15),ETU(15),DET(15),DETU(15),DYW,NJP,NJP1,NJPM1,IWALL,          DIM3.16
                   1ROJTER,RINNER,ECCEN,ES,NJO,YTOTO,EXCHAW,NJOM1                      DIM3.17
 6.  0000008        COMMON  OLDU(30),OLDV(30),OLDW(30),OLDP(30),                       DIM3.18
                   1        OLDUU(30),OLDUV(30),OLDUW(30),OLDVV(30),OLDVW(30),         DIM3.19
                   1        OLDWW(30),OLDTE(30),OLDED(30),OLDFF(30),                   DIM3.20
                   1        OLDDEN(30),OLDVIS(30),OVISUU(30),OVISVV(30),               DIM3.21
                   1        OLDUTA,OOPDZ                                               DIM3.22
 7.  0000008        LOGICAL INCALU,INCALV,INCALW,INCALP,INCALC,INPRO,                  COMALL.32
                   1        INCALR,INTURB,INDIFF                                       COMALL.33
 8.  0000008        EQUIVALENCE (X(1),SAVE(1))                                         COMALL.34
 9.  0000008        EQUIVALENCE (OLDU(1),TRANS(1))                                     DIM3.23
10.  0000008        DIMENSION AT(30),OU1(15,30),OU2(15,30),OU3(15,30),OU4(15,30),      DIM3.162
                   1                  OU5(15,30)                                      DIM3.163
11.  0000008        REAL MINC,MAXC                                                     DIM3.164
               C*********************************************************************  OUTPUT.4
               C                          SINGLE VARIABLES                             OUTPUT.5
               C*********************************************************************  OUTPUT.6
12.  0000008        WRITE(6,010)                                                       OUTPUT.7
13.  0043558        ZD=Z(2)/YTOT/2.                                                    OUTPUT.8
14.  0043568        WRITE(6,020) ISTEP,ZD,DZ,DPDZ,UT(3)                                OUTPUT.9
15.  0043708        IF(IU.EQ.0.AND.INDEX.NE.0) GO TO 110                               OUTPUT.10
16.  0043728        DO 100 I=IU1,IU2                                                   OUTPUT.11
17.  0043748        TAU=UT(I)*UT(I)*DENSIT                                             OUTPUT.12
18.  0043758        IF(.NOT.INTURB) TAU=VISCOS*(W(I,NJM1,2)-W(I,NJ,2))                 OUTPUT.13
```

```
                  1                    /(Y(NJ)-Y(NJM1))                    OUTPUT.14
 19.  0044138        CF=TAU/(0.5*DENSIT*W(I,1,K)*W(I,1,K))                OUTPUT.15
 20.  0044208        DEL1=0.0                                             OUTPUT.16
 21.  0044218        DEL2=0.0                                             OUTPUT.17
 22.  0044228        DO 100 J=2,NJM1                                      OUTPUT.18
 23.  0044258        WR=W(I,J,2)/W(I,1,2)                                 OUTPUT.19
 24.  0044308        DEL1=DEL1+(1.0-WR)*SNS(J)                            OUTPUT.20
 25.  0044348    100 DEL2=DEL2+WR*(1.0-WR)*SNS(J)                         OUTPUT.21
 26.  0044438        EH=DEL1/(DEL2+1.E-30)                                OUTPUT.22
 27.  0044458        WRITE(6,030) CF,DEL1,DEL2,EH                         OUTPUT.23
 28.  0044558    110 IF(IHT.EQ.0) GO TO 140                               OUTPUT.24
 29.  0044568        CFLUX=0.0                                            OUTPUT.25
 30.  0044568        DELC=0.0                                             OUTPUT.26
 31.  0044568        DO 120 I=IC1,IC2                                     OUTPUT.27
 32.  0044618        DO 120 J=2,NJ                                        OUTPUT.28
 33.  0044648        CFLUX=CFLUX+W(I,J,2)*C(I,J,2)*RCV(J)*SEW(I)*SNS(J)*DEN(I,J,2)  OUTPUT.29
                  1          *SPHEAT                                     OUTPUT.30
 34.  0044768        WR=W(I,J,2)/W(I,1,2)                                 OUTPUT.31
 35.  0045008        CR=(C(I,J,2)-C(I,1,2))/(C(I,NJ,2)-C(I,1,2)+SMALL)    OUTPUT.32
 36.  0045078    120 DELC=DELC+WR*CR*SNS(J)                               OUTPUT.33
 37.  0045168        WRITE(6,040) DELC,CFLUX,CT(3)                        OUTPUT.34
 38.  0045248        CBULK=CFLUX/(VMEAN*R(NJ)*R(NJ)*0.5*(XU(I2+1)-XU(I1)))/DENSIT  OUTPUT.35
                  1          /SPHEAT                                     OUTPUT.36
 39.  0045348        WRITE(6,50)                                          OUTPUT.37
 40.  0045418        DO 130 I=1,NI                                        DIM3.165
 41.  0045438        THETA=X(I)/3.14159*180.                              OUTPUT.39
 42.  0045458        CDIFF=(C(I,NJ,2)-CBULK)/(CBULK+SMALL)                OUTPUT.41
 43.  0045538        STAN=QUE(I)/(C(I,NJ,2)-CBULK+SMALL)/(DENSIT*VMEAN*SPHEAT)  OUTPUT.42
 44.  0045638        ENUSS=STAN*PRANDT*DENSIT*VMEAN*2.0*YTOT/VISCOS       OUTPUT.43
 45.  0045708        IF(STAN.GE.1.E+20) STAN=6H                           OUTPUT.44
 46.  0045758        WRITE(6,060) I,THETA,QUO(I),QUE(I),CT(I),CDIFF,CBULK,STAN,ENUSS  OUTPUT.45
 47.  0046148    130 CONTINUE                                             OUTPUT.46
 48.  0046168    140 CONTINUE                                             OUTPUT.47
 49.  0046178        WRITE(6,10)                                          OUTPUT.48
 50.  0046228        IF(MOD(ISTEP,INOPRI).EQ.0.AND.MOD(ISTEP,NUMPRI).NE.0) RETURN  OUTPUT.49
            C*********************************************************************  OUTPUT.50
            C                 OUTPUT FROM HYDRODYNAMIC CALCULATIONS                OUTPUT.51
            C*********************************************************************  OUTPUT.52
            C*****MEAN VELOCITY FIELD                                      OUTPUT.53
 51.  0046348        IF(IU.EQ.0.AND.INDEX.EQ.1) GO TO 500                 OUTPUT.54
 52.  0046378        WRITE(6,240)                                         OUTPUT.55
 53.  0046428        DO 200 I=IU1,IU2                                     OUTPUT.56
 54.  0046448        DO 200 J=1,NJ                                        OUTPUT.57
 55.  0046478        OUT1=Y(J)/Y(NJ)                                      OUTPUT.58
 56.  0046508        OUT2=W(I,J,2)/UT(I)                                  OUTPUT.59
 57.  0046548        OUT3=(Y(NJ)-Y(J))*UT(I)/VISCOS                       OUTPUT.60
 58.  0046568        OUT4=W(I,J,2)/W(I,1,2)                               OUTPUT.61
 59.  0046608        WRITE(6,250) J,Y(J),U(I,J,2),V(I,J,2),W(I,J,2),PE(I,J,2),PP(I,J)  OUTPUT.62
                  1              ,OUT1,OUT2,OUT3,OUT4                     OUTPUT.63
 60.  0047128    200 CONTINUE                                             OUTPUT.64
 61.  0047178        IF(.NOT.INTURB) GO TO 500                            OUTPUT.65
            C*********************************************************************  OUTPUT.66
            C*****TWO-EQUATION MODEL                                       OUTPUT.67
 62.  0047208        IF(MODEL.NE.3) GO TO 390                             OUTPUT.68
 63.  0047228        WRITE(6,340)                                         OUTPUT.69
 64.  0047268        DO 300 I=IU1,IU2                                     OUTPUT.70
 65.  0047308        DO 300 J=1,NJM1                                      OUTPUT.71
 66.  0047338        OUT1=Y(J)/Y(NJ)                                      OUTPUT.72
```

```
 67.  0047348        OUT2=TE(I,J)/UT(I)/UT(I)                                  OUTPUT.73
 68.  0047418        OUT3=ED(I,J)*Y(NJ)/UT(I)**3                               OUTPUT.74
 69.  0047448        OUT4=VIS(I,J,2)/UT(I)/Y(NJ)                               OUTPUT.75
 70.  0047508        OUT5=-(VIS(I,J,2)+VIS(I,J+1,2))*0.5*(W(I,J+1,2)-W(I,J,2))/ OUTPUT.76
                    1      (Y(J+1)-Y(J))/UT(I)/UT(I)                          OUTPUT.77
 71.  0047618        WRITE(6,350) J,OUT1,TE(I,J),ED(I,J),OUT2,OUT3,OUT4,OUT5   OUTPUT.78
 72.  0050018    300 CONTINUE                                                  OUTPUT.79
 73.  0050068        RETURN                                                    OUTPUT.80
 74.  0050108    390 CONTINUE                                                  OUTPUT.81
                C*********************************************************** OUTPUT.82
                C*****REYNOLDS STRESSES                                        OUTPUT.83
 75.  0050108        WRITE(6,440)                                              OUTPUT.84
 76.  0050138        DO 400 I=IU1,IU2                                          OUTPUT.85
 77.  0050158        DO 400 J=2,NJ                                             OUTPUT.86
 78.  0050208        OUT1=YV(J)/Y(NJ)                                          OUTPUT.87
 79.  0050218        OUT2=UU(I,J)/UT(I)/UT(I)                                  OUTPUT.88
 80.  0050258        OUT3=VV(I,J)/UT(I)/UT(I)                                  OUTPUT.89
 81.  0050278        OUT4=WW(I,J)/UT(I)/UT(I)                                  OUTPUT.90
 82.  0050318        OUT5=TE(I,J)/UT(I)/UT(I)                                  OUTPUT.91
 83.  0050338        OUT6=-VW(I,J)/(W(I,J,2)-W(I,J-1,2)-SMALL)*(Y(J)-Y(J-1))/  OUTPUT.92
                    1         R(NJ)/UT(I)                                      OUTPUT.93
 84.  0050468        WRITE(6,450) J,OUT1,UU(I,J),VV(I,J),WW(I,J),OUT2,OUT3,OUT4 OUTPUT.94
                    1        ,OUT5,OUT6                                        OUTPUT.95
 85.  0050728    400 CONTINUE                                                  OUTPUT.96
                C-----SOME DETAILED INFORMATION                               OUTPUT.97
 86.  0050778        WRITE(6,460)                                              OUTPUT.98
 87.  0051028        DO 470 I=IU1,IU2                                          OUTPUT.99
 88.  0051048        DO 470 J=2,NJ                                             OUTPUT.100
 89.  0051078        OUT1=YV(J)/Y(NJ)                                          OUTPUT.101
 90.  0051108        OUT2=VW(I,J)/UT(I)/UT(I)                                  OUTPUT.102
 91.  0051148        OUT3=-VW(I,J)*(W(I,J,2)-W(I,J-1,2))/(Y(J)-Y(J-1))/(ED(I,J)+SMALL) OUTPUT.103
 92.  0051278        OUT4=ED(I,J)*Y(NJ)/UT(I)**3                               OUTPUT.104
 93.  0051328        OUT5=VISUU(I,J)/UT(I)/Y(NJ)                               OUTPUT.105
 94.  0051338        OUT6=VISVV(I,J)/UT(I)/Y(NJ)                               OUTPUT.106
 95.  0051358        OUT7=VW(I,J)/(SQRT(ABS(WW(I,J)*VV(I,J)))+SMALL)           OUTPUT.107
 96.  0051478        WRITE(6,480) J,OUT1,VW(I,J),UW(I,J),ED(I,J),OUT2,OUT3,OUT4 OUTPUT.108
                    1             ,OUT5,OUT6,OUT7                              OUTPUT.109
 97.  0051718    470 CONTINUE                                                  OUTPUT.110
 98.  0051768    500 CONTINUE                                                  OUTPUT.111
                C*********************************************************** OUTPUT.112
                C                  OUTPUT FROM SCALAR TRANSPORT CALCULATIONS  OUTPUT.113
                C*********************************************************** OUTPUT.114
                C*****MEAN SCALAR FIELD                                        OUTPUT.115
 99.  0051768        IF(IHT.EQ.0) RETURN                                       OUTPUT.116
100.  0052018        IF(IHT.EQ.2) GO TO 800                                    OUTPUT.117
101.  0052028        WRITE(6,640)                                              OUTPUT.118
102.  0052068        DO 600 I=IC1,IC2                                          OUTPUT.119
103.  0052108        DO 600 J=2,NJ                                             OUTPUT.120
104.  0052138        OUT1=Y(J)/Y(NJ)                                           OUTPUT.121
105.  0052148        OUT2=(C(I,NJ,2)-C(I,J,2))/(CT(I)+SMALL)                   OUTPUT.122
106.  0052258        OUT3=(C(I,NJ,2)-C(I,J,2))/(C(I,NJ,2)-C(I,1,2))            OUTPUT.123
107.  0052338        OUT4=(VW(I,J)*(C(I,J,2)-C(I,J-1,2)))/                     OUTPUT.124
                    1      (VC(I,J)*(W(I,J,2)-W(I,J-1,2))+SMALL)              OUTPUT.125
108.  0052458        WRITE(6,650) J,OUT1,C(I,J,2),OUT2,OUT3,OUT4               OUTPUT.126
109.  0052638    600 CONTINUE                                                  OUTPUT.127
110.  0052708        IF(.NOT.INTURB) RETURN                                    OUTPUT.128
                C*************************** ***************************************** OUTPUT.1
                C*****SCALAR FLUXES AND SCAL  FLUCTUATIONS                    OUTPUT.13
```

```
111.  005273B        WRITE(6,740)                                          OUTPUT.131
112.  005276B        DO 700 I=IC1,IC2                                      OUTPUT.132
113.  005300B        DO 700 J=2,NJ                                         OUTPUT.133
114.  005303B        OUT1=YV(J)/Y(NJ)                                      OUTPUT.134
115.  005304B        OUT2=UC(I,J)/(UT(I)*CT(I)+SMALL)                      OUTPUT.135
116.  005312B        OUT3=VC(I,J)/(UT(I)*CT(I)+SMALL)                      OUTPUT.136
117.  005314B        OUT4=WC(I,J)/(UT(I)*CT(I)+SMALL)                      OUTPUT.137
118.  005317B        OUT5=C2(I,J)/(CT(I)*CT(I)+SMALL)                      OUTPUT.138
119.  005322B        OUT6=-VC(I,J)/(C(I,J,2)-C(I,J-1,2)+SMALL)*(Y(J)-Y(J-1))  OUTPUT.139
                    1     *DENSIT/VISCOS                                  OUTPUT.140
120.  005336B        WRITE(6,750) J,OUT1,UC(I,J),VC(I,J),WC(I,J),C2(I,J),EC(I,J),  OUTPUT.141
                    1             OUT2,OUT3,OUT4,OUT5,OUT6                OUTPUT.142
121.  005366B    700 CONTINUE                                              OUTPUT.143
                C                                                         OUTPUT.144
122.  005373B        RETURN                                                OUTPUT.145
123.  005375B    800 CONTINUE                                              OUTPUT.146
124.  005375B        IF(INDEX.NE.0) GO TO 805                              DIM3.166
125.  005376B        DO 804 I=1,IT                                         DIM3.167
126.  005400B        DO 804 J=1, JT                                        DIM3.168
127.  005403B        OU1(I,J)=0.0                                          DIM3.169
128.  005405B        OU2(I,J)=0.0                                          DIM3.170
129.  005406B        OU3(I,J)=0.0                                          DIM3.171
130.  005406B        OU4(I,J)=0.0                                          DIM3.172
131.  005407B        OU5(I,J)=0.0                                          DIM3.173
132.  005407B    804 CONTINUE                                              DIM3.174
133.  005413B        NT=NJO                                                DIM3.175
134.  005413B    805 CONTINUE                                              DIM3.176
135.  005415B        MAXC=-GREAT                                           DIM3.177
136.  005416B        MINC=GREAT                                            DIM3.178
137.  005416B        DO 810 J=1,NJ                                         DIM3.179
138.  005421B        AT(J)=YV(J)/Y(NJ)                                     DIM3.180
139.  005422B        DO 810 I=1,NI                                         DIM3.181
140.  005425B        MINC=AMIN1(MINC,C(I,J,2))                             DIM3.182
141.  005431B        MAXC=AMAX1(MAXC,C(I,J,2))                             DIM3.183
142.  005433B    810 CONTINUE                                              DIM3.184
143.  005437B        DO 820 J=1,NJO                                        DIM3.185
144.  005441B        DO 820 I=1,NI                                         DIM3.186
145.  005444B        OU1(I,J)=C(I,J,K)/(CBULK+SMALL)                       DIM3.187
146.  005453B        OU2(I,J)=(C(I,J,K)-MINC)/(MAXC-MINC+SMALL)            DIM3.188
147.  005463B    820 CONTINUE                                              DIM3.189
148.  005467B        IF(INCALC) CALL PRINT(1,1,NI,NT,IT,JT,KT,X,Y,C,HEDC,2)  DIM3.190
149.  005472B        IF(INCALC) CALL PRINT(1,1,NI,NT,IT,JT,KT,X,Y,OU1,HEDC,1)  DIM3.191
150.  005475B        IF(INCALC) CALL PRINT(1,1,NI,NT,IT,JT,KT,X,Y,OU2,HEDC,1)  DIM3.192
151.  005500B        IF(INCALR(JUC))CALL PRINT(1,1,NI,NJ   ,IT,JT,KT,X,AT,UC,  DIM3.193
                    1             40H          TANGENTIAL SCALAR FLUX     ,1)  DIM3.194
152.  005503B        IF(INCALR(JVC))CALL PRINT(1,1,NI,NJ   ,IT,JT,KT,X,AT,VC,  DIM3.195
                    1             40H            RADIAL SCALAR FLUX       ,1)  DIM3.196
153.  005506B        IF(INCALR(JWC))CALL PRINT(1,1,NI,NJ   ,IT,JT,KT,X,AT,WC,  DIM3.197
                    1             40H            AXIAL SCALAR FLUX        ,1)  DIM3.198
154.  005511B        IF(INCALR(JC2))CALL PRINT(1,1,NI,NJ   ,IT,JT,KT,X,AT,C2,  DIM3.199
                    1             40H       ( SCALAR FLUCTUATION )**2     ,1)  DIM3.200
155.  005514B        IF(INCALR(JEC))CALL PRINT(1,1,NI,NJ   ,IT,JT,KT,X,AT,EC,  DIM3.201
                    1             40H        SCALAR DISSIPATION RATE      ,1)  DIM3.202
156.  005517B        DO 825 I=1,NI                                         DIM3.203
157.  005521B        DO 825 J=1,NJ                                         DIM3.204
158.  005524B        OU1(I,J)=0.0                                          DIM3.205
159.  005526B        OU2(I,J)=0.0                                          DIM3.206
160.  005527B    825 CONTINUE                                              DIM3.207
```

```
161.  0055328        DO 830 I=IC1,IC2                                          DIM3.208
162.  0055348        DO 830 J=2,NJM1                                           DIM3.209
163.  0055378        DU1(I,J)=-VW(I,J)*(Y(J)-Y(J-1))/(W(I,J,K)-W(I,J-1,K)-SMALL)  DIM3.210
164.  0055528        DU2(I,J)=-VC(I,J)*(Y(J)-Y(J-1))/(C(I,J,K)-C(I,J-1,K)-SMALL)  DIM3.211
165.  0055658        DU3(I,J)=-UC(I,J)/(C(I,J,K)-C(I-1,J,K)+SMALL)*SEWU(I)*RCV(J)  DIM3.212
166.  0056008        DU4(I,J)=DU1(I,J)/(DU2(I,J)+SMALL)                        DIM3.213
167.  0056028        DU5(I,J)=DU3(I,J)/(DU2(I,J)+SMALL)                        DIM3.214
168.  0056058    830 CONTINUE                                                  DIM3.215
169.  0056118        IF(ISTEP.LE.1) CALL PRINT(1,1,NI,NJ,IT,JT,KT,X,AT,DU1,    DIM3.216
                    1              40H     MOMENTUM DIFFUSIVITY -RADIAL-      ,1)  DIM3.217
170.  0056158        CALL PRINT(1,1,NI,NJ    ,IT,JT,KT,X,AT,DU2,               DIM3.218
                    1              40H      SCALAR DIFFUSIVITY -RADIAL-       ,1)  DIM3.219
171.  0056178        CALL PRINT(1,1,NI,NJ    ,IT,JT,KT,X,AT,DU3,               DIM3.220
                    1              40H    SCALAR DIFFUSIVITY -TANGENTIAL-     ,1)  DIM3.221
172.  0056218        CALL PRINT(1,1,NI,NJ    ,IT,JT,KT,X,AT,DU4,               DIM3.222
                    1              40H         PRANDTL NUMBER -RADIAL-        ,1)  DIM3.223
173.  0056238        CALL PRINT(1,1,NI,NJ    ,IT,JT,KT,X,AT,DU5,               DIM3.224
                    1              40HRATIO OF DIFFUSIVITIES,TANGENTIAL/RADIAL,1)  DIM3.225
174.  0056258        RETURN                                                    OUTPUT.147
                C*****************************************************************  OUTPUT.148
                C                          FORMAT STATEMENTS                    OUTPUT.149
                C*****************************************************************  OUTPUT.150
175.  0056278     10 FORMAT(///1H0,120(1H*)///)                                OUTPUT.151
176.  0056278     20 FORMAT(1H ,20X,*STEP=*,I4,3X,* ZD=*,1PE10.3,*  DZ=*,1PE10.3,  OUTPUT.152
                    1        *  DPDZ=*,1PE10.3,*  UTAU=*,1PE10.3)              OUTPUT.153
177.  0056278     30 FORMAT(1H ,32X,* CF=*,1PE10.3,*DEL1=*,1PE10.3,*  DEL2=*,   OUTPUT.154
                    1        1PE10.3,*    EH=*,1PE10.3)                        OUTPUT.155
178.  0056278     40 FORMAT(1H ,31X,*DELC=*,1PE10.3,*CFLUX=*,1PE10.3)           OUTPUT.156
179.  0056278     50 FORMAT(34X,*I      THETA       QO        QI        CTAU     (CW-CB)/CB*  OUTPUT.157
                    1  ,*        CBULK        STAN        NUSS*)                OUTPUT.158
180.  0056278     60 FORMAT(33X,I2,1P8E11.3)                                   OUTPUT.159
181.  0056278    240 FORMAT(//2X,* J      Y           U           V           W*  OUTPUT.160
                    1      ,*          P           PP          Y/R        WPLUS*  OUTPUT.161
                    1      ,*      YPLUS       W/WMAX    */)                    OUTPUT.162
182.  0056278    250 FORMAT(2X,I2,1P10E11.3)                                   OUTPUT.163
183.  0056278    340 FORMAT(//2X,* J     Y/R        K.E.         ED         K/UT2*  OUTPUT.164
                    1      ,*      ER/UT3      VIS/UT/R  SHEAR/UT2*/)           OUTPUT.165
184.  0056278    350 FORMAT(2X,I2,1P7E11.3)                                    OUTPUT.166
185.  0056278    440 FORMAT(//2X,* J     YV/R        UU          VV          WW*  OUTPUT.167
                    1      ,*         UU/UT2      VV/UT2      WW/UT2      TE/UT2*  OUTPUT.168
                    1      ,*  W-DIFFUSIVITY*/)                                 OUTPUT.169
186.  0056278    450 FORMAT(2X,I2,1P9E11.3)                                    OUTPUT.170
187.  0056278    460 FORMAT(//2X,* J     YV/R        VW          UW          ED*  OUTPUT.171
                    1      ,*       VW/UT2       P/E       ER/UT3    VIUU/UTR*  OUTPUT.172
                    1      ,*   VIVV/UTR     VW/V/W*/)                         OUTPUT.173
188.  0056278    480 FORMAT(2X,I2,1P10E11.3)                                   OUTPUT.174
189.  0056278    640 FORMAT(//2X,* J     Y/R          C         CPLUS       CBAR*,  OUTPUT.175
                    1        *      PR*/)                                      OUTPUT.176
190.  0056278    650 FORMAT(2X,I2,1P5E11.3)                                    OUTPUT.177
191.  0056278    740 FORMAT(//2X,* J   YV/R         UC          VC          WC*,  OUTPUT.178
                    1        *          C2          EC       UC/UTCT     VC/UTCT*,  OUTPUT.179
                    1        *     WC/UTCT     C2/CTCT     VC/DCY*/)            OUTPUT.180
192.  0056278    750 FORMAT(2X,I2,1P11E11.3)                                   OUTPUT.181
193.  0056278        END                                                       OUTPUT.182
```

```
  1.  000000B        SUBROUTINE LISOLV (ISTART,JSTART,PHI1,N,KP,NS,IM1,IM2)                LISOLV.2
              C*********************************************************************       COMALL.2
              C                              COMMON BLOCKS                                  COMALL.3
              C*********************************************************************       COMALL.4
  2.  0000008        DIMENSION SAVE(20229)                                                  DIM3.1
  3.  0000008        DIMENSION TRANS(512)                                                   DIM3.2
  4.  0000008        COMMON                                                                 COMALL.6
                    1X(15),Y(30),Z(02),XU(15),YV(30),ZW(02),                                DIM3.3
                    1DXEP(15),DXPW(15),DYNP(30),DYPS(30),SEW(15),SNS(30),                   DIM3.4
                    1DXEPU(15),DXPWU(15),SEWU(15),DYNPV(30),DYPSV(30),SNSV(30),             DIM3.5
                    1R(30),RV(30),RCV(30),WFN(30),WFS(30),WFE(15),WFW(15),                  DIM3.6
                    1U(15,30,2),V(15,30,2),W(15,30,2),PE(15,30,2),C(15,30,2),PP(15,30),     DIM3.7
                    1UU(15,30),UV(15,30),UW(15,30),VV(15,30),VW(15,30),WW(15,30),           DIM3.8
                    1ED(15,30),TE(15,30),FF(15,30),UC(15,30),VC(15,30),WC(15,30),           DIM3.9
                    1C2(15,30),EC(15,30),RS(15,30),                                         DIM3.10
                    1DEN(15,30,2),VIS(15,30,2),GAM(15,30,2),VISUU(15,30),VISVV(15,30),      DIM3.11
                    1AW(15,30),AE(15,30),AN(15,30),AS(15,30),AD(15,30),AU(15,30),           DIM3.12
                    1AP(15,30),SU(15,30),SP(15,30),                                         DIM3.13
                    1UT(15),CT(15),QUE(15),DCDZB(15),QUO(15),                               DIM3.14
                    1DENSIT,VISCOS,PRANDT,SPHEAT,EXCHAT,                                    COMALL.19
                    1CMJ,CR1,CR2,CRS,CR1W,CR2W,CEPS1,CEPS2,CEPS,CAPPA,ELOG,                 COMALL.20
                    1CC1,CC2,CC,CC1W,CC2W,CG2,CG,CAPPAC,ELOGC,                              COMALL.21
                    1JUU,JUV,JUW,JVV,JVW,JWW,JED,JTE,JFF,JUC,JVC,JWC,JC2,JEC,               COMALL.22
                    1NI,NIM1,NIM2,NJ,NJM1,NJM2,NK,NKM1,IT,JT,KT,IJT,                        COMALL.23
                    1HEDU(4),HEDV(4),HEDW(4),HEDP(4),HEDC(4),HEDE(4),HEDD(4),HEDVIS(4),     COMALL.24
                    1INCALU,INCALV,INCALW,INCALP,INCALC,INPRO,INCALR(14),INTURB,INDIFF,     COMALL.25
                    1NSWPU,NSWPV,NSWPW,NSWPP,NSWPC,NSWPR,                                   COMALL.26
                    1MODEL,MJDEC,MRW,MCW,IQUE,IDIF,IJET,ITEST,ITESU,ITESC,ICON,             COMALL.27
                    1IRUN,IU,IHT,IU1,IU2,IC1,IC2,I1,I2,INDCOS,FRA,                          COMALL.28
                    1K,DZ,ISTEP,ISTP1,NRS,INDEX,DPDZ,                                       COMALL.29
                    1FLOWIN,VMEAN,QLENTH,SMALL,GREAT,XTOT,YTOT,RSWALL(14),                  COMALL.30
                    1ZDPRO(18),IPRO,IEND,INDPRI,NUMPRI,BVE,BVW,BVS,BWS                      COMALL.31
  5.  0000008        COMMON                                                                 DIM3.15
                    1ET(15),ETU(15),DET(15),DETU(15),DYW,NJP,NJP1,NJPM1,IWALL,              DIM3.16
                    1ROUTER,RINNER,ECCEN,ES,NJO,YTOTO,EXCHAW,NJOM1                          DIM3.17
  6.  0000008        COMMON  OLDU(30),OLDV(30),OLDW(30),OLDP(30),                           DIM3.18
                    1        OLDJU(30),OLDUV(30),OLDUW(30),OLDVV(30),OLDVW(30),             DIM3.19
                    1        OLDWW(30),OLDTE(30),OLDED(30),OLDFF(30),                       DIM3.20
                    1        OLDDEN(30),OLDVIS(30),OVISUU(30),OVISVV(30),                   DIM3.21
                    1        OLDUTA,OOPDZ                                                   DIM3.22
  7.  0000008        LOGICAL INCALU,INCALV,INCALW,INCALP,INCALC,INPRO,                      COMALL.32
                    1        INCALR,INTURB,INDIFF                                           COMALL.33
  8.  0000008        EQUIVALENCE (X(1),SAVE(1))                                             COMALL.34
  9.  0000008        EQUIVALENCE (OLDU(1),TRANS(1))                                         DIM3.23
 10.  0000008        DIMENSION PHI1(15,30,2),PHI(15,30,2),A(30),B(30),CA(50),D(30)          DIM3.226
              C*********************************************************************       LISOLV.6
              C*****WEST-EAST SWEEP                                                         LISOLV.7
 11.  0000008        JSTM1=JSTART-1                                                         LISOLV.8
              C   INITIALISE PHI ARRAY.                                                     LISOLV.9
 12.  0020218        DO 10 I=1,NI                                                           LISOLV.10
 13.  0020238        DO 10 J=1,NJ                                                           LISOLV.11
 14.  0020268        IF(N.EQ.1)PHI(I,J,1)=PHI1(I,J,1)                                       LISOLV.12
 15.  0020358     10 PHI(I,J,2)=PHI1(I,J,KP)                                                LISOLV.13
 16.  0020518        A(JSTM1)=0.0                                                           LISOLV.14
              C-----COMMENCE W-E SWEEP                                                      LISOLV.15
 17.  0020518        DO 100 I=IM1,IM2                                                       LISOLV.16
 18.  0020548        CA(JSTM1)=PHI(I,JSTM1,K)                                               LISOLV.17
```

```
LISOLV                **SUBROUTINE LISOLV (ISTART,JSTART,PHI1,N,KP,NS,IM1,IM2)**
                                                                          LISOLV.18
              C-----COMMENCE S-N TRAVERSE                                 LISOLV.19
 19.   002060B        DO 101 J=JSTART,NJM1                                LISOLV.20
              C-----ASSEMBLE TDMA COEFFICIENTS                            LISOLV.21
 20.   002064B        A(J)=AN(I,J)                                        LISOLV.22
 21.   002067B        B(J)=AS(I,J)                                        LISOLV.23
 22.   002070B        CA(J)=AE(I,J)*PHI(I+1,J,K)+AW(I,J)*PHI(I-1,J,K)+    LISOLV.24
                     1AU(I,J)*PHI(I,J,K-1)+SU(I,J)                        LISOLV.25
 23.   002103B        D(J)=AP(I,J)                                        LISOLV.26
              C-----CALCULATE COEFFICIENTS OF RECURRENCE FORMULA          LISOLV.27
 24.   002104B        TERM=1./(D(J)-B(J)*A(J-1))                          LISOLV.28
 25.   002107B        A(J)=A(J)*TERM                                      LISOLV.29
 26.   002111B    101 CA(J)=(CA(J)+B(J)*CA(J-1))*TERM                      LISOLV.30
              C-----OBTAIN NEW PHI*S                                      LISOLV.31
 27.   002116B        DO 102 JJ=JSTART,NJM1                               LISOLV.32
 28.   002120B        J=NJ+JSTM1-JJ                                       LISOLV.33
 29.   002121B    102 PHI1(I,J,KP)=A(J)*PHI1(I,J+1,KP)+CA(J)              LISOLV.34
 30.   002132B    100 CONTINUE                                            LISOLV.35
 31.   002135B        IF(NS.EQ.2) GO TO 150                               LISOLV.36
 32.   002137B        DO 11 I=ISTART,NIM1                                 LISOLV.37
 33.   002141B        DO 11 J=JSTART,NJM1                                 LISOLV.38
 34.   002144B        PHI1(I,J,KP)=PHI1(3,J,KP)                           LISOLV.39
 35.   002153B     11 PHI(I,J,K)=PHI1(3,J,KP)                             LISOLV.40
 36.   002165B        RETURN                                              LISOLV.41
 37.   002167B    150 CONTINUE                                            LISOLV.42
 38.   002167B        DO 155 I=ISTART,NIM1                                LISOLV.43
 39.   002171B        DO 155 J=JSTART,NJM1                                LISOLV.44
 40.   002174B    155 PHI(I,J,K)=PHI1(I,J,KP)                             LISOLV.45
              C*********************************************************** LISOLV.46
              C*****SOUTH-NORTH SWEEP                                     LISOLV.47
 41.   002212B        ISTM1=ISTART-1                                      LISOLV.48
 42.   002213B        A(ISTM1)=0.0                                        LISOLV.49
              C       COMMENCE S-N SWEEP                                  LISOLV.50
 43.   002213B        DO 200 J=JSTART,NJM1                                LISOLV.51
 44.   002216B        CA(ISTM1)=PHI(ISTM1,J,K)                            LISOLV.52
              C       COMMENCE W-E TRAVERSE                               LISOLV.53
 45.   002222B        DO 201 I=ISTART,NIM1                                LISOLV.54
              C       ASSEMBLE TDMA COEFFICIENTS                          LISOLV.55
 46.   002226B        A(I)=AE(I,J)                                        LISOLV.56
 47.   002230B        B(I)=AW(I,J)                                        LISOLV.57
 48.   002232B        CA(I)=AN(I,J)*PHI(I,J+1,K)+AS(I,J)*PHI(I,J-1,K)     LISOLV.58
                     1     +AU(I,J)*PHI(I,J,K-1)+SU(I,J)                  LISOLV.59
 49.   002245B        D(I)=AP(I,J)                                        LISOLV.60
              C       CALCULATE COEFFICIENTS OF RECURRENCE FORMULA        LISOLV.61
 50.   002246B        TERM=1.0/(D(I)-B(I)*A(I-1))                         LISOLV.62
 51.   002251B        A(I)=A(I)*TERM                                      LISOLV.63
 52.   002253B    201 CA(I)=(CA(I)+B(I)*CA(I-1))*TERM                     LISOLV.64
              C       OBTAIN NEW PHI,S                                    LISOLV.65
 53.   002260B        DO 202 II=ISTART,NIM1                               LISOLV.66
 54.   002262B        I=NI+ISTM1-II                                       LISOLV.67
 55.   002263B    202 PHI1(I,J,KP)=A(I)*PHI1(I+1,J,KP)+CA(I)              LISOLV.68
 56.   002274B    200 CONTINUE                                            LISOLV.69
 57.   002277B        RETURN                                              LISOLV.70
 58.   002301B        END
```

```
  1.  0000008        SUBROUTINE PRINT (ISTART,JSTART,NI,NJ,IT,JT,KT,X,Y,PHI,HEAD,K)          PRINT.2
  2.  0000008        DIMENSION PHI(IT,JT,KT),X(20),Y(50),HEAD(4),STORE(50)                   PRINT.3
  3.  0000008        DIMENSION F(7),F4(11)                                                   PRINT.4
  4.  0000008        DATA F/4H(1H ,4H,A6,,4HI3, ,4H11I ,4H10, ,4H7X, ,                       PRINT.5
                    14HA5) /                                                                 PRINT.6
  5.  0000008        DATA F4/4H 1I ,4H 2I ,4H 3I ,4H 4I ,4H 5I ,4H 6I ,                      PRINT.7
                    1        4H 7I ,4H 8I ,4H 9I ,4H10I ,4H11I /                            PRINT.8
  6.  0000008        DATA HI,HY/6H  I = , 6H Y =  /                                          PRINT.9
  7.  0000008        ISKIP=1                                                                 PRINT.10
  8.  0001068        JSKIP=1                                                                 PRINT.11
  9.  0001073        WRITE(6,110)HEAD                                                        PRINT.12
 10.  0001158        ISTA=ISTART-12                                                          PRINT.13
 11.  0001168    100 CONTINUE                                                                PRINT.14
 12.  0001178        ISTA=ISTA+12                                                            PRINT.15
 13.  0001208        IEND=ISTA+11                                                            PRINT.16
 14.  0001218        IEND=MIND(NI,IEND)                                                      PRINT.17
 15.  0001238        F(4)=F4(IEND-ISTA)                                                      PRINT.18
 16.  0001258        WRITE(6,F) HI, (I,I=ISTA,IEND,ISKIP), HY                                PRINT.19
 17.  0001458        WRITE(6,112)                                                            PRINT.20
 18.  0001508        DO 101 JJ=JSTART,NJ,JSKIP                                               PRINT.21
 19.  0001538        J=JSTART+NJ-JJ                                                          PRINT.22
 20.  0001548        DO 120 I=ISTA,IEND                                                      PRINT.23
 21.  0001608        A=PHI(I,J,K)                                                            PRINT.24
 22.  0001658        IF(ABS(A).LT.1.E-20) A=0.0                                              PRINT.25
 23.  0001728    120 STORE(I)=A                                                              PRINT.26
 24.  0001768    101 WRITE(6,113)  J,(STORE(I),I=ISTA,IEND,ISKIP),Y(J)                       PRINT.27
 25.  0002178        WRITE(6,114) (X(I),I=ISTA,IEND,ISKIP)                                   PRINT.28
                C-----------------------------------------------                              PRINT.29
 26.  0002328        IF(IEND.LT.NI)GO TO 100                                                 PRINT.30
 27.  0002348        RETURN                                                                  PRINT.31
 28.  0002368    110 FORMAT(1H0,20(2H*-),5X,4A10,5X,20(2H-*))                                PRINT.32
 29.  0002368    112 FORMAT(3H  J)                                                           PRINT.33
 30.  0002368    113 FORMAT(1H ,I3,1P12E10.2,0PF7.3)                                         PRINT.34
 31.  0002368    114 FORMAT(4H0X= ,12E10.3)                                                  PRINT.35
 32.  0002368        END                                                                     PRINT.36
```

0 0 0 0 4 9 0 2 3 8 5 - 7 1

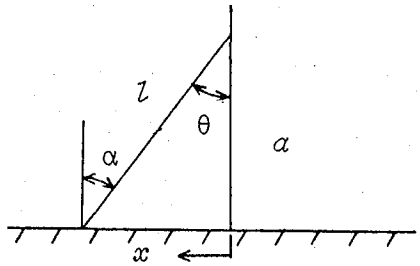

(a) Single Wall

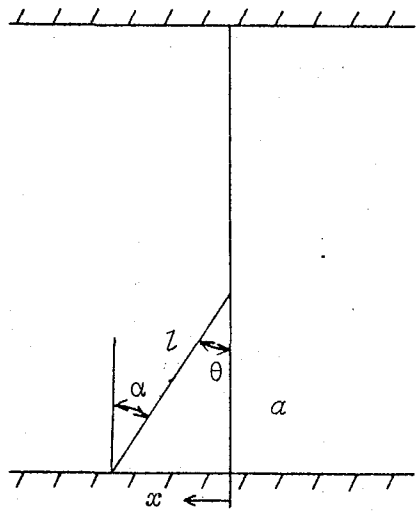

(b) Two Parallel Walls

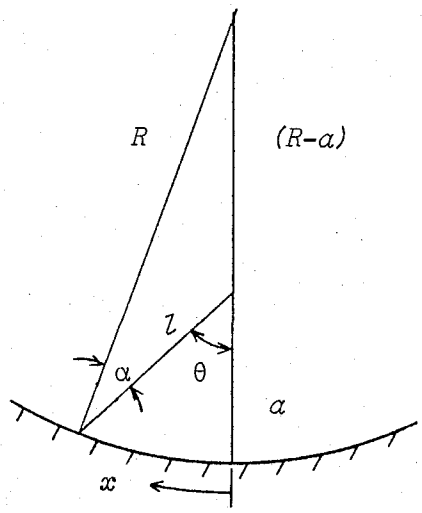

(c) Inside a Cylinder

Fig. A.1 Near-Wall Geometries

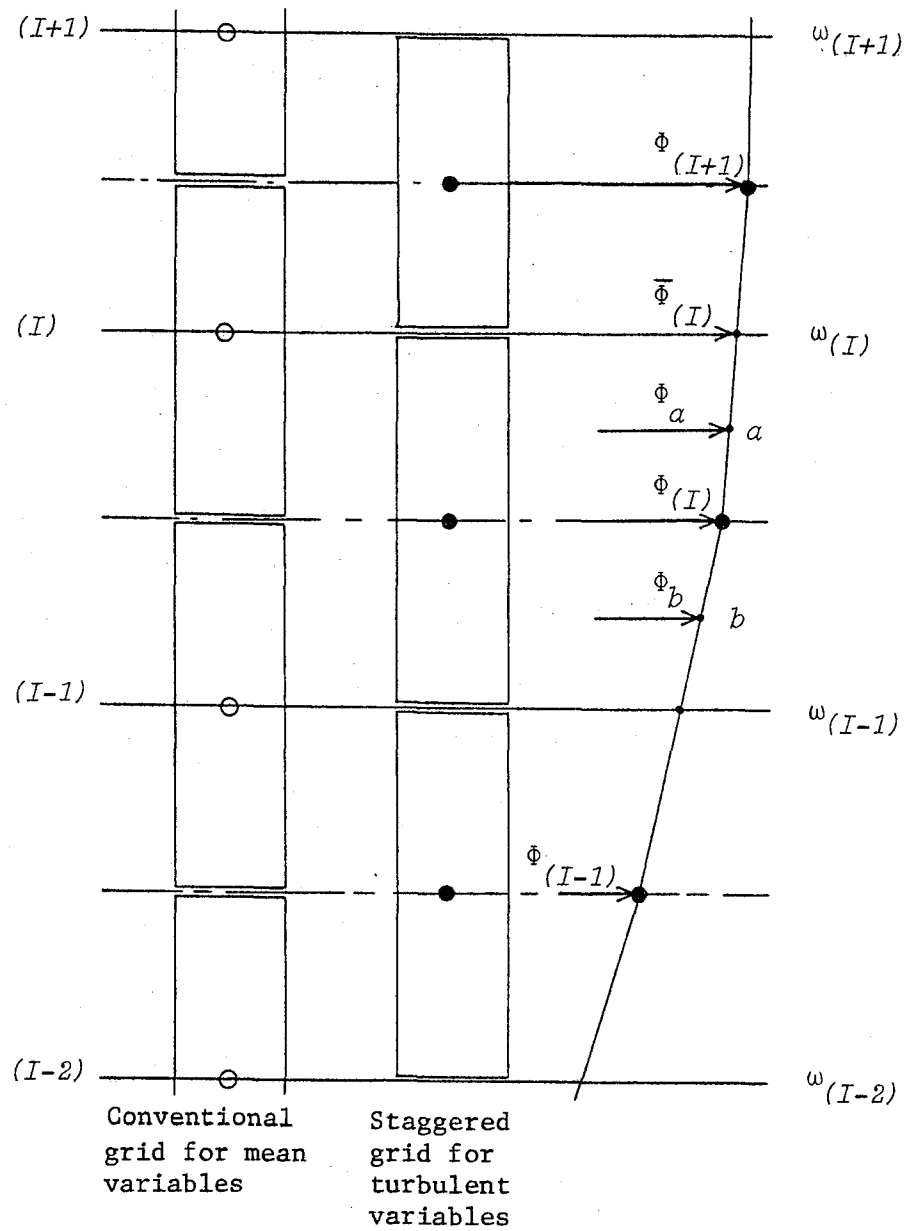

Fig. E.1 Staggered Grid in ω-Space

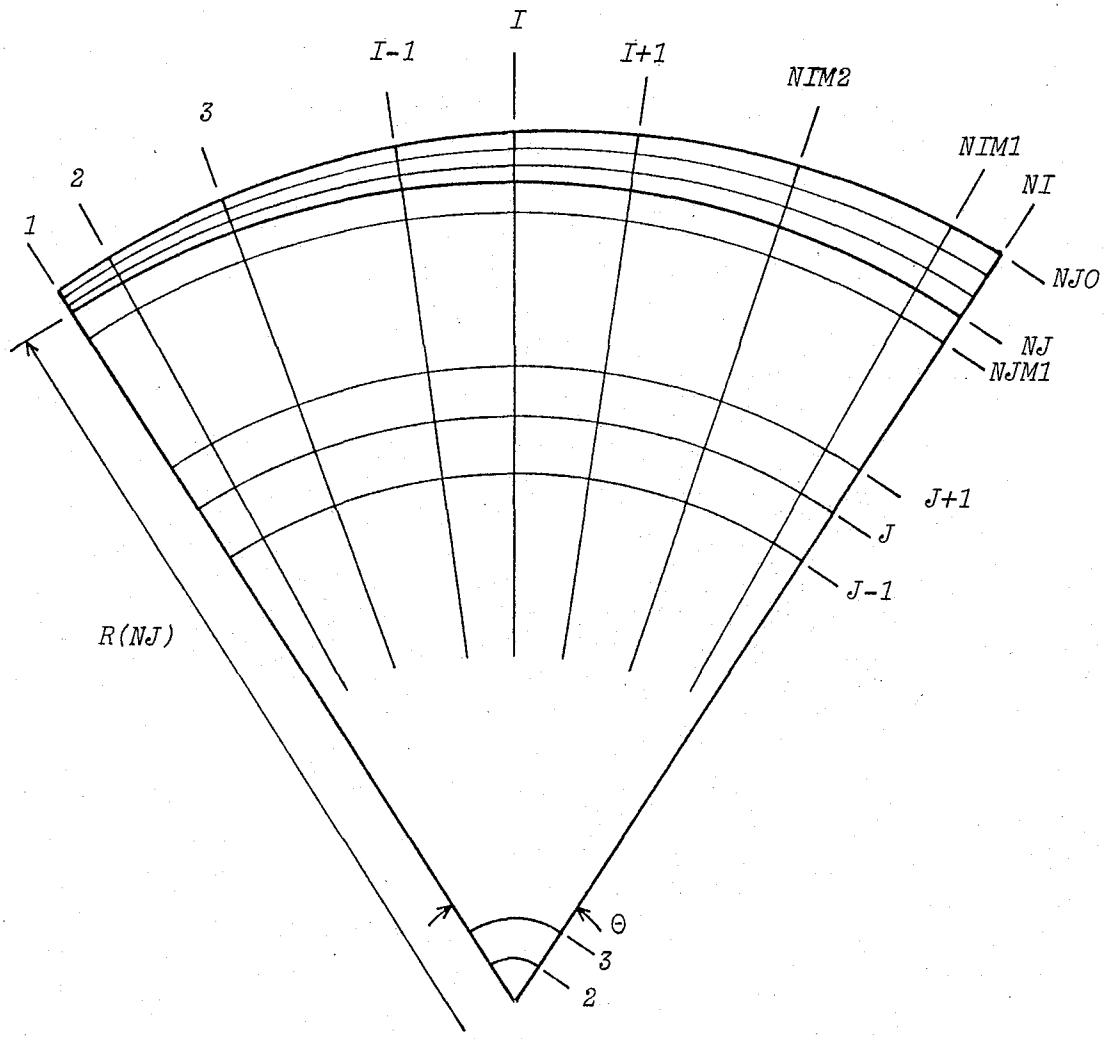

Fig. F.1 Calculation Domain

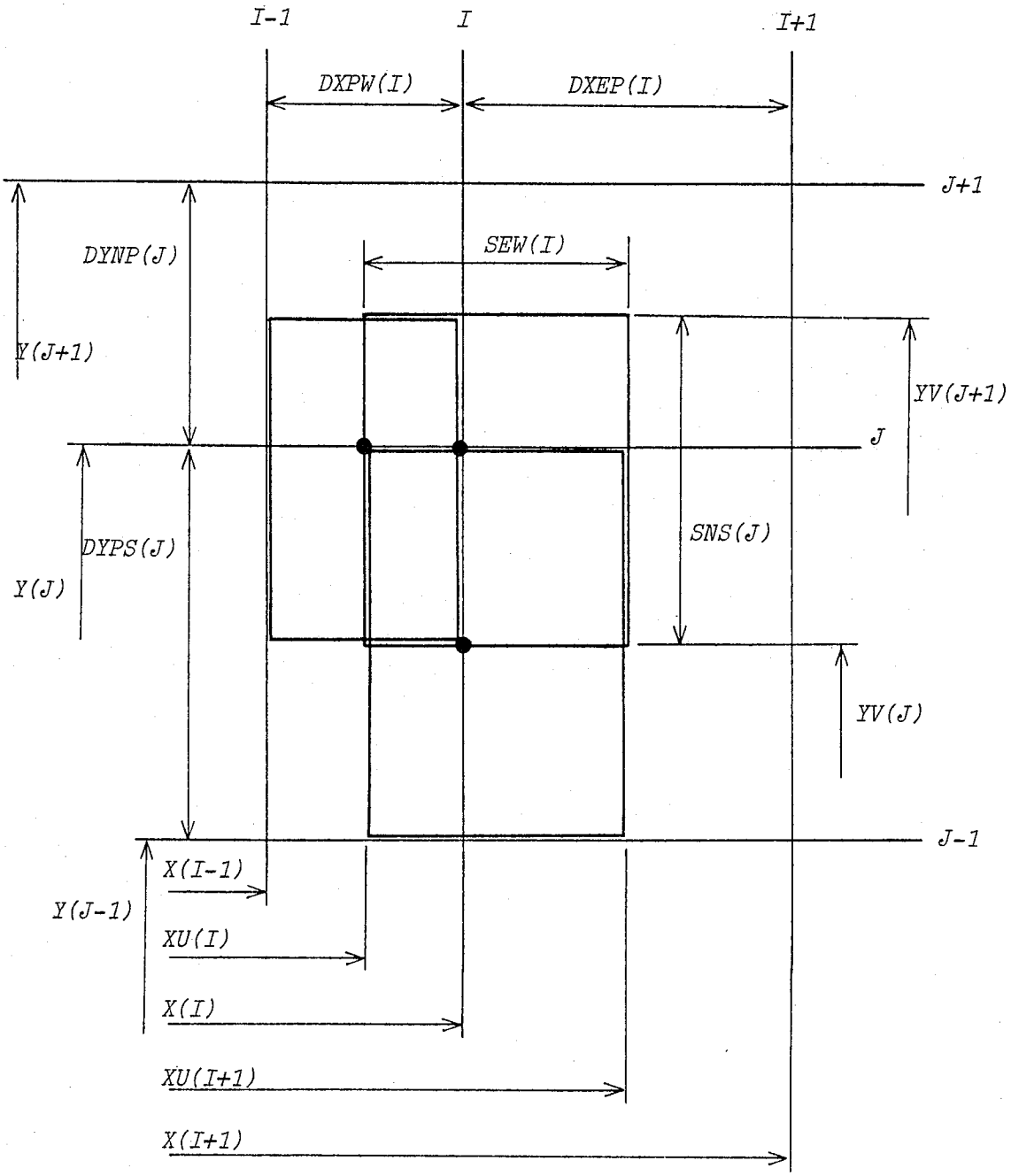

Note:

$DXEPU(I) = SEW(I)$;	$DYNPV(J) = SNS(J)$;
$DXPWU(I) = SEW(I-1)$:;	$DYPSV(J) = SNS(J-1)$;
$SEWU(I) = DXPW(I)$;	$SNSV(J) = DYPS(J)$.

Fig. F.2 Grid and Related Dimensions.

This report was done with support from the United States Energy Research and Development Administration. Any conclusions or opinions expressed in this report represent solely those of the author(s) and not necessarily those of The Regents of the University of California, the Lawrence Berkeley Laboratory or the United States Energy Research and Development Administration.

0 0 0 0 4 5 0 2 2 9 4